CORROSION PERFORMANCE OF EPOXY-COATED REINFORCEMENT

by

KHALED ZUHAIR KAHHALEH, B.Sc., M.S.

DISSERTATION

Presented to the Faculty of the Graduate School of

The University of Texas at Austin

in Partial Fulfillment

of the Requirements

for the Degree of

DOCTOR OF PHILOSOPHY

THE UNIVERSITY OF TEXAS AT AUSTIN

May 1994

CORROSION PERFORMANCE OF EPOXY-COATED REINFORCEMENT

Approved by
Dissertation Committee:

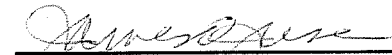

James O. Jirsa, Supervisor

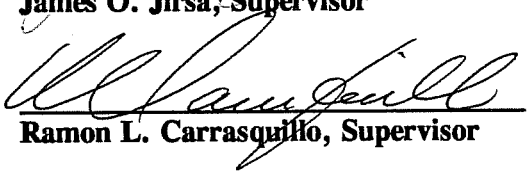

Ramon L. Carrasquillo, Supervisor

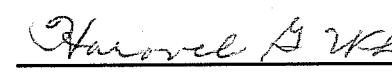

Harovel G. Wheat

John E. Breen

David W. Fowler

Copyright

by

Khaled Zuhair Kahhaleh

1994

CORROSION PERFORMANCE OF EPOXY-COATED REINFORCEMENT

by

KHALED ZUHAIR KAHHALEH, B.Sc., M.S.

DISSERTATION

Presented to the Faculty of the Graduate School of

The University of Texas at Austin

in Partial Fulfillment

of the Requirements

for the Degree of

DOCTOR OF PHILOSOPHY

THE UNIVERSITY OF TEXAS AT AUSTIN

May 1994

This book is dedicated to the following people,
with love and lifelong devotion.

My wife, ***Siba,***
for her love, warmth, support,
devotion, encouragement, faith,
and above all patience.

My children, ***Mo'men*** *and* ***Zain.***
They have made my life rich and full.

My parents, and my in-laws,
for their love and support.

K.K.

ACKNOWLEDGMENTS

The financial support of the Texas Department of Transportation and the Federal Highway Administration which made this research project possible is greatly acknowledged.

A large number of people contributed in significant ways towards the execution and completion of this work. My sincere appreciation and gratitude go to both Dr. James O. Jirsa and Dr. Ramon L. Carrasquillo, co-chairmen of my supervising committee. Dr. J. Jirsa was instrumental in providing help and support to alleviate problems that came my way, and from the beginning of this research to its completion, his continuing advice has been most generous. His dedication to research has been a source of inspiration and motivation. The help and guidance of Dr. R. Carrasquillo were also indispensable to the completion of this work. His encouragement gave me the thrust to pursue excellence. I am greatly indebted to both of them for their suggestions, humor, exemplary characters, generosity and friendship which made the course of this study very enjoyable.

Particular thanks go to Dr. Harovel G. Wheat for her help and interest. Her comments and contribution to the project were most appreciated. My special thanks are also extended to Dr. John E. Breen and Dr. David W. Fowler, for their guidance, advice, and very constructive comments. My sincere thanks are extended to all the staff members at Ferguson Structural Engineering Laboratory and the Materials Research Group who cooperated to make this project possible. The assistance of both Faisal Sayed and Hasan Pasha was invaluable. Also, special thanks are due to Heng-Yih Chao, Robert Frosch, Wanzhi Li, Trey Hamilton, and Enrique Vaca for their help during various phases of the project. Great gratitude is extended to Marwan Awad, Basim Mekha, Riyad Aboutaha, Elias Saqan, Hakim Bouadi, Osama Hamzeh, Ghiath Mansour, Asif Wahidi, Todd and Karen Helwig, Raj Valluvan, and many other fellow graduate students for their friendship.

I am especially indebted to my wife and parents for their love and faith. I am also deeply thankful to Dr. Seyfeddin Muaz, the administration, and colleagues at The Royal Scientific Society in Jordan for their encouragement and support.

Austin, Texas
April, 1994

Khaled Z. Kahhaleh

CORROSION PERFORMANCE OF EPOXY-COATED REINFORCEMENT

Publication No. _____

Khaled Zuhair Kahhaleh, Ph.D.
The University of Texas at Austin, 1994

Supervisors: James O. Jirsa, Ramon L. Carrasquillo

The long-term corrosion resistance of fusion-bonded epoxy-coated reinforcement in concrete exposed to chlorides has recently been questioned. Damage to coating, primarily during fabrication, handling, and construction, is considered to be the most serious factor affecting performance. In this study, the integrity of epoxy-coated bars in various corrosive environments was examined. The effects of coating damage, exposure conditions, and cracking due to structural loading on corrosion performance of coated bars were investigated experimentally.

The level of damage to the coating governed the resistance to corrosion. The larger the areas damaged and percentage of damage on a bar surface, the higher was the corrosion rate. Bent bars with damage concentrated at the bends exhibited extensive debonding of the coating from the bar and widespread corrosion on the steel substrate. Concrete cracking, regardless of the width, led to an accumulation of chlorides at the bar surface and accelerated initiation of corrosion. Significant pitting corrosion was observed on stressed coated bars with 3% surface damage embedded in concrete beams with crack widths about 0.33 mm (0.013 in.). Electrical continuity between coated and uncoated bars located in different chloride environments, or exposure of damaged coated bars to chloride concentration cells, promoted macrocell activity. Also, variations in concrete consolidation around coated bars facilitated initiation of corrosion and increased possibility of void formation at the underside of the bar where corrosion spotting was noted most.

The epoxy coating, however, improved the performance of reinforcement in concrete exposed to chloride compared with bare reinforcement. Corrosion initiation was delayed and the severity of bar surface degradation and metal loss was reduced on coated bars compared to uncoated bars. Corrosion-induced deterioration of concrete members with coated reinforcement was reduced. Patching of damaged areas reduced corrosion activity but did not stop it completely. The performance of coated bars will be improved by coating after fabrication, minimizing damage to coating, avoiding mixing coated and uncoated reinforcement, improving coating repair materials and application, tightening current specification requirements regarding coating quality and acceptable damage limits, and improving concrete consolidation around bars.

TABLE OF CONTENTS

CHAPTER 1
INTRODUCTION

1.1 Research Objectives

1.1.1 General. Epoxy-coated reinforcement is being used extensively in construction to protect the steel from corrosion. If structures constructed with coated reinforcement prematurely deteriorate because of corrosion, the economic impact will be immense. The research work described herein is focused on the following two important issues:

- determination of the performance of epoxy-coated reinforcement in corrosive environments; and,
- evaluation of the effect of potential corrosion of coated reinforcement on the integrity of structure.

1.1.2 Objectives. The main objective of this study was to investigate the integrity and performance of epoxy-coated reinforcement in corrosive environments. The purpose was to indicate the conditions which influence performance of coated reinforcement so that proper precautions can be taken in design, construction, and maintenance to maximize the service life of structure.

The main objective of the study was divided into the following key points:

- Identifying conditions that produce damage to epoxy coating and evaluating some techniques for inspection of the quality of coating application. Of concern was damage introduced during coating, fabrication, handling, transportation, storage, installation, and concreting procedures.

- Identifying conditions conducive to corrosion of epoxy-coated bars. An experimental program was established to evaluate performance of coated bars with various levels of coating damage (and repair) and under different loading conditions.

- Providing guidance for improving performance of epoxy-coated bars.

The findings of this study are expected to benefit practioners in the selection and detailing of coated bars. The findings are also expected to aid in improving procedures critical to performance of coated bars from coating to final use in the field. In addition, the information provided in this study can be used to modify current specifications and inspection techniques.

1.2 Nature of Corrosion Damage Problem

1.2.1 Corrosion of Steel in Concrete. Conspicuous brown-red rust stains, scaling, and crumbling of concrete on bridge decks and parapets are all too common in much of the northern US where deicing salts are used or along the coastal marine environments. During the past three decades, deterioration of bridge decks has become expected in the first 2 to 3 years following construction.[1-3] The problem has been traced to corrosion of reinforcement caused by chlorides present in deicing salts. In the early 1960's, the Federal Highway Administration (FHWA) instituted the "bare pavement" or "clear road" policy; *i.e.* keeping all roads open all year round. Ever since, the use of deicing salts has increased tremendously and so have the repair costs of corrosion-induced damage as shown in Fig. 1.1. Despite its detrimental effect on bridge structures, salt is still used extensively to keep the roads clear!

In the late 1970's, *Engineering News Record,*[4] reported that: "... chloride corrosion of reinforcing steel in concrete is much like cancer. Dissolved deicing salt seeps into pavement concrete and creates a tumor-like rust on the steel and breaks the concrete apart."

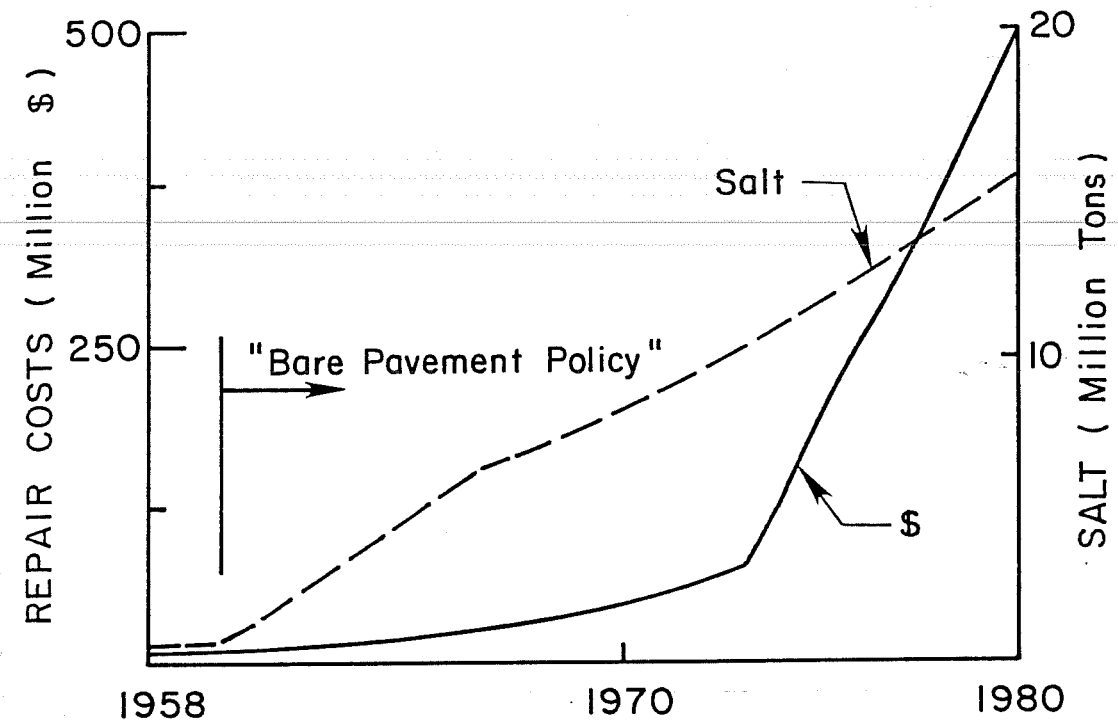

Figure 1.1 Increase of Repair Costs of Bridge Deck Deterioration Related to Salt Application.[4]

It was soon known that chlorides attacked all elements of reinforced concrete highway structures. Bridge decks, sidewalls, pier caps, piers, pilings, slab soffits, and even foundations suffer from salt water splashing and surface run off. Salt transported by automobile tires to parking structures during winter has precipitated damage and early degradation in those structures. Figure 1.2 shows examples of structures suffering excessive damage due to reinforcement corrosion.

The problem is growing: approximately half of the 575,000 bridges in the US Federal Aid Highway System are structurally deficient or functionally obsolete.[5,6] The FHWA has estimated that one of every four bridge decks in the US is badly deteriorated. Expensive repairs are often required after only 5 to 10 years in operation.[2,3]

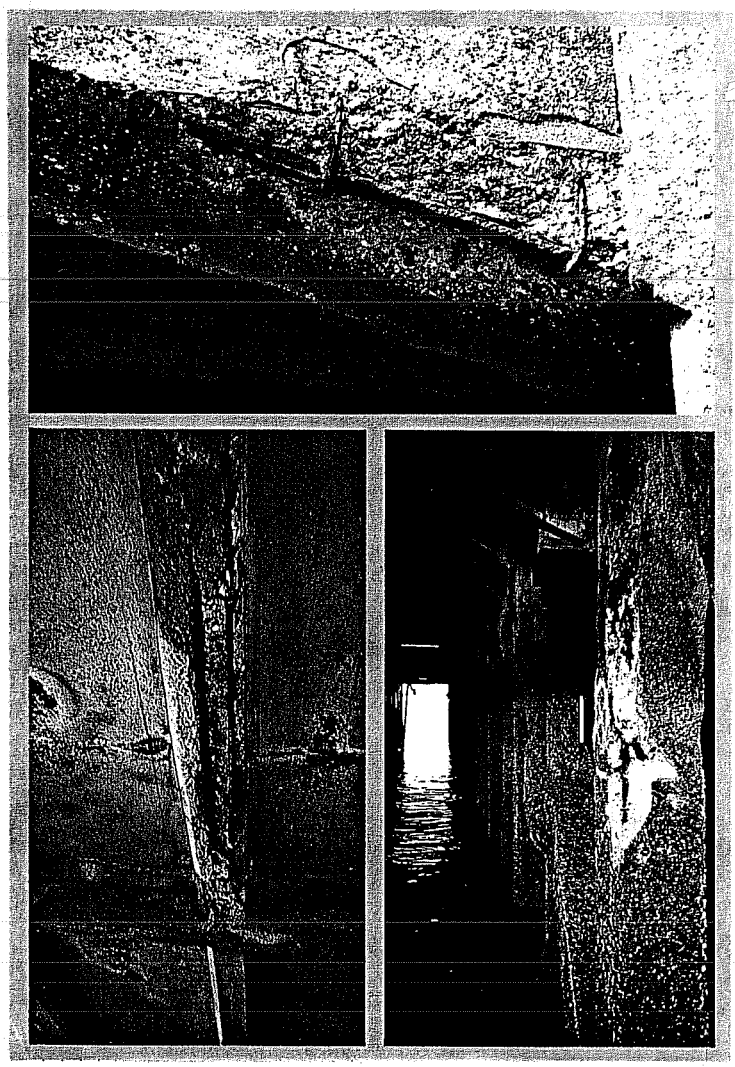

Figure 1.2 Examples of Structures Suffering Excessive Damage Due to Reinforcement Corrosion (Courtesy of Sealocrete Corp. Ltd.).

Corrosion problems occur worldwide largely due to chlorides. Research in Saudi Arabia and elsewhere in the Middle East indicated that the service life of buildings in the Arabian Gulf may be expected to be between 10 and 15 years,[7] and sometimes only 5 years![8] What could be more frustrating than knowing that corrosion was, in some cases, so severe that concrete damage occurred even before the completion of construction?![9]

In the Greater Copenhagen area of Denmark, half of the bridges with columns are expected to have corrosion-induced damage.[10] In Japan, rapid deterioration has been observed on prestressed and reinforced concrete bridges near the seashore after only about 10 years in operation.[11] Eleven viaducts built in the UK in 1972 for £28 million deteriorated within two years because of winter salting of roadways.[12] In 1985, over 40% of the turnover of the UK construction industry involved the repair and maintenance of existing structures.[13] Numerous conferences, workshops, seminars, and committee meetings were held, on a global level, to express concern, bring awareness, and exchange thoughts about an effective means of solution.

At present, the greatest extent of natural damage to reinforced concrete structures can be attributed to chloride ions. Transportation structures and parking garages in cold countries are damaged because of deicing salts. Coastal structures and bridge substructures in marine environments are damaged by seawater and salt spray. In addition, structures are often constructed with a built-in destructive agent: a chloride-based accelerating admixture. Moreover, self-contaminated aggregates and brackish water set the stage for advanced corrosion and premature durability problems.

Deterioration of structures is hastened by inferior concrete quality, inadequate cover to reinforcement, cracking, and adverse service conditions. Harsh environments, such as salt water splashing, tidal waves, and hot and moist climates promote corrosion and subsequent degradation. As more chloride ions penetrate to the steel, corrosion accelerates, rust products form, concrete cracks and delaminates, and the integrity of the structure is threatened.

The phenomenon of corrosion has been known for centuries as a natural process of metal decay. Although viewed by many as a negative action, corrosion may be used in a positive way, as in dry-cell batteries. Preventing corrosion is warranted only when its consequences are intolerable. In structures, corrosion itself need not be stopped: as long as the structure's life or function or aesthetics is not jeopardized, corrosion is tolerable. Therefore, corrosion of reinforcing steel may *not* always be a problem, but will be if damage is produced.

1.2.2 The Need to Control Corrosion in Reinforced Concrete Structures. Different estimates of the economic loss due to corrosion of steel in concrete have been reported in the literature. There is general agreement that the problem in the US is costing millions of dollars per annum. The cost of metallic corrosion alone is greater than the costs of floods, hurricanes, tornadoes, fires, lightning, and earthquakes and is substantially escalating.[14] Metallic corrosion cost was appraised at $70 billion per year (more than 3.5% of the Gross National Product as shown in Fig. 1.3). Corrosion-induced damage of bridge decks, in particular, costs about $500 million per year.[4,5,14]

Bridges are wearing out much faster than they can be repaired; restoration costs are, many times, prohibitive. In 1972, repair of deteriorated structures due to chloride attack was estimated at $3 to $4 billion.[1] The annual cost of repairs on interstate highways only was estimated to be more than $70 million.[15] In 1978, it was estimated that 40% of all steel production was being used to replace corroded steel.[4,16] In 1979, the cost to restore surfaces on 160,000 Federal Aid System bridges was estimated to be $6.3 billion.[17]

In 1981, a published study indicated that the restoration cost of all distressed bridges in US was estimated to be about $10 billion.[18] This estimate was based on the assumption that 40% of all bridges suffer distress. The study was skeptical about the effectiveness of the

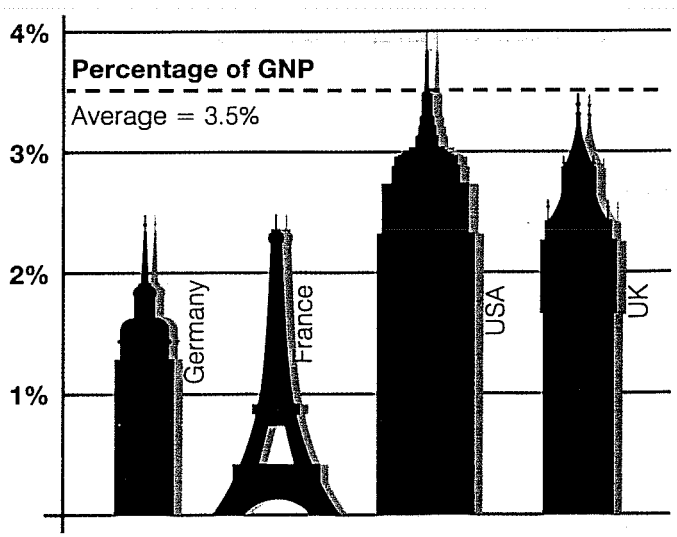

Figure 1.3 Cost of Corrosion (Courtesy of Schlumberger Technologies).

rehabilitation procedures employed at that time; the rehabilitation procedures provided no technical guarantee that the restoration would be effective for more than a decade! Other studies estimated the cost of correcting existing bridge problems in 1982 to be in the neighborhood of $47 to $60 billion.[19]

In 1983, according to one study, the estimated number of deficient bridges was in excess of 100,000 and the cost of their rehabilitation or replacement was to be around $33 billion.[20] The projected cost directly related to bridge deck deterioration was about $11 to $17 billion. Another study estimated the cost of repair to some 300,000 bridge decks at over $100 billion.[21] According to a third study, it was calculated that the interstate highway system that stretched over 64,000 km (40,000 miles) across the country would require close to $500 billion in repair over a decade.[4]

In the UK, surveys showed that repairs to just a tiny fraction of the national highway bridges and motorway structures exhibiting chloride attack would cost about £600 to £800 million over 10 years.[3,22] In Switzerland, it was estimated that the annual costs of inspection and maintenance of bridge decks only to be about 80 million Swiss francs.[23]

Another problem related to corrosion-induced deterioration is unscheduled shutdown. Bridges are frequently shut down for remedial work or unexpected failure. Closing a bridge in a busy area will incur a huge indirect cost for traffic rerouting and will inconvenience a large number of people. For example, over 240,000 people who used the Williamsburg Bridge in New York every day were affected when the bridge was closed for rehabilitation for nearly four months in 1988.[24]

The serious economic implications of reinforcing steel corrosion to the existing stock of bridges and buildings worldwide warranted the development of some effective techniques for corrosion control. The approach for dealing with the corrosion damage problem has not been well-defined or agreed on. After 30 years of experience, Buslov[25] stated that "The corrosion damage problem will not go away; since it cannot be eliminated, the goal is to find the most efficient way of living with it". Buslov decided that ".. the execution of repairs of

corrosion deterioration based on a regular maintenance cycle is the most efficient way of dealing with this problem".

On the other hand, El-Metwally and Schlaich[26] called for the adoption of the concept of designing structures to be repair-free. They suggested that dealing with the corrosion damage problem during the design stage is the cheapest and most efficient way to prevent corrosion.

The FHWA considered eliminating the problem of bridge deck deterioration as one of the top priority efforts.[27] In search of an effective means to solve the problem, fusion-bonded epoxy-coated reinforcement emerged as a promising solution. Epoxy-coated reinforcement is a "positive" corrosion preventive system mandated by the necessity to resist corrosion when concrete cracking permits chlorides to reach the steel.

It has been more than a decade since coated steel gained popularity and reputation as a cost-effective technology to prevent corrosion. In 1982, the Transport and Road Research Laboratory Supplementary Report 667 stated that:[12] "Epoxy coating of the top steel in addition to current waterproofing practice would provide -at relatively little extra cost- additional assurance that the reinforcement would be adequately protected throughout the life of the bridge." As a result, epoxy coating plants were set up in the US and in many parts of the world such as Canada, Europe, the Middle East, Japan, and Australia.[28]

Initially, the cost of coated reinforcement ranged from 40 to 100% more than conventional reinforcement.[4,29] Recent contacts with the Texas Department of Transportation (TxDOT) indicated that the cost of coated reinforcement dropped from 50% more than conventional in the early 1990's to only 25% in 1992. Considering the total cost of typical bridge structures, it is expected that the increase in cost due to use of coated reinforcement does not exceed 3%. Such an increase is insignificant compared to the potential savings in maintenance during the useful life of a bridge structure.

1.1.3 Corrosion of Epoxy-Coated Reinforcing Steel. Unfortunately, instances of premature failure of the epoxy coating and significant corrosion of steel substrate have occurred recently. The premature deterioration of the substructures of the Florida Keys bridges in the late 1980's was the first major incident. Four bridge substructures in the Florida Keys deteriorated significantly after about 6 to 10 years in service. Corrosion was noted on both straight and bent coated bars. It is likely that the high water salinity and high temperature in Florida promoted corrosion, but several other factors were raised as possible causes that precipitated failure. Damage and debonding of epoxy coating prior to concrete placement were major factors.

Other corrosion problems related to epoxy failure were also reported in Oregon and New York.[30] Three bridge decks and one noise barrier wall constructed with epoxy-coated bars were identified, with at least a portion of each structure suffering from reinforcement corrosion or corrosion-related distress, or both.[31] These structures were subjected to both freeze-thaw cycles and deicing salt applications.

In the Middle East, some epoxy-coated bars coated and stored outdoors for over six months exhibited cracking and debonding, as well as severe underfilm corrosion.[12] The coating was discolored and debonded on one side of the bar. Fine cracking of the substrate, in addition to crystalline deposits, was discovered beneath the coating. The major cause of coating failure was attributed to inadequate surface preparation.

In spite of these incidents, there is no published evidence to date of any corrosion-related damage in bridge decks incorporating coated bars within the US. Apparently, the coated bars provide a high degree of protection in chloride-contaminated bridge decks.[32] However, it has been debated whether the generally good corrosion performance of sampled coated bars from bridge decks was due to epoxy coating or to improved concrete quality and deeper cover![31]

The deterioration of bridge substructures in Florida has raised concern about the effectiveness of the epoxy coatings to prevent chloride-induced corrosion of reinforcement

in highly corrosive environments. The concern over performance of coated bars was heightened after new observations by a principal researcher regarding the propensity of the coated reinforcement to lose its protection.

Clear[33-37] has recently reported that fusion-bonded epoxy coatings will not be effective in providing long-term (50 years or more) protection to reinforcement in salt-contaminated concrete. It has been said that an unexpected failure mechanism involving progressive loss of coating adhesion and underfilm corrosion occurs even in high quality coated bars. A highly corrosive environment can cause a pattern of debonding, blistering, and cracking of the epoxy film.

According to Clear, the projected increase in life of structures constructed with epoxy-coated reinforcement over those with uncoated reinforcement in the northern US and Canadian environments (marine and deicing salt) is in the range of 3 to 6 years. Further, Clear has indicated that strict and tightly enforced specifications will not assure long-term, maintenance-free service life. Clear concludes that coated bars will not be effective for more than 15 years in northern environments, or more than 5 years in hot, salty, and moist southern exposures.

The fact that corrosion of epoxy-coated bars has caused damage in existing structures indicates that, at present, there is probably no single method of corrosion prevention that can be presumed to be effective throughout the life of a structure.

1.3 Research Significance

1.3.1 Technical Concerns. At present, there are several standard specifications and recommended practice documents prepared by ASTM, AASHTO, National Association of Corrosion Engineers (NACE), and Concrete Reinforcing Steel Institute (CRSI) endorsing the production and use of epoxy-coated reinforcement. Although these specifications are, more or less, similar to each other, there are some important variations. The major specification requirements that affect the performance of coated steel are: the condition of

bar surface before and after blast cleaning during the coating operation; thickness of coating; bend test to check coating flexibility and adhesion; and permissible damage criteria.

The adequacy of current specifications has been widely questioned and the need for modification them has been advocated by many researchers and Federal transportation officials.[33] Arguments have arisen for tightening the specifications, addressing all phases of the coating process and use of bars in field, and improving quality control to avoid unexpected failures. Examples of the requirements proposed for modification are the ASTM A775[38] bend test radii which are less than those used in practice for fabrication, and the ASTM D3963[39] permissible damage criteria.

Commonly, bars are coated before bending. Subsequent fabrication may introduce damage to coating and weaken adhesion to steel substrate. Handling, transportation, storage, installation, and concrete placement and vibration may produce further damage, mainly by abrasion. Exposed steel at damaged areas reduces resistance to corrosion.

Corrosion of coated bars at crack locations in concrete bridge decks has been observed.[31] Excessive amounts of chlorides may penetrate through the cracks and accumulate in high concentrations at the bar surface initiating corrosion. The problem is particularly relevant to coated bars since wider flexural cracks have been observed on concrete members reinforced with coated bars relative to uncoated bars. The problem could be aggravated by both freeze-thaw action and damage to the coating.

To summarize, many concerns about long-term protection of coated bars have been expressed. Of particular interest was the susceptibility of epoxy-coated bars to:

- excessive defects and damage from production stage to embedment in concrete; and,
- undercutting (propagating underfilm corrosion) after corrosion starts on exposed steel at defects and damaged spots (Fig. 1.4).

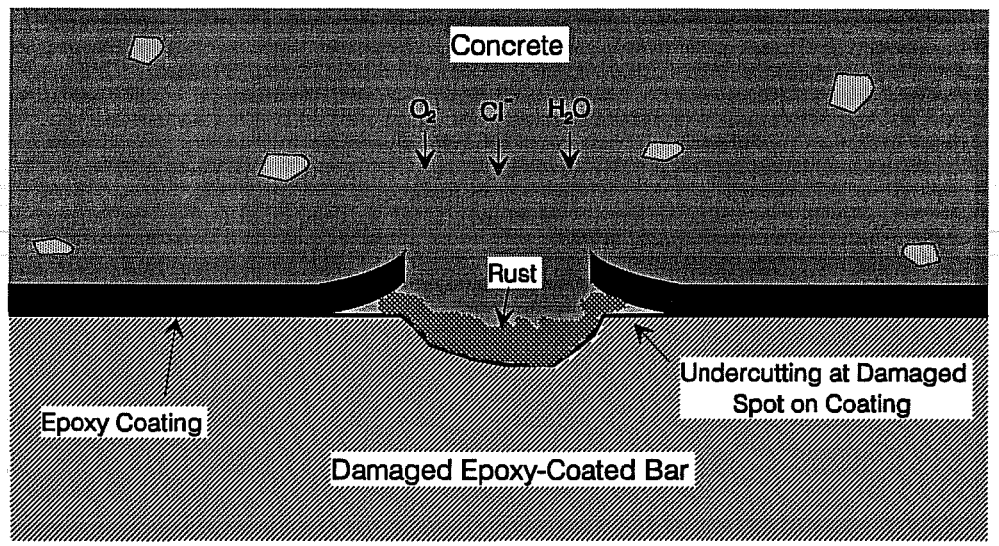

Figure 1.4 Corrosion Propagation Under Epoxy Coating.

In addition, it is vital to understand the effects of the following on the resistance of coated bars in concrete to corrosion:

- exposure of coated bars to high and variable concentrations of chloride ions; and,
- coupling coated bars to uncoated bars which may drive an intensive corrosion activity at the exposed steel areas on the coated bars under certain exposure conditions. Commonly, epoxy-coated bars are installed in the top mat reinforcement of bridge decks with possible electrical contact with the uncoated bars in the bottom mat.

Despite the numerous papers published on corrosion performance of epoxy-coated bars, the information concerning its long-term durability is incomplete.[40] The need to understand the corrosion mechanism(s) of coated reinforcement is as great as ever. Early studies have indicated that epoxy-coated reinforcement has good potential as a corrosion resistant material. Recent findings, however, are not consistent with the early findings and disagreement is growing regarding the effectiveness of coated steel in controlling corrosion. The construction industry in general, and transportation agencies in particular, need to know that coated reinforcement will perform as desired.

1.3.2 Economic Concerns. CRSI,[32,41] has indicated that during 18 years of use of epoxy-coated reinforcement, there are more than 100,000 structures in US and Canada constructed with coated steel. This figure equates to over 1.8 million metric-tons (2 million tons) of coated steel.

There is an increasing demand for coated bars. The yearly consumption of coated bars in the US has increased by a factor of 180 over the last 15 years. In 1987, the total tonnage of coated bars exceeded 160,000 metric-tons (180,000 tons), which was about 7% of the total reinforcing bar market.[29,42] USA and Canada together consume approximately 4.5 million metric-tons (5 million tons) per annum of reinforcing steel of which over 270,000 metric-tons (300,000 tons) per annum is epoxy-coated bars.[1] Today, most state transportation agencies specify coated steel in projects in harsh environments exemplifying the widespread acceptance of this corrosion protection system.[30]

Epoxy-coated reinforcing steel is presently used extensively in bridge decks, parking garages, waste-water treatment plants, chemical plants, cooling towers, subways, and marine structures. Public funds already invested and future investments in construction using epoxy-coated reinforcement are large. Corrosion problems will lead to major losses.

1.4 Research Organization

An extensive literature review and some field visits were carried out to gather information for the study. First, the corrosion phenomenon and methods of corrosion detection and monitoring were reviewed. Second, critical aspects of performance of coated bars were studied, and general information on epoxy-coated reinforcement were presented. Third, previous studies on durability of epoxy-coated bars were reviewed, and the mechanisms proposed in the literature for corrosion of coated bars were summarized.

Next, a series of tests was conducted to evaluate some inspection techniques and field operations relevant to coating damage determination. The widely-used holiday detectors and

another test of potential future use, the hot water immersion test, were examined. Damage to coating due to concrete placement and vibration was evaluated.

Finally, a three-part corrosion experimental program to study performance of coated bars in highly corrosive environments was established. First, damaged coated bent bars were exposed to chloride solution and their deterioration was examined and reported in the immersion test. Companion bent bars were embedded in concrete prisms exposed to chloride solution while being linked to uncoated bars. The corrosion currents were monitored and reported in the macrocell test. Straight bars and stirrups were placed in beams that were partially exposed to chloride solution. The beams were subjected to different loading conditions. The steel electrical potential was monitored and the effects of concrete cracking, and cycles of loading and unloading, on the deterioration of performance of coated bars under conditions simulating service conditions were examined. The results were reported in the beam exposure test.

A summary of the study, conclusions and recommendations are presented.

CHAPTER 2
LITERATURE REVIEW OF THE BASICS OF REINFORCEMENT CORROSION IN CONCRETE

2.1 Steel Corrosion Cell Development in Concrete

2.1.1 General. Corrosion of metals is a natural process known as extractive metallurgy in reverse.[14] In the steel making process, a large amount of energy is used to drive off oxygen. As a result, a high level of potential energy is stored in the steel. The iron becomes thermodynamically "anxious" to return to iron oxide.[16] Figure 2.1 illustrates this process in which the iron goes through an energy cycle reversing the metallurgy.

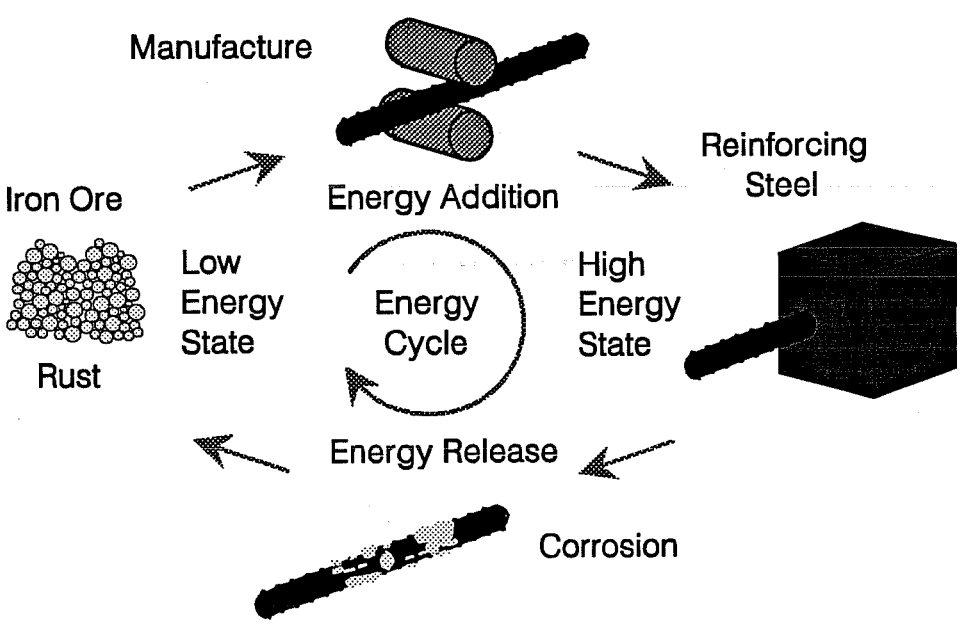

Figure 2.1 The Energy Cycle of Iron.

2.1.2 Corrosion Cell Components. There are three essential components for a simple corrosion cell. These are:

- An anode; the site which looses metal (the corroding surface).
- A cathode; the site which is not consumed (the passive surface).
- An electrolyte; the medium in which the corrosion process takes place.

The basic corrosion cell is also called the electrolytic or galvanic cell because of the electrochemical nature of corrosion or the galvanic action involved.

2.1.3 Corrosion Process. To understand the mechanisms involved in steel corrosion in concrete, it is necessary to know how steel corrodes in general. As a first step, an active iron atom on the steel surface oxidizes, *i.e.* loses electrons, to become an iron (or ferrous) ion Fe^{+2}. The oxidation reaction is half of the overall corrosion reaction and is called the anodic reaction. The oxidized area is, thus, the anode. Such conversion in the state of iron occurs under a certain electromotive force.

The other half of the complex corrosion reaction is the cathodic (or reduction) reaction. Most often oxygen molecules, in the presence of moisture, on the steel surface consume the liberated electrons in the reduction reaction. The product of such half-cell reaction is the hydroxyl ion OH^-. Thus, the electrochemical corrosion process involves the movement of electrons within the metal being corroded. The area of the steel where oxygen reduction occurs is the cathode.

The electrolyte is a conductive material that permits ionic diffusion between the anode and cathode. The electrolyte must have a specific minimum ion content and a minimum water content to be conductive.[43] It may exist in a bulk form, such as a corrosive solution in contact with the steel bars, or a conductive concrete surrounding the reinforcing bars. It may also be present as a thin condensed or adsorbed film on the steel surface.[16]

The overall corrosion reaction is the sum of the anodic and cathodic half-cell reactions also called redox reactions. No corrosion process is complete without both reactions occurring simultaneously at the respective electrodes. A metallic conductor must also exist to allow electron transfer. The surplus electrons freed at the anode pass through the metal to the cathode. Likewise, the conductive electrolyte facilitates ion transfer. The hydroxyl ions migrate towards the dissociated iron to combine, in a series of intermediate steps, to form rust. The resulting rust products precipitate back to the surface (see Fig. 2.2 and the reactions included in Section A.2). These products are, more or less, water-containing compounds. It follows that only oxygen is consumed to form rust.[29]

The active element is depicted as a short-circuited galvanic element. The charge transfer obeys Ohm's Law. The law describes the current that will flow under a certain driving force, or voltage, and path resistance. The driving force (or electromotive force) is the potential difference between the anode and cathode. In essence, it is a measure of the tendency of the reaction to occur. The ionic current flows through the electrolyte in an opposite direction to the electrical current. The number of ions that pass between the electrodes is a measure of the corrosion current. High corrosion currents correspond to high corrosion rates. The resistance of the electrolytic path, among other factors, governs the corrosion rate.

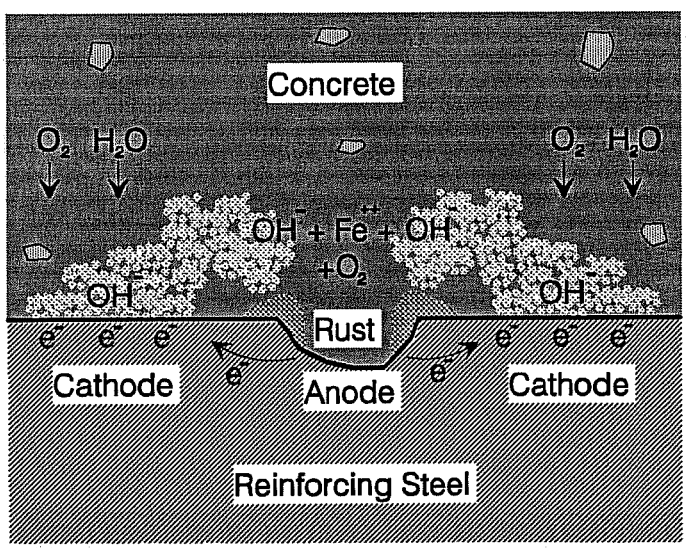

Figure 2.2 Precipitation of Rust.

The conductivity of the concrete as an electrolyte comes from the ingress of salt and retained moisture. Salt reduces the concrete resistivity, *i.e.* increases the conductivity, which accelerates the corrosion rate.[16] Moisture also increases the conductivity besides taking part in the reduction reaction. Therefore, the dryer the concrete, the more the corrosion process is retarded. Under saturated conditions, on the other end, the deficiency of the oxygen supply reduces the process. However, the concrete zone that undergoes a successive wetting and drying regime will produce a high rate of reinforcement corrosion.

Cathodic reactions in reinforced concrete are very likely to occur on uncoated bars. First, the steel surface is exposed and available for reaction. Second, both oxygen and water can naturally occur in a form capable of permeating the concrete to reach the steel surface. Notice however, that oxygen consumed in the cathodic reaction has to be in a dissolved state.[44] Hence, it is the concentration of dissolved oxygen, not the gaseous oxygen, that is important for the corrosion process. Once corrosion is initiated, the cathodic process and the electrical resistivity of concrete control the rate of corrosion.[45,46]

Concrete is capable of retaining a significant proportion of its sorbed water even in arid environments. Accordingly, water is present in concrete virtually anywhere.[20] Any degree of moisture in concrete is enough to support corrosion.[47] Actually, this relation between corrosion of embedded steel and moisture in concrete make it possible to classify the corrosion process as "wet corrosion".[14]

Oxygen is also available in sufficient amounts in concrete to permit corrosion to proceed. Remember that both water and oxygen are needed at the cathode. They do not participate, at least initially, in producing corrosion products at the anode. In fact, the initial presence of oxygen at the anode can limit or prevent corrosion.[46] The reason is ascribed to the possible formation of an oxide layer of iron that protects the steel. However, oxygen migrating to the anode, or penetrating through a crack to an anodic site, usually reacts with the corrosion product to form red rust Fe_2O_3. Oftentimes, the cracks that allow oxygen to migrate are developed as a result of expansion of the corrosion products.[46] Figure 2.3 shows a corroded section of a reinforcing bar in a cracked section.

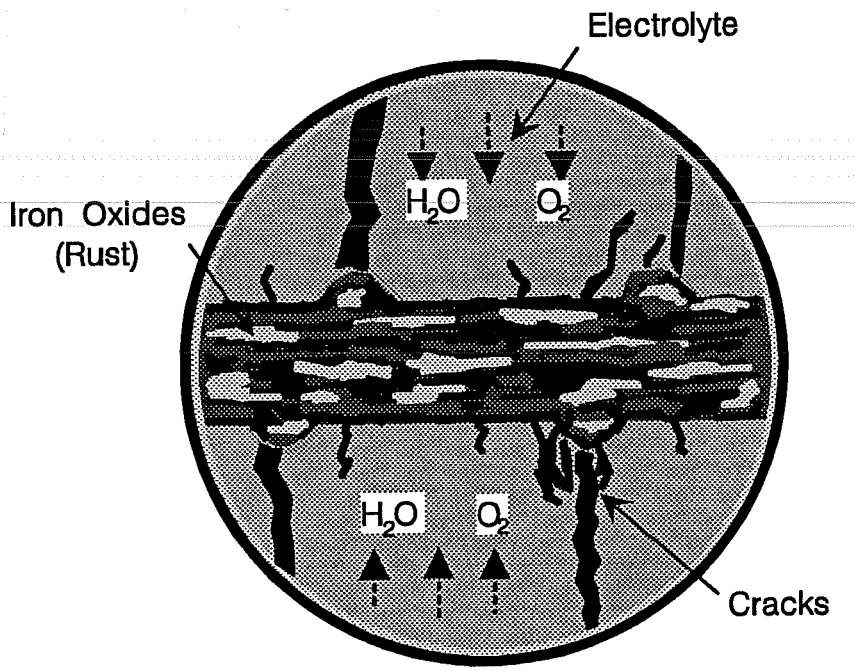

Figure 2.3 Rust Formation on Reinforcing Bar and Cracking of Concrete.

One important characteristic of steel corrosion is that the resulting products occupy a larger volume than the reactants. The increase in volume of the corrosion products cited in the literature ranges from 2 to 20 times the original volume of the steel.[13,48] One reason for this large discrepancy is that corrosion products may take different forms at several oxidation states. Therefore, the volumetric changes associated with the formation of different iron oxides are unequal.

The discussion so far has been limited to rust formation as a natural process without accelerating agents such as chlorides. The corrosion process requires only water and oxygen in contact with iron. In this case, corrosion activity is described as the "oxygen-absorption corrosion cycle".[16] When chlorides are present, however, the process is complicated. The role of the chloride ion in the corrosion of reinforcing steel is discussed in Section 2.4.

2.1.4 Micro- and Macro-Corrosion Cells. Anodically and cathodically active areas on the steel surface may be adjoining or far apart. If they are in the immediate vicinity of each other, *i.e.* on a microscopic scale, then the corrosion cell formed is called a micro-corrosion cell or a *microcell*. On the other hand, if they are separated, even over a relatively large distance, then the cell created is called a macro-corrosion cell or a *macrocell*. Generally, the surface of active reinforcing steel in concrete will corrode under the effect of a combination of many microcell and macrocell interactions.[43]

A microcell is composed of a tiny anode and an adjacent or surrounding cathode. The distance between the two sites may be a micron. An illustration of a microcell is that given in Fig. 2.2. Usually, numerous small corrosion cells form on the same metal surface. Figure 2.4 shows a number of adjacent microcells.

A macrocell comprises an anode and a cathode separated by a finite distance, which may be centimeters or meters (inches or yards). The anode and the cathode may occur on the same bar or on different bars in contact. For the latter case, an example is when one layer of reinforcement becomes anodic with respect to another layer that behaves as the cathode (see Fig. 2.5).

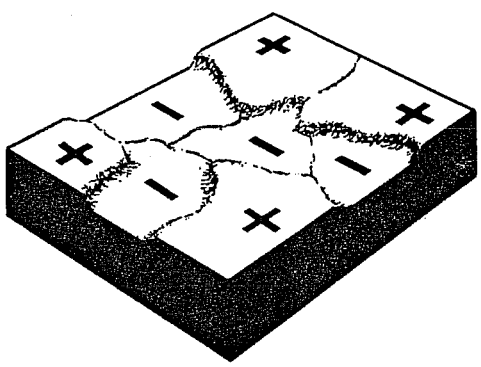

Figure 2.4 Steel Surface Corrosion by Multi-Microcells.[16]

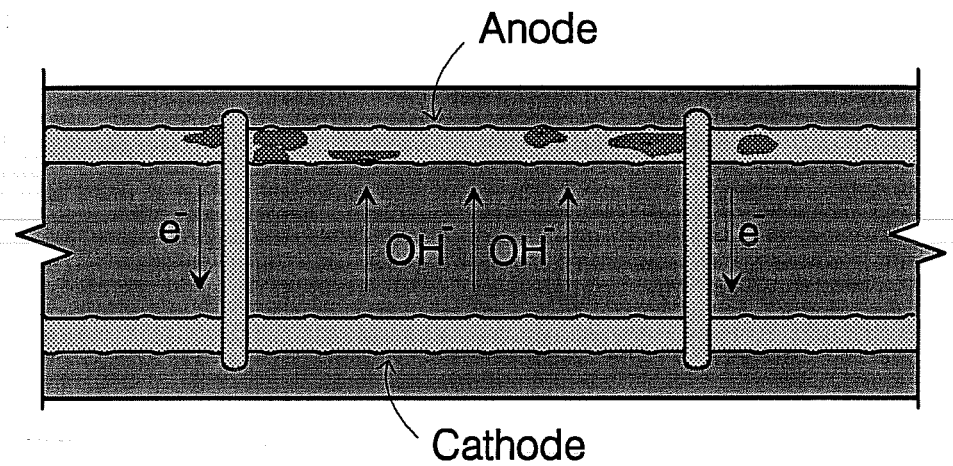

Figure 2.5 Steel Mesh Corrosion by Macrocell Action.

The formation of microcells and macrocells is dependent on many factors affecting the environment surrounding the steel. The primary consideration is the development of a potential difference between candidate anodic and cathodic sites. The significance of such a potential difference lies on the ohmic resistance and the area ratio between the anode and cathode (see Section 2.6.4).[29] Normally, microcells result in relatively low corrosion rates.

In bridge decks, experience has shown that potentials of the top steel vary considerably across the surface of the deck.[17] The horizontal variation of the potentials, sometimes in the order of 300 to 400 mV, creates conditions conducive to strong galvanic action. Corrosion is accelerated because of macrocell formations. Another more serious macrocell action is set up in bridge decks between the top and bottom steel reinforcing layers. Large potential differences develop between these two electrically continuous layers as a result of different chloride concentrations: The top steel is exposed to chlorides from deicing salts, while the bottom steel remains in an uncontaminated concrete. The potential of the top steel shifts to a more negative value when contacting the chlorides, whereas the bottom steel retains a passive potential. This vertical variation of the potential, and the resulting macrocell action, has caused most of the damage to bridge decks in the Northern US.[44]

2.2 Passive State of Steel in Concrete

2.2.1 General. Under normal conditions, concrete provides the embedded reinforcing steel with a protective mechanism against corrosion. In other words, concrete has inherent protective attributes. Borgard *et al.*,[49] reviewed the corrosion-in-concrete literature and arrived at three possible mechanisms for steel protection. These mechanisms are summarized as follows:

- The alkalinity of concrete causes the steel to form a passive, protective film (oxidation layer) which prevents the metal from further reaction with the environment.
- The high electrical resistance of concrete makes it a low conductive electrolyte, which limits ionic flows necessary to complete the corrosion process.
- The high calcium content in the pore solution of concrete causes mineral scales to form on the steel surface and prevents the metal from reacting with the environment.

Understanding these mechanisms is very important for any corrosion study of reinforced concrete, particularly when using epoxy-coated reinforcement. The coated steel is deprived of the natural protection concrete affords. Whether or not exposed steel at damaged areas of the coating becomes protected needs close examination. The following review will help uncover the basics of steel protection in concrete to better understand this matter.

2.2.2 Passivation Film. It has been widely accepted that steel is passive towards corrosion because of the pH environment inherent in portland cement concrete. Typical alkalinity of concrete ranges between pH 12 and 13. It is believed that at this alkalinity level, a tightly adhering, invisible layer of metal oxide forms around the reinforcing bar surfaces. This protective layer is called the passivation film. The stability of the layer depends on maintaining alkalinity of the environment and ionic concentrations.[43,50]

The sequence of development of the passivation film starts at a pH of 9.5 or more.[51] At the beginning, a ferrous hydroxide $Fe(OH)_2$ compound is produced in an initial stage of corrosion. Ferrous hydroxide has low solubility and is oxidized by the oxygen and moisture present in concrete. The oxidation converts the hydroxide to iron oxide Fe_2O_3 which forms the passivation film. As the layer forms uniformly around the bar, the rate of oxygen diffusion to the steel surface decreases and the rate of corrosion is reduced. Accordingly, the passivation of steel in concrete is a special case of activation polarization (see Section 2.9.3).

Oxygen and water are essential elements for steel corrosion in concrete. Ironically, in order for the steel passivity to persist, both elements must be present.[52] Lack of oxygen to maintain steel passivity could initiate corrosion.[21] However, the corrosion rate would, presumably, be negligible due to the limited oxygen supply. An example of this case is concrete permanently submerged in seawater.

The steel passivation layer, which is an oxide of the metal itself, is characterized by its protective influence; it behaves like a nobel metal.[16] It is a submicroscopic layer of rust estimated to be approximately 30 angstroms or less.[43] This minute, non-conductive layer prevents oxygen from contacting the steel, and deters iron ions from escaping into the electrolyte solution.[43] Thus, as long as the passivation layer is intact, no steel dissociation will occur.

The concept of steel passivity in concrete has become the most popular explanation of how alkaline concrete protects steel from corrosion. Almost every recent publication on reinforcement corrosion mentions the concept of passivity. This concept was based on potential/pH (Pourbaix) diagrams developed for *iron in water*, with iron oxide Fe_2O_3 as a protective (passive) film.[49] These diagrams are founded on principles of thermodynamic equilibrium and are discussed further in Section 2.9.2. The passivation film of steel in concrete is often expressed as gamma iron oxide γ-Fe_2O_3; however, passivation may not always involve γ-Fe_2O_3 product.[46] Furthermore, passive films may not be the prime source of protection in concrete. Although the concept of passive film formation seems

unquestionable, little or no information has been cited to explain the mechanism of passivation.

When the passivity concept was first introduced in 1964 by Cornet and co-workers, it was not supported by experimental evidence.[49] The validity of extrapolating thermodynamics in water to the complex environment of concrete is arguable. Even if a passive film does form around the steel, as suggested or accepted by many scientists and engineers, the function or breakdown of this film has not been elucidated.[49,50] If the passivation process was better known, ways to enhance it would probably have been developed.

For a long time, alkalinity in concrete has been attributed to the large amount of calcium hydroxide $Ca(OH)_2$ produced by cement hydration. Moreover, the pore solution, an alkaline solution with a pH of 13.5-13.8, was thought to be composed of saturated $Ca(OH)_2$. Accordingly, the concrete environment was simulated by a saturated $Ca(OH)_2$ solution with a pH of 12.5. However, a well-hydrated portland cement may contain only 15-30% $Ca(OH)_2$ by weight of the original cement.[44,51] In addition, the pore solution is primarily a mixture of KOH and NaOH.[17] Knowledge of the exact concrete composition is important to understand the mechanism of steel protection and how to prevent corrosion. The corrosion process, its initiation and propagation, is controlled by the concrete environment surrounding the reinforcing steel.

In the case of epoxy-coated reinforcement, development of a passivation film on the entire length of bar is impossible. Even when limited areas of steel are exposed, the extent to which the passivation film may form on these areas is unknown. More importantly, whether such a localized surface oxidation may protect the underlying steel or not is debatable.

*2.2.3 **Electrolyte Conductivity.*** The electrical resistivity of concrete, in addition to the availability of oxygen and moisture, controls the corrosion process. The lower the concrete permeability, the higher the electrical resistivity which impedes the ionic corrosion

current flow.[44,47] The ingress of chlorides, however, can reduce the electrical resistivity and enhance corrosion activity.

There is a correlation between concrete electrical resistivity and corrosion rate.[49] The AC impedance method of corrosion monitoring is based on this relationship (see Section A.5).

2.2.3 Mineral Scales. It is suggested that protective scales, high in calcium, form on metal surfaces embedded in concrete.[49] The likelihood of scale formation is attributed to the presence of low soluble calcium products in the pore solution of concrete. Page supported this idea by indicating that protection to reinforcing bars in concrete is provided by a continuous lime-rich layer around the bars.[17] The concept of the formation of protective mineral scales to prevent corrosion of metals is known in the industry of water distribution pipes, oil field tubing, and boiler walls.

An important aspect of this theorized protection mechanism is that corrosion initiation will only be possible if voids at the steel/mortar interface are formed. Voids expose parts of the metal surface which will then come in contact with aggressive species like chlorides. Therefore, corrosion of steel in concrete is possible if calcium carbonates $CaCO_3$ fail to adequately cover the steel surface. A similar phenomenon is observed in the corrosion of oil and gas tubing where turbulence wears the carbonate scales away and allows deep pitting.

Observations from a case study of a deteriorated structure support the above discussion. A durability study was conducted on a 34-year-old bridge constructed with prestressed concrete.[53] The cracks and expansion joints passed water and chlorides to the prestressing tendons. Some of the tendons were not grouted in their sheaths. As expected, corrosion was evident on the wires contained in the chloride contaminated grout. Surprisingly, there was no corrosion on the non-grouted tendons.

With this concept of protective scales, there is little difference between the protection of epoxy-coated (but damaged) and uncoated reinforcing bars. Voids in contact with the steel

may form in either case. The matter depends primarily on concrete consolidation and how well concrete encases the reinforcement. Weak adhesion between concrete and the coated bars may signify plastic concrete settlement. If this happens, relatively large air pockets will develop particularly under the coated bar. Steel exposed at pinholes and damaged areas will not be *passivated* at these air pockets.

2.3 Active State of Steel in Concrete

2.3.1 General. Corrosion of metals, *per se*, is a complex phenomenon and corrosion of reinforcing steel in concrete is no exception. This is so because it occurs under structural, physical, electrochemical, and environmental influences.[50] Thus, there is no single underlying cause for the corrosion of reinforcement in concrete. Generally, a combination of factors yield corrosion and result in deterioration.

In order for corrosion to take place, steel has to be *depassivated*, moisture and oxygen have to be available, and concrete resistivity has to be in the low range, all occurring simultaneously.[45] Depassivation occurs when the alkalinity of concrete surrounding reinforcement falls below approximately pH 9.[29,46,54] This marks an acidic or mildly-alkaline concrete medium. Carbonation of concrete, due to the ingress of carbon dioxide CO_2, is a primary source of pH neutralization. Harmful halides, such as chlorides and bromides, can also break steel passivity and trigger corrosion activity.[46] This latter incidence may happen in spite of a high pH.[18]

Under the conditions mentioned above, concrete ceases to protect the embedded reinforcing bars from dissociation, and the steel corrodes. However, most of today's reported cases of corrosion and the related deterioration of reinforced concrete structures have been associated with the presence of salts in concrete. The association with salt has resulted in a "false sense of security" for concrete structures in the absence of salt.[49] Salt, particularly chloride, is not always necessarily the culprit. Besides chloride, there are other means by which concrete protection to steel is lost.

Several factors promote corrosion activity on reinforcing steel. Poor quality concrete, as well as reduced cover thickness can greatly accelerate depassivation of the steel. Aerated wet concrete acts as an electrolyte facilitating the corrosion process. Cracking of concrete also plays a significant role in breaking down the passivity of reinforcement as it permits the ingress of water, air, and deleterious chemicals.[51]

The presence of cracks and voids, the level of chloride ions, and pre-existing coating damage seem to be important factors in depassivating the epoxy-coated reinforcing steel. The presence of oxygen at a crack location or air pocket may establish a cathode. Any potentially active site, even if remote from the cathode, may start corroding (see the illustration in Fig. 2.6). Some field observations support this idea (see Section 4.2.17).

2.3.2 Corrosion Initiation by Halides. Since steel passivity in concrete is, by large, related to the formation of an oxidation layer, then it is logical that corrosion occurs as a result of breakdown of such a protective layer. One unique destroyer of the passive layer is the chloride ion. Steel depassivation became associated with the presence of chlorides, a concept widely accepted now. However, the level of chloride associated with the onset of corrosion of steel in concrete varies considerably. This variation indicates that corrosion activity is not exclusively related to the breakdown of passivation films.[49]

To strengthen this argument, reference can be made to other research studies which show a diversity of trends. Some researchers reported high levels of chloride content associated with corrosion initiation (see Section 2.5.4). These chloride levels even exceed the levels necessary to depassivate corrosion-resistant alloys, such as stainless steel and titanium. Ironically, others found that chloride can *reduce* corrosion in some cases; chloride

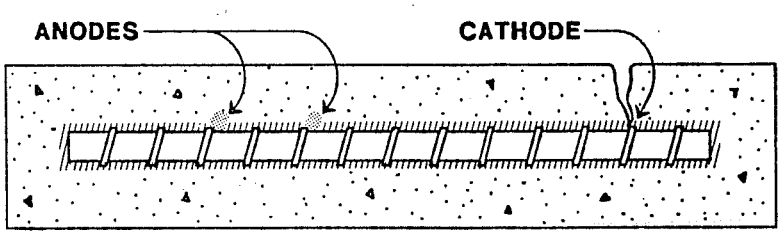

Figure 2.6 Corrosion of Epoxy-Coated Steel in Cracked Concrete.[46]

salts may act as corrosion inhibitors ! Based on the foregoing discussion and those presented in Ref. 50 and 55, the steel passivity concept appears to be insufficient to explain thoroughly how concrete protects steel from corrosion.

Chloride ions contaminate concrete from either internal or external sources. The internal sources are summarized by the following:

- use of contaminated aggregates;
- use of seawater for mixing or curing;
- use of calcium chloride as a set accelerator; and
- use of steel contaminated by salt-laden dust.

External sources, on the other hand, may be in the form of:

- exposure to deicing salts;
- exposure to a marine environment, such as seawater spray or splashing, tidal waves, air-borne moisture and precipitates; and
- exposure to a chloride containing material such as in chemical plants and chlorinated freshwater swimming pools.

Deicing salts are applied to bridge decks and roadways in winter to keep the roads open for traffic. The consumption rate of road salt each winter in the US exceeds 9.1×10^9 kg (10^7 tons).[20] Bridges in the snow belt states may receive 1.2 to 4.9 kg/m^2 (0.25 to 1 lb/ft^2) each winter season. A typical use of deicing salts involves about 40 salt applications per year.[20]

Chloride-contaminated aggregates cause detrimental corrosion progression. The chlorides contained in the aggregate may be freed in concrete to attack the reinforcing steel. This problem is particularly serious in lightweight concrete exposed to moisture and changes in temperature.[44]

Sufficient concentrations of chloride ions relative to hydroxyl ions are necessary at the steel surface to destroy passivity in a high pH environment.[56] In addition, there must be a sufficient oxygen supply to sustain the corrosion activity. Oxygen is the fuel necessary to support the metal dissociation process. No significant pH change associated with chloride attack was observed in the concrete environment.[30] However, the following paragraph illustrates how the steel/concrete interface exhibits a drop in pH where corrosion occurs.

In some studies, the pH on or near corroding reinforcing steel in chloride-contaminated concrete was measured and invariably found in the range of 4.8-6.0.[57] These values are very acidic. However, they were restricted to localized regions in the vicinity of the anodes. The cause of the acidity was attributed to the iron chloride complexing and water hydrolysis which generate hydrogen ions H^+. On the other hand, pH measurements at the non-corroding sites of steel in the same concrete varied between 11.5 and 13.0 regardless of the chloride level. This result confirms that oxygen reduction (cathodic reaction) in concrete liberates hydroxyl ions OH^- which maintain the high pH level. The reduction of pH at the anodic areas allows the corrosion to proceed more easily.[58] Oxygen reduction controls the rate of corrosion, but chloride distribution affects the number or extent of active sites.

The mechanism through which the steel passivity, or protective film, is destroyed by chloride ions is not fully understood, nor agreed upon.[50] Chlorides are thought to react directly with the steel causing its depassivation.[30] One mechanism proposed is the "complex ion formation" originally attributed to Hoar and Foley, and expanded by Hime.[55] According to this theory, chloride ions break down the passivity of steel by "complexing" with the ferrous ion. More information is given in Section 2.4.2 and the details of the possible reactions are shown in Section A.2.

2.3.3 Depassivation by pH Drop. Lixiviation of the hydroxides in concrete leads to a drop of pH or loss of alkalinity.[29,44,54] Water penetrating concrete (or running through cracks) dissolves the alkaline products and moves out to the surface where it evaporates. This leads to leaching out of limes (a process known as efflorescence) which reduces the pH of the aqueous phase of concrete. Some acids also cause chemical reactions with the

hydrated calcium hydroxides. The reactions produce water-soluble compounds susceptible to leaching out by aqueous solutions.[47] Acid attack may occur from acid formations such as dissolution of free carbon dioxide in streams, sulfuric acid from fuel combustion, acid rain, *etc.*[43,47]

When concrete pH is about 9 or lower, active corrosion conditions prevail. There is a postulated relationship between the state of steel, concrete pH, and steel potential. The relationship is based on Pourbaix diagrams discussed in Section 2.9.2. The change in the reinforcement state, for example from the passivation state to the corrosion state, in relation to the pH of the environment, and the potential of steel is shown in Fig. 2.7.

2.3.4 Corrosion Activity due to Carbonation. Atmospheric carbon dioxide CO_2 dissolves in the pore solution of concrete to form carbonic acid. The acid reacts with cement alkalies to produce carbonates. Consequently, the pH of the cement matrix drops to the range 8.5-10.[30,44,59-61] At this low alkalinity level, maintenance of steel passivity ceases and corrosion proceeds in the presence of oxygen and moisture.

Carbonation increases concrete shrinkage on drying and, thus, tends to enhance cracking.[47] Cracking will allow other harmful substances to penetrate and aggravate

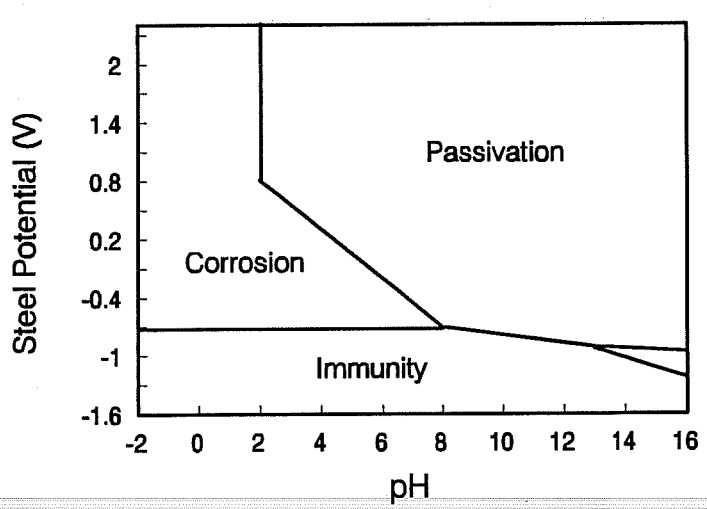

Figure 2.7 Steel Corrosion as a Function of pH Value and Potential.

corrosion. Carbonation progress in concrete does not depend on chloride content.[62] The presence of moisture accelerates the carbonation process; however, maximum carbonation occurs at 50% water saturation.[44]

The use of thick, dense concrete covers to reinforcement eliminates the carbonation-related corrosion problem. The carbonation front advances very slowly in sound concrete. The rate of advancement is nearly proportional to the square-root of the exposure time.[60] Hence, it will take longer than the design life for the carbonation front to reach the deeply embedded reinforcement to cause corrosion. The present specifications for the construction of highway structures call for adequate cover thicknesses and concrete quality that the carbonation problem is of no concern.

2.4 Chloride Role in Steel Corrosion in Concrete

2.4.1 General. One of the significant and most controversial issues of corrosion of reinforcing bars in concrete is the role of chloride ions. Present discussions focus on the determination of safe limits of chlorides and their impact on corrosion. Therefore, a thorough understanding of the chloride effects and corrosion threshold limits becomes very important.

2.4.2 Chloride Effects on Steel Depassivation. The chloride-related corrosion mechanism of reinforcing steel is still not well understood and the chloride role is not agreed upon. ACI committee 222[44] presented three modern theories to explain the effects of chloride ions on steel depassivation. These theories are:

<u>The Oxide Film Theory</u>

This theory is founded on the concept of formation of a passivation film around the steel in concrete which normally protects the steel from corrosion. The breakdown of this film by chloride ions is the postulated action causing corrosion. The oxide film may have pores or defects through which the chloride ions can penetrate. Alternatively, the chloride

ions may colloidally disperse the oxide film, thereby making it easier to penetrate. Depassivating the oxide film is the most common theory of corrosion initiation.[43]

The Adsorption Theory

The chloride ions may be adsorbed on the steel surface to promote the hydrolysis process of the metal ions. The catalytic action of the chlorides leads to metal dissociation. In this theory, chlorides attack the steel directly.

The Transitory Complex Theory

Since chloride ions and hydroxyl ions are both negatively charged, then both compete for the ferrous ions produced by corrosion. The reactions result in complex formation of soluble iron chloride compounds such as $FeCl^-_3$. The complex ions diffuse away from the anode, then breakdown to allow iron hydroxide $Fe(OH)_2$ precipitation. The chloride ions become free again to transport more metal ions from the corrosion site. Here, the chloride ion acts as an essential catalyst (accelerating agent). The corrosion rate is multiplied by a factor of about 10 to 100.[63]

2.4.3 Controversial Issues on Chloride Role. While it is agreeable that chlorides accelerate steel corrosion in concrete, it is not clear yet whether chlorides initiate the corrosion process or not. Corrosion may still occur at the depassivated steel in the presence of moisture and oxygen without chlorides. Moreover, there are many examples of concrete structures which withstood severe chloride environments and remained serviceable for their design life.[50]

Some investigators suggested that the chloride ions diminish the alkalinity of the pore solution surrounding the steel, leaving it susceptible to corrosion.[17,43] When chloride ions concentrate at the steel surface, the pH drops at the points of corrosion initiation. This leads to further breakdown of steel passivity. As a result, pitting corrosion occurs. However, a direct reduction of alkalinity is not necessary for the chloride ion to cause depassivation. In addition, the situation may, sometimes, depend on the type of cation used with the chloride.[46] It was found that the common deicer salt, NaCl, does not cause a significant reduction of the

pH. It is further suggested that if iron chlorides hydrolyze to form hydrochloric acid HCl, then the reserve calcium hydroxide $Ca(OH)_2$ in the cement paste will quickly normalize the acid.

The nature of the chloride ion may affect the severity of the corrosion process. Calcium chloride $CaCl_2$ seems to be more aggressive than sodium chloride NaCl.[17,64] This may relate to the different chloride binding capacities of the portland cement depending on the type of chloride ion present. In terms of ion diffusivity, chloride with calcium diffused 3-4 times greater than chloride with sodium. However, in a different study, it was found that NaCl reacts very slowly with tricalcium aluminate C_3A in the presence of free lime.[65] This means that a larger fraction of chloride will tend to stay in the pore solution of concrete to cause faster corrosion development than in the case of $CaCl_2$. Furthermore, when the chloride source is internal, *i.e.* from contaminated mix constituents, corrosion-induced deterioration is generally slower.[66]

Chloride-based salts can promote corrosion of reinforcement both directly and indirectly. It has been discussed above how chloride ions work as a catalyst for local pitting corrosion. This is the most serious harmful direct effect. Indirectly, the salt in concrete increases freeze-thaw cycling and freeze shock.[59,60,67] Hence, the salt contributes to increased micro-cracking of concrete. Freezing of the concrete surface which contains salt leads to the formation of thermo-cracks. Cracking, in turn, allows the ingress of salt and other deleterious materials which enhance corrosion.

Another harmful effect is that salt causes a high degree of saturation in concrete.[47] When salt penetrates moist concrete, it retains water for a longer time making the concrete a stronger electrolyte. This hygroscopic property of salt enhances the corrosion reactions and other deterioration mechanisms such as frost damage. The cause of this problem is attributed to the lower vapor pressure of salt solutions relative to water which causes little or no drying between wetting periods.

In short, the chloride ions are very aggressive on both the electrochemical dissociation of the reinforcing steel and the physical disintegration of the concrete. With severe corrosion and concrete spalling, the safety margin is reduced and the structural integrity is threatened.

2.5 Chloride Threshold Concentration for Corrosion Initiation

*2.5.1 **Background.*** In 1972, Stratfull did not find a correlation between the amount of chloride extracted from bridge decks and the extent of corrosion detected.[49] His data suggested that a minimum level of chloride was necessary to break down steel passivity to initiate corrosion. The minimum chloride ion concentration to initiate corrosion, also called the corrosion chloride threshold, was proposed by Clear in 1974.[50] It was defined as the minimum quantity of total chloride required to initiate reinforcing bar corrosion when other factors are present.

The term total chloride means the total amount of chloride in concrete determined by special analytical methods.[44] The acid-soluble chloride refers to the chloride extracted by acid (usually nitric acid) used in the test. Acid-soluble tests are described in ASTM C114 and AASHTO T260. The total chloride and acid-soluble chloride are often used interchangeably in the literature. Water-soluble chloride, on the other hand, denotes extractable chloride in water under defined conditions. Determining water-soluble chloride is time-consuming and difficult to control; several factors significantly affect the results.[47]

ACI 222[44] approximated the water-soluble chloride to be 75-80% of the acid-soluble chloride. The variation in the given range is dependent on the amount of chloride in concrete, the mix ingredient, and test method. Gaynor,[68] on the other hand, estimated the water-soluble chloride to be only 50-75% of the acid-soluble chloride. ACI 201[47] confirmed that 50-85% of the total chloride is water-soluble (with some exceptions).

*2.5.2 **Factors Affecting Chloride Threshold Concentration.*** The relation of chlorides to reinforcement corrosion in concrete is unclear. Confusion exists in interpreting

the chloride concentration values reported in test results and even in the specifications. A major reason for this confusion is the different ways of expressing the chloride ion content.

Despite the introduction of the concept of chloride threshold value, establishing a chloride content below which the risk of corrosion is negligible is difficult. There cannot be one limit which is adequate for all mix ingredients, under all exposure conditions, and can be measured by a standard test.[44] The factors involved in corrosion initiation are numerous and interrelated. Some of these factors are:[17,49,64] concrete composition; moisture level and atmospheric conditions; and type and source of chloride ion in contact with concrete. Variations in these factors, and others, led to wide discrepancies in the chloride levels associated with the onset of corrosion. In addition, high localized variations in chloride content are quite possible. These variations are difficult to detect by commonly used techniques.

To illustrate the influence of one of these factors, the water to cement ratio (w/c) in concrete is considered. Increasing w/c results in a lower pH of the pore solution. This influences both the degree of chloride binding and the critical chloride concentration required to depassivate steel.[64] The net effect is unfavorable, as both the time to corrosion initiation and chloride threshold value are reduced. It can be concluded that the harmful effects of chlorides must be considered in conjunction with the level of water present.

The chloride threshold concentration is dependent on the pH level and oxygen concentration. The relationships were found by testing steel corrosion in solutions with variable pH and oxygen content.[58] The test data are summarized in the plot of Fig. 2.8. The plot depicts a three-dimensional space within which corrosion will not occur. The conditions outside the envelop are conducive to corrosion. This figure clearly shows that the critical chloride concentration varies as the pH and oxygen concentrations are varied as well.

Hausmann and co-workers found that the chloride/hydroxyl ion Cl^-/OH^- ratio is the critical parameter affecting the loss of passivity.[30,55] It was proposed that a ratio of Cl^-/OH^-

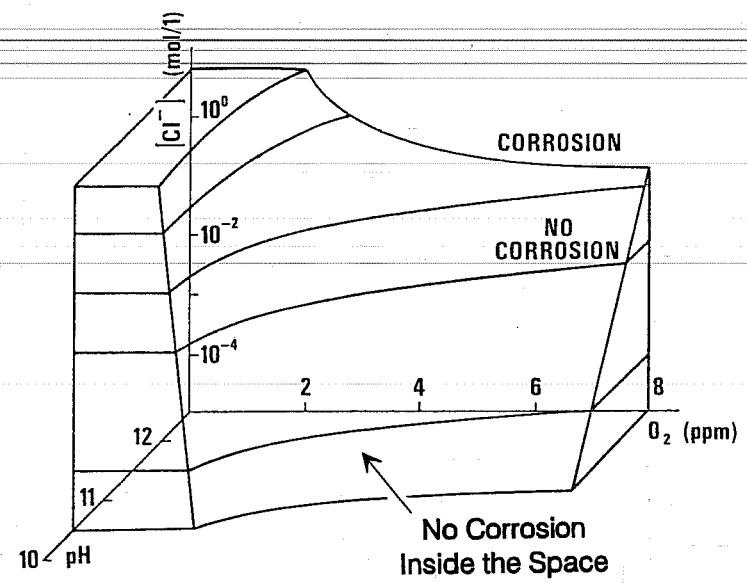

Figure 2.8 Three-Dimensional Space for No Corrosion of Steel.[58]

greater than 0.6 is required to initiate corrosion. Arup[52] suggested that the chloride threshold is a function of the potential, among other things, and active potential is a function of chloride content. Others found that the cation initially combined with the chloride ion, such as sodium Na^+ or calcium Ca^{++}, will also affect the chloride amount required for the onset of corrosion.[64]

2.5.3 Chloride State in Concrete. To control the reinforcement corrosion in concrete, it is necessary to understand the mechanism of chloride intrusion into concrete. Such information, and the chloride state in the concrete matrix, is needed to predict chloride penetration, and the possibility of corrosion initiation. At present, the mechanisms of chloride intrusion into concrete are not fully understood.

The two generally proposed phenomena for chloride penetration into concrete submerged in seawater are chloride ion diffusion and chloride binding in concrete. Quite recently, two more phenomena were added. These are condensation of the water-soluble chloride in the concrete matrix and on the embedded steel bars.[69]

It generally has been believed that chlorides in concrete exist as free ions or as ions bound to the cement. With the newly added phenomena, chloride condensations in concrete and around the reinforcing bars are two other possible states. The significance of the condensation phenomenon is that concrete exposed to continuous wetting by seawater may result in chloride concentration in the pore solution many times higher than that of the seawater.[69] Unfortunately, whether this phenomenon will result in a positive or negative effect on the corrosion of steel is not yet known.

From the corrosion initiation standpoint, different chloride concentrations are required to start corrosion depending on the chloride state in concrete. Chlorides that diffuse through concrete from an external source trigger corrosion at a lesser amount than that of the chlorides mixed in concrete.[17] The difference in chloride content is about 1 to 2 orders of magnitude.

Besides the chloride state, the uniformity of chloride distribution may also affect corrosion activity. If chloride distribution in concrete is uniform (as in the case of mixed chloride), a higher chloride content is required to produce, substantially, the same corrosion current as intruded chloride.[46]

One explanation given to the effect discussed above is binding of chloride ions with tricalcium aluminate C_3A in cement when concrete is still fresh. Such binding immobilizes chlorides.[43] The amount of chloride bound to the cement is not considered a contributor to the onset of corrosion.[64] The binding reaction is not speculated to occur to any great extent when chloride ions diffuse through the hardened concrete. It should be cautioned, however, that chloride tied up by reacting with cement aluminates in fresh concrete could be released again. If concrete was exposed to sulfate and atmospheric carbon dioxide, then the calcium chloroaluminate hydrates (Friedel's salt) could dissolve to free the chloride.[55,65]

Anyway, only a given amount of chloride ions becomes fixed in the hardened cement regardless of the chloride content of the concrete.[11] Therefore, increasing the quantity of chlorides in concrete (for example by a longer exposure period) will increase the risk of

activating corrosion. In addition, the larger the chloride ion content in concrete, the earlier the time to onset of corrosion and the larger the number of corrosion sites.[58]

The amount of free chloride which is the soluble chloride present in concrete pore solution is more critical than bound chloride. However, when concrete is cracked, the cracks provide direct access for the chlorides to the steel level. Therefore, it is normal to find a greater chloride concentration on a crack surface at the bar level than in the surrounding uncracked area. The higher the chloride concentration at the bar surface, the more is the likelihood of reinforcement corrosion.

*2.5.4 **Proposed Chloride Limits.*** The chloride ion threshold concentration vary considerably in literature. Even the well-recognized standards and specifications contain different safe limits of chloride contents in concrete. There is not a clearer example of the uncertainty of the chloride amount needed to promote corrosion of reinforcement than the disagreement among ACI committees. The controversy about this matter has not yet been resolved.

The limit of water-soluble chloride ions for reinforced concrete in a moist environment and exposed to chlorides is one example of the discrepancy among the ACI committees. ACI 201[47] recommends a limit of 0.1% by weight of cement. ACI 318[70] requires a maximum of 0.15% by weight of cement. ACI 222[44] expresses the limit in terms of acid-soluble chlorides which is 0.2% by weight of cement. This limit is claimed to be more conservative; it is based on realizing the serious consequences of corrosion. It has been questioned whether or not a factor of safety should be imposed on these recommended maximum chloride concentrations. These values are specified for concrete prior to service exposure and, perhaps, the environment may change with time. At least, the problem of uncertainty can be alleviated when such a factor is introduced.

The specified chloride limits are given for uncoated reinforcing steel. There is not enough information to generalize these limits to include epoxy-coated reinforcement. It is

expected, though, that higher chloride concentrations can be tolerated by coated bars before the onset of corrosion because the coating is a physical barrier that covers the steel.

Despite the concern that chloride limits specified by the different ACI committees are sometimes non-conservative, other national codes and publications suggest more liberal limits. The Norwegian code N5 3474, for example, permits acid-soluble chlorides up to 0.6% by weight of cement.[71]

2.5.4 Data on Chloride Levels at Onset of Corrosion. Data on corrosion threshold values are conflicting. The critical chloride content for corrosion initiation falls mostly in the range of 0.02-0.05% by weight of concrete (equivalent to approximately 0.14-0.35% by weight of cement). The following is a summary of the chloride threshold values reported in the reviewed literature:

- Munjal[72] referred to FHWA laboratory results that indicated values between 0.89 and 1.19 kg/m^3 (1.5 to 2 lb./yd^3).
- A field study of bridge decks in Pennsylvania revealed moderate corrosion associated with as little chloride content as 0.06 kg/m^3 (0.1 lb./yd^3).[73]
- Berke[74] reported experimental results of severe corrosion occurring at values between 0.12 and 15.6 kg/m^3 (0.2 and 26 lb./yd^3).
- Weyers and Cady[75] noted the value 0.71 kg/m^3 (1.2 lb./yd^3).
- Al-Qadi, Peterson, and Weyers[6] reported values in the range of 0.2-2.8 kg/m^3 (0.3-4.7 lb./yd^3).
- Fraczek[43] gave the range of 0.59-0.83 kg/m^3 (1-1.4 lb./yd^3).
- Hagen[76] referred to a threshold range of 0.65-0.95 kg/m^3 (1.1-1.6 lb./yd^3).
- An article in *World Construction* magazine suggested values in the range of 0.6-0.9 kg/m^3 (1.01 to 1.52 lb./yd^3).[8]

The wide variation in the reported chloride threshold concentration explains why the reinforcement was not corroding in some cases despite a high chloride content. Many field studies showed that corrosion was not evident although the chloride concentration was above

the established corrosion threshold limit.[10,50,65] In contrast, even minor amounts of chlorides can destroy steel passivation.[50,77] This means that severe corrosion can occur even where the chloride content in concrete is within acceptable limits.

Erlin[65] summarized the inconsistency of associating reinforcing bar corrosion with a certain chloride limit by stating: "Just because chloride is within the limit does not necessarily mean that steel will not corrode. And just because the concrete contains chloride does not necessarily mean there will be corrosion." It appears that each concrete component may have a unique chloride threshold concentration. Such a concentration is related to the particular composition, exposure conditions, and the influencing factors discussed above.

The concept of chloride threshold concentration has been particularly applied to bridge decks exposed to deicing salts. Many of these decks are scheduled for replacement just because of their level of contamination. However, based on the above views, it is suggested that replacement of bridge decks and other structures should not be undertaken solely on the basis of their high chloride content. The concept of the chloride threshold in concrete, and its practical applications, may have to be revised.

2.6 Corrosion Driving Force

2.6.1 General. Corrosion ensues when a potential difference is developed on the steel surface. Virtually, any dissimilar steel surface conditions can cause a potential difference to build up. Local variations in steel composition are one factor that creates a potential difference. These variations may be caused by differences in the constituent phases of the material itself. Else, they may occur as variations in natural films on the metal surface.[16] Differences in pH, oxygen concentration, chloride concentration, or moisture differential, and temperature differential are examples of variations in the surrounding environment. Galvanic coupling of dissimilar metals in concrete can also produce corrosion.

2.6.2 Potential Difference. The driving force in the electrolytic corrosion cell is the difference in nonpolarized potentials between the anode and the cathode.[78] The value of

the driving force indicates the potential energy pushing the corrosion reaction in a particular direction.[43] Once the potential difference is developed, one area undergoes anodic behavior and the other cathodic behavior. The resulting corrosion action is known as sacrificial corrosion. The metal with high potential is preferentially consumed while the metal with low potential remains unaffected.

The corrosion rate depends on the amount of actual charge passed through the corrosion cell, *i.e.* the flowing current. According to Faraday's Law,

$$W = kIt \tag{2.1}$$

the weight of the metal corroded, W, is proportional to the amount of current I passing in a period of time t.

2.6.3 Concentration Cells. A concentration cell is an electrolytic corrosion cell that builds up a potential difference, *i.e.* electromotive force, due to a difference in concentration of some component in the electrolyte.[79] Any nonuniformity in the chemical or physical environment of the surrounding concrete leads to this concentration difference. For example, a difference in the concentration of chloride, oxygen, water, iron ion, *etc.* results in corrosion cell formation. Temperature gradients and different strains of steel are also other possible factors for corrosion cell development.

Emphasis is put on the concentration cells created by differences in the availability of oxygen at the steel surface. Finley found extensive evidence that oxygen concentration cells cause most of the corrosion.[50] Others demonstrated that corrosion does not occur unless oxygen bubbles are trapped against the steel surface. Their observations were based on testing reinforcing bars immersed in a simulated chloride-bearing concrete environment. They found that oxygen bubbles created oxygen concentration gradients along the steel.[50]

Concentration cells can lead to severe macrocell corrosion action. If steel is continuous through wet and dry sections of concrete, then the nonuniform moisture and oxygen (and maybe salt) distributions are likely to develop corrosion macrocells. Leaky

joints in concrete bridge decks saturate adjacent portions of the concrete and cause such corrosion conditions to arise.

2.6.4 Area Ratio. Area ratio is the ratio between the surface area of the anodic and cathodic regions. As the anodic area decreases with respect to the cathodic area, the current density (current per area of anode) increases. An increase in the corrosion current density denotes an increase in the corrosion rate.

2.7 Effects of Environment and Cracking on Corrosion

2.7.1 Environment. Temperature and relative humidity are among the most serious parameters affecting the rate of corrosion. Exposure of the concrete surfaces to wetting with a chloride solution, followed by partial drying can promote corrosion. Frequent wetting and drying leads to further aggravated corrosion cell development. Where more than one side of the concrete member is exposed to the environment, the penetration and accumulation of the aggressive substances in concrete will be increased. This is particularly associated with corners such as in bridge piers exposed to seawater splashing.

Temperature has direct and indirect effects on corrosion rate. Increasing the amount of heat energy accelerates the corrosion reaction; the rate of oxidation is accelerated under elevated temperatures. Indirectly, increasing the temperature reduces concrete resistivity which promotes the corrosion reaction. Temperature also affects the relative humidity in the concrete and the mobility of the ions in the pore solution.[22] Corrosion testing has shown that the typical corrosion rate at a concrete temperature of 35° C (95° F) was about 2.5 times greater than at a temperature of 16° C (60° F). Concrete resistivity at 35° C (95° F) was less than half of that at 16° C (60° F).[57]

Relative humidity dictates how much moisture is available in the pores of concrete to be conductive and function as an electrolyte. The maximum corrosion activity associated with chloride attack is believed to occur when relative humidity within the concrete is around 60%.[22] This relative humidity is different from the atmospheric relative humidity. The

relative humidity in concrete is influenced by many factors such as splash water, run off, capillary action, and dew formation.

Total saturation as well as total desiccation normally stop corrosion. Oxygen is not available in such situations and the corrosion reaction cannot be sustained. Suppressing corrosion activity due to unavailability of oxygen is called oxygen starvation. The higher the moisture content of concrete, the less the concrete resistivity and the higher the ionic conduction. This leads to higher corrosion rates.[17] The resistivity of dry concrete is about 5 orders of magnitude higher than that of water saturated concrete.

2.7.2 Concrete Cracking. The role of concrete cracking in the corrosion of reinforcing steel is controversial. In one point of view, cracks are thought to permit rapid penetration of corrosion-inducing substances. Thus, the onset of corrosion is accelerated. At the same time, the cracks provide space in which corrosion products deposit. The other viewpoint is that corrosion is only localized at crack locations. After a few years of service, little difference would exist between corrosion in cracked and uncracked concrete exposed to chlorides. In any case, the effects of cracks on corrosion should be evaluated in relation to the cause, width, and orientation of the crack.

Some investigators think cracks less than about 0.3 mm (0.012 in.) wide have little influence on the corrosion of reinforcing steel.[44] Therefore, they suggest restricting design crack width to such a limit. For wider cracks, there is a recognized tendency for the amount of local corrosion to increase with the increase in crack width.[11] Other studies, however, have shown that there is no relationship between crack width and corrosion.[44] Additionally, there is no direct relationship between crack width at surface and at the reinforcement level. It follows that controlling surface crack widths by structural design is immaterial. It may not be the crack width, but the total area covered by cracks, especially near the steel, that is most important for corrosion to progress.

Cracks parallel to the direction of embedded steel bars are more serious, from a corrosion standpoint, than cracks transverse to the bars.[45,47] Wide cracks forming directly

above and along the direction of reinforcement allow large amounts of corroding substances to reach the steel surface and promote corrosion. Plastic settlement (or subsidence) cracks are of this type. They are considered as the most important type of cracks that affect corrosion progression on embedded reinforcement.[20]

Transverse cracking in bridge decks is a prime example of plastic settlement cracks.[75] They form during the initial hours of concrete solidification. Chlorides filling such cracks at the surface rapidly reach the reinforcement level. The factors that affect settlement crack formation are cover, bar diameter, and concrete slump. For a 16 mm (#5) reinforcing bar diameter, and a 50 mm (2 in.) slump, cracking probability of a 25 mm (1 in.) cover is as high as 71%.[20]

Mehta[45] indicated that cracks allow large amounts of chloride to penetrate into concrete in contrast to uncracked areas which exhibit slow diffusion processes. In addition, an increase in the crack width leads to an increase in chloride concentrations in the vicinity of the crack. Thus, larger cracks may cause a fast breakdown of steel passivity and early corrosion initiation. At present, no relationship exists between surface crack width and corrosion rate, unless surface cracks represent widespread internal cracking.

The deterioration of bridge decks related to corrosion is a problem aggravated by truck traffic loads. Transverse and longitudinal cracking have been associated with increased truck traffic.[50] Overloading the trucks is an important factor contributing to the increased damage of the bridge decks. Cracking is interrelated with progressive corrosion-related deterioration.

It should be remembered that reinforced concrete is intrinsically a cracked material. Concrete cracking greatly interferes with its durability under severe exposure conditions. Whether corrosion leads to cracking, or cracking precedes corrosion, is another controversial issue.

Data are extensive to support the idea that corrosion results in cracking. After corrosion initiation, steel is converted to rust. The oxidized metal accumulates at the steel/concrete interface. The produced solid corrosion products are expansive and exert high radial pressures inside the concrete pores. When the generated tensile stresses exceed the concrete strength, rupture occurs. Local disintegration creates internal weak spots in concrete. With time, the process propagates away from the corroded bar leading to surface cracking. Figure 2.9 presents the mechanism of corrosion-induced deterioration in concrete.

On the opposite side, some believe that microcracks are inherently present in concrete. These microcracks become progressively large due to structural or environmental exposure conditions. As a result, concrete disintegrates. Thus, damage propagates from the concrete surface towards the reinforcing bar. Freeze-thaw cycles are an example of this type of damage.[18] Chloride ions find free and direct routes to the steel to initiate corrosion.

During some investigations, cores obtained from building walls, marine pipes, and highway bridge decks commonly showed cracks which were wider away from the corroded steel.[49] It was doubted that corrosion had caused these cracks since otherwise the cracks would have been wider near the steel. These results suggested to the researchers that corrosion was caused by cracking.

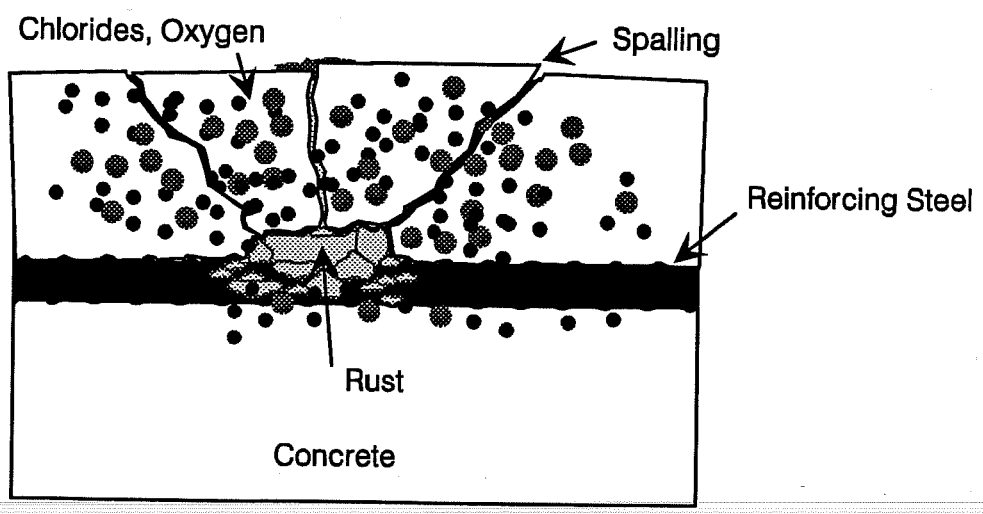

Figure 2.9 Cracking of Concrete Due to Rust Formation on Reinforcing Steel.

Certainly, cracks present before the onset of corrosion will assist the corrosion process. After a fairly prolonged period of exposure, corrosion develops along a greater length of the reinforcement. Longitudinal cracks develop as a consequence of corrosion and corrosion then progresses rapidly with increasing damage to the concrete. It has been surmised that increase in the reinforcement corrosion and expansion of the cracks cause deterioration to progress synergistically affecting each other.[11]

The corrosion-cracking cycle may start with concrete that contains networks of microcracks. The cracks widen under service conditions and lead to corrosion initiation. Corrosion, in turn, leads to further cracking. Figure 2.10 shows the diagrammatic presentation of this cycle. In essence, both cracking and corrosion aid each other in escalating their respective destructive mechanisms.[18]

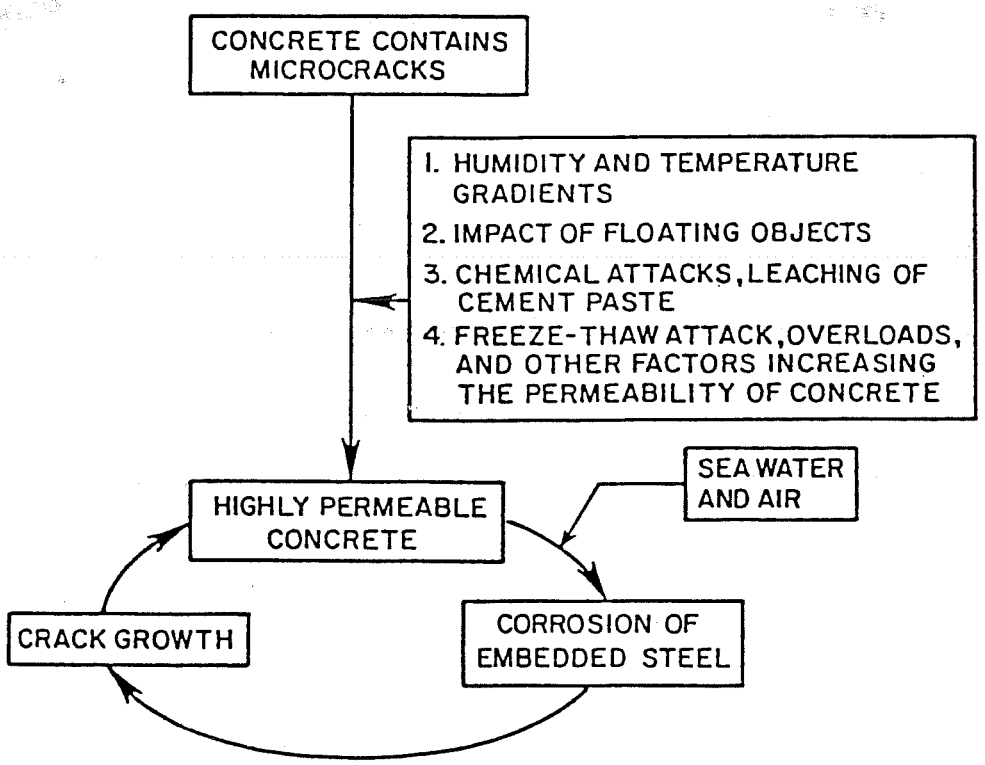

Figure 2.10 Cracking-Corrosion Cycle in Reinforced Concrete Exposed to Seawater.[45]

2.8 Pitting Corrosion

2.8.1 Definition. Pitting is a form of extremely localized attack that results in holes in the metal.[14] Pits may exist as isolated or interconnected holes that they look like a rough surface. Generally, the pit has a surface diameter about the same as or less than the depth.

2.8.2 Pit Development. Pitting occurs as steel passivity is destroyed only locally, forming a small anodic area. The larger surrounding cathodic areas drive a substantial anodic action resulting in a pit. Chloride ions play an important role in depassivating the steel and concentrating metal dissociation in active pits. The chloride ions accelerate the process and make it self-perpetuating.

Pitting is more likely to occur where chlorides reach only isolated areas of the reinforcement.[52] Once a pit is initiated, corrosion is promoted by an oxygen gradient between the electrolyte and the oxygen-starved electrolyte at the bottom of the crevice.[16] Figure 2.11 illustrates schematically the pitting process. The following factors maintain or aggravate the development of an existing pit:[52]

- Acid production at anode (pit) and alkali at cathode cause the pH to shift in opposite directions. Acidity at anode is enhanced by the high current density and because of the hydrolysis associated with ferrous ion Fe^{+2} oxidation to ferric ion Fe^{+3} at the edge of the nodule.
- Migration of chloride towards the anode and away from the cathode.

Pits usually grow in the direction of gravity.[14] In addition, they tend to undermine or undercut the metal surface as they grow. The pits may be difficult to detect under visual examination because they are usually covered by caps of corrosion products.

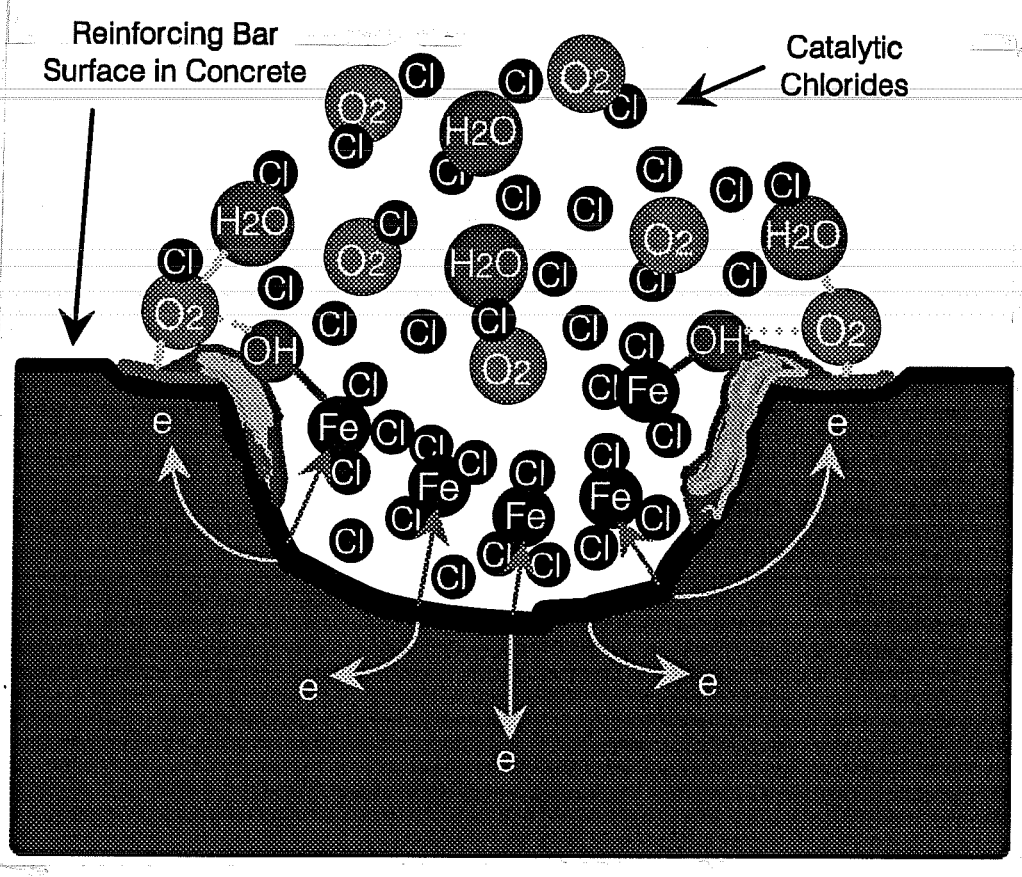

Figure 2.11 Schematic Illustration of Pitting Corrosion of Steel in Concrete.

2.8.3 Pitting Consequences. Once pitting corrosion starts, it is nearly always progressive; the pitting process is an autocatalytic process. Pitting is a highly localized and intense form of corrosion. It can result in substantial local reductions in cross sectional areas of the steel reinforcing bars.

As the metal dissolutes in the pit, oxygen reduction takes place on the adjacent surfaces. The cathodic reactions tend to suppress corrosion on these adjacent surfaces. In a sense, pits cathodically protect the rest of the metal surface.[14] This phenomenon is very important when contrasting the performance of coated and uncoated steel bars. The above description applies perfectly to the uncoated reinforcement. In the case of coated reinforcement, however, only limited areas may be exposed for pitting. If these areas are

relatively small, the coating (as a barrier) on the adjacent surfaces restricts further cathodic activity. As a result, the severity of corrosion may be alleviated.

2.9 Corrosion Thermodynamics and Electrode Kinetics

2.9.1 Corrosion Thermodynamics. The corrosion electrochemical reaction is described mathematically using thermodynamics principles in the form of the following equation,[80]

$$E = 1.255 - \frac{0.059}{4} \log \frac{1}{[O_2][H_2O]^2} \qquad (2.2)$$

This equation is known as Nernest equation, in which E is the corrosion potential or voltage, and O_2 and H_2O are the concentration values of oxygen and water available at the corroding steel interface. This equation can be viewed as the "map" to controlling or stopping corrosion.[80] It can be put in the form,

$$E = A - B \qquad (2.3)$$

By principle, to stop corrosion, the voltage or driving force must be reduced to less than or equal to zero. Maintaining a negative potential means that the reinforcing steel must be negatively charged. This is the basic concept of cathodic protection. Steel is negatively charged to remain a cathode all the time thereby arresting corrosion. In essence, controlling part A in the equation is a viable option to "lock" the electrons in the reinforcing steel body.

The reinforcing bars must be made electrically continuous to ensure effective cathodic protection. With epoxy-coated reinforcement, cathodic protection is difficult. The current practice of installing individually coated bars will not guarantee full electrical continuity among the bars. Charging the entire reinforcement assembly may not be achieved. More information about cathodic protection is given in Section A.7.

The coated reinforcement represents another method to control corrosion by considering part B of the Nernst equation. The coating is simply a barrier to keep oxygen

and water concentrations in contact with steel very low. The coating is also intended to guard against the chlorides reaching the steel surface. However, it is very important to realize that the coating still has a finite permeability to oxygen and water vapor. Organic coatings, such as the epoxy coating, function well by keeping O_2 and H_2O low enough that the corrosion rate remains insignificant.

If the coating material is intact, the rate of corrosion will be negligible. This should be the case at least for the intended design service life. However, if damage occurs to the coating, from various sources before or after installation in the field, the concentrations of oxygen and water at the steel surface will increase. The corrosion rate may then become significant.

2.9.2 Potential-pH (Pourbaix) Diagrams. The potential-pH diagrams were prepared for iron in an aqueous solution. Three metal states are defined based on thermodynamic equilibria in the potential/pH space:[49]

- Immunity. The metal is stable and is immune to corrosion.
- Corrosion. The metal ions are stable.
  Metal dissociation occurs but its rate is not predictable.
- Passivity. The metal compounds are stable.
  Passive films are formed which may be protective against corrosion.

The application of "thermodynamic passivity" to the kinetic nature of steel electrodes in concrete has serious limitations. One of these limitations is the inability to predict whether or not a passive film will be protective of its substrate.[49]

2.9.3 Potential Polarization. Polarization is the shift of the half-cell potential of an electrode from the equilibrium (reversible or open-circuit) potential due to current flow.[43,44,79] The final potential is called the polarized potential.

The anodic and cathodic reactions can be represented by intersecting curves on the potential (y-axis) vs. corrosion current (x-axis) plot. Each curve indicates the polarized half-cell reaction (see Fig. 2.12). The intersection point refers to the new equilibrium state at which no net external current flows. The corresponding y-intercept is the rest, or static, or open-circuit potential E_{corr} of the corroding element. The x-intercept is the corrosion current I_{corr}. The potential value E_{corr} is the mixed potential of the anode and cathode which can be measured by a reference half-cell electrode.

The electrochemical polarization is divided into activation and concentration polarization. Any kinetic hinderance of the rate controlling step of a half-cell reaction results in activation polarization.[44] In other words, the electrochemical process is controlled by the reaction sequence at the metal/electrolyte interface. If the anodic process is the slow process in corrosion reaction, then the corrosion rate is said to be anodically controlled. Figure 2.13 illustrates the polarized curves of anodically controlled corrosion on a potential-current logarithm plot.

If the reactions are controlled by diffusion of ions in the electrolyte, then the process is under concentration polarization. The polarization is especially large for half-cell reactions which are almost irreversible such as that of oxygen.[44] When oxygen is depleted at the

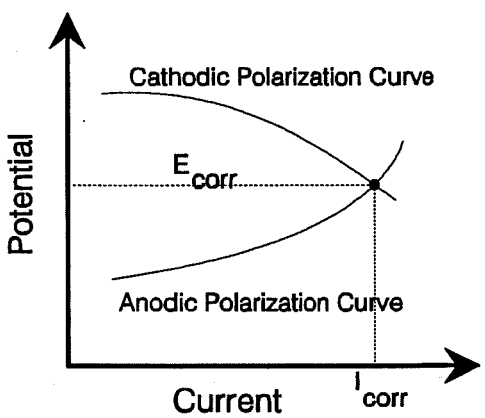

Figure 2.12 Polarized Anodic and Cathodic Curves of Steel Corrosion.

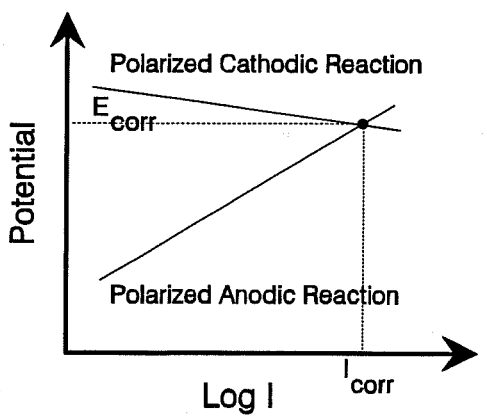

Figure 2.13 Polarized Curves of an Anodically-Controlled Steel Corrosion.

cathode, the rate of oxygen diffusion through concrete determines the rate of corrosion. If the cathodic process is the slow process in the corrosion reaction, then the corrosion rate is said to be cathodically controlled. Similar to Fig. 2.13, Fig. 2.14 illustrates this other kinetic situation on a potential-current logarithm plot.

The total polarization of an electrode is the sum of the activation and concentration polarization. The activation polarization usually controls at low reaction rates, while the concentration polarization becomes controlling at higher rates.[43] For the corrosion of reinforcing steel in concrete, the corrosion rate is usually governed by the cathodic reaction.[16,78]

The presence of the epoxy coating as an isolator around the reinforcing bar restricts the access of oxygen to the steel surface. The reduction reaction of oxygen is essential to complete the corrosion process. The scarcity of the cathodic area, therefore, slows the cathodic reaction and consequently the overall corrosion activity. Here, cathodic polarization predominates the process; *i.e.* the corrosion rate is cathodically controlled.

The slope of the polarized cathodic curve increases and may approach infinity. The mixed potential E_{corr} approaches the potential of the anodic potential of the corrosion cell. The corrosion cell may be developing at a holiday or damage in the coating. The intersection point lies in the more negative potential but in a low corrosion current region (see Fig. 2.15). Hence, highly negative potential measurements on epoxy-coated bars are not necessarily associated with high corrosion currents as is the case with uncoated bars.[81]

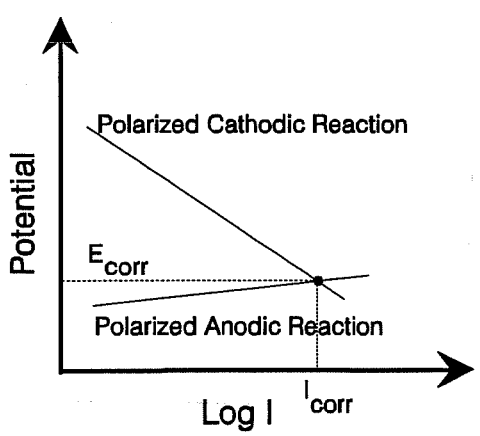

Figure 2.14 Polarized Curves of a Cathodically-Controlled Steel Corrosion.

Corrosion of epoxy-coated steel in concrete is a system that involves complex corrosion reactions subject to mixed polarization conditions.[82] Because of such complexity and the multiple polarization effects, the early attempts to evaluate the corrosion rate of the coated reinforcement were approximate. They were based on many assumptions. Models were proposed for coated bars with perforations or a partially debonded area of the epoxy coating.[82-84] Electrochemical impedance measurements were applied to determine their validity in evaluating the corrosion rate of the coated reinforcement. Such measurements were limited by the complexity of the response encountered. Concrete resistivity is one important factor affecting current distribution and diffusion.

Concrete may develop a high resistance path that could be a corrosion-rate-controlling mechanism.[44] The ohmic resistance of the moist concrete results in a potential drop through concrete known as IR drop. It obeys Ohm's Law; the potential drop is equal to the product of concrete resistance times the ionic flow. In a macrocell corrosion action, the potential difference, which drives corrosion between distinctly spaced anodic and cathodic sites, is reduced by this potential drop in the intervening electrolyte (see Fig. 2.16).

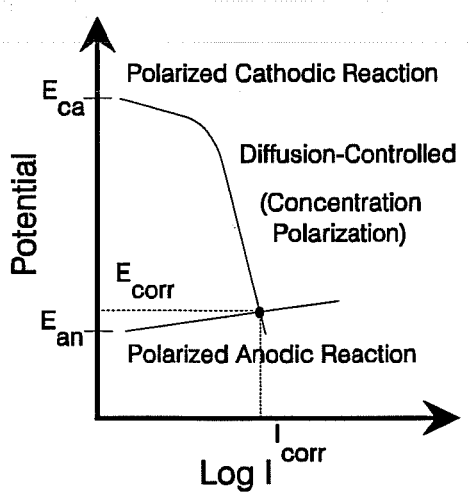

Figure 2.15 Polarized Curves of a Diffusion-Controlled Steel Corrosion.

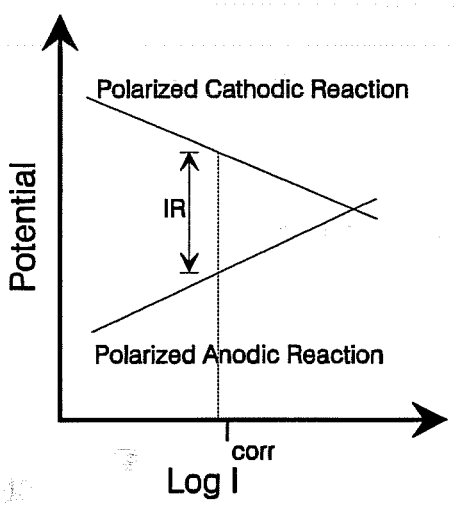

Figure 2.16 Potential Drop Due to Ohmic Resistance of Electrolytic Concrete.

CHAPTER 3
CRITICAL ASPECTS TO PERFORMANCE OF EPOXY-COATED REINFORCEMENT

3.1 General

Corrosion resistance of epoxy-coated reinforcement depends highly on its quality. To obtain a high-quality product, coating defects and damage must be minimized. This necessitates proper execution of the coating process, and careful treatment of the coated bars in subsequent stages. Damage to coating cannot be totally eliminated; therefore, detection and repair of damage become issues of concern. Quality control procedures are very effective in reducing the occurrences of coating imperfections. Strict specifications can result in further improvement to the final product.

The coating process involves several major steps. A schematic presentation of these steps is given in Fig. 3.1. The reinforcing bar is first cleaned and roughened by abrasive blasting. Then it is heated to a required temperature before coating application. Following coating, the bar is given a thermal treatment to ensure full curing of the epoxy film. These steps are discussed in detail in the sections to follow. The discussion includes a review of

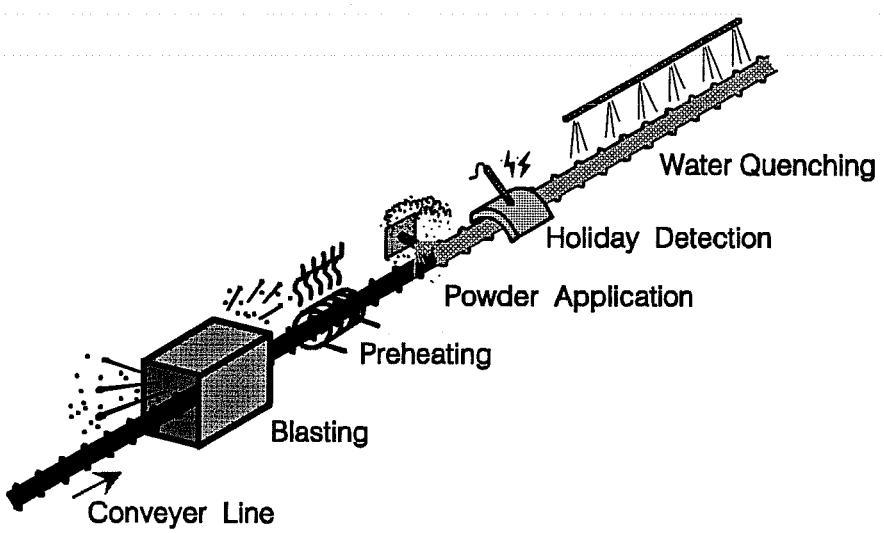

Figure 3.1 Fusion-Bonded Epoxy Coating Process.

current practice and prevailing specifications. The discussion also highlights important aspects of the coating process that can influence the quality of coating and effectiveness of the coated bars in resisting corrosion.

Even if epoxy coating were perfectly applied, damage to coating can still occur anytime the bar is carelessly handled. The major operations that may cause considerable damage are: fabrication; handling and transportation; storage; installation; and concrete placement. These operations are examined in this chapter to pinpoint how damage can occur or be prevented. Successful performance of coated reinforcement relies greatly on the quality of workmanship at all stages.

Careful inspection and repair of damage to coating are essential for improving the performance of the coated bars. Quality control tests are useful means for an inspector to determine conformance of the material with the approved standards and specifications. Repair materials, systems, and techniques are not yet widely addressed in different documents governing the production and use of the epoxy-coated reinforcement. Although repair of damage is required, it is not certain whether damage can be detected effectively or not. Such issues are presented here to shed some light on current practice and to make suggestions for future requirements.

3.2 Coating Process

3.2.1 Surface Preparation. In order for the epoxy coating material to realize its full potential, proper surface preparation must be obtained. Surface preparation is an extremely important factor which affects adhesion of the coating and bending characteristics of the coated reinforcing bar. Surface preparation involves adequate blasting to remove mill scale and surface contaminants. Additionally, it produces a rough surface for stronger coating adhesion. An example of a clean, roughened bar surface is shown in Fig. 3.2. Total debonding was observed on bent bars coated without any surface preparation.[15,85] It was stated that while the epoxy adheres tenaciously to mill scale, the mill scale debonds from the steel substrate.

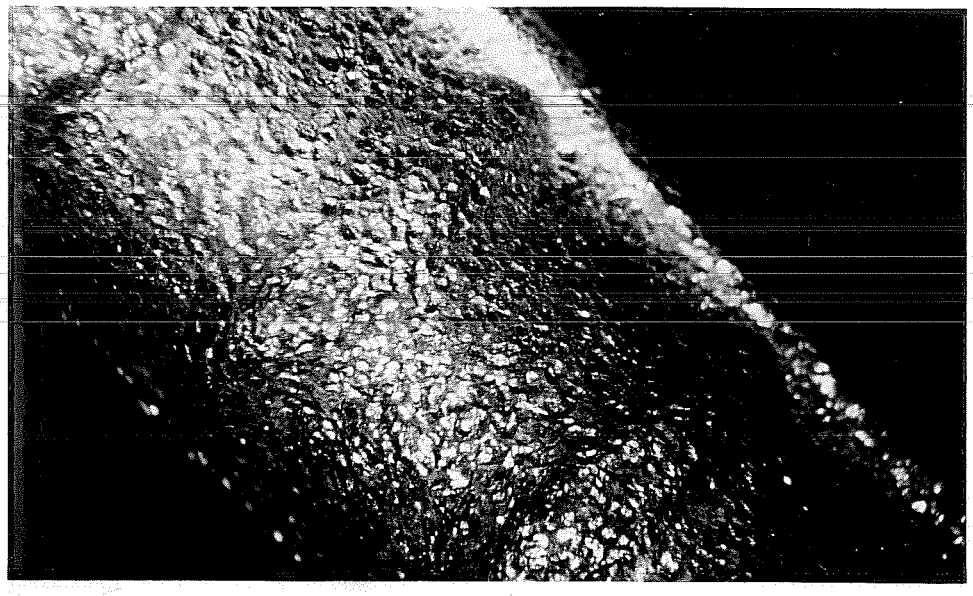

Figure 3.2 Blast-Cleaned Reinforcing Bar.

Cleaning the reinforcing steel surfaces by blasting is normally the first step in the coating process. The reinforcing bars are brought to the production line where a conveyor system carries them through the blasting chamber. The bar surfaces get blast-cleaned to remove rust, mill scale or loosely adhering deposits, oil, grease, and similar surface contaminants or foreign matter. If solvents are used to wipe visible oil and grease spots, care should be exercised not to leave a residue.

Various specifications and job documents require that surfaces be blast-cleaned to "near-white" finish.[12,18,38,39,86] This is usually done in accordance with the Steel Structure Painting Council Surface Preparation Specification SSPC-SP10.[87] The degree of cleanliness can be checked against the visual standard SSPC-VIS 1.[88] It should be remembered that cleaning to "near-white" finish permits a small specified amount of streaking and shadowing. Thus, this level of cleaning is not the most effective method of preparing steel surfaces for maximum coating adhesion and durability. Cleaning to "white" finish provides a thorough cleaning which is the only method to ensure maximum coating performance under severe service conditions.[89] Combining thorough cleaning with chemical pretreatment gives the ultimate surface preparation that will prove more economical in the long run.

All traces of blast particles, dust, airborne contaminants, or other debris from cleaning can cause defects in the coating if not properly removed prior to coating. To decontaminate the steel surfaces, a high pressure air jet (air-knife) or a high pressure liquid blasting, or simply brushing or vacuuming may be used.[30,89] If it is necessary to remove moisture from the bars, they need to be preheated to a sufficient temperature near 232° C (450° F).[18,72]

The freshly cleaned bare metal surface is very susceptible to corrosion and will rust quickly if wet or exposed to high humidity.[89] Therefore, the application of coating should proceed as soon as possible (within 90 minutes) after cleaning and before surface oxidation discernible to the unaided eye occurs.[30,86,90] ASTM specifications A775[38] and D3963[39] permit delaying coating application up to 8 hours after cleaning. Surface oxidation after blasting is known as "blueing" or "flash rust".

The degree of roughness of the steel surface during blasting is controlled to optimize the anchor pattern for coating bond. The number of peaks and valleys on the steel surface, as well as their depths, has a direct effect on the surface area available for molecular bond with the coating. Therefore, the surface profile should be kept within a specified range for maximum adhesion. The range is normally a small fraction of the required thickness of coating to avoid interference with its protective property. The amplitude of the anchor pattern is required to be in the range of 0.04 to 0.06 mm (1.5 to 2.5 mils) or approximately one-third of the coating thickness.[12,18,38,39,86] Recent proposed modifications to the specifications and proposed NACE specification for epoxy-coated bars raised the limits of the anchor pattern to a range of 0.05 to 0.1 mm (2.0 to 4.0 mils).[91,92]

Surface measurements to check the surface profile are important to assure quality of adhesion. Replicating tapes are commonly used on blasted areas to reproduce the surface profile.[30,90] The depth of the valleys is then measured using a dial-type micrometer. Other electronic measuring devices are available, such as the "Profilometer" and the "Perthometer".[30,90]

Selection of the type of abrasive is critical for producing a proper anchor pattern. The shape, size, and hardness of the abrasive affect the height and frequency of the peaks, as well as the angularity of the profile. Grit blasting, for example, produces an angular shape better for adhesion than the rounded profile of a shot blast.[30] A consistent surface finish can be obtained by a stabilized mix of abrasive (steel shot and grit) maintained by frequent small additions of new grit commensurate with consumption. Operation of blasting machine scalping and air wash separators is necessary to avoid contamination of the abrasive.

The quality of the base steel is also of importance to the overall quality of the coating, especially the adhesion. Steel surface defects such as shelling, rolling laps or flaws, blowholes, fissures, slag inclusions, slivers, and scabs can impair coating adhesion and its subsequent protective qualities.[11,12] Figure 3.3 shows an example of a defect at intersection of ribs on bar surface. Even excessively sharp and angular deformations can be difficult to coat properly.[90] Sharp edges cause the coating to flow away resulting in an inadequate film thickness. These defects are usually promoted by the rolling processes which produce the deformations. If left undetected, the flaws become sources of macroscopic defects in the epoxy coating films.[11] For ease of detection, inspection for these flaws can be made after blast cleaning. The Japanese standard JSCE EP20 covers checking for surface defects in detail.[12]

Figure 3.3 Steel Surface Defect at Rib Intersection.

Checking surface preparation immediately prior to coating is very important. This is normally done by quality control personnel at the coating plant. CRSI has a quality control plan[90] in which it recommends several test methods to check chloride contamination, as well as mill scale, dirt, and backside contamination. Skimping in any phase during surface preparation should be avoided. Strict control must be practiced in this regard if premature breakdown is to be circumvented.

*3.2.2 **Heating.*** Heating the reinforcing steel bars is the second important step in the coating process. The flexibility, quality of adhesion, and performance of the cured epoxy coating is affected by the temperature of the steel substrate when being coated.[15,30,85,93] The optimum bar temperature at the entrance of the coating station varies with the epoxy type, but is generally between 232° and 246° C (450° and 475° F).[18,86] To heat the steel to this level, ovens (such as gas fired) or electrical induction coils are often used. Figure 3.4 shows reinforcing bars being heated by induction coils during the coating process. Monitoring of the application temperature is possible through infra-red heat sensors, optical pyrometer, contact thermocouple, and temperature indicating crayons.[30]

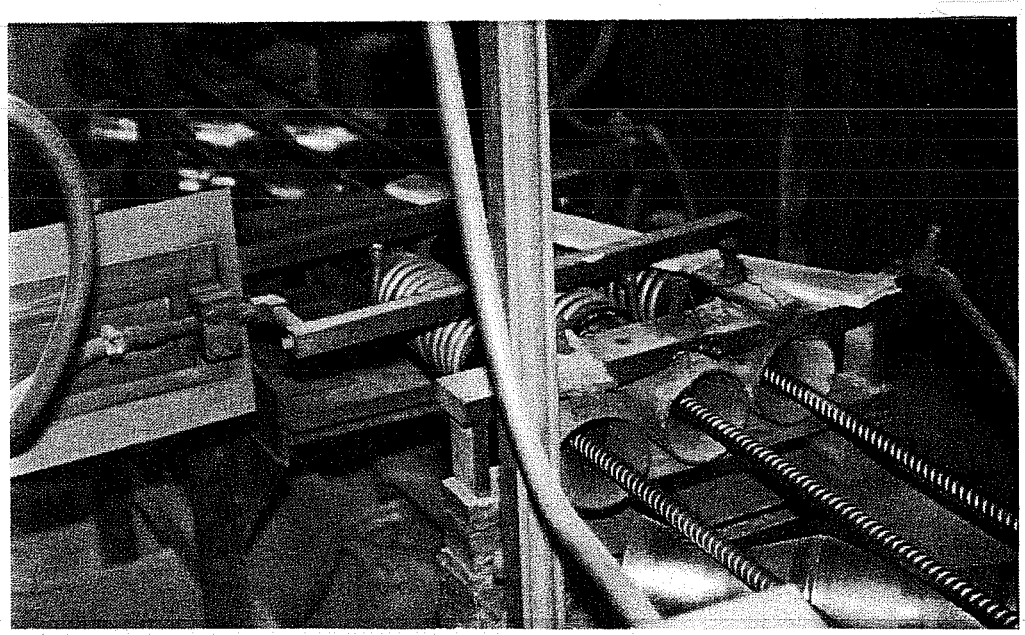

Figure 3.4 Heating of Reinforcing Bars by Induction Coils During Coating Process.[30]

It is important to maintain a constant even heat to assure proper thermosetting action of the epoxy resin.[86] Some powders are very tolerant of temperature fluctuations while others perform poorly if not applied within 3° to 5° C (5° to 10° F) temperature range.[30] It has been found that bars brought up to near 232° C (450° F) may form sizable oxide layers on the steel surface that constitute the metallic interface boundary.[93] Dissolution of these oxides at the boundary layer results in loss of adhesion. In order to control the heat, the speed at which the bar travels and the heat generated by the source need to be varied according to the bar steel mass. Small size bars require less heat and can travel at a faster speed, while large size bars require more heat and need to travel at a slower speed.

Underheating will result in poor performance because of the incomplete reaction and cure of the powder. There are two major sources for underheating: the heating source may be inadequate; or the steel itself may be too thick causing a heat sink. The surface temperature should be monitored so as not to drop off rapidly immediately prior to, or after coating application.[30] Surprisingly, ASTM D3963[39] allows the application of the epoxy powder to cold bars. It is believed that this provision is incorrect. The proposed revision of this standard specification has corrected this error.[91]

Overheating is also undesirable since it will cause severe damage to the coating. Consequences of coating application at elevated temperatures are: excessive foaming; poor "bendability"; lack of adhesion and blistering.[30,90] It is also possible to cause "burning" of the coating which appears as surface discoloration or rippling.

3.2.3 Coating Application. Several pre-approved epoxy powders are available for use in Texas Department of Transportation (TxDOT) projects. These powders meet the pre-qualification requirements specified by ASTM A775[38] (see Appendix B for more details). The powder used in a coating plant should be stored in the original unopened containers according to the manufacturer's instructions. The powder should not be used if its shelf life has expired.

There are different methods of epoxy powder application to preheated reinforcing bars. The main methods discussed in literature are: fluidized powder bed dipping; electrostatic spraying; and tribostatic spraying.[12,48] Dipping in a fluidized powder bed is suitable for coating fabricated steel in complex shapes, fittings, and welded mesh cages. The bed is a bath full of suspended epoxy powder granules that are aerated and kept well agitated by dry air streams blowing up from the bottom (see Fig. 3.5). When the preheated reinforcement is dipped into the bath for a sufficient time, the even flow of the powder allows fusion to take place. Therefore, the epoxy particles need not be electrically charged in this method.

Although dipping is a fast and relatively simple method of coating, it is difficult to control. Many factors affect the coating thickness and uniformity. These factors are: composition and viscosity of the coating material; rate of withdrawal of the object; and effectiveness of drainage in preventing drips and thick edges.[89] For best results, the temperature of the fluidized material should be well controlled, withdrawal of the object should be at a slow uniform speed, and the hanging system should be carefully designed to avoid unsightly drip beads or thick edges.

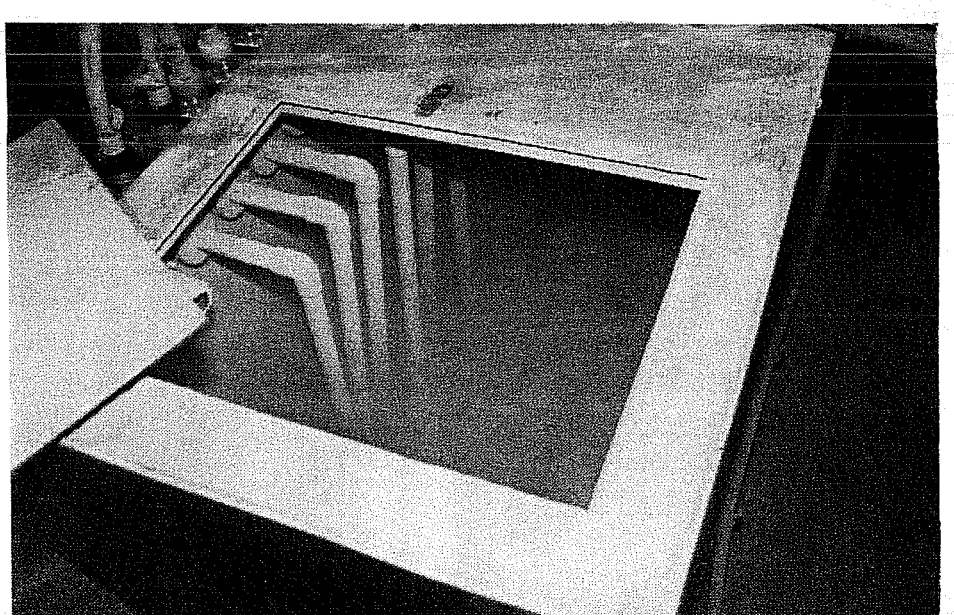

Figure 3.5 Fluidized Epoxy Powder Bed.[30]

Electrostatic spray coating is the more common method of powder application in the US and Japan. It is used to coat straight bars running in production lines. Spraying is done by drawing out the aerated powder, by means of a venturi-system, into specially designed nozzles (guns). The dry epoxy powder is injected into an air stream and is electrostatically charged to enhance attraction to the grounded steel surface.[12,30,86,89] Figure 3.6 illustrates the nozzle spraying system used on a production line of a Canadian coating plant. If moisture gets trapped in the air supply to epoxy particles, clumping may result which leads to defective coating. The powder particles are charged as they are sprayed. A small wire electrode at the tip of each nozzle induces a constant static charge of approximately 20,000 volts.[30] The charging practices may differ from one coating plant to another. A charging system which imparts a charge of about 45,000 volts has been reported.[12]

The speed of bars moving through the spray chamber and the orientation of the electrostatic spray guns are among the important factors that influence uniform coating application. Insufficient exposure time in chamber can result in thin coatings such as shown in Fig. 3.7. Rib geometry and deformation pattern complexity may also affect the thickness and uniformity of the coating. Mill marks are examples of complex, oftentimes sharp, surface irregularities where defects, mainly pinholes, are commonly found (see Fig. 3.8).

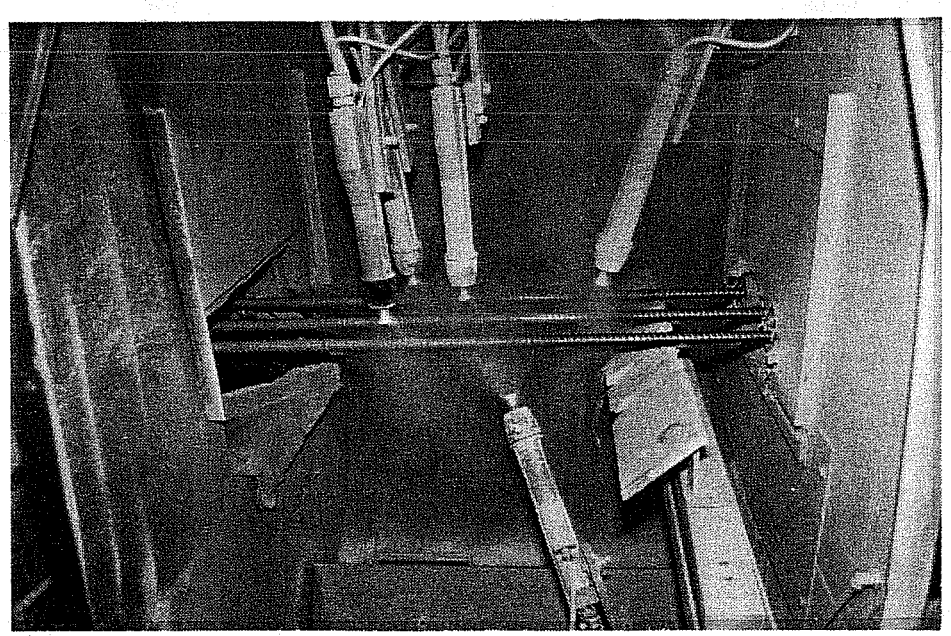

Figure 3.6 Electrostatic Epoxy Powder Spraying.[30]

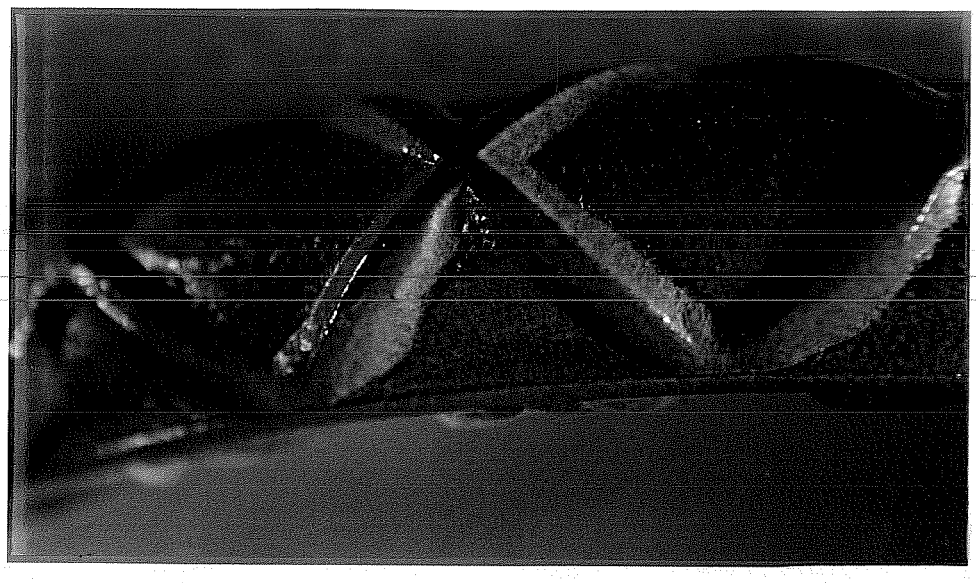

Figure 3.7 Thinly-Coated Steel Reinforcing Bar.

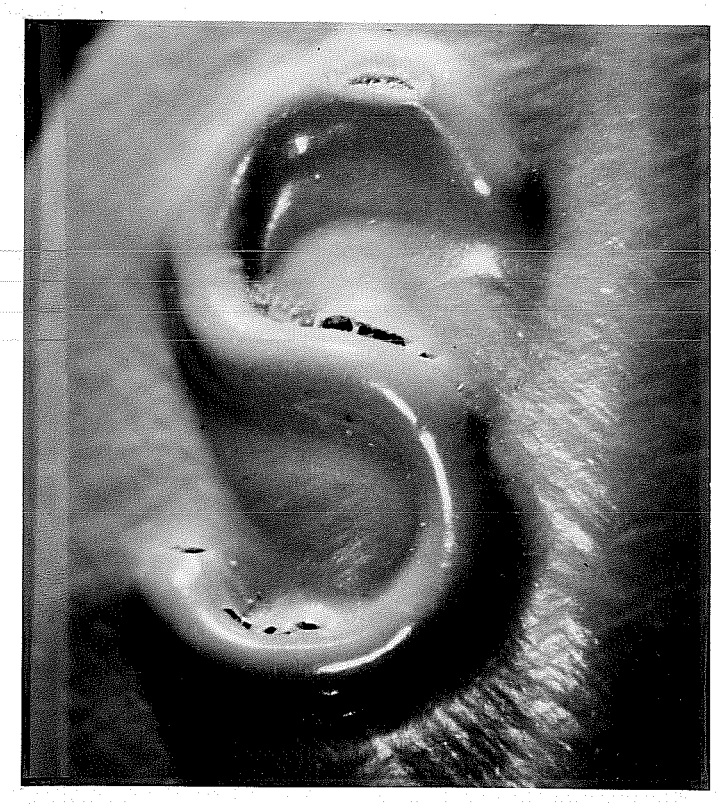

Figure 3.8 Typical Pinholes at Mill Marks on Bar Surface.

Experience has shown that worn out dies produce reinforcing bars that have less sharp edges and are thus preferred.

When the charged epoxy particles come in contact with the heated bar, they melt instantly and flow into the steel anchor profile. The resin gels in about five to seven seconds and solidifies within 15 to 25 seconds.[29,86] The time elapsed to turn the material from a liquid form to a gel is called the gel time, and is the first phase of the curing process.[90] During the gel time, the coated bars should not be disturbed by any contact between the bar and hard surfaces which might cause damage to the coating. After seven seconds of coating application, the bars may be supported on wetted, non-metallic rollers to be conveyed to the second curing phase.[18]

Depending on the system of conveying, the bar ends may not be properly coated. A system with rotating rollers forces the bars to rotate as they advance through the coating chamber. Normally, the last 3 m (10 ft.) piece of the bar is not well supported while it is being coated. The violent rotation of the end piece inhibits uniform coating application. Figure 3.9 shows a typical improperly-coated bar surface near the end.

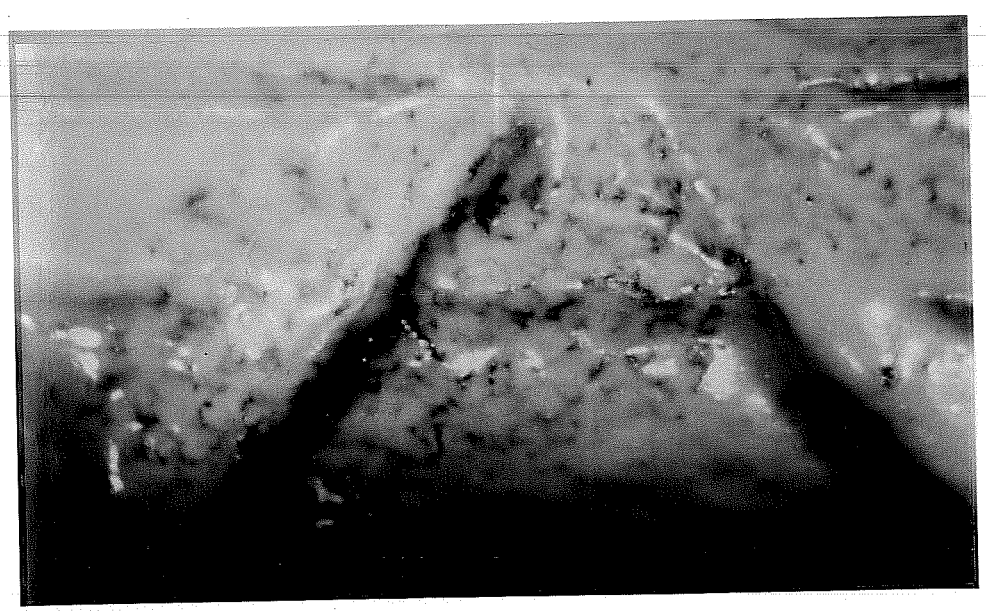

Figure 3.9 Improperly-Coated Reinforcing Bar Surface Near the End.

For tribostatic spraying, the operation is considerably different from the electrostatic spraying by the method of charge induction. In tribostatic spraying, charge is induced by circulating the powder in a spiral mode so that the granules become charged by friction with the charged surfaces of the gun barrel.[12] The charge imparted in this case is about 25,000 to 30,000 volts. Figure 3.10 delineates the principles of the two spray methods. It is important to note that the equipment needs to be different for each coating method, as well as the formulation of the epoxy powder itself.

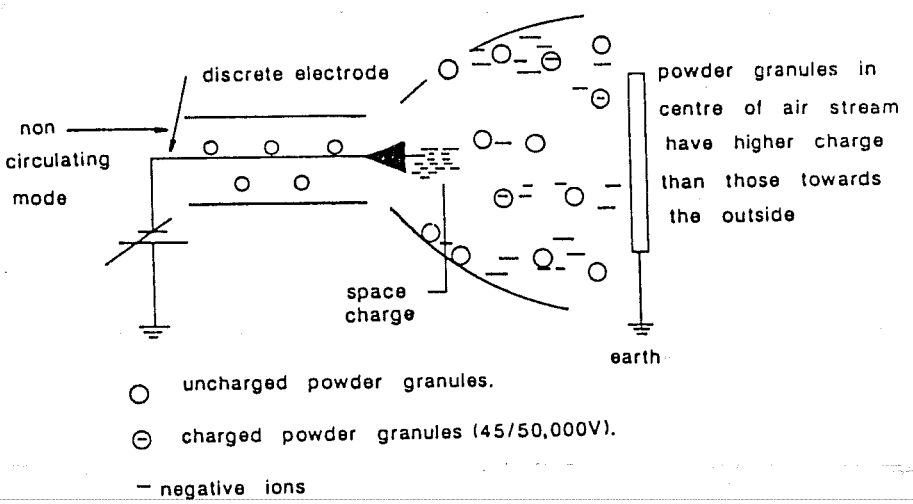

(a) Electrostatic Spraying

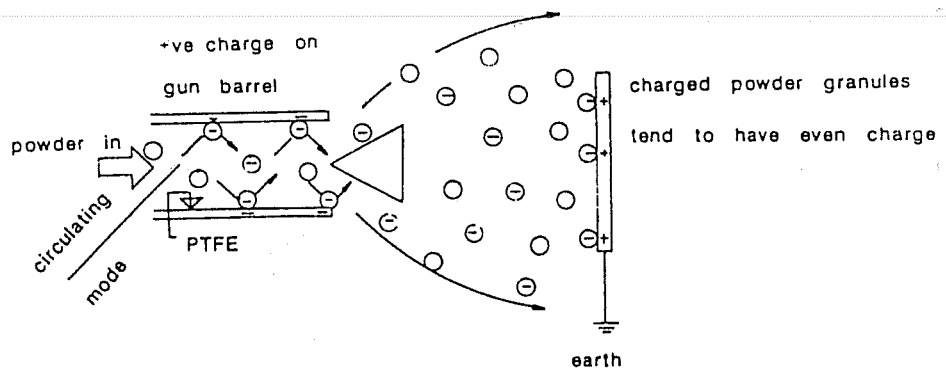

(b) Tribostatic Spraying

Figure 3.10 Principles of Electrostatic and Tribostatic Spray Coating.[12]

The tribostatic spraying technique is an alternative method of coating encouraged in Europe and is suited for straight bars. This technique requires more spray nozzles than the electrostatic technique but provides much more uniform charge, deposition, and thickness to the final coating.[48] Thus, it is especially effective for non-standard deformation patterns and complex surface configurations.

Reclaiming and reusing oversprayed powder may cause coating defects if not properly done. When oversprayed powder is collected in the coating chamber, it should be filtered and screened very well before it is ready for reuse.[30]

Coating discontinuity and coating thickness should be checked and maintained within specification allowable limits. These limits are discussed in detail in Sections 3.4.1 and 3.5.1, respectively. Coating thickness measurement and holiday detection are the duties of the quality control personnel at the coating plant.

3.2.4 Water Quenching. After coating, the bars are given a thermal treatment to provide a fully cured finished coating. Water quenching is normally used to cool the steel and coating to a temperature typically around 95° C (203° F).[29,30] The epoxy powder manufacturer usually specifies the temperature range at which the coated bar should be cooled to enable handling.

At the beginning of the water quench area, the epoxy is in a semi-set stage, and direct water spill on the bars may damage the uncured coating.[86] Therefore, the bars are moved on water-moistened, soft-covered rollers for about 30 seconds to allow slow curing. The bars should not be forced to cool sooner than 28 seconds after coating at optimum application temperature.[18,29] Cooling too soon may stop the cure reaction before it is complete.

In a second cooling stage, the bars are brought under direct water spray to cool to the required handling temperature. High temperatures exceeding 200° C (383° F) should be avoided during cure. It has been found that above this temperature limit, undesirable changes

in the resin structure are introduced which will affect the coating performance. Figure 3.11 shows the water quenching stage.

It takes approximately one minute for the bar to travel from the powder spray head to the end of the water bath.[72,86] In this short time, the epoxy melts, flows, and cures on the bar. The time between melting to final cross-linking of the epoxy molecule is known as the cure time.[30,90] It is generally recognized that a coating material with slower curing possesses better mechanical and chemical resistance properties. One way to increase the curing time is to slow the production speed.

The degree of epoxy curing can be checked reliably by differential scanning calorimetry (DSC) tests on epoxy samples.[48] The equipment involved is very specialized and is usually available at the epoxy powder manufacturer.[94]

3.3 Post-Coating Operations

3.3.1 ***Fabrication.*** The operation of bending coated bars almost always produces surface damage to the coating. Damage takes two forms: direct abrasion of the bar against

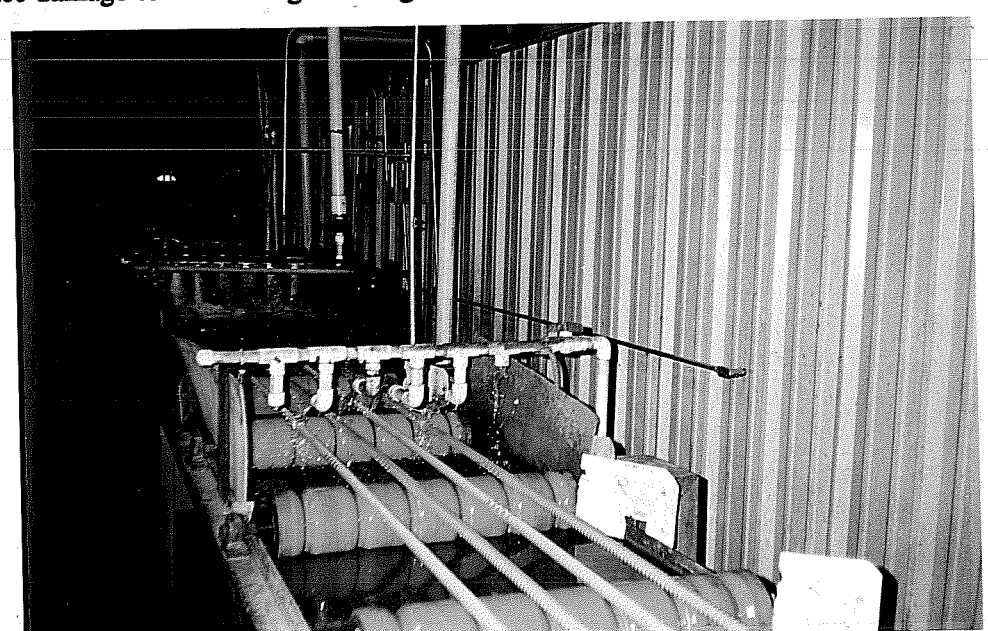

Figure 3.11 Water Quenching at the End of the Production Line.

the mandrels; and cracking of coating due to intolerable stretching. Besides the mechanical damage, bending may affect the adhesion state between the coating and the steel substrate. Bond weakness is manifested in film cracking and partial flaking or debonding.

During bending, the coated bar bears against the mandrel at the center pin and backup barrel (back stop) which often results in scraping or compression damage. Contact points on the bar are normally limited to the ribs. Consequently, damage appears as scraped or mashed spots on the transverse ribs on both the inside and outside of bends. To illustrate this type of damage and coating separation at weak locations, Fig. 3.12 shows the inside portion of a bent bar. Damage on the inside of bends is nearly always neglected in inspection.

On the outside of bends, the epoxy film may be stretched beyond its limit, particularly along the rib bases. Poor surface preparation aggravates loss of adhesion under the stretched coating. Hairline cracks or micro-tears form at these locations indicating inadequate "bendability" characteristics of the coating. Figure 3.13 shows two examples of coating cracking on bent bars with parallel and cross deformations.

Many coating plants provide fabrication services. The plants are usually equipped with the proper tools to minimize coating damage due to fabrication. When nylon, plastic,

Figure 3.12 Damage on the Inside Surface of Bent Bar.

(a) Bar with Parallel Deformations

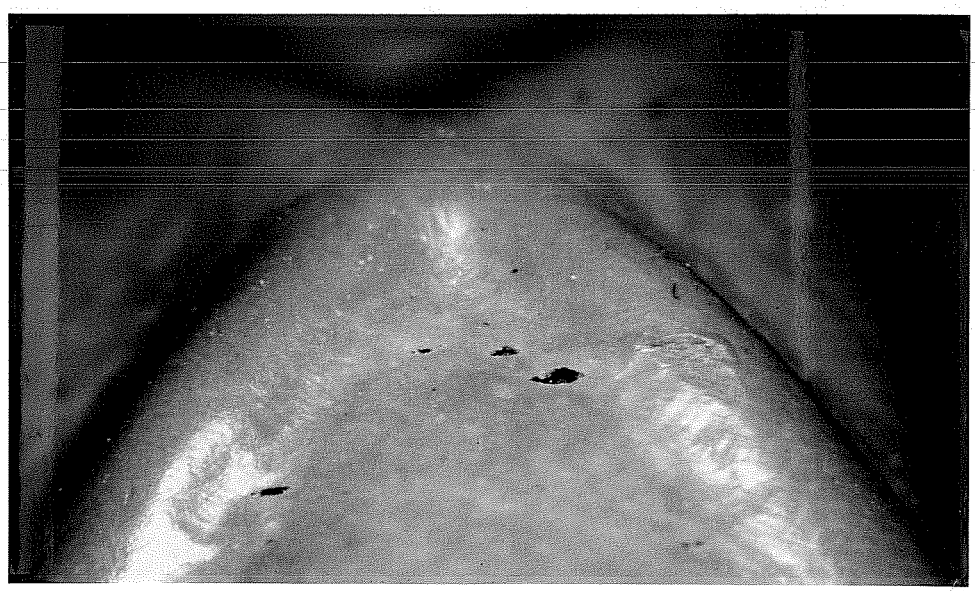

(b) Bar with Cross Deformations

Figure 3.13 Examples of Coating Hairline Cracking Due to Bending.

or urethane sleeves are used over the mandrels, the direct abrasion damage can be greatly reduced. Combined with proper flexibility of the coating, the high density plastic sleeves have proven to be effective. The use of a coating of paraffin wax to eliminate abrasion on the bending table has also been recommended.[86] Non-revolving back stops should not be used as they can cause considerable damage by abrasion.[48] Figure 3.14 shows the bending table with protective sleeves over the mandrels.

For greater efficiency, the bars are often bent at a fast rate. The effect of speed of bending on the degree of damage that may occur during fabrication is not fully understood. However, it is generally accepted that faster rates of bending cause more damage.[48] The normal shop rates of bending are between one to five seconds. These rates need to be modified if they result in damage to the coating. A rate of bending coated bars of 15 to 20 seconds may improve results. For large size bars, and tight bends, such as 180°, fabrication times greater than 50 seconds may be needed.

Bending at lower temperatures increases the tendency of the coating to crack.[11,29] Lowering the temperature causes the epoxy film to become brittle and more vulnerable. The best operating temperature for bending coated bars is in the range of 12° to 15° C (54° to 59° F).[29] The coating thickness affects the susceptibility of the coated bar to crack during bending. Increasing the coating thickness reduces the ability of the bar to be bent without cracking.[11,29] In Section 3.5.3, the effects of bar condition on the bending characteristics are discussed.

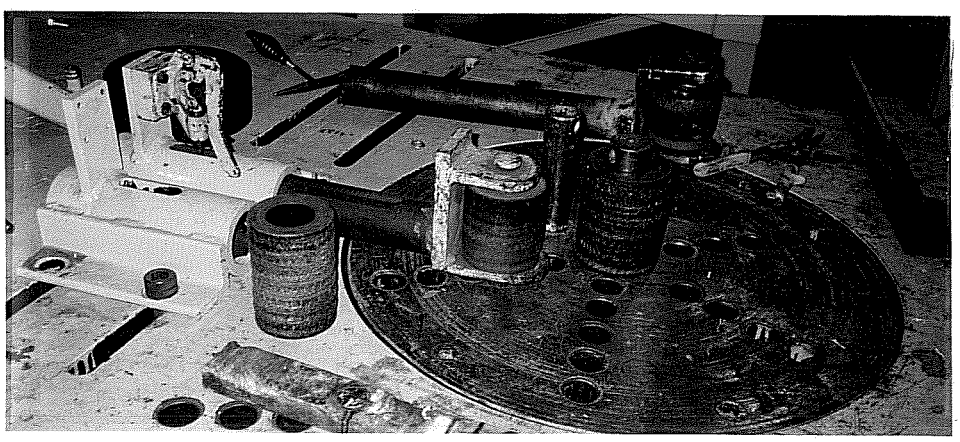

Figure 3.14 Fabricating Table with Protective Sleeves on Mandrels.

Additionally, the degree to which coated bars are damaged when fabricated depends on the bar diameter and radius of bending. Usually, tighter radii of bending are allowed for smaller diameter bars. As a result, more damage in the form of hairline cracking occurs on the outer surfaces of tight bends of smaller diameter bars. Hence, coated bars used in construction sites should not be bent tightly unless required by structural design. The intention is to minimize the potential of damaging coated bars by unnecessary practices.

Shearing coated bars also requires careful operation to avoid damaging the coating. Saw cutting is common at fabrication plants. Sheared bars need to be moved on protected conveyors, such as rubber-coated rollers, and collected in padded bins to prevent coating damage.[86]

*3.3.2 **Handling and Transportation.*** Damage to epoxy coating during handling the coated bars may occur due to:

- scraping or skidding of bar bundles;
- bar-to-bar abrasion from sags in the bundles;
- dropping or dragging of bars; and
- using unprotected contact areas of the handling equipment.

In general, any form of collision or violent rubbing with bars or other hard surfaces may chip the coating. Good practice should be followed when handling the bars at the coating plant and after they arrive at the construction site.

At the coating plant, bars should be bundled and banded with padded materials to protect the bars during handling and transportation. Nylon strings, padded straps, or padded wire rope slings are acceptable alternatives.[18,86,95,96] If the coating plant does not fabricate the bars, they are usually shipped to a steel fabricator prior to the final delivery to the construction site.

Loading and unloading the coated bars require close attention and proper precautions against damaging the coating. Skidding the bars from the truck bed could produce severe damage. Power-hoisting equipment should be used to move the bars. Bundled bars should be lifted with a strong back, a platform bridge, or a spreader beam that has multiple lifting points to prevent sagging of bundles during hoisting (see Fig. 3.15). In lieu of a spreader beam, spreader cables with at least two-point lifting can be used.[86,95] Wood cribbing minimizes damage and should be encouraged in place of chains or cable chokers.[86] Bundles should also be smaller than normally associated with uncoated bars.

Figure 3.15 Hoisting of Coated Bars with Multiple Lift Points.[86]

Sagging of the bundled bars during shipping can be prevented by placing a sufficient number of wood blocks on the truck. Nylon tie-downs need to be tightened across the trailer load at sufficient intervals to reduce vibration during transit.[86] Figure 3.16 shows bundles of coated bars loaded on a trailer.

3.3.3 Storage. The exposure conditions and period of storage may affect the long-term performance of the epoxy-coated bars. In particular, exposure to ultra-violet rays and

salt water spray during prolonged storage can degrade the protective qualities of the coating. Bars exposed to such adverse pre-service conditions may not perform well later in service when subjected to excessive amounts of chlorides.

Figure 3.16 Transportation of Epoxy-Coated Reinforcement.

Long periods of exposure to sunlight may cause fading or "chalking" of the epoxy color. According to CRSI Guidelines for Inspection and Acceptance of Epoxy-coated Bars at the Job Site,[95] discoloration does not harm the coating nor affect its corrosion protection properties. Therefore, outdoor exposure periods extending to one season of construction are allowed. The CRSI document does not specify the time limits of exposure beyond which the protective qualities of the coating become seriously impaired. On the other hand, recent studies have indicated that deterioration of coating may result from heating/cooling cycles and exposure to ultra-violet rays.[93] The conclusions were based on observations of the exposure conditions during storage of coated bars in a marine environment. Formerly, Lee and Nivelle[97] cited that chemical changes in epoxy films can be observed as a result of exposure to ultraviolet, and these changes might well be expected to adversely affect performance.

In their recently introduced certification program, CRSI recommends a maximum limit of outdoor exposure of 30 days.[90] However, stricter limits of only one to two weeks

prior to installation were suggested by others.[93] Hence, shipments of coated bars should be planned with minimum storage on site, and direct installation on formwork is preferred. It is clear that minimizing the time of storage at the construction site is a very good practice.

Exposure to chlorides during storage of coated bars can promote coating debonding and initiate corrosion of the substrate. Moisture alone may cause corrosion to begin at holidays and/or damaged areas. An actual documentation of the conditions prevailing at one construction site revealed that prolonged open storage at elevated temperatures, and exposure to salt water spray caused unexpected breakdown of the coating and corrosion of the steel.[98] The bars were shipped to the site in excellent condition, *i.e.* with minimum damage (less than 2%). It was concluded that even bars conforming to the specifications would incur considerable coating damage and degradation of bond if stored in a severe environment.

Apparently, storage is a very important source of damage to coating and to the future performance of coated bars. Storage conditions should be controlled in terms of preventing both direct physical damage caused by impact of other objects, and indirect damage induced by rigorous exposure to the environment. For the latter, bundled bars or assemblies stored in a construction yard in a marine environment should be protected from sunlight and possible exposure to salt water. Suitable protective materials should be used to cover the bars and allow adequate ventilation. The degree to which adverse storage conditions can affect coating adhesion and steel corrosion depends on the epoxy properties, the coating process, and the exposure interval whether continuous or intermittent.[93]

To prevent direct physical damage during storage, it is important to specify where and how the coated bars are stored. Storage locations on the job site should be away from traffic and equipment, and close to final position of installation. The coated bars should be separated from uncoated bars and grouped in small manageable bundles. Access should be available to any group of bars without having to dislodge or move others. Bent bars should be stored with additional care to avoid damaging the bends. Situations such as the ones disclosed in Fig. 3.17 must be avoided. It requires effort on part of the contractor and the inspector to ensure proper storage of coated bars during the entire construction phase.

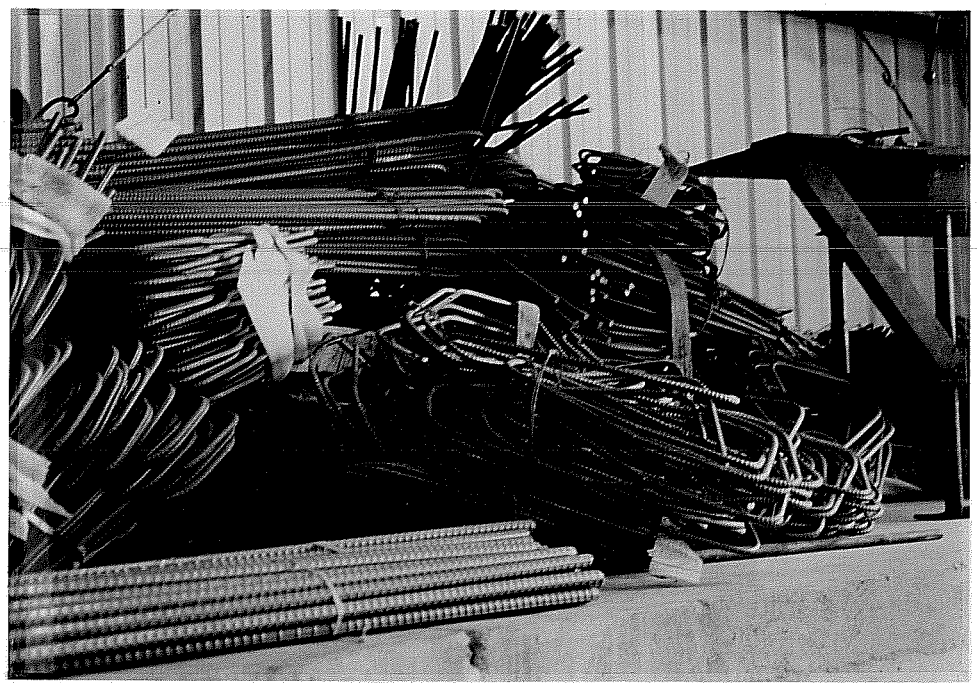

(a) Inadequate Storage of Bent Bars at the Coating Plant

(b) Inadequate Storage of Coated Bars at the Job Site

Figure 3.17 Examples of Inadequate Storage of Coated Reinforcement.

Proper storage at both the coating plant and the construction site is largely a common sense procedure as illustrated in CRSI published guidelines.[95] For example, storage should be on timber (wood blocks) or other protective cribbing above ground (as demonstrated in Fig. 3.18). Sags in the bundles should be prevented, and non-metallic tags should be used for bar identification.

Figure 3.18 Proper Storage of Coated Reinforcement.[84]

3.3.4 Installation. Reinforcing bar cage assembly, procedures, and positioning in concrete forms may add to the mechanical damage to coating.[93] The contractor should follow all the necessary precautions to avoid damaging the coating. For example, coated bars should be carried not dragged to their final locations. Walking on coated bars should be minimized, and care should be exercised not to drop heavy tools on the bars.

Tie wires should be of a special covered type capable of being twisted around bars without damage to either one. The covering material on the wire is usually epoxy, plastic, or nylon. A commonly used tie wire is black-annealed, 16.5 gauge or heavier wire.[95] However, this type of wire may cause cutting into the bar coating if tightened vigorously. Development of plastic clips and tie wires are still under way.[29]

Bar chairs, supports, and spreader bars for use with epoxy-coated reinforcement should be made of a non-corrosive or non-metallic material. Often, these are protected by either epoxy or plastic coating compatible with the bar epoxy coating. If galvanized steel was used, then it is required to coat the cradle and the upper part with epoxy or plastic.[18] Installation of these parts should proceed without causing physical damage to the coated reinforcing bars. In this regard, chairs carrying the top coated bars should rest on the formwork instead of the bottom reinforcing bars. Avoiding contact between the bars would help reduce the possibility of developing electrical continuity. Figure 3.19 demonstrates an acceptable detail for installed coated bars.

Splicing or coupling systems should be carefully used with the coated reinforcement. Fusion-bonded, epoxy-coated couplers are now available for use in construction. Careful installation is required to avoid introducing damage to the coated surfaces. It is strongly recommended that all parts of the installed splice be properly coated with a compatible patching material using appropriate tools. Inspection of splices prior to concrete placement is necessary to assure good quality patching.

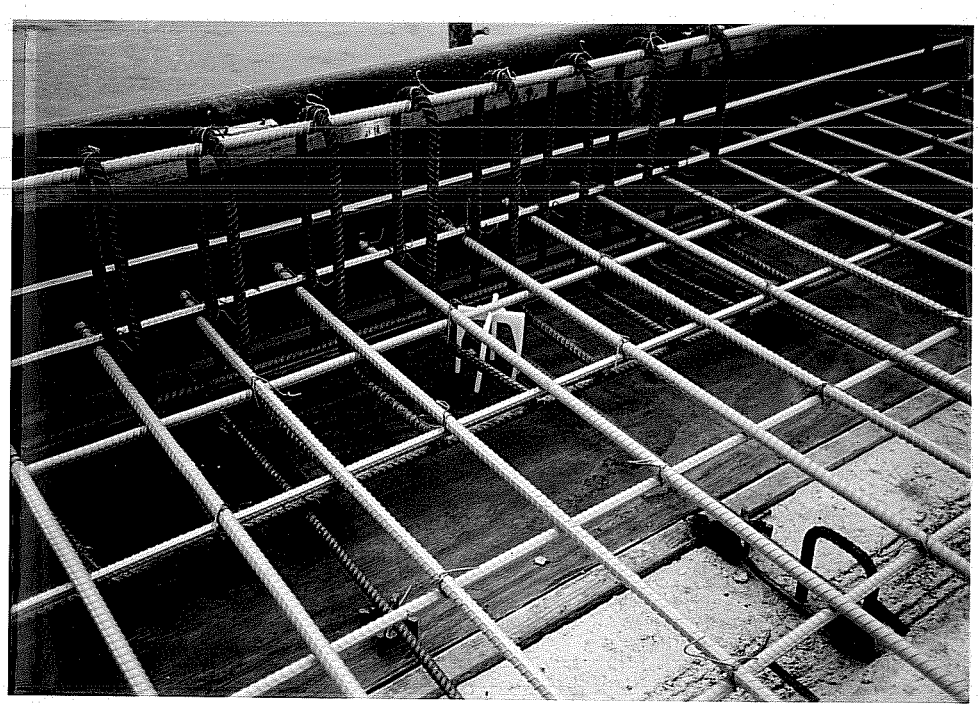

Figure 3.19 Proper Installation of Coated Reinforcement.

Field operations involving cutting, fabrication, and welding of coated bars are conducive to damage that can be detrimental to future performance. These operations must be minimized and well-controlled. Field cutting can be done only as permitted by the engineer. Using saw cutting rather than flame cutting can reduce the area that needs repair or touch-up. Field bending or straightening should be avoided if possible. An example of an improper field procedure of prying a coated bar is shown in Fig. 3.20. Even when damaged areas are patched, these areas will have a greater propensity for corrosion, especially if located in the vicinity of a construction joint.

It is worth emphasizing that coating damage at all stages prior to placing concrete can be cumulative from the various sources discussed. Proper inspection before placing concrete is, thus, essential to detect and repair the damage. This single step may considerably improve the long-term performance of the coated bars. Hence, job specifications should require that after completion of field installation of coated bars, all damaged areas should be patched with the repair epoxy compatible with the original.

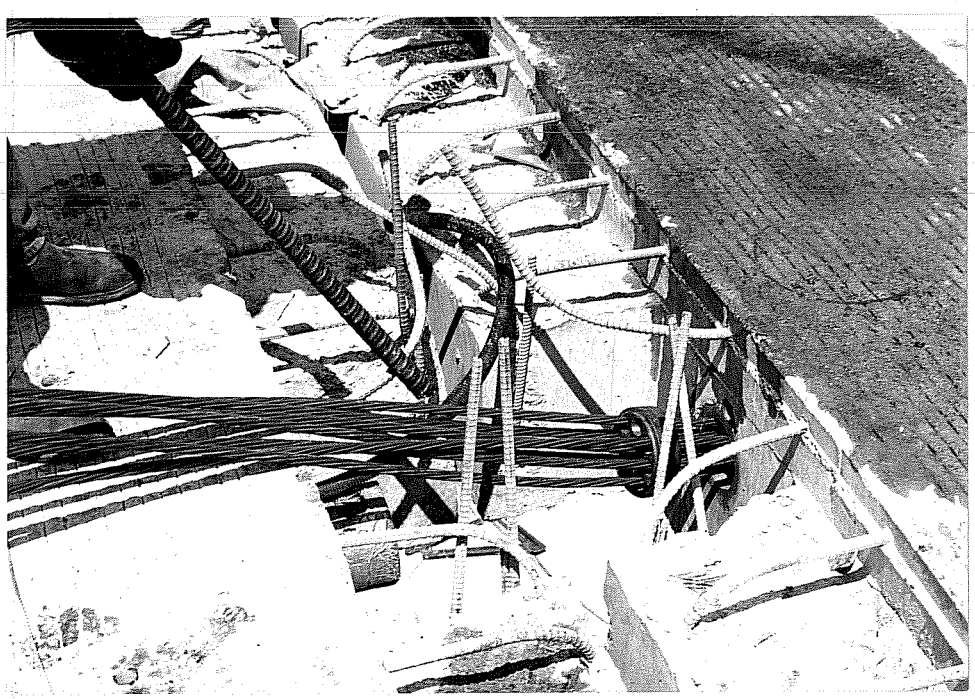

Figure 3.20 Improper Field Procedure of Prying Coated Bars.

3.3.5 Concrete Placement. A source of damage to the epoxy coating usually neglected is the conveying and placement of concrete. Damage due to this source is not observable and often underestimated. The equipment used to transport concrete during casting can damage the coated bars. Improper placing of concrete or dropping concrete on the coated steel may create additional surface damage.[93,95] Vibrating freshly placed concrete can also introduce significant levels of damage. Vibrators with metallic heads may damage epoxy coating. Direct impact between the vibrator's head and the coated surfaces will result in abrasion and steel exposure. The more area in contact, or the greater the pressure of the vibrator against the bar, more damage will result and increase the potential for corrosion initiation. Greater care should be exercised when vibrating concrete containing coated reinforcement than that containing uncoated reinforcement.

3.4 Repair of Coating Damage

3.4.1 Damage limits and Repair Requirements. A great deal of discussion appears in the literature concerning the effects of coating damage on the performance of coated bars. Coating damage has received close attention during the past few years, and the intention is to enforce tighter limits on acceptable damage to coating in the future. Current specifications, such as ASTM A775,[38] ASTM D3963,[39] AASHTO M284,[99] and industry recommendations, such as CRSI guidelines for inspection and acceptance of epoxy-coated reinforcing bars at the job site[95] set limits on acceptable coating damage and repair.

The aforementioned documents have different damage limits and repair requirements. The differences are clear with respect to specified acceptable damage in three separate stages. These stages are: damage incurred during the coating process only; damage due to fabrication and handling to the point of shipping; and damage incurred after shipping. As for the damage allowed in the coating process, ASTM A775 specifies a limit of 0.5% of the coated surface area of bar. Such unrepaired damage may be in the form of holes, voids, cracks, and deficient areas discernible to the unaided eye. Regarding the inevitable holidays (pinholes not visually discernible), both ASTM A775 and D3963 allow for a maximum of 6 holidays/m (2 holidays/ft.) in any production run.

According to ASTM A775, all damage caused by fabrication and handling to the point of shipping shall be repaired. The total permissible coating damage is limited to 1% of the bar surface area. Acceptable damage due to fabrication is given in detail in all the specifications and guidelines mentioned earlier. Hairline cracks without debonding from substrate during fabrication need not be repaired. Only when the coating looses adhesion and damage beyond hairline cracking occurs within any fabricated area, repair is required.

ASTM A775 does not deal with permissible damage incurred after the bars are set for shipping. However, according to ASTM D3963, damage caused by shipment of epoxy-coated bars need not be repaired in cases where the damaged area is 6 x 6 mm (1/4 x 1/4 in.) or smaller, and the sum of all damaged areas in each 0.3 m (1 year) length of bars does not exceed 2% of the bar surface area.[39] It follows that damage needs to be repaired with a patching epoxy material if any individual damaged spot exceeds the size limit of 36 mm^2 (0.063 $in.^2$) or the total damaged area per 0.3 m (1 ft.) of bar is over the 2% percentage limit.

CRSI guidelines agree with ASTM D3963 on the specified limits of coating damage that requires patching. However, the former TxDOT specifications[100] were more stringent allowing only up to 0.5% of damage without patching. Further, recent proposals for modifying existing specifications,[91] coupled with initial results of research work presented here, has led TxDOT to revise limits. The new TxDOT specifications[101] require that all visible damage shall be repaired. Similarly, the proposed NACE specification[92] for epoxy-coated reinforcement requires patching all visible damage.

There has been a trend to reduce the maximum allowable limit on patched surface area. When coated reinforcement was first used, job specifications limited the total damaged area acceptable for patching to 10% of the total coated area.[18] Any damage to coating beyond this limit results in bar rejection. CRSI guidelines limit the amount of damaged coating, including repaired and unrepaired areas, to 2% of the surface area per 0.3 m (1 ft.) of bar, whereas ASTM 3963 limits the maximum surface area of patched damage to 5%.

The most recent TxDOT specifications limit the acceptable amount of patched area at the applicator to 6 mm (1/4 in.) total length in any linear 0.3 m (1 ft.).

Repairing minor damaged areas and sheared or sawed bar ends is normally done using an epoxy patching compound. The patching material must be compatible with the original coating and inert in concrete. It should also be capable of being applied at the coating plant and in the field. The common types of the patching materials consist of two-component mixtures, supplied by the manufacturer of the epoxy powder, and are cold applied according to his recommendations. The same patching material is often specified for use in the field and in the fabrication shop.

At present, the current specifications governing use of epoxy-coated bars do not include provisions for repair materials and techniques. It is usually left to the epoxy powder and patching material manufacturer to specify which materials are compatible and how they should be applied. However, even when a selected patching material was used according to the manufacturer's instructions, a number of pinholes was discovered on the patched bar surface under microscopic examination (see Fig. 3.21). It is recommended that the effectiveness of the commercially available patching materials be evaluated. Formal guidelines should also be issued to govern assessment of repair materials and methods of application.

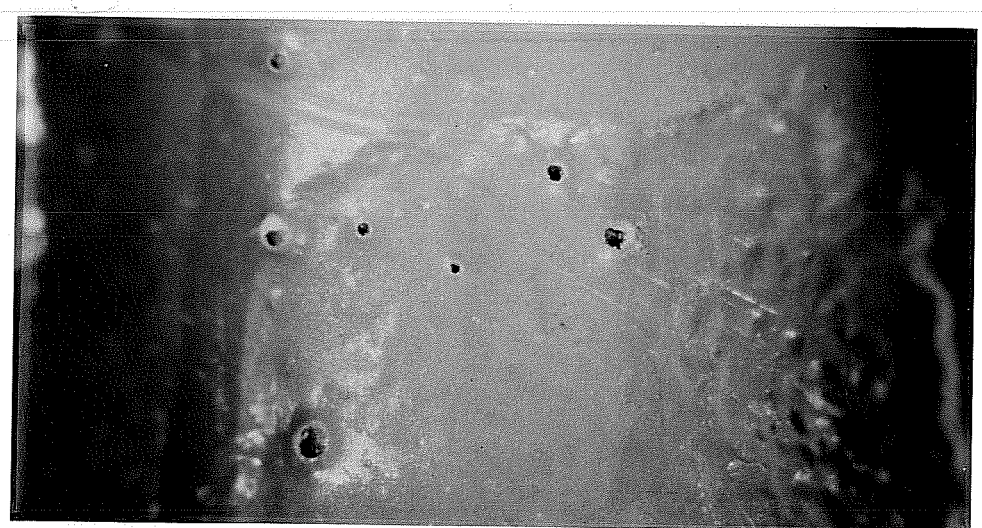

Figure 3.21 Pinholes on Patched Bar Surface.

Only minor coating defects should be repaired. Examples of defects that require limited repair are: scars; slivers; and minor surface imperfections. Major coating defects, such as unbonded coating, or inadequate film thickness should not be repaired. The protective qualities of coating with such defects remain questionable.

Patching the exposed steel areas needs to be performed as soon as practical before surface oxidation occurs. However, it is important to properly prepare the surface. Areas to be repaired should be clean and free of surface contaminants. Small spots may be cleaned by surface grinders, coarse files, or other suitable means to expose steel and remove dirt and damaged coating. Larger areas may be roughened with emery cloth or sandpaper.[30] The dust generated during preparation should be carefully wiped off. The presence of dirt, oil, grease, and other detrimental contaminants can impair adhesion of the patching material. In cases where rust is present, ASTM D3963 requires that rust be removed by blast cleaning prior to repair. Proper surface preparation is as important to successful repair as it is to the original coating process.

The recommended minimum thickness of liquid epoxy patching compound varies from one type to another. A thickness between 250 to 380 μm (10 to 15 mils) was required by previous specifications.[18] Both former and current TxDOT specifications require at least the same thickness of patching as specified for the original coating. It should be noted, however, that bar cut ends do not have an anchor profile and cutting produces very sharp edges. Therefore, patched cut ends tend to be thin and weak. Additional measures should be taken, such as covering bar ends with protective caps, to completely reduce the risk of corrosion progressing from these regions

Patching application temperature may also affect the quality of repair. Early job specifications specified a minimum application temperature of 13° C (55° F).[18] For some types of patching compounds, heating of the repair areas to a specified temperature may be necessary. In any case, all patched areas should be allowed to cure, cool, and dry before handling and storage.

Before shipping the steel, inspection for holidays and imperfections on the coating, as well as patching damaged areas, are the duties of the plant inspector. Inspection of the coated reinforcement following installation and prior to placing concrete is also necessary to patch any minor damaged areas.

3.4.2 Repair Systems. Two repair systems are widely used to patch damaged areas of the epoxy-coated reinforcement:

- Two-component patching compound; and
- Thermoplastic repair stick.

The two-part patching liquid epoxy is generally preferred for large repairs or when used on hot steel.[30] However, it is characterized by slow setting on cold steel, which reduces its field practicality.

3.4.3 Repair Techniques. Repairing damaged areas using two-part patching liquid epoxy is done by first blending the exact required proportions of the two components. Then, the thoroughly mixed compound is applied generously on the prepared surfaces. A spray gun or brush is usually used to obtain an even and smooth finish. The method of application is sometimes dictated by the pot life of the patching compound. It is important that the application of the material be in strict accordance with the manufacturer's instructions for best results. It is important to allow the mixture to stand a certain period of time before using it, and waiting till the patched areas are dry prior to handling and storage.

Using the melt stick to repair damaged areas requires a higher level of skill than the first method. Patching is done by covering the entire patch area with a propane torch, without scorching or charring the coating.[30] A repair stick is then heated and worked in a circular motion to obtain smooth even flow of molten material into the substrate. Any roughness in the patch could be smoothened by gentle post heating. It is important that patching covers the entire prepared area and runs onto the sound coating.

3.5 Quality Control

3.5.1 Coating Thickness. To ensure adequate protection, the epoxy film should be cured with a minimum number of defects. In the past, a range of coating thicknesses which satisfied these requirements without adversely affecting the structural behavior was defined between the limits 100 to 300 μm (4 to 12 mils).[62] Current ASTM[38,39] and AASHTO[99] specifications and CRSI guidelines[95] allowed values between 125 and 300 μm (5 to 12 mils). In addition, it is required that the deviation of individual thickness measurements not to exceed $\pm$ 30% or $\pm$ 50 μm ($\pm$ 2 mils) from average thickness, whichever is less. There is a tendency to raise the minimum acceptable thickness to 175 μm (7 mils) to attain a better minimum level of corrosion resistance.[91,92] Recent TxDOT specifications[101] have adopted this new thickness lower limit.

The method outlined in ASTM G12 for measurement of film thickness of pipeline coatings on steel is normally applied for epoxy-coated reinforcing bars.[18,30,38,39,96] Representative bar samples from each production lot are usually checked for film thickness and uniformity. ASTM A775 specifies checking coating thickness on a minimum of two bars of each size from each production shift. A test specimen is defined in Annex A of ASTM A775 as a 1.2 m (4 ft.) long, 19 mm diameter (#6) deformed reinforcing bar. Coating thickness must be checked on the straight body of the bar between the deformations and ribs, or both.

The calibrated "Mikrotest" magnetic gages are widely used for film thickness measurement. Their accuracy is within $\pm$ 10% of the true thickness of the coating.[30] Therefore, a number of readings should be taken and then averaged for better accuracy. The average of three readings of thickness obtained from three adjacent areas between deformations is considered a single measurement.[38,39] Usually, a minimum of five measurements (*i.e.* 15 readings) approximately evenly spaced along each side of a test bar are required. This is equivalent to obtaining a single measurement every 0.3 m (1 ft.). ASTM specifications further require that at least 90% of the measurements be within the specified limits.

It should be noted that common measurement techniques of coating thickness may not always yield reliable results. Undesirable thin films, for instance, may not be detected by magnetic gage measurements.[94] Studies performed in the UK on several types of thickness measurement gages indicated that these instruments were unsatisfactory.[48] The probes seem to be inaccurate for thickness measurements on and between the ribs. As an alternative, laboratory optical microscopes can be used to examine bar cross-sections for evidence of thin film regions. There are indications that magnetic gage measurements consistently give higher thickness values than obtained by direct microscopic measurements.[48] It should be recognized, however, that the surface configuration of the reinforcing bar affects the coating film thickness. Films at the ribs were found to be considerably thicker than at the corners of ribs or lugs.[11]

Very thick coatings have many undesirable effects. Thick films raise the propensity of the coated bar for cracking during fabrication (see Section 3.3.1). Films that are more than 500 μm (20 mils) may produce porous structures. The cause is attributable to the possibility of vaporizing some curing components at curing temperatures yielding the formation of porous expandable solids.[85]

3.5.2 Holiday Detection. Cured epoxy-coated bars are usually checked for continuity of coating at the plant. The coatings must be free of pinholes, flaws, voids, contamination, cracks, and damaged areas. These defects, or discontinuities, may jeopardize the performance of the coated bars. Examples of microscopically-detected pinholes are shown in Fig. 3.22.

The term frequently used to describe tiny discontinuities in the coating is "holiday". A holiday is a very small discontinuity (pinhole) of the coating that exposes the metal surface to the environment or exhibits electrical conductivity when exposed to a predetermined voltage. This means that holidays are openings in the coating capable of transmitting corrosion currents.[94] The size limits of holidays are not precisely defined but usually they are so small they cannot be detected with the unaided eye.

Figure 3.22 Microscopically-Detected Pinholes on Coated Bar Surface.

ASTM and AASHTO specifications[38,39,99] require routine checks for holidays during production using a 67.5 volt DC, 80000 ohms, wet-sponge type holiday detector. The detector is a device that electronically examines the reinforcing bar for minute discontinuities. The device comes with an audible or visual signal. The holiday detection requirements were originally taken from ASTM G62 that covers holiday detection in pipeline coatings. Inspection for holidays is recommended after coating has cooled to 120° C (250° F) or lower, depending on the powder manufacturer's instructions.[18] This usually takes place once the coated bar has passed through the cooling tank (see Fig. 3.23). Holiday detection of hot bars may show false defects because the dielectric strength (resistivity) of the coating is low at high temperatures.[30] In the holiday count, holidays at cut ends are excluded.[100]

Detection and correction of defects in protective coating are important factors in an effective corrosion control system. Holidays are not inspected as often at the job site as at the coating plant. At best, holiday detection indicates the continuity of epoxy coating and does not provide information on coating resistance, bond, physical characteristics, or the overall application quality. It is used to detect voids, cracks, foreign inclusions, or

contamination in the coating that are of such a size, number, or conductivity as to significantly lower the electrical resistance or dielectric strength of the coating.[102]

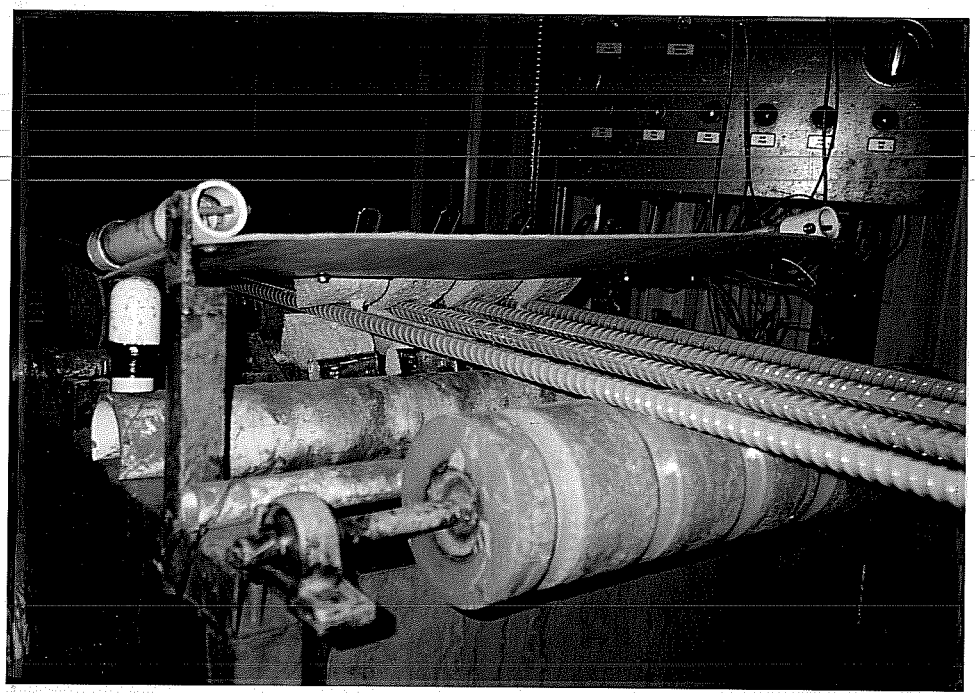

Figure 3.23 In-Line Holiday Detection.

When in-line detection is used, the major problem lies in achieving continuous contact with the bar base metal. One possibility is to use the metallic rollers that push the bar into the coating chamber to make electrical contact between the holiday detector and the bar metal surface. The sponge electrode is normally placed at a point away from the coating chamber to inspect the coated surface after the bar cools down by water-quenching. Once the bar end passes the last metallic rollers to enter the coating chamber, the electrical contact is lost. The distance between the sponge and the bar's end will not be inspected. Another possibility of grounding is to utilize the water bath system as part of the electrical circuit. The water is electrically charged so that when it comes in contact with conductive defects in the coating at the same time the sponge electrode is passing over a holiday, the detection signal is triggered. This solution may not be practical because of the difficulty in isolating water from the metal frame of the production line. In addition, water contact points need to be closely spaced to allow for continuous detection.

The film thickness influences the number of pinholes developed in the coating. Increasing the film thickness tends to reduce the frequency of pinholes. A Japanese study has shown that, under similar production conditions, thicker coating films exhibited less pinholes and better coating uniformity.[11] For a coating thickness of 300 μm (12 mils), practically no pinholes were formed.

3.5.3 Coating Flexibility and Adhesion. The flexibility of the coating is evaluated by the bend test. The test is also useful to detect poor surface preparation and inadequate epoxy cure, which will result in a poor bond between the epoxy coating and the steel. For this later objective, the test became a measure of the "bendability" of the reinforcing bar, *i.e.* the ability to fabricate the coated bar. The bend test is included in ASTM and AASHTO specifications.

To conduct the test, a representative number of bars is selected from each production lot. Normally, one bar of each size from each production shift is tested. The bar is bent 120° according to ASTM specifications,[38,39] or 180° according to TxDOT specifications[100] around a specified mandrel diameter according to bar size. It is noted in ASTM A775 that the specified mandrel diameters for the bend test of bars 10-25 mm in diameter (#3 to #8) are not compatible with fabrication bending practices. Tighter bends are customarily used in construction. Hence, the finished bends of smaller size bars need to be closely examined. If hairline cracking were detected, they should be repaired with the specified patching material.

The bend test is conducted at room temperature between 20° to 30° C (68° to 86° F) on bars that have reached thermal equilibrium. The bending rate needs to be uniform and may take up to one minute or 90 seconds to complete.[18,30,38,39,90] The bar passes the test if no cracking, tearing, or debonding on the outside surfaces of the bends was discernible to the unaided eye. Evidence of cracking or debonding would be a cause for rejection of the lot represented by the bar specimen. In regard to the test criterion, concerns have been expressed about detecting cracking at a delayed time after bending. Small-scale tears probably develop after some relaxation of the stretched coating takes place. Two retests of

random specimens are allowed if the first test specimen from a particular lot fails. If both specimens pass the test, the bars are accepted.

Several factors affect the performance of coated bars in the bend test. The most important factors are: bending radius; angle of bend; bending rate; bar temperature; and coating thickness. It has been mentioned earlier that thicker films are more prone to cracking during fabrication. However, for inspection purposes, the severity of the test can be increased by: reducing the bending radius; tightening the angle of fabrication; increasing the speed of bending to develop higher stresses at the steel/coating interface; and lowering the bar temperature to reduce the coating flexibility. In the new certification program for coating applicators developed by CRSI, an outstanding rank is assigned for those bars that pass a rigorous bend test. Such a test is performed in 30 seconds instead of 90 seconds, and by bending the bars 180° rather than 120°.[90]

Another method of testing coating adhesion on straight and bent bars is the "knife test". This test is not part of the current coated reinforcing bar specifications, but has originally been used with coated pipes. It requires making an X-shaped cut in the coating using a sharp knife. The coating is then peeled off by exerting pressure on the knife while its pointed edge is bearing against the sheared coating. A subjective rating system is used to evaluate the state of adhesion by assigning a numerical value for the following conditions:[30]

- Rank 1: well adhered coating; cannot be stripped from the substrate.
- Rank 2: coating pried from substrate in small pieces, leaving some residue in the anchor pattern.
- Rank 3: coating easily peeled from substrate leaving no residue behind.

3.5.4 CRSI Certification Program. In 1991, the Concrete Reinforcing Steel Institute established a program under which steel coating plants can be certified for maintaining a required level of quality.[103] The objective of the program was to ensure production commensurate with the latest approved standards and specifications. By encouraging a quality product, public investment in the infrastructure would be protected.

Participation in the program for certification was left voluntary. In order for a plant to be certified, it must have a written quality control policy statement, keep careful records, and post a quality inspector on every work shift.[103] In general terms, the assessment includes the equipment, technology, and operators involved in the coating process.

The certification program addresses most of the plant's procedures and quality control tests. The issues of concern covered in the plan are the following:[90,103]

- Abrasive blast cleaning of the steel before coating, including testing for chlorides and copper sulfate contamination.
- The temperature at which the steel is coated.
- The coating thickness.
- Handling of the coated steel, including checking for holidays, and the bend test.

Although the program is concerned with producing a quality product, it does not certify the product itself. However, participating plants will benefit from this program and the quality of their products are expected to improve with better in-house quality control procedures and record-keeping. Figure 3.24 shows the difference in the quality of the fabricated coated bars at one plant before and after the initiation of the certification program.

Unfortunately, the program is intended to result in high quality of coated reinforcing bar as it leaves the coating plant. Damage to coating during handling, transportation, installation, and concrete placement is almost certain. The program alone will not be sufficient to ensure satisfactory future performance. The efforts spent on assuring compliance with quality standards during coating will be wasted if no equivalent care has been given to the bars at all stages until they are embedded in concrete.

3.5.5 Inspection. An inspection scheme should be prepared to ensure that coated bars conform to recognized standards and specifications. An effective inspection scheme would include the following items:

- Plant inspection for initial production approval.
- Approved quality control plan on produced coated reinforcement.
- Transport and job site control.

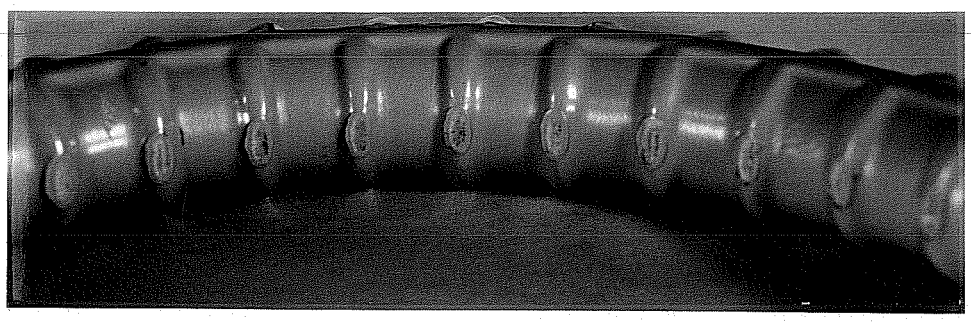

(a) Bar Bent Before the Certification Program

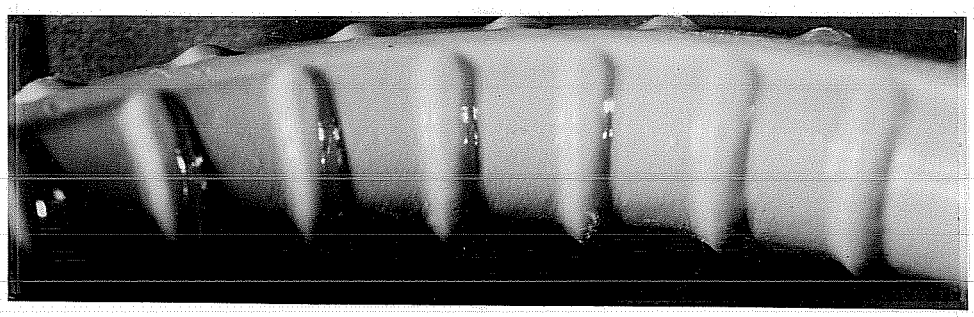

(b) Bar Bent After the Certification Program

Figure 3.24 Comparison of Damage Due to Bending Before and After CRSI Certification Program.

For TxDOT projects, the epoxy powder used for coating reinforcing bars must be pre-approved. Approved powder types are in accordance with the requirements of ASTM A775 Annex A1 which involves pre-qualification testing of the coating material. In Texas, the Materials and Tests Division of TxDOT has the responsibility for checking the production of the coated reinforcement up to the point of shipment to the fabricator or the construction site. Coating defects resulting from process imperfections are the primary concern at this stage. The duties of the division's personnel include shop inspection and sampling bars for

quality testing. The inspectors observe the full process of coating, starting with surface preparation till coating curing. They take samples from bar lots at the coating plant to conduct some verification tests. Typical tests include: yield and ultimate strength; elongation; coating film thickness; and bend test. Besides these tests, checking for deviation in the coating thickness is also important.

At the job site, the project engineer is responsible for checking and maintaining the quality of the used coated bars. In addition, project engineers should educate the people involved in the construction about the requirements for avoiding damage to the coating. For this purpose, the CRSI published Guidelines for Inspection and Acceptance of Epoxy-Coated Reinforcing Bars at the Job Site have been used. The primary use of the guidelines is to determine whether the repair of individual damaged areas is required, and if the total amount of damaged coating is permissible.[95] Visual examination of the coated bars for damaged areas should be done twice on the job site: first, when the bars are received; and second when the bars are ready to be covered with concrete. Furthermore, rejected coated bars should be removed from the site so that they are not accidentally reused.

CHAPTER 4
LITERATURE REVIEW OF PERFORMANCE OF EPOXY-COATED REINFORCEMENT IN DURABILITY STUDIES

4.1 General

Prior to investigating the adequacy of organic coatings for corrosion prevention, much attention was given to metallic coatings such as zinc, cadmium, and nickel.[15,85,104] The use of organic coatings on reinforcing bars was only briefly studied before the early 1970's. The idea did not gain wide acceptance until the National Bureau of Standards (NBS) study[15] reported in 1974. After this initial effort by NBS, many studies were conducted internationally to further explore the performance of coated bars under different conditions. Much of today's knowledge about the performance of epoxy-coated reinforcing bars was accumulated over the last 20 years of research.

This chapter contains summaries of a number of previous durability studies that focused on the performance of epoxy-coated bars in corrosive environments. The studies include both laboratory and field evaluations. The aim is to examine the earlier testing conditions, procedures, assessment techniques, results, and conclusions. Information in the literature is helpful in understanding research interests and implications of results to practice. Gaps in these efforts and current research needs can then be identified to select variables, test setups, type of measurements, and methods of analysis.

While providing a broad overview of the historical performance of epoxy-coated reinforcement, similarities among reported results and controversial issues pertaining to the early findings will be pointed out. Comments are made to help explain, scrutinize, emphasize, and question some of these findings.

Many of the studies included an evaluation of other corrosion protection systems besides epoxy-coated reinforcement. Examining the performance of these other systems in

details is beyond the scope of this study. For further information on any of these studies, the reader is referred to the references noted at the beginning of each section. The NBS study was a landmark in the history of development of the epoxy-coated reinforcement. Today's specifications of coated bars are still greatly influenced by the evaluation criteria of this first study. Inspection and quality control tests emerged from the same testing procedures. Hence, the NBS study deserves attention and will be reviewed in detail.

4.2 Laboratory and Field Studies

4.2.1 National Bureau of Standards, US, 1974.[15,85,104]

Study. Under the auspices of the Federal Highway Administration, the NBS performed an exploratory program aimed at identifying organic coatings, especially epoxy systems, suitable for protecting steel reinforcing bars in concrete. The study program included: the selection and procurement of promising coating materials; evaluation of the physicochemical durability and protective qualities of the coatings; identification of the most practical methods of testing such coatings; and determination of whether or not coated reinforcement would affect the structural integrity of concrete bridge decks.

The tests included liquid and powdered epoxy, polyvinylchloride powder, polyurethane liquid, polypropylene powder, phenolic nitrile liquid, and zinc rich liquid coatings. Altogether, there were 47 different coatings of which 36 were epoxy coatings. Emphasis was placed on epoxies because they seemed to best satisfy the selection criteria in terms of: inertness towards the constituents of cement paste and chloride ions; film integrity and protective qualities; bond to steel; creep characteristics; resistance to damage by rough handling; and feasibility of applying the coating commercially.

Findings. *Chemical Resistance.* Cured epoxy bar specimens were immersed for a year in selected chemicals most deleterious to epoxy coatings. The chemicals were aqueous solutions of the following: 3M NaOH; saturated $Ca(OH)_2$; and 3.5% 0.7M NaCl. In general, the epoxy coatings applied to sandblasted surfaces were not affected by these

chemicals. In addition, absorption tests were conducted on disks coated with epoxy which confirmed previous findings that **epoxies absorb measurable amounts of water**. Weight gain of the tested epoxy specimens was between 0.8 to 16%; therefore, thin epoxy films, *i.e.* 50-250 μm (2-10 mils) thick, were not entirely impervious to moisture.

Chloride Permeability. Cured powder epoxy films, 75 to 180 μm (3 to 7 mils) thick, were essentially impervious to chloride ions during an exposure period of at least 37 weeks in special permeability cells. However, the researchers stated that unequivocal interpretations of the chloride permeability values were not possible, but that epoxy films with low values would probably provide the best protection for reinforcing bars.

Film Integrity. Measurements of the coating film thickness, and the number of holidays per unit length of bar, in additional to visual examinations of the coating condition were performed to assess film integrity. The powder epoxy coatings produced films of moderate thickness 180 $\pm$ 50 μm (7 $\pm$ 2 mils) which were free of defects or holidays, and reasonably uniform when applied electrostatically by spray guns. Bar surface deformations, in addition, were not obscured by this coating material. The overall film integrity and covering characteristics of coating were better achieved by the electrostatic spray method than by the fluidized bed method of application.

Bend Test. The most discriminating test used in the NBS evaluation program was the bend test. Coated bars, 19 mm diameter (# 6), were bent through an angle of 120° over a 75 mm (3 in.) radius mandrel using a manually-operated hydraulic bending machine. Bends were then checked visually for any evidence of cracking or debonding of the coatings. This test particularly reveals the adequacy of the inherent flexibility of the coating, film thickness, cure, and surface preparation of the steel substrate. Powder epoxy coatings of moderate thicknesses, generally performed satisfactorily. Film thicknesses over 250 μm (10 mils) generally failed the test.

Abrasion and Impact Resistances. The abrasion resistances of epoxy coatings on steel panels were determined in accordance with ASTM D1044-56. None of the powder epoxy

coatings failed the test. Damage to coating on reinforcing bars caused by an impact of a 1.8 kg (4 lb.) weight falling a distance of 0.75 m (30 in.), according to ASTM G14-69T, was considered an indication of the abuse reinforcing bars receive during handling, shipping, and installation. The powder epoxy coatings, again, showed satisfactory results as the damage area did not exceed an arbitrarily chosen limit of 95 mm^2 (0.15 $in.^2$). Impact resistances were also evaluated by dropping, lengthwise, a piece of a coated bar on a concrete slab from different heights and inspecting damage after each drop. The relative ratings of the coatings were found to correlate closely with the bend test results.

Applied Voltage Studies. A potential of two volts was applied between two 19-mm (#6) coated bars (anode and cathode electrodes) immersed in 7% NaCl electrolytic solution. The applied voltage was used to assess the effects of electrochemical stresses on the bond of epoxy coatings on steel. Corrosion initiated on the anode if holidays in a film were developed because of degradation of the coating. In addition, coatings that permitted evolution of hydrogen gas at the cathode within 15 minutes were considered of doubtful value. No signs of corrosion were apparent on the powder epoxy coatings thicker than 125 μm (5 mils) after one month of testing. Consequently, single intentional holes 6 mm (1/4 in.) in diameter were introduced in both electrodes and the test was continued for an additional 24 hrs. Undercutting in the area around the holes was insignificant.

Electrical Potential and Resistance Measurements. Simultaneous measurements of the electrical potentials and resistances of the epoxy films were taken on coated reinforcing bars partially immersed in 3.5% NaCl solutions. The test served as a means of assessing the protective qualities of the barrier coatings. Resistances below 500 ohms were considered indicative of films which either had many holidays, or were permeable to water and chloride ions. Observance of several corrosion sites on coated bars was also correlated with potential readings below -600 mV with reference to a saturated calomel electrode (SCE). Companion specimens showed wide variance in the initial millivolt and ohmic readings which decreased with time ending with good agreements. Figure 4.1 illustrates the potential and resistance data of two sets of reinforcing bars coated with different epoxies. In general, properly

applied powder epoxy coatings with thicknesses between 150 to 280 μm (6 to 11 mils) performed well.

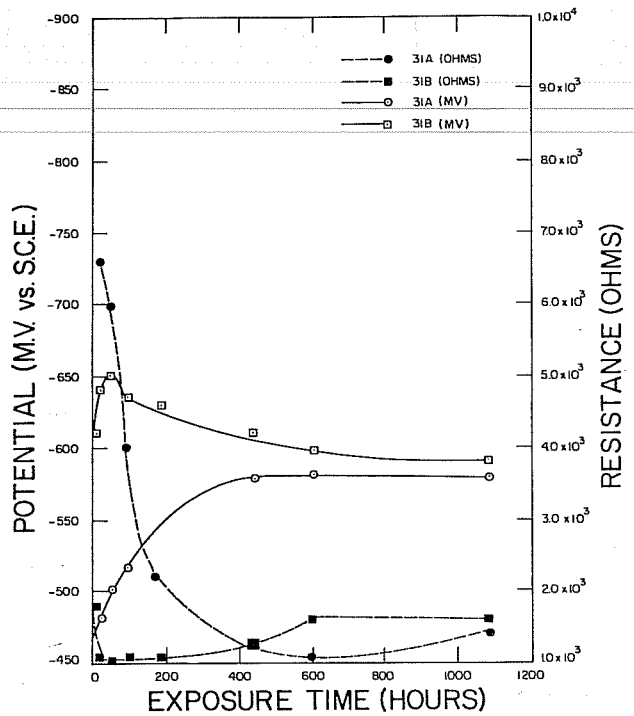

Figure 4.1 Electrical Potential and Resistance Measurements of a Group of Epoxy-Coated Bars Immersed in 3.5% NaCl.[15]

Bond and Creep Tests. Bond characteristics of coated bars in concrete were compared with uncoated bars by pullout tests. These tests were conducted using a type of specimen and methods developed earlier by Mathey and Watstein. In these tests, the bond strengths developed on coated bars with film thicknesses below 250 μm (10 mils) were essentially equal to those developed on uncoated bars. Furthermore, such coating thicknesses showed acceptable creep characteristics. Epoxy films with a thickness of about 630 μm (25 mils) developed bond strengths which were only about 60% of those of uncoated bars.

Overall Conclusions. It was concluded that properly formulated and properly applied powder epoxy coatings should be satisfactory for the intended application. The epoxy coating

provides an inert barrier sufficiently tough to allow bending of bars and to withstand abuse of normal construction practice. Coated bars with a maximum film thickness of 250 μm (10 mils) can be incorporated in bridge design without compromising the bridge structural integrity. The optimum film thickness of epoxy films is 180 $\pm$ 50 μm (7 $\pm$ 2 mils), with 100 μm (4 mils) being the limit below which corrosion protection will not be secured. Four epoxy resins suitable for use in reinforced concrete construction were identified in this study.

Comments. Although this study recognized that epoxy coatings tend to be permeable and absorb measurable amounts of water, the effects of such tendencies on softening, debonding, and ultimately the performance of coating were not clarified. The chemical immersion tests did not fully represent the concrete environment; the composition, physical restraint and homogeneity were quite different. Therefore, materials performing well in the immersion tests may not necessarily do so after long-term embedment in concrete. The pore solution of a portland cement paste or mortar contains a mixed solution of NaOH, KOH, and very little $Ca(OH)_2$.[93,105] An approximate composition is given as:

0.6M KOH + 0.2M NaOH + 0.001M $Ca(OH)_2$

Projected evaluations of the long-term durability of coatings in concrete, using simulated solution environments, need to be carefully carried out. Nevertheless, immersion of bars in aqueous solutions, such as salt water, will provide a discriminatory criterion and a basis on which comparison between different specimens can be satisfactorily made.

The chloride permeability tests were not conclusive. Indications of low chloride permeability were obtained only for a group of coated bars with coatings 75 to 180 μm (3 to 7 mils) thick.

The susceptibility of the coating to debond from the substrate during bending could not be determined satisfactorily by the bend test. Visible cracking in the coating was construed as the failure criterion. However, some degree of debonding during bending could still occur and might have detrimental effects. If corrosion is initiated at some breaks in the

coating, its progression under the coating would be facilitated by debonding. This condition may be evaluated better by using the applied voltage test on bent bars.

The applied voltage test can be useful for accelerated macrocell corrosion testing. Originally, the applied voltage test was used to investigate the development of holidays in a film because of degradation of the coating. Hence, the test was based on forcing potential anodic and cathodic formations to occur on two coated bars initially damage-free. In essence, the test served as a sensitive holiday detector. However, by changing some test parameters, it can be used to accelerate macrocell corrosion between coated and uncoated bars brought in contact with each other under a corrosive environment. Further, if the coated bars were damaged to simulate actual field conditions, the test conditions would be more severe.

Electrical potential measurements seem to be a valid means to monitor the condition of the coating. Likewise, electrical resistance measurements may be effective in monitoring corrosion activity of the coated bars. Interestingly, the potentials reported in the NBS study started much more negative than normally the case with uncoated reinforcement.

4.2.2 Virginia Department of Transportation, US, 1977.[96]

Study. Encouraged by the Federal Highway Administration, the Virginia Department of Transportation made a trial installation of epoxy-coated reinforcing bars on the twin bridges carrying Route I-77 over Route 620 in Carroll County, Virginia. During the experimental installation, a study was carried out to record any problems encountered during fabrication and shipment of steel and during placement of concrete.

The scope of the study included observation of the deck construction and measurements of electrical resistivity, potentials, cover depths, and chloride contents. Such base data could be used for further evaluation of the effectiveness of the coated reinforcement under service conditions. The use of deicing salts was conceived as the primary source of chloride ions into concrete.

Transverse and longitudinal steel in the decks tested, including the negative moment reinforcement over the piers was epoxy-coated. The parapets, however, were constructed with uncoated reinforcement. SKOTCHKOTE 202 epoxy material, with a specified film thickness of 180 $\pm$ 50 μm (7 $\pm$ 2 mils), was used on the test bridges.

To study the performance of the coated bars, a comparison was made with the performance of uncoated bars under similar salt application histories. The bridge structures on Route I-77 closest to the tested bridges were chosen as control structures. The chloride contents in the decks of both sets of bridges were determined.

Findings. *Resistivity Measurements.* Resistivity measurements were taken along some instrumented bars after placement of concrete. The readings were obtained using a DC electrical procedure. These readings were of the magnitude normally measured on bare concrete over uncoated bars, *i.e.* below 10,000 ohms. This indicated that the epoxy was not intact. It was suspected that patching carried out before steel embedment did not seal all the holidays completely. It was also possible that many flaws in the coating existed. Damage during concrete placement was not ruled out, even though visual inspection of uncovered bars at various spots disclosed no distress.

Electrical Potential Measurements. Electrical potential measurements were also taken along the instrumented bars. The readings were below the value of -300 mV CSE- the threshold of probable corrosion. Therefore, initiation of corrosion was not suspected.

Chloride Contents. The chloride contents were within the range normally associated with chlorides chemically bound in Virginia aggregates. Such chlorides were not expected to take part in steel attack.

Observations. With reasonable care exercised by the applicator and contractor, no damage occurred in moving the bars from plant to final position in deck. Suggestions were made to eliminate the coated chairs and ties and to reduce the amount of patching required.

Many of these requirements were dropped from later editions of the Virginia Department of Highways and Transportation specifications.

Comments. The suitability of using a DC electrical procedure versus an AC technique to obtain the resistivity readings was questioned in the study report. The measured resistances might not be accurate enough to pass a judgement on the integrity of the epoxy coating.

The study raised some doubts about the effectiveness of the patching material to seal coating defects. Such concerns still exist today, and the demand is high for improved patching materials and techniques.

Good practice in handling the coated bars at the applicator and the job site can result in limited induced damage to the coating. Similar shipping and handling procedures need to be enforced in all applications of the coated reinforcement to assure a quality product. Relaxing requirements related to patching damage and use of coated chairs and ties does not appear to be justified.

4.2.3 Oklahoma Department of Transportation, US, 1981.[18]

Study. A monitoring system was established on a rehabilitated bridge on I-35 in Noble County, Oklahoma. The objective was to study the durability of the epoxy-coated reinforcement under corrosive influences. The stability of the epoxy film in concrete was monitored by taking electrical resistances measurements. Only the top mat of reinforcement in the bridge deck was epoxy-coated using SCOTCHCOTE 213.

Six coated bars were selected at random for AC resistance measurement. Each measurement cell consisted of two coated bars tied to copper conductors. The resistance measured between the coated bar and the copper conductor was used as an indicator of the integrity of coating film. A drop of resistance was considered to signal the onset of deterioration. In addition to these measurements, wet mop AC resistance readings were

obtained on 14 other bars randomly selected. A commonly used wet, conductive sponge connected to a copper plate was used for these latter measurements.

Findings. Data collected during the first nine months of monitoring were plotted as resistance curves. These curves were, generally, flat indicating stable conditions within the deck. However, there was a notable increase of the resistance in the month of January and during July.

Comments. The study referred to several mechanisms that could alter resistance readings. It was stated that a rapid decrease of the resistance can be attributed to emergence of holidays. On the other hand, an increase in resistance might possibly indicate some type of holiday healing mechanism. Another proposed explanation was a thorough drying of the deck especially during the driest month, January. Moreover, freezing of the remaining water in the concrete voids might have raised the resistance since January is also the coldest month.

The experience of the Oklahoma Department of Transportation with the first installation of coated reinforcement, and the initial results of monitoring, were encouraging. No problems or difficulties during all stages of construction were encountered.

4.2.4 Maryland State Highway Administration, US, 1981.[72]

Study. An experimental study was conducted on 11 selected bridges constructed with epoxy-coated reinforcement coated with two different materials (FLINTFLEX 531-6080 and SCOTCHKOTE 202). For comparison, a bridge constructed with conventional reinforcement was also selected. Furthermore, a total of 21 additional bridges were visually examined. All these bridges were in the Baltimore metropolitan area.

Because the coated reinforcing bars for one bridge did not pass the bend test, the coating process was modified to coat the bars after fabrication. The fabricated bars that could not pass through the electrostatic spraying system were coated by hand using spray

guns. During construction, caution was exercised to prevent scuffing of the coated bars. All supporting chairs were epoxy-coated, and all tie wires were plastic coated.

In each bridge deck, 14 bars were monitored. Twelve bars were touched up before concrete placement and two were left unrepaired for comparison. Both electrical resistances and potentials of the selected bars were measured annually for five years. The surface condition of deck and chloride content were also determined.

Findings. *Electrical Resistances.* The measured resistances increased during the period of monitoring. After four years of service, the average readings on most of the tested bars (including coated and uncoated bars) were indicative of no corrosion activity.

Electrical Potentials. The initial potentials were considerably more negative than the subsequent potentials in all of the evaluated bridge decks. The range of the initial readings was between -200 and -770 mV CSE. After one year of service, the readings dropped to an average level of -100 to -200 mV. In the following three years of service, the majority of the tested bars maintained a potential less negative than -350 mV. There were some cases, however, in which the final potentials, after four years of service, were more negative than -350 mV.

Chloride Penetration. After three and four years of service, the chloride ion concentration at the bar level was found to be below the known threshold level for corrosion initiation.

General Surface Conditions. No spalling was observed on any of the bridge decks. However, cracks ranging from 0.3 to 6 m (1 to 20 ft.) in length, and from hairline to 1.6 mm (1/16 in.) in width were developed on all of the decks. The causes of these cracks were not attributed to corrosion activity.

Comments. The high initial potentials and their subsequent drop observed in this study were attributed to two factors: the deck being too wet; and the presence of pinholes

in the coating. The first factor may explain the behavior of both the coated and uncoated steel, whereas the second factor is limited to the coated steel. It was stated that mill scale formation at the holidays or other breaks in the coating caused the potentials to rise at the beginning of monitoring. However, the effects of the detected cracks on the resistances and potentials were not discussed in the study. It cannot be established if high potentials were associated with bars that had cracks running along their axes.

In general, the measurements obtained do not indicate corrosion initiation even for the uncoated reinforcement. The conditions after five years of service were not conducive to corrosion. Therefore, the effectiveness of the epoxy coating to control corrosion was not demonstrated by this study. However, it can be observed that the electrical potentials require a period of time to reach a consistent trend, and readings in excess of -350 mV CSE may be obtained without further signs or indications of active corrosion.

4.2.5 Federal Highway Administration, US, 1983.[106,107]

Study. In 1980, an outdoor exposure study of concrete slabs with epoxy-coated bars not conforming to the specifications or with concrete containing a calcium nitrite admixture with uncoated steel was carried out. The study was aimed at evaluating the performance of both corrosion protection systems in comparison with uncoated steel in concrete without admixtures. The exposure conditions simulated those found in typical highway bridge decks.

A total of 31 relatively large reinforced concrete slabs was fabricated for testing. The slabs were placed in two lifts: a chloride-free bottom lift; and a chloride-contaminated top lift with 8.9 kg/m^3 (15 lb/yd^3) of chloride ions admixed during mixing. Each concrete lift contained a mat of reinforcing steel. Both mats were connected externally to allow monitoring of the corrosion current. Acceleration of the corrosion process was made possible by using poor quality concrete (w/c = 0.53), epoxy-coated bars with too many holidays and which had failed the bend test, and good electrical coupling between the reinforcing mats. Damage to coating was limited to 0.22 and 0.80% of the surface area of tested bars.

The slabs were placed outdoors in Washington, D.C. They were ponded with a 3% salt solution for 46 days and then exposed to natural weathering to enhance the corrosive conditions. Several slabs showed cracking and debonding between concrete lifts during curing. Subsequently, angle iron clamps were used to maintain contact at crack interface. The data collected on these slabs were not included in the calculations. The corrosion current flow was monitored for about two years to determine the corrosion rate. At the end of the exposure period, some selected slabs were demolished for visual inspection of the reinforcing bars. The measurements taken in this study included:

- corrosion current;
- open-circuit or instant polarized corrosion driving voltage;
- electrical potential of top mat with respect to a standard half-cell electrode;
- electrical potential of bottom mat with respect to a standard half-cell electrode;
- mat-to-mat electrical resistance; and
- slab temperature.

Findings. Both epoxy-coated reinforcing steel and calcium nitrite were quite effective in reducing the corrosion rate. The reduction was at least an order of magnitude relative to the case of unprotected steel. The differences in performance between coated bars with holidays only and those with holidays and visible bare areas were insignificant. The presence of the epoxy coating increased the mat-to-mat resistance which resulted in lower macrocell driving voltages and half-cell potential differences between the mats compared to the control specimens.

For the case of only the top mat epoxy-coated, it would take 12 years on the average to consume an amount of iron equal to that consumed from uncoated steel in one year. The corrosion rate was controlled by path resistance with the absence of cathodic polarization at the top mat micro-cathodes. When both mats were coated, 46 years would be required to consume equal amounts of iron. The system in this case involved both resistance effects and cathodic polarization at the bottom macro-cathode. Cracking between concrete lifts in some

specimens caused a shift in the balance of corrosion rate control from predominantly cathodic control to predominantly resistance control.

Slab demolition and visual examination of the retrieved bars showed light rusting under the epoxy coating at certain locations. Underfilm corrosion was possible because of the inadequate bond between the coating and the steel. Any hole in the epoxy film would allow corrosion to initiate and advance beneath the coating.

Comments. The levels of damage to coating included in the macrocell test (below 1%) were not severe. The specifications permit a total damaged area of 2% of the bar surface area, and bars damaged to this specification limit are expected to show worse performance. The study, however, emphasized the validity of specification requirements to guard against long-term development of corrosion beneath the coating surface. Such corrosion progress "might become detrimental".

The ratio of the amount of iron consumed between the uncoated and the coated steel was used in the study to express the improvement of performance due to coating. However, relating this ratio to the number of years required to consume equal amounts of iron from both types of steel is based on the assumption that the corrosion rate remains constant. Such an assumption may not be valid.

One important conclusion of the study is that the **epoxy-coated reinforcement should be many times more resistant to corrosion-induced damage than uncoated reinforcement even if the coated bars did not meet the specifications.** The best situation for field applications was pointed out as the one in which all the bars are epoxy-coated or the coated bars are electrically isolated from any other metal in the structure.

4.2.6 University of Tokyo, Japan, 1984.[11]

Study. The corrosion performance of epoxy-coated and galvanized reinforcing steel in a marine splash zone exposure was studied over a three-year period. Beam specimens,

each reinforced with two separate bars, were used for the study. Three types of reinforcing bars were included, namely: uncoated; galvanized with 150 μm (6 mils) plating thickness; and epoxy-coated with 100 and 200 μm (4 and 8 mils) coating thickness. Two depths of concrete cover of 20 and 30 mm (0.8 and 1.2 in.) were provided. The beams were stressed back-to-back in a four-point flexural loading arrangement. The maximum crack widths at mid-span of beams were about 0.2 to 0.3 mm (0.008 to 0.012 in.).

The specimens were visually inspected every six months, and the state of cracking and crack widths were documented. The corrosion condition of bars was determined by removing concrete and measuring the corroded areas and weight loss.

Findings. Corrosion occurred on several locations along the epoxy-coated bars with coating thickness of 100 μm (4 mils) and concrete covers of 20 and 30 mm (0.8 and 1.2 in.). The corroded spots coincided with the introduced flexural cracks. At one year of exposure, the epoxy film slightly debonded from the steel substrate at the corroded locations. Underfilm corrosion extended to about 150 mm (6 in.). After three years of exposure, the epoxy film debonded completely from considerable areas and prominent corrosion of the steel substrate was evident. However, metal loss and corrosion depth were substantially reduced relative to the uncoated bars.

The epoxy-coated bars with coating thickness of 200 μm (8 mils) performed much better than those uncoated or galvanized. The corroded sites were very small on some of the bars, underfilm corrosion was limited, and metal loss was negligible. It was concluded that a coating thickness of at least about 200 μm (8 mils) was necessary for complete corrosion protection.

Comments. The test conditions promoted microcell formations along the tested epoxy-coated bars. The results confirmed that corrosion initiates at weak points in the coating concurrent with crack locations. In the cases where underfilm corrosion extended over large areas, metal dissociation was only superficial. In addition, the greater the coating thickness, the more underfilm corrosion progression will be limited. The coated bars were

not initially damaged, nor linked to uncoated steel to develop macrocell action. Therefore, the test conditions did not enhance corrosion activity on the tested bars.

4.2.7 University of Texas at Austin, US, 1984.[4]

Study. A large-scale durability test study was conducted outdoors at the University of Texas. The objective was to study the performance of transversely prestressed slabs relative to non-prestressed slabs when subjected to a severe corrosive environment under varied loading conditions. A total of 24 slab specimens were included in the study of which 16 were prestressed and eight were non-prestressed. All of the slabs contained some non-prestressed bars which were either uncoated or epoxy-coated. The slabs were cracked prior to exposure to salt water solution. The crack widths were limited to 0.05 and 0.4 mm (0.002 and 0.015 in.) by controlling the imposed loads on the slabs.

The exposure conditions consisted of periodical wet-dry cycles. Each test cycle extended 14 days with three days continuously wet and 11 days of natural drying. The number of cycles ranged from eight to 14. During each cycle, the specimens were loaded and unloaded to facilitate the penetration of chlorides and oxygen to the steel surface. Half-cell potentials were recorded for the different types of reinforcement at various locations in each slab. The slabs were destructed for postmortem examination at the end of the exposure period. Chloride samples were also taken to determine the chloride concentration at the reinforcement level.

Findings. Both transverse prestressing and epoxy coating were effective in reducing the corrosion risk. While transverse prestressing limited crack width on the deck slab, epoxy coating provided the reinforcement with satisfactory protection from chloride-induced corrosion.

Corrosion initiation and spreading on non-prestressed steel started at flexural cracks. The uncoated reinforcement showed a much greater corrosion than the epoxy-coated reinforcement. At some crack locations, the epoxy coating chipped off the bar deformations

revealing minor surface corrosion. In these cases, the chloride concentrations exceeded 7.1 kg/m^3 (12 lb/yd^3).

Comments. Although the corrosion testing was accelerated, the duration of the exposure period was relatively short due to time constraints. Therefore, the effects of long exposure of the coated steel to contaminated concrete could not be assessed. However, the study revealed that the epoxy coating might have a limited tolerance to chlorides. Corrosion resistance of stressed bars in excessively contaminated concrete may possibly deteriorate with time. The study reported the surface condition of the tested bars without examination of the underfilm corrosion. The condition of adhesion of the coating and the extent of corrosion progression on the underlying steel were not indicated.

4.2.8 Pennsylvania State University, US, 1987.[75]

Study. A field study was performed to evaluate the performance of epoxy-coated bars in concrete bridge decks in service for about 10 years. Twenty-two major bridge decks in the state of Pennsylvania were selected for the study. Half of the bridge decks were constructed with coated steel and the other half with uncoated steel. After all bridge decks were visually inspected, only four were thoroughly evaluated.

For comparison, the chosen bridge decks had approximately the same average daily traffic count, superstructure type, depth of concrete cover, w/c, and exposure to deicing salts. The length of each bridge was between 30 and 61 m (100-200 ft.).

Findings. The visual inspection indicated that 40% of the decks containing uncoated steel were in the initial stages of deterioration. None of the decks containing epoxy-coated bars showed any sign of corrosion-induced deterioration.

The detailed study revealed extensive corrosion of the uncoated steel and deterioration of the bridge decks, whereas no corrosion was found on the epoxy-coated steel. The chloride

content at the level of reinforcement in all of these bridge decks was predicted to be higher than the known corrosion threshold value.

Comments. This investigation indicated that the use of the coated reinforcement in bridge decks provided a level of satisfactory corrosion resistance. The epoxy coating protected against corrosion-induced deterioration at a time concrete with uncoated steel suffered from severe deterioration. The study, however, did not report whether the coated bars were used only in the top reinforcing mat or in both top and bottom, and if there was any electrical contact between the bars.

4.2.9 Simitomo Metal Industries Ltd., Japan, 1988.[51,108]

Study. A comprehensive study was carried out on the corrosion resistance of uncoated, galvanized, and epoxy-coated reinforcing bars embedded in concrete prisms and exposed to a corrosive environment. Two exposure conditions were selected: natural splashing in a tidal zone; and a laboratory accelerated wetting and drying cyclic regime in seawater. In the laboratory test, specimens were repeatedly immersed for six hours in 60° C (140° F) seawater, then allowed to dry in air for six hours.

Each prism contained a central reinforcing bar. The prisms were pre-cracked and loaded to a steel tensile stress of 200 MPa (29 ksi) during exposure. Some of the coated bars were artificially damaged prior to testing. Some of the prisms was made with concrete containing chloride contaminated aggregate. Three epoxy coating thicknesses were chosen, 100, 200, and 300 μm (4, 8, and 12 mils). Further, concrete cover thicknesses were 20, 40, and 70 mm (0.8, 1.6, and 2.8 in.).

The results were reported for a natural exposure period of three years, and accelerated corrosion testing for two years. Six test specimens were used for each variable in the test.

Findings. The undamaged epoxy-coated bars in cracked specimens exposed to the natural environment remained totally unaffected by rust irrespective of film thickness and depth of cover. The bars retained their original gloss and initial adhesive strength and hardness. Similar bars in cracked specimens exposed to accelerated corrosion testing also showed excellent performance. Only two to four small blisters were formed on the 100 μm (4 mils) thick coating without pitting even at 20 mm (0.8 in.) concrete cover. Red rust percentage of the surface area of the bar did not exceed 0.1%. Bars with coating thicknesses of 200 μm (8 mils) and above, remained completely unaffected irrespective of the concrete cover. The coatings of these bars maintained their initial characteristics in terms of gloss, adhesive strength, and scoring and peeling hardness. Figure 4.2 shows the percentage of the surface area covered with red rust for all types of tested bars.

Tests on artificially damaged coatings under natural exposure conditions showed that red rust formation varied mainly with concrete cover thickness. The development of rust ranged between 22 and 45% of the damaged area at cover thickness of 20 mm (0.8 in.), compared to less than 5% at cover thicknesses 40 and 70 mm (1.6 and 2.8 in.). There was no visible evidence of undercutting. Rust was limited to areas in the vicinity of the cracks.

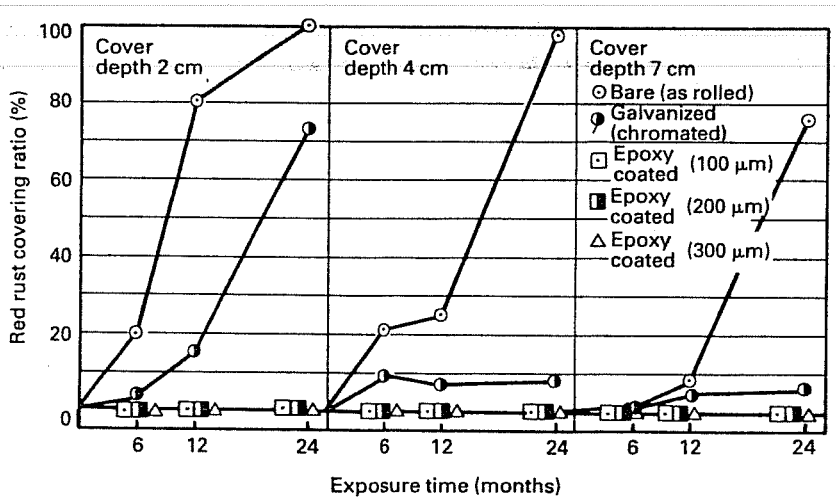

Figure 4.2 Red Rust Covering Ratio on Test Bars (Accelerated Exposure Test).[51]

When the artificially damaged coatings were subjected to accelerated exposure conditions for 12 months, the bars with 100 μm (4 mils) coating thickness and concrete covers 20 and 40 mm (0.8 and 1.6 in.) were severely damaged. Almost all of the damaged area was covered with rust. The investigators detected a layer of black rust (referred to as magnetite Fe_3O_4) under the coating. This form of rust product indicated the lack of oxygen under the coating. Bars with 200 and 300 μm (8 and 12 mils) coating thicknesses and concrete covers 40 and 70 mm (1.6 and 2.8 in.) had less than 20% of the damaged area covered with rust.

Comments. The results of this study confirmed that undamaged epoxy-coated bars provide excellent corrosion protection even in cracked concrete under severe chloride accumulation. The fact that the coating maintained its original characteristics such as the initial adhesive strength is surprising. Such behavior may be due primarily to the excellent epoxy resin, adequate steel surface preparation, and proper coating procedure.

Although the testing exposure conditions were extremely corrosive, the use of single coated bars with uniform exposure did not produce the worst conditions for severe corrosion activity. If the damaged coated bars were linked to uncoated bars, macro-corrosion cell formation could have developed higher corrosion currents and further deterioration. In addition, no information was provided on the level of introduced coating damage (size, frequency or percentage). The level of damage might affect the integrity of the coating during exposure to a salt solution. Despite the limited observations, the researchers determined that properly coated bars, even under very severe marine exposure conditions and localized coating damage, can "provide long-term protection against corrosion".

A comparison between the results of both exposure regimes (the natural and accelerated regimes) indicates that the laboratory accelerated exposure testing produced worse conditions than the natural exposure testing. This justifies carrying out controlled, accelerated corrosion tests in a relatively short time, without jeopardizing the validity of the results for real life situations. However, no simple correlation exists at present between the two exposure regimes.

The study show that even with coated bars, the use of thicker concrete cover to reinforcement can improve the corrosion resistance. While the uncoated bars corroded extensively at all cover depths, the epoxy-coated bars with 200 μm (8 mils) coating thickness had the best performance where the concrete cover was 70 mm (2.8 in.).

4.2.10 Florida Department of Transportation, US, 1988.[12,29,30,42,98,109,110]

Study. The first signs of corrosion of epoxy-coated bars were evident in 1986 on the substructure of the Long Key Bridge in the Florida Keys only six years after construction. Subsequent investigations conducted by Florida Department of Transportation (FDOT) revealed that significant corrosion of the coated reinforcement occurred in four of the five major bridge substructures in the Florida Keys. Tables 4.1 and 4.2 show the bridges and approximate number of piers exhibiting corrosion. The observations reported here are limited to the deteriorating major substructures.

Findings. Corrosion was limited to a 0.6-2.4 m (2-8 ft.) length above the mean high water level on the substructure, *i.e.* only in the splash zone. The visual examination indicated that corrosion may have initiated in the fabricated bars at bends and then progressed to the straight bars. The corrosion products were usually in the form of a black-green paste, but sometimes quite solid. Acidic water (pH of 5) was often found trapped between the coating and the underlying steel indicating corrosion progression in an acidic environment.

Table 4.1 The Five Major Florida Keys Bridges.[98]

Bridge	Construction Period	No. of Piers In Water	First Signs of Corrosion
Long Key	1979-1981	101	1986
Seven Mile	1979-1982	263	1988
Niles Channel	1981-1983	37	1988
Channel Five	1981-1983	34	None
Indian Key	1979-1981	18	1990

Table 4.2 Number of Piers Corroded in Four Florida Keys Bridges.[98]

Bridge	1986	1987	1988	1989	1990	1991
Long Key	1	3	17	--	31	31
Seven Mile	--	--	8	--	58	60
Niles Channel	--	--	17	*	17**	17
Indian Key	--	--	--	--	2	2

* All corrosion spalls repaired.
** New corrosion spalls.

The steel substrate was covered by a thin black, relatively dry layer of a corrosion product. Severe pitting was also found on some of the bars with metal dissociation rates -of thickness- exceeding 25 μm/y.

Corrosion was in an advanced stage and caused concrete delamination and spalling. The spalled areas were relatively larger than those previously experienced with uncoated reinforcement. Corrosion also spread to the steel in sound concrete areas adjacent to the spalled areas. Figure 4.3 shows typical corrosion-induced deterioration common to the affected bridge substructures. According to FDOT, some spalls occurred in areas with insufficient concrete cover and where concrete quality was poor. However, corrosion was mainly observed in sound concrete areas with up to 0.1 m (4 in.) cover. In addition, large delaminations of concrete were detected in areas free of visible cracking.

There is disagreement among the various references about the concrete cover thickness. Some said the cover was 0.05 m (2 in.) on the average with values as high as 0.15 m (6 in.) over the reinforcement in the affected locations. Others claimed the cover was 25 mm (1 in.) or less and below in the corroded areas, and in all cases was below the specifications.

Chloride ions found at the reinforcement level were unusually high. Chloride concentrations varied between 3-11 kg/m^3 (5-18.5 lb/yd^3) with a typical value of 9 kg/m^3 (15

lb/yd^3). One reason for the high chloride content in concrete was the high salinity of the seawater in the Florida Keys. Reports showed the chloride content in the seawater to be as high as 29,000 ppm which is 70% more saline than the normal ocean seawater. The other major contributor to the high chloride content at the steel surface was the early concrete cracking. The widths of the detected early cracks were more than twice the size tolerable in a corrosive environment.

Figure 4.3 Typical Corrosion-Induced Deterioration of Some Major Bridge Substructures in Florida Key.[98]

Complete coating debonding was observed on bar samples extracted from regions above the deteriorating splash zone. Areas of coating debonding revealed bright, dull, or slightly darkened metal underneath and raised concern about the initial quality of the coated

reinforcement. However, the initial conditions of the bars before placement could not be accurately determined. Some references indicated that the quality of the coating was acceptable. The differential thermal analyses performed on coating samples did not reveal any abnormal product characteristics. Other references stated that the cleaning and blast profile were found to be marginal and the coating foam level was excessive. These observations raised the doubts about the cleanness and anchor profile of the bars. Moreover, damage to coating during construction could not be quantified. Data on damage indicated that the damage did not exceed the 2% limit allowed in the prevailing specifications.

It is worth noting that some of the above observations were similar for other undamaged substructures in Florida. Debonding with underlying darkening, without advanced corrosion, was a common finding. These substructures were in service for only 7-11 years.

Comments. No information was provided in the cited references about the fifth major bridge (Channel Five) which did not show signs of corrosion. Knowing the similarities and differences between this bridge and the other deteriorating bridges can help understand the causes of the unexpected corrosion problem.

The weak bond between concrete and the coated steel could probably be the reason for the larger spalls and delamination areas experienced. Concrete surrounding the coated bars is expected to be less resistant to corrosion-induced pressures than in the case of uncoated bars. In addition, the lack of bond may affect the degree of plastic settlement and concrete consolidation around the bars and may result in further weakening of concrete in the plane of reinforcement.

Based on the observations and concerns discussed above, it is prudent to apply stringent quality control measures to protect the coated reinforcement from damage at the job site. Currently, more attention is paid to producing high quality product than assuring that what goes in concrete has the same initial quality.

4.2.11 Pennsylvania Department of Transportation, US, 1988.[73]

Study. A field study was performed in Pennsylvania to evaluate and compare several bridge deck corrosion protection systems. The systems included reinforcing steel coatings, concrete overlays, and waterproofing membranes. Overall 169 bridge decks were visually inspected, some of which were also tested. Field measurements consisted of half-cell potential and electrical resistance measurements. In addition, 125 cores representing 23 different bridge decks were submitted for laboratory testing and visual examination of the reinforcing bar samples. The chloride content at reinforcing bar level, as well as the concrete permeability were determined from the concrete cores.

Finding. Reinforcing bars treated by coating, namely, fusion-bonded epoxy and hot dip galvanizing provided the most effective corrosion protection. Both materials performed well despite the high chloride contents in the concrete. The decks reinforced with epoxy-coated steel were found performing better than expected based on deterioration rate and life expectancy calculations.

Half-cell readings evaluated according to ASTM C876 did not correlate with visual bar ratings. Potentials more negative than -350 mV CSE were measured on bars with excellent appearance.

Comments. The locations of the cores, if given, would have helped to interpret the results more accurately. Bar samples retrieved from crack locations would have more tendency to show signs of corrosion activity. Restrictions on the number of cores, grid size for half-cell measurement, and visual inspection of embedded bars preclude generalizing the findings.

4.2.12 Building Research Establishment, UK, 1989.[62]

Study. The Building Research Establishment in England conducted a corrosion study to evaluate the performance of fusion-bonded epoxy-coated steel alongside high yield

uncoated and galvanized steel bars. The study involved the examination of concrete specimens containing these types of reinforcing bars after five years of natural exposure to the atmosphere. Both concrete slabs and prisms were used to test bent and straight epoxy-coated bars (including cut ends). The epoxy-coated bars were coated to a minimum thickness of 100 μm (4 mils). Concrete cover thicknesses were 10, 20, and 25 mm (0.4, 0.8, and 1.0 in.). Two concrete mixtures were used with three levels of chloride contamination.

A comprehensive examination of the specimens was undertaken by visual, electrochemical (half-cell potential measurements), and destructive methods. Weight loss was calculated for the different bars to evaluate the severity of the corrosion activity.

Findings. The half-cell results of the epoxy-coated bars varied more than those of the galvanized and uncoated bars. Moreover, a wide range of potentials was obtained between similar slabs.

The straight epoxy-coated bars recovered from the prisms were free of corrosion along most of the bar at all chloride levels. Some blisters were found on the coating which were possibly associated with defects in the coating. The untreated ends of the bars were corroded in the highly-contaminated concrete. In these cases, a black corrosion product (magnetite) was visible in small pits. Patching the bar ends, also, was not totally effective.

Upon removal of the coating, the steel was found bright and untarnished in the low chloride level prisms. In the highly-contaminated prisms bars were corroded. A black underfilm corrosion product was detected in areas along axial and transverse ribs extending up to 65 mm (2.6 in.) from the cut ends. Bars recovered from the richer, but more contaminated, mix were corroded over a greater length than those from the leaner, and less contaminated, mix. Pits under blisters were also found on some epoxy-coated bars.

Bent epoxy-coated bars recovered from the slabs showed some bubbles of corrosion products adjacent to coating defects. Corrosion was limited to the curved length of the bar.

Again, a black corrosion product was found to extend under intact areas of the coating with some slight pitting.

In spite of the damage to the coated bars in highly-contaminated concrete, their performance was significantly better than the galvanized or untreated bars. The conclusions of the study stated that "the use of fusion-bonded epoxy coatings on steel reinforcement provides a significant reduction in the rate of deterioration of reinforced concrete containing high levels of chloride, although the use of these coatings **does not provide total protection.**"

Comments. Damage to epoxy coating prior to embedment of bars in concrete was not reported. Therefore, it is difficult to relate the extent of bar deterioration to a certain condition of initial damage or defects in the coating. This is particularly important in the case of bent bars, where debonding is likely to occur in addition to possible coating damage in the curved portion. In addition, it was not specified whether the epoxy-coated bars were coated before or after bending.

The study concentrated on the performance of the individual coated bars in isolation from any other metal in concrete. Corrosion activity, in this case, was governed by microcell formations. A more critical testing condition would be linking the coated steel to uncoated steel to set up a more destructive macrocell.

Test specimens (prisms and slabs) were not subjected to any structural loads during exposure. Therefore, simulation of service conditions during corrosion testing was not attempted. The results may be affected by the loading and cracking conditions of the tested elements.

4.2.13 Ontario Ministry of Transportation, Canada, 1989.[81]

Study. The Ontario Ministry of Transportation carried out a field investigation of the condition of epoxy-coated reinforcement in barrier walls expected to be highly-

contaminated by chlorides. Barrier walls were advantageous for the study because of their ease of access, low cover requirements, and vulnerability to rapid chloride ion attack. Deficiencies in the construction of the barrier walls, in the form of extensive shrinkage and plastic settlement cracks and voids, facilitated the ingress of chlorides directly to the reinforcing bars.

The investigation included sections of three reinforced concrete barrier walls constructed in the late 1970's and subjected to very corrosive environments. Two of these sections had epoxy-coated reinforcement, while the third one had uncoated reinforcement for comparison. The locations were selected after a preliminary investigation of 14 structures in search of the worst cases.

Epoxy-coated crossing and overlapping bars within the study areas were tested for electrical continuity. Half-cell potentials were also measured along each bar in the study areas. Based on the findings of the above tests and measurements, the rate of corrosion of each bar in the most active location was determined using the three electrode linear polarization method.

Following the measurements described above, concrete cores were extracted from critical locations. The chloride profile in concrete was determined, and the condition of the reinforcing steel and its coating were examined.

Finally, the concrete cover was removed from the study area of the most corrosive environment. Visual inspection of the exposed coated bars and correlation with the results of the half-cell potentials and the rate of corrosion measurements were made. To complete the study, the results of the investigation of the coated reinforcement were compared with those obtained from investigating the wall section with uncoated reinforcement.

Findings. The barrier walls with epoxy-coated bars did not show serious premature corrosion-induced deterioration of the concrete. In contrast, the wall with uncoated bars

suffered from severe rust staining. The chloride content at the level of the bars in all walls examined was well beyond the known threshold value for corrosion initiation.

Samples of the coated bars recovered in cores showed no evidence of corrosion activity except at one bar where minor surface corrosion of a small bare area was found. The epoxy coating was in very good condition with no evidence of debonding. The epoxy film thickness was generally found within the specification requirements. The uncoated bar samples, on the other hand, showed extensive and severe corrosion activity.

Only superficial corrosion activity was found on a section of a stirrup when all the reinforcement in a study area was exposed. Upon careful examination, no pitting or underfilm activity was detected in the vicinity of the damaged area, *i.e.* corrosion was insignificant and localized. Prying the coating with a knife revealed that coating adhesion was stronger between the transverse ribs than on the ribs themselves.

Visual examination of the coated bars in the study areas showed evidence of mechanical damage to the coating. The damage appeared to be the result of bar-to-bar abrasion and fabrication. Damage on the outer surfaces of the bends of the stirrups was in the form of extensive lateral hairline cracking and damaged ribs. On the inner surfaces of the bends, a few hairline longitudinal cracks and debonded areas were detected.

High negative potentials were measured on the coated bars (in the range of -122 to -540 mV CSE) without visual evidence of corrosion activity. The more negative values might be linked with oxygen restriction on the steel surface to support the cathodic reaction. The oxygen deficiency slowed the cathodic reaction which, in turn, increased the cathodic polarization causing such potential readings. Therefore, applying ASTM C876 to epoxy-coated reinforcement would lead to inconsistent results. However, the measurements might still provide useful information on corrosion activity of the steel.

The satisfactory performance of the epoxy-coated bars was characterized by the limited microcell corrosion activity on small exposed steel areas. Maintaining the insulative

properties of the coating in spite of the presence of damage was the key factor for this performance. The epoxy coating had successfully reduced the corrosion activity on the reinforcing steel during the first nine years of service. However, the effectiveness of the coating over the life of the structure remained uncertain.

Comments. This field investigation provided valuable information on the performance of epoxy-coated reinforcement in a harsh service environment. The importance of this study stems from the fact that factors such as the condition of the embedded coated bars, the presence of cracks in concrete, and the natural exposure to salt, are in-situ examples. When accelerated corrosion studies are to be performed in a laboratory, these factors need to be considered to yield meaningful results that correlate well with actual practice.

The study revealed that the embedded coated bars suffered from mechanical surface damage to the coating. Fabrication was a serious source of damage as it caused loss of adhesion as well as cracking and chipping on both the inside and outside of the bends. Therefore, more attention should be paid to the effects of fabrication on corrosion resistance.

4.2.14 University of South Florida, US, 1989.[30,42,109]

Study. The performance of straight and bent epoxy-coated bars in concrete prisms exposed to salt solution was studied. The bars were 22 mm in diameter (#7) collected from two suppliers of coated bars. The bars from one supplier had more holidays than the other. The bend angles were 180° before rebound and bend diameters were 110, 130 and 165 mm (4.4, 5.25 and 6.5 in.). Uncoated bars, and bars coated after fabrication were included in the study. Damage was introduced on some bars on the outer bend surfaces. Patching of the bent portions was done before introducing damage.

The concrete specimens (w/c = 0.5) were partially immersed in 5% NaCl solution with the apex of the bend at the waterline (see Fig. 4.4). This arrangement facilitated

chloride accumulation at the bar level by capillary action of solution and water evaporation. Some specimens were cracked before exposure.

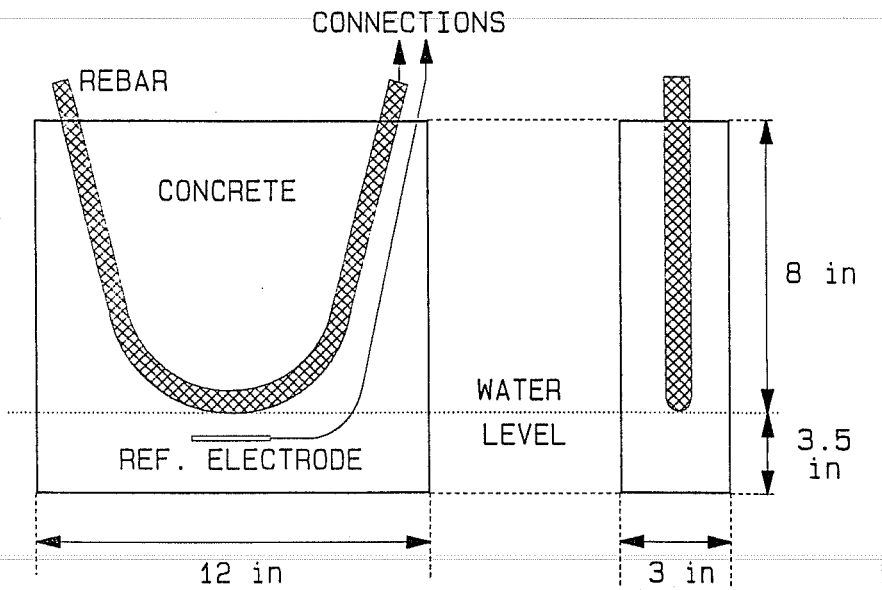

Figure 4.4 Specimen Configuration and Test Arrangement.[109]

Open circuit potentials and Electrochemical Impedance Spectroscopy (EIS) measurements were taken during the test. Autopsy of the specimens was done at 300 days and followed up at 600 days.

Findings. Fabrication of the coated bars resulted in reduced adherence of the coating and formation of cracks and holidays on the outer bend surfaces. Consequently, corrosion resistance of the bent bars was considerably reduced.

Time-to-onset of corrosion was comparable for both coated (damaged) and uncoated bars. Coating defects tended to shorten the time for corrosion initiation. The corrosion rate,

however, was one order of magnitude higher for the uncoated bent bars relative to that for coated bars bent after coating.

The performance of the coated bars varied significantly, especially at the beginning of the test. The performance was also different between the bars from the two different suppliers. However, corrosion was more severe for bars fabricated after coating than for straight bars or bars coated after fabrication. The tighter was the bend, the more was the tendency to develop corrosion.

Corrosion was evident at the exposed steel spots. Adjacent steel surfaces were darkened and the coating was loosely adhered. Coating separation was also observed at areas with bright metal substrate.

Comments. Open-circuit potentials and EIS measurements were effective in this experiment to show corrosion development in the coated bars. A potential drop was indicative of corrosion initiation. The initial performance of the coated bars in cracked concrete specimens was different than in uncracked specimens. Cracking led to a shift in the potential towards more negative readings.

4.2.15 University of South Florida, US, 1990.[42,110]

Study. An investigation was initiated after detecting the failure of the epoxy-coated reinforcement used in marine bridge substructures in the Florida Keys. The objective was to study the effects of pre-service and in-service conditions on corrosion of coated bars. Epoxy-coated bar specimens, 31 mm in diameter (#10), were immersed in three solutions to simulate three environments. These environments were:

- 3.5% NaCl , pre-service weathering near coast;
- saturated $Ca(OH)_2$, uncontaminated concrete; and
- saturated $Ca(OH)_2$ with 3.5% NaCl, chloride-contaminated concrete.

The as-received condition of the tested bars complied with FDOT specifications at the time of construction of the deteriorated structures. The epoxy film was typically 150 μm (6 mils) in thickness and showed no visible surface damage. A controlled amount of damage to coating was introduced on some of the bars exposing about 0.25% of the underlying steel.

The specimens were tested under both open-circuit (free corrosion) and polarized conditions. Potentials were varied between -750 to -400 mV SCE for the intentionally damaged bars and between -1000 to +100 mV SCE for the as-received bars. The test duration was 30 days.

Findings. The coating of specimens in $Ca(OH)_2$ solution, under all test conditions, did not show any changes in the appearance or mechanical integrity. The exposed metal remained uncorroded.

Specimens immersed in NaCl solution showed the following:

Anodic Polarization.

- at +100 mV for as-received coating only: Corrosion products covered imperfections with significant pitting underneath. No significant debonding around the pits.
- at -500 mV: Corrosion products covered imperfections and bare spots. Pits formed at damaged spots without debonding in the surrounding regions.

Open-Circuit.

- at -645 mV: Corrosion products covered imperfections and about two-thirds of the bare metal spots with only shallow pits underneath. Coating debonded to about 3 mm (0.1 in.) away from defect edges and around imperfections. Metal under debonded coating was generally bright.

Cathodic Polarization.

- at -750 mV (also at -1000 mV for as-received coating only): No corrosion was visible. Coating debonded to about 10 mm away from defect edges and around imperfections. Metal under debonded coating was bright.

Specimens immersed in NaCl/ $Ca(OH)_2$ solution showed the following:

Anodic Polarization.

- at -400 mV: Large, mostly black corrosion products formed over all damaged spots and holidays. Pits were developed on the damaged spots with a size reaching 6 mm (0.2 in.) wide and 3 mm (0.1 in.) deep. Coating debonded to about 10 mm (0.4 in) away from defect edges. Metal immediately surrounding the pits was blackened but was bright further into the debonded region. A few small blisters were observed at surface imperfections with bright metal underneath. A clear liquid with pH 3.5-5 was detected under the coating and in some blisters.

Open-Circuit.

- at -625 mV: Minor corrosion was visible on about one-third of the introduced spots. Coating debonded to about 1 mm (0.04 in.) around all spots with bright metal underneath.

Cathodic Polarization.

- at -750 mV (also at -1000 mV for as-received coating only): No corrosion was visible. Some debonding was observed at the damaged spots with bright metal underneath.

Comments. Pore solution in concrete contains different cations than those used in the test solutions. Therefore, the performance of the specimens should not be viewed as an accurate presentation of the actual behavior in concrete. According to the researchers, testing coated bars in solutions served as a first approximation approach.

Exposures at potentials more negative than -650 mV SCE (the free corrosion potential) seemed to effectively detect the susceptibility of the coating to cathodic debonding. Investigating the behavior under predominantly anodic conditions seemed also to be possible by polarizing test specimens to potentials around -400 mV.

There was close similarity between the corrosion morphology depicting the failure of the coated bars in the field (Florida Keys) and in the laboratory experiments. Hence, anodically polarized epoxy-coated bars exposed to NaCl + $Ca(OH)_2$ solution may reasonably simulate the anodic behavior of a portion of a coated bar galvanically coupled to cathodic regions elsewhere in the structure. However, perfect resemblance may not be possible unless actual concrete elements are tested under conditions very similar to field conditions.

4.2.16 University of South Florida, US, 1991.[93]

Study. A new study was carried out at the University of South Florida to determine key aspects of the mechanism of corrosion of epoxy-coated reinforcement in marine bridge substructures. The main items considered for study were: the causes of coating debonding; the mechanism of corrosion progression; corrosion prediction; and evaluation of a corrosion control method suitable for affected substructures.

To study coating debonding before placing concrete, the effects of exposure to salt water either continuously or intermittently, and the effects of variable bar sources were examined. Bar specimens were subjected to 3.5% NaCl solution for four weeks. The test bars were first damaged mechanically to about 1% of the surface area. The open-circuit potential was monitored during the exposure period. Samples were removed at different times to determine the extent of debonding using a sharp knife.

The scope of testing coating debonding after placing concrete, but prior to chloride attack, included three exposure conditions. These were: damaged bars exposed to 3.5% NaCl solution to resemble pre-existing corrosion, and then placed in $Ca(OH)_2$ solution; damaged bars exposed to Na(OH) solution to explore the effects of Na^+ cations in concrete

pore solution in promoting debonding without chloride ions; and cured-free films of an epoxy compound subjected to various chemical species relevant to the concrete environment to test film absorption. The test bars were damaged to about 0.25% of the surface area before being submerged vertically in test tanks under variable potentials. The bars were removed after 30 days to determine the extent of debonding using a sharp knife.

To examine coating debonding after chloride attack, bar specimens were first exposed to 3.5% NaCl solution and then submerged in a $Ca(OH)_2$ + NaCl solution. It was required to establish whether the extent of pre-existing debonding could be significantly aggravated by exposure to chloride ions in service.

The macrocell and pre-existing corrosion effects on corrosion progression of damaged coated bars embedded in concrete and exposed to marine substructure conditions were also studied. Test specimens were eight concrete columns that contained multiple reinforcing bar segments placed at various levels. The columns were submerged at the bottom in 5% NaCl salt water solution (see Fig. 4.5). The lower parts of the columns had 11.9 kg/m^3 (20 lb/yd^3) of added chlorides in the concrete mixture. Water rising by capillary action evaporated leaving behind dissolved salts and a moisture gradient. Such conditions promoted anodic activity in the lower parts of the columns. Measurements for corrosion monitoring included macrocell currents flowing between bar elements, concrete resistivity, and half-cell potentials.

The tested bars were damaged intentionally to expose approximately 2% of the total surface area of each bar element. Half of the bars had pre-existing corrosion on the exposed steel areas. Two of the columns which contained bars not corroded before placing concrete were subjected to water application above the waterline on one side after 295 days of exposure. One of the columns in the group of two was demolished after one year for visual inspection of the bars.

Findings. *Causes of Debonding.* The amount of debonding of coating caused by continuous or intermittent exposure to NaCl solution varied considerably from one product to another. Debonding was proportional to the exposure time. The maximum total

debonding at the end of the test was 16%. The results indicated that degradation of the coating due to weathering before placing concrete may occur. Pre-existing corrosion of the coated bars did not aggravate debonding in $Ca(OH)_2$ solution regardless of the potential used.

The amount of debonding caused by exposure to either Na(OH) or NaCl solution was comparable at similar potentials. The difference was that no corrosion products were formed

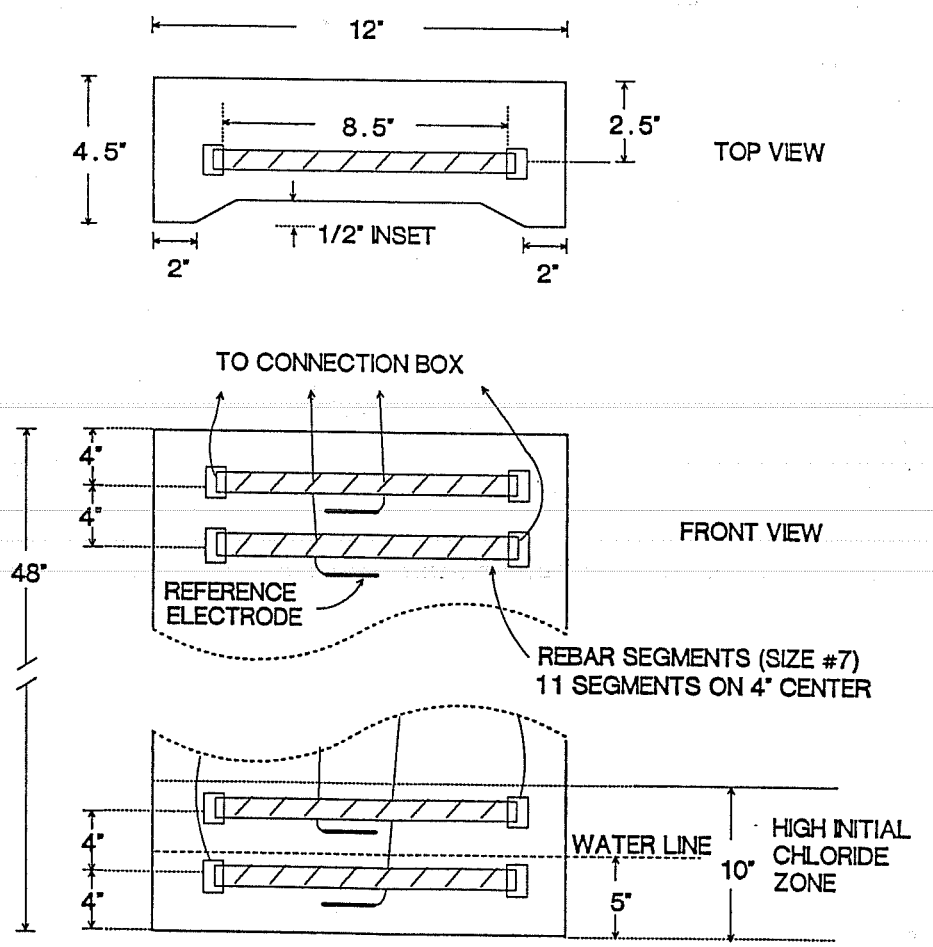

Figure 4.5 Column Configuration and Test Arrangement.[83]

under the coating in the case of Na(OH) solution suggesting cathodic debonding conditions. The presence of Na^+ cations in the pore solution of concrete in significant amounts may, therefore, cause debonding of a previously damaged coating after a prolonged service period.

Weight increases on the order of 1% were observed in the absorption tests of cured films. Changes of the solution pH had no significant effects. Therefore, debonding in the cathodic potential range was probably an oxide dissolution mechanism at the steel/coating interface rather than by alkaline degradation of the coating itself.

Pre-existing corrosion of coated bars significantly enhances the total amount of debonding upon exposure to an NaCl + $Ca(OH)_2$ mixed solution under anodic conditions. It follows that the initiation of corrosion on the coated bars before placing concrete may lead to aggravated corrosion later in service. Underfilm corrosion was characterized by dark dissolution and accumulation of low pH liquid. The extent of the debonded area was found to increase linearly with the time of exposure.

Mechanism of Corrosion Progression. During early exposure, pre-existing corrosion (and consequent debonding) tended to facilitate cathodic reactions at the cathodic portion of the macrocell in concrete. Surfaces under debonded coating were available for oxygen reduction which increased the rate of cathodic reactions and, ultimately, overall corrosion activity. Figure 4.6 shows the corrosion macrocell current flowing between the anodic and cathodic portions of the columns.

Coating debonding at cathodic sites in concrete increased with time. Thus, cathodic efficiency was raised to the extent that similar appreciable macrocell currents were developed later in the exposure period for both cases of bars with or without pre-existing corrosion. Visual inspection of recovered bars from the cathodic end of one column revealed almost complete coating debonding without corrosion traces. The anodic end, on the other hand, showed debonding over about two-thirds of the coating with underfilm corrosion. A few small blisters, up to approximately 3 mm (0.1 in.) in diameter, were observed facing air voids in the concrete. Furthermore, an acidic liquid was found in some of these blisters.

Corrosion progression on the steel surface below debonded coating was relatively uniform without gross pitting. Potential measurements were consistent with the level of macrocell activity observed in each column; more negative potentials were associated with larger macrocell currents.

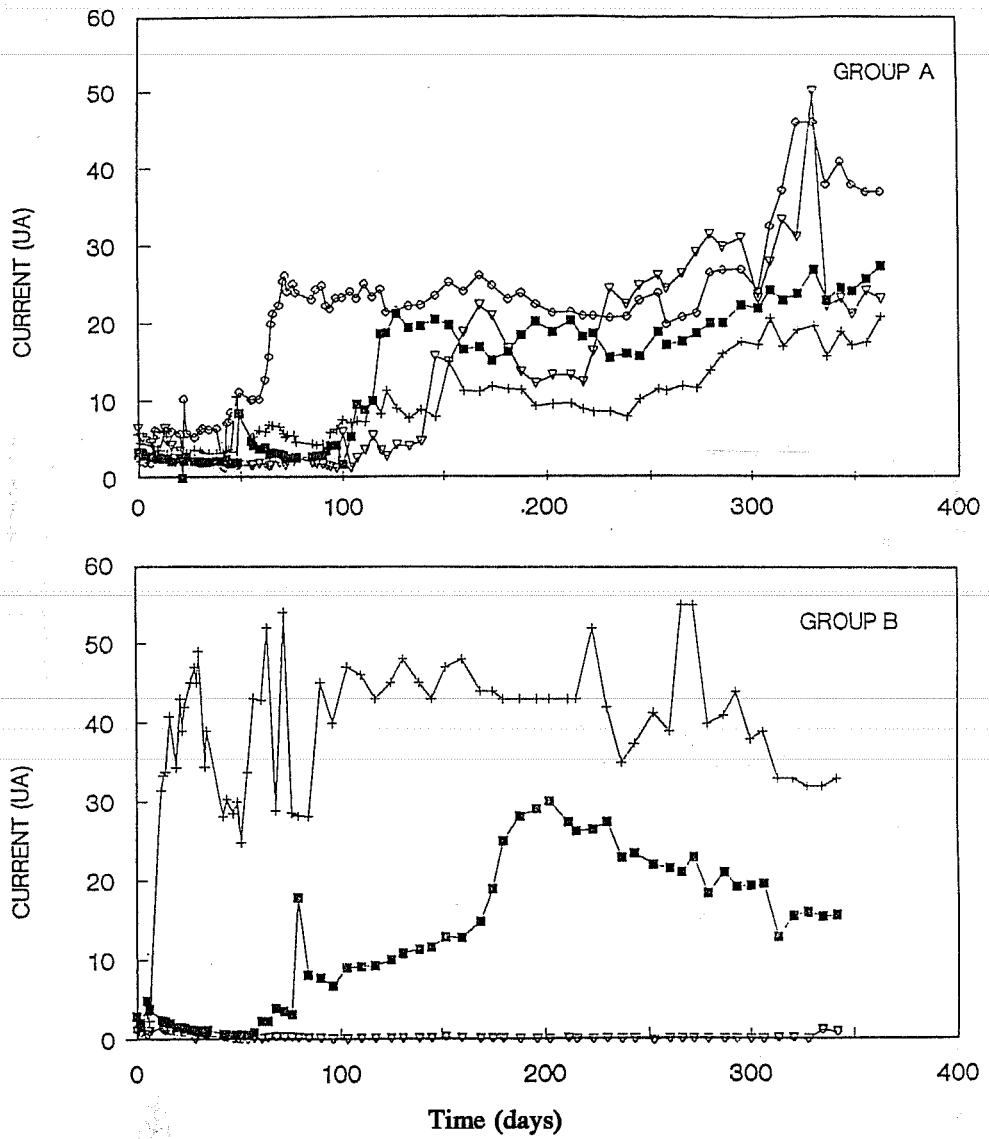

(Group A: Bars without pre-existing corrosion;
Group B: Bars with pre-existing corrosion)

Figure 4.6 Corrosion Macrocell Current Flowing Between Anodic and Cathodic Portions of Tested Columns.[93]

Comments. Debonding of coating caused by fabrication was addressed in the study. However, the effects of mechanically produced debonding on enhancing corrosion under service conditions were not evaluated experimentally. The coexistence of surface damage produced by bending and debonding around curved areas may also result in aggravated corrosion development.

Surprisingly, two of the columns which contained corroded bars before placing concrete developed only marginal anodic action during the entire exposure period. There was only one column in this four-column group that showed corrosion currents significantly higher than those of the four columns in the other group (see Fig. 4.6). The data of this single column were the basis of the conclusion that "precorroded segments developed at early times a distinctly larger apparent current density". Further, no comparison was made between the actual bar conditions in both groups since only one column was destructed for visual examination.

Results from immersion tests and concrete exposure tests were somehow different. Immersion of pre-corroded coated bars in a $Ca(OH)_2$ + NaCl solution (resembling a contaminated concrete environment) showed aggravated coating debonding. On the other hand, corrosion currents of similar bars in two of the column exposure tests did not reveal measurable corrosion activity. Therefore, the actual concrete environment strongly influenced the performance of the embedded coated bars. The physical and chemical conditions of the concrete can be quite different from the solution environment. Corrosion of reinforcing bars may be best studied in concrete where heterogeneities would play an important role in the overall electrochemical process.

4.2.17 Concrete Reinforcing Steel Institute, US, 1992.[30,111,112]

Study. Extensive research was undertaken on the effectiveness of epoxy-coated reinforcement over a period of nine years. The research was conducted by Kenneth C. Clear, Inc., and published by Concrete Reinforcing Steel Institute. The study concentrated on:

- Long-term outdoor exposure evaluation of macrocell slabs subjected to a deicing salt and freeze-thaw environment.
- Corrosion macrocell evaluation of slabs containing straight and bent reinforcing bars from different suppliers.
- Bridge deck performance evaluation.

A review of these studies and subsequent laboratory work were carried out by Wiss, Janney, Elstner Associates, Inc. The observations and conclusions from the follow up investigation are given at the end of the comments section.

Long-Term Outdoor Exposure Study. Besides the epoxy-coated bars, some of the outdoor exposure test slabs contained uncoated and galvanized bars. The bars were straight and reported to be in accordance with the applicable specifications. The exposure conditions consisted of 3.1 years of cyclic ponding with a 3% NaCl solution (three days wet, four days natural weathering per week). The ponding was terminated and the test continued for 5.4 more years. Macrocell currents and half-cell potentials were monitored with time. Autopsies were made at the end of the period for verification of the test data.

Macrocell Study. Twenty variables were included in a three-year study of straight and bent epoxy-coated bars procured from eight US suppliers. Two bar sizes, 13 mm (# 4) and 16 mm (# 5), were selected for the study. Some of the test variables were: epoxy film thickness; bend speed and temperature; patching damaged areas; coating before and after fabrication; and bend diameter. The test slabs (two per variable) were subjected to 70 weeks of Southern Exposure cycling (ponding with 15% NaCl at room temperature for four days followed by three days dry exposure to 38° C (100° F) and ultraviolet light per week). Macrocell currents, driving voltage, electrical half-cell potentials, and mat-to-mat AC resistance were measured during the test to monitor corrosion.

After the 70 weeks exposure, some slabs were ponded continuously with tap water for 4.5 months and others for 10.5 months. Then, the slabs were moved outdoors for 9.5

months of natural weathering. Selected slabs were demolished and autopsied at different intervals during the test period.

Bridge Deck Field Study. The condition of the epoxy-coated bars in 13 bridge decks constructed in the Eastern US between 1974 and 1981 was evaluated. Eighty-five cores were taken from sound and unsound areas, including cracks, for comparison. In addition, the chloride content at bar level was determined from a limited number of uncracked locations.

Findings. *Long-Term Outdoor Exposure Study.* The only slabs which did not crack during the entire period of testing were those slabs with epoxy-coated bars either at top mat only or both mats. The measured corrosion currents on these uncracked slabs were negligible or very low. In comparison, the corrosion currents of the cracked slabs with uncoated reinforcing bars were more than 100 times greater. The best performance was that of both mats epoxy-coated.

Minor surface corrosion was observed on the epoxy-coated bars, presumably at small coating imperfections. The corrosion activity was not sufficient to cause significant metal consumption and disruptive internal pressure. Softening of the epoxy coating of both top and bottom bars was observed without underfilm corrosion or obvious detrimental effects.

Macrocell Study. Unlike the uncoated bar specimens, all slabs of the epoxy-coated bars showed no rust staining or cracking during the Southern Exposure cycling. The macrocell corrosion currents were negligible for the coated bar slabs except two which exhibited moderate corrosion currents. The overall average corrosion current for the coated bar slabs was about 80 times less than that for the uncoated bar slabs. Mat-to-mat resistance did not indicate coating degradation. However, autopsies disclosed minor corrosion at damaged areas and holidays on the bent and straight coated bars.

During and after the continuous ponding with tap water, the performance of the coated bar specimens changed. Significant reductions in mat-to-mat resistances accompanied by high corrosion currents and corrosion-induced cracking were observed on the majority of

these slabs. Source was the only variable which correlated with the change in performance. Factors which seemed important were: the presence of chloride at the steel/coating interface; and the number of coating imperfections prior to exposure.

Bridge Deck Field Study. After 9-16 years of service, 87% of the top mat epoxy-coated bars -in cores- were found with minimal or no corrosion and corrosion-induced distress. Other bars located at cracks showed significant localized corrosion (but without significant section loss). In some instances, bar portions away from the cracks showed some corrosion. The water-soluble chloride content at bar level of half of the cores did not exceed the concentration commonly associated with corrosion initiation. The rest of the cores had a chloride content that ranged from 0.6 to 4.7 kg/m^3 (1-8 lb/yd^3) which could be very corrosive to uncoated bars.

Under the coating, the steel surface was bright and shiny except at some vertical cracks. Despite the presence of numerous holidays, mashed areas, and small bare steel areas, the performance of coated bars in uncracked sections was generally unaffected. The condition of the epoxy coating was described as follows: underfilm contamination varied from 10 to 70%; anchor pattern varied from 30 to 55 μm (1.2 to 2.2 mils); and average thickness ranged between 130 and 360 μm (5.1 to 14.3 mils). Further, the minimum bar trace pH was 9 indicating no acidic corrosion products.

Comments. *Long-Term Outdoor Exposure Study.* The test utilized an unusually small distance of 45 mm (1.75 in.) between the two reinforcing mats. Such a short distance might have affected conditions controlling the anodic and cathodic reactions and the severity of corrosion development.

The reported overall average number of holidays per lineal meter of bar was 10.8 (3.3 per ft.). This indicates that part of the tested coated bars, if not all, was not in accordance with the specifications- limiting holidays to 6/m (2/ft.).

Softening of the epoxy coating could be a sign of physical alteration of the coating material which may affect its long-term performance. Since softening took place on both anodic and cathodic bars without underfilm corrosion, factors other than corrosion activity might have contributed to this phenomenon. It should also be noted that only cores were taken from the slabs for bar autopsy. The condition of the coating along the total 2.4 m (8 ft.) top and 3.7 m (12 ft.) bottom bars in each slab might not have been adequately represented.

Macrocell Study. A large number of variables (20) was studied in a relatively small number of test specimens (40). It would be difficult to conclude what factors, or combinations thereof, lead to successful or detrimental performance. The study indicated that the deterioration of the epoxy-coated bars (loss of electrical insulative properties) was probably the result of continuous wetting of already salt-contaminated concrete. The conditions might have created osmotic pressures due to the semi-permeable coating membrane. This needs to be studied further to better understand the mechanism of failure. However, effects of chloride saturation on concrete conductivity and electrolytic properties might also be important and should be studied.

Test data indicated that mat-to-mat AC resistance was an important controlling factor in determining corrosion performance of coated bars. Specimens which did not crack maintained an average resistance more than an order of magnitude higher than cracked specimens (for both bent and straight bars). However, large variability existed among all of the measured initial resistances. Specimens with bent bars, in general, had lower resistances than those with straight bars.

Bridge Deck Field Study. The observations were different on coated bar portions retrieved from cracked and uncracked areas of the same bridge. Corrosion spots were concurrent with crack locations where chlorides are usually more concentrated. Therefore, it is important to include the state of stress and cracking in the criteria of performance evaluation in both field and laboratory corrosion studies. Furthermore, the "real world"

condition of coating was that which contained numerous holidays and defective areas and measurable amounts of underfilm contamination.

Based on the given counts of the number of holidays, bare areas, and mashed areas on bar specimens from each bridge, it can be conservatively estimated that the total number of defects was over 115. If the length of bar specimens recovered in the 0.1 m (4 in.) cores was assumed 0.1 m (4 in.), then the equivalent length of 107 specimens is about 10.7 m (35 ft.). The average number of defects per lineal meter is thus about 10.7 (3.3 per lineal ft.) which exceeds the limit for holidays in the specifications- a maximum of 6/m (2/ft.).

Findings of Wiss, Janney, Elstner Associates, Inc., 1993.[94] Corrosion performance of coated specimens was dominated by the holiday count. In both the long-term outdoor exposure test and the macrocell test on straight and bent coated bars from different suppliers, macrocell corrosion current development was directly related to the number of holidays determined on tested bars. An examination of the retained coated bars from different sources (untested companions to the ones in slabs) revealed large numbers of holidays in excess of specification limits. Therefore, numerous as-received epoxy-coated bars were of questionable quality.

Electrical resistance was an effective means to measure and monitor the potential corrosion protection qualities of the coated bars. A good correlation was found between initial resistance and final corrosion current test results. Further, differences in measured initial resistances among tested slabs correlated with number of holidays on companion retained bars. There seems to be good agreement between area of metal exposed and electrical resistance properties of the coated bar.

Based on the discussion above, film thickness, surface preparation, and holiday count had a direct influence on the value of electrical resistance. Thin films, for example, may develop holidays which contribute to poor corrosion performance. Microscopic examination of tested bars found numerous corrosion spots that relate to thin film regions- 50 μm (2 mils).

The scanning electron microscopic examination of the cross section of some epoxy chips removed from the tested bars indicated that chloride did not penetrate through the epoxy coating. This finding suggested that chloride ions reached the substrate steel surface through breaks in the coating.

Factors that did not have a significant influence on the variability of test results were: cover thickness differences; concrete water absorption; epoxy water absorption; surface roughness profile; film backside contamination; and curing of epoxy coating. The role that osmotic pressure played in aggravating corrosion during tap water ponding is still unknown.

4.2.18 King Fahd University of Petroleum and Minerals, Saudi Arabia, 1992.[113]

Study. The performance of uncoated mild, galvanized, epoxy-coated, and stainless clad reinforcing bars was evaluated after seven years of embedment in chloride-contaminated concrete. Specimens were concrete prisms with four pre-weighed straight bars at the corners and 25 mm (1 in.) clear cover. Type V cement was used throughout, and sodium chloride was added to mix water. Three levels of chloride content were included: 2.4, 4.7, and 19 kg/m^3 (4, 8, and 32 lb/yd^3) corresponding to 0.6, 1.2, and 4.8% by weight of cement, respectively.

All reinforcing bars were procured from commercial sources. The epoxy-coated bars, equally divided between parallel and cross deformation patterns, conformed to ASTM A775-81 specification. Three replicate specimens were used for each steel type and chloride level.

Test specimens were exposed outdoors on a site at King Fahd University of Petroleum and Minerals, Dhahran, Saudi Arabia. During exposure the onset of cracking and crack widths were monitored through periodic inspection and measurement. At the end of the seven-year period, the specimens were demolished and the reinforcing bars retrieved. Weight measurement and condition examination of each bar were carried out. Corrosion

performance was based on the following criteria: the onset and propagation of concrete cracking; weight loss of steel; and percentage of bar surface covered by rust and pitting.

Findings. Specimens containing epoxy-coated bars and chloride contents of 2.4 and 4.7 kg/m^3 (4 and 8 lb/yd^3) did not crack. The retrieved bars were corrosion-free and had shiny, undamaged coating. However, significant corrosion was observed on the bars embedded in concrete containing 19 kg/m^3 (32 lb/yd^3) chloride ions concentration. Buildup of corrosion products on the underlying steel caused breakdown of the coating and subsequent concrete cracking. This indicated that epoxy coatings have a finite tolerance limit for chlorides. Damage morphology of corroded epoxy-coated bars was described by the following:

- Corrosion was observed at the base of lugs. Where damage to coating had occurred at some cut ends before casting concrete, corrosion was severe and cracking always started radiating from these locations.
- Underfilm corrosion was significant.
- Coating was breached systematically from mechanical pressure of underlying corrosion products.
- Damage was noticeably greater in bars with parallel deformations pattern than in bars with cross deformations pattern. The coating broke down along the longitudinal lug parallel to the bar.

In comparison, specimens containing mild and galvanized bars suffered from variable corrosion-induced damage at all three chloride levels. Significant pitting and rib degradation were observed on both bar types in the highly-contaminated concrete. Use of galvanized bars merely delayed concrete failure by only a finite period of time. On the other hand, the best performance was exhibited by the stainless-clad bars which did not show any sign of corrosion even at elevated chloride levels.

Comments. The study did not reveal whether or not sites where corrosion on epoxy-coated bars was observed were initially undetected holidays and coating imperfections.

Corrosion would be expected to start at points of weakness along the coated bar. Corrosion initiation depends on many factors some of which are presence of coating defects, film thickness, and uniformity of coating.

The fact that corrosion was severe at some damaged bar ends indicates the importance of patching cut ends and any damage thereto. If left unrepaired, these ends would allow corrosion progression under the coating with subsequent breakdown of coating.

When comparing the performance of bars with different deformation patterns (parallel and cross deformations), the following factors may be of significance in addition to evaluation of the observed corrosion on each bar type:

- rib geometry (height, angle) and sharpness;
- surface preparation;
- coating thickness, uniformity, and consistency; and
- quality of the base metal (mill tests).

The study did not show a comparison between the bars of the two deformation patterns with regard to these factors. One reason for greater attack along the longitudinal rib parallel to the bar may be the angularity of the rib resulting in a very thin coating at the rib/bar junction.

4.2.19 University of South Florida, US, 1992.[114]

Study. Extensive investigations were conducted following unexpected corrosion problems of epoxy-coated bars in the Florida Keys bridges. The most compelling finding was that coating debonding occurred prematurely under both anodic and cathodic conditions, *i.e.* with or without chloride ions. To this end, concerns were raised about the susceptibility to similar early deterioration of the other 300 bridges constructed in Florida using epoxy-coated reinforcement. A new investigation was then launched to determine the extent of the problem statewide, and to evaluate viable solutions. Thirty bridges were scheduled for field

examination of which 13 were reported. The investigation is still in progress and only initial efforts are presented here.

Besides visual examination of the bridge structure and sampling concrete and reinforcement, measurements included electrical continuity, half-cell potentials, electrical resistances, electrical currents, as well as, polarization resistance. Laboratory assessment of field specimens included testing adhesion of coating to underlying metal, measuring concrete conductivity, and other specialized analyses on coating properties and quality. Experiments to determine the mechanism of corrosion had been initiated using immersion solutions, impressed current methods, macrocell activity monitoring, and special apparatus for measuring corrosion conditions inside crevices.

Findings. A variable degree of electrical continuity between epoxy-coated bars was detected in field structures. Measured electrical continuity ranged from 0 to 100%, with a median of 27%.

Epoxy coating had undergone significant loss of adhesion in virtually all structures examined. Debonding was observed even when the chloride content at bar level was still low. These findings were confirmed by laboratory tests using solutions to simulate concrete environment. The results suggested that debonding occurred due to the presence of Na and K ions in the concrete pore solution. In addition, the laboratory tests indicated that debonding can result under anodic polarization conditions once chloride ions attack the bar. It was observed that one coating material performed consistently better than other types included in the debonding tests.

The experiments further showed that mechanical aspects of corrosion-induced fracture were nearly the same for both the epoxy-coated and the uncoated bars. Time to cracking was comparable when similar corrosion-impressed currents were used. Moreover, the macrocell tests in progress were showing a cathodic current activity at coated bars equivalent to about 15% of that at uncoated bar specimens. The ratio of initial surface area exposed on the coated bar to that of the uncoated bar was only 2%.

Comments. Test solutions used to determine the tendency of epoxy-coated bars to debond in concrete were more representative of the concrete pore solution than those used in earlier studies (such as NBS study in 1974). Earlier attempts to evaluate performance of the coated bars in a simulated concrete environment did not include all important cations such as Na and K. Unlike previous studies, the results of this study showed that coating could be affected by the simulated concrete environment. Actual concrete specimens are also being tested to confirm these findings. The fact that one coating material consistently behaved better than other types in debonding tests indicates that a wide variability in quality exists among commercially available products.

4.2.20 University of New Brunswick, Canada, 1993.[56]

Study. Research is being conducted on corrosion of epoxy-coated bars in concrete exposed to seawater in both laboratory and field tests. Test specimens consisted of small-scale concrete blocks containing a single U-shaped epoxy-coated bar with 20 mm (0.8 in.) clear cover. Three conditions of damage to epoxy coating were used: no damage; 1%; and 2% surface area damage. Companion specimens were also cast with uncoated reinforcement. A w/c of 0.6 was utilized in the concrete mixture. The details of the experimental program are given in Table 4.3.

Table 4.3 Layout of Experimental Program.[56]

Type of Exposure		Number of Concrete Slabs Cast			
		Uncoated Rebar	Epoxy-Coated Rebar		
			No Damage	1% Damage	2% Damage
ASTM Seawater (MESS) (SERIES-C)		4	4	2	2
Treat Island	Mid-Tide (SERIES-D)	4	2	2	2
	0.5 m below High-Tide (SERIES-E)	4	4	2	2
	0.5 m above High-Tide (SERIES-F)	4	4	2	2

Laboratory testing utilized a simulated marine environment (tidal effects) with four wetting and drying cycles each day. Each cycle consisted of two hours wetting with seawater and four hours natural drying. The exposure period in accelerated laboratory tests extended over two years. Field testing involved placing specimens at a natural marine environment exposure station in Treat Island, Maine. Specimens were subjected to an average of 130 freeze-thaw cycles per year.

Corrosion activity was monitored using electrochemical techniques including measurements of open-circuit potentials, linear polarization resistance, and AC impedance. At the end of one year and two years of exposure, some concrete specimens were demolished to expose bars for visual and microscopic examination

Findings. The results of both natural and laboratory exposure testing were in good agreement. The open-circuit potentials, after two years of measurement indicated that initially undamaged coated bars remained passive (around -120 mV SCE). The 1% and 2% damaged coated bars behaved similarly and became active (more negative than -270 mV SCE). Figure 4.7 shows potentials measured on various test bars.

The linear polarization measurements and AC impedance measurements confirmed the above findings. No measurable corrosion current densities were obtained for the undamaged bars, whereas current densities higher than 0.01 $\mu A/cm^2$ (0.01 mA/ft^2) but not exceeding 0.05 $\mu A/cm^2$ (0.05 mA/ft^2) were estimated for both the 1% and 2% damaged bars.

No cracking or corrosion staining was observed on the concrete surfaces of all specimens containing coated bars for the entire period of testing. Visual examination of recovered bars showed no corrosion on the undamaged bars. Rust products (usually black) with localized pits at the damaged spots were seen on both the 1% and 2% damaged bars.

Comments. Input data used to calculate the corrosion current density of the coated bars utilizing the polarization resistance technique were originally derived for uncoated bars.

Nevertheless, the correlation between the results of the various electrochemical techniques and the visual observations was good.

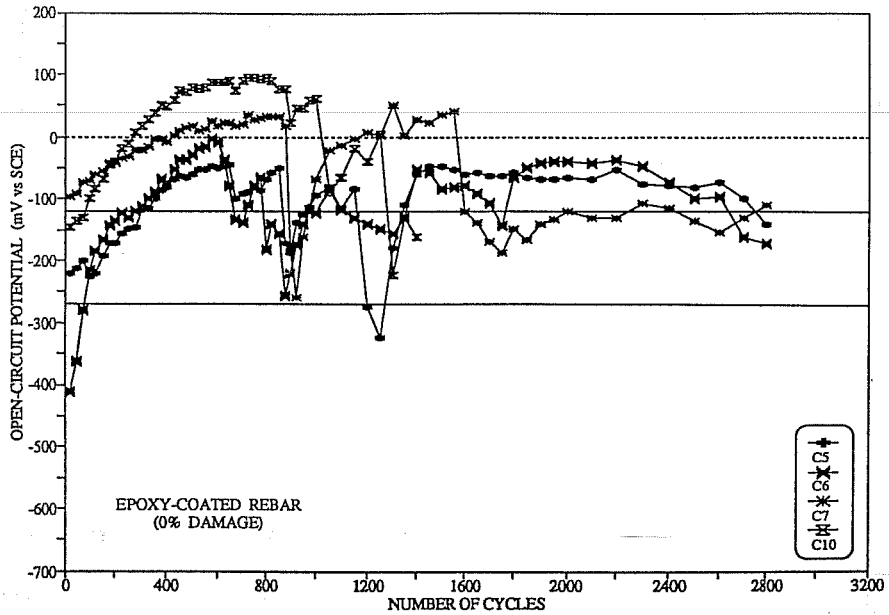

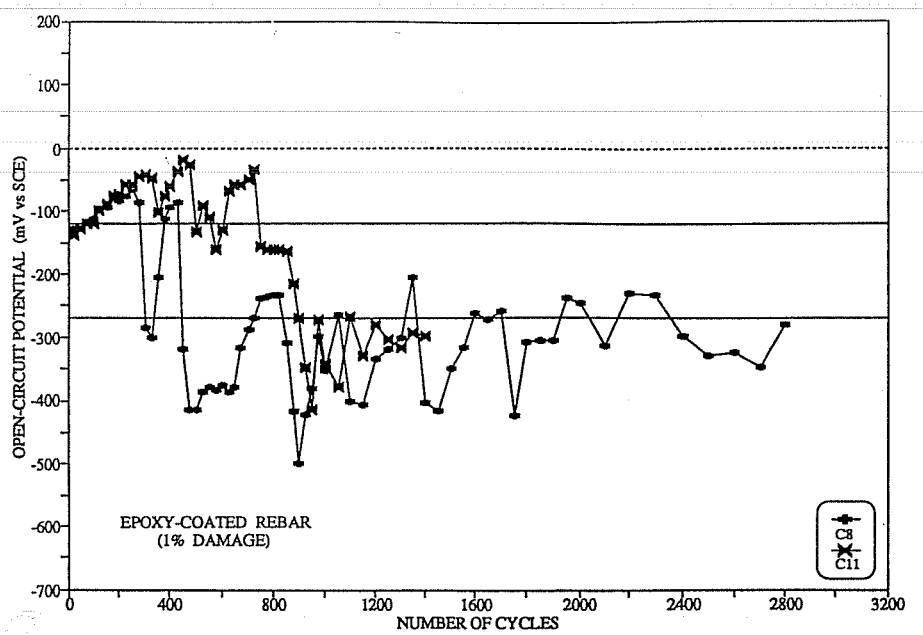

Figure 4.7 Potential Measurements on Slab Test Bars.[56]

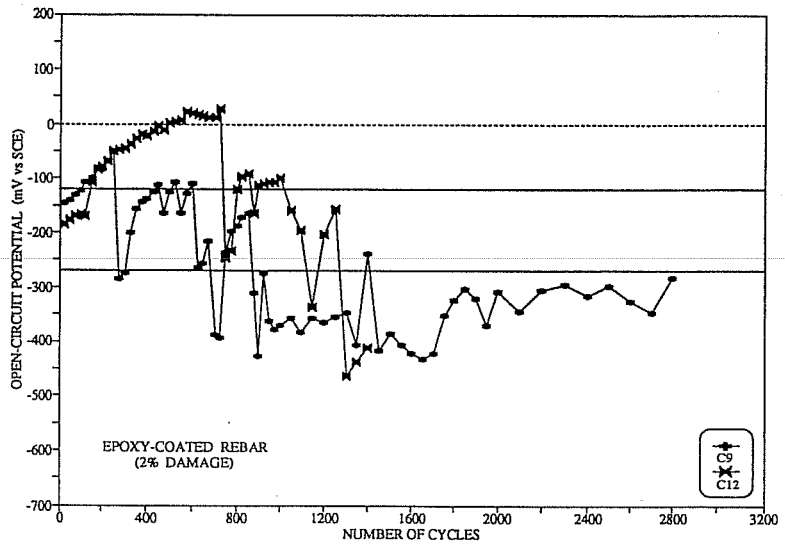

Figure 4.7 (Cont'd) Potential Measurements on Slab Test Bars.[56]

In the same fashion, the open-circuit potential measurement seems to be effective in monitoring the corrosion activity on the coated bars although the technique was originally used on uncoated reinforcement. Long-term potential monitoring tends to yield consistent trends of half-cell potentials measured against a saturated calomel electrode.

4.2.21 Berkshire Transport Research Laboratory, UK, 1993.[115]

Study. The effects of defects on the performance of epoxy-coated reinforcement commercially produced in UK is being studied. Concrete beam and slab specimens were cast containing coated bars with the following conditions: uncoated bar ends; repaired ends; damage spots in the coating; and bent bars. Salt was introduced by either mixing it with concrete ingredients (3.2% by weight of cement), or ponding the top surfaces of the specimens with salt water solution. The w/c ratio was 0.58.

Each beam specimen contained four electrically isolated coated bars. Two cover thicknesses were used 10 and 20 mm (0.4 and 0.8 in.). The coating of one bar at each cover

depth was damaged by introducing four 1 mm (0.04 in.) diameter holes. The bar cut ends were either patched or left bare.

Slab specimens had the configuration shown in Fig. 4.8. The two halves of the slab were either cast with added salt or left uncontaminated. In some slabs, only one half was salt-contaminated. Some slabs were ponded with 3% NaCl solution weekly to contaminate the chloride-free portion. Half-cell potentials on the straight bars, and macrocell corrosion currents flowing between the bent bars were measured.

Both beam and slab specimens (including companions containing uncoated bars) were placed outdoors in Southern England for weather exposure. Visual inspection and electrochemical measurements were carried out every three months for two years. At one and two years, some beam and slab specimens were opened for a detailed examination of the bars.

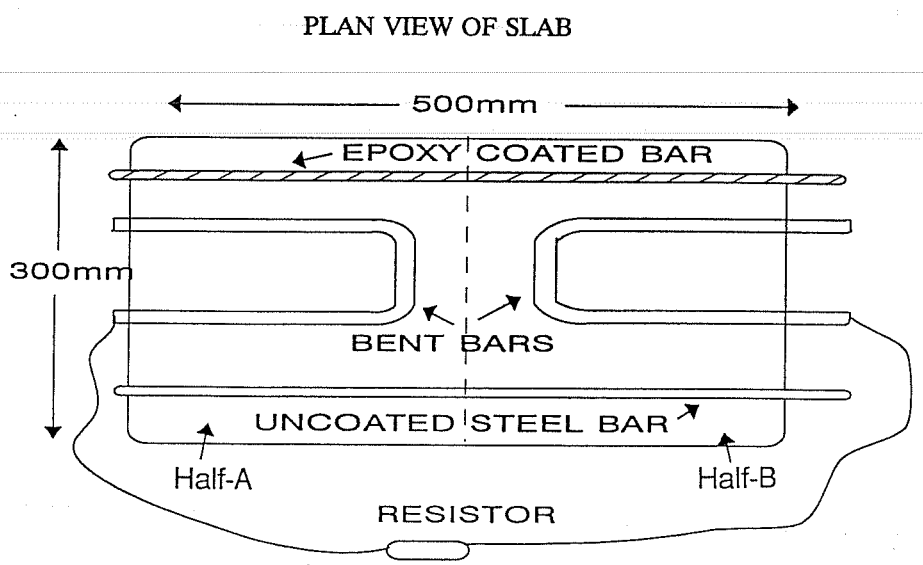

Figure 4.8 Slab Test Configuration.[115]

Findings. The performance of the coated reinforcement outweighed that of the uncoated reinforcement. The extent of concrete cracking and the severity of corrosion were reduced for the coated bars compared with the uncoated bars after two years of testing in chloride-contaminated specimens.

Half-cell potential measurements on chloride-free slabs were in the range of +50 to -300 mV SCE for both coated and uncoated bars. Potentials were inconsistent on slabs with cast-in chlorides. Uncoated bars exhibited more negative potentials than coated bars. For slabs ponded with chloride solution, potentials became more negative with time. In all these cases, potentials on coated bars showed a wider variation with time than uncoated bars. Typical results are shown in Fig. 4.9. It follows that a single set of potential measurement on epoxy-coated bars would be difficult to interpret. Periodic surveys are then necessary to detect significant changes in potentials.

The maximum average macrocell corrosion current measured on coated-uncoated bent bar combinations in the slabs was about 1 μA. This current is approximately 50 times lower than the maximum average current measured on uncoated-uncoated bar combination. Figure 4.10 shows measured average corrosion currents in the slabs.

Underfilm corrosion was detected adjacent to coating defects, and beneath repaired coating, as well as beneath the coating on bent bars. However, corrosion of the coated bars was light surface rusting without peeling or blistering of the coating, and less than that of uncoated bars. In most cases, there were no visible signs of corrosion before coating was removed.

Comments. Damage introduced on the beam bar specimens was very small approximating production defects rather than handling and placement damage. Experience has shown that coated bars are usually subjected to damage many times greater than the damage used in this study.

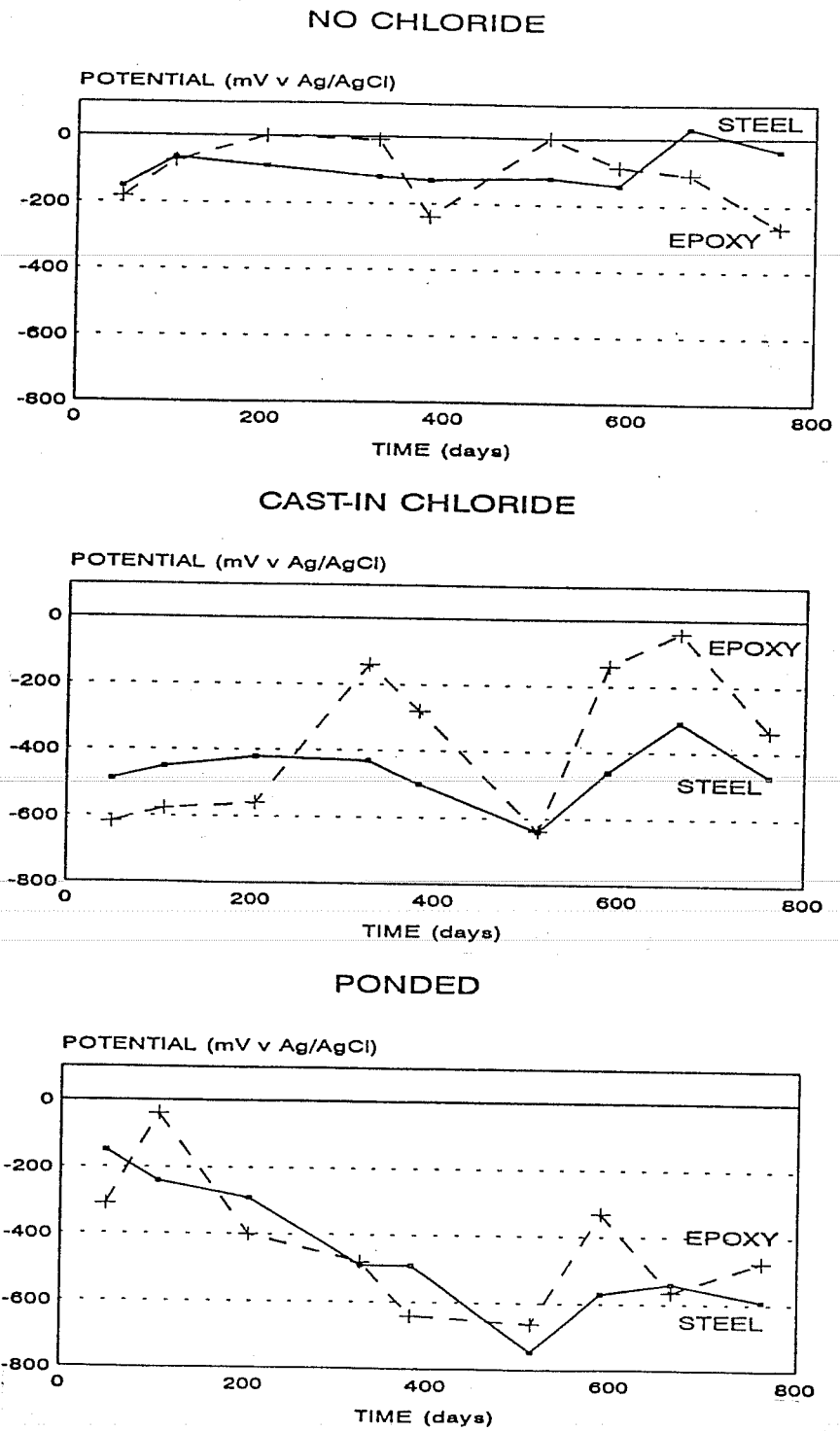

Figure 4.9 Typical Potential Measurements on Single Slab Specimens.[115]

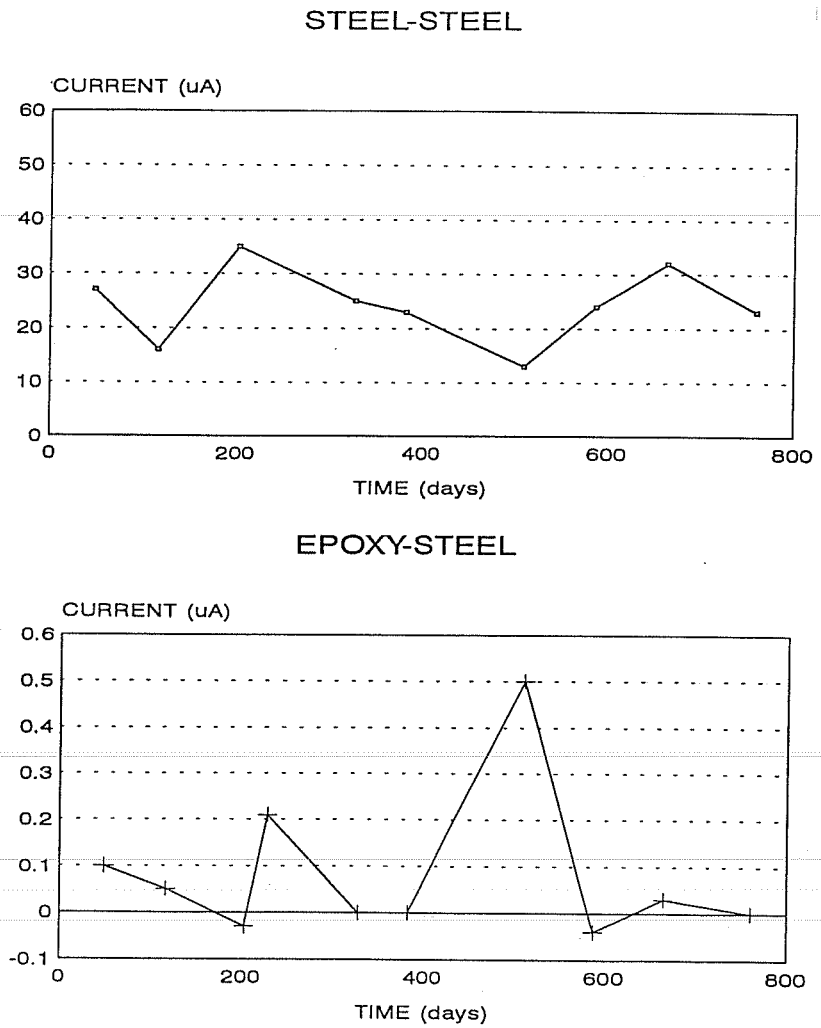

Figure 4.10 Average Corrosion Current in Slab Specimens (Cast-In Chloride in the Side of the First Named Bar).[115]

Potential and corrosion current graphs show how different exposure environments cause different histories of corrosion development. While the cast-in chloride environment tended to produce potentials and currents that fluctuate with time, continuous ponding with chloride solutions tended to shift the graphs consistently towards more negative values. It can also be observed that measuring positive potentials against a saturated calomel electrode is possible.

4.2.22 Building Research Institute, Germany, 1993.[116]

Study. Limited tests were conducted at the Institute für Bauforschung (Building Research Institute- IBAC) in Germany to investigate the performance of damaged epoxy-coated bars under different chemical environments. Immersion of straight coated bars in 3.5% NaCl solution was selected to evaluate the effects of exposure to a marine environment prior to embedment in concrete. A chloride-free concrete environment was simulated with KOH + NaOH solution. The third test solution was a combination of KOH + NaOH + NaCl to resemble a chloride-contaminated concrete. Coated bar specimens immersed in these solutions were procured from two sources. Source A produced coated bars according to ASTM standards, while source B produced coated bars according to the German guidelines.

Damaged bars were tested under both open-circuit and polarized conditions. The potential ranged between -1800 mV (cathodic polarization) to +100 mV (anodic polarization). Immersion tests lasted 30 days after which bar specimens were compared in terms of amount of debonding and surface condition.

Findings. The results of the immersion tests are shown in Fig. 4.11. The differences in performance of the bars between source A (US) and source B (Germany) were obvious. The amount of debonding was expressed as a percentage of the total immersed surface of the bar.

Comments. The results show, in general, that the bars from source B performed better than those from source A. Bars from source B exhibited less pitting corrosion under anodic polarization in NaCl solution, and less coating debonding in the cathodic polarization range. It is evident that the stricter German requirements for the epoxy-coated bars result in an improved performance compared with the American requirements.

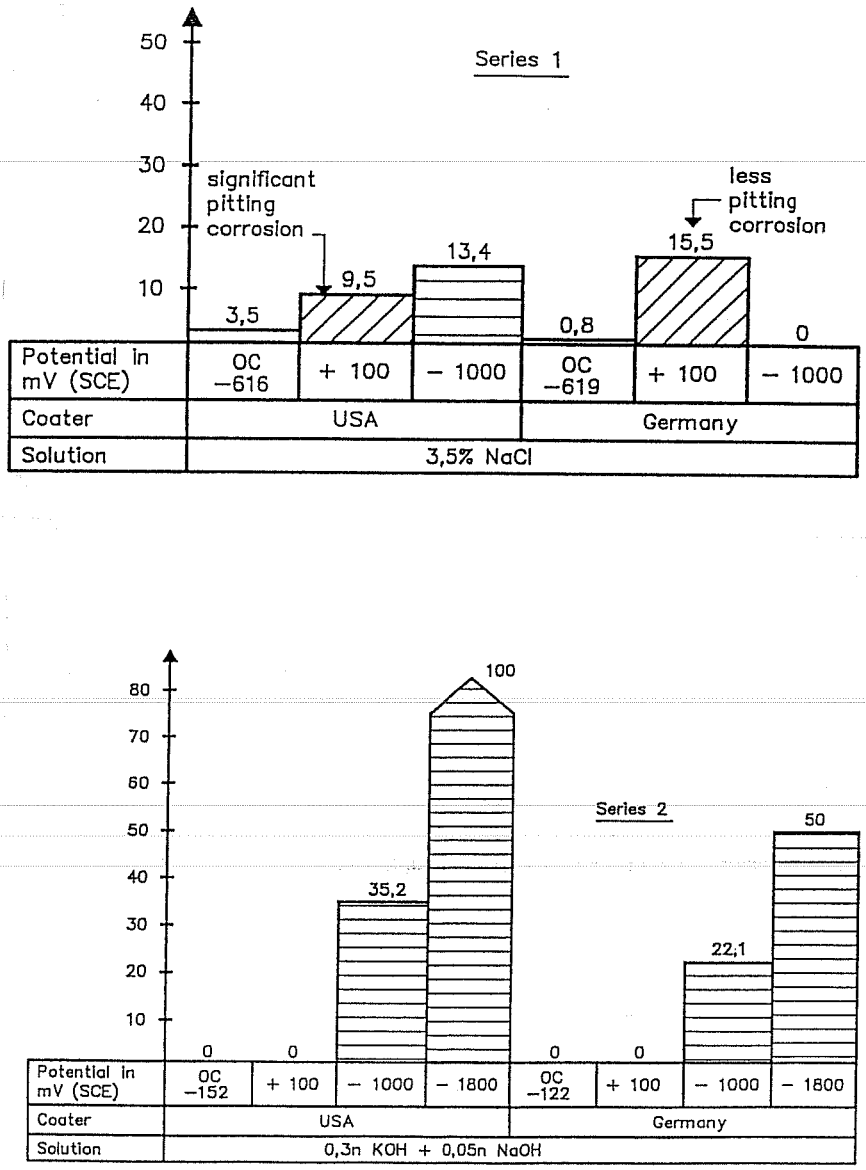

Figure 4.11 Percentage of Coating Debonding After 30 Days Exposure in Test Solutions at Different Potentials.[116]

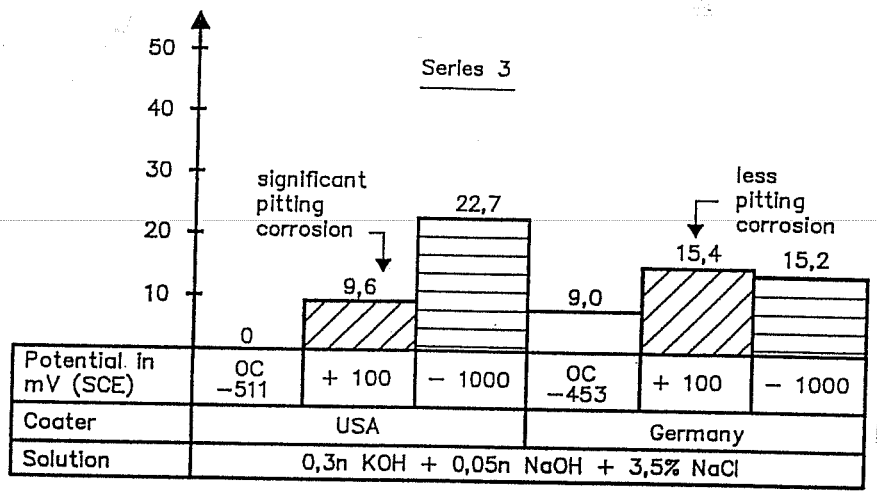

Figure 4.11 (Cont'd) Percentage of Coating Debonding After 30 Days Exposure in Test Solutions.[116]

4.3 Overview

4.3.1 Historical Perspective. Initial research studies generally addressed bridge deck construction. Results of laboratory accelerated corrosion tests showed that performance of epoxy-coated reinforcement could be significantly better than conventionally uncoated reinforcement. Early field observations and evaluation studies of bridge decks were very supportive of these findings; the performance of the epoxy-coated bars was satisfactory. In other words, coated reinforcing steel successfully reduced the risk of corrosion due to deicing salt application. It is important to note, however, that many of the inspected bridge decks were not yet contaminated with chlorides to serious levels at the time of inspection.

In the context of the early studies, corrosion observed on the coated bars was found to be of no concern. Because of its limited extent of severity, corrosion was described as "minor", "very slight", "insignificant", or "superficial". Little damage morphology was given in terms of the state of coating adhesion, underfilm corrosion, blister formation, and accumulation of salt water beneath the coating. The absence of damage on the outer surface

of the coating cannot necessarily be considered to mean that the epoxy film or the substrate were completely unaffected.

The premature corrosion of the epoxy-coated bars in the substructures of four major bridges in the Florida Keys was a shocking incident to the construction industry. It can be considered a milestone in the history of application of coated bars. Skepticism about how well epoxy coating can function in severe environments resulted in a diversity of opinions. In response to the demand for a better understanding of the mechanism of corrosion of coated bars, research has continued and more tests are being performed.

At this time, accelerated tests are addressing conditions more conducive to corrosion than before. Coating defects are being given more consideration, especially those caused by mechanical fabrication. Loss of adhesion and underfilm corrosion were a new focus of the studies. Effects of surface corrosion or coating debonding before embedment of bars in concrete on the performance of bars are also being examined. Recent findings have confirmed that, even when coating material itself is visually unaffected, underfilm corrosion development associated with debonding is possible.

4.3.2 Parametric Variations. To date, different corrosion test concepts and procedures have been employed to study performance of coated bars. Variations in test methods have led to a wide range of results with little or no correlation possible. The following comments address some parameters that differ, were not controlled, or were not reported in the corrosion studies summarized in this chapter.

Concrete Specimens. Concrete quality (*e.g.* w/c), cover thickness, loading condition (*e.g.* at rest or stressed or cracked).

Coated Steel. Surface area, configuration (*e.g.* straight or bent), arrangement (*e.g.* anode or cathode or both), surface complexity and sharpness of edges.

Epoxy Coating. Type, film thickness, coating application method, holiday count, surface damage, degree of debonding, patching

Exposure Conditions. Natural environment, accelerated corrosive conditions (*e.g.* cyclic salting or impressed voltage or current), test period, chloride contamination (*e.g.* included or intruded salt), chloride concentration.

Corrosion Monitoring. Half-cell potentials, resistances, currents driving voltages, crack width and propagation.

Corrosion Assessment. Observations and autopsy examination, metal loss measurement or calculation, corrosion current rate, half-cell potential levels, electrical resistance changes.

Tests with different or varying parameters produce different corrosive conditions. Therefore, the performance of coated bars can best be evaluated based on a comparison with a control test (uncoated steel) under the same test conditions. This is particularly useful when direct measurement of corrosion current, or corrosion rate, is involved. However, no reliable means has yet been established to relate half-cell potentials measured on coated bars to known states of corrosion activity. In case of uncoated bars, ASTM C876[117] provides a standard method for potential measurement and interpretation.

The superiority of the epoxy-coated bars over uncoated bars in reducing or preventing corrosion has been demonstrated in many laboratory studies. Even when the coated bars did not conform to specifications, performance of the bars was generally improved compared to bare steel bars. Epoxy-coated bars with little or no coating damage performed well, even in very aggressive environments and embedded in concrete of low quality.

Much effort has been allocated to study condition and corrosion performance of coated reinforcing steel samples obtained at the coating plant. The main intention was to gain

confidence in the finished product. Therefore, the laboratory reported performance of the coated bars related directly to the adequacy of the coating process and plant quality control measures. The studies often referred to the coating thickness and holiday count as being major considerations for evaluation.

Indeed, the quality of the produced material is important, nonetheless, the quality of materials in the reinforced concrete is more important. The condition of the coated bars at the job site could be different from that at the coating plant. Conditions at the construction site are expected to be more conducive to damage to coating. When carelessly handled, stored, placed and embedded in concrete, the coating could be in a state of damage or debonding far exceeding acceptable limits. Recently, more emphasis has been put on studying condition and corrosion performance of coated reinforcing steel sampled at the construction site.

The quality of base steel may have an impact on quality of coating which, in turn, affects corrosion performance. Surface complexity and sharpness of edges were not usually reported in cited references. Excessively sharp and angular deformations are more prone to corrosion initiation because of the difficulty in coating to required thicknesses. Furthermore, mechanical properties of the steel may affect its propensity to corrosion. Any significant variations in properties of the parent metal (such as yield strength) need to be documented.

From reported studies, it is evident that the type of environment used in the experiment has an impact on results. Solutions used to simulate concrete environment may fail to do so. It is cautioned against extrapolating results of tests with aqueous solutions to actual concrete systems. In concrete, several physical and chemical inhomogeneities may create a complex situation of interfering oxidation-reduction systems.

Polarizing the potentials of the coated bars while in different environments seems to be a useful technique. Polarization in both the anodic and cathodic ranges can shed light on performance of coated bars subjected to various conditions. Changes in chemical and physical properties of the coating, as well as changes at the epoxy/metal interface and

corrosion development can be examined. Future developments of new standard tests for coating quality or performance may adopt a similar approach.

4.3.3 Test Conditions. Conditions used in previous tests can be grouped to find combinations of factors that lead to satisfactory, or unsatisfactory, performance. Corrosion resistance of coated bars (initially damaged or undamaged) was satisfactory under the following conditions:

- Concrete specimens uncracked. Only limited amounts of chlorides reach the bar surface through diffusion.
- Microcell corrosion formation. This is characterized by cathodic areas remote from the active reaction front insufficient to drive large corrosion currents.

Unsatisfactory performance of coated bars was obtained under the following conditions:

- Damaged and debonded coating. Coating defects reduce the level of protection. Underfilm corrosion can spread from the defects and beneath the debonded coating.
- Excessive chloride contamination. Large amounts of chloride ions at the bar surface resulting from initial high dosage of salt in concrete mixture, reduced cover thickness, or cracked concrete under salt exposure.
- Macrocell corrosion formation. A sufficient supply of hydroxyl ions from abundant cathodic areas can sustain large corrosion current flows.

4.3.4 Evaluation Criteria. Many criteria have been used to define performance of reinforcing bars in the studies reported. The following list provides a means of assessing the corrosion resistance of the epoxy-coated reinforcement:

- Corrosion time development. Time-to-onset of corrosion
  Time-to-cracking
  Crack width and propagation

	Delamination or spalling of cover
- Metal loss.	Measured weight loss
	Estimated section loss
	Calculated metal consumption
- Reinforcing bar conditions.	Appearance of coated surfaces
	Rust coverage percentage of steel area
	Pit size
	Coating condition or integrity
	Coating adhesion or extent of debonding
	Blister formation

The peeling resistance of the epoxy film can be used as an indicator of the adhesive strength. Unfortunately, there is no standard at present to specify the way coating should be peeled and evaluated. One study provided the following categorization of the substrate surface condition at prying or peeling the coating loose using an "X-Acto" knife (No. 11 fine blade):[94]

- Intact: impossible to dislodge the coating without leaving some coating residue adhering to the steel and otherwise disrupting the remaining coating.
- Poor bond: coating can be pried loose from the steel without leaving residue on the bright-steel surface.
- Corroded: steel surface is discolored by corrosion products and there is a general loss of bond between epoxy coating and steel.

CHAPTER 5
FAILURE MECHANISMS OF EPOXY-COATED REINFORCEMENT IN CONCRETE

5.1 General

Several hypothetical failure mechanisms of epoxy-coated bars in concrete have been proposed in the literature and are presented in this chapter. The failure mechanisms include: cathodic debonding; anodic activity under macrocell action; secondary cathode development at low pH in advanced corrosion; anodic activity in metal/coating crevices; and filiform corrosion. At present, the information is incomplete as to whether multiple failure mechanisms occur at one time, whether one mechanism follows another, or whether coated bars conforming to specification undergo some changes in coating properties prior to significant corrosion.[31] Lack of knowledge is due in part to the fact that corrosion activities below the concrete surface are difficult to monitor. Therefore, it is hard to predict the performance of coated bars using current evaluation procedures. The susceptibility of the coated bars to one or more failure mechanisms is not well defined.

Failure of epoxy coating may be influenced by several factors related to the surrounding concrete, the coating material itself, and the steel substrate. The quality of concrete, particularly the void structure, surface cracking, moisture content, and level of chloride contamination are among the most influential factors in the environment. Uniformity, consistency, adhesion, and coating blemishes are other important factors related to the coating material. Finally, the presence of flaws in the base steel can also affect the vulnerability of the coated bar to corrosion initiation.

All commercial epoxy-coated reinforcing products are not the same. They vary in quality and performance under different test conditions. Therefore, the failure mechanism of one product may be different from another. Research studies should not generalize a

certain failure pattern unless a consistent trend is apparent for many coated bars obtained from different sources.

5.2 Cathodic Debonding

Cathodic debonding refers to loss of adhesion of coating at cathodic sites. This condition was detected when damaged epoxy-coated bars were exposed to neutral 3.5% NaCl solutions under variable potentials.[93] Significant debonding occurred around existing or introduced coating imperfections with bright metal underneath. Debonding was a result of cathodic reactions. The cathodic activity continued as the cathodic area expanded further under the coating.

Cathodic debonding has also been observed on epoxy-coated bars placed in concrete for some time even in the absence of chloride ions.[93,114] This interesting observation was made during the investigation of several bridge substructures in Florida. In this case, the tendency for the coating to loose adhesion to the steel substrate is not directly related to corrosion activity. Hence, the concrete environment, and any changes thereto, may have a primary role in initiating coating debonding. Cathodic debonding may be construed as an indicator of coating degradation in concrete.[114]

Based on observations of debonding of organic, polymer coatings, two possible mechanisms were suggested for the cathodic debonding phenomenon.[110] The first mechanism is related to the effect of alkalinity on the polymer/metal interface. Reactions at the cathodic site, such as oxygen reduction, generate alkalinity by producing hydroxyl ions OH^-. These ions, by saponification or other adverse interactions, may cause separation between the coating and the substrate. The other mechanism involves the reduction of oxides to which the epoxy coating is adhered. Alteration of the boundary layer at the steel surface may result in separation.

Cathodic debonding takes place in an ionic environment. Accordingly, charge flow must be in equilibrium. Charge balance at the epoxy/metal interface is maintained by the

presence of a cation, such as Na^+. Calcium cations were not found to promote cathodic debonding. Furthermore, the pore water solution in hardened concrete is richer in Na^+ and K^+ ions than in Ca^{++} ions. Therefore, cathodic debonding of epoxy-coated bars embedded in concrete is more likely.

Coating resistance to cathodic debonding depends mainly on substrate surface preparation and the coating itself. Factors such as film thickness, cure, water and vapor penetration, dielectric strength, as well as the formulation of the coating significantly affect susceptibility to debonding.[32,97] Hence, the diffusivity of the various ions and water permeation characteristics of the epoxy film become very important for long-term corrosion resistance.

Tests have shown that the moisture absorption of epoxy coatings 125 to 250 μm (5 to 10 mils) thick from six suppliers varied between 2.04 and 20.34% by weight with an average of 10.58%.[112] These results clearly indicate that commercially-produced epoxy films absorb relatively large amounts of water; the normal absorption being 2 to 3%. Water absorption and water permeation cause loss of adhesion. Usually, the higher the water absorption and water permeability, the more rapid is the adhesion loss.[97] It follows that exposure of epoxy coating to high humidities impairs adhesion.

It has been observed that water penetrates epoxy paint films very quickly and probably spreads along the boundary layer.[97] Consequently, it was theorized that adhesion loss is caused by water action on the boundary layer. Data have shown that the boundary layer was more water-sensitive than the bulk polymer and contained water-soluble constituents. The manner in which water operates on the boundary layer was not established. However, it was suggested that water might displace polar groups and reduce van der Waals forces; or it might swell the boundary layer to set up high stress concentrations; or it might physically alter the boundary layer in a way that weakens it mechanically.[97]

In this research, the effects of water on the adhesion of the epoxy coating was studied briefly. Several epoxy-coated reinforcing bars were continuously immersed in tap water at

room temperature. Two bar diameters, 19 and 25 mm (#4 and #8), with both parallel and cross rib deformations were selected for testing. The bars were bent to 180° at the coating plant before immersion. After about 135 days of testing, the coating was pried from different spots along the bar using a sharp blade. It was found that the coating on the bent portions was relatively easier to pry compared to companion bars not tested. The coating was also easier to pry on the bent portions than on the straight portions for both bars immersed or not. It was concluded that bending had weakened the coating adhesion along the bent portions. Subsequently, the coating in these areas softened and debonded upon exposure to water. The bars were then allowed to dry in room temperature for about 75 days. The coating was found to retain the initial adhesion characteristics after drying. Therefore, coating softening may be a reversible phenomenon.

Coating debonding may have serious consequences. Loss of adherence between the steel and the epoxy film generates a potential for electrochemical activity at the steel surface and can limit the usefulness of the epoxy coating. The debonded coating becomes an isolator of the alkaline concrete from the steel surface. The steel is, thus, deprived from the passivity effect offered by concrete pore solution in conventional construction using uncoated steel. If the chloride-laden electrolyte penetrates the debonded coating, then corrosion may start and progress along the bar surface.[98] It is imperative that coatings have the lowest possible moisture and oxygen permeability and remain intact for maximum corrosion resistance.

5.3 Anodic Activity Under Macrocell Action

Localized damage to the epoxy coating exposes only a small area of the steel substrate. If the bar is subjected to a corrosive environment, then such an exposed area is likely to show corrosion activity. When the damaged bar is electrically isolated from other bars, and is exposed to a uniform corrosive environment, part of an exposed area becomes the cathode. The severity of the corrosion activity depends on the potential difference between the micro-anode and micro-cathode sites within the exposed area. Since no significant potential difference is likely to develop on a small area, the microcell corrosion

activity tends to be negligible. Cathodic reactions are restricted by the non-conductivity of the coating and isolation from other bare metals.

When the damaged bar is in electrical contact with other uncoated bars, a macro-corrosion cell is likely to develop. Intensive corrosion activity is expected to take place if sufficient cathodic areas are available to sustain large macrocell corrosion currents. After corrosion initiation at the exposed steel area, corrosion beneath the coating (undercutting) progresses. The coating loses its insulative properties and further corrosion spreading takes place. It is feared that the intensive metal dissociation at the initially corroded sites on the exposed steel may lead to serious pitting. Macrocell action has been reproduced in many laboratory experiments. Test results showed good correlation with actual observations of corroded bars in bridge substructures in the Florida Keys.[93] Figure 5.1 depicts the hypothetical conditions discussed in terms of coating damage, electrical continuity, and micro- vs. macro-corrosion activities.

The quality of the concrete mixture seems to have an influence on the extent of corrosion of the epoxy-coated bars. More underfilm corrosion spreading was observed in concrete mixtures with higher cement contents.[62] Coating blistering was also observed where voids in concrete were in contact with the bar's surface.[93]

5.4 Secondary Cathode Development at Low pH in Advanced Corrosion.

A secondary destructive mechanism may initiate at an advanced stage of corrosion of the coated bars. When corrosion propagates under the epoxy film, the oxygen supply becomes scarce. At the same time the pH drops locally at the anodic sites. Acidification occurs because of the evolution of hydrogen in the corrosion process. Water transformation into hydrogen is another probable process.[29] Due to the deficiency of oxygen and the acidity of the media, hydrogen evolution becomes an alternative cathodic reaction.[16,43,82]

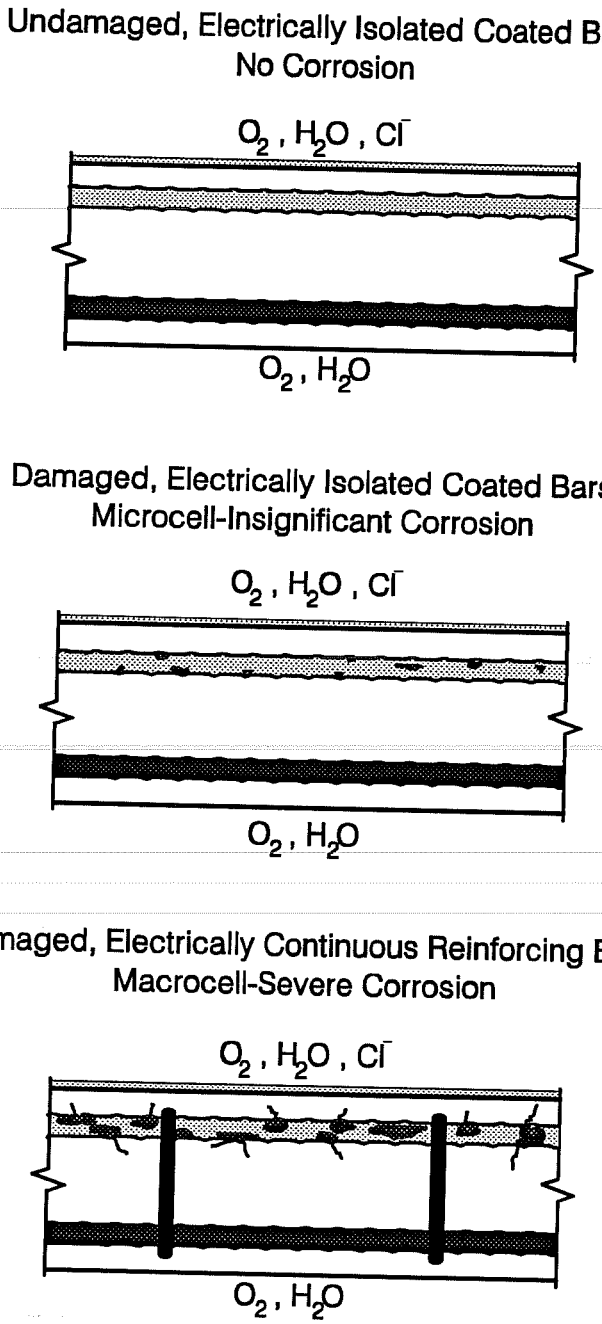

Figure 5.1 Microcell and Macrrocell Corrosion on Epoxy-Coated Reinforcement.

5.5 Anodic Activity in Metal/Coating Crevices.

Areas of debonded coating may experience enhanced corrosion by the crevice effect.[93] Crevices are formed in the restricted regions between the steel and the debonded coating. These crevices promote the anodic reactions that result in wider debonded areas. As more crevices develop beneath the coating, additional metal surface areas become available for corrosion activity.

The proposed failure mechanism was based on laboratory observations and field examination of corroded coated bars. Epoxy-coated bar specimens exposed to $Ca(OH)_2$ + NaCl mixed solution became debonded around defects and showed pits filled with black corrosion products, and a low pH liquid trapped between the coating and the underlying steel.[93] The process was found to be anodically controlled, i.e. under anodic activation polarization conditions. This was indicated by a black corrosion product which was at a low oxidation state.[81,108]

Observations made on corroded coated bars from a deteriorated structure suggested that crevice or occluded cell corrosion occurred under the debonded coating.[114] In another case, crevice corrosion was found adjacent to bare cut ends acting as cathodes in the corrosion cell.[115] Crevice corrosion is characterized by a self-propagating mechanism in the confined crevice environment. Knowledge is limited on the behavior of steel under crevice conditions in concrete. Studies are in progress to investigate this corrosion mechanism.[114]

5.6 Filiform Corrosion

Filiform corrosion is another form of corrosion expected to take place on epoxy-coated reinforcement.[94] This form of corrosion is not widely discussed in published corrosion studies performed on coated bars. Filiform corrosion can be regarded as a special type of crevice corrosion or filamentary corrosion.[14] It most often occurs under protective films in humid environments. It only affects the metal surface appearance; thus, it does not weaken the metallic component.

Filiform corrosion appears as a network of corrosion product trails or hair-like tracks. The corrosion originates at a break in the coating. The filament or corrosion track consists of an active head and a tail. Figure 5.2 shows a magnified schematic diagram of a filament growing on an iron surface. Corrosion takes place only at the head with the tail being primarily cathodic. The head usually appears with a blue-green color indicating active conditions of iron dissociation into ferrous ions. The inactive tail is usually red-brown as a result of precipitation of ferric oxide or hydrated ferric oxide.

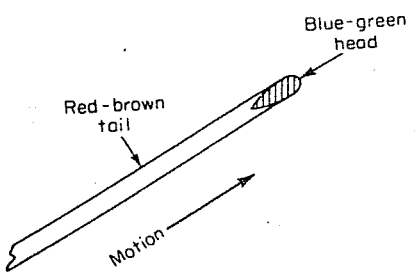

Figure 5.2 Schematic Diagram of a Corrosion Filament on an Iron Surface.[14]

Corrosion filaments tend to move beneath the coating in straight lines. Several possibilities of interaction between the filaments are depicted in Fig. 5.3. Active heads do not cross inactive tails. The growth of the filaments depends on the humidity of the environment and the available space for movement. Generally, the higher the humidity, the more rapid is the growth. The lower relative humidity limit for filiform corrosion on steel is approximately in the range between 60 and 65%. At such humidity levels, the filiform corrosion cell dries out and stops. Higher relative humidities result in wider corrosion filaments. Above 90% humidity, corrosion appears primarily as blistering.[14]

Oxygen and water are necessary for filament propagation. Oxygen and water are supplied to the head through breaks in the coating and by osmosis which tends to remove water from the inactive, porous tail.[94] The osmotic action is due to the high concentration of dissolved ferrous ions in the head and the low concentration of soluble salts in the tail. Figure 5.4 illustrates water diffusion into the active head and oxygen lateral diffusion under

the debonded coating. Although the mechanism of filiform corrosion is not completely understood, it is viewed as a self-propagating crevice.[14] Hydrolysis of the corrosion products at the head produces an acidic environment. Corrosion becomes restricted to the head, while oxygen reduction takes place at the tail.

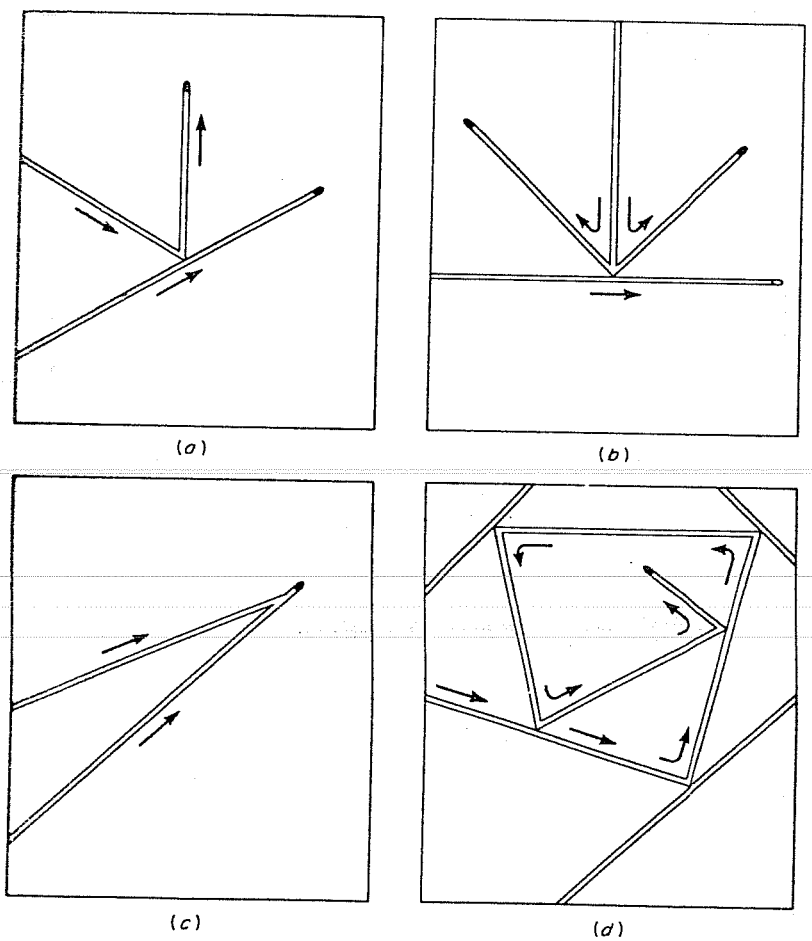

(a) Reflection of a corrosion filament; (b) Splitting of a corrosion filament; (c) Joining of corrosion filaments; (d) "Death trap".

Figure 5.3 Schematic Diagrams of Possible Interaction Between Corrosion Filaments.[14]

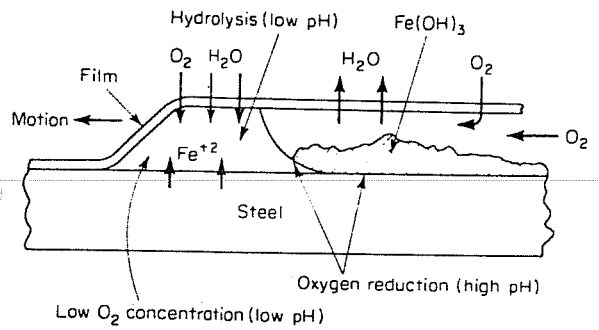

Figure 5.4 Underfilm Corrosion on a Steel Surface.[14]

Filiform corrosion is relatively insensitive to the type of protective coating on the metal surface. However, there is a tendency for coatings with low water permeability to suppress underfilm corrosion propagation.[14] Lowering the humidity of the surrounding concrete during service can reduce the risk of filiform corrosion. Minimizing damage to the coating surface further reduces chances of admitting water and oxygen necessary for active corrosion. Further studies are needed to explore this form of corrosion of the epoxy-coated reinforcement, particularly in the presence of chlorides.

CHAPTER 6
QUALITY OF COATING APPLICATION

6.1 General

In order for the epoxy coating to perform as a corrosion "barrier", a continuous sound layer of epoxy material must be well-adhered to the surface of the reinforcing steel. Satisfactory performance of coated bars in concrete is due, primarily, to the intrinsic protective properties of the epoxy material. However, poor application of even the best materials will render the coating ineffective. Thus, the quality of coating application is of utmost importance to the performance of the product.

In addition, coating imperfections and damage need to be controlled. These requirements call for effective inspection tools that can be conveniently used, especially in the coating plant. This chapter deals with an evaluation of two quality control measures specifically devised to detect coating imperfections resulting from improper application. The two techniques studied in this program are the widely-used holiday detector and a European quality control test known as the hot water immersion test.

6.2 Evaluation of Holiday Detection Process

6.2.1 Study Objectives. Although holiday detectors have been in use in reinforcing bar coating plants for some time, their effectiveness has not been well established. Concerns have been raised about the accuracy and reliability of such devices in detecting coating defects. The main objective of this part of the study was to evaluate the effectiveness of the typical holiday detectors in inspecting the integrity of the coating after application. Several factors that may influence the detection process were investigated. The full details of the study are given in Ref. 118.

6.2.2 Operation of Holiday Detectors. The operation of a holiday detector is based on the conductivity of defects present in a coated surface. Current passes through bar from the grounded end and the exploring electrode (usually with a damp sponge). Proper electrical grounding of the holiday detector to the base metal of the tested bar as well as conductive defects in coating are necessary to complete the electrical circuit. The exploring electrode is the means by which an electrical potential is applied to the surface of the coating. Normally, 67.5 volts DC are applied to the dampened sponge. Then the sponge electrode is either moved over the surface to be inspected or kept stationary while the rolling bar touches it. The latter arrangement is common at coating plants and is referred to as in-line detection. As the sponge passes over a void, the dampness provides the electrical conductivity to permit a small current to pass. As a result, a transistor oscillator is triggered, generating an 800-cycle audio signal. The low voltage and current involved qualify this as a nondestructive test.

Some important guidelines for improving the effectiveness of the electrode in holiday detection are:[102]

- the construction of the exploring electrode should be such that contact between the electrode and the entire circumference of the coated surface is maintained at all times; and,
- the exploring electrode should be kept clean and free of coating material and/or rough surfaces that might damage the coating.

In addition, grounding the holiday detector with the base metal should be properly maintained to allow continuous detection of the coated surfaces.

For the purpose of this study, the device selected for testing was a sponge-type, hand-held holiday detector (see Fig. 6.1). For use with reinforcing steel bars, the sponge was modified to provide closer contact between the coated surface and the sponge electrode. Two different sponges were used to fit the sizes of bars tested.

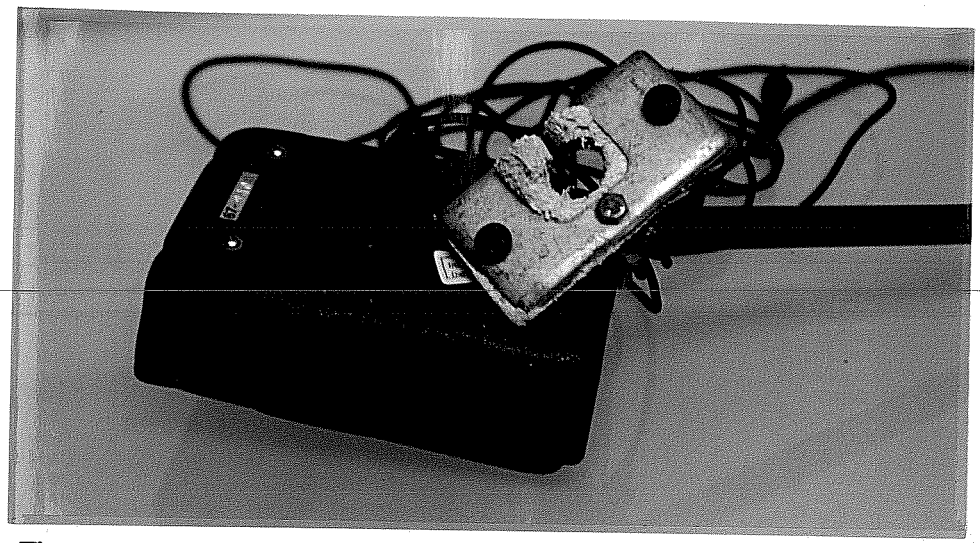

Figure 6.1 Holiday Detector Used for Experiment.

6.2.3 Evaluation Tests.

Test Parameters. Controlled holiday detection tests were conducted in which a number of variables were considered. A group of coated control bars was set up with differing types of damage. Bars were of two sizes and two deformation patterns. Operating conditions were varied in terms of the degree of moisture in sponge, speed of detection, and different operators.

Test Control Bars. A total of 12 epoxy-coated bars with two diameters, 13 mm (#4) and 25 mm (#8), and with parallel- and cross-type deformations were selected. These bars came from the same lot and were coated under identical conditions. The average coating thickness was about 250 μm (10 mils). Since the current use of holiday detectors is generally limited to inspecting straight bars during the coating process, the control bars were also straight. The length of each bar was 0.6 m (2 ft.). Five approximately equal regions were marked along each bar to facilitate data collection.

Different types of coating damage were deliberately introduced on some bars using a utility knife. The damage conditions included in the tests were as follows:

As-received: no additional damage introduced.
Hairline cuts: several short hairline cuts introduced.
Pinholes: small pinholes introduced.

Test Conditions. *Moisture in Sponge*. Moisture in the electrode sponge is necessary to complete the electrical circuit where discontinuities in the coating have been spotted by the holiday detector. The conditions of moisture affect the sensitivity of the electrical continuity and may, consequently, affect the reliability of the detection. No response is expected when the electrode sponge is completely dry. Varying moisture conditions need to be tested to establish their influence on the detection. In this study, three levels of moisture were selected. The following terms were used to describe the dampness of the sponge:

Wet: sponge dipped into water, removed without squeezing, and used when no excess water was dripping from sponge.
Squeezed once: sponge dipped into water and squeezed once.
Well-squeezed: sponge dipped into water and squeezed to remove as much water as possible.

Speed of Operation. Varying the time the sponge is passed over the whole bar may affect the ability of the operator to distinguish the number of signals. Three different speeds of detection were used to assess the differences in responses as a function of travel time. The following notations were used to describe travel speed along the test bar:

Fast: sponge electrode passed in 1 to 2 seconds.
Medium: sponge electrode passed in 3 to 4 seconds.
Slow: sponge electrode passed in 5 to 6 seconds.

Operator. Three different operators C, K, and R conducted the same detection tests to evaluate repeatability of the test results.

Test Procedure. Each operator inspected the 12 control bars using the three different speeds of operation, and for each speed three different moisture conditions of the sponge. As the holiday detector was passed along each bar, the operator counted the sound signals in each region. The number of these signals was considered to be equivalent to the number of discontinuities detected. Every pass at a certain speed and with a particular sponge dampness was repeated five times to generate enough data for comparison.

Data Analysis. The results of the detection tests were fully presented in Ref. 118. To summarize the information obtained from the large number of data points, only average numbers are furnished here. The responses from the five passes along each bar were added. Then, the results were accumulated for each bar group (a bar group consists of three bars of the same size and deformation pattern). The net sum was divided by 5 and again by the total length of the bars in the group. The resultant was the average number of defects detected per unit length. Such calculations were repeated for each sponge moisture condition and speed of detection for each operator. Only selected examples of the results are presented in the following section.

6.2.4 Test Results and Discussion.

Effects of Variable Moisture in Sponge. Figures 6.2 shows the responses obtained by operators C and K for 25 mm (#8) bars with parallel deformation pattern. It can be seen that the deviation was not significant for different moisture conditions when the detector was operated at a fast speed. However, when the speed of operation was lowered, the responses showed more deviation for different moisture conditions. Interestingly, opposite trends can be seen for the deviation of the responses obtained by the two operators. There was also no clear trend for the results obtained from the other groups of bars.

From these observations, it appears that moisture conditions did not have a distinct influence on the results. As long as there was moisture in the sponge, the detector was able to locate discontinuities in the coating.

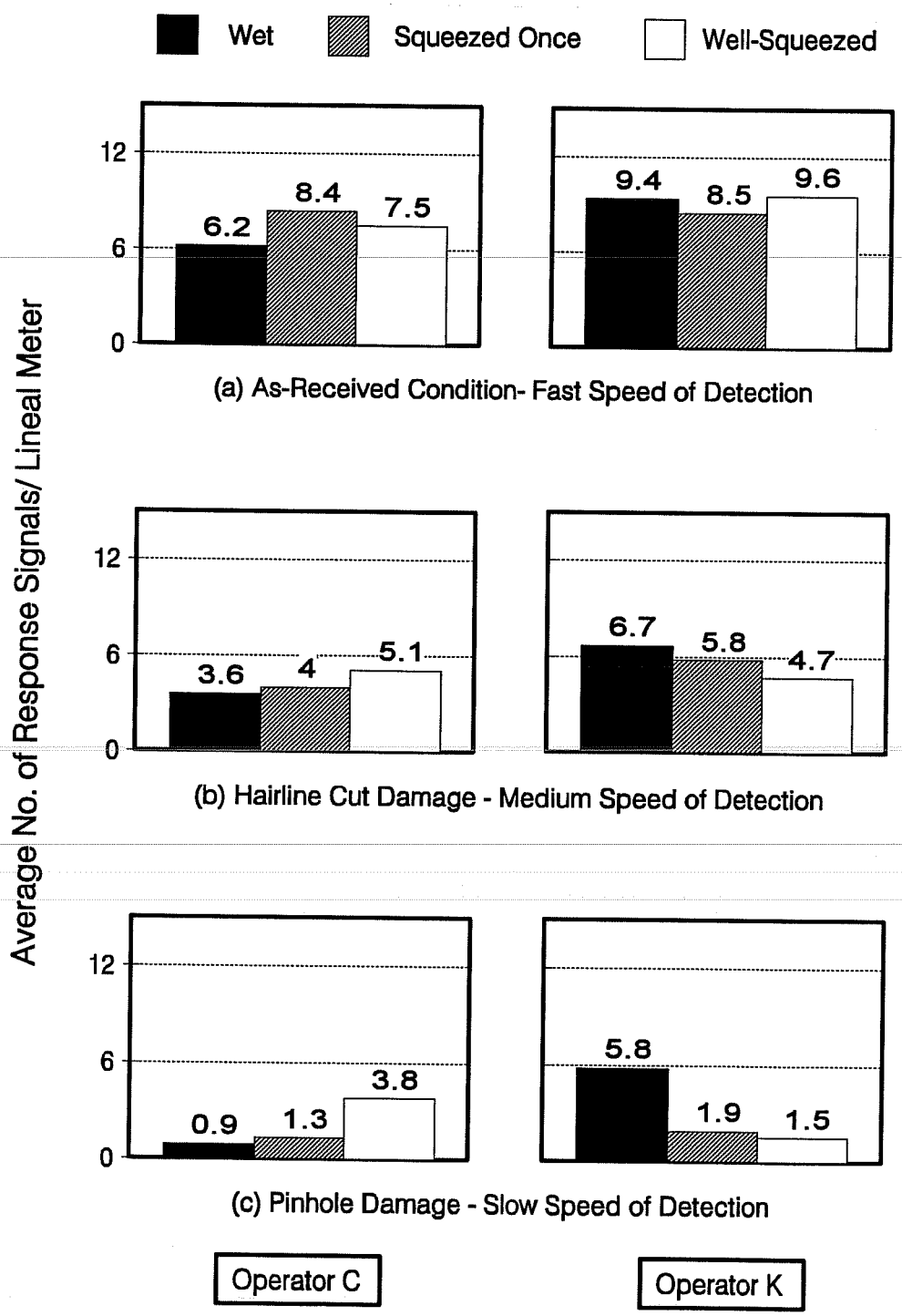

Figure 6.2 Holiday Detector Responses on 25 mm Bars with Parallel Deformations Using Variable Misture in Sponge.

Effects of Variable Speed of Detection. Figure 6.3 shows the responses collected at different speeds for 25 mm (#8) bars by both operators C and K. Generally, the slower the speed of detection, the higher the number of responses obtained. Slow detection was more reliable.

Effects of Different Operators. The use of a holiday detector depends primarily on the operator. Therefore, human errors were very significant in this test. Since personal judgements are heavily involved in determining the number of signals heard, and in assuring proper sponge/surface contact, considerable deviations between operators were expected.

As can be seen from Figures 6.2 through 6.4, responses counted by different operators deviated considerably. In addition, there was no clear tendency for one operator to consistently obtain higher or lower responses than the others. One operator might obtain maximum responses with one condition and minimum responses with another.

6.2.5 Conclusions. The effectiveness of the holiday detector was evaluated considering three main variables: moisture in the sponge; operating speed; and operator. The only clear trend involved the speed of detection.

Varying the moisture conditions gave inconsistent results. In some cases, higher responses were obtained with more moisture in the sponge while in others the opposite was found. Therefore, no general trend can be identified. Whenever there was moisture in the sponge, moisture was not a critical factor. However, the user of the holiday detector should know that, while ordinary tap water would suffice to wet the sponge on a coating up to 10 mils thick, a non-sudsing wetting agent should be used for thicker coatings. Moisture should penetrate any possible voids in the thicker coating and sudsy aqueous liquids will increase this ability. Usually, the manufacturer of the holiday detector suggests an acceptable wetting agent. The manufacturer should also instruct the user to make several passes with the sponge electrode to assure that moisture has penetrated all existing voids.

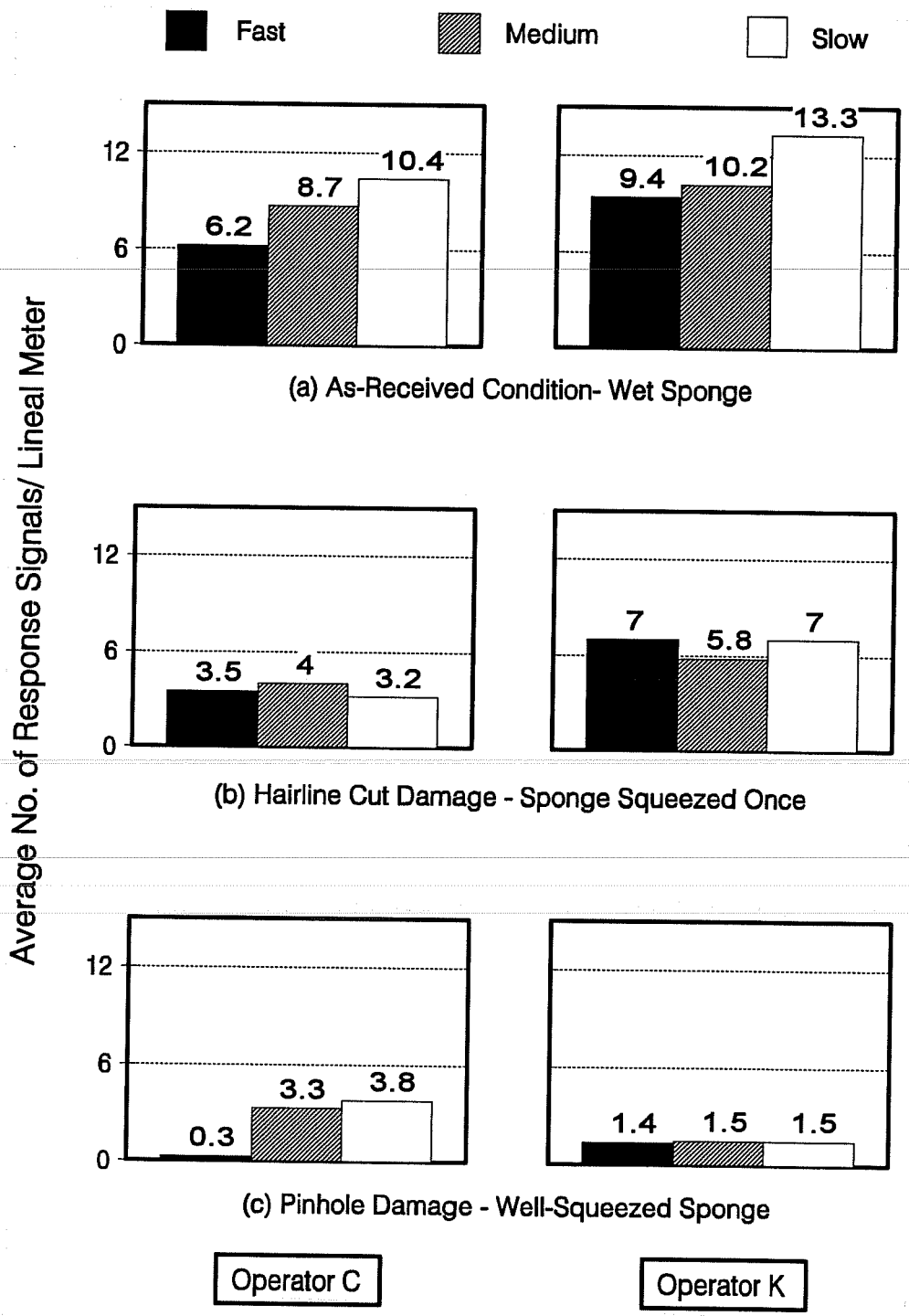

Figure 6.3 Holiday Detector Responses on 25 mm Bars with Parallel Deformations Using Variable Speed of Detection.

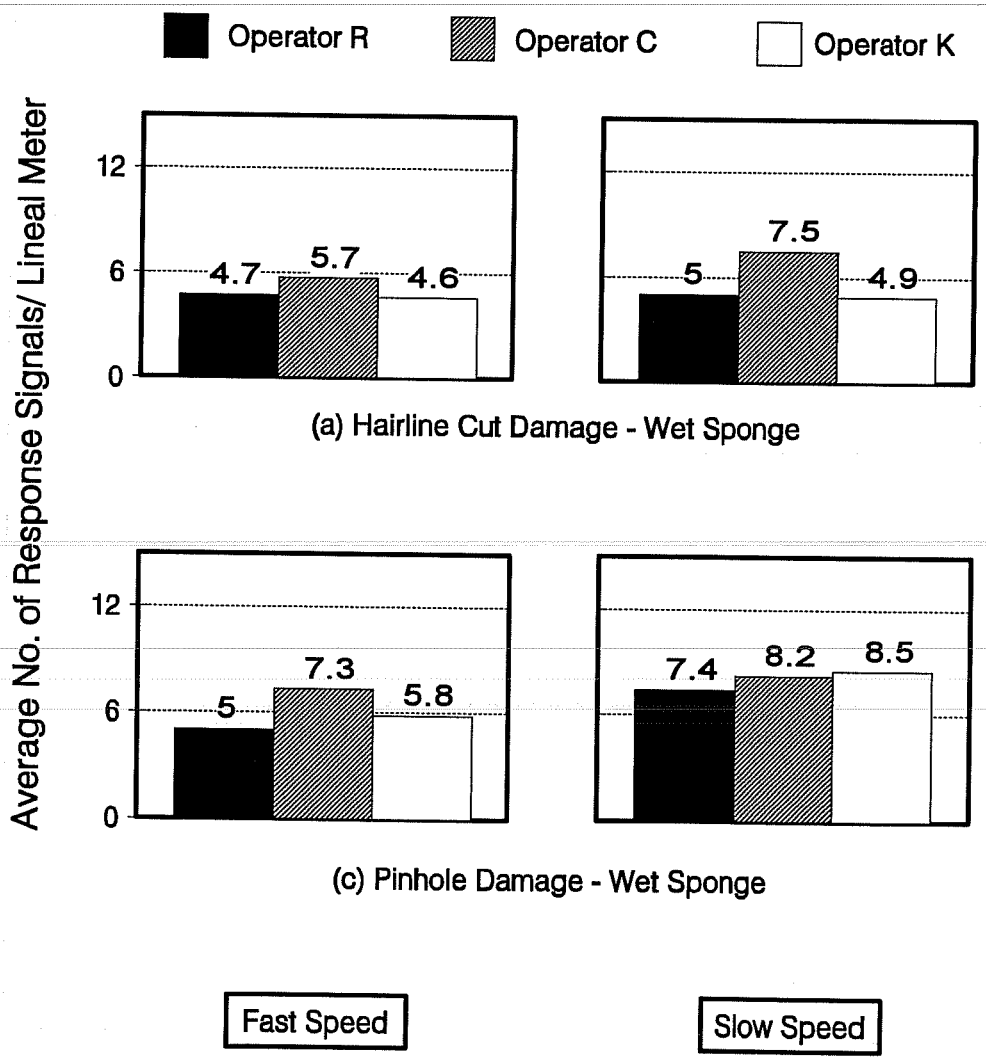

Figure 6.4 Holiday Detector Responses on 25 mm Bars with Cross Deformations Using Wet Sponge and Variable Operators.

Another critical factor when using a holiday detector is signal adjustment. This factor was not considered in this study, but it is important when testing bars with coatings thicker than 250 μm (10 mils). The detector's signal is usually factory set to trigger at an external resistive load of 80,000 ohms $\pm 5\%$, which is the standard for coating up to 250 μm (10 mils) thick. To accommodate coatings in excess of this thickness, the sensitivity of the device needs to be adjusted. A signal actuation load of 100,000 ohms is adequate for coatings up to 500 μm (20 mils) thick.

Generally, a slower operating speed led to more responses. Large deviations of responses were obtained for different detection speeds. What complicates the problem of having consistent responses is that a long signal may be treated as two or more short signals due to different operating speeds and different orientations of the sponge which may, occasionally, lose contact with the bar. It is worth noting here, that such a problem is especially cumbersome when inspecting bent bars. The inner and outer surfaces of bent bars usually have a large number of closely-spaced damage spots which are hard to detect separately.

The response distributions were, generally, dissimilar for different operators. Therefore, the number of signals counted may not accurately reflect the number of possible voids in the coating. Each operator detected the bars differently and used different judgment regarding the number of signals heard. Even when the responses of several passes were averaged, the deviations of the results among the different operators were still significant. This implies that repeatability of the holiday detection results is very poor.

In the study reported here, the number of responses obtained can only indicate possible defects in the coating. The readings gave no indication of the location and the size of existing defects.

An interesting observation was that the number of defects detected on the "as-received" coated bars was unexpectedly high. In many cases, the responses even exceeded the specified maximum allowable limit of the number of holidays per unit length, which is

6/m (2/ft.) on the average. This indicated that the bars did not meet the specifications at the time of the test. However, these bars passed the in-line holiday check at the coating plant before they were shipped and cut to size in the laboratory.

Based on the discussion above, a holiday detector generally cannot be considered a reliable device for detecting voids or pinholes in epoxy coating applied to steel bar surfaces. However, the general quality of the coating can be evaluated by careful holiday detection accompanied by visual inspection. It follows that the use of the in-line holiday detector may be continued by virtue of being a quality "indicator" during production. For acceptance or rejection purposes, however, random samples of coated bars need to be carefully checked by a separate holiday detector along with visual examination.

6.3 Proposed Hot Water Immersion Test

6.3.1 Study Objectives. The application of epoxy-coated reinforcing bars in the United States has drawn the attention of many European countries including Germany, Denmark, the Netherlands, and Switzerland. In search of an effective quality control test, one country has introduced the hot water immersion test. The purpose of the test is to check quality of coating application. Areas of the bar where coating defects usually appear are mill marks, sharp rib edges, bent portions, and the first and last coated straight lengths of the bar.

The use of this test in Europe deserves serious consideration for adoption in the US. The objective of this part of the study is to explore the usefulness of this test and its applicability to bent bars. The thrust for this work is based on the demand for a relatively quick and reliable quality control/quality assurance test.

6.3.2 Test Description and Criteria. Coated bar specimens (straight or bent) are placed in a hot water bath having a temperature of approximately 80° C (176° F) for seven days. The visual appearance of the bars at the end of this period indicates whether coating application was successful or not. According to Swiss guidelines for epoxy-coated

reinforcement,[119] a successful coating application should meet the following visual acceptance requirements:

- in previously undamaged areas, no deterioration is acceptable (inspection by microscope); and,
- in patched areas, deterioration such as the formation of blisters and damage visible to the unaided eye is acceptable.

The procedure of the hot water test may differ slightly from one country to another. Schiessl and Reuter[116] from Germany, mentioned the use of demineralized water warmed to 90° C (194° F) for testing coated bars by the immersion test.

6.3.3 Evaluation Tests.

Test Preparations. Six bent bars, four 13 mm in diameter (#4) and two 25 mm in diameter (#8) were used in the test. The radii of bending were 25 and 75 mm, respectively. These values are in accordance with ACI 318-89[70] requirements for minimum bend diameters. Each bar was deliberately damaged with the introduction of two 6 x 6 mm (1/4 x 1/4 in.) damaged areas. One of the damaged areas was patched with the same repair material used at the coating plant, while the other area was left with the steel exposed.

Test Setup. All bars were immersed for a week. The water temperature was maintained at 80° C (176° F) by a circulating heater connected to a preset temperature gage (see Fig. 6.5). The immersion tank was a 5-gal. plastic bucket.

6.3.4 Test Results and Discussion.

13-mm (#4) Bars. Before immersion, numerous hairline cracks were present on the bent portions of the bars with parallel deformations. After immersion, deterioration was observed at the cracks and the exposed damaged areas on both the inside and outside of bends (see Fig. 6.6). The patched areas did not deteriorate during the test.

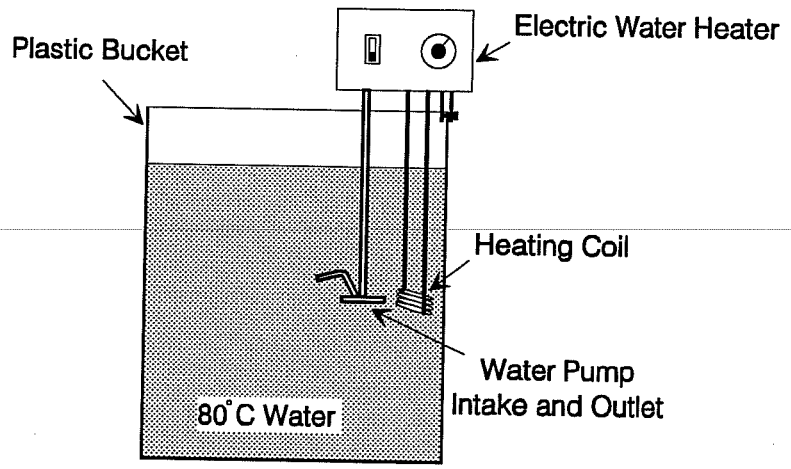

Figure 6.5 Schematic Illustration of Hot Water Immersion Test Apparatus.

On the bars with cross deformations, no hairline cracks were observed initially, but holiday damage was evident after testing as indicated by rust build-up at the holidays (see Fig. 6.7). Damaged areas with exposed steel deteriorated during this test as expected, but patched areas did not.

25-mm (#8) Bars. No visible signs of deterioration were observed on any bar where the damaged area was patched. However, damage on a few holidays was evident especially on bars with cross deformations. In addition, a considerable amount of rust was seen on the exposed steel areas (see Fig. 6.8 and 6.9). Minor deterioration occurred on the damaged areas on the inside of bends.

6.3.5 Conclusions. Based on the above observations, it is clear that all of the tested bars did not satisfy the requirements of the hot water immersion test. The quality of coating application was not satisfactory because of the deterioration that appeared on pinholes and cracks in previously undamaged areas. Integrity of coating was not maintained, especially along the sides of the lugs.

Figure 6.6 Deterioration of Exposed Areas on 13-mm Bar with Parallel Deformations.

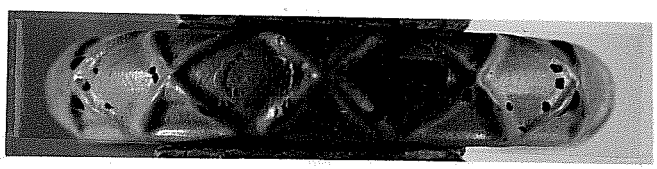

Figure 6.7 Deterioration of Exposed Areas on 13-mm Bar with Cross Deformations.

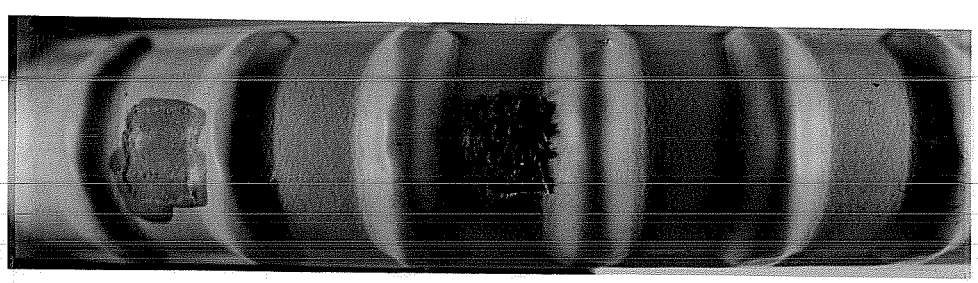

Figure 6.8 Deterioration of Exposed Areas on 25-mm Bar with Parallel Deformations.

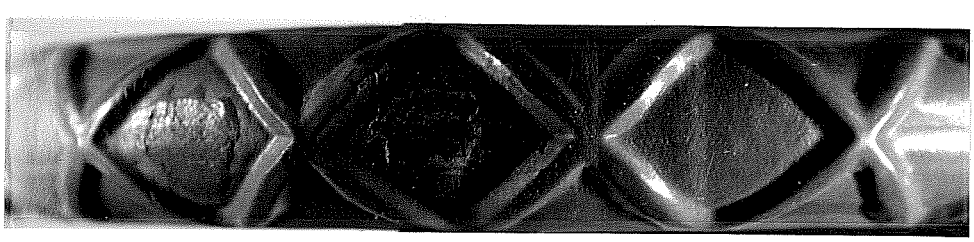

Figure 6.9 Deterioration of Exposed Areas on 25-mm Bar with Cross Deformations.

It is worth mentioning in this context that the hot water test is one of 16 different tests in the Swiss guidelines for coating quality control. Application of all these tests is meant to assure a high quality level in the coating system. The tests supplement each other by putting various constraints on the end product. With regard to bending of bars, for example, the Swiss guidelines require that a visual inspection of the coating does not show any signs of deterioration or damage in the curved area. This requirement would immediately cause the rejection of any bars with cracks or damaged spots anywhere on the inside or outside of bends produced by bending to certain mandrel diameters.

In conclusion, the hot water immersion test for coated bars (straight or bent) seems to provide an objective indication of the quality of coating application. The test was especially effective in identifying pinholes in the coating on bent bars. The convenience of this short test and its reliability indicate that further development should be undertaken to produce a coating quality control test. Future efforts should also reexamine acceptance criteria to remove ambiguity concerning checking the quality of application of patching material.

CHAPTER 7
EVALUATION OF DAMAGE TO EPOXY COATING DUE TO CONCRETE PLACEMENT AND VIBRATION

7.1 General

Vibration is used to eliminate voids and trapped air while consolidating the concrete in the forms and around reinforcing bars. The vibrator has an eccentric rotating mass which applies periodic force to the concrete. The concrete flows (or "liquefies") under the force and consolidates away from the vibrator. Internal or immersion vibrators (often called "spud" or "poker" vibrators) operate at a frequency in the range of 4,000-12,000 rev/min.[120] These vibrators are usually preferable in construction. The head of the vibrator imparts enough energy to excite and move the solid particles in the concrete mix. Although concrete flows, it does not move uniformly. The coarse aggregate particles are propelled from the vibrator head preferentially because of their greater mass.[120] Often, the vibrator operator forces the vibrator to contact the reinforcement cage to improve concrete consolidation around the bars.

It is expected that during casting and vibrating concrete, the aggregate particles and the vibrator will come in violent contact with the coated reinforcement. As a result, coating damage will occur. Damage at this stage of construction cannot be inspected or repaired, and it can be a major cause of poor performance in the future. Particularly, excessive damage on bent bars close to the concrete surface may lead to corrosion initiation and propagation.

This chapter summarizes a preliminary experimental study conducted to evaluate the degree of mechanical damage caused by concrete placement procedures. Recommendations to reduce this type of damage are also presented. Finally, future efforts for further examination of some solutions to the problem will be highlighted.

7.2 Damage to Coating Prior to Concrete Placement

Casting and vibrating concrete are the last conceivable sources of damage in the construction process. Any damage resulting is added to previous damage. In order to weigh this additional damage with respect to the overall coating damage, it is important to establish the amount of damage prior to concrete placement.

Earlier surveys were carried out in the states of Kentucky and Iowa in which epoxy-coated reinforcement installations were measured immediately prior to concrete placement to define the actual damaged areas.[106,107] In Kentucky, representative areas of about 2.3 m^2 (25 ft^2) of the 16 bridge decks were selected for visual inspection of bar damage. Several areas were studied on some bridges for more data. Coated bars with bare areas of different percentages were used to aid inspection.

Twelve decks showed an average damage between 0 and 0.010% of the bar surface area. Three other decks showed average damage between 0.011 and 0.04%. The worst damaged area on a single deck was 0.4%. It should be born in mind, however, that damage determination in the field based on visual inspection only is very difficult and, perhaps, inaccurate. The major problem is detecting damage on the underside of the bar mat once it has been installed. Therefore, it is anticipated that actual damage was greater than reported.

In Iowa, 36 individual bars were randomly chosen from a job site immediately prior to installation into columns. The estimation of damaged area in this case was based on an area representation card. Each damaged area on the bar was compared to 18 shaded squares or rectangles varying in area from 2.5 to 60.6 mm^2 (0.0039 to 0.094 $in.^2$). The maximum percentage of damage in 0.3 m (1 ft.) length was 1.08% of the surface area for the 48 mm (#15) bars and 0.88% for the 35 mm (#11) bars.

The surveys discussed above and other studies[93,96] show that damage levels prior to casting may vary considerably. The values fell close to zero when careful procedures were followed during the entire stages of production and construction. It was assumed that

normal good practice results in negligible damage to the coating in the order of 0.1%.[121] However, the aftermath of the Florida Keys bridge substructure investigations[93] revealed that a damage level of 1% was unavoidable before embedment of bars in concrete.

7.3 Evaluation Tests of Damage to Coating During Concrete Placement

7.3.1 Test Specimens. A series of three tests was conducted in this study to examine the damage that may be produced during vibration. The details of these tests were reported in Ref. 118. The first test simulated a column base with two mats of bars. The top mat consisted of 25-mm (#8) bars and the bottom mat consisted of 13-mm (#4) bars. Each mat consisted of two layers of bars in a perpendicular grid. Figure 7.1 shows the configuration of the formwork and the arrangement of bars used. All reinforcement was epoxy-coated. It was carefully examined and damage prior to placement of concrete was marked. Five vertical 13-mm (#4) bars were positioned at one corner. These bars were tied to the horizontal layers of bars by plastic-covered wire to avoid damage during the assembly of the bars.

The second and third tests simulated partial slab sections with one top mat of bars in each specimen. The mat consisted of 13-mm (#4) bars in one case, and 25-mm (#8) bars in the other. The bars were placed at different spacings and in perpendicular directions forming an irregular grid as shown in Fig. 7.2 and 7.3. An equal number of bars with parallel deformations and with cross deformations was used in both mats. Again, all the reinforcement was epoxy-coated and was examined in advance for any existing damage.

7.3.2 Test Procedure. Concrete was placed in the three prepared forms directly from the ready-mix truck. Figure 7.4 shows the specimens during vibration after placing concrete. A 50-mm (2-in.) immersion-type vibrator was used. Starting from the middle of the form, the vibrator was gradually moved around to consolidate the entire volume of concrete. For the column base specimen, concrete was placed and vibrated in several lifts. When the vibrator was wedged into the space between the cage and the form, it shook violently due to the limited space available. The most critical spaces in all the specimens

were the corners where the vibrator had little clearance between the bars and the forms. The concrete was vibrated for a few minutes in the slab specimens and for about 15 minutes in the column base specimen. The concrete was removed promptly and the bars were washed carefully. A thorough inspection was then carried out to document the coating damage due to vibration.

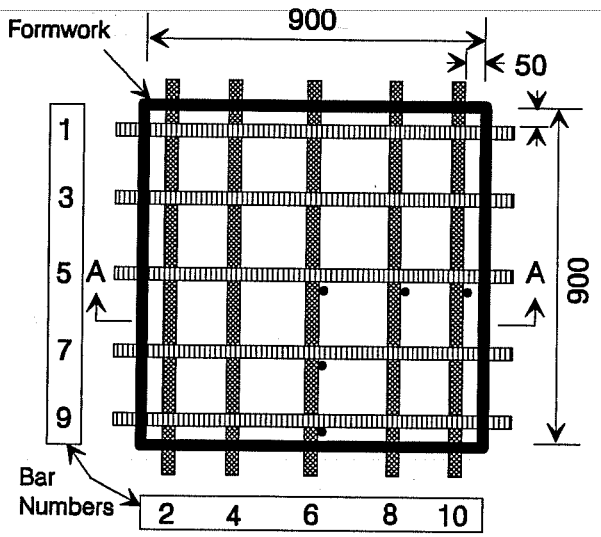

(a) Plan View

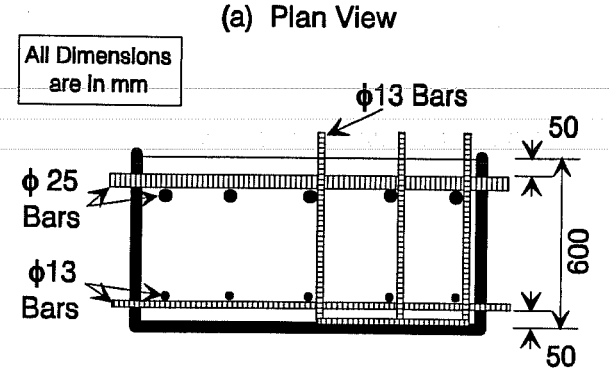

(b) Section A-A

Figure 7.1 Details of the Column Base Specimen.

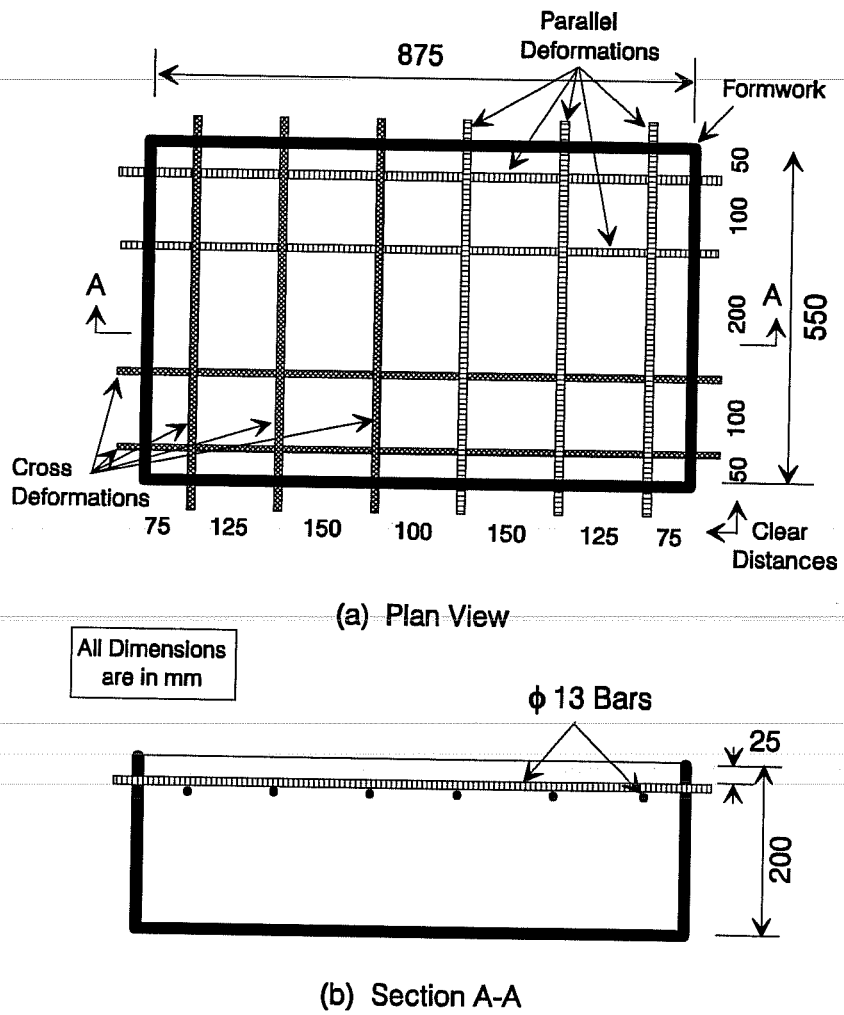

Figure 7.2 Details of the Slab Specimen with 13-mm Bars.

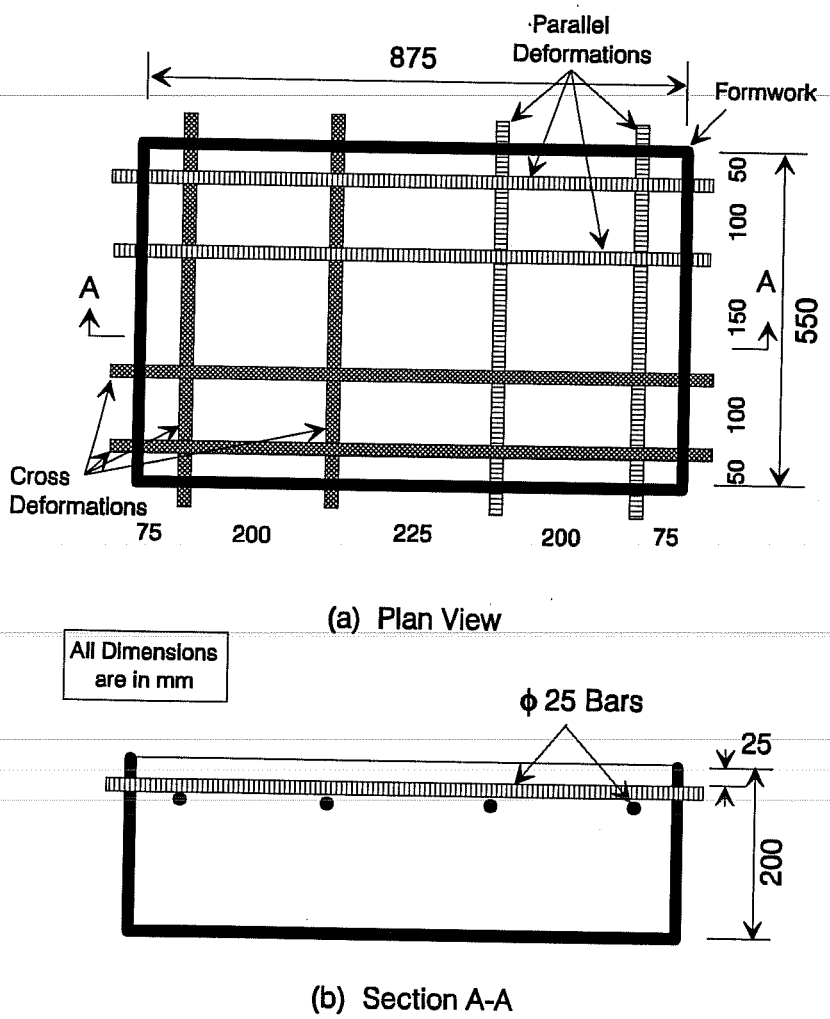

Figure 7.3 Details of the Slab Specimen with 25-mm Bars.

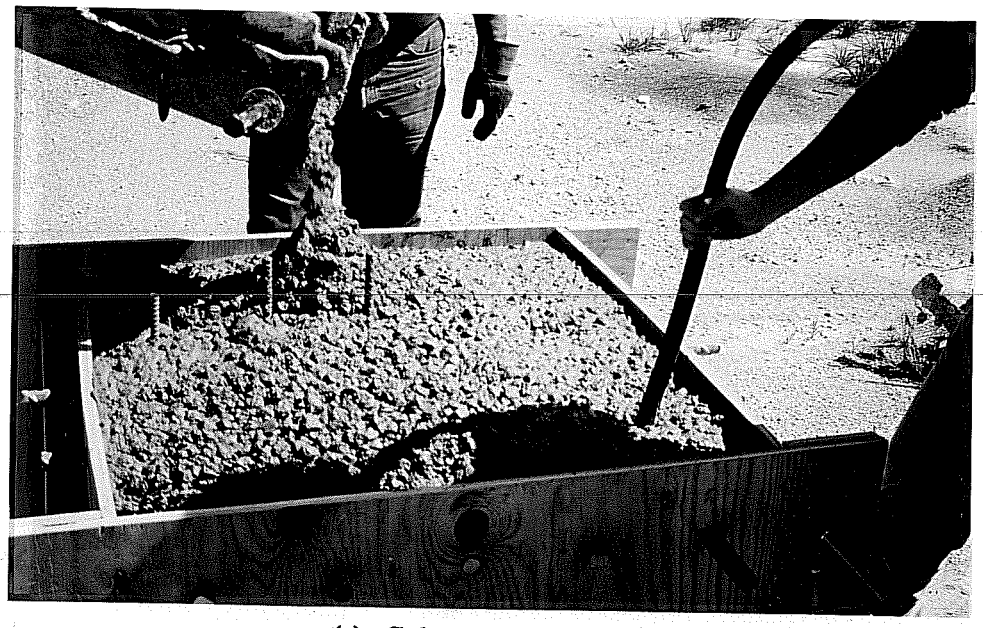

(a) Column Base Specimen

(b) Slab Specimen

Figure 7.4 Vibration of the Test Specimens.

7.4 Test Results

7.4.1 General Observations. Damage due to vibration appeared to have been caused by the abrasion between the vibrator and the bars. Bars located along the edges had the worst damage, especially those adjacent to corners.

7.4.2 Column Base Specimen. Damage caused by the vibrator during concrete placement could be generally identified by the rough surfaces of the coating. Some of these rough surfaces revealed considerable damage in which the bare steel surface had been exposed. The total damaged area of the coating on each bar ranged from 0.1 to 3.0% of the bar surface area.

The four bars on the side of the top mat (numbers 1, 2, 9, and 10) were significantly damaged. Several rough areas were observed along each bar. These areas were concentrated at the middle and near the ends of the bars. Damaged spots larger than 6 x 6 mm (1/4 in. x 1/4 in.) were found near the ends. Bars in the middle of the top mat (numbers 3-8) showed less damage due to vibration. However, several rough spots on the surface of the coating were found with the bare steel surface exposed.

Bottom mat bars showed a damage pattern similar to that of top mat bars. Bars on the sides were subjected to more violent contact with the vibrator than bars in the middle. Damaged spots measuring approximately 3 x 6 mm (1/8 x 1/4 in.) were observed especially near the corners.

7.4.3 Slab Specimen With 13-mm (#4) Bars. Similar to the column base specimen, damaged areas were easily identified by the rough surfaces of the coating caused by the vibrator. Isolated or inter-connected spots of variable sizes were found distributed along the bars. The majority of these spots had a size equal to or less than 1.5 x 1.5 mm (1/16 x 1/16 in.). Only a few damaged areas were relatively worrisome with the bare steel surface exposed. However, the largest spot did not exceed 6 x 6 mm (1/4 x 1/4 in.), which occurred at the end of one middle bar.

The total damaged area of the coating on each bar ranged from 0.1% to 1.1% of the bar surface area, whereas the maximum percentage of damage per linear 0.3 m (1 ft.) ranged from 0.2% to 1.7%. The distribution of total damage revealed no significant difference between the bars on the side and the bars in the middle. However, the most damaged lineal 0.3 m (1 ft.) of each bar almost consistently occurred near the end, indicating that damage was more concentrated in the areas of limited spaces for vibration.

An important observation is that the average percentage of damage of the bars with cross deformations was almost three times that of the bars with parallel deformations. Although this is highly dependent on the operator who controls the movement of the vibrator, the bar deformation pattern may be a contributing factor. For most angles of attack of the vibrator head, a bar with cross deformations will have a larger area of the lugs per unit length exposed for contact with the vibrator. For this reason, bars with cross deformations may be damaged more than those with parallel deformations under similar conditions of vibration.

7.4.4 Slab Specimen With 25-mm (#8) Bars. Damaged spots on 25 mm (#8) bars were larger and more frequent than those on 13-mm (#4) bars. The largest spot was a little less than 13 x 6 mm (1/2 x 1/4 in.) which occurred on one side bar with cross deformations. The side bars, in general, had the worst damage, especially near the ends.

For this specimen, the total damaged area of the coating on each bar ranged from 0.3% to 1.7% of the bar surface area. The maximum percentage of damage per linear 0.3 m (1 ft.), however, ranged from 0.4% to 2.2%. The distribution of total damage indicated that the side bars had, on average, three times the amount of damage found on the middle bars. Most of the damage was on the side bars with only 50-mm (2 in.) clearance.

The upper bars in the mat were, generally, more damaged than the lower bars. Damage on the bars with either type of deformation (the parallel or cross deformations) was not significantly different. In any case, the pattern of damage or roughening of coating surface was typical of that observed in the other two specimens.

7.5 Discussion of Results

The three specimens consistently showed that vibration of concrete during placement can produce considerable damage to coated reinforcing bars. Typical damage due to vibration consisted of abrasion and roughening of the surface of the coating. Damage was generally limited to the lugs, as they were the most likely part of the bar to come in contact with the vibrator. Where space for motion of the vibrator was limited, damage was the worst as indicated by damage concentrated near the ends on the side bars at form corners. Examples of the damage observed on the test bar specimens are shown in Fig. 7.5.

The total damaged area of the coating on each bar in the three specimens ranged from 0.1% to 3.0% of the bar surface area. The distribution and average percentage of damage for each group of bars (on the side or away from the edge) is delineated in Fig. 7.6. According to ASTM D3963 specification,[39] bars with a damaged area larger than 2% of the total surface area per linear 0.3 m (1 ft.) and damage spots with a size greater than 6 x 6 mm (1/4 x 1/4 in.) should be repaired. In the tests performed damage to some of the bars was greater than 2% of the total surface area and some bars had damage spots exceeding the size limit.

Different bar sizes have different surface curvature which results in unequal contact areas between the bar and the vibrator head. Larger size bars have more contact areas and, therefore, more chances of locking small aggregate particles in between the two colliding surfaces than small size bars. Therefore, the 25-mm (#8) bars are more susceptible to damage due to vibration than the 13-mm (#4) bars. This trend is clear in Fig. 7.6. The smaller size bars, in the three specimens, did not show damage that exceeded both the 2% limit and the spot size limit. Damage to some 25-mm (#8) bars, on the other hand, exceeded both limits.

In addition, damage on the side bars tended to be worse than on the middle bars, especially where the side clearance is limited to 50 mm (2 in.). Damage average percentages were clearly higher for side bars than for middle bars for both bar sizes as shown in Fig. 7.6.

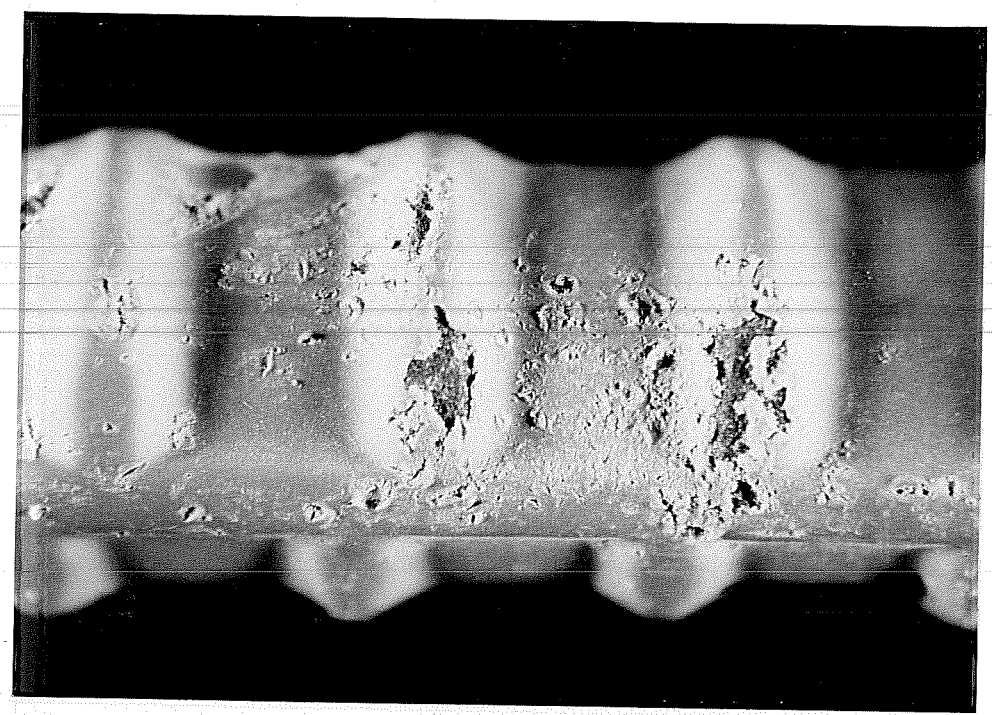

(a) Bar with Parallel Deformations

(b) Bar with Cross Deformations

Figure 7.5 Examples of Damage Due to Vibration.

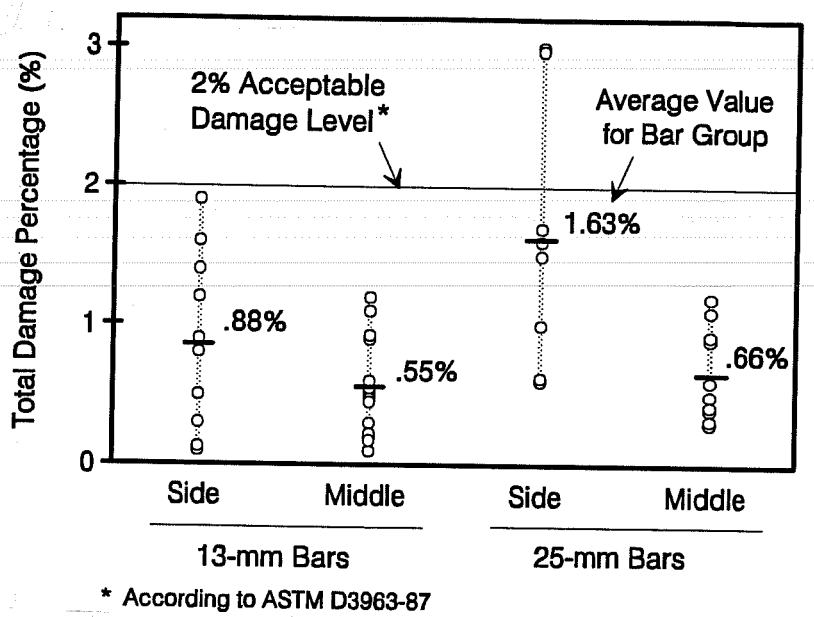

Figure 7.6 Total Coating Damage Percentage for All Tested Bars.

The largest damaged spots in the three tests occurred on bars with cross deformations. Since the database is quite small, more tests may be needed if the effects are to be quantified.

To study the occurrences of certain levels of damage, a histogram was prepared (see Fig. 7.7) combining the results of both bar sizes. A total of 70% of the bars (two-thirds of which were the smaller size) did not exceed 1% total damage of the bar surface. One-quarter of the bars fell in the damage range of 1.1-2%. Only 5% of the bars (all the larger size) exceeded the 2% specification limit.

It is important to notice that the above discussion of results referred to the total damage percentage with respect to the embedded surface area of bar. The specification limit of 2%, however, applies more specifically to the worst 0.3 m (1 ft.) length. If the results were expressed in terms of the worst (most damaged) 0.3 m (1 ft.) length of bar, the effect would be as shown in Fig. 7.8 for the slab bars. Only 61% of the bars instead of 83% fell in the damage category of 0-1%. The number of bars with damage between 1.1 and 2%

increased from 20 to 28%. Most importantly, the fraction of bars which exceeded the 2% limit rose from zero to 11%. Therefore, considering the worst 0.3 m (1 ft.) damaged piece of the bar tends to shift the results towards more rejected bars.

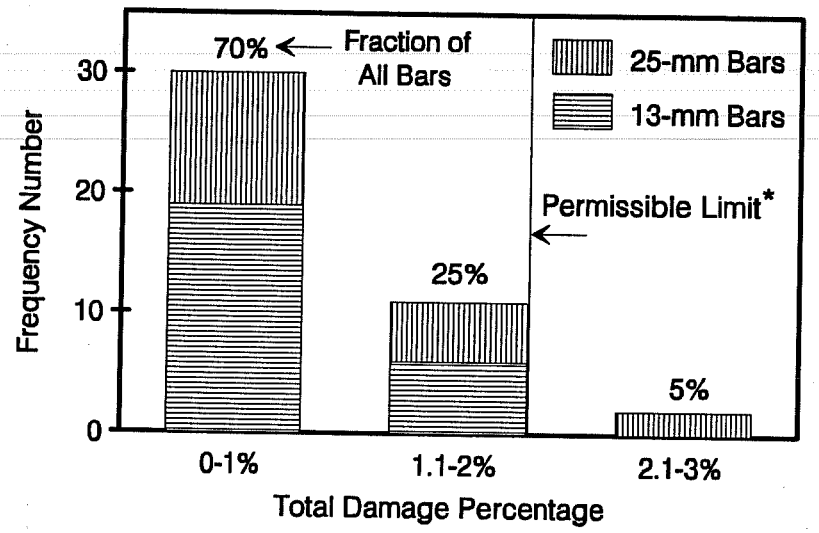

Figure 7.7 Histogram of Total Coating Damage Percentage for All Tested Bars.

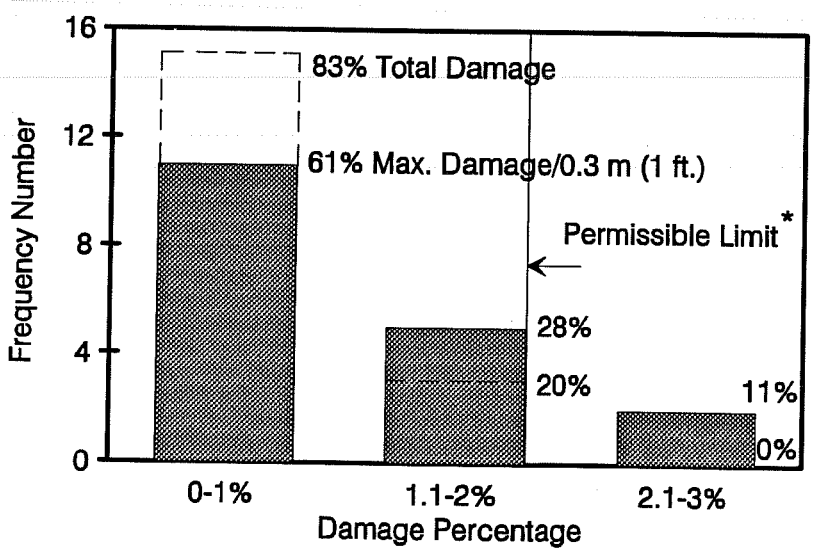

Figure 7.8 Histogram of Coating Damage Percentage for Slab Tested Bars.

7.6 Conclusions

The most important conclusion is that even if the bars were carefully handled and all visible damage was patched before placing concrete, the bars might still be subjected to considerable damage during concrete placement. Therefore, damage due to vibration should not be ignored. Damage of this sort cannot be repaired and can have a detrimental effect on the performance of epoxy-coated reinforcement. It is reasonable to expect that the most damaged bars will be those near the surface of concrete.

Based on the limited number of tests performed, damage due to concrete placement and vibration can, on the average, reach from 0.85 to 1% of the total surface area of bar. Adding this damage to the estimated 1% damage before casting would raise the total defective surface area to about 2%; which is the current specification limit.

It is believed that damage due to vibration can be reduced by proper precautions. By following standard operating procedures and using common sense, damage can be effectively minimized. The vibrator should be lifted up and down to avoid dragging the vibrator head over bars, which causes damage. Special care should be taken when the vibrator is used in a confined space to avoid violent contact between the vibrator and the bar.

Additional techniques for improving vibrating practice may also be adopted. Some equipment suppliers are proposing the use of "soft" vibrator heads for use with epoxy-coated reinforcement, but such equipment was not evaluated in this study. It was seen from the experience with bending operations that protective sleeves (high density plastic rings) on mandrel greatly reduced damage on the inside of the bends, and it may be possible to obtain similar results with nonmetallic vibrator heads. However, it is recommended that "soft" vibrator heads be investigated before implementation to determine whether they actually prevent damage and still produce well-consolidated concrete.

CHAPTER 8
IMMERSION TEST OF BENT EPOXY-COATED REINFORCEMENT

8.1 General

One method of quickly examining the effectiveness of epoxy coating in protecting underlying steel from corrosion is to subject coated bars to a severely corrosive environment. A commonly used corrosive environment for rapid testing is submersion in a sodium chloride solution (3.5% NaCl). Although this environment is not the same as that for epoxy-coated reinforcing bars in service, it provides a means for studying corrosion behavior. This chapter describes an experimental study undertaken to evaluate a few key aspects of corrosion of fabricated epoxy-coated reinforcement. A chloride solution was used as a testing environment to accelerate corrosion and to allow continuous visual monitoring of the behavior of the coated bars.

The immersion test was performed in conjunction with tests of companion bar specimens embedded in concrete prisms and subjected to alternate wetting and drying cycles. The macrocell corrosion study is described in Chapters 9 and 10. A background for both tests, including factors for selecting study variables, and emphasis on testing damaged fabricated bars are presented in Chapter 9. The bars used for the immersion test were procured and prepared following procedures similar to those described for the macrocell test in Appendix C. In addition, the details of the immersion test, and the interim results were reported in Ref. 118.

In the immersion test, bars bent 180° were artificially damaged to levels comparable with acceptable damage limits in current specifications. These limits were discussed in Section 3.4.1. Three replicate specimens were tested for each condition of damage. Table 8.1 summarizes the test variables and Fig. 8.1 shows the configuration and dimensions of the test bars. A total of 66 bars were included in the study.

Table 8.1 Immersion Test Variables

Group No.[a]	Deformation Pattern	Damage Category Size or Percentage[b]	Damage Condition
1	Parallel	Control (Uncoated Bars)	-
2	Parallel	Spots > 6 x 6 mm	Patched
3	Parallel	Spots > 6 x 6 mm	Exposed
4	Parallel	Small Spots > 2%	Patched
5	Parallel	Small Spots > 2%	Exposed
6	Parallel	Cracks < 1%	Exposed
7	Parallel	Small Spots < 2%	Exposed
8	Cross	Control (Uncoated Bars)	-
9	Cross	Spots > 6 x 6 mm	Patched
10	Cross	Small Spots > 2%	Exposed
11	Cross	Pinholes < 1%	Exposed

a The same for bars 13 mm in diameter (#4) and 25 mm in diameter (#8)
b Area damaged/total area immersed

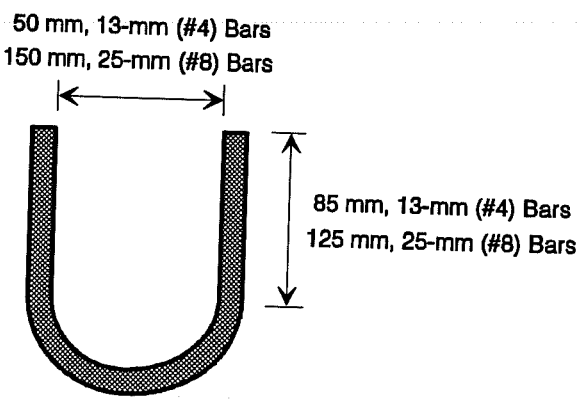

Figure 8.1 Configuration and Dimensions of Immersion Test Bars.

The amount of damage caused originally by bending varied according to deformation type and bar size. Bars with cross deformations showed pinholes concentrated at lug/bar intersection (lug base), especially where lugs crossed. Bars with parallel deformations showed rows of tiny cracks at transverse lug bases. The size of bar also affected the formation of hairline cracks. Tightly bent small diameter bars showed more cracking than those with larger diameter bent to a larger radius.

For the test specimens, the initiation and progression of corrosion with time was studied by visual examination. A detailed visual examination was carried out at the end of specified periods of exposure. The behavior of the different groups of bars was compared on the basis of corrosion characteristics of each group. Evidence of softening, discoloring, debonding, and changes in film integrity was recorded for assessment of relative durability of the coating. Further, the degree of rusting on coated and uncoated bars was assessed qualitatively. Removal of bars for detailed investigation of surface condition and underfilm corrosion was done at three exposure periods: 8 months; 18 months; and 24 months.

8.2 Test Setup and Procedure

The bent epoxy-coated reinforcing bars were immersed in a naturally aerated 3.5% NaCl solution with the outer surfaces of bends facing down. The solution was stagnant and exposed to laboratory air in a temperature-controlled room. To further accelerate the test, the exposure regime consisted of cycles of immersion for four days followed by drying in air for three days.

In order to prevent damage to coating during testing, the bars were hung from a wooden frame using nylon strings. The frame was built to permit lifting the bars out of the solution during drying periods. The bars were suspended above the saltwater level so that any solution on the bars would drop into the immersion bucket. To account for possible evaporation of water, a constant concentration of the solution was maintained by adding water to a fixed depth. Figures 8.2 and 8.3 show the test setup.

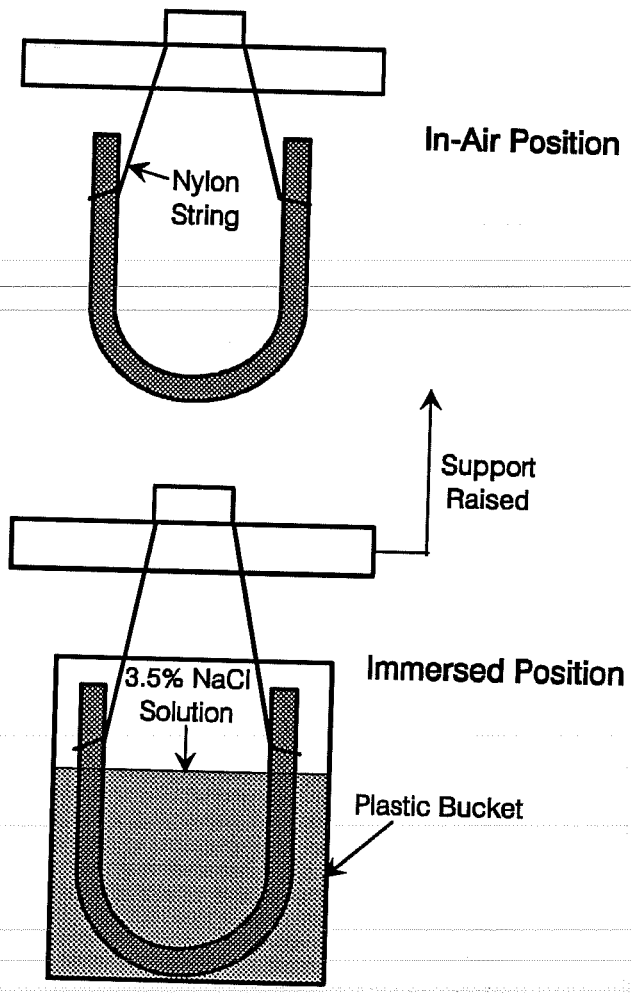

Figure 8.2 Schematic Drawing of Immersion Test Setup.

8.3 Observations of Immersed Bars

8.3.1 Initial 8 Months. The uncoated bars, as well as the damaged areas on the coated bars started to corrode immediately after submersion in salt solution. Brown corrosion products began to build up over the damaged areas, but were brittle and easy to remove. Figure 8.4 shows examples of the damaged areas of both deformation types and the progression of corrosion in these areas after 8 months of testing. Both the inside and outside portions of bends were similar in their behavior. The inside portions of bends were as

susceptible to corrosion as the outside portions, even though it appeared that the coating on the outside of the bend had only been compressed.

Figure 8.3 View of Immersion Test Setup.

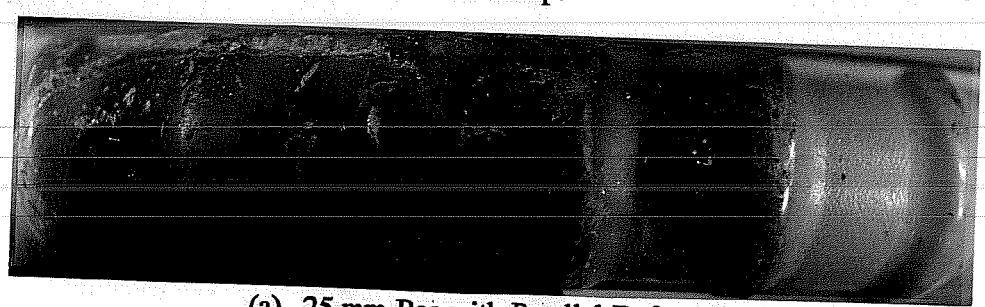

(a) 25-mm Bar with Parallel Deformations

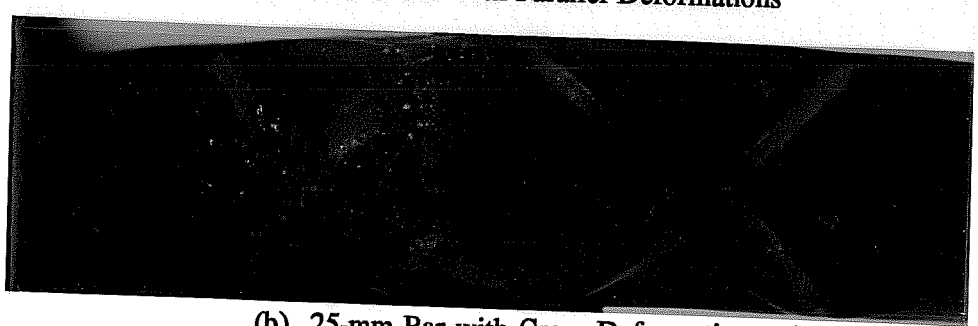

(b) 25-mm Bar with Cross Deformations

Figure 8.4 Corrosion on Damaged Areas of Coating After 8 Months of Exposure.

Patched areas showed no signs of corrosion for the first few weeks, but then corrosion was evident at the patches. At first, the patched surface was smooth and shiny. With time, bubbles and brown spots developed, and then the coating started to break down where the bubbles formed. At this stage, corrosion was accelerated as saltwater penetrated the damaged coating. After 8 months of immersion, a considerable amount of corrosion products had accumulated on the patched areas (see Fig. 8.5).

Corrosion was also apparent at holidays in the coating that were not detected in advance. Corrosion on holidays was evident from small brown spots scattered along the bar (see Fig. 8.6). It was evident that most of the holidays were located on the deformations or along their sides. In general, more holidays existed on bars with cross deformations than on bars with parallel deformations. It was also noticed that as the area of introduced damaged decreased, corrosion on holidays and small damaged spots increased.

In comparison with coated bars, uncoated bars corroded severely with considerable rust buildup on their surfaces. Bar features, such as deformation lugs, were degrading.

8.3.2 After 18 Months. Conspicuous corrosion products built up to a thickness of about 1.6 mm (1/16 in.) over the damaged areas and pinholes all around bar. The corrosion products were solid and were brown to dark-brown on the surface but darker inside. The coating appeared more discolored than in earlier stages of immersion testing. No appreciable difference of corrosion between the two deformation patterns existed.

Generally, corrosion on the inside of bends was intense. The damaged areas showed corrosion product buildup to various degrees. Many swelling spots were visible on the bar surface between lugs, particularly along the longitudinal rib where pinholes were most concentrated (see Fig. 8.7). The swelling areas were more prominent on the inner side of bend than on the outer side, and on bars with parallel deformations compared with cross deformations.

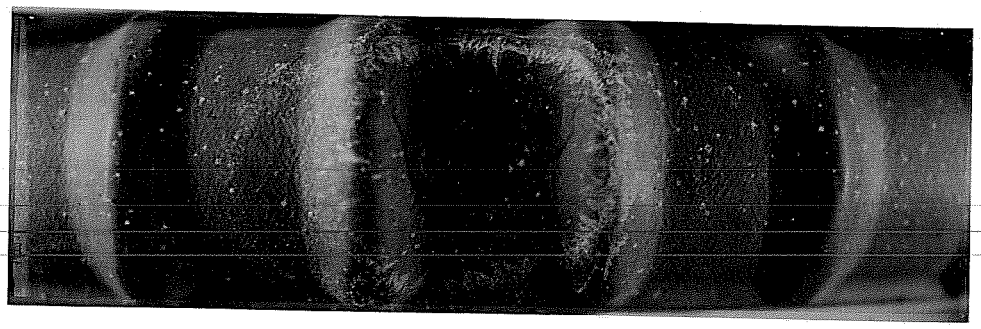

Figure 8.5 Corrosion on Patched Damaged Area of Coating After 8 Months of Exposure.

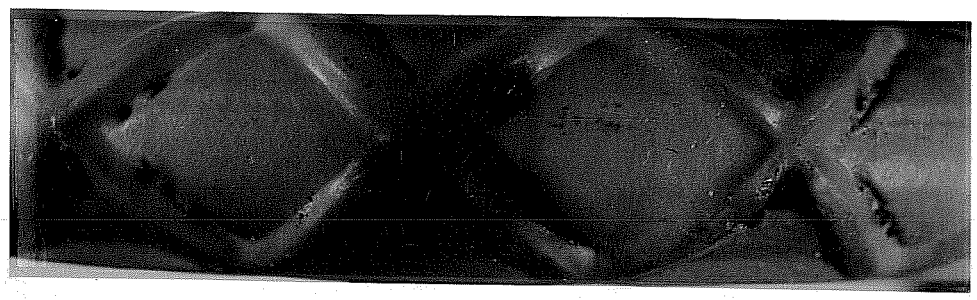

Figure 8.6 Corrosion on Holidays After 8 Months of Exposure.

Figure 8.7 Swelling Areas on 25-mm Bar After 18 Months of Exposure.

Patched areas showed less corrosion than unrepaired areas. Corrosion also continued to progress on holidays and hairline cracks in the coating which were more obvious on small bars than on large bars.

For comparison, the uncoated bars suffered severe corrosion with considerable rust buildup on their surfaces. Corrosion was general, causing uniform degradation of the deformations. The severity of corrosion activity on uncoated bars was greater than that on coated bars.

Of interest were the patterns of coating failure observed on new 13-mm (#4) bent bars added to the immersion test. These bars were coated with materials from different suppliers and bent on properly protected mandrels. The new bars were also damaged to various levels (above 2% and below 1%) and some were patched. Although corrosion product buildup on the outer surfaces of bends was similar to that described above, the epoxy film cracked alongside the continuous rib in the bent area (Fig. 8.8). Further, tiny longitudinal cracks, sometimes associated with swelling spots, were observed at different locations where corrosion products accumulated and breached the coating. Figure 8.9 shows an example of these cracked areas. Only minor corrosion was observed on the inside of bends as they were almost free of initial damage.

8.3.2 After 24 Months. Corrosion products built up to about 2.4 mm (3/32 in.) over the damaged areas and pinholes all around bar. The brown crests were solid but cracked revealing granular black corrosion products inside. The crests on pinholes were mostly brittle and easy to remove. The coating broke down and was discolored over considerable portions of length. The patched areas showed extensive corrosion roughly similar to that on unrepaired areas. Figure 8.10 shows examples of corrosion progression in damaged and patched areas of both deformation types after 24 months of testing.

In a few cases, corrosion buildup on the inside of bends was, greater than that on the outside. Swelling areas were largely concentrated along the continuous rib which exhibited cracking and corrosion spotting (Fig. 8.11).

Figure 8.8 Coating Cracking Along Continuous Rib Due to Corrosion.

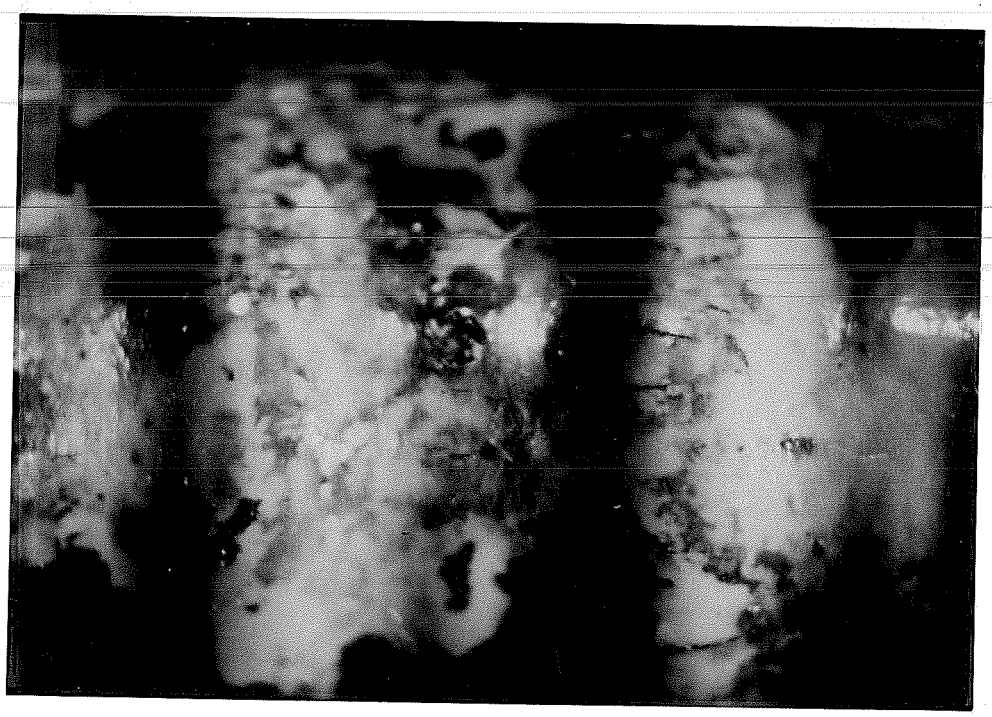

Figure 8.9 Coating Longitudinal Cracking Due to Corrosion.

The condition of uncoated bars was similar to that after 18 months of exposure. Thick layers of solid brown, orange, and black corrosion products covered the bars. The lug profiles were also degraded uniformly. Figure 8.12 shows an example of an uncoated bar after 24 months of cyclic exposure to salt solution.

Figure 8.11 Coating Cracking and Corrosion Spotting Along Continuous Rib.

Figure 8.12 Corrosion on Uncoated Bar After 24 Months of Exposure.

8.4 Condition of Bar Under the Coating

Generally, observations of the steel substrate under the coating revealed surface conditions that were not considerably different at the three times specimens were removed from the solution and examined (autopsy). The observations are combined in this section and only major differences are noted. The surface condition under the coating was inspected to qualitatively evaluate the extent of corrosion.

During coating removal, it was noticed that coating on the bend peeled off much more easily than coating on the straight portion. Bar size and deformation type also affected the ease or difficulty of coating removal. Generally, the coating on large bars with parallel deformations was the easiest to remove. In all cases, the epoxy coating was more difficult to remove before immersion testing than afterward.

Underfilm corrosion was identified by dark brown spotting. In general, corrosion penetrated under the coating about 6-13 mm (1/4-1/2 in.) from the edge of the damaged area. Where damaged areas were close to each other, undercutting was continuous (see Fig. 8.13). This condition was common inside bends where damage due to bending existed on every transverse lug. Undercutting was similar outside and inside the bends.

Brown corrosion spots spread on substrate steel mainly where damage (or an undetected defect) or loss of adhesion occurred. Surface corrosion was minor with insignificant pitting, even after 24 months of testing. Bars with minimum surface damage, for example holidays and pinholes only, had limited underfilm corrosion progression. The rest of the bar surface appeared dull or covered with a very thin dark layer. Figure 8.14 shows the condition of steel surface around minor coating defects. Generally, the straight portions of the bars remained unaffected with a bright or slightly dull surface underneath the coating.

In addition to these observations, bars examined after 18 and 24 months disclosed some wet areas with black-greenish products under the coating. There were also other areas

The 25-mm (#8) bars showed fewer cracks and less corrosion at the lug/bar intersection compared to 13-mm (#4) bars. The tighter bending radius of small bars is likely the main reason for developing more cracks in the coating. The bending radius was 4d (d=diameter of bar), or 50 mm (2 in.), for the small bars compared to 6d, or 150 mm (6 in.), for the large bars. The type of deformation also affected the formation of cracks. Bars with parallel deformations exhibited more hairline cracking along the lugs.

It seems that adhesion was initially weakened because of bending (stretching of coating) and it continued to deteriorate as corrosion (undercutting) developed with time. The bent portions exhibited extensive coating debonding after exposure to alternate wetting by salt solution and drying, and at locations where corrosion on damaged spots inevitably occurred. In their corrosion experiments, Zayed and Sagues,[84,109] also indicated that corrosion proceeded along metal-epoxy crevices developed by coating delamination during deformation.

8.5.2 Surface Corrosion. It appeared that surface corrosion at the exposed steel areas occurred to different oxidation levels. The outer brown layer indicated a higher oxidation level of ferric compounds, while the inner dark product indicated a lower oxidation level of ferrous compounds. It was suggested that the brown product was hydrated hematite, while the darker product was magnetite.[84]

The patched areas showed corrosion shortly after the immersion test was started which indicated that patched areas were vulnerable to corrosion. When the liquid coating material was applied, it did not harden quickly enough to avoid flowing from the top of the lugs which resulted in a thin layer of coating over the lugs. Additionally, liquid epoxy contains solvents that evaporate after application resulting in pore formation.[29]

Corrosion morphology of the tested bar specimens was very similar to that described by other researchers. Early in the immersion test, corrosion with minimal metal loss appeared on exposed steel and coating imperfections, but debonding was significant. The same observations were made by Sagues *et al.*,[83,93] in similar tests. Failure of the epoxy coating in the form of tiny longitudinal cracks was also described by Hededahl and

Manning.[81] It is reasonable to assume that the planes of weakness of the coating are perpendicular to the direction of epoxy flow during coating application and curing. As the epoxy flows on the rotating bar and rapidly starts to cure, the frictional stresses create planes of weakness between the parts that cure successively. In addition, coating on the longitudinal rib is prone to break as noted by Treadaway and Davies,[62] and Rasheeduzaffar, *et al.*[113]

The epoxy coating is particularly weak at surface defects and excessively sharp edges of the reinforcing bar. Examples are rolling flows, sharp angularity of deformations, and mill marks. Failure of the coating and corrosion are often triggered at these weak points. Corrosion then propagates to adjacent areas which become debonded. The quality of the base steel is important and should be carefully considered at the coating stage. CEB bulletin No. 211 states that there should be controls to the type of steel to be coated, especially its rib profile.[29] Experience has shown that longitudinal ribs frequently result in higher levels of pin holes in the coating. It is difficult to thoroughly clean and coat at longitudinal rib bases.

The sides of lugs are areas where coating is usually difficult to apply uniformly; therefore, holidays tend to concentrate more in these areas than elsewhere. Cross deformations are more complex than parallel deformations and, hence, are more prone to have holidays. However, the variation in performance of bars with different deformation patterns may also depend on many other factors such as coating operation, coating thickness, and the ability of coating to "stretch" without breaking during bending.

Early in the test, corrosion on holidays and on tiny damaged areas increased as the introduced damaged area decreased. This could be due to the effect of unfavorable area ratio between large cathodes and small anodes. For a given current flow in a corrosion cell, the current density is greater for a small corroding electrode than a large one. The greater the current density in an anodic area, the greater the corrosion rate. For the test bars, corrosion was initiated by anodic and cathodic reactions on exposed steel areas. The coating was debonded and the electrolytic solution penetrated beneath the coating, through the damaged areas. As more surface area was available for cathodic reactions, corrosion on small anodic sites became more severe.

Another explanation is that the probability to nucleate a corrosion cell on a larger damaged area is higher than on a smaller area (such as a holiday). Once corrosion is initiated, the potential difference between the anode and surrounding cathodes increases. Consequently, corrosion activity increases and results in more metal dissociation on larger damaged areas.

8.6 Corrosion Mechanism

From observations of corrosion progression on damaged coated bars immersed in salt solution, it is likely that the corrosion mechanism proceeded as follows:

Due to the uniformity and high conductivity of the electrolytic solution, no significant potential differences between exposed steel areas were generated. As a result, many small pits were initiated simultaneously at an early stage, but corrosion activity was not sufficient to cause severe pitting. The anodic reactions were under simple activation control, while the cathodic reactions were under mixed activation and diffusion control. Corrosion products accumulated with time as more steel dissociated from the base metal.

Coating debonded around exposed steel surfaces and small coating imperfections and extended over much of the bent portion. Coating separation might have been initiated and aggravated by one or more of the following processes:

- fabrication;
- anodic activity extending under the coating (undercutting); and,
- cathodic activity extending under the coating.

Cathodic debonding, which was indicated by bright metal and untarnished backside of pried coating, permitted additional reduction reactions to take place on the metal surface. Anodic activity or undercutting, however, was marked by a stained backside of pried coating and extended 6 to 13 mm (1/4 to 1/2 in.) from the edge of the exposed area. Corrosion was enhanced as more anodic and cathodic areas became available. The accumulation of

electrically conductive corrosion products in contact with the underlying steel might also have promoted corrosion activity.[84,110] Further, Stratmann, indicated that the reduction of ferric oxides might be an important cathodic reaction in rust layers on iron.[84] The cathodic activity was probably restricted by the resistivity of the electrolyte layer migrating under the coating, oxygen diffusion through the epoxy film and into coating crevices, and the ohmic polarization encountered in the corrosion products.[84]

8.7 Conclusions

The immersion test of damaged bent bars was conducted over a period of two years. The following conclusions were based on visual inspection and comparisons among tested bars.

A severe corrosive environment will initiate corrosion on any damage to epoxy coating (pinholes, cracks, and damaged spots). No exception is made regarding the size of damaged area or its location. However, during the initial stage of exposure, corrosion activity at pinholes and cracks tended to be higher on bars with smaller areas of introduced damage. With time, the differences of apparent corrosion between all bars with variable surface damage or defects tended to even out.

Current repair practices for damaged coating proved to be ineffective. All patched areas showed corrosion activity after a few weeks of immersion.

Long-term exposure of damaged coated bars to wet and dry cycles in chloride solution resulted in deterioration of the protective qualities of the coating. Undercutting spread around damaged areas and holidays undetected before testing. Swelling spots formed on the coating surface, especially on the compressed side of bar. The coating cracked along the longitudinal rib in the bent area. The coating also debonded extensively due to subsurface anodic and cathodic activities. A solution was found trapped beneath the debonded coating. A thin dark layer covered parts of the steel substrate, but the remaining parts were only dull.

Bars with cross deformations were more susceptible to pinhole (holiday) development in the coating than bars with parallel deformations. In general, coating is more difficult to apply uniformly to the sides of lugs. For bars with more complicated lug patterns such as the cross pattern, the coating on the sides of lugs appeared to be of poorer quality. As a consequence, cross deformations were more prone to corrosion initiating on coating breaks and holidays.

Corrosion on damaged spots introduced during bending on the inside of bends was as severe as on the outside. However, when bars were bent with properly equipped mandrels, corrosion on the inside of the bends was greatly reduced. Therefore, the surfaces against which the bars are bent should be protected to assure that damage does not occur.

The 13-mm (#4) bars were more susceptible to hairline cracking when bent to a smaller radius than the 25-mm (#8) bars. This was especially true for bars with parallel deformations where hairline cracks along deformation lugs were very common. Bending epoxy-coated bars to minimum radii should, therefore, be avoided unless required for structural purposes.

Quality of the base steel is very important for producing good quality coated bars. Rib profile, particularly the longitudinal rib, may affect corrosion performance significantly.

Corrosion on uncoated control bars was very severe and uniform with extensive degradation of bar profile. Qualitatively, the performance of all damaged epoxy-coated bars was much better than uncoated bars over two years of continuous testing.

Exposing reinforcing bars to a uniform corrosive environment did not promote concentrated chloride attack which is more typical in concrete. The physical and chemical properties of any electrolyte affect the corrosion process significantly. Therefore, the performance of coated bars in chloride solution should not be extrapolated to that in concrete.

CHAPTER 9
MACROCELL CORROSION STUDY: CONCEPT AND TEST RESULTS

9.1 General

The effects of coating damage and debonding on the long-term corrosion performance of epoxy-coated reinforcement are major concerns to the industry. As shown earlier, damage to coating during fabrication, transportation, handling, storage, and concrete vibration is almost inevitable. Damage due to fabrication is particularly important because damage and debonding may coexist at critical regions. During bending, bars may be damaged either mechanically or by forming small fissures or holidays, or both, in the stretched coating. Hence, steel becomes exposed within the bent portion. In addition, the common practice of bending coated bars to tight radii results in weakening of the coating adhesion to underlying steel. Although damaged spots are normally patched manually, little has been done to prove the effectiveness of patching. Bent bars are particularly vulnerable because they may be located where chlorides are most likely to attack.

In Florida bridge substructures, the first signs of corrosion of coated reinforcement were observed on fabricated bars. Subsequent investigations revealed that fabrication of coated bars reduces their protection abilities.[30,42,109] The susceptibility of coated bent bars to early corrosion development became a major concern. This necessitated evaluating the allowable coating damage limits in the specifications.

This part of the study focuses on assessing current specification limits on acceptable damage to epoxy-coated bent bars. These specification limits were discussed in Section 3.4.1. In order to evaluate the criteria of the specifications, the effects of the following factors on corrosion initiation and progression were considered:

- Extent of coating debonding relevant to bending radius.

- Level of mechanical damage.
- Repair of damage.
- Bar size.
- Bar deformation pattern.

An accelerated corrosion test was designed to study these variables in view of governing standards and specifications. This test utilized the concept of macrocell formation between different reinforcing layers in concrete to aggravate corrosion. Bars bent 180° were used to represent the worst conditions of fabrication. Two bar diameters, 13 and 25 mm (#4 and #8), and two deformation patterns, parallel and cross ribs, were selected for the study.

All details of the test, such as test variables, steel preparation, material characteristics, specimen design and preparation, test setup, routine monitoring, and postmortem examination procedure are included in Appendix C. Some of this information is presented here for clarity.

The coated bars were damaged to various levels between 0.5 and 2.2% of bar surface area. Some damaged spots were patched while others on identical bars were not. The test bars were embedded in concrete prisms exposed to intruded chlorides. The macrocell corrosion performance of coated bars was compared to that of uncoated bars under similar testing conditions. Table 9.1 summarizes the variables included in the different test groups. There were three replicate specimens in each group of both series A (13-mm bars) and B (25-mm bars).

9.2 Test Concept

9.2.1 Macrocell Action. In the corrosion electrochemical process, the availability of a cathodic area drives corrosion at anodic sites. Therefore, large quantities of cathodic steel are apt to drive high corrosion at anodic steel. Such macrocell activity is very destructive in concrete. It is the primary cause of early bridge deck deterioration (concrete cracking and spalling) where chloride-based deicing salts are used.[44,106,112]

Table 9.1 Summary of Macrocell Study Variables, Series A and B

Group No.[a]	Deformation Pattern		Epoxy Coating Damage Level					Damage Condition	
	Parallel Ribs	Cross Ribs	Spots > 6x6 mm	Spots > 2%	Cracks < 1%	Spots < 2%	Pinholes < 1%	Patched	Not Patched
1	●		Control Specimens - Uncoated Bars						
2	●		●					●	
3	●		●						●
4	●			●				●	
5	●			●					●
6	●				●				●
7	●					●			●
8		●	Control Specimens - Uncoated Bars						
9		●	●					●	
10		●	●						●
11		●					●		●

a Series A: 13-mm (#4) "U" bent bar; Series B: 25-mm (#8) "U" bent bar.

The destructive action of macrocell formation is also envisaged as a possible major cause of corrosion of epoxy-coated reinforcement mainly in bridge decks and marine applications. When damaged coated bars in contact with chlorides are electrically coupled to uncoated bars away from chlorides, the large cathode (uncoated steel) may drive corrosion on the small potentially active anode (damaged spots). However, corrosion of epoxy-coated steel may be governed by physical restraint of ion transport to the damaged spots. This restraint can lead to different corrosion performance characteristics compared to uncoated steel.

Progression of corrosion after initiation is also related to anode potential. The kinetics of anodic polarization can dictate the severity of corrosion activity. Therefore, it is important to investigate the performance of coated bars at the anodic end of corrosion

macrocells in concrete. With the availability of cathodic steel, the mechanism of corrosion of coated steel may be controlled by anodic polarization. The macrocell test provides an opportunity to study the anodic performance of fabricated epoxy-coated bars in concrete.

9.2.2 Test Conditions. In order to simulate a bridge deck for macrocell testing, and accelerate corrosion at the same time, the following factors were implemented:

- High permeability concrete. The diffusion of chloride ions is faster in less water-tight concrete.
- Reduced concrete cover. The time of penetration of chlorides to steel level is reduced.
- A large cathodic steel area coupled to a small anodic steel area. This ensures a large corrosion driving force.
- Reduced concrete path between anode and cathode. The ionic flow path through electrolytic concrete becomes shorter.

The reality of having a direct electrical contact between reinforcing layers, in the form of metal to metal contact, can be demonstrated by previous field observations. In bridge decks that contained uncoated steel, top and bottom, contact was available in virtually every instance.[81,106] Such contact was provided by truss bars, tie wires, bar chairs, bar ends in contact with expansion dams or scuppers, or both.[106,107]

On the other hand, partial contact was the most common situation found with epoxy-coated bars.[81,106,107] Even when nonmetallic-coated tie wires and bar chairs were used, mat-to-mat coupling was not always eliminated. Therefore, assuming full contact between reinforcing layers covers the worst conditions. Figure 9.1 shows an example of mixing coated with uncoated steel in bridge deck construction. Sagüés,[114] has recently found a considerable degree of electrical contact between epoxy-coated bars in the same structure.

Damage to epoxy coating is expected. A damage level of 1% of bar surface area was considered to be representative of the unavoidable mechanical damage prior to casting.[93]

Damage introduced during concrete placement may, moderately, add another 1% (see Chapter 7). Thus, coating damage may eventually reach as high as 2%. This percentage is equivalent to the highest allowable damage limit in current specifications.

Figure 9.1 Bridge Deck Slab with Coated (Top) and Uncoated (Bottom) Reinforcement.

Subjecting concrete to a wet-dry cyclic regime using a chloride solution promotes corrosion. An earlier study showed that the drying period locally concentrates chloride and oxygen and eventually leads to corrosion initiation.[58] Concentration of chlorides is favorable in corrosion testing for triggering corrosion activity in a short period.

When chlorides penetrate concrete, their accumulation at reinforcing bar level is gradual and nonuniform. The rate of accumulation affects the initiation and development of corrosion and should be accounted for when designing a laboratory experiment. Therefore, ponding a relatively strong salt solution on the concrete surface with shallow depth to reinforcement will reproduce the exposure conditions in the field in a shorter time.

9.3 Test Setup and Procedure

9.3.1 Test Setup. Concrete prisms were designed and prepared to simulate the conditions of a bridge deck slab exposed to salt solution. A model of the test specimen and a view of actual specimens are shown in Fig. 9.2 and 9.3, respectively. Only one coated bent bar was used in each specimen at the top, and two (for series A) or three (for series B) uncoated straight bars were placed at the bottom.

A total of 68 macrocell specimens was included in the test. The exposure conditions consisted of cycles of ponding a 3.5% NaCl solution on the top surfaces followed by removing the solution and allowing the specimens to dry in a temperature-controlled room. Each cycle lasted four weeks, with two weeks wet and two weeks dry. In order to monitor the macrocell corrosion current, the two reinforcing layers were linked via a known resistor and the voltage drop across this resistor was measured periodically. The voltage was converted to current using Ohm's Law.

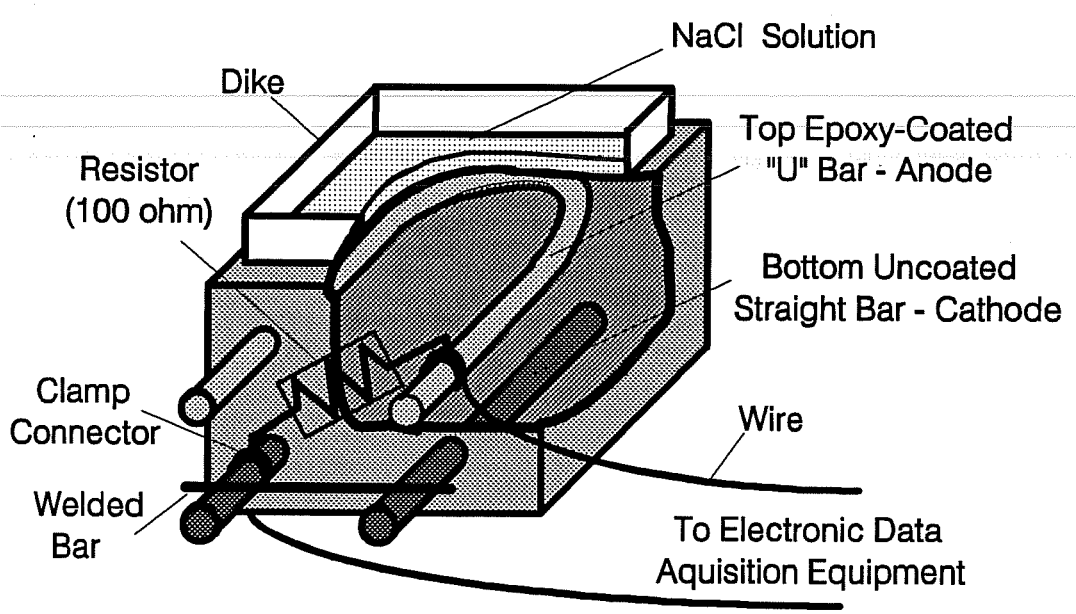

Figure 9.2 Macrocell Specimen Model.

Figure 9.3 Macrocell Test Setup.

9.3.2 Measurements and Observations. Time development of macrocell corrosion was studied over a two-year period. Time-to-onset of corrosion, and time-to-cracking were the two important observations of particular interest during the first period of the test.

The measured macrocell current served as an excellent indicator of time-to-corrosion. Some of the control (uncoated steel) specimens exhibited steadily increasing currents shortly after the test was started. Others showed a delay in the onset of corrosion. In Table 9.2 the time periods elapsed before increasing corrosion currents began to flow are listed.

Periodical visual inspection of the concrete specimens allowed the determination of time-to-cracking. The first signs of concrete staining and cracking due to corrosion were visible on the large bar control specimens. The small bar control specimens were the second to exhibit similar corrosion manifestations. The recorded time-to-cracking for all the specimens are also shown in Table 9.2. Further descriptions of crack initiation and

propagation are given in Section 9.5. The epoxy-coated bar specimens remained uncracked during the two-year observation period.

Measuring the macrocell current between anode bars and cathode bars offered quantitative means to evaluate the corrosion rate of the anode bars. The corrosion rate was used to study the relative performance between the coated and uncoated bars and within the variably damaged coated bars.

Table 9.2 Time to Corrosion and Cracking
(Time in Days)

Group No.	Damage Category and Condition	Series A		Series B	
		Time-to-Corrosion	Time-to-Cracking	Time-to-Corrosion	Time-to-Cracking
1	Control	63 - 98	350 - 518	7 - 56	210 - 224
2	Spots > 6 x 6 mm, Patched	N[a]	-	182 - 350	-
3	Spots > 6 x 6 mm	469	-	154 - 266	-
4	Spots > 2%, Patched	N	-	266 - 462	-
5	Spots > 2%	238-350	-	98 - 154	-
6	Cracks < 1%	539 - 616	-	245 - 280	-
7	Spots < 2%	294	-	84 - 399	-
8	Control	14 - 126	343 - 532	7 - 42	210 - 427[?]
9	Spots > 6 x 6 mm, Patched	N	-	203 - 294	-
10	Spots > 6 x 6 mm	245 -504	-	98 - 273	-
11	Pinholes < 1%	N	-	182 - 231	-

a N means consistently very low (below 10 μAmp) corrosion current.
? 427 is uncertain. Cracking is suspected earlier.

9.4 Macrocell Corrosion Currents

9.4.1 General. Examples of macrocell corrosion currents versus time of exposure up to two years are shown in Fig. 9.4 and 9.5. A complete set of results for all specimens is given in Section C.8. The corrosion currents illustrate macrocell action development as a function of exposure time. The results provided valuable information on corrosion behavior and support the findings from specimen autopsy.

9.4.2 Control Bar Specimens. All control specimens developed consistent macrocell current patterns after some time of exposure. The small bar specimens showed more steady currents than the large bar specimens. However, corrosion currents in the small bar specimens increased rapidly after about 1.5 years of testing. For the large bar specimens, the general tendency was for the current to increase progressively in the second half of the first year, and again after 1.5 years although there were appreciable fluctuations of currents with time.

9.4.3 Epoxy-Coated Bar Specimens. Many specimens with epoxy-coated bars followed patterns similar to the ones described above but to lesser magnitudes and at delayed times. Group B.5 specimens (25-mm bars with coating damage slightly exceeding 2%) showed the worst performance of all coated bar specimens. Series A specimens with total coating damage less than 2%, and those with damaged spots smaller than 6 x 6 mm (1/4 x 1/4 in.), and all patched bars, exhibited the best performance with negligible currents. The patched bars of series B exhibited activity much lower than identical unrepaired bars. There was no appreciable difference in performance between bars with different deformation patterns. However, the difference in performance between bars of different sizes was significant.

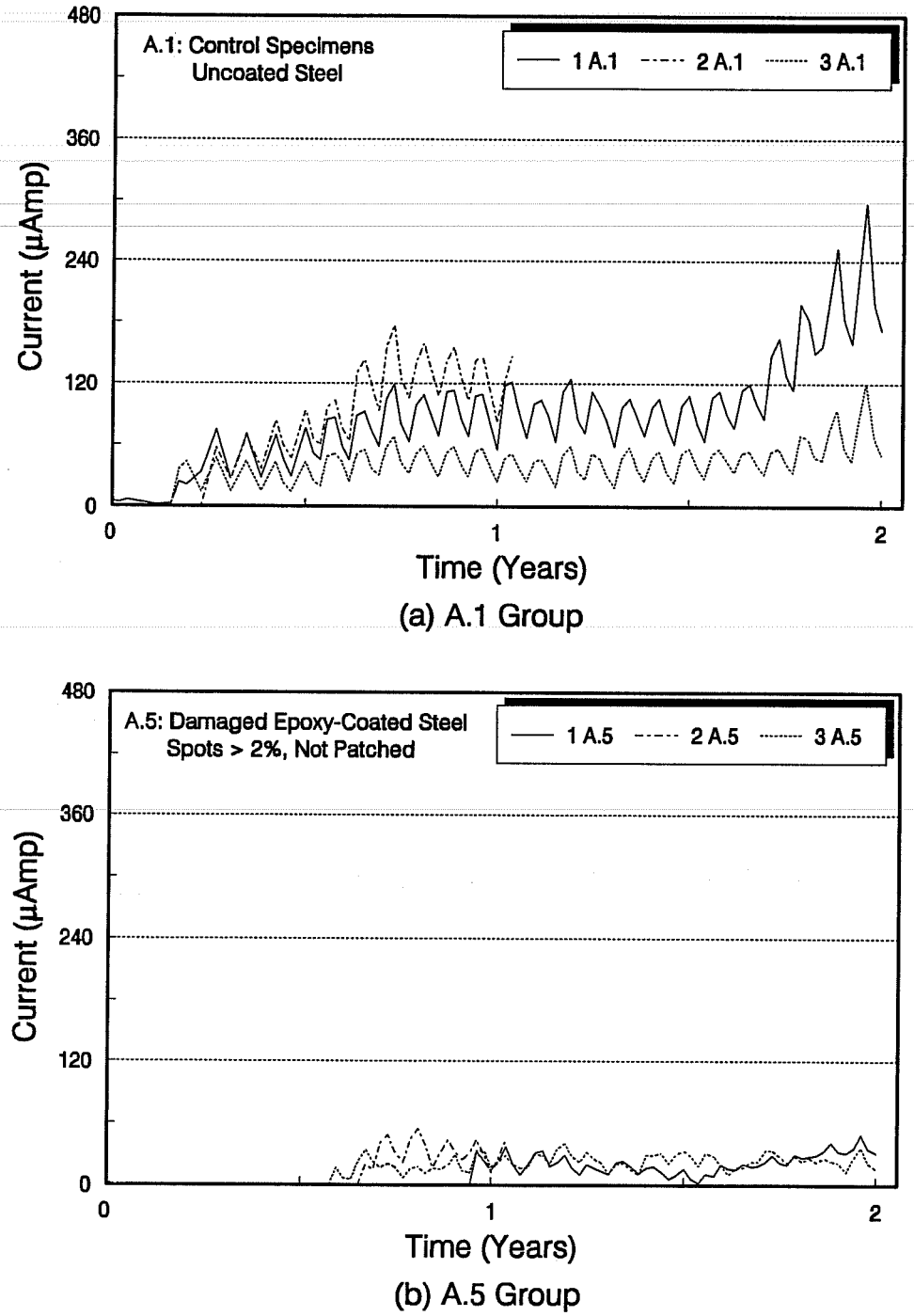

Figure 9.4 Examples of Macrocell Corrosion Currents for Series A.

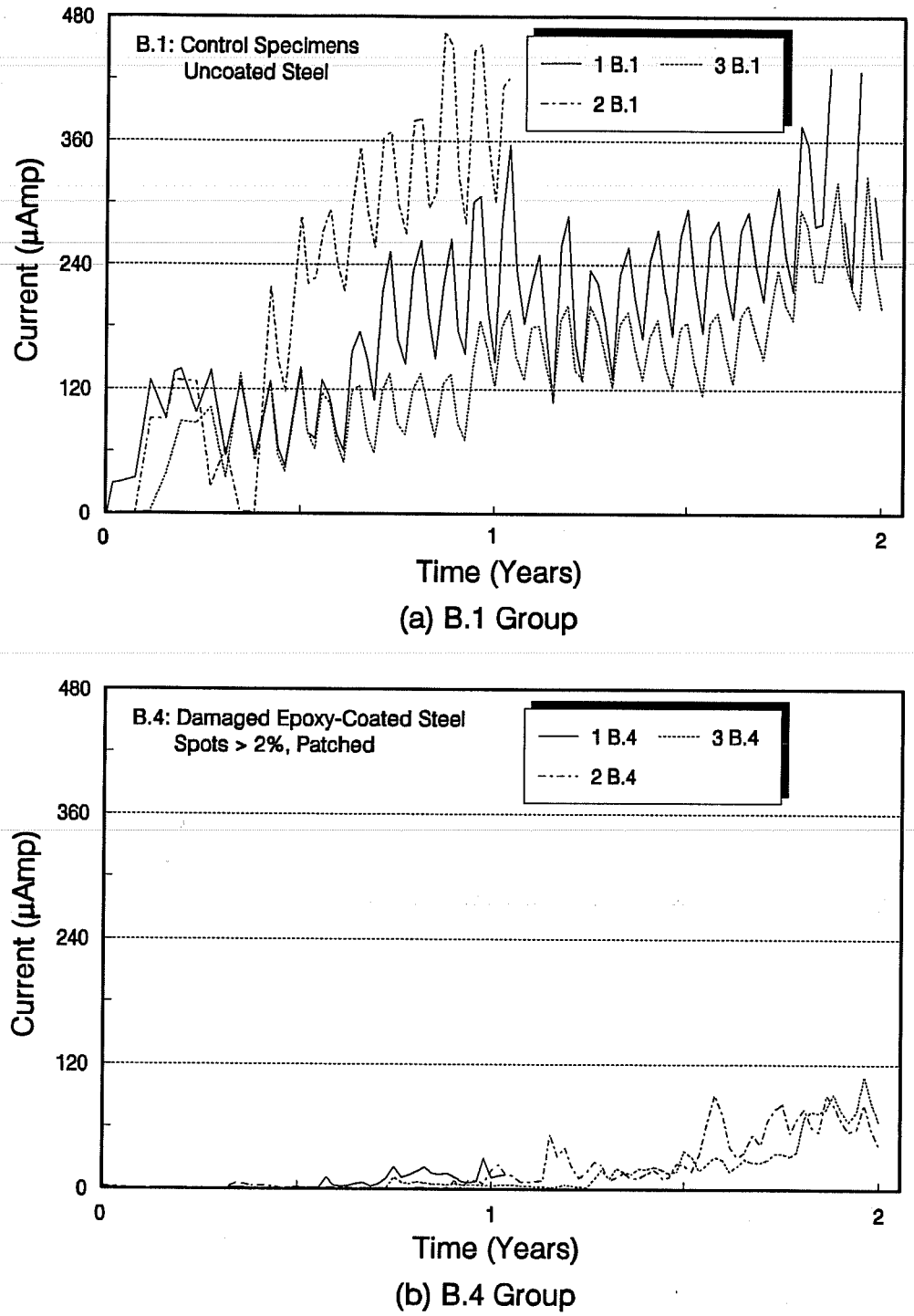

Figure 9.5 Examples of Macrocell Corrosion Currents for Series B.

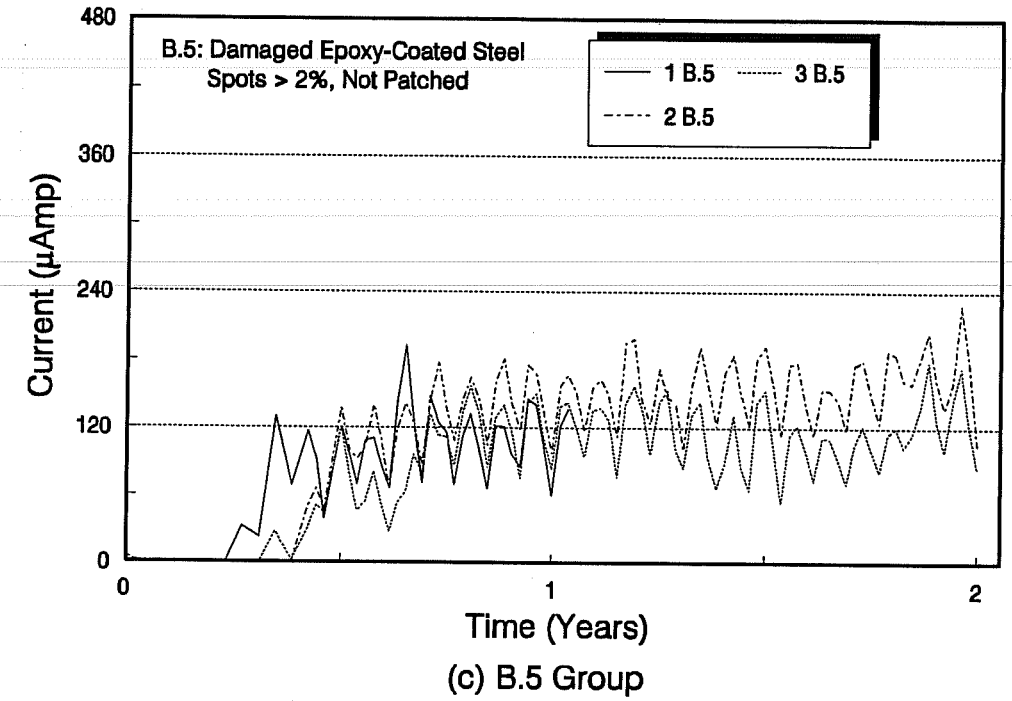

(c) B.5 Group

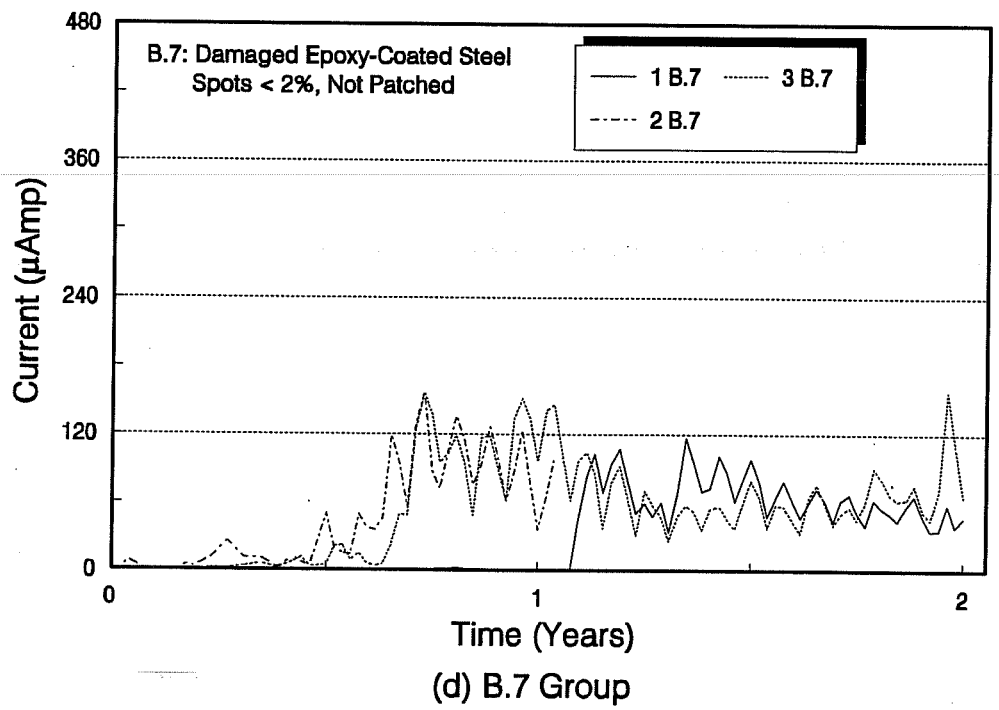

(d) B.7 Group

Figure 9.5 (Cont'd) Examples of Macrocell Corrosion Currents for Series B.

For all specimens where corrosion activity was evident, the electric currents flowed from the top reinforcing bar to the bottom bars as expected. This pattern was maintained throughout the test period. Current fluctuations with time are due to alternate wetting and drying in each exposure cycle. The differences in currents observed within one group reflect variations in the extent of corrosion activity experienced during the time period of testing. These differences could be attributed to variations in concrete cover due to finishing after concrete pouring. Generally, the differences in behavior tended to even out with time.

9. 5 Concrete Cracking and Rust Staining

9.5.1 Control Bar Specimens. The first outward signs of corrosion on the macrocell specimens containing uncoated reinforcement became apparent after about 100 days of exposure. The large bar specimens, in particular, showed minor brown spots on the concrete surface around the protruding ends of top bars. After about 170 days of exposure, larger brown stains were apparent at the same locations. Rust staining on the top concrete surfaces was visible after about 200 days of exposure. The small bar specimens showed staining on the top concrete surfaces after about 330 days of exposure.

Fine corrosion-induced cracks showed up on the top concrete surfaces of some of the large bar specimens at approximately 210 days. The fine cracks gradually developed larger areas of rust staining and widened. The cracks generally formed parallel to the embedded bars and along the straight portions of the bars. Cracking was first evident on the top surfaces of the smaller bar specimens after about 340 days of testing.

The surface condition of the specimens after one and two years of exposure is depicted in the sketches presented in Section C.9. Figure 9.6 shows two examples of these specimens removed at different times for forensic examination.

(a) Specimen 2 B.1, One year of Exposure

(b) Specimen 2 B.8, Two Years of Exposure

Figure 9.6 Examples of Autopsied Uncoated Steel Specimens.

9.5.2 Epoxy-Coated Bar Specimens. None of the epoxy-coated bar specimens showed surface staining or cracking beyond the plastic settlement and shrinkage cracks detected at the beginning of the test. These initial cracks are described in Section C.8. Figure 9.7 shows two examples of specimens inspected after two years of exposure.

9.6 Forensic Examination

9.6.1 General. Forensic examination was carried out for three reasons:

- to correlate the corrosion current measurements to actual bar condition;
- to determine the relative corrosion activity on the test bars with various surface conditions; and,
- to investigate the condition of the epoxy coating.

One specimen in each group of three was removed for autopsy after one and after two years of exposure. Generally, the specimen selected was the one showing maximum corrosion activity indicated by the history of the macrocell corrosion current. The bars were carefully removed following the procedure outlined in Section C.9. The forensic examination was documented by visual observations, microscopic examination, and photographs.

9.6.2 Concrete Delamination. Prior to destruction, delamination of concrete was checked by hammer sounding but did not indicate concrete delamination in any of the specimens after one and two years of exposure. It is believed that any corrosion which occurred in the specimens was not sufficient enough to cause delamination.

9.6.3 Chloride Content at Steel Level. Chloride samples were drilled out from each specimen before demolishing. The concrete surfaces at the drilled locations were uncracked; therefore, the chloride concentrations should represent quite closely the general distribution of ingressive chlorides. The measured acid-soluble chloride concentrations are tabulated in Section C.9.

(a) Specimen 2 B.5, Two Years of Exposure

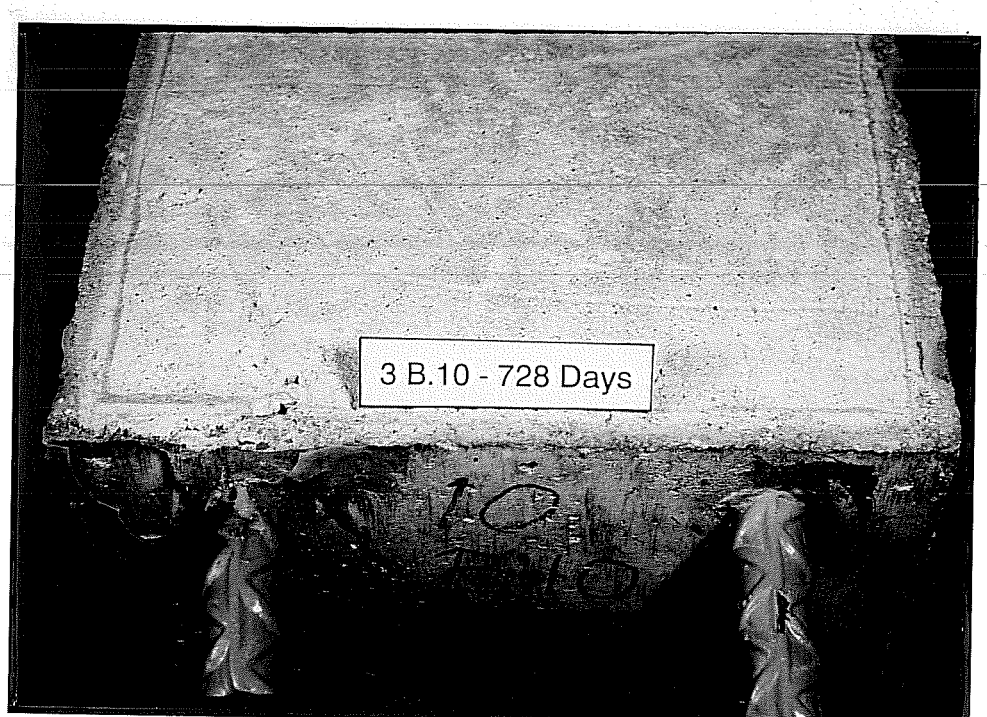

(b) Specimen 3 B.10, Two Years of Exposure

Figure 9.7 Examples of Autopsied Epoxy-Coated Steel Specimens.

The chloride contents at top steel level varied considerably and were, on the average, 3.8 kg/m^3 (6.4 lb./yd^3) for series A, and 4.8 kg/m^3 (8.1 lb./yd^3) for series B after one year. The respective values after two years were 5.7 kg/m^3 (9.6 lb./yd^3) and 5.4 kg/m^3 (9.1 lb./yd^3). The chloride profiles in concrete based on average chloride concentration values are shown in Fig. 9.8 and 9.9.

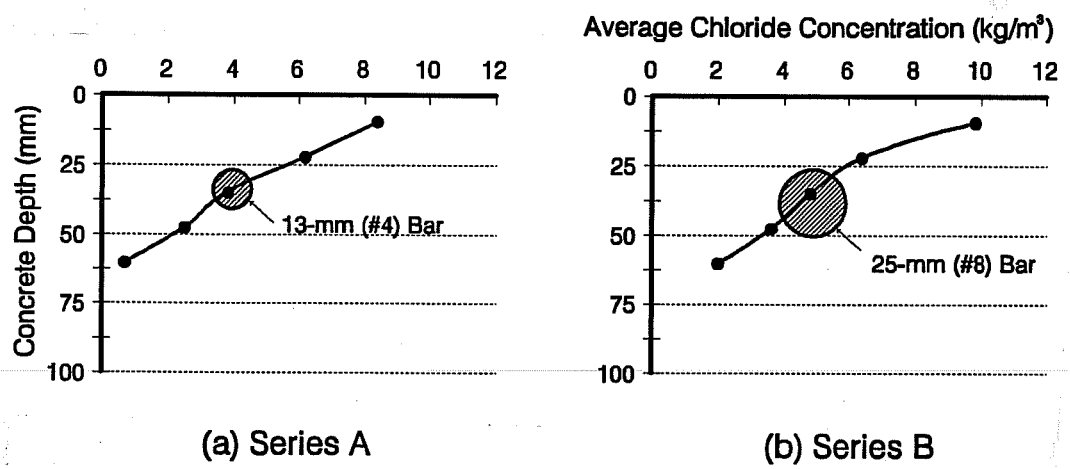

Figure 9.8 Chloride Profile in Macrocell Specimens After One Year of Exposure.

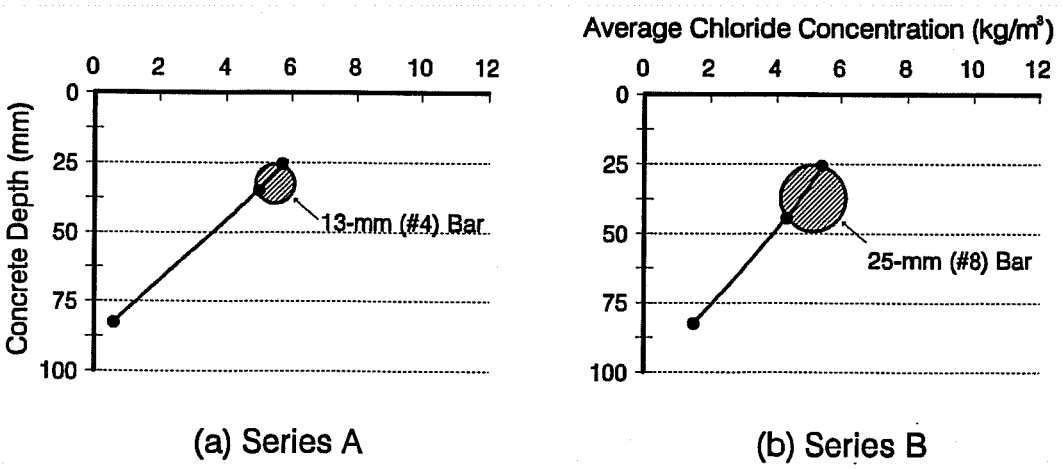

Figure 9.9 Chloride Profile in Macrocell Specimens After Two Years of Exposure.

9.6.4 Steel Surface Corrosion.

Control Bars. The uncoated bars showed relatively high levels of corrosion with discernable extensive degradation and localized loss in section, especially after two years. As shown in Fig. 9.10, corrosion was concentrated mostly at the straight portions of the bar. Figure 9.11 shows an area of aggravated pitting corrosion on uncoated bar surface. In general, more pitting corrosion occurred on the top side than the bottom side of the bar. Larger bars were more severely attacked than the smaller bars. The corrosion products were a mixture of black and brown products.

Epoxy-Coated Bars. Summarized descriptions of the bar *surface* condition are tabulated in Section C.9. It was decided that the commonly used ratio of area covered by red rust (ratio of corroded area to bar surface area) as a measure of the state of corrosion was inaccurate for coated bars. The apparent corrosion at coating breaks does not represent the actual extent of substrate metal corrosion.

After one year of exposure, the small coated bars showed either no apparent corrosion or minor surface corrosion on the introduced damage and other defective areas of coating (inside and outside of bend). Figure 9.12 shows two examples of the 13-mm (#4) bars exposed for one year. At the damaged locations, steel was only discolored or had suffered minor (shallow) loss of metal.

The large bars showed relatively more corrosion activity; however, metal loss was also minor as shown in Fig. 9.13. Rust spotting at some patched areas was visible. On the majority of the large bars, many variable size blisters distributed on the coated surface were noted. The blisters formed at spots facing air voids in concrete as shown in Fig. 9.14. Based on appearance, the worst bars, from both series, were those with exposed damaged areas slightly exceeding 2% of the bar surface area.

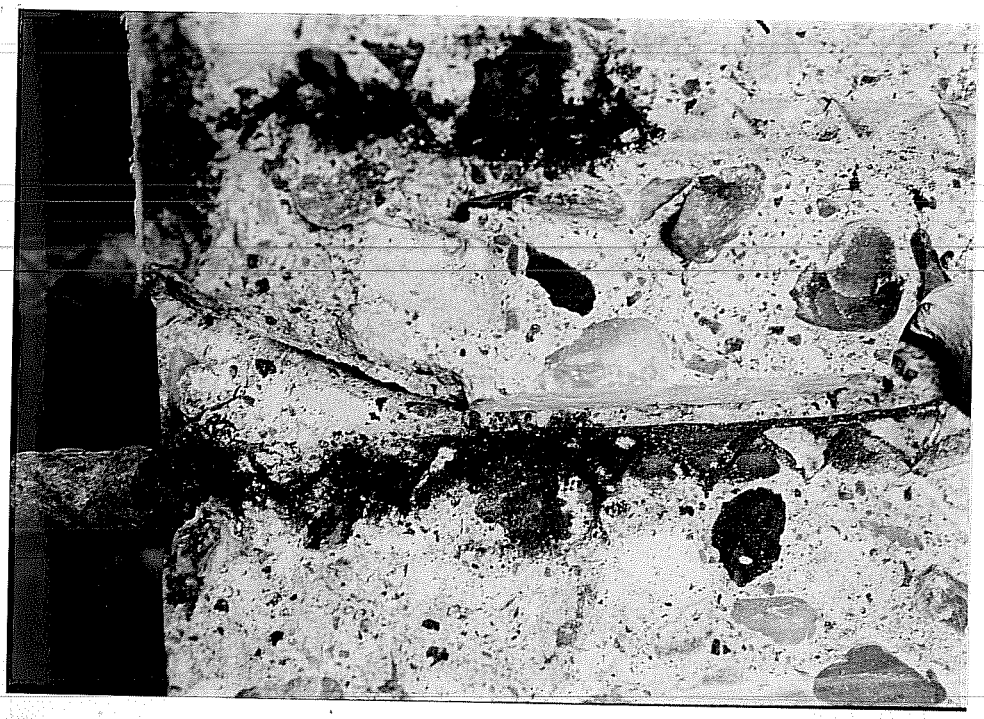

Figure 9.10 Corrosion of Uncoated Steel Bar (2 A.8) After Two Years of Exposure.

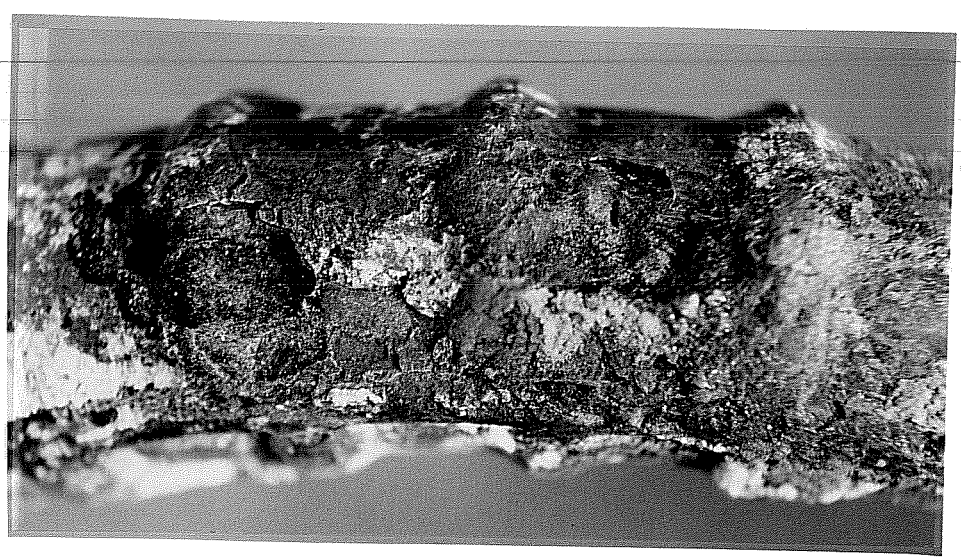

Figure 9.11 Severe Pitting Corrosion on Uncoated Steel Bar (1 B.1) After Two Years of Exposure.

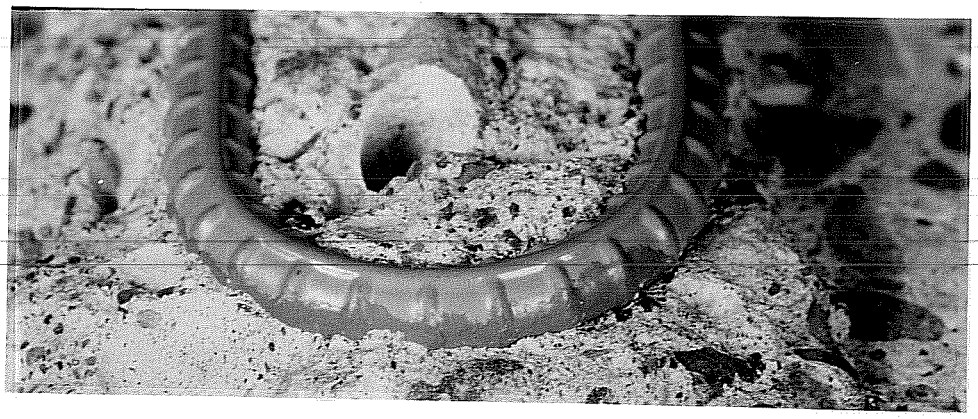

(a) Specimen 1 A.4

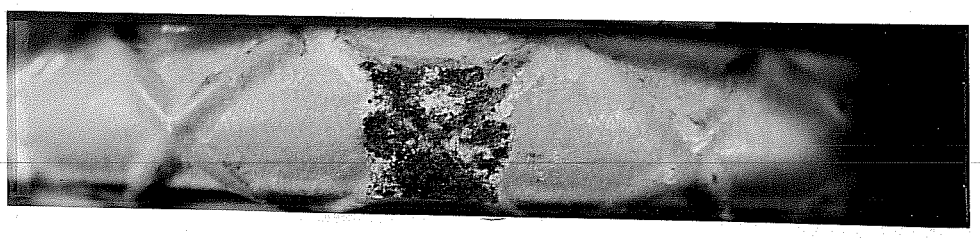

(b) Specimen 3 A.10

Figure 9.12 Examples of 13-mm Coated Bar Specimens Autopsied After One Year of Exposure.

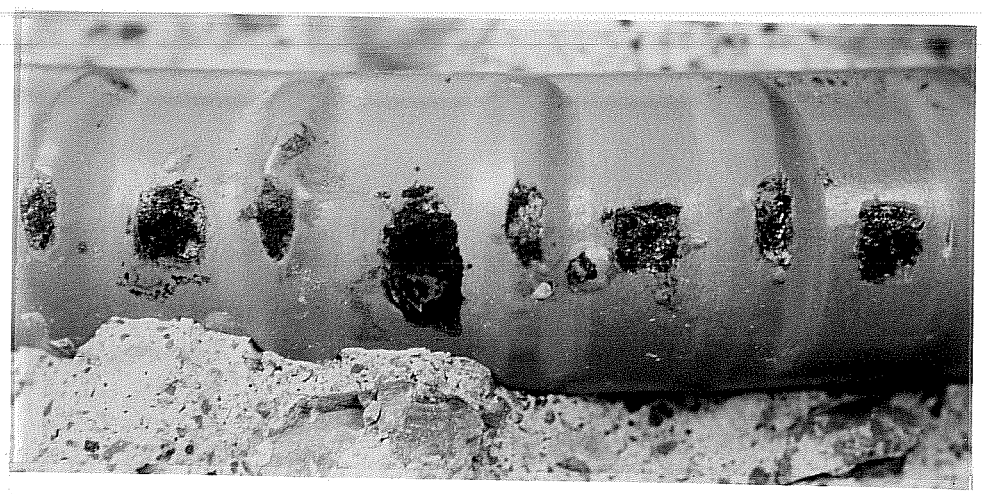

Figure 9.13 Example of 25 - mm Coated Bar Specimens After One Year of Exposure.

(a) Blister on a Coated Bar Surface

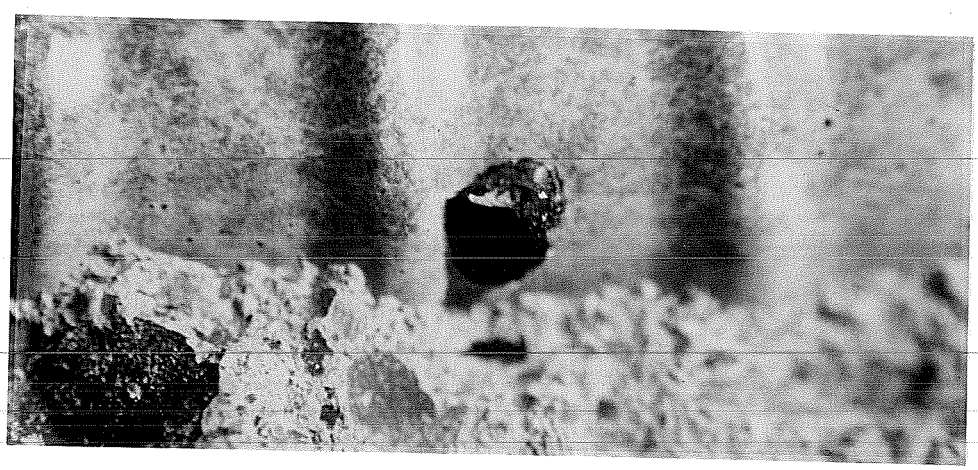

(b) Void in Concrete at Blister Formation

Figure 9.14 Coating Blistering at Voids in Concrete.

More corrosion activity was visible after two years than after one year. After two years, it was clear that pitting corrosion was occurring on the exposed areas of some specimens. Rust spotting at some patched areas was also observed, particularly on the larger size bars. These observations are illustrated in Fig. 9.15. Again, blisters of variable sizes formed on the coated bar surface at locations facing voids in concrete. These voids were more concentrated on the underside of the bar as shown in Fig. 9.16. The blisters were also

much more apparent after two years than after one year for the corresponding specimens indicating further breakdown of the coating with longer exposure. Figure 9.16 shows a bar with many blisters formed on the bottom side.

As for the specimens examined after one year, small size bars examined after two years exhibited less corrosion than the large size bars. The only bars which appeared in excellent condition were the small bars with parallel deformations and repaired damaged areas. One of the damaged small bars showed fine cracking of the coating along the longitudinal rib in the bent area.

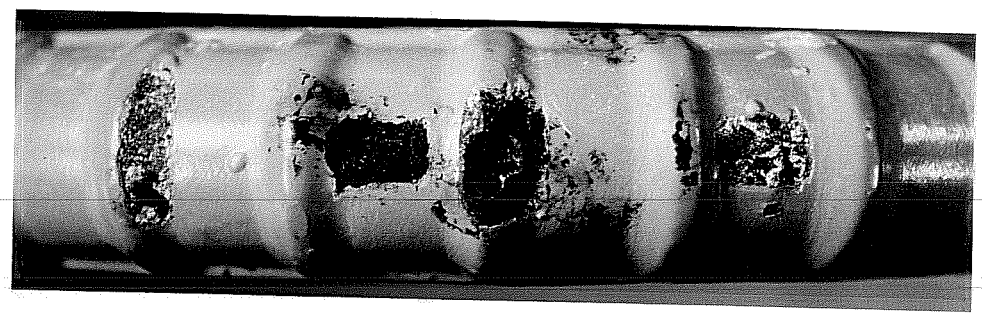

(a) Pitting Corrosion on Specimen 3 B.3

(b) Rust Spotting on Specimen 1 B.2

Figure 9.15 Examples of 25 mm Coated Bar Specimens After Two Years of Exposure.

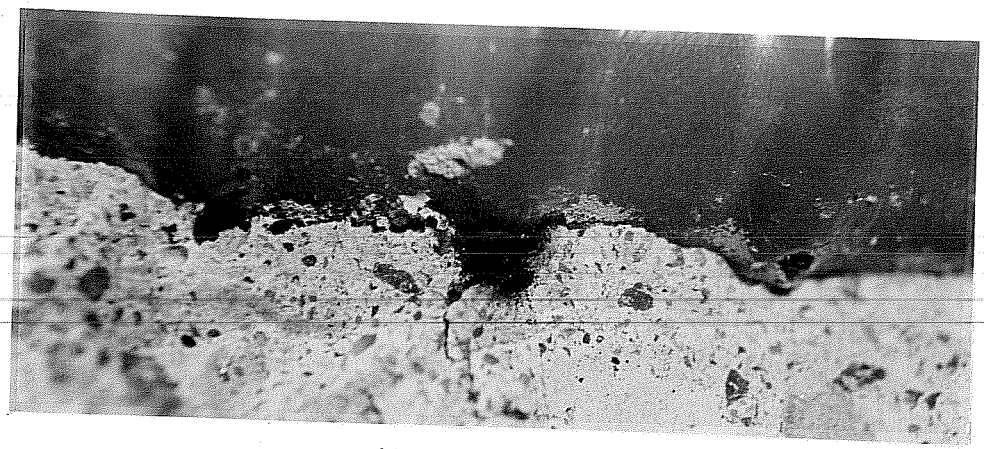

(a) Specimen 3 B.7

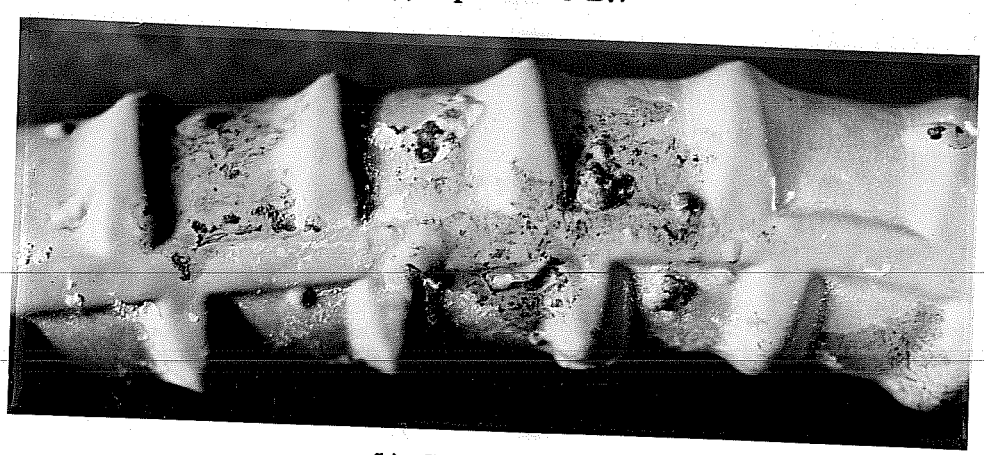

(b) Specimen 2 B.5

Figure 9.16 Blister Formation at Bottom Side of Coated Bars After Two Years of Exposure.

After one and two years, corrosion products were dark green-black and brown solid products. However, upon exposing the epoxy-coated bars, in many instances, a dark greenish-blue corrosion product was found in a soluble form. The dark greenish product rapidly converted to brown on contact with air. In addition, a clear solution spilled from damaged spots and pinholes at the bottom side of some bars. Furthermore, steel corroded spots almost always coincided with gaps in the surrounding concrete through which the corrosion products dispersed as shown in Fig. 9.17. In addition to corrosion on the exposed steel areas (inside and outside of bend), the bottom side of bar generally showed the worst rust spotting and blistering.

(a) Specimen 3 B.10 (Bottom side facing up)

(b) Specimen 2 B.5 (Inside of bend facing up)

Figure 9.17 Rust Spotting on Bottom Sides of Coated Bars Coincident with Voids in Concrete.

One interesting phenomenon was that a soft swelling spot with rust stain exudations formed on the coated bar surface either exactly where the bar protruded from the specimen, or about 3 mm (1/8 in.) from the concrete edge. These spots were first observed after about 600 days of testing and only on the larger size bars. The solution filling these spots must have passed under the coating from the embedded portions where damage existed or corrosion was taking place. Figure 9.18 shows one of the swelling spots.

Cathodic Bars. The cathodic uncoated bars at the bottom were, as expected, free of rust as shown in Figure 9.19.

9.6.5 Coating Prying. The coating was removed around exposed spots and from originally undamaged areas using a sharp blade. In general, loss of adhesion along the bend for both bar sizes was extensive. The debonded areas were relatively easy to pry and were characterized by noticeable separation from the metal. In contrast, cutting through the well-bonded coating near the straight ends was difficult and caused cohesive separation of the coating material itself. However, even the straight portions of the bars became mostly debonded after two years of exposure. Scraping the coating after two years was easier than after one year and resulted in larger chipped off pieces. Figure 9.20 illustrates the extent of debonding of the epoxy coating.

9.6.6 Underfilm Corrosion. Short descriptions of the condition of steel substrate are given in Section C.9. Generally, the small bars, after one year of exposure, appeared in good condition. The substrate metal either remained bright with no visible corrosion activity, or was slightly discolored with minor surface disruption.

Many of the large bars, however, exhibited moderate to widespread underfilm corrosion starting from the exposed steel areas and defects on both the inside and outside of bends. The metal underneath the coating, including patching, appeared dull and darkened with some brown rust spotting. A thin black layer was observed, particularly in the cases with high percentage or large size of coating damage. Despite this appearance, surface rusting was light without significant loss of bar section. Additionally, a clear or whitish

trapped solution was found underneath the coating of many bar specimens. The solution dried fast upon exposure to the atmosphere leaving whitish deposits which turned to orange, and then to brown. Figure 9.21 shows an example of undercutting on a large bar specimen.

After two years, specimens showed moderate underfilm activity and pitting. There was a clear distinction between the appearance of the top and bottom sides of the bar. The top side was black, and sometimes moist, while the bottom side was dull with sporadic rust spotting as shown in Fig. 9.22. Even the patched large bars showed surface darkening with minor metal loss or slight pitting as shown in Fig. 9.23. Whitish and orange residue was occasionally observed in some pockets forming alongside the bottom continuous rib (see Fig. 9.24). The blisters were often full of corrosion products and some had an acidic (pH 2 to 4) trapped solution. Figure 9.25 shows a close up of the solution detected underneath the coating.

9.6.7 Bar Trace in Concrete. The bar trace of uncoated steel was porous, dusty, and generally well adhered to the steel surface. Exudation of some black and brown corrosion products in concrete pores was extensive around the locations of corroded steel. Figure 9.26 shows that the concrete/bar interface at the areas adjacent to the corrosion sites was slightly darkened.

The bar trace on top of the coated steel appeared glossy, smooth and generally free of voids as shown in Fig. 9.27. The bottom trace appeared dull with laitence and many voids of different sizes as shown in Fig. 9.28. Bar imprints (rib marks) were clearer on the top side than the bottom side of the bar. Sometimes white deposits, probably salt, accumulated on the underside bar trace as shown in Fig. 9.29. In general, more rust products were visible in and around the voids at the bottom trace than at the top.

The bottom (cathodic) bars had a completely different trace in concrete. The layer at the concrete/bar interface seemed dark, probably because of the alkalinity produced by the cathodic activity at the steel surface. Figure 9.30 shows the cathodic bar imprint in concrete.

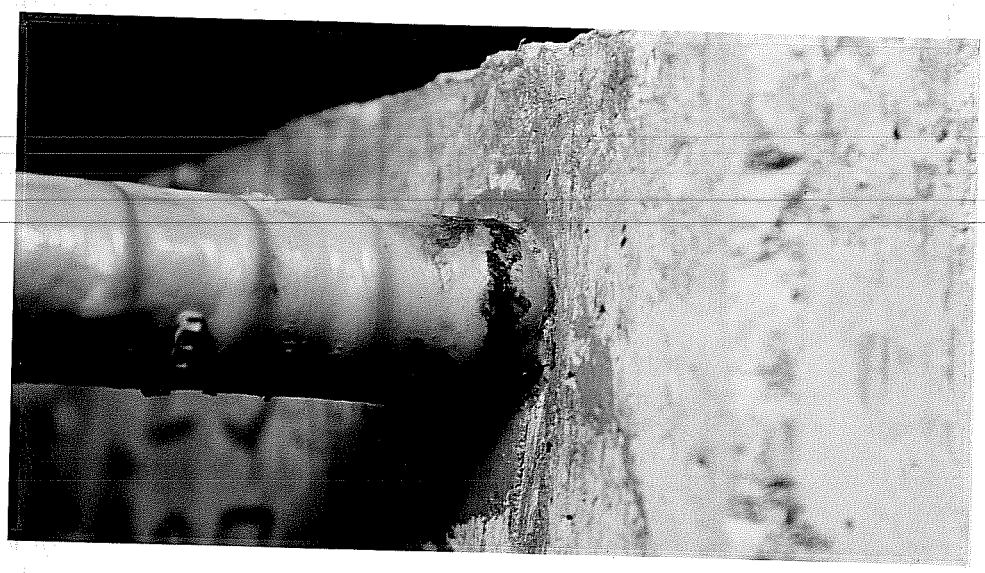

Figure 9.18 Example of Swelling Spots on bar Surface Outside Concrete Specimen.

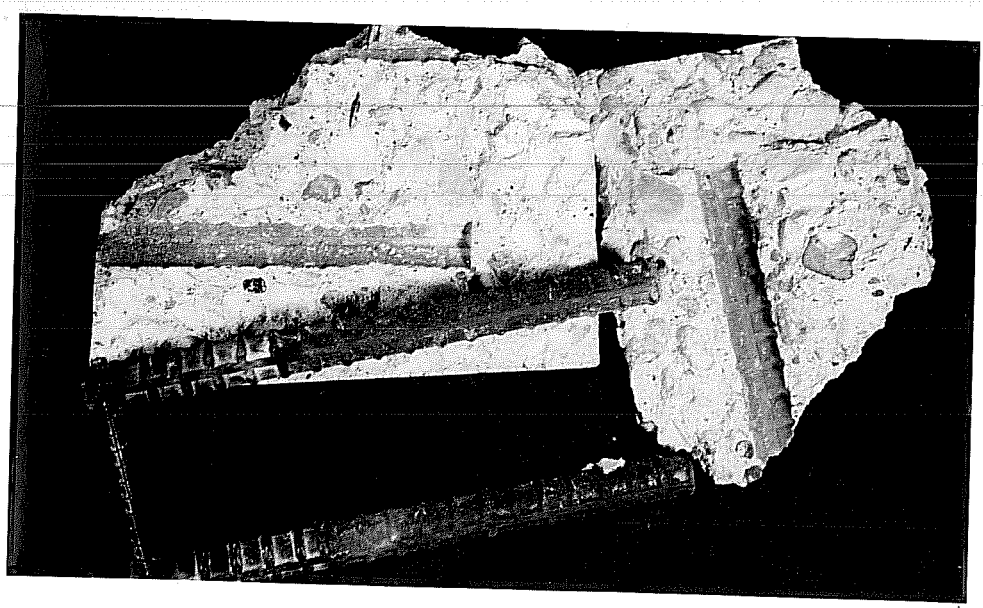

Figure 9.19 Cathodic Uncoated Bars at Bottom of Macrocell Specimens.

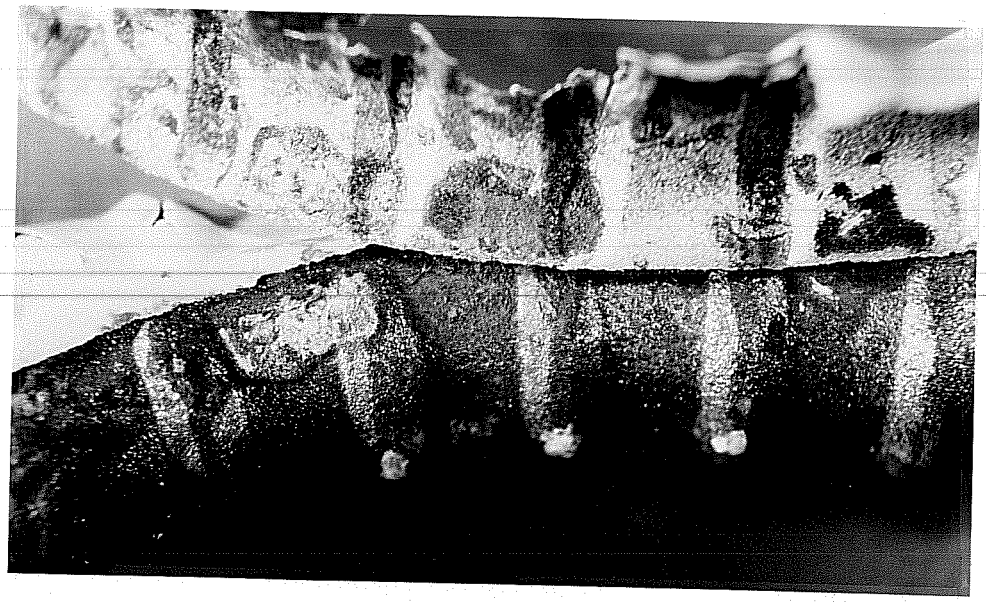

(a) Specimen 2 B.4

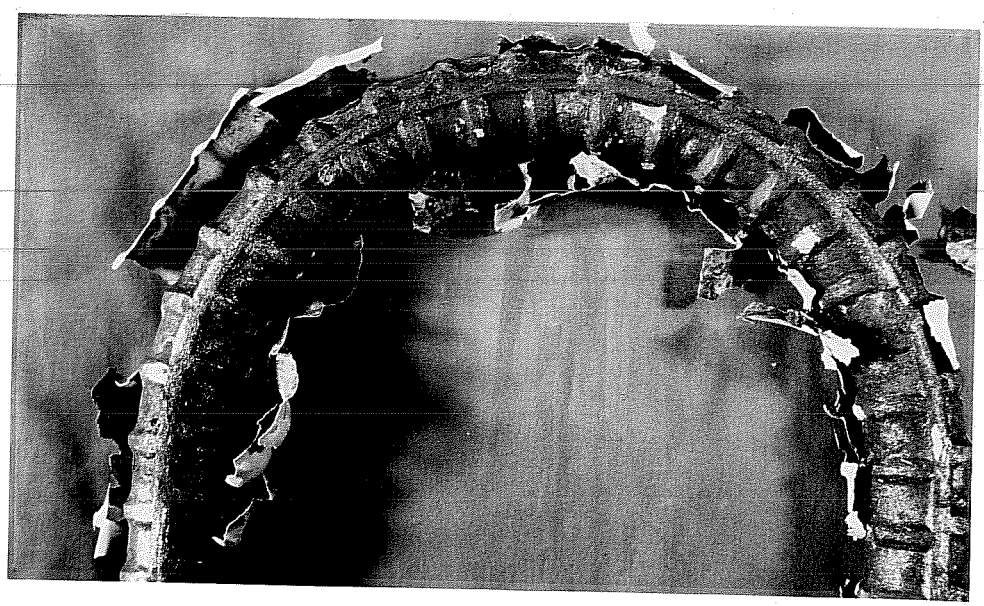

(b) Specimen 2 B.5

Figure 9.20 Coating Debonding After Two Years of Exposure.

Figure 9.21 Underfilm Corrosion (Undercutting).

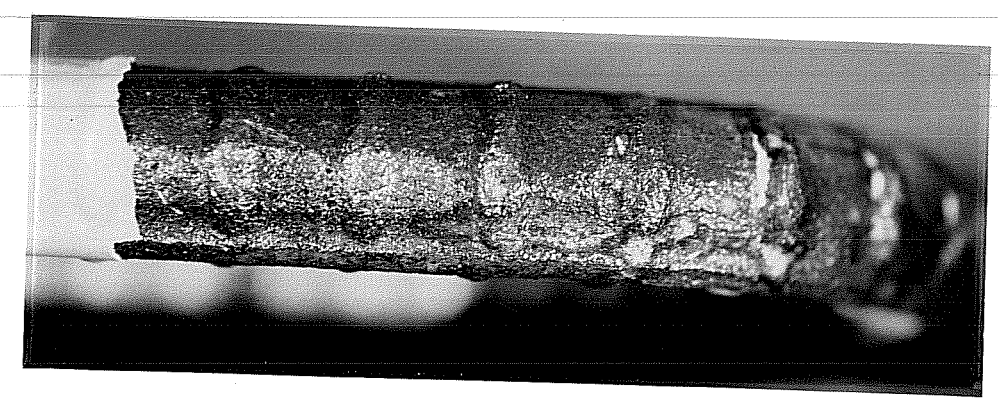

Figure 9.22 Thin Black Layer on Top Side of Steel Surface.

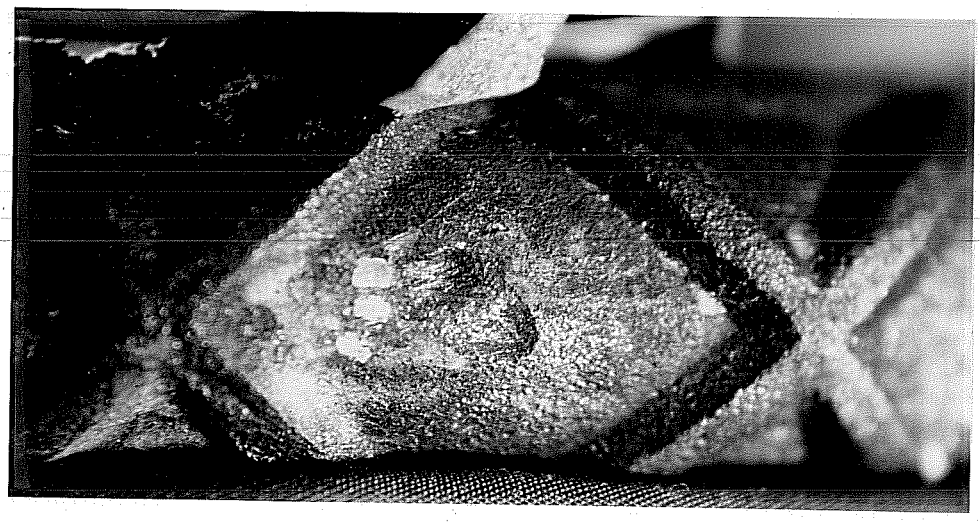

Figure 9.23 Darkening and Pitting Underneath Patching.

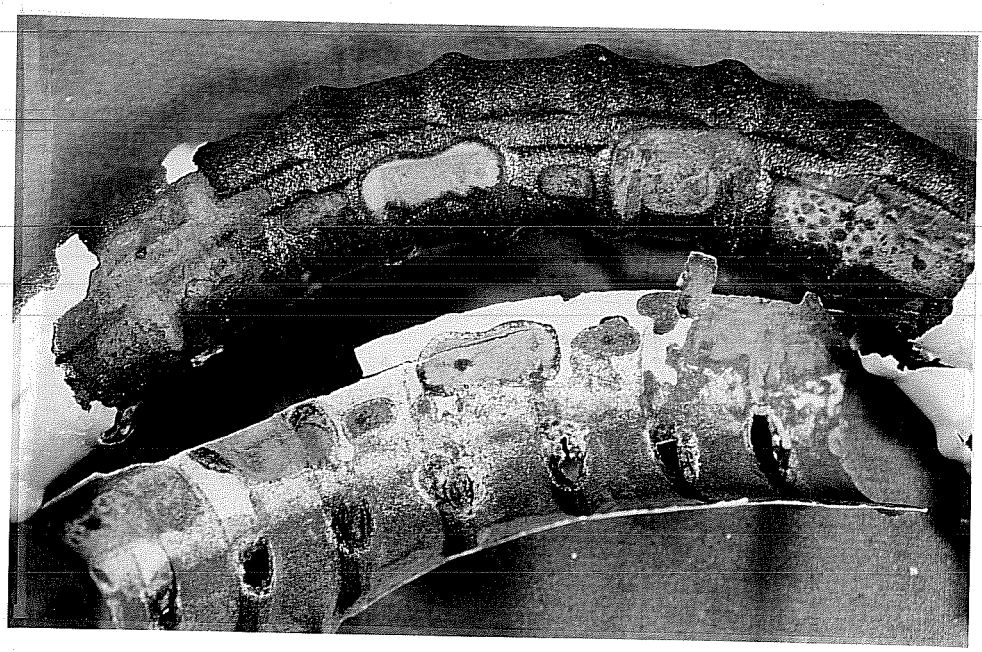

Figure 9.24 Corrosion Deposits on Bottom Side of Steel Surface.

Figure 9.25 Trapped Solution Beneath Epoxy Coating.

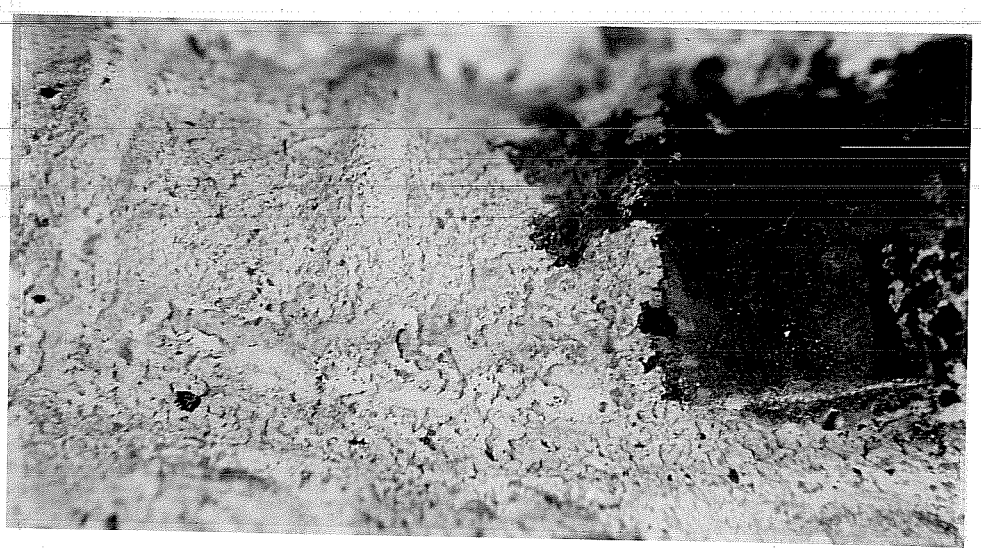

Figure 9.26 Uncoated Top Bar Trace in Concrete.

Figure 9.29 White Deposits Accumulated Under Coated Bar.

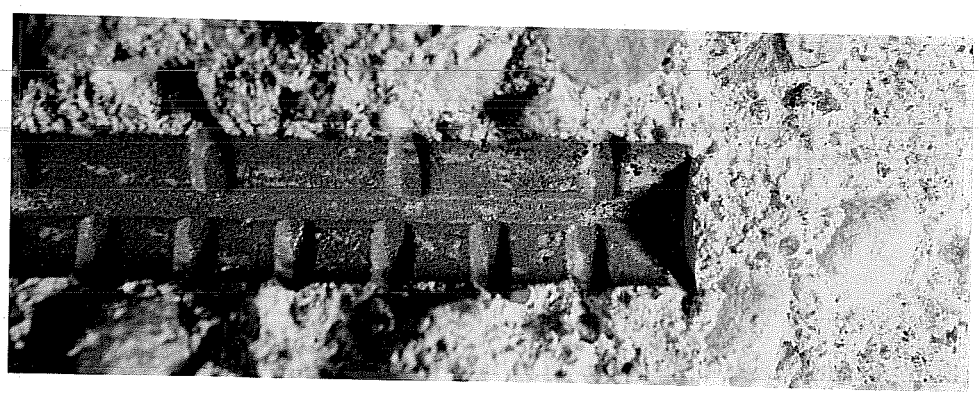

Figure 9.30 Cathodic Bar Trace in Concrete.

CHAPTER 10
MACROCELL CORROSION STUDY: ANALYSIS AND DISCUSSION OF TEST RESULTS

10.1 General

Variables in the macrocell study, such as bar size, deformation pattern, level of coating damage, and patching could have affected the test results significantly. Other factors, including the chloride distribution, coating thickness, and material properties could have also played a role in the corrosion process. These factors may act together or individually, leading to complex behavior of the corrosion systems. In this chapter, the macrocell test results are analyzed and the effects of the various factors are evaluated.

The macrocell corrosion phenomenon was studied in terms of the corrosion system parameters and how they influenced the corrosion mechanism. Time development of the corrosion process, level of corrosion activity and intensity, and observations of the corroded metal and its environment were systematically evaluated. Then, conclusions were drawn as to the causes of coating debonding and loss of integrity which led to corrosion of the metal substrate. The data and observations were used to develop a hypothesis for the corrosion mechanism.

10.2 Time Development of Corrosion

10.2.1 Time-to-Corrosion. Time-to-onset of corrosion varied considerably. It was noted that the less the degree of damage to coating, the longer corrosion initiation was delayed. In other words, the more steel area was exposed, the higher was the potential for earlier corrosion initiation. All specimens with patched damage in series A, the 13-mm (#4) bars, showed negligible activity throughout the two-year period. Patching of bars in series B, the 25-mm (#8) bars, merely delayed the onset of corrosion compared to bars with exposed steel areas.

In general, earlier corrosion initiation was noticed in series B than in A. This reflects the combined effects of many factors: bar size and area of exposed metal; steel metallurgy; variation in coating thickness; and variability of the surrounding concrete environment. The smaller bars had smaller total area of steel exposed, better mechanical properties (yield strength), slightly thicker coatings, and better concrete consolidation.

Epoxy-coated reinforcement showed a greater tolerance to chloride accumulation in the surrounding concrete than uncoated reinforcement. The epoxy film isolated the steel from the contaminated environment and delayed corrosion. When sufficient amounts of chloride ions reached the exposed steel areas, corrosion was initiated. Acid-soluble chloride concentrations associated with the onset of corrosion in the control specimens ranged from below 0.08 to 0.12% by weight of concrete, which is equivalent to 1.8 to 2.7 kg/m^3 (3.0 to 4.6 lb./yd^3). The corresponding average chloride content for onset of corrosion of the epoxy-coated bar specimens was about 0.18% , *i.e.* 4.0 kg/m^3 (6.7 lb./yd^3). Hence, corrosion started on the damaged epoxy-coated bars when chlorides had reached about 1.5 to 2 times the levels corresponding to uncoated bars.

10.2.2 Time-To-Cracking. The control specimens showed surface cracking and staining at ages that varied between approximately 210 and 532 days of exposure. Not surprisingly, the large bar specimens cracked much earlier than the small bar specimens at the same cover depth. This observation agrees with previous findings that the smaller the cover-to-bar diameter ratio, the earlier cracking will occur.[22] Corrosion activity increased noticeably after concrete cracking. Corrosion currents for the small bar specimens increased after about 1.5 years which is roughly the average time to cracking for the six control specimens.

Based on the established relation that each amp-hour of corrosion current consumes 1.04 gm (0.037 oz.) of iron,[106] the average consumption of iron of the control bars at the time of cracking was 0.6 gm (0.021 oz.). As a percentage of the total bar weight or volume, the consumption was as low as 0.05% for 25 mm (#8) bars and 0.1% for 13 mm (#4) bars.

This consumption yields an average yearly rate of thickness loss from the metal surface area of 3.6 μm/yr for all control bars.

As stated earlier, none of the epoxy-coated bar specimens exhibited corrosion-related staining or cracking during two years of exposure. Interestingly, some of the coated bar specimens reached higher levels of metal consumption than those associated with control bar cracking and yet did not crack. Possible explanations of this phenomenon are presented in Sections 10.4.4 and 10.7.1.

Concrete cracking occurred at a much lower rate of consumption of iron than stated by other researchers. Clear and Virmani[57,106,107] indicated that concrete cracking occurs at total iron losses as low as 0.5-2% of bar volume. Broomfield *et al.*[22] found that cracking can occur at steel consumption of 10-100 μm/yr depending on geometry (cover to bar diameter), concrete quality, and oxygen access.

However, Spellman and Stratfull, as reported in Ref. 113, showed that a conversion of as little as 25 μm (1 mil) of steel into its characteristic corrosion products can cause cracking in a 22 mm (7/8 in.) thick concrete layer. More recently, Hime[55] has indicated that although cracking was suggested to occur at a rust thickness of 25-500 μm (1-20 mils), evidence has been gathered that even below 2.5 μm (0.1 mil) cracking can occur. These observations indicate that cracking may occur at significantly lower metal losses than often reported in literature. In this study, the main reasons why cracking occurred at a low metal consumption rate may be attributed to the low strength of concrete and small cover to reinforcement.

10.3 Corrosion Activity

10.3.1 General. In principle, a direct measurement of the corrosion current can be obtained by reading the voltage drop across the resistor in the macrocell specimen. The magnitude of the current reflects the severity of corrosion activity. When monitored versus

time, the corrosion current indicates the amount of iron consumed from the top anode bar under macrocell action.

Besides the cathodic bottom bars in the macrocell specimen, other cathodes may also have developed at the top bar. In this case, the net reaction of the anodes and cathodes on the same bar would not result in a net current flowing to the bottom reinforcement. Such activity is not expected to be critical for coated bars because of the very limited surface area available for oxygen reduction. For uncoated bars, the actual corrosion activity would be underestimated by the measured corrosion current. It is conservative then to compare the performance of coated bars to that of uncoated bars on the basis of the measured macrocell currents.

The rate of corrosion can be expressed in different forms. The commonly-used expressions are: weighted average current; corrosion current density; and amount of metal consumed. These are discussed in the following sections.

10.3.2 Weighted Average Current. The weighted average corrosion current I_{wa} for any specimen was evaluated by the following expression,

$$I_{wa} = \frac{\Sigma I_{ai} T_i}{\Sigma T_i} \qquad i = 1, n \tag{10.1}$$

where, I_{ai} = average current in time interval i,
T_i = time interval i,
n = total number of time periods of measurements.

The magnitude of the weighted average current reflects the severity of corrosion activity over the increment of time under test. The weighted average current provides a measure of the net electrons released by the corrosion process and flowing through the external link. The calculated values of the current (the group averages) at one and two years are listed in Table 10.1.

Table 10.1 Weighted Average Corrosion Current for Macrocell Specimens (μAmp)

Group No.	Damage Category and Condition	Series A		Series B	
		1 Year	2 Years	1 Year	2 Years
1	Control (Uncoated Bars)	55.70	64.51	143.01	164.17
2	Spots > 6 x 6 mm, Patched	0.08	0.62	6.26	20.11
3	Spots > 6 x 6 mm, Exposed	0.64	7.42	35.34	69.50
4	Spots > 2%, Patched	0.11	0.50	3.28	17.96
5	Spots > 2%, Exposed	7.41	13.68	69.32	94.39
6	Cracks < 1%, Exposed	0.50	4.02	9.04	8.90
7	Spots < 2%, Exposed	1.18	1.41	29.04	41.13
8	Control (Uncoated Bars)	44.93	62.59	104.88	151.35
9	Spots > 6 x 6 mm, Patched	0.43	1.88	17.25	14.54
10	Spots > 6 x 6 mm, Exposed	3.30	3.14	27.84	48.32
11	Pinholes < 1%, Exposed	0.04	0.39	14.63	26.72

The table shows that the control bars exhibited much higher corrosion currents than the coated bars. The larger bars performed worse than the smaller bars. In both series, the highest corrosion currents among the coated bars were those associated with highest damage percentage (2%) followed by those with large spots of damage (6 x 6 mm). Patching the small bars was effective in suppressing the corrosion current, whereas patching the large bars merely reduced the current. Data from both deformation patterns were not much different. The rate of increase of the corrosion current at the end of two years suggests that the performance of the coated bars was deteriorating.

10.3.3 Corrosion Current Density. When the weighted average current is divided by the total (nominal) surface area of the anodic bar, the product is defined as the corrosion current density. From information (Ref. 22, 6, and 112) on the rate of corrosion of

reinforcing steel in concrete, corrosion current densities up to 0.1 $\mu A/cm^2$ denote a negligible corrosion rate, between 0.1 and 0.2 $\mu A/cm^2$ indicate a low corrosion rate and a threshold for active deterioration mechanism, and between 0.2 and 0.5 $\mu A/cm^2$ disclose a shift to a moderate corrosion rate. The average current densities obtained for the different groups are plotted in Figs. 10.1 and 10.2. In each figure, a comparison can be made between the results at one and two years of exposure.

For the small bar series, the control bars exhibited moderate corrosion rates with a modest increase in the current density over the second year of exposure. Generally, the corrosion rate of all coated bars was negligible. After two years, the severely damaged bars showed an increase in the corrosion rate towards the low range. Bars with patched damage performed excellently.

For the large bar series, the performance of the control bars was similar to that of the small control bars. However, the coated bars clearly showed a rise in the corrosion rate from negligible to low, and tended to rise rapidly during the two years. The corrosion rates of bars with patched damage, and those with exposed damage less than 1%, remained negligible with a tendency to increase. While the control bars in both series displayed comparable rates, the heavily damaged large bars exhibited about 2-3 times higher corrosion rates than the small bars. Again, deformation pattern had no consistent effect on corrosion.

10.3.4 Metal Loss. The integration of the current-time relationship gives the amount of electrical charge (flux) exchanged in a certain period of time. The amount of charge, *i.e.* number of electrons, correlates with the amount of metal consumed. Therefore, charge flux can be used as a measure of corrosion severity. The average amounts of charge passed in one and two years for the test groups are plotted in Figs. 10.3 and 10.4. In the same figures, the amounts of charge of the coated bars are given as percentages of the uncoated bars. The plots confirm the previous discussion and show that the coated bars varied widely in their performance. At worst conditions, the heavily damaged large bars exhibited corrosion in the range of 25-57% of the uncoated bars. Patching damage reduced corrosion to about 10%.

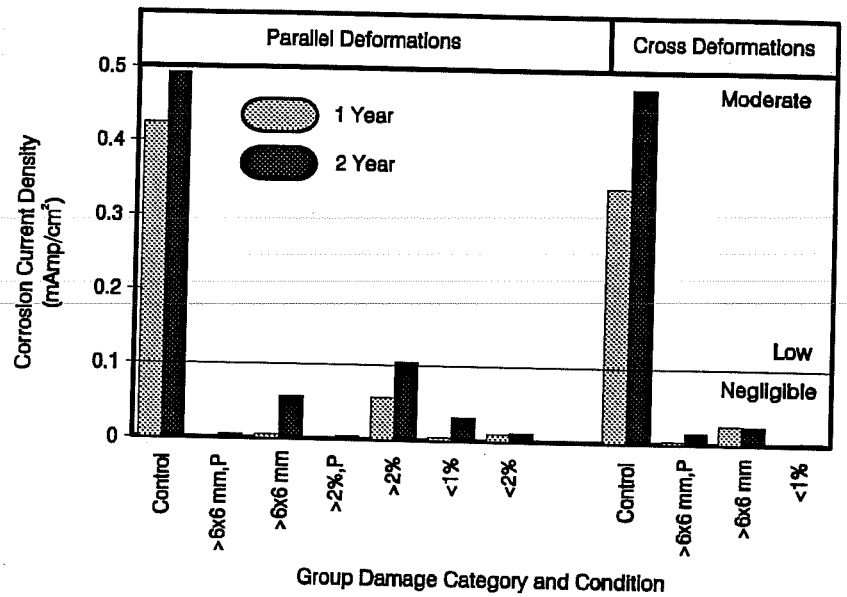

Figure 10.1 Average Corrosion Current Densities for Series A.

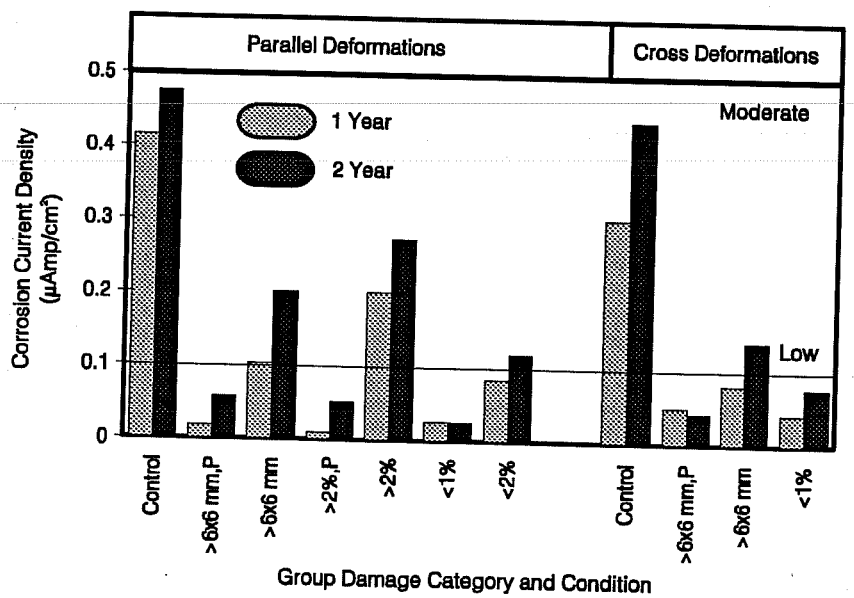

Figure 10.2 Average Corrosion Current Densities for Series B.

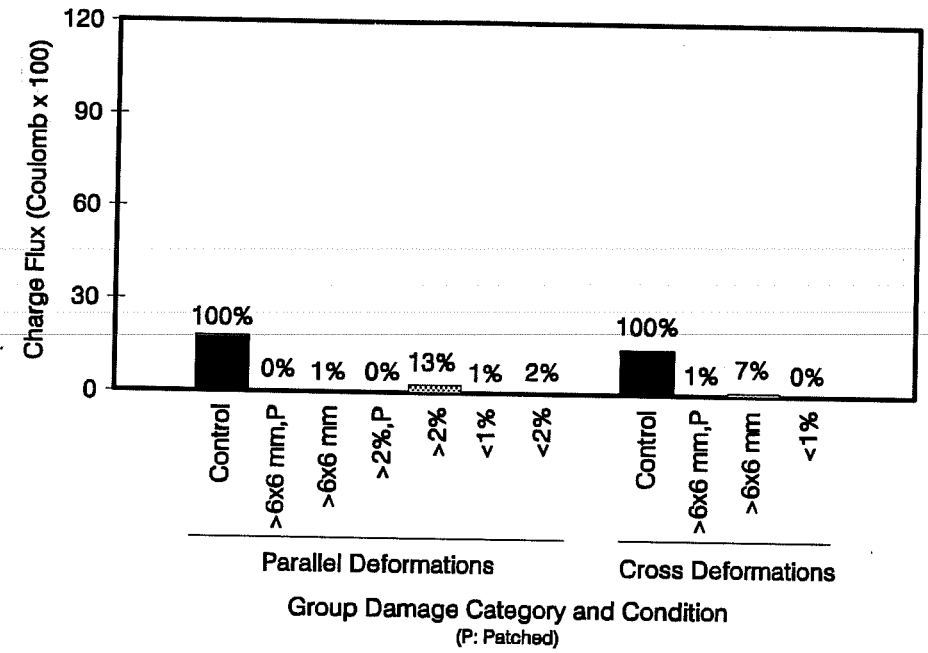

(a) One Year of Exposure

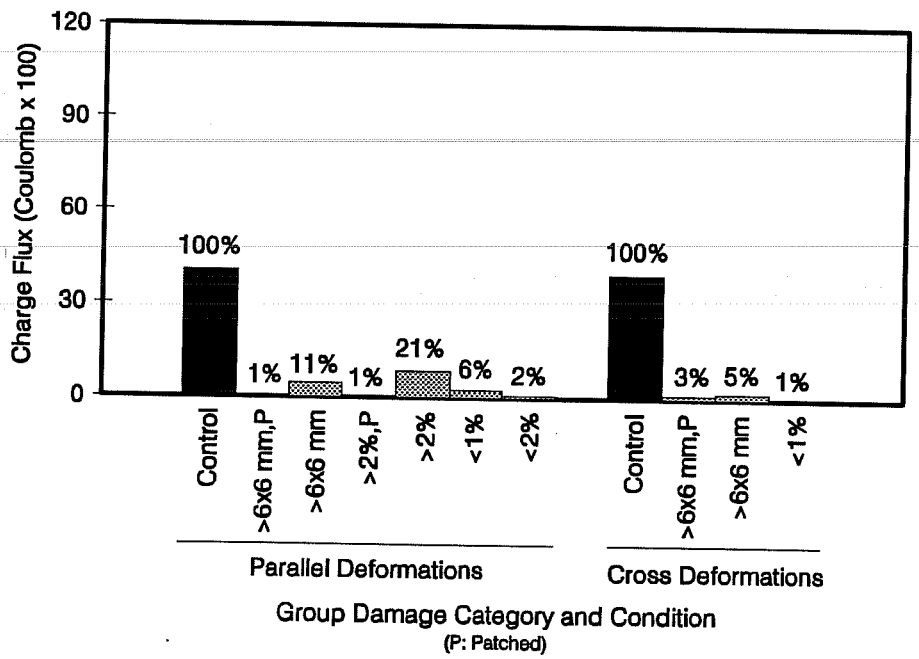

(b) Two Years of Exposure

Figure 10.3 Average Charge Flow for Series A.

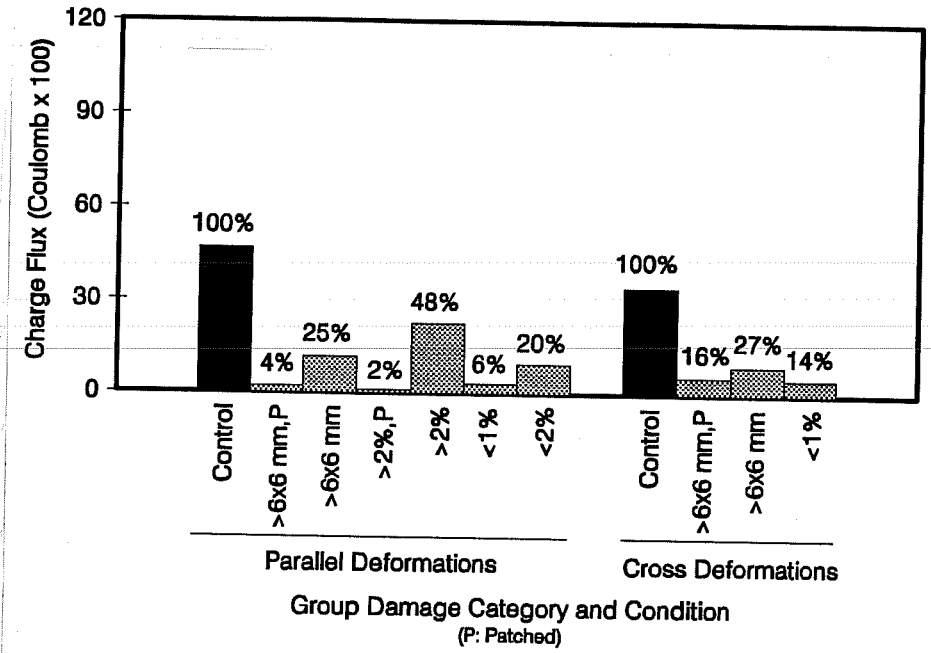

(a) One Year of Exposure

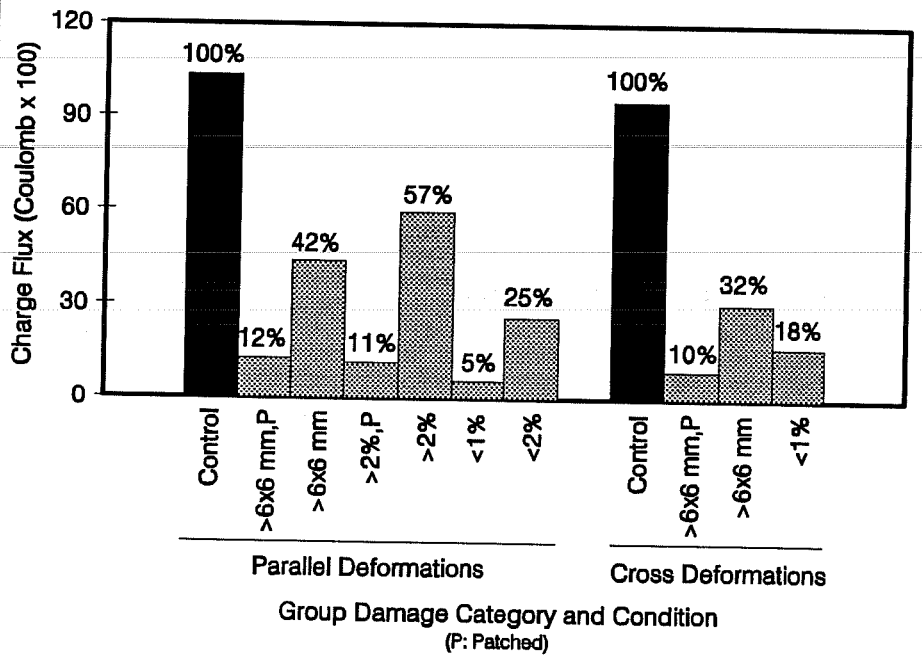

(b) Two Years of Exposure

Figure 10.4 Average Charge Flow for Series B.

The amount of metal lost, in grams, from any specimen during the test period was estimated by multiplying the area under the current-time (Amp-hr) diagram by 1.04.[106] The average values of the consumed metal for each group, after one and two years of exposure, are listed in Table 10.2.

The performance of epoxy-coated bars relative to uncoated bars is clearly better. Based on the amounts of iron lost in corrosion during the test period for the different groups, it is evident that coating reduces metal consumption. This important finding agrees with previous findings that epoxy-coated reinforcement exhibits less corrosion than uncoated reinforcement.[11,56,62,106,108,109,112,115]

Table 10.2 Metal Consumed by Corrosion
(Amounts in mg)

Group No.	Damage Category and Condition	Series A		Series B	
		1 Year	2 Years	1 Year	2 Years
1	Control (Uncoated Bars)	526	1,172	1,349	2,983
2	Spots > 6 x 6 mm, Patched	0.7	11	59	365
3	Spots > 6 x 6 mm, Exposed	6.0	135	334	1,263
4	Spots > 2%, Patched	1.1	9.1	31	326
5	Spots > 2%, Exposed	70	249	654	1,715
6	Cracks < 1%, Exposed	4.7	73	85	162
7	Spots < 2%, Exposed	11	26	274	747
8	Control (Uncoated Bars)	424	1,137	990	2,750
9	Spots > 6 x 6 mm, Patched	4.1	34	163	264
10	Spots > 6 x 6 mm, Exposed	31	57	263	878
11	Pinholes < 1%, Exposed	0.4	7.0	138	486

However, the improvement of performance due to coating application needs to be quantified. The effectiveness of epoxy-coated reinforcing steel to resist corrosion relative to uncoated steel can be assessed in terms of the metal consumption ratio. This ratio, called the performance ratio in Table 10.3, shows the improvement of performance of each group of coated bars relative to the control group. The performance ratio is simply the reciprocal of the charge percentage given in Figs. 10.3 and 10.4. The values are tabulated for both one and two years of exposure and include group averages.

The values in Table 10.3 indicate that most of the patched small bars performed about two orders of magnitude better than the uncoated bars. The corresponding improvement for the patched large bars is about one order of magnitude. Even in the worst conditions, where

Table 10.3 Performance Ratio of Epoxy-Coated Bars to Uncoated Bars Based on Amounts of Consumed Steel

Group No.	Damage Category and Condition	Series A		Series B	
		1 Year	2 Years	1 Year	2 Years
1	Control (Uncoated Bars)	1.0	1.0	1.0	1.0
2	Spots > 6 x 6 mm, Patched	739	104	23	8.2
3	Spots > 6 x 6 mm, Exposed	88	8.7	4.0	2.4
4	Spots > 2%, Patched	497	129	44	9.1
5	Spots > 2%, Exposed	7.5	4.7	2.1	1.7
6	Cracks < 1%, Exposed	112	16	16	18
7	Spots < 2%, Exposed	47	46	4.9	4.0
8	Control (Uncoated Bars)	1.0	1.0	1.0	1.0
9	Spots > 6 x 6 mm, Patched	104	33	6.1	10
10	Spots > 6 x 6 mm, Exposed	14	20	3.8	3.1
11	Pinholes < 1%, Exposed	1,059	162	7.2	5.7

damage slightly exceeded 2% of the surface area, there was an improvement in the performance of epoxy-coated reinforcement over uncoated reinforcement in the time frame of the test. However, performance ratios as low as 1.7 are undesirable. Results from previous testing using both epoxy-coated bars conforming and not conforming to specifications showed about an order of magnitude improvement in the performance of coated bars.[106,112]

The performance of the epoxy-coated bars in a corrosive test environment seems to deteriorate with time. The rate of increase of metal consumption of coated bars is higher than that of uncoated bars. Lower performance ratios are obtained after two years of exposure than at one year. Therefore, longer exposure periods are necessary to determine whether or not the corrosion rates of coated bars will rise to the levels found on uncoated bars.

Metal loss reflects the reduction of bar diameter or bar cross section and can be a decisive parameter for determining the deterioration rate. However, this parameter fell short of indicating whether metal loss was concentrated or distributed. Concentration of metal loss is very important from the viewpoint of structural load-carrying capacity. It has been surmised that damaged coatings could concentrate corrosion in few spots thereby intensifying localized metal loss, whereas the loss would be distributed on uncoated steel. The estimated amounts of metal loss discussed above do not necessarily support this. In fact, visual observations revealed that the uncoated bars suffered more severe pitting corrosion than damaged coated bars! Explanations for this phenomenon are given below.

10.4 Condition of Reinforcing Steel.

10.4.1 Apparent Surface Corrosion. Forensic examination of bar specimens, in general, confirmed the findings of the rate of corrosion analysis. All epoxy-coated bar specimens experienced less steel corrosion than control specimens. Figures 10.5 and 10.6 show close ups of surface corrosion of an uncoated bar and a damaged coated bar specimens,

respectively. The figures illustrate severe surface degradation of the uncoated bar relative to superficial corrosion on the exposed steel of the coated bar.

Figure 10.5 Surface Corrosion of Uncoated Bar After One Year of Exposure.

Figure 10.6 Surface Corrosion of Coated Bar After One Year of Exposure.

Based on visible degradation of steel, the coated bar specimens can be ranked in an order of increasing degree of corrosion damage similar to their order of increasing macrocell activity or amount of steel consumed. The test technique was effective in determining the magnitude and severity of corrosion of the embedded reinforcing bars.

Some epoxy-coated bar specimens, particularly some of the small bars, retained their original appearance without corrosion or blistering despite the high chloride content. There was no undercutting even though the coating was debonded around the bend. This observation agrees with some field studies which demonstrated that epoxy-coated bars extracted from deck slabs were also in excellent condition despite a chloride content between 2 and 7 kg/m^3 (3.3 and 11.7 lb./yd^3).[73] These results indicate that epoxy coating can provide full protection to reinforcing steel from chloride-induced corrosion. Nevertheless, certain conditions should exist pertaining to coating quality, level of damage, and quality of surrounding concrete.

10.4.2 Coating Adhesion to Steel. There are indications that coating bond strength to steel is weakened by fabrication. Bending coated bars causes stretching of the coating at the rib bases (rib-bar intersections) on the outer surface of bend. The regions at the rib bases of the test bars seemed slightly discolored which indicated thinning of the coating and a tendency for debonding. A recent study has demonstrated that coating films are consistently thinner at deformation edges than in the areas between the deformations.[94] The difference in coating thickness averaged about 23 μm (0.9 mils) for straight bars, and about 55 μm (2.2 mils) for bent bars.

The initiation of corrosion activity in thin film regions is a consequence of developed holidays. This is a common observation in corrosion studies.[94] A thin film spot is a point of weakness where holiday formation is most likely to occur. The indicators to debonding are the micro-tears in the coating and the more noticeable cracking. Even if the film remains unbroken, it probably allows oxygen and water to cross the film. With debonding, the condition becomes worse; moisture and oxygen can be retained beneath the coating and

corrosion is more likely to initiate. Figure 10.7 illustrates stretching and debonding in the rib base region on the outside of bend.

Damage on the inside of bend is usually neglected mainly because the region is compressed instead of stretched. However, coating debonding may still occur. Bending a coated bar generates high shear stresses at the steel/coating interface on both sides of the bend. The stresses may break the adhesion creating paths for oxygen and water migration to the debonded region. Figure 10.8 shows the microscopic ripples that form on a compressed coated surface. Localized compressive residual stresses at the metal surface have been recognized as a factor to initiate corrosion at the inside of bends.[16] Such a phenomenon explains why sheet steel often rusts first at bent edges.

Exposure of the coated bars to the corrosive test environment seriously impaired coating adhesion to steel. The epoxy coating flaked away from exposed bars more readily than from similar unexposed bars. Coating softening and debonding after exposure to a chloride-contaminated concrete was also reported by Clear,[112] and Sagüés, *et al.*,[84,110] Further, coating debonding was observed by others in "perfect" condition bars that had passed the standard bend test.[98] It was suggested that an alteration to the epoxy/steel interface boundary occurs in the concrete environment. Reference 111 refers to Romano's suggestion that "cathodic disbondment of epoxy coatings can occur adjacent to damaged areas because of the galvanic process occurring between the cathodic and anodic sites on the steel."

The straight portions of the embedded test bars initially had very strong coating adhesion relative to coating on the bent portions. These straight ends exhibited significant debonding after two years of exposure, compared to limited debonding after the first year. However, underfilm corrosion on the straight portions was negligible. It appeared that well-adhered, damage-free coatings suppressed corrosion even after adhesion was lost. Conversely, defective areas with initially weakened adhesion (the bent portions) suffered widespread corrosion.

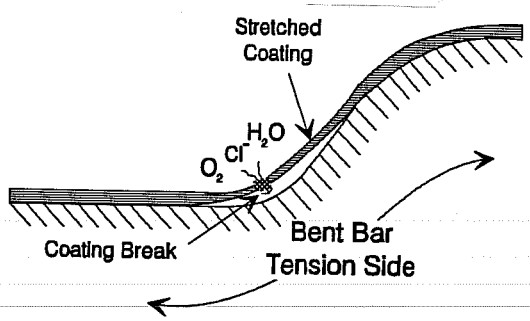

Figure 10.7 Coating Thinning and Debonding at Rib/Bar Interface.

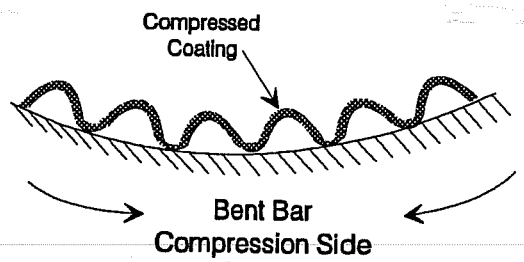

(a) Schematic Drawing

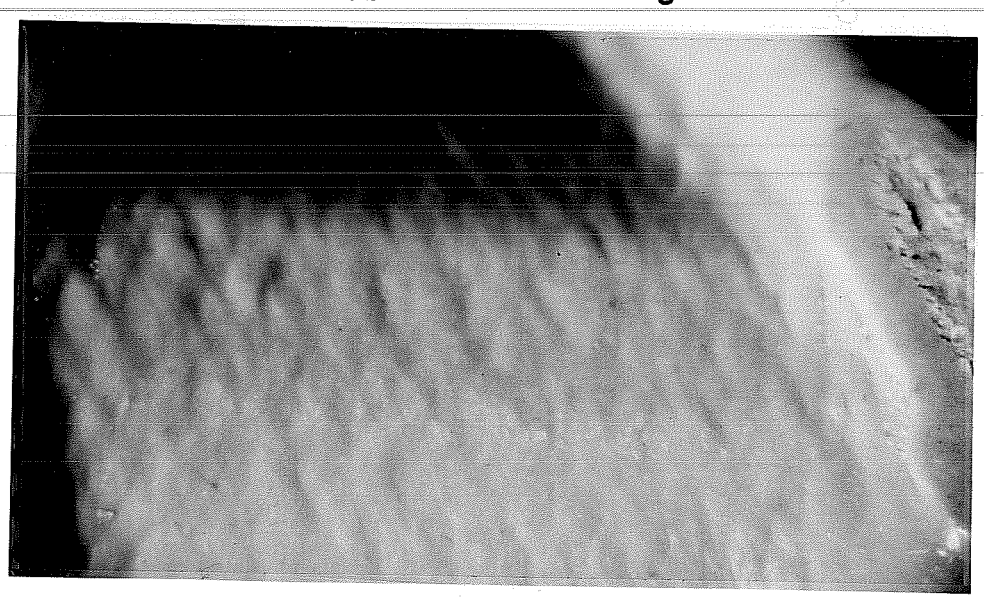

(b) Inside of Bend

Figure 10.8 Compressed Coating Surface.

The degree of debonding may affect the extent of undercutting. A precursor to this is the premature failure incidence of the coated bars which were generally related to some problem in coating adhesion.[41] The key factors to achieving proper adhesion are steel cleanliness prior to coating, anchorage profile, and coating curing.

10.4.3 Undercutting. Although large parts of the coating seemed unaffected when visually examined, the subsurface conditions indicated corrosion activity at various stages. Corrosion which may have started at defects and exposed metal areas spread beneath the epoxy coating. For some coated bar specimens, after the first year of testing, undercutting was confined to the vicinity of exposed steel areas, and coating defects and breaks documented before testing. Other bars, including the majority of those inspected after two years, showed either widespread underfilm corrosion or localized corrosion around pinholes not detected prior to exposure.

Underfilm corrosion (further from exposed steel areas) was, generally, in the form of light surface rusting with no significant loss in bar section. Coating protected the steel surface from direct attack by chloride ions. Similar observations were reported by Sagüés, Powers, and Zayed,[42,93,109] Mckenzie,[115] Sohanghpurwala and Clear,[111] and Kobayashi and Takewaka.[11] It has been suggested that corrosion results in the formation of flat cavities under the coating where there is little oxygen and therefore the corrosion process is slow.[29]

The corrosion morphology of steel substrate was in many aspects similar to that described by Zayed and Sagüés,[109] in a corrosion study of epoxy-coated bars. The bars with cross deformations showed corrosion spots at holidays at the crossing of deformations. Corrosion spread on both the inside and outside bent portions. The coating could be easily peeled around the bend with a sharp blade. The corrosion products building up on the exposed steel were dark red-brown; however, the metal under the coating was covered with a greenish-black product. Away from the corroded spots, the metal was usually bright.

10.4.4 Black Corrosion Products. Corrosion spreading underneath the epoxy coating, as noted above, was characterized by the formation of a thin black (greenish-black)

corrosion layer. The black corrosion product has been identified by others as magnetite Fe_3O_4. Swamy *et al.*,[108] Treadaway and Davis,[62] Rasheeduzzafar *et al.*,[113] Clear and Virmani,[57] and Erdoğdu and Bremner[56] made the same observation.

The black product is indicative of corrosion in a restricted oxygen environment of crevices that form under the coating. Such a corrosion product is in a low state of oxidation generated from ferrous ions Fe^{+2} present in $Fe(OH)_2$ or $FeCl_2$ or $FeCl_2.H_2O$.[62,113] Upon exposure to open air, the complex ferrous chloride ion converts instantly to a black granular product Fe_3O_4. Further oxidation to ferric ions Fe^{+3} after some time of exposure to air produces the more usual and stable red-brown corrosion product Fe_2O_3.

Because of its low state of oxidation, the ratio of the volume of black corrosion product to the volume of the parent iron is small compared to that of developed red rust. The volume of rust product Fe_3O_4 is about twice as much as the original steel as shown in Fig. 10.9. In saturated concrete, the increase in rust volume is only 20-50%.[60] In comparison, the reddish rust $Fe(OH)_3.3H_2O$ has a volume 6-7 times greater than the original steel. When concrete is very wet, the volume increase of black corrosion product may either reside under the coating or diffuse through the pore network of concrete. Consequently, less internal pressure is exerted on concrete in the case of the black product than higher iron oxidation products.

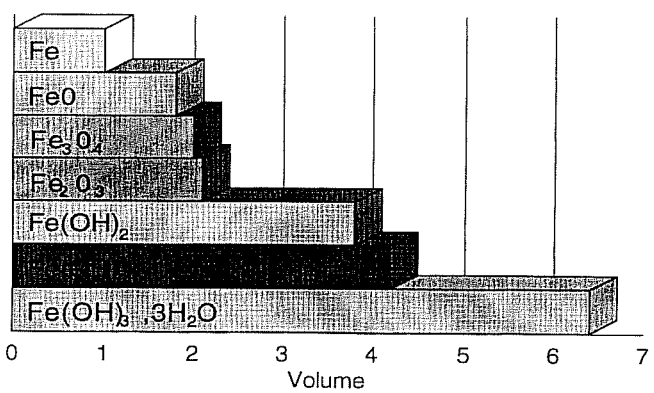

Figure 10.9 Volume Ratio of Corrosion Products.[60]

It follows that the corroded epoxy-coated bars produced smaller amounts of corrosion products than uncoated bars (which agrees with visual observations made on opened concrete specimens). The associated volume increase with the black product was not substantial and was insufficient to develop high enough stresses in concrete to cause cracking. This explains why some of the coated bar specimens reached higher levels of steel consumption than those associated with control bar cracking and yet did not crack. Another supplementary explanation for this phenomenon is related to the configuration of the corrosion system and is given in Section 10.7.1.

It is suspected that the formation of the greenish-black corrosion product was a result of two factors, the restricted oxygen diffusion to anodic sites and the possible high corrosion rate. Oxygen diffusion to the anodic sites (developed in the crevices underneath the coating) was limited by the coating barrier. Therefore, more ferrous ions were produced than could be oxidized to ferric ions. As a result, the corrosion products remained in the lower state of oxidation.

In addition, the large cathode to small anode ratio increased the *local* corrosion rate in the limited anodic steel (at damaged spots and to some extent beneath the coating). Thus, more of the lower level oxidized iron was produced before it could be converted to an oxide of higher level. In other words, the electrochemical reactions were controlled by activation polarization.

10.4.5 Coating Blistering. Blisters were found spreading on the coating surface indicating pitting corrosion. The pits were generally very slight (shallow depth) covered with black and brown brittle corrosion products. Figure 10.10 shows a blister under microscopic examination. At some locations, the buildup of corrosion products breached the epoxy film. At other locations, the blisters were soft and full of liquid. The majority of blisters were formed on the lower half of the bar surface where voids developed at the coating/concrete interface.

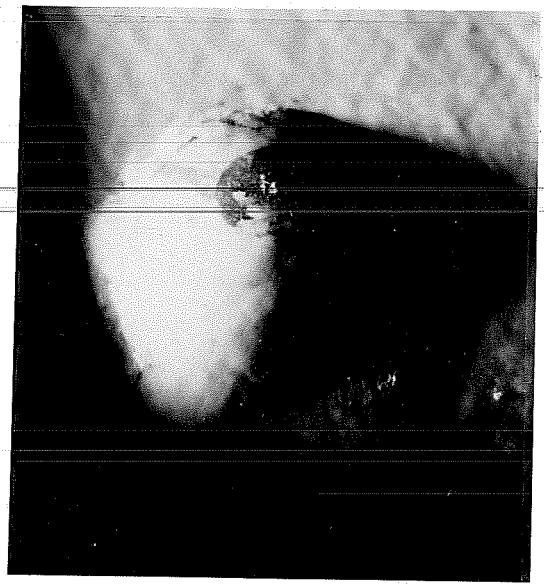

(a) Blister on Coating Surface

(b) Corrosion Product Buildup in Blister

(c) Pitting Inside Blister

Figure 10.10 Blister Under Microscopic Examination.

Blisters were formed because of the increase in volume of the corrosion products in the vicinity of coating defects. Sohanghpurwala and Clear,[111] and Treadaway and Davies[62] reported similar observations. Pfeifer *et al.*[94] also observed blistering and cracking of the coating over a corroded bar which exhibited a high macrocell corrosion current during their experiment. Clear noticed rust stains exiting from the edges where the bars protruded from concrete similar to the swelling spots observed in this study.

A clear or pasty (whitish) liquid was frequently found trapped under freshly chipped epoxy coating and inside blisters. The surrounding concrete was relatively dry indicating the ability of the coated bar to retain the solution between the epoxy film and steel surface. This solution was also observed by other researchers such as Sagüés,[42,93,109,110] who described it as acid moisture accumulation or "local acidification". He also noticed that blisters formed at locations facing air voids in concrete. Treadaway and Davies[62] indicated that the green product was always found in concrete with high chloride concentration and in association with very localized regions of lower pH (*i.e.* acid solution).

10.5 Concrete Consolidation Around Reinforcing Bars

10.5.1 General. The effects of concrete placement and consolidation on corrosion performance of embedded steel has not been strongly emphasized in literature. In this study, it was found that the condition of the concrete region surrounding the coated bars played a significant role in the corrosion process. The following discussion will expose the factors that had profound effects on corrosion initiation and coating degradation observed in the macrocell test.

10.5.2 Differences in Concrete Consolidation. During concrete consolidation and setting, water migrates towards the top concrete surface. Some of the bleed water is trapped under the horizontal epoxy-coated bars. As fresh concrete settles, small gaps are formed under the coated bar. Gap formation is enhanced by lack of interlock and cohesion between cement mortar and coated bar surface. Free water may then accumulate in that zone underlying the bar. When water eventually evaporates, it leaves voids or air pockets adjacent

to bar surface. These voids will not be filled during hydration similar to the voids forming around the aggregates due to bleeding and inefficient packing of the cement mortar. As a result, a weak porous zone, with possible interconnected cavities, forms underneath the bar. This zone is characterized by a dull, light gray appearance as shown in Fig. 10.11.

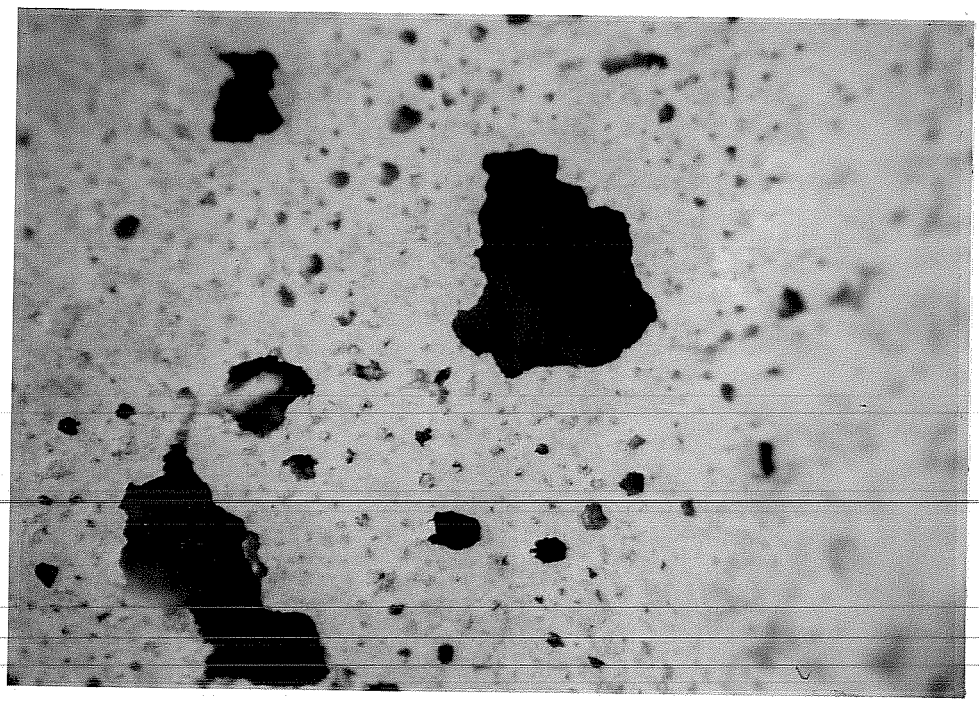

Figure 10.11 Concrete Below Coated Bar.

Based on observations from the opened macrocell specimens, initial efforts were taken in this study to investigate the possibility of gap formation beneath the coated bars. One concrete prism of similar dimensions to the macrocell specimens was cast with an individual coated bent bar typical of those bars used in series B. Concrete was vibrated as in a normal casting procedure. The prism was sawcut after few days in a plane perpendicular to the bar axis. The condition of concrete above and below the bar was microscopically inspected. Although concrete was compacted well above the bar, a gap was found underneath the bar. A view of the gap is shown in Fig. 10.12.

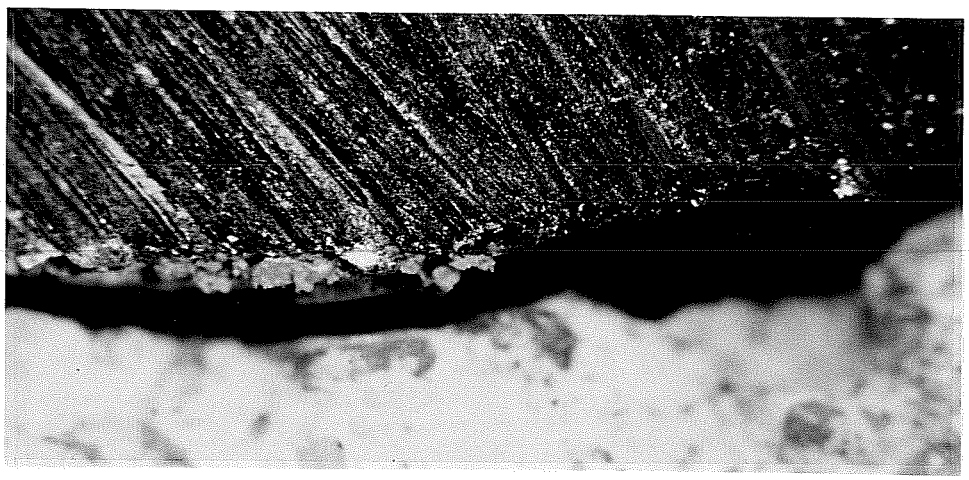

Figure 10.12 Gap Formation below Coated Bar.

The zone under the bar may trap relatively large amounts of harmful substances very close to the bar surface. Moisture, oxygen, and chlorides are the specific agents necessary for corrosion. With time, these agents penetrate to the metal surface mainly through damaged spots, coating defects, and holidays. Salt solution may also accumulate under the bar and beneath the coating bridging between concrete and the corroded sites. Corrosion commences and progresses causing widespread undercutting.

In contrast, concrete resting on top of the coated bar will be more dense and closely-packed than that below the bar. Concrete consolidates as it builds up on top of the bar. The smoothness of the coated surface facilitates displacement of concrete to the sides of the bar. With vibration, more cement paste concentrates at the bar/concrete interface. As a result, the condensed fine mortar on top of the bar will generally have a smooth and continuous interface layer. This layer appears glossy and relatively dark gray when cover is removed as shown in Fig. 10.13.

10.5.3 Influence of Concrete Consolidation on Corrosion. The differences in concrete environment above and below the coated bar are expected to influence the corrosion performance negatively. First, any steel exposed (at holidays or damaged areas) facing the

gaps may be more prone to corrode upon exposure to salt than steel covered by alkaline concrete. Second, differences in the electrolytic concrete surrounding the bar, even if slight, may promote concentration cell development (see Chapter 2). Variations in concrete above and below the bar, related to moisture distribution, oxygen supply, and chloride concentration, are most likely to occur. Therefore, steel areas exposed on the top and bottom of the bar have a potential for macrocell activity.

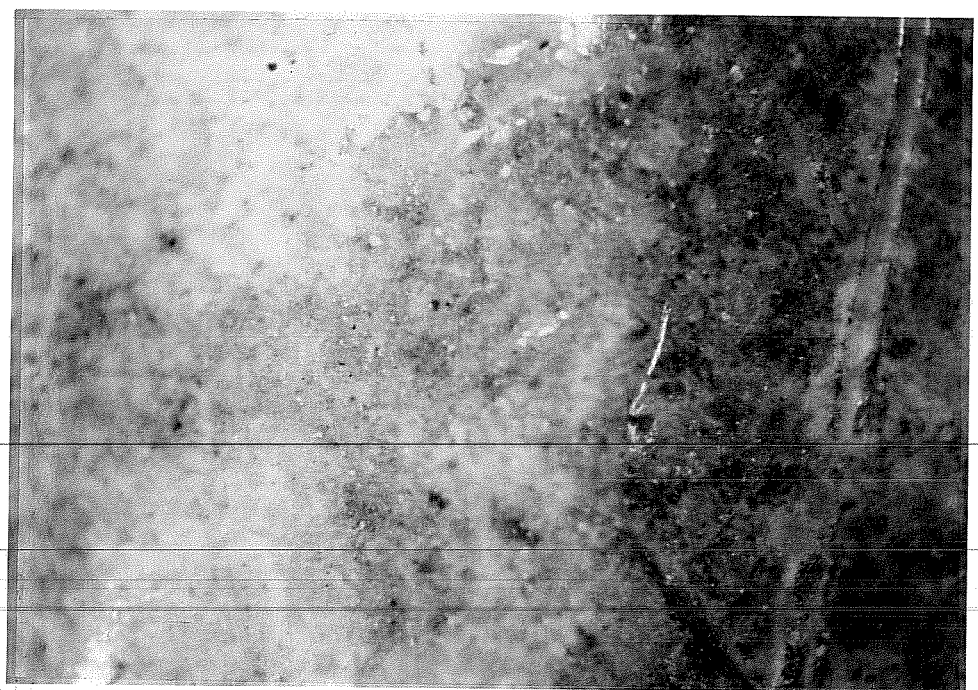

Figure 10.13 Concrete Above Coated Bar.

Chloride ions, for example, have restricted movement in dense mortars.[50] This suggests that the amount of chloride in the zone immediately above the bar may be limited. However, the porous zone below the bar, as stated earlier, can retain deleterious materials such as chlorides. Fraczek[43] also indicated that high localized concentrations of chlorides occur primarily in voids in concrete that are in direct contact with steel. Hence, there is probably less chloride concentration at the top side of bar than at the bottom, even though chlorides are penetrating from the top concrete surface!

There is evidence that corrosion activity takes place in voids in concrete facing embedded steel. Escalante and Ito[58] illustrated the process as it might occur adjacent to a steel surface in concrete. They showed that moisture saturated concrete will have solution-filled voids containing low concentrations of chlorides and oxygen. However, as the concrete dries, salts concentrate and precipitate an the walls of the voids as shown in Fig. 10.14.

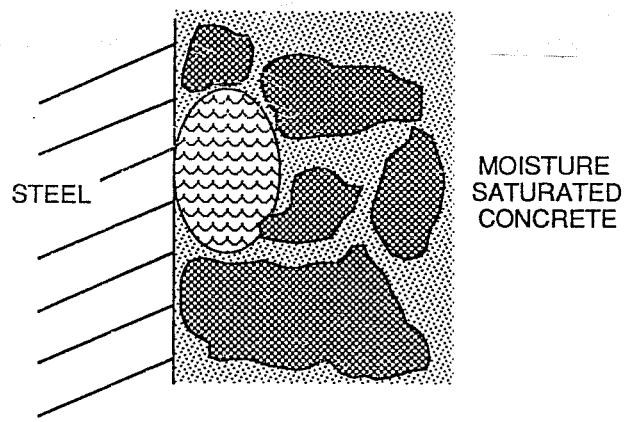

(a)

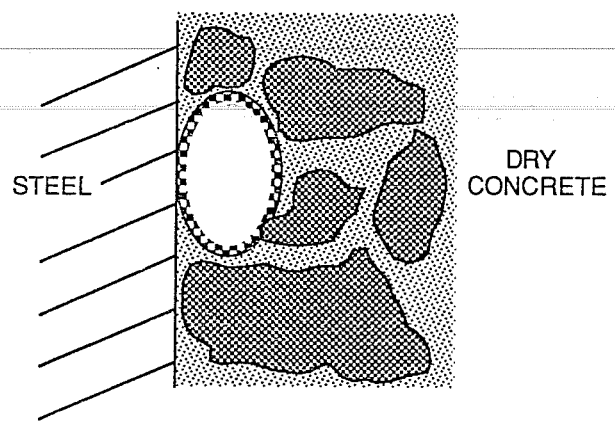

(b)

(a) Void adjacent to steel containing a solution of low concentration of salts and oxygen; (b) Concentration of salts on walls of void during drying cycle.

Figure 10.14 Voids Promoting Steel Corrosion in Concrete.[58]

Oxygen diffuses into the concrete and concentrates in these voids. Thus, both wetting and drying, and concentration of chlorides and oxygen in voids, promote corrosion. Figure 10.15 shows corrosion products found in voids in contact with exposed steel on a coated bar specimen.

Figure 10.15 Corrosion Products Found in Voids at Coated Bar Surface.

Based on the concept of corrosion protection by a steel passivation film, steel will not be passivated at the spot where a void exists. Hime and Erlin[46] illustrated the formation of the oxide film over a steel surface fully embedded in a high pH concrete as shown in Fig. 10.16. In their illustration, a void at the steel surface which interrupted the formation of the oxide film is shown. Hence, discontinuity of the protective layer is attributed to the void formation. Hime[55] also suggested that a possible cause of localized corrosion on a steel bar in concrete is an attached air bubble that does not allow penetration of the alkaline paste.

The discussion above agrees fully with the observations of autopsied bar specimens presented in Sections 9.6.4, 9.6.6, and 9.6.7, and the discussion in Section 10.4.1. Corrosion was worse on the lower half of the coated bars than on the upper half. Blisters formed in voids in contact with the bar surface, particularly at the bottom side. A trapped solution was detected beneath the coating with different precipitates along the bottom surface of the bar. More voids existed at the bar/concrete interface below the bar than above it. Laitence and some whitish deposits were observed underneath the coated bars.

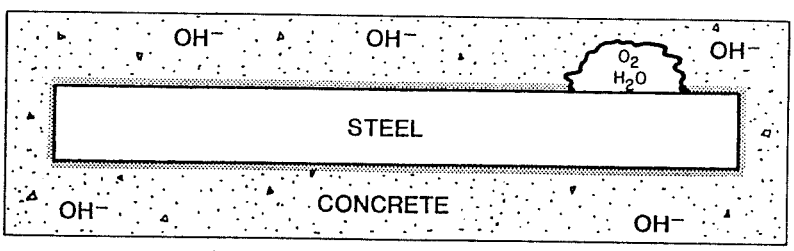

Figure 10.16 Steel depassivation at Void Formation in Concrete.

In addition, photographs of the exposed steel areas on bar specimens retrieved after one year of testing were re-examined. The purpose was to confirm that corrosion initiated generally at the edges of the open areas, *i.e.* around the perimeter of the cut in coating (see an example in Fig. 10.17). It is possible that while casting concrete, the cement paste filled these open areas but bridged over the sharply cut edges. If this happened, both the gaps that were formed and the crevice effect at the coating edges encourage corrosion initiation as shown in Figure 10.18.

The discussion above may also explain why pitting corrosion was observed primarily on large damaged spots. The larger the damaged area of coating, the more it is exposed to the electrolyte. Then, chances are higher for chloride solution to accumulate excessively in the pores or voids in contact with steel. As soon as an anodic potential develops, corrosion starts and accelerates under the catalytic action of chlorides. Hence, the size of the defect

or damaged area is a physical constraint which governs the severity of chloride attack. Both the frequency and size of the damaged areas need to be controlled to reduce probability of corrosion .

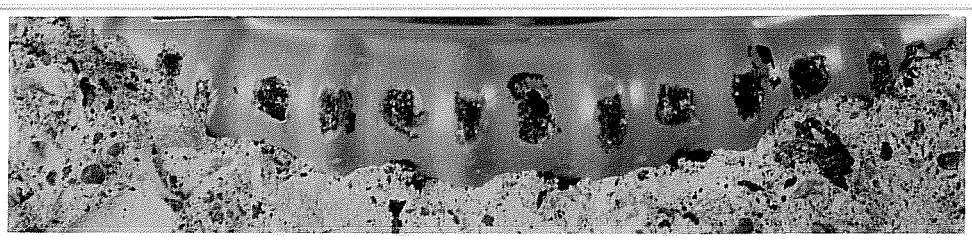

Figure 10.17 Corrosion Initiation Around Exposed Steel Areas on Damaged Coated Bars Embedded in Concrete.

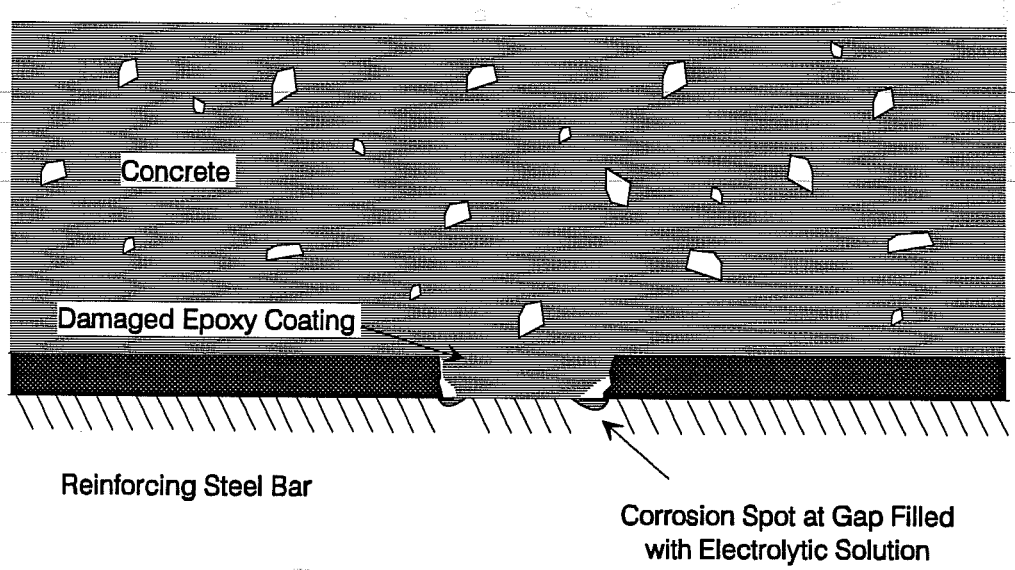

Figure 10.18 Schematic Diagram of Corrosion Initiation Around Exposed Steel Areas on Damaged Coated Bars Embedded in Concrete.

10.6 Influence of Initial Concrete Cracking on Corrosion

10.6.1 General. Cracks which follow the line of reinforcing bar, for example plastic shrinkage cracks and plastic settlement cracks, are very damaging in a corrosive environment.[44] These cracks are frequently wide, and allow corrosion to spread appreciably along the bar. They also reduce concrete resistance to spalling. The relation between these types of cracks and the susceptibility of epoxy-coated bars to corrosion need to be examined.

10.6.2 Crack Formation and Consequences. Excessive amounts of deep cracking have been observed on bridge decks constructed with epoxy-coated bars.[29] The cracks were developed during the early stages of curing. This may indicate a serious problem involving plastic settlement cracks. In addition, research conducted on bond characteristics of coated bars in beams indicated that flexural cracking occurred at every section containing a coated stirrup.[122] In effect, the coated transverse reinforcement, tie or stirrup, tends to act as a crack inducer. Additionally, the crack widths were larger than those associated with uncoated bars.

In the macrocell study, relatively wide plastic settlement cracks were observed on the top concrete surfaces of some specimens (see Appendix C). The width of the cracks varied considerably but were as large as 0.4 mm (0.015 in.). This observation and the preceding ones above suggest that coated bars are more prone to develop wide plastic settlement cracks and flexural cracks in the same planes of the bars. This tendency has a negative influence on the corrosion performance of coated bars.

When plastic settlement cracks are present, chloride contamination is virtually instantaneous. Cady and Weyers[20] predicted that, due to plastic settlement cracking, a bridge deck with 25-mm (1 in.) average cover will be critically contaminated with chloride over more than 50% of the deck from the very first season of deicer application. Excessive levels of chloride contamination at bar surface can be reached within a very short time of service.

10.7 Aspects of Corrosion of Epoxy-Coated Bars

10.7.1 Conceptual Behavior. From the preceding sections, it seems that many unfavorable conditions may combine where epoxy-coated bars are used beginning with wide plastic settlement cracks, frequent gaps beneath the bar, lack of adhesion to concrete, and instantaneous contamination by intruding chlorides. From the standpoint of preparing for the worst case, epoxy-coated steel used as top reinforcement in slabs, may develop the conditions depicted in Fig. 10.19 (with exaggeration for clarity).

A few interesting key points emerge from the preceding diagram. First, corrosion products that develop on the lower half of the coated bar may turn brownish if moisture and oxygen were available in the voids to further oxidize the initial black corrosion products. In addition, the availability of *space* in these voids allows friable corrosion products to build up.

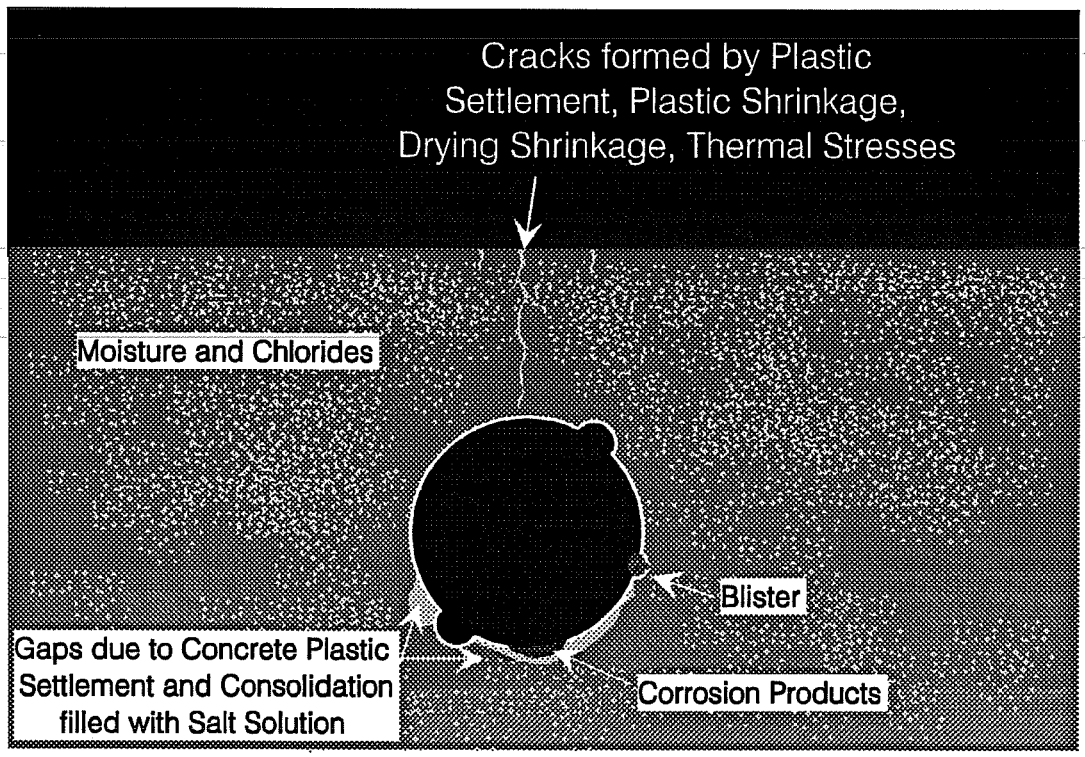

Figure 10.19 Conditions Developing for Coated Bars Embedded in Concrete.

Conversely, the steel substrate at the upper half of the bar, where concrete is well consolidated, remains in an air-tight zone suffering from oxygen starvation. As a result, a very thin black layer forms underneath the coating. Moisture may also reach to the upper surface by means of capillary action or "web effect", or simply permeation through the coating.

Second, a fundamental difference in corrosion behavior between epoxy-coated bars and uncoated bars can be deduced. With all other variables being equal, the uncoated bars tend to suffer more corrosion at the upper half of the bar, where intruding chlorides attack first. Corrosion builds up voluminous solid products that exert radial pressure against concrete cover causing early cracking (see the illustration in Fig. 10.20).

The opposite is true for the epoxy-coated bars placed near the top concrete surface. Unless the coated bars are heavily damaged at random, corrosion tends to commence at the lower half of the bar. The corrosion products remain in a low state of oxidation and may diffuse through concrete pores; the volume of the corrosion products is nearly always small. Consequently, the generated internal pressure is low and in an inward direction (see the illustration in Fig. 10.20). Therefore, the risk of developing corrosion-induced cracking and deterioration is lower for coated bars than uncoated bars. This explains again why concrete specimens containing coated bars with large amounts of lost steel did not crack during the macrocell test.

Based on the foregoing discussion, concrete cracking should not be construed as a principal criterion of comparison between the corrosion performance of coated and uncoated bars. Cracking simply does not indicate the true level of corrosion activity of coated bars. The amount of metal lost is a more reliable indicator of the severity of corrosion, although it does not correlate with the intensity of corrosion at the exposed metal surface.

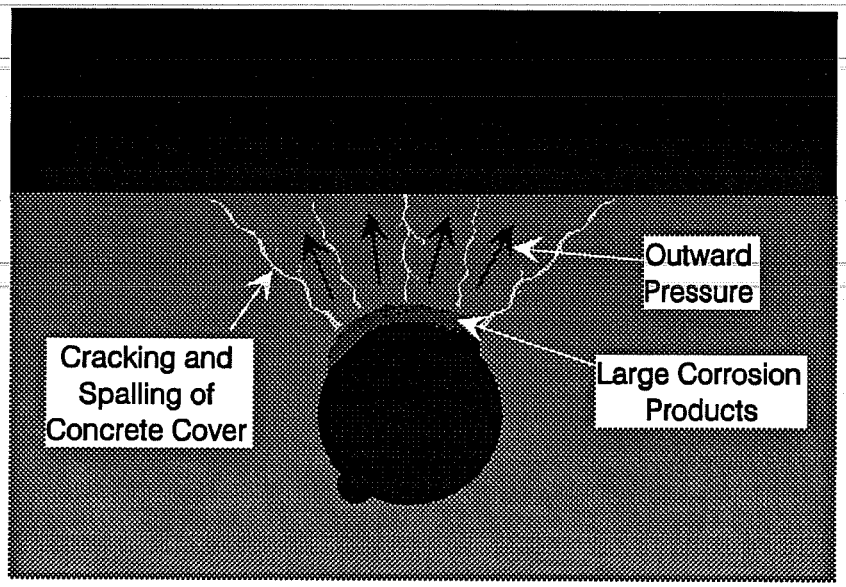

(a) Uncoated Bar

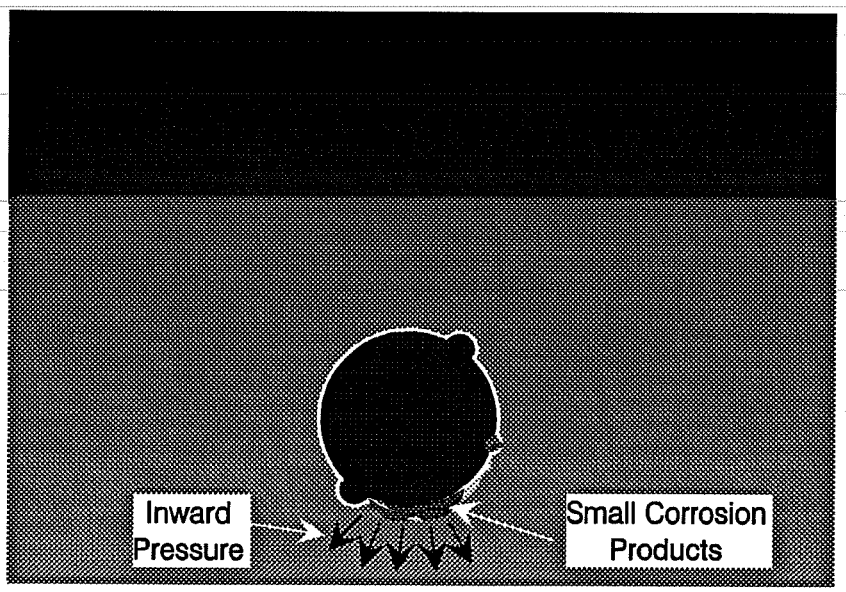

(b) Coated Bar

Figure 10.20 Differences of Corrosion Behavior Between Uncoated and Coated Bars in concrete.

This consideration has a significant impact on the evaluation of bridge decks based on surface condition surveys only. The absence of cracking, despite being a positive sign of good performance, may actually be a deceptive sign! This should not be interpreted, however, to devalue the benefit of using coated bars, as they still show improved performance over uncoated bars. Until this time, there has been no better alternative to detect the condition of coated bars in the field than visual inspection at some check points.

10.7.2 Effects of Bar Size on Corrosion. The smaller bar specimens developed less corrosion than the larger bar specimens. This observation has been pointed out earlier based on comparisons of both visual appearance and corrosion rate data. One significant factor for the discrepancy is that the concrete environments surrounding the two different bar volumes were different. Concrete consolidation around the top reinforcement is affected by the bar size. Variations in consolidation will, in turn, affect the formation of plastic settlement cracks and the void structure in contact with the reinforcing bar. From the forensic examination, there were smaller and fewer voids around the 13-mm (#4) bars than the 25-mm (#8) bars. Other contributing factors for the difference in behavior between the two bar sizes may be their different metallurgy and the dissimilar concrete electrical resistivity in the two different concrete mediums.

10.8 Corrosion Mechanism

10.8.1 General. The following sections will describe a hypothesis of macrocell action on the test bars (both uncoated and coated). The scenario of the hypothesis reconstructs the most likely sequence of steps that lead to the observed behavior. The first part of the hypothesis is based on published research findings on the causes of rapid concrete distress in bridge decks presented by Clear and Virmani[57] more than a decade ago.

10.8.2 Macrocell Action on Uncoated Bars. The uncoated bars corroded more severely than the coated bars, *i.e.* showed deeper pits and worse surface degradation. The surface area of rust on the uncoated bars was not significantly larger than that of the coated bars extending beneath the coating. A likely mechanism for this behavior is presented below:

When sufficient amounts of chloride ions penetrated the concrete cover and reached the top uncoated reinforcement, they initiated micro-corrosion cells. The potentials of the micro-anodes decreased rapidly and reached highly negative values (say more negative than -350 mV CSE). Consequently, there was a large potential difference between the anodic sites and the large cathodic steel at the bottom of the specimen. A macrocell corrosion current flowed between the two reinforcing layers.

The periodic wetting and drying promoted corrosion activity. As the pH of the local anodes dropped due to hydrogen ion H^+ generation by the corrosion reaction, the remaining steel area on the top bar maintained a relatively high pH value. This created another macrocell on the top bar which intensified metal dissociation at the same anodes. In the end, the corroded areas covered only a fraction (1/10 to 1/5) of the total surface area of the top bar before concrete cracking occurred.

After cracking, excessive amounts of chlorides and oxygen reached the top steel to accelerate the corrosion process and convert the corrosion products to higher oxides. Perhaps, as concrete further disintegrated and separated from the metal surface, new anode sites developed and corrosion propagation continued on the surface.

Two observations strongly support the above hypothesis. First, the surface of the top bar was virtually free of rust everywhere but the small fraction of corroded sites. This indicated that steel next to the pits was cathodically protected. Second, concrete darkening around the unaffected steel (similar to that observed around the cathodic bars at the bottom), provided further evidence of the second macrocell formation. Also, it has been established by test results that the pH at the bar/rust interface reaches 3.0 or lower, while the pH of the neighboring concrete remains at 12 or more.[123]

10.8.3 Macrocell Action on Coated Bars. The initiation of corrosion on the exposed metal areas of the epoxy-coated bars followed the same sequence of steps described for the uncoated bars. A probable distinction is the chloride concentration associated with the onset of corrosion. The limited areas available for reaction on the coated bars necessitated higher

levels of chlorides to accumulate sufficiently in the vicinity of these exposed areas to depassivate the steel. The potential difference was almost exclusively developed between the corroding anodes and the bottom macro-cathodes.

The macrocell current flowed and the anodic activity spread to adjacent areas beneath the coating. The weak coating adhesion in the bent area (due to fabrication) facilitated migration of chloride ions, and other species in the electrolyte, to new locations under the coating. The pH at the anodic sites and their vicinities dropped to acidic levels due to ferrous ion hydrolysis in chloride solution. As acidification continued, the oxygen supply became deficient in flat crevices under the coating and created a self-perpetuating corrosion environment. Corrosion products formed in small quantities in a low oxidation state. The volume of the corrosion products was not large enough to breach the coating. The steel surface remained isolated from the alkaline pore solution of concrete. Thus no second macrocell was formed due to variation of pH along the bar surface.

Corrosion activity continued causing further metal dissolution at the exposed anodic sites and light surface degradation beneath the coating. Voids in the surrounding concrete provided opportunities for expansion where shallow pits started to form and corrosion products grew inside the cavities; thus, blisters were formed.

Under repeated wetting periods, the debonded coating retained an aqueous solution which became acidic. As the acid solution travelled freely along the steel surface, a probable secondary cathodic reaction involving hydrogen reduction might have occurred. However, corrosion activity was still below the level found on uncoated steel. Corrosion products either diffused in concrete at coating breaks, or deposited at the bottom cavities alongside the continuous rib.

Both oxygen starvation at the anodic end (beneath the coating), and the high electrical resistivity of the path between anodes and macro-cathode (due to dielectric properties of the coating) lessened the severity of corrosion action. The fact that concrete did not crack

indicated that further oxidation of ferrous hydroxide $Fe(OH)_2$ to red rust Fe_2O_3 was not supported and iron remained in the ferrous state.[43]

There are three observations that support the mechanism described above. First, the ferrous hydroxide corrosion product was seen under the loosely-adhered coating as indicated by some white pasty deposits. Second, an acidic solution was found trapped beneath the coating and blisters. Third, chloride ions were also traced in the same trapped solution by other researchers.

An irony and a dilemma coexist in the preceding description of the corrosion mechanism of coated bars. The irony is that the same coating which is used to protect steel from corrosion becomes the cause of undercutting due to expansion of the anodic area in the debonded regions. The epoxy film deprives the steel from the natural protection afforded by concrete and this allows the creation of a self-propagating corrosion mechanism in the flat crevices beneath the coating.

The dilemma arises in that the reason why epoxy-coated bars performed better than uncoated bars is that corrosion was distributed behind the coating rather than concentrated in limited steel areas. This means that debonding may actually help the coated bar to perform better than to be detrimental to performance! Further illustration of this point is given below.

The anodic area increased in the debonded region due to migration of low pH solution. The acid solution nucleated new pits so large in number and closely spaced that a general corrosion state rather than localized pitting was approached. This condition was exactly opposite to that occurring on the uncoated bar which developed a second macrocell. In effect, the extra driving force of a second macrocell was eliminated on the coated bar and corrosion was distributed. Figure 10.21 shows a bend on a control bar free of rust (because localized severe pitting occurred at the straight ends), and a corroded bend after stripping the damaged coating.

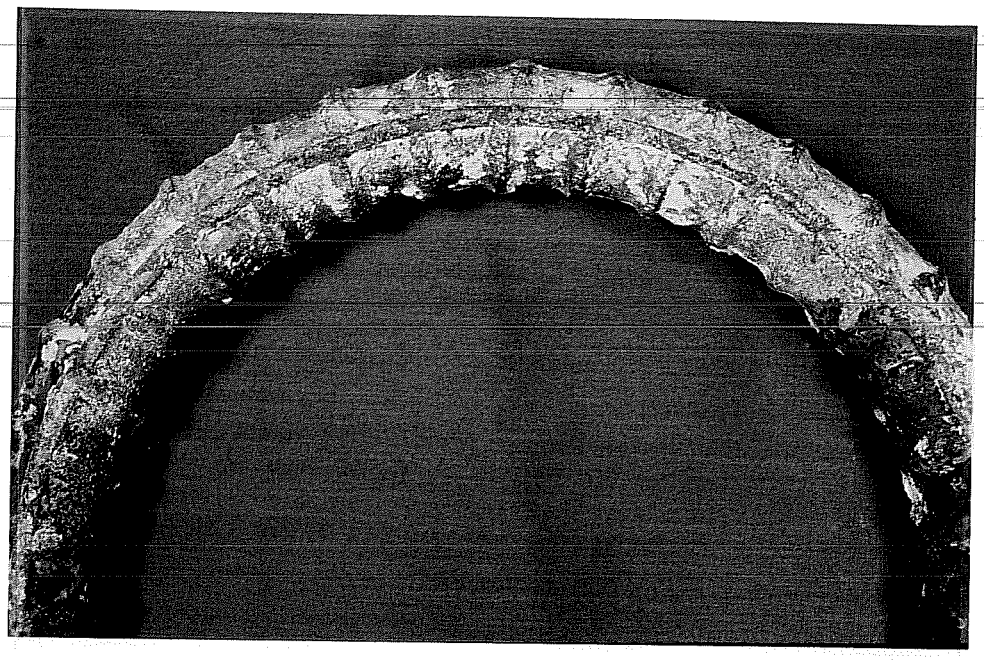

(a) Uncoated Bar Free of Rust at Bend

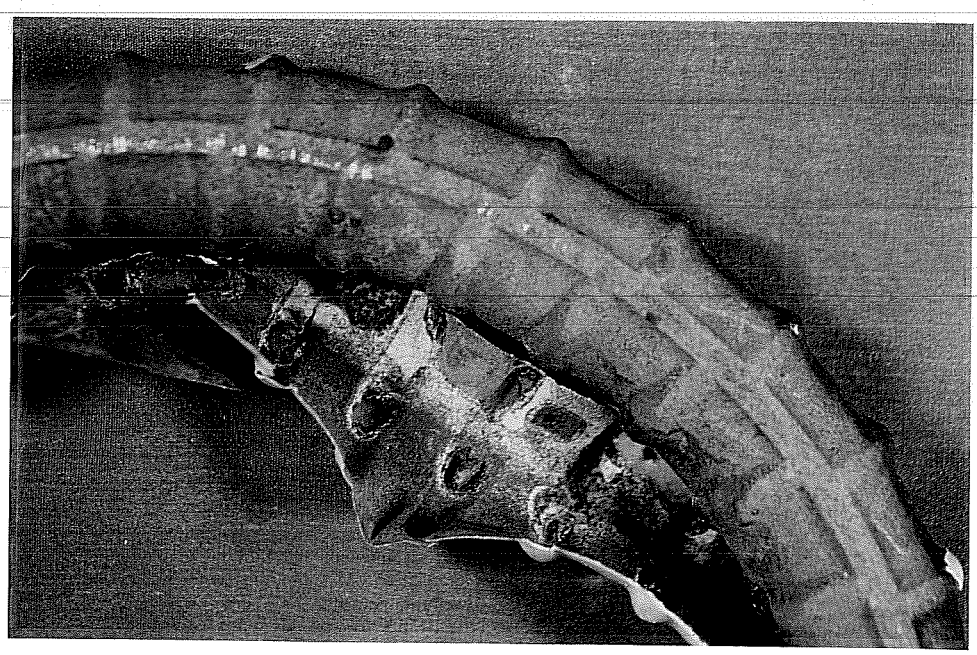

(b) Coated Bar with Corroded Bend

Figure 10.21 Comparison of Corrosion Distribution Along Bends of Uncoated and Coated Bars.

It must not be forgotten that the overall performance was better for the coated bars. Even when a large anodic area was formed, the restricted oxygen supply forced the corrosion products to remain in a low state of oxidation. These products were soluble when moisture was available, so corrosion occurred without exerting high enough pressure to crack or spall the concrete. Bars with less coating damage performed better than those heavily damaged which emphasized the fact that a better initial product results in better corrosion resistance.

10.9 Summary and Conclusions

10.9.1 Summary. To study the performance of bent epoxy-coated bars damaged to various levels, a macrocell corrosion experimental program was conducted. The coated bars were embedded in concrete and subjected to intruded chlorides while being in contact with uncoated bars resting in chloride-free concrete. Time development of corrosion, as well as the corrosion rate were monitored through two years of exposure. Selected specimens were opened to examine the actual bar condition. The main conclusions of this study pertaining to bent coated bars are given in the following sections.

10.9.2 Onset of Corrosion. Corrosion of damaged epoxy-coated steel in concrete was delayed and started at chloride concentrations around twice the levels associated with the onset of corrosion of uncoated steel.

10.9.3 Effectiveness of Epoxy-Coated Steel. The epoxy coating, even if damaged, was effective in reducing the severity of reinforcement corrosion under macrocell action in chloride-contaminated concrete over a two year period. However, corrosion resistance was governed by the degree of damage to coating Both the frequency and size of damage were dominant factors to performance. As the percentage of coating damage was reduced, the performance was improved.

Patching of damage reduced corrosion substantially, but did not provide full protection to the bare areas. The common practice of patching only the damage on the outside of the bend did not prove to be sufficient; corrosion spread from both damage on

outside and inside of bend. The results encourage the practice of patching all visible damage to further improve performance.

No corrosion-induced cracking at the concrete surface was observed with epoxy-coated reinforcement. The corrosion products associated with coated bars were at a low state of oxidation which suppressed surface damage manifestation.

The limits on allowable damage to coating in the current specifications are not strict enough. Damage close to these limits, if concentrated at critical locations such as on bent bars near the concrete surface, provides access to deleterious substances that can cause breakdown of the coating adhesion and widespread underfilm corrosion. To improve corrosion resistance of coated bars, both stringent specification limits and better field practice are required.

The performance of damaged coated bars seemed to be deteriorating with longer periods of exposure. The rate of metal consumption of heavily damaged coated bars was increasing and approaching that of uncoated bars. The long-term integrity of damaged coated bars could be jeopardized by corrosion initiation and progression.

10.9.4 Effects of Bar Size and Deformation Pattern. Coated reinforcing bars with smaller diameters exhibited less corrosion than bars with larger diameters. The influence of bar size on corrosion severity was significant. Test data on the relative performance of bars with parallel and cross deformations did not show a consistent trend .

10.9.5 Effects of Concrete Environment. The quality of concrete at the bar interface has a significant effect on protection of the epoxy-coated reinforcement from corrosion at high levels of chlorides. There was a tendency for the epoxy coating to develop blisters and to breakdown at air pockets in contact with the bar surface. The more the likelihood of void formation around the bar (particularly in the vicinity of a damaged spot), the higher the chances of developing a corrosion cell.

The coated bars consistently showed high propensity for plastic settlement cracking, gap formation below the bar, and corrosion product accumulation at the lower side of the bar. These observations were most probably due to lack of adherence between the epoxy coating and concrete, and differences in concrete consolidation above and under the coated bars.

10.9.6 Coating Debonding. Exposure of epoxy coating to increasing amounts of chloride solution in concrete caused debonding. Adhesion was first weakened by fabrication, then further reduced by exposure. Surface defects and mechanical damage to coating permitted the corrosive substances to penetrate the coating, initiate underfilm corrosion, and increase coating delamination. Debonding did not correlate with the level of coating damage or extent of undercutting, nor was it a consistent indicator of poor performance.

10.9.7 Corrosion Mechanism. Corrosion commenced at exposed steel areas in contact with sufficient chloride ions, and spread to adjacent areas undercutting the epoxy coating. While corrosion products gradually built up on the exposed steel, debonding and underfilm corrosion progressed in crevices at the coating/metal interface. Corrosion became more distributed on the coated bar than on the uncoated bar.

Crevice acidification took place in the form of accumulated low pH solution trapped under the coating and in blisters. The low oxygen supply beneath the coating deterred the corrosion products (mostly black) from converting to expansive red rust. In addition, corrosion concentrated more on the lower part of the bar than on the top. Hence, corrosion proceeded without early signs of cover cracking.

CHAPTER 11
BEAM EXPOSURE STUDY: CONCEPT AND TEST RESULTS

11.1 General

Concrete components are sometimes subjected to partial wetting and drying in a corrosive environment where chlorides are present in solution. This condition is typical of marine splash zone exposure where concrete within the tidal zone undergoes cyclic wetting and drying and significant localized chloride accumulation. Figure 11.1 portrays a concrete pier in such a hostile environment. The configuration of the reinforced concrete member directly influences the chloride transport mechanism to the steel surface. The presence of cracks facilitates chloride penetration which eventually precipitates corrosion. Concrete members exposed to such adverse service conditions, even if encompassing epoxy-coated bars, may exhibit severe corrosion and rapid deterioration. An example is the corrosion-induced damage to some bridge substructures in the Florida Keys in only a few years following their completion.

The basic components of the corrosion system mentioned above are: the wet-dry region; the relatively dry region; and the continuous steel network passing through both regions as shown in Fig. 11.1. The wet-dry region allows salt accumulation as a result of direct intrusion and capillary action followed by water evaporation. The dry region provides an adequate medium for oxygen passage to reinforcing steel. Finally, steel continuity between the frequently wetted zone and the permanently dry zone encourages the development of a corrosion cell stretching over the two regions.

Corrosion behavior of the depicted system is influenced by several factors. Among these factors, the following may have pronounced effects on the level of corrosion activity on the epoxy-coated reinforcement:

- Concrete permeability.
- Concrete cover and surface cracking.
- Loading condition.
- Level of coating damage and amount of damage patched.
- Level of salinity of chloride solution.
- Degree of electrical continuity of steel.

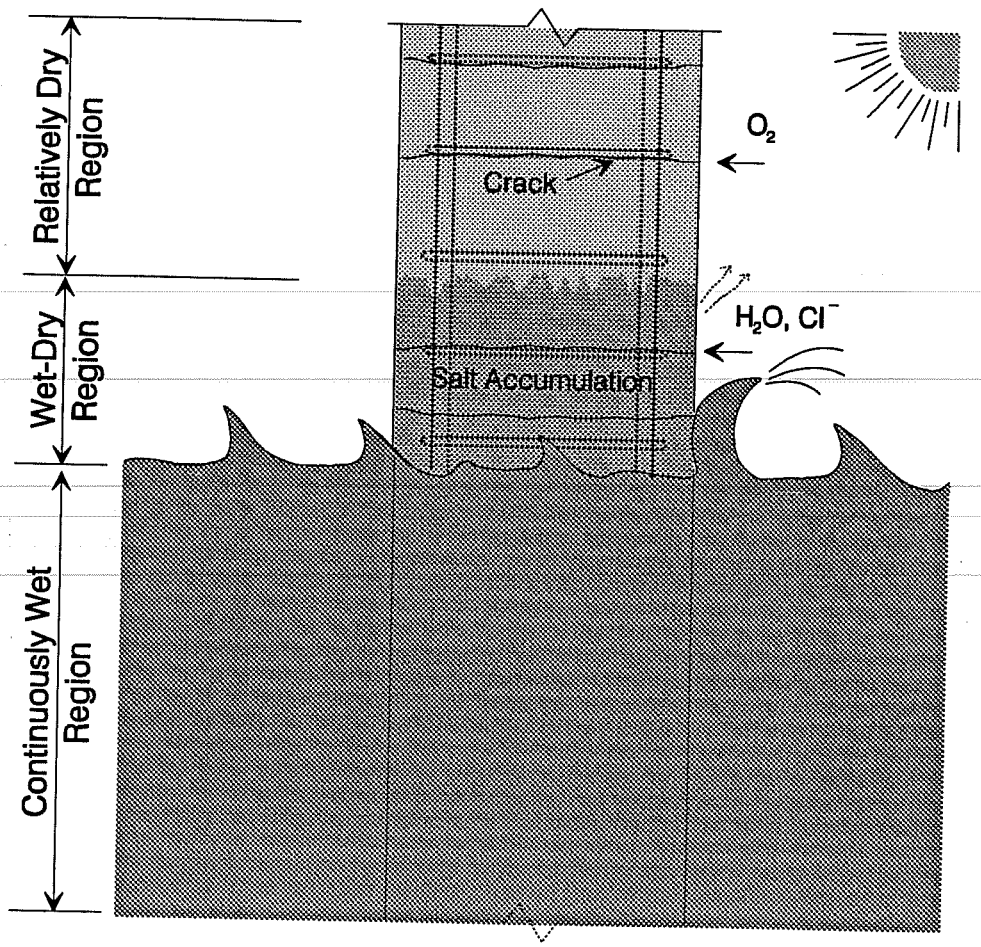

Figure 11.1 Exposure of Concrete Pier to Marine Environment.

In previous studies, Swamy[51,108] and Poston[4] showed that epoxy coating greatly reduced the incidence and extent of corrosion in cracked structural members. Poston also reported that subjecting test members to cycles of loading and unloading during exposure to salt solution resulted in minor chipping and flaking of the epoxy coating on the ribs of bars. Two aspects needed further research: the effects of previous mechanical coating damage during handling on performance; and the effects of structural loading on inducing further damage to the coating.

If cyclic loading affects the condition of a coated reinforcing bar in concrete, then the long term performance of the bar may be seriously impaired. One concern is that the coating may flow away from high stress locations, such as the base of a transverse lug on a ribbed bar.[29] Chloride ions can penetrate easily through the weak coating zone, where epoxy has "squeezed out", thus resulting in localized spots of high concentrations. Large chloride accumulations increase the probability of corrosion initiation. In addition, localized stresses in steel promote an anodic behavior and, in fact, stressed areas generally become the anodes.[16] The critical aspect of corrosion of highly stressed steel is that metal degeneration occurs where the strength is needed most.

Most field reinforced concrete structures are designed to function in a cracked condition. Therefore, testing uncracked concrete in the laboratory satisfies what is called "laboratory curiosity".[49] Cracking is part of the actual service conditions and should be considered in laboratory corrosion studies. Two important aspects of cracking that deserve attention are crack width and crack propagation.

Controversy exists as to the width of a crack necessary to lead to significant corrosion.[77] It is also argued that unloaded cracks in a laboratory test may heal and produce misleading results.[49] Field observations of bridge deck construction have revealed that deep cracks form in association with the use of epoxy-coated reinforcement.[29] In addition, experience with corrosion of coated bars has shown that corrosion concentrates at crack locations. Therefore, it was prudent to investigate the corrosion performance of coated reinforcing steel under laboratory exposure conditions involving cracked, loaded specimens.

With relatively wide cracks, the coated reinforcement may be exposed to large amounts of salt within a very short period.

In the beam exposure study, beams with separate arrangements of straight, bent, and spliced coated bars were tested. The beams were designed to simulate cracked, loaded concrete components exposed to high corrosive environments. A schematic conceptualization of the test is depicted in Fig. 11.2. All details of the test, such as description of test variables, steel preparation, material characteristics, specimen design and preparation, test setup, routine monitoring, and postmortem examination procedure are included in Appendix D. The following section summarizes the corrosion systems and the conditions included in the test.

11.2 Test Concept

11.2.1 Corrosion System. The environment in which epoxy-coated reinforcement is normally used is quite heterogeneous; the concrete alone being nonhomogeneous and the exposure conditions being diverse. In effect, an appreciable potential difference may develop between relatively close anodic and cathodic sites on the same bar. Hence, mixed material and exposure conditions are likely to exist in which a single coated bar may exhibit a strong macrocell action. To investigate the susceptibility of coated bars to such behavior, electrically isolated bars with various levels of coating damage were included in the test. The idea was to simulate field applications where all reinforcement was epoxy-coated and proper precautions were taken to keep the bars electrically discontinuous.

Coated fabricated bars, such as stirrups and ties, may also be subjected to adverse conditions. First, a stirrup is likely to perform as a crack inducer in a flexural member. As a result, the stirrup lies in the same crack plane. Second, the stirrup is the closest part of the steel cage to the concrete surface exposed to chlorides. Third, damage to coating due to fabrication, vibration, or other causes tends to occur on the outer stirrup surfaces. Fourth, common practice of patching the outside bent areas may not always be effective. Fifth, electrical continuity between coated and uncoated reinforcement may exist if stirrups were

tied to uncoated bars. Thus, stirrups become a weak link in construction where coated reinforcement is the primary protection system used against corrosion. The performance of fabricated bars under such conditions was also studied in the beam exposure test.

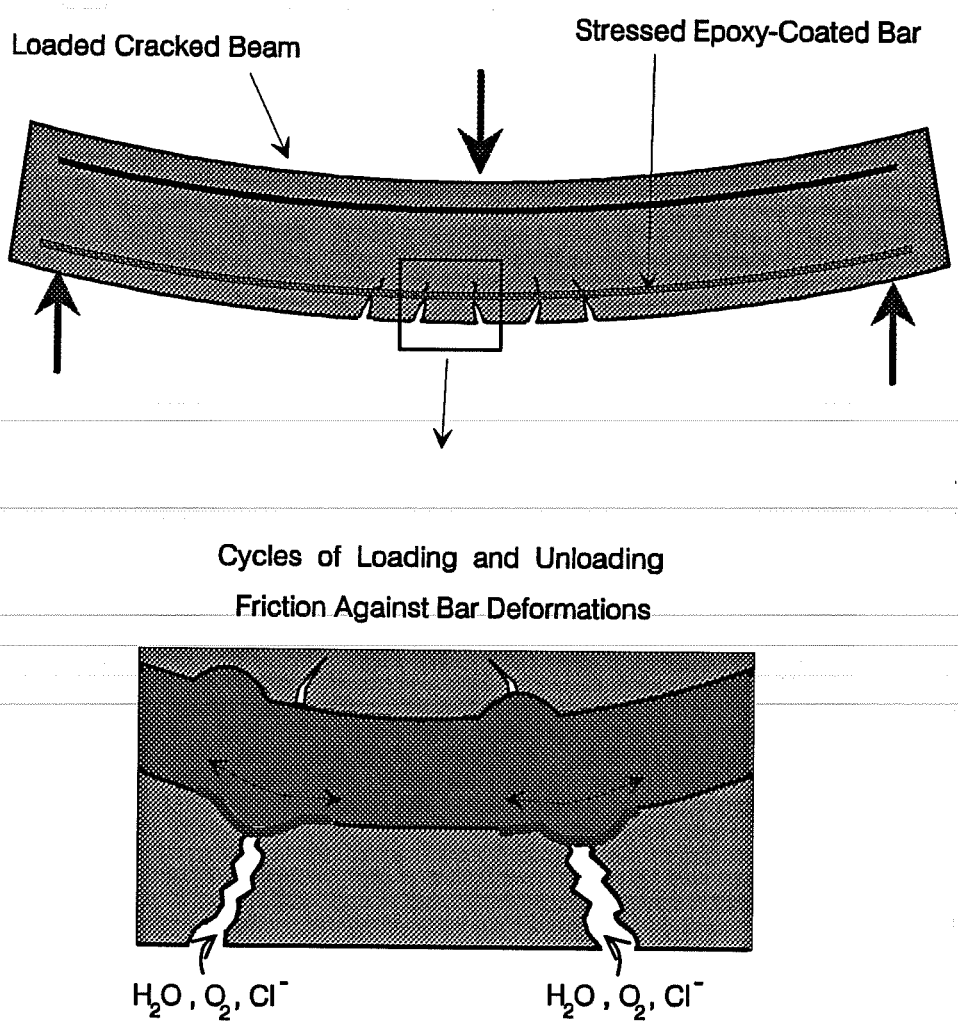

Figure 11.2 Concept of Beam Exposure Test.

Another weak link in the corrosion resistance system is spliced bars located in high moment regions. These regions are normally cracked close to the patched bar ends. The steel surface at cut bar ends has very sharp edges and does not exhibit the roughness usually produced by blasting prior to coating. Hence, patching saw cut bars may fail to provide adequate protection against corrosion initiation at the bar end followed by corrosion propagation beneath the coating along the bar. This aspect of failure was also investigated in the beam exposure test.

11.2.2 Test Conditions. Thirty-four beam specimens were included in the test program. Beams were divided into three groups according to the corrosion systems described above. Table 11.1 summarizes the variables included in each beam group. The test variables were as follows:

Coating Damage

- Longitudinal bars with no visible damage or "as received" condition.
- Longitudinal bars severely damaged (3% of bar surface area) with or without patching. The introduced coating damage was limited to the middle 0.91 m (3 ft.) length of the bar.
- Stirrups in as received condition with or without patching the bends.
- Stirrups severely damaged (3% of stirrup surface area) with patching. The introduced coating damage was limited to the outer bends at one side of the stirrup.
- Splice bars with patched ends.

Loading Condition (Loading as a test variable refers to imposed loads causing bending about strong axis. All beams were carrying their own weight)

- Uncracked Unloaded: At rest condition (no cracks or imposed loads) during exposure.
- Cracked Unloaded: A load was applied to produce a crack of 0.33 mm (0.013 in.) width then the load was removed during exposure.

- Cracked Loaded: A load was applied to produce a crack of 0.33 mm (0.013 in.) width then the load was held during exposure.

The crack width used in the test conforms to ACI 318-89[70] crack limit for exterior exposure. Cycles of loading and unloading to the same crack width specified were performed during

Table 11.1 Summary of Beam Exposure Study Specimens

Bar Condition (Damage Level and Condition)	Loading Condition[a]		
	Uncracked Unloaded	Cracked Unloaded	Cracked Loaded[b]
Group I Beams, Monitoring Longitudinal Bars (Stirrups were Covered)[c]			
As Received[d]	B1, B2	B3, B4	B5, B6
3% Damaged	B7, B8	B9, B10	B11, B12
3% Damaged, Patched		B13, B14	
Group II Beams, Monitoring Stirrups (Longitudinal Bars were Covered)[c]			
As Received[e]	B15, B16	B17, B18	B19, B20
As Received, Patched	B21, B22	B23, B24	B25, B26
3% Damaged, Patched		B27, B28	
Group III Beams, Monitoring Longitudinal Bars and Stirrups			
Mixed Longitudinal Bars and Stirrups			
Both 3% Damaged, Patched		B29, B30	
Mixed Splice Bars and Stirrups			
Stirrup 3% Damaged, Stirrup and Splice Bar End Patched		B31, B32	B33, B34

a Loading condition refers to imposed loads causing bending about strong axis. All beams were supporting their own weights.
b Loads were imposed to open cracks to 0.33 mm.
c Cover was provided by a heat shrink tube.
d No visible damage.
e No patch on bends.

exposure (explained in the following section). Loading and unloading may promote physical damage to coating and to concrete at crack locations and increase exposure to corrosive substances.

Beams were subjected to a laboratory cyclic wet-dry exposure regime using 3.5% NaCl solution. Periodic wetting and drying ensures continuous transport of corrosive substances to steel surfaces to promote corrosion. To further accelerate corrosion initiation, concrete with high permeability was used. For corrosion monitoring, periodic visual inspection and half-cell potential measurements were made.

11.3 Test Setup and Procedure

11.3.1 Test Setup. Reinforced concrete beams were designed and prepared for assessment of the durability of coated bars in concrete under conditions simulating loaded structural elements. There were two replicates for each test condition. The two replicates were stressed back to back as in the model shown in Fig. 11.3. A view of the beam specimens under test and the loading process are shown in Fig. 11.4 and 11.5. Only two longitudinal coated bars were used in the tension side of each beam and one coated stirrup at midspan. The two compression reinforcing bars were uncoated.

The exposure conditions consisted of 3.5% NaCl solution flowing over the beam surfaces (within a defined exposure area) continuously for 3 days followed by air drying for 11 days. The cracked beams were subjected to cycles of loading and unloading twice during each exposure cycle: one time during wetting and the other during drying. Five load cycles were imposed each time up to a level producing the selected maximum crack width.

11.3.2 Measurements and Observations. In Chapter 4, it was shown that potential measurements provided a means of monitoring corrosion activity on coated bars. Generally, steel exhibits a potential that falls in a range that indicates passive, active, or unstable active-passive conditions. The potentials may be particularly useful in indicating time-to-corrosion initiation which is marked by significant drop in the potential value. After corrosion has

started, the activity may progress to a point causing distress to concrete. Therefore, monitoring the state of corrosion activity by observing changes in the potential readings can provide valuable information on the effectiveness of epoxy coating.

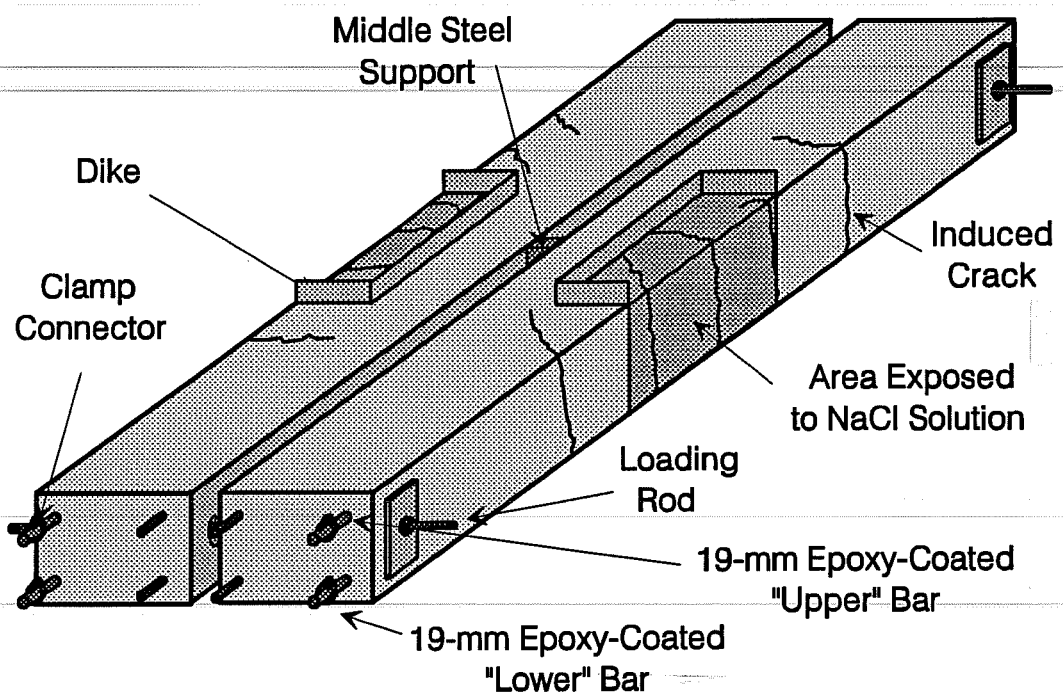

Figure 11.3 Model of Beam Exposure Test Specimens.

Electrical half-cell potentials of longitudinal bars and stirrups embedded in beams were measured periodically against a saturated calomel reference electrode (SCE). Figure 11.6 shows the process of taking half-cell measurement. Spacing between the points of measurement along the concrete surface along the longitudinal reinforcement was 150 mm (6 in.) and from 50 to 100 mm (2-4 in.) for stirrups. The spacing influences the interpretation of the results. If measurement points are too far apart, areas of localized corrosion could be easily missed. Field experience has shown that the detection of all corrosion spots is likely when a grid dimension of 150 mm (6 in.) or less is used for potential mapping.[23]

Figure 11.4 Beam Exposure Test Setup.

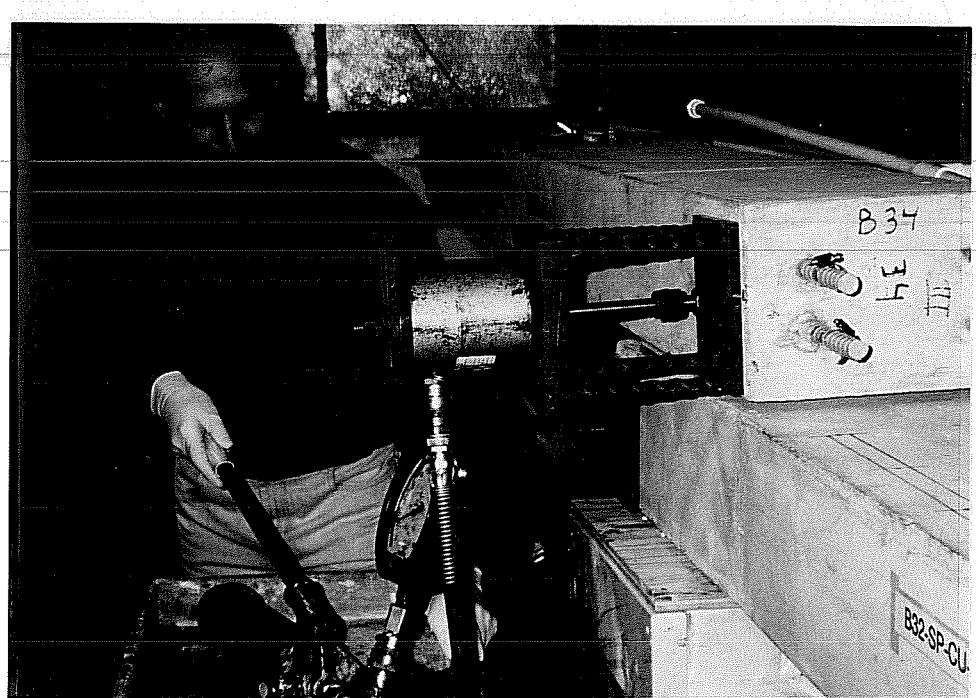

Figure 11.5 Loading Beam Test Specimens.

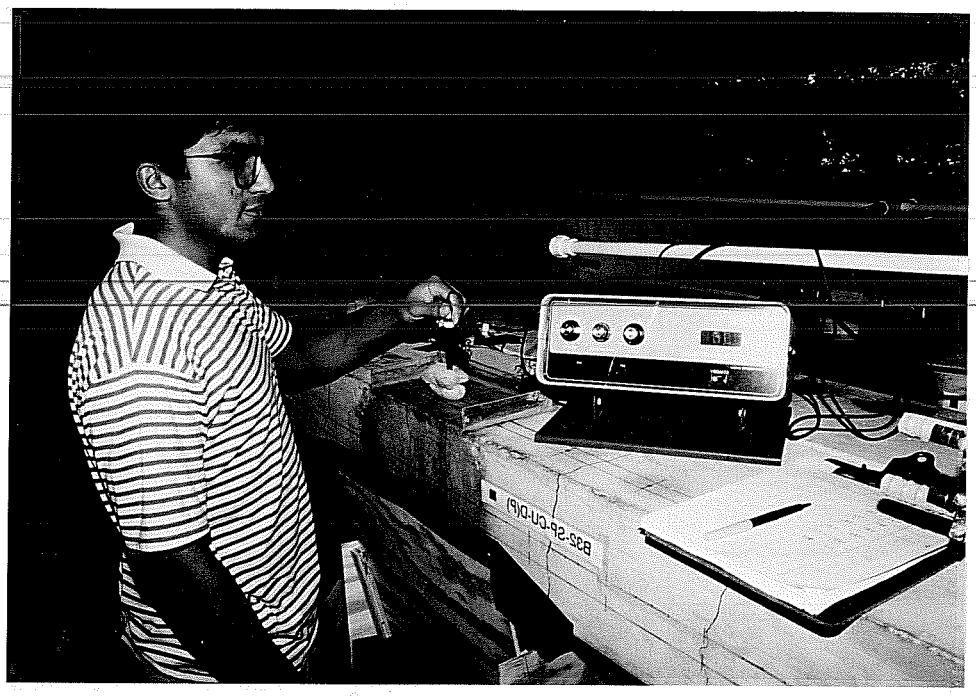

Figure 11.6 Half-Cell Measurement.

The surface of the beam specimens was visually inspected periodically for any signs of staining or crack development due to corrosion but none showed such activity during the 400-day observation period. In addition, crack maps and crack widths were documented and updated during the exposure period. Crack widths of a few selected cracks were measured periodically.

11.4 Half-Cell Electrical Potentials

11.4.1 General. Examples of half-cell electrical potentials versus time of exposure up to about 400 days are shown in Fig. 11.7 to 11.13. The average potentials of the four points in the "dry regions" and the five points in the "wetted region" for the longitudinal bars are also shown in these figures. Further, the graphs show the change in average potentials. The same information was gathered for the stirrups but all points marked for potential measurement (seven points) were included in the calculation of averages. A complete set of results of half-cell potentials of beams removed for autopsy to date is given in Section D.8.

The electrical potentials illustrate corrosion development as a function of exposure time. The results provided valuable information on corrosion initiation and support the findings from the beam autopsies.

Half-cell potentials demonstrate the thermodynamic behavior of reinforcing steel in concrete. According to ASTM C876,[117] the probability of corrosion of uncoated steel in concrete is determined by the empirical half-cell potential criteria shown in Table 11.2. Caution is required in the interpretation of half-cell potential measurements with epoxy-coated bars. The reason for caution is that the coating is non-conductive and the electrochemical activity polarizes (see Section A.4). In absence of more reliable criteria for evaluation of potentials measured on epoxy-coated bars, those displayed in Table 11.2 will be used in this study for comparison of performance of tested bars.

The results of half-cell potential measurements given below are expressed in terms of the average wetted region potentials (for points within the exposure area) over an observation period of about 400 days. The initial potentials refer to those potentials measured after the first wetting period. Some positive half-cell readings were obtained using the saturated calomel reference electrode. Several studies have reported positive potential measurements on epoxy-coated bars ranging between zero and +100.[56,106,109,115]

The development of a highly negative potential was considered to be a signal of the onset of corrosion although it may not necessarily indicate significant corrosion activity. Some bars exhibited highly negative wetted region potentials at the beginning or shortly after the test was started. Other bars showed a delayed potential drop to high negative ranges. Time to measure a drop in the wetted region potential to a consistent high negative value or to a fluctuating potential (successively changing potential approximately 100 mV or more) are listed in Tables 11.3 to 11.5.

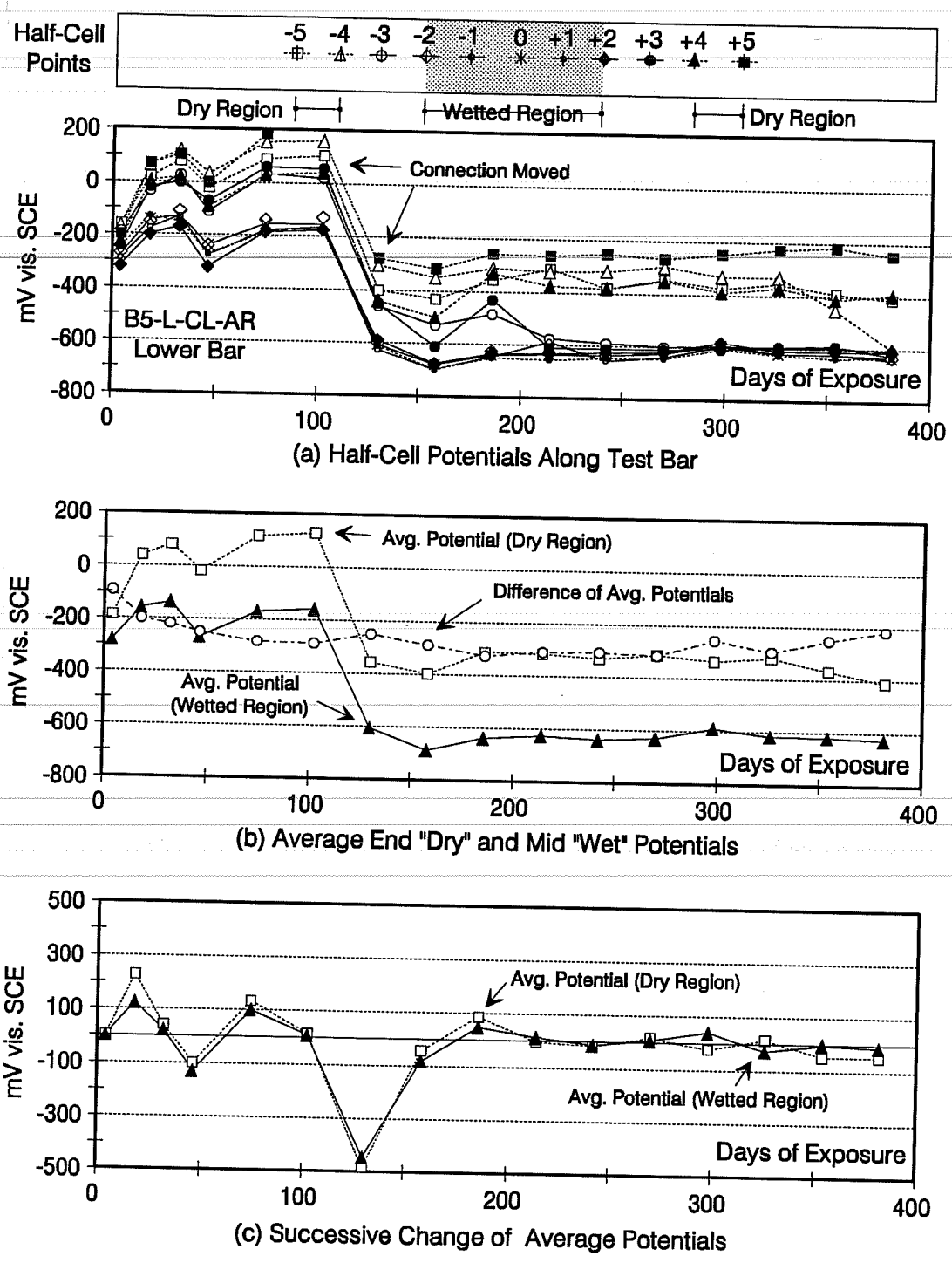

Figure 11.7 Half-Cell Potentials for Beam B5 Lower Bar.

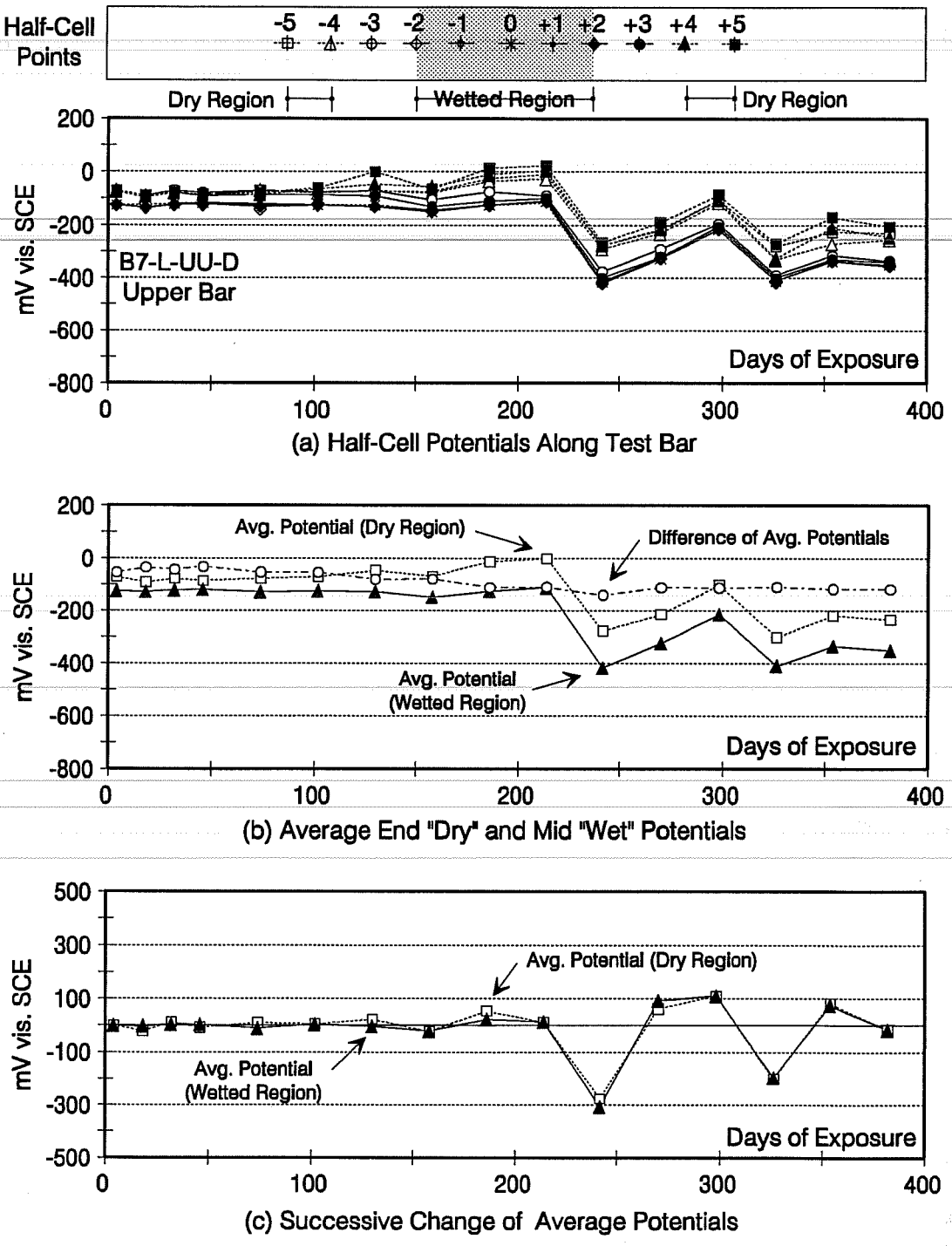

Figure 11.8 Half-Cell Potentials for Beam B7 Upper Bar.

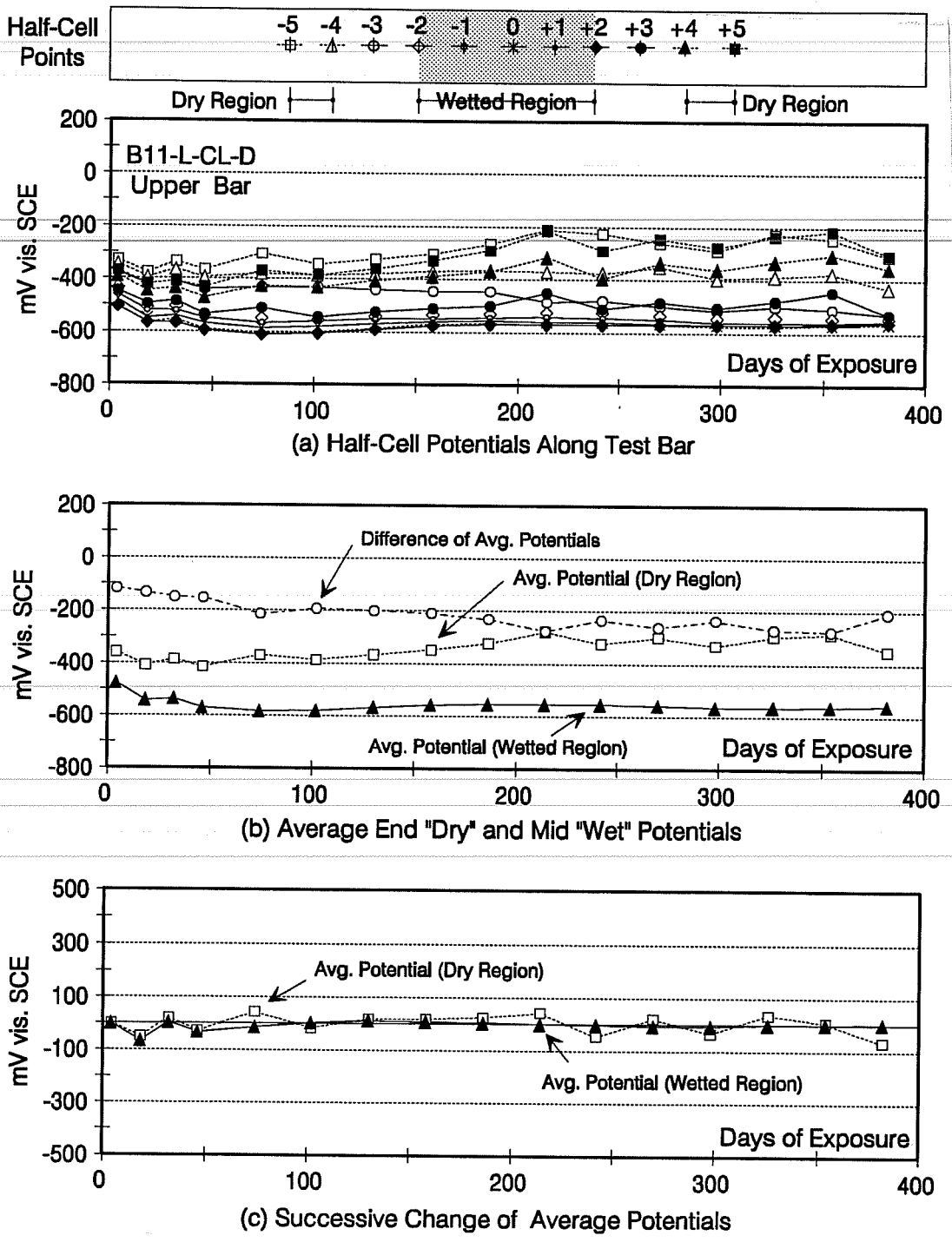

Figure 11.9 Half-Cell Potentials for Beam B11 Upper Bar.

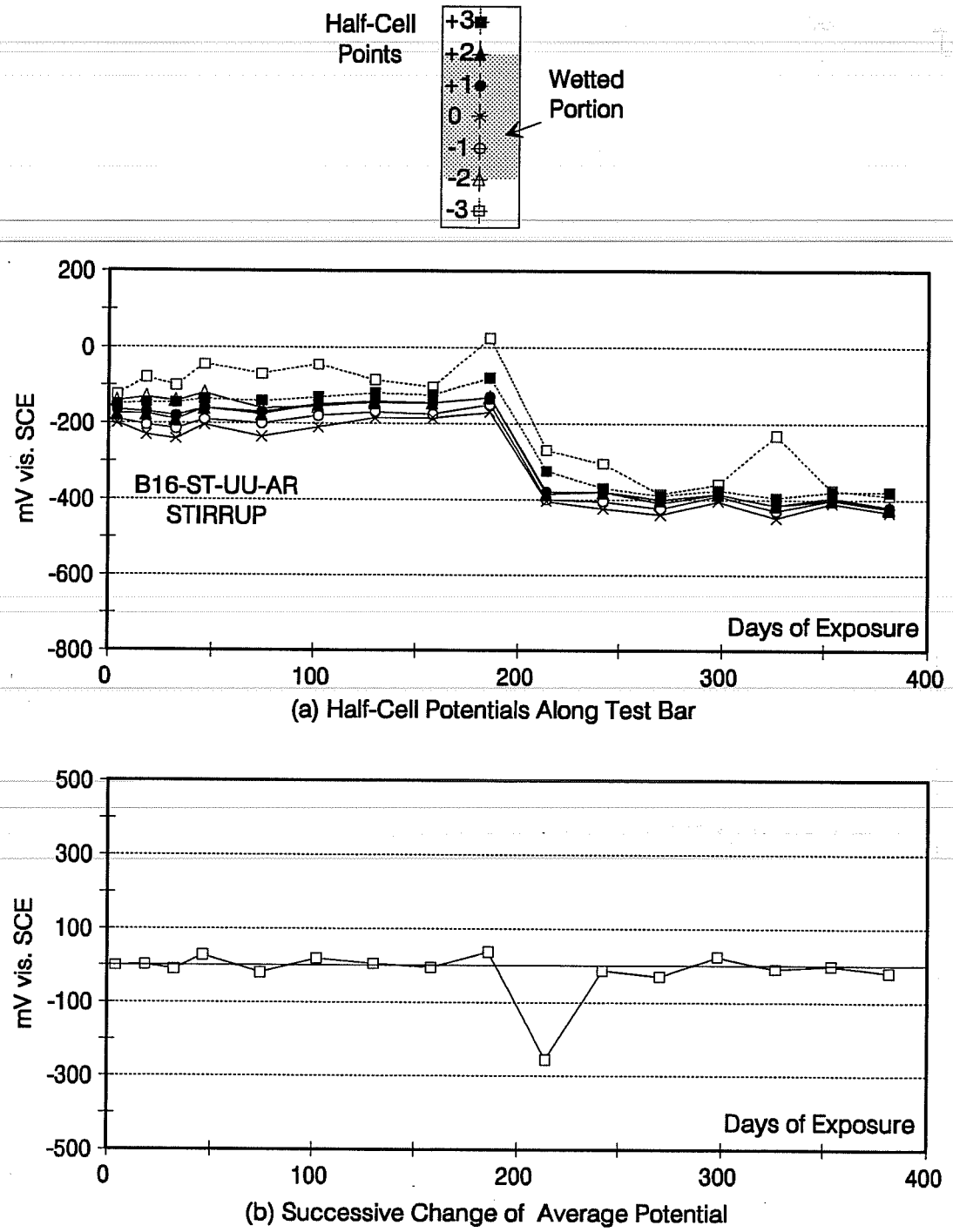

Figure 11.10 Half-Cell Potentials for Beam B16 Stirrup.

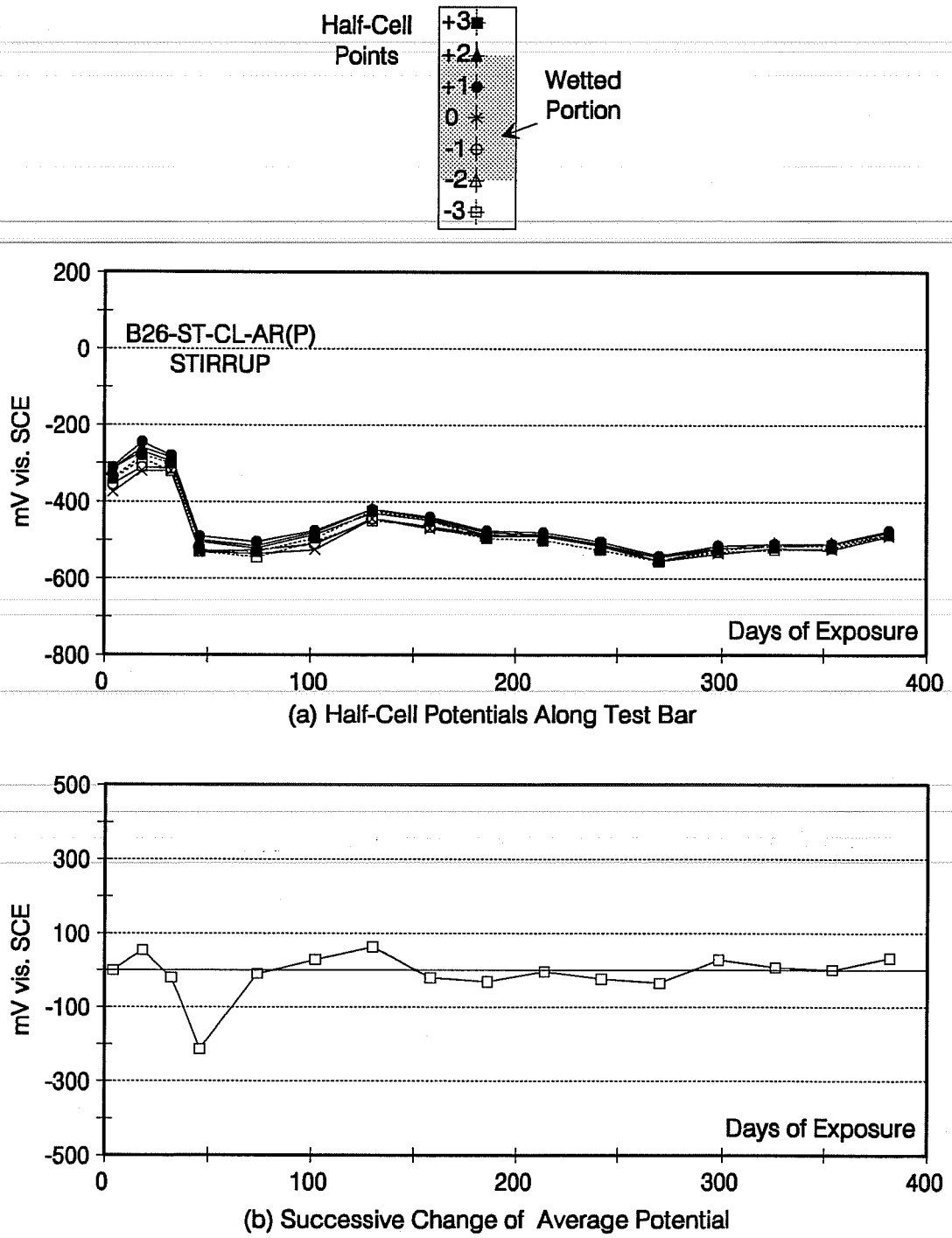

Figure 11.11 Half-Cell Potentials for Beam B26 Stirrup.

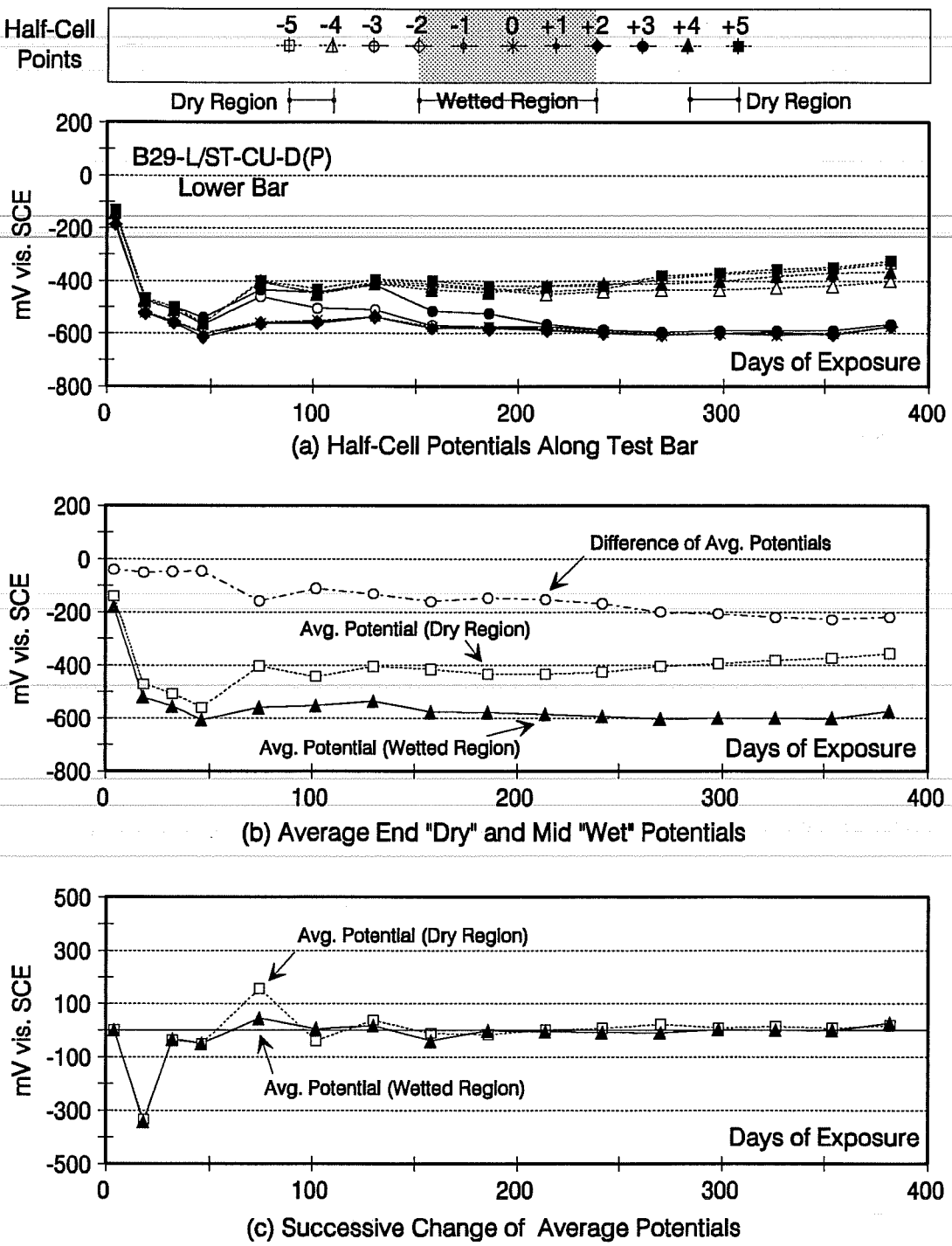

Figure 11.12 Half-Cell Potentials for Beam B29 Lower Bar.

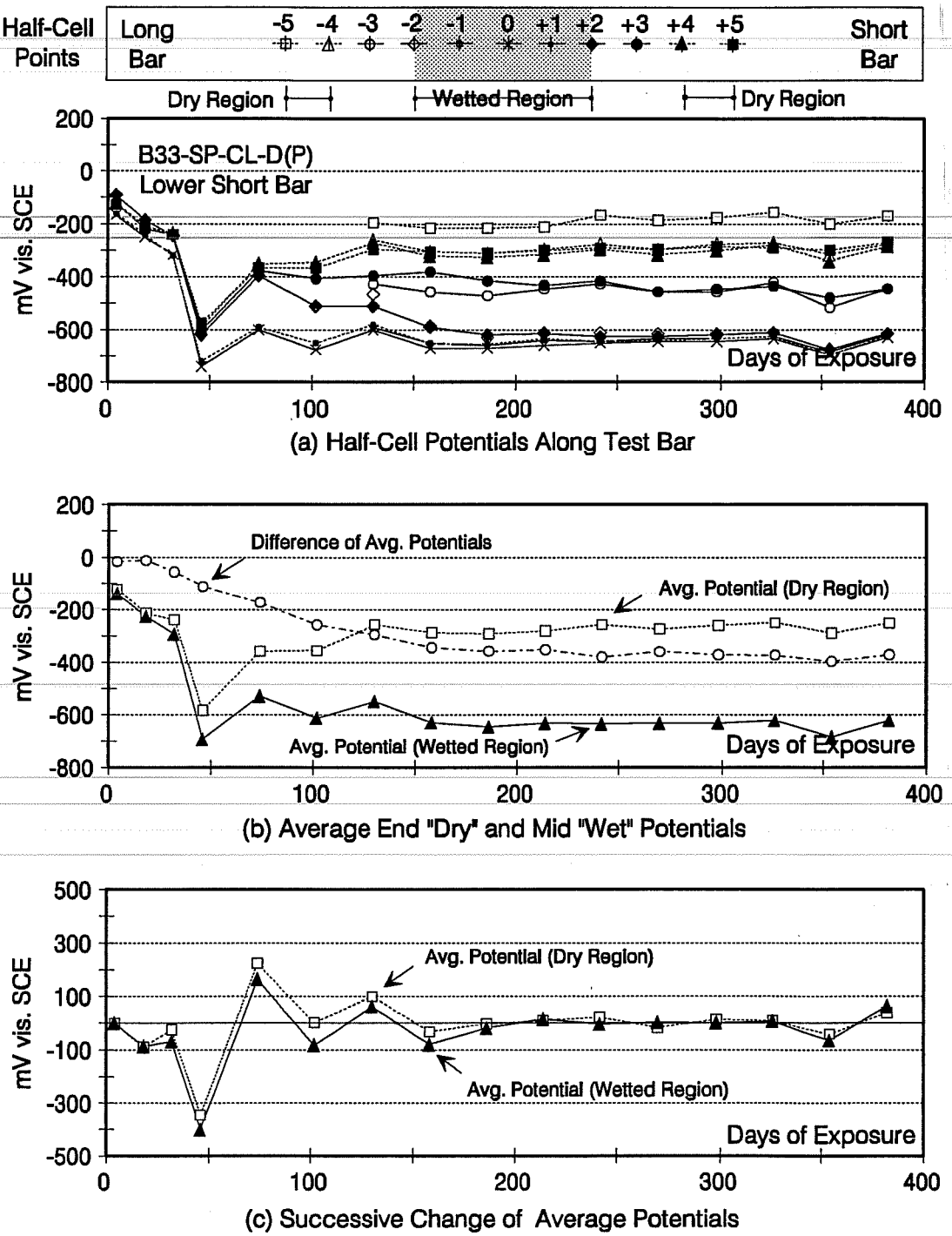

Figure 11.13 Half-Cell Potentials for Beam B33 Lower Short Bar.

Table 11.2 Interpretation of Half-Cell Potentials Based on ASTM C876-87

Probability of Corrosion	Half-Cell Potential Reference	
	Copper/Copper Sulfate, CSE (mV)	Saturated Calomel, SCE (mV)
Less than 10% if potential is less negative than	-200	-125
More than 90% if potential is more negative than	-350	-275
Uncertain if potential is between	-200 and -350	-125 and -275

11.4.2 Group I Specimens. The results show that the two longitudinal bars in each beam generally exhibited slightly different potential change with time. The lower bars tended to exhibit more negative potentials; however, this trend was not consistent.

Bars in As Received Condition. There was a clear difference in performance of bars in uncracked and cracked beams. The potentials of bars in uncracked beams were mostly steady in the low negative range (below -125 mV) but some started to fluctuate late during the exposure period. The potentials of bars in cracked beams either fluctuated early or late in the test and some dropped then remained steady for the rest of the exposure time.

Bars with 3% Unrepaired Damage. There was another clear difference in performance of bars in uncracked and cracked beams. The potentials of bars in uncracked beams were mostly steady below -200 mV then dropped and fluctuated. The potentials of bars in cracked beams were either in a high negative range initially or dropped shortly after and remained stable around -500 to -600 mV for the rest of the exposure period.

Bars with 3% Repaired Damage (Cracked Unloaded Beams only). The trend of potentials was very similar to that of bars in cracked beams with unrepaired damage. The potentials dropped early in the test and remained steady in the high negative range for the rest of the exposure period.

Table 11.3 Time-to-Corrosion Initiation of Beam Bar Specimens
Group I, Longitudinal Bars (Upper-Up, and Lower-Lw)

Beam No.	Initial Average Potential After 4 Days of Exposure (mV)	Maximum Average Potential (mV)	Exposure Time to Maximum Drop of Average Potential (Days)	Time-to-Corrosion Initiation (Days)
B1-Up	-60	-430[a]	270	270
B1-Lw	-65	-160	270	Uncertain
B2-Up	-80	-100	46	Unsuspected
B2-Lw	-95	-230	270	Uncertain
B3-Up	-115	-590	74	74
B3-Lw	-105	-630	102	102
B4-Up	-65	-620	74	74
B4-Lw	-100	-615	18	18
B5-Up	-190	-380	102	102
B5-Lw	-280	-685	130	130
B6-Up	-430	-620	18	4
B6-Lw	-105	-505	46	46
B7-Up	-125	-415	242	242
B7-Lw	-120	-465	186	186
B8-Up	-115	-455	326	326
B8-Lw	-95	-460	270	270
B9-Up	-410	-555	130	4
B9-Lw	-470	-565	32	4
B10-Up	-170	-550	18	18
B10-Lw	-395	-590	18	4
B11-Up	-475	-585	18	4
B11-Lw	-425	-605	46	4
B12-Up	-250	-550	18	18
B12-Lw	-440	-590	18	4
B13-Up	-385	-600	32	4
B13-Lw	-500	-615	46	4
B14-Up	-205	-590	18	18
B14-Lw	-125	-595	18	18

a The underlined potentials in the table indicate probable corrosion initiation.

11.4.3 Group II Specimens.

Stirrups in As Received Condition. The potentials for stirrups in uncracked beams were steady in the low negative range except for one stirrup which exhibited a drop in potential around the middle of the exposure period. The performance of stirrups in all cracked beams (loaded and unloaded) was not significantly different. The potentials for stirrups in cracked beams either fluctuated for a considerable period of time or dropped steadily then remained stable between -400 and -600 mV.

Stirrups in As Received-Patched Condition. Stirrups in this category exhibited similar performance to that of stirrups with as received condition. The potentials for stirrups in uncracked beams were steady in the low negative range except for one stirrup which exhibited a sudden drop in potential after the middle of the exposure period. The potentials for stirrups in cracked beams fluctuated gradually for a considerable period of time before they reached a steady state between -200 and -600 mV.

Stirrups with 3% Repaired Damage (Cracked Unloaded Beams only). The performance of stirrups in replicate beams was different. The initial potentials were -185 and -285 mV, while the final potentials were -325 and -535 mV. The potential for the stirrup which exhibited less negative initial potential remained steady for a long time before gradually declining. The potential for the other stirrup dropped early in the test and fluctuated gradually for a considerable period of time before reaching a steady state.

11.4.4 Group III Bar Specimens.

Bars and Stirrups with 3% Repaired Damage (Cracked Unloaded Beams only). The performance of bars and stirrups was similar to that of bars in group I beams and stirrups in group II beams with similar damage condition, perhaps with slightly more negative final potentials.

Table 11.4 Time-to-Corrosion Initiation of Beam Bar Specimens Group II, Stirrups

Beam No.	Initial Average Potential After 4 Days of Exposure (mV)	Maximum Average Potential (mV)	Exposure Time to Maximum Drop of Average Potential (Days)	Time-to-Corrosion Initiation (Days)
B15	-165	-165	74	Uncertain
B16	-165	-415[a]	214	214
B17	-245	-355	74	74
B18	-220	-465	74	74
B19	-190	-555	46	46
B20	-240	-570	46	46
B21	-135	-280	242	Uncertain
B22	-190	-190	-	Uncertain
B23	-215	-425	130	130
B24	-245	-510	46	46
B25	-205	-365	46	46
B26	-335	-550	46	4
B27	-185	-325	18	18
B28	-285	-590	46	46

a The underlined potentials in the table indicate probable corrosion initiation.

Table 11.5 Time-to-Corrosion Initiation of Beam Bar Specimens Group III, Longitudinal/Splice Bars (Upper-Up, and Lower-Lw) and Stirrups

Beam No.	Initial Average Potential After 4 Days of Exposure (mV)	Maximum Average Potential (mV)	Exposure Time to Maximum Drop of Average Potential (Days)	Time-to-Corrosion Initiation (Days)
		Longitudinal Bars Including Splice Bars		
B29-Up	-350[a]	-600	18	4
B29-Lw	-180	-605	18	18
B30-Up	-135	-705	18	18
B30-Lw	-80	-625	18	18
B31-Up	-230	-740	18	18
B31-Lw	-390	-650	18	4
B32-Up	-340	-605	32	4
B32-Lw	-180	-645	18	18
B33-Up	-465	-720	46	4
B33-Lw	-140	-695	46	46
B34-Up	-280	-835	18	18
B34-Lw	-500	-660	46	4
		Stirrups		
B29	-460	-635	46	4
B30	-145	-515	46	46
B31	-400	-545	32	4
B32	-120	-525	102	102
B33	-440	-630	46	4
B34	-220	-545	46	46

a The **underlined** potentials in the table indicate probable corrosion initiation.

Bars in Splice Zone and Stirrups with 3% Repaired Damage. The change of potential with time for short bars was characterized by an early drop, followed by large fluctuation, and then stability. In contrast, the change of potential with time for long bars was characterized by a delayed drop, followed by slight fluctuation, and then stability.

No appreciable difference in performance of longitudinal bars existed between bars in cracked unloaded and cracked loaded beams, except that bars in cracked loaded beams exhibited the highest drops in potentials (maximum potentials reached -835 mV). The performance of stirrups in all cracked beams was very similar. The potentials of stirrups in cracked beams generally fluctuated for some time then stabilized around -500 to -600 mV.

11.5 Crack Widths

11.5.1 General. Crack maps and crack width measurements during the exposure period were made and are included in Section D.8. An examples of these crack maps is shown in Fig. 11.14 for one of the beams removed for forensic examination after about 400 days of exposure. Average crack width measurements for selected cracks identified on the map are listed in Tables 11.6.

11.5.2 Crack Width Change with Time. Crack width change with time was particularly monitored for the cracked unloaded beams to detect any crack movement caused by corrosion activity. In general, the cracks tended to be slightly wider near the lower longitudinal coated bar than the upper one due to beam deflection under its own weight. Often, it was difficult to measure crack width accurately because of both salt accumulation and concrete disintegration at the crack surface. Load cycling, in addition to salt crystallization in concrete pores near the surface, resulted in concrete scaling at the crack surface. Therefore, crack width measurement might not have reflected the exact crack opening; however, it indicated that no unusual crack movement due to corrosion activity had occurred.

Table 11.6 Average Crack Width Measurement Across Beam Tension Side for B29-L/ST-CU-D(P), Group III

Days of Exposure	Crack 1 (mm)	Crack 2 (mm)	Crack 3 (mm)	Crack 4 (mm)
162	0.08	0.17	0.06	0.11
193	0.10	0.20	0.07	0.13
220	0.08	0.19	0.07	0.15
252	0.10	0.20	0.07	0.13
277	0.10	0.19	0.08	0.15
305	0.11	0.20	0.07	0.15
333	0.10	0.19	0.07	0.13
361	0.10	0.17	0.07	0.13
381	0.10	0.17	0.08	0.12

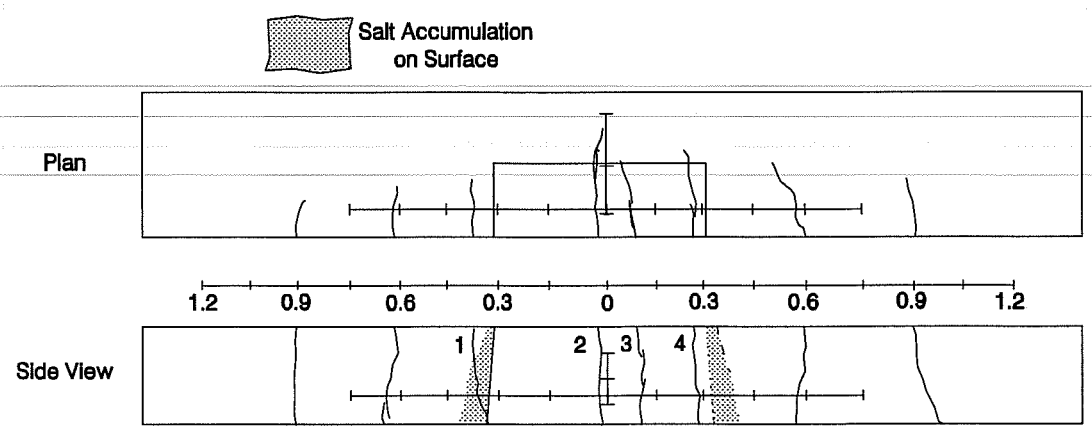

Figure 11.14 Surface Condition of Beam 29 (Group III) After One Year of Exposure Showing Monitored Cracks.

11.6 Forensic Examination

11.6.1 General. Forensic examination of beams was carried out for three reasons:

- to correlate the steel potential measurements to actual bar condition;
- to document the extent of corrosion activity on test bars with various surface conditions after being subjected to different stress histories; and,
- to investigate the condition of the epoxy coating.

One of each of the coupled replicate beams was removed for autopsy after about 400 days of exposure. The bars were carefully removed following the procedure outlined in Section D.9. The forensic examination was documented by visual observations, microscopic examination, and photographs.

11.6.2 Concrete Delamination. Prior to destruction, each beam was examined for surface delamination by hammer sounding. No concrete delamination in any of the beams after 400 days of exposure was detected.

11.6.3 Chloride Content at Steel Level. Chloride samples were obtained by drilling from each beam after testing. The concrete surfaces at the drilled locations were either cracked or uncracked to determine the relative amounts of chlorides in each case. The measured acid-soluble chloride concentrations are tabulated in Section D.9.

Chloride contents at different depths are shown in Figs. 11.15 and 11.16. These chloride contents were determined at crack locations in the exposure area and are plotted as a function of crack width and loading condition. The average chloride contents near the upper longitudinal bar or stirrup bend for the cases of cracked unloaded and cracked loaded beams were 12.00 kg/m^3 (20.2 lb./yd^3) and 15.3 kg/m^3 (25.7 lb./yd^3), respectively. The respective values for the lower longitudinal bar or stirrup bend were 11.0 kg/m^3 (18.5 lb./yd^3) and 14.0 kg/m^3 (23.5 lb./yd^3).

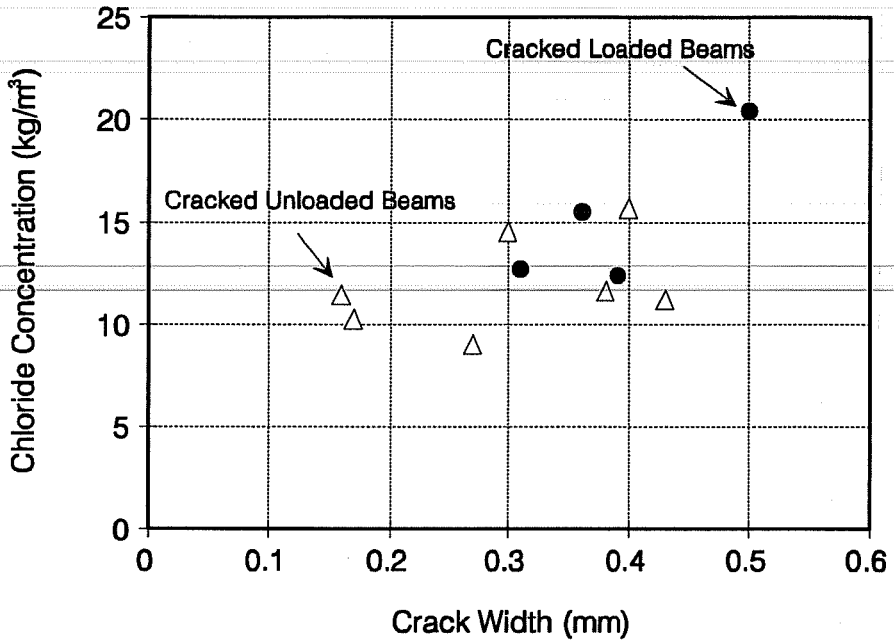

Figure 11.15 Chloride Concentration at Crack Locations Near Beam Upper Bars.

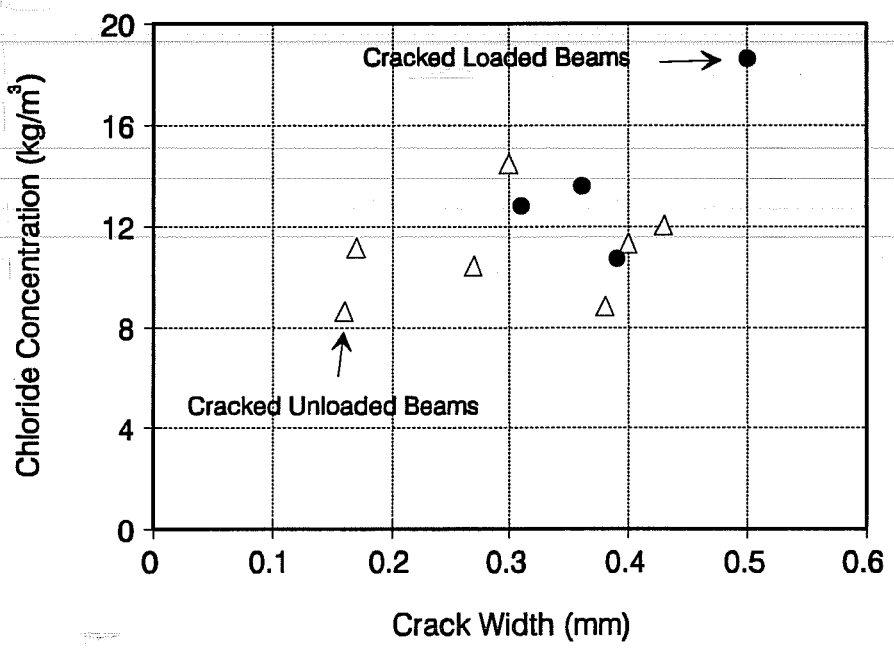

Figure 11.16 Chloride Concentration at Crack Locations Near Beam Lower Bars.

Chloride contents determined at uncracked surfaces in the exposure area did not correlate with the loading condition. The average chloride contents near the upper and lower longitudinal bar or stirrup bend were 5.2 kg/m^3 (8.7 lb./yd^3) and 5.9 kg/m^3 (9.9 lb./yd^3), respectively. At other locations (cracked or uncracked), within approximately 0.3 m (12 in.) outside the exposure area, chloride contents at the upper and lower steel were 2.0 and 3.9 kg/m^3 (8.7 lb./yd^3), respectively. No chlorides were detected at locations more than 0.3 m (12 in.) from the exposure area.

11.6.4 Steel Surface Corrosion. Information on bar *surface* condition after testing are tabulated in Section D.9. A summary of the observations is given below:

Bars in As Received Condition. Bars in as received condition in uncracked beams were almost unaffected. Only one very minor rust spot appeared at a mill mark on one bar. More rust spots were apparent on bars in cracked unloaded and cracked loaded beams, particularly on mill marks, within about 40 mm (1.5 in.) from the crack location.

Bars with 3% Damage. Bars in uncracked beams showed rust spotting on some exposed steel areas facing the concrete cover. It was evident that blisters were also forming on the coating on the same side of the bar. Again, more corrosion spots and blisters (facing the concrete cover) were visible on bars in beams with opened and unopened cracks within about 40 to 60 mm (1.5 to 2.5 in.) from crack location. Figure 11.17 shows examples of damaged bars removed from cracked beams (notice the approximate crack location marked by a thick line around the bar). Bars with patched damage showed minor rust spotting on the patched areas with evidence of coating cracking and blistering as shown in Fig. 11.18.

Stirrups in As Received Condition. Stirrups in uncracked beams showed corrosion spots, blisters and coating cracking at the hook end closest to the lower concrete surface. In addition to blistering, stirrups in beams with unopened cracks disclosed corrosion spots at areas of contact with uncoated bars as shown in Fig. 11.19. Similar but worse corrosion appeared along the continuous ribs, hook end, and bends of stirrups in beams with opened cracks as shown in Fig. 11.20.

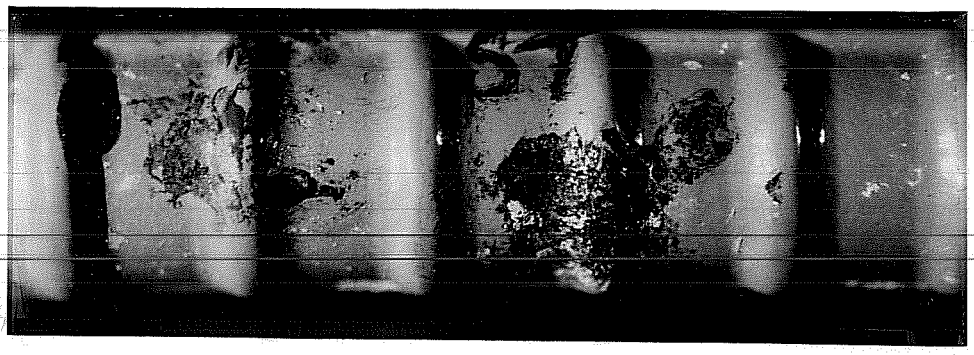

(a) Damaged Upper Bar from Cracked Unloaded Beam B9

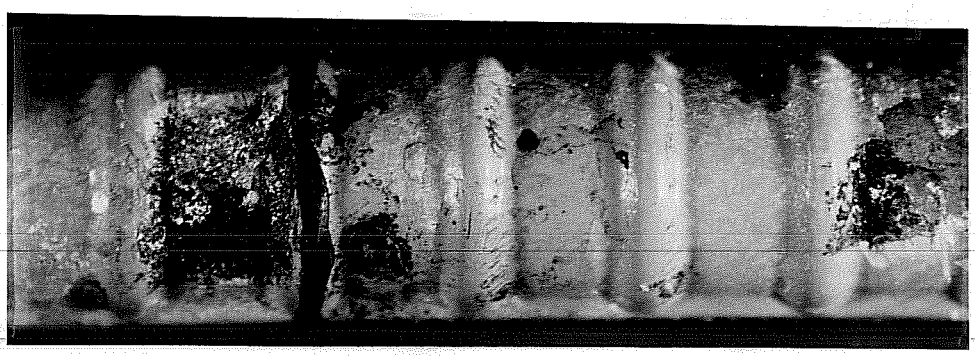

(b) Damaged Upper Bar from Cracked Loaded Beam B11

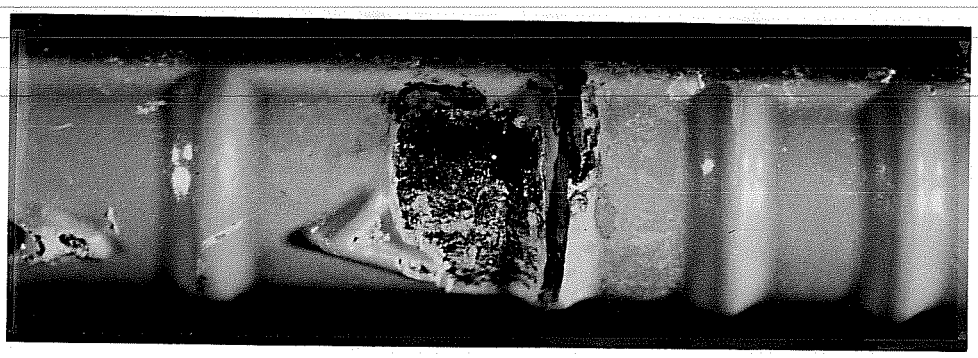

(c) Damaged Lower Bar from Cracked Loaded Beam B11

Figure 11.17 Corrosion on Lower Side of Bars Removed from Beams After One Year of Exposure.

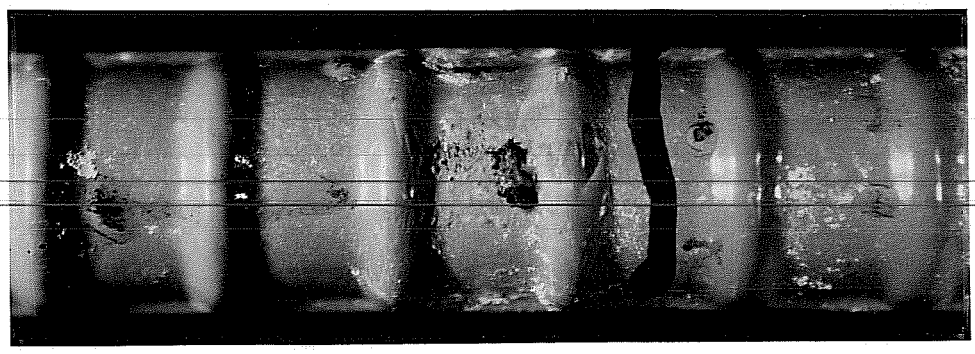

Figure 11.18 Corrosion on Lower Side of Patched Bar Removed After One Year of Exposure.

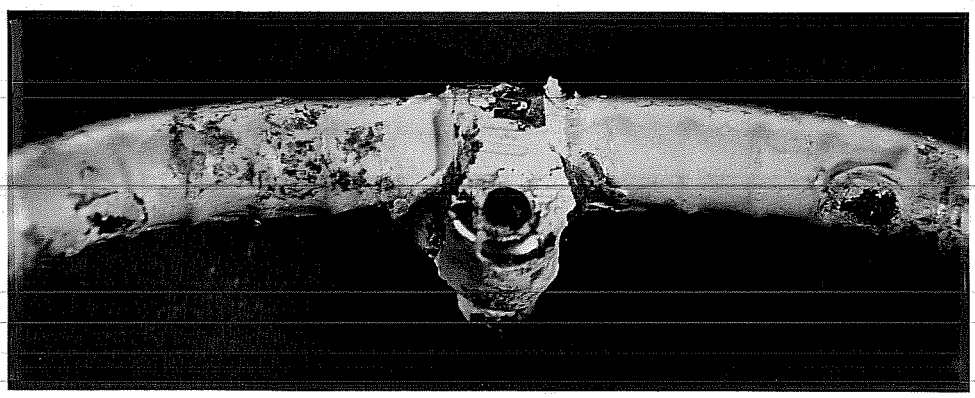

Figure 11.19 Corrosion at Areas of Contact Between Stirrup and Uncoated Bars.

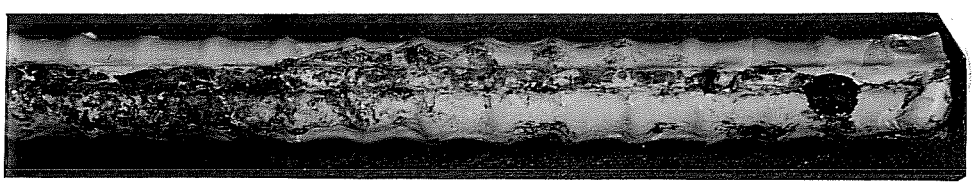

Figure 11.20 Corrosion on Hook End of Stirrup Removed from Cracked Loaded Beam After One Year of Exposure.

Stirrups with patched bends in uncracked beams were free of visible corrosion. Other patched stirrups in cracked beams had a similar condition to that described above for stirrups without patching. Figure 11.21 shows corrosion spots on the inside surface of patched bends in contact with uncoated bars.

Stirrups with 3% Repaired Damage. These stirrups had similar but more visible signs of corrosion as the stirrups in as received condition. Stirrups used in splice regions at midspan, in particular, showed the worst rust spotting (breakdown of coating) along hook ends, continuous ribs, and bends, and longitudinal cracks in the coating. The patched damaged areas were severely corroded as shown in Fig. 11.22.

Bars in Splice Zone. As shown in Fig. 11.23, rust had covered about 10 to 60% of the patched cut ends of bars. Additionally, coating cracking and blistering were visible up to about 140 mm (5.5 in.) from the bar end.

The corrosion products in all cases were black and brown. The products were mostly brown in the vicinity of cracks. In some instances, upon exposing the bars around stirrups in beams with splice bars, a greenish-black corrosion product was found in a soluble form. The dark greenish product rapidly converted to brown on contact with air. Similar to macrocell observations, steel corroded spots on the longitudinal bars almost always coincided with voids in the surrounding concrete as shown in Fig. 11.24. Of particular interest was that corrosion occurred at holidays and exposed steel areas mainly on the side of the bar facing concrete cover on the short side of beam, *i.e.* the lower side of the bar in casting position. Even at crack locations, where corrosion was apparent on exposed steel areas facing the cover, no corrosion occurred on exposed areas on the other side. Figure 11.25 shows the two sides of a damaged bar at the crack location with rust only on one side.

Uncoated Bars in Compression Zone. During removal of stirrups, short lengths of the uncoated bars in the compression zone were uncovered. In many cases, the uncoated bars were severely corroded with extensive surface degradation and loss of metal around contact points with the stirrup. Corrosion was spread along the bar about 75 mm (3 in.) and it was

associated with chloride solution transport through the wide transverse cracks near beam midspan as shown in Fig. 11.26.

Figure 11.21 Corrosion at Areas of Contact Between Patched Stirrup and Uncoated Bars.

Figure 11.22 Corrosion on Patched Damaged Areas of Stirrup After One Year of Exposure.

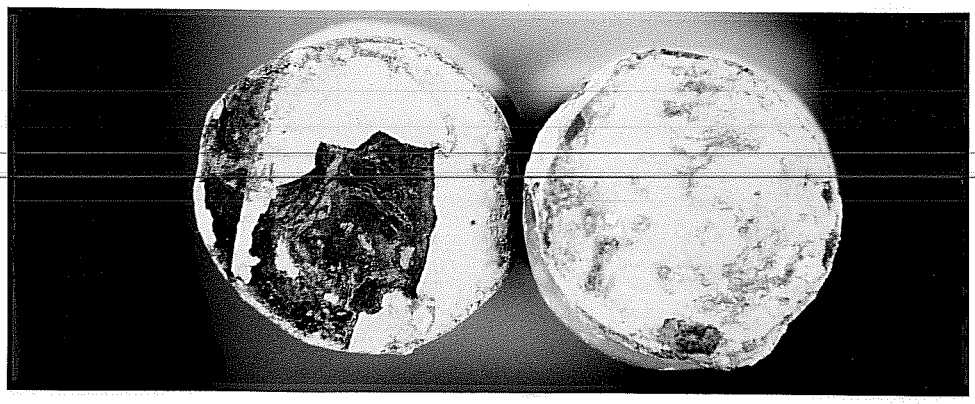

Figure 11.23 Corrosion on Patched Cut Ends of Splice Bars After One Year of Exposure.

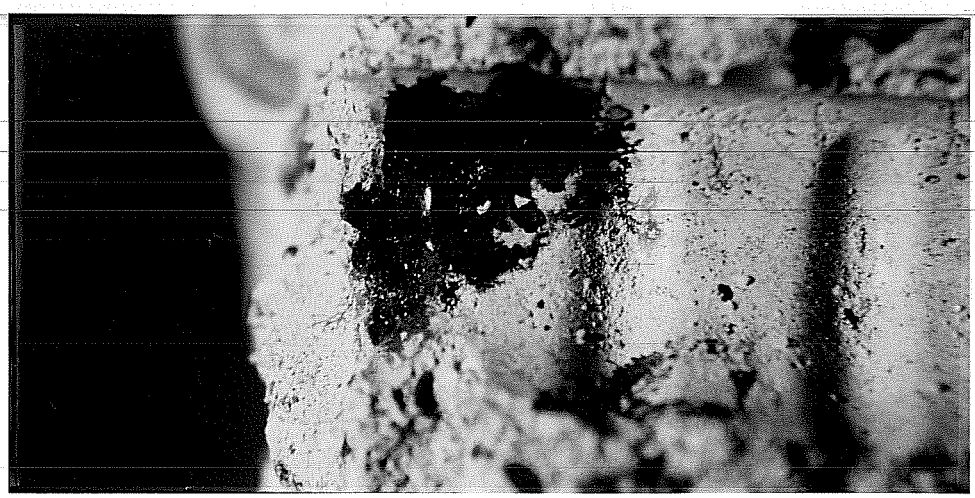

Figure 11.24 Corrosion Spots Coincident with Voids in Concrete.

(a) Corrosion on Lower Side of Bar (Facing Cover)

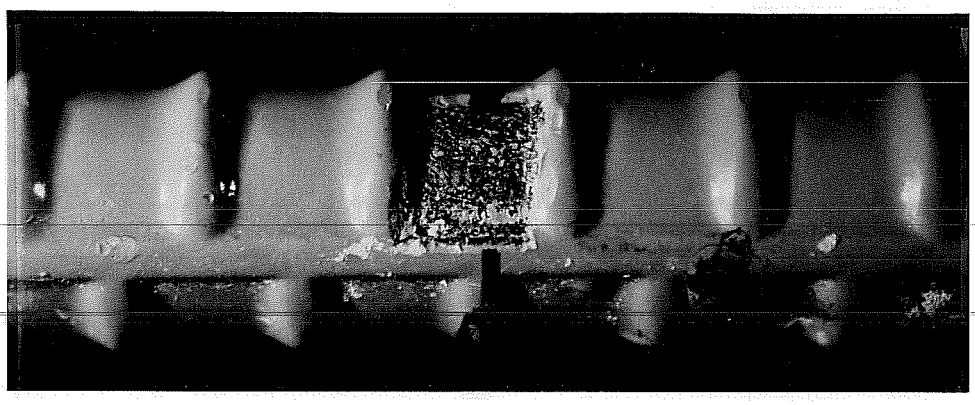

(b) No Corrosion on Upper Side of Bar (Facing Inward)

Figure 11.25 Difference of Corrosion Performance Between Upper and Lower Sides of Bar at the Same Crack Location.

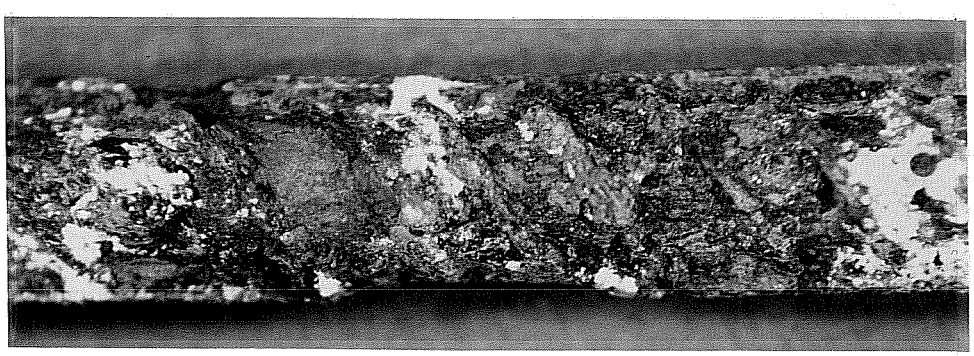

Figure 11.26 Corrosion of Uncoated Compression Bars at Crack Location.

11.6.5 Coating Prying. A sharp blade was used to remove the debonded coating and to inspect areas of intact coating. In general, loss of adhesion on the longitudinal bars was limited to about 10 mm (3/8 in.) around all exposed steel areas, and to some length along the corroded sites. Even where damage was repaired, debonding reached about 15 mm (1/2 in.) around the patched areas. Debonding was proportional to apparent corrosion along the bar: the more surface corrosion, the larger the debonded area.

For stirrups, coating debonding was much more prevalent on stirrups in cracked beams than in uncracked beams. The areas of stirrup most vulnerable to coating debonding were the bent portions and the patched ends. In addition, the coating was debonded to some extent along the rust areas. Debonding was particularly extensive (over 60% of stirrup surface) in those specimens where stirrups were used with longitudinal or splice bars. For cut bar ends, debonding took place along the cracked coating extending from the cut end.

As described for the macrocell specimens, the debonded areas were relatively easy to pry and were characterized by noticeable separation from the metal. In contrast, cutting through the well-bonded coating was difficult and caused cohesive separation of the coating material itself. Figure 11.27 illustrates the extent of debonding of the epoxy coating on a longitudinal bar and a stirrup.

11.6.6 Underfilm Corrosion. Short descriptions of the condition of steel under the coating are given in Section D.9. Generally, bars and stirrups in uncracked beams suffered the least substrate corrosion. The metal either remained bright with no visible corrosion activity, or was slightly discolored with minor surface disruption at sporadic locations as shown in Fig. 11.28.

Metal corrosion on the longitudinal bars in cracked beams was mainly concentrated on the bar side facing concrete cover. Thin black -sometimes brown- corrosion products covered the metal surface around the affected sites. Underfilm corrosion spread to about 75 mm from crack location, and up to about 45 mm from the edge of the damaged areas. There was not any appreciable difference in the extent or severity of substrate corrosion between

as received bars in beams with opened or unopened cracks. However, bars with intentionally introduced damage showed more substrate corrosion in cracked loaded beams than in cracked unloaded beams as illustrated in Fig. 11.29.

(a) Upper Longitudinal Bar (B29)

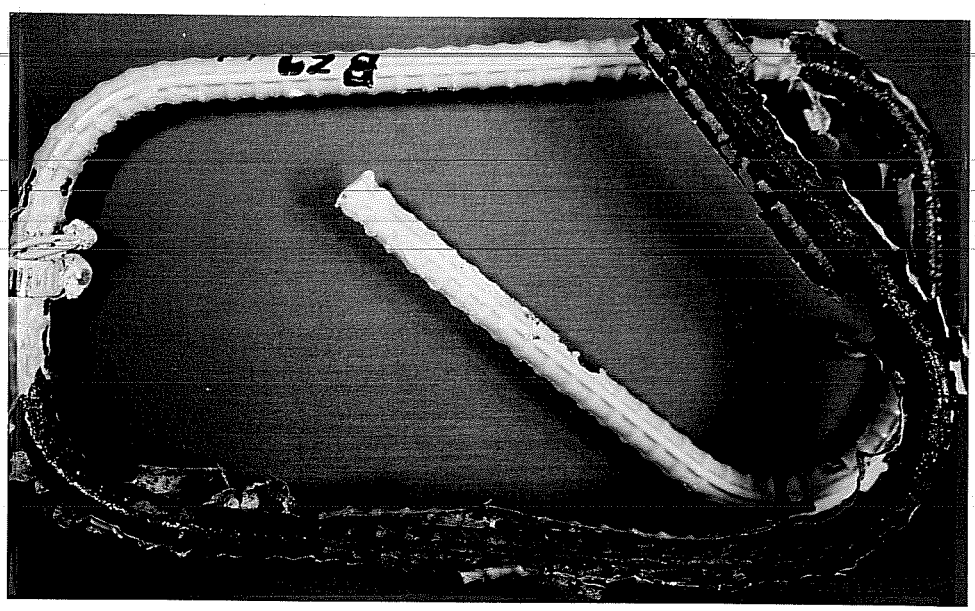

(b) Stirrup (B29)

Figure 11.27 Coating debonding After One Year of Beam Exposure.

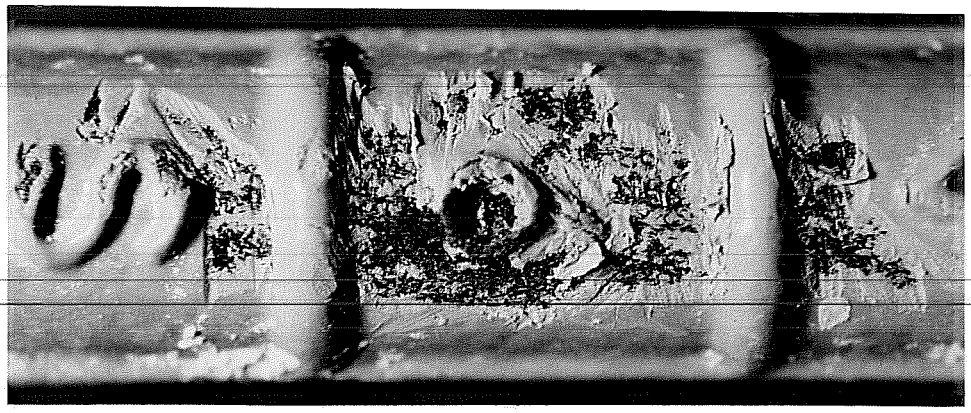

(Coating Scraped Away)

Figure 11.28 Minor Surface Corrosion of Undamaged Bar Removed from Uncracked Beam After One Year of Exposure.

Indeed, the severest metal corrosion was found on the damaged bars retrieved from the cracked loaded beam. Significant pitting occurred at the edges of the exposed steel areas intercepting wide cracks. These pits were elliptical measuring about 6 x 9 mm (1/4 x 3/8 in.) in perpendicular directions and up to 1.25 mm (0.05 in.) in depth as shown in Fig. 11.30. Several smaller pits existed beneath the coating in adjacent areas. The pits were covered with dark brown corrosion products.

Longitudinal bars with patched damage showed dark steel surfaces around the patches on the bar side facing cover. Steel under the patching material away from the exposure area and on the bar side facing inward was mostly bright. Rust extended to about 60 mm (2.4 in.) from crack locations and up to 25 mm (1 in.) from the edge of the patched area. Only shallow pits were evident under the film near the affected sites.

Occasionally, a clear trapped solution was found underneath the coating. The solution dried fast upon exposure to the atmosphere leaving a white residue which turned to brown as shown in Fig. 11.31. Except for the bars that exhibited considerable pitting as mentioned above, steel corrosion was generally superficial without significant metal loss.

Many of the stirrups exhibited moderate to widespread underfilm corrosion starting from the hook ends and from defects on both the inside and outside of bends. The metal underneath the coating, including patching, appeared dull and darkened with some brown rust spotting. A rust layer was observed particularly on stirrup parts closest to a crack or lower concrete surface. Corrosion was also obvious around points of contact between stirrup and uncoated bars. Slight pitting was observed along the continuous ribs of some stirrup legs. Stirrup surface rusting ranged from minor to severe but without significant localized loss of bar section. Figure 11.32 shows an example of undercutting on a stirrup specimen with 3% patched damage.

For bar ends at splice zones, a black corrosion product covered up to about 70% of bar surface area at the lower side. The maximum undercutting length was about 165 mm (6.5 in.) from the cut end as shown in Fig. 11.33. Again, corrosion was light without significant metal loss.

11.6.7 Bar Trace in Concrete.

Bar traces of coated steel confirmed the previously mentioned findings from the macrocell study. Concrete on top of the coated steel (in casting position) appeared glossy, smooth and generally free of voids. Concrete on the underside of the coated steel appeared dull with laitence and many voids of different sizes. In general, more rust products were visible in and around the voids at the bottom trace than at the top.

The stirrup trace did not have a similar distinct pattern. There were some voids distributed along the stirrup legs and concrete was not as glossy as it appeared on top of the longitudinal bars. Figure 11.34 shows an example of stirrup trace in concrete. An interesting observation was that the patching material used at the coating plant to repair stirrup ends remained on the stirrup imprint in concrete as shown in Fig. 11.35.

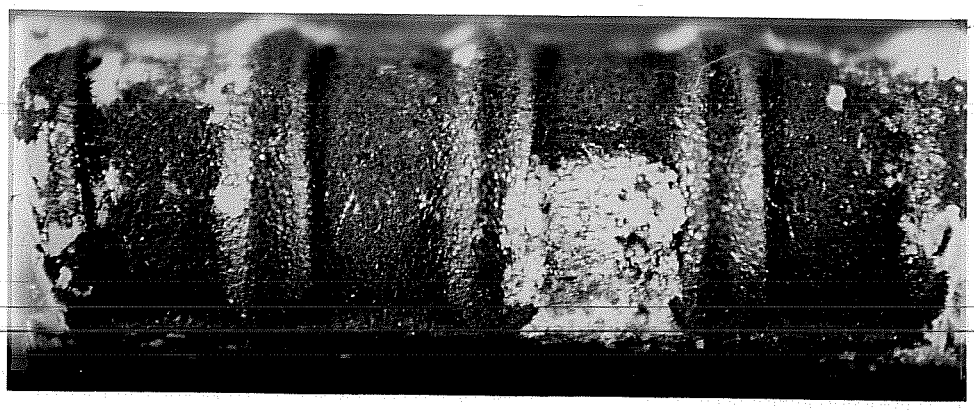

(a) Corrosion on Bar from Uncracked Beam B7

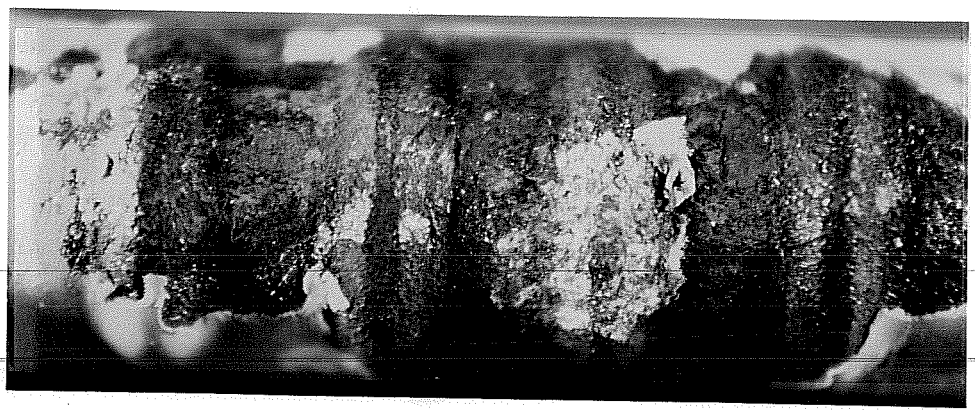

(b) Corrosion on Bar from Cracked Unloaded Beam B9

(c) Corrosion on Bar from Cracked Loaded Beam B11

Figure 11.29 Substrate Corrosion on Bars with Introduced Damage and Variable Beam Loading Condition.

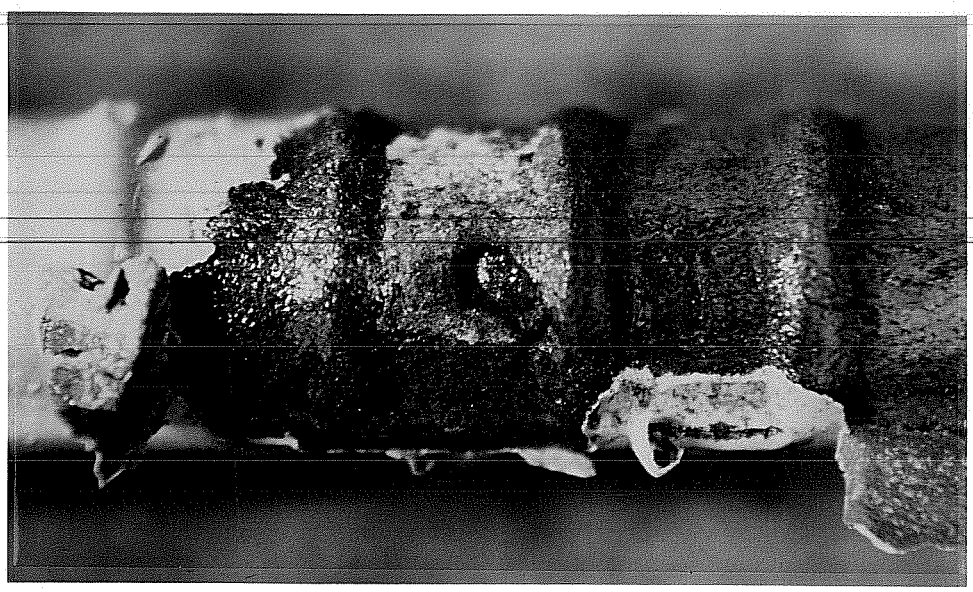

(a) Pitting on Upper Longitudinal Bar

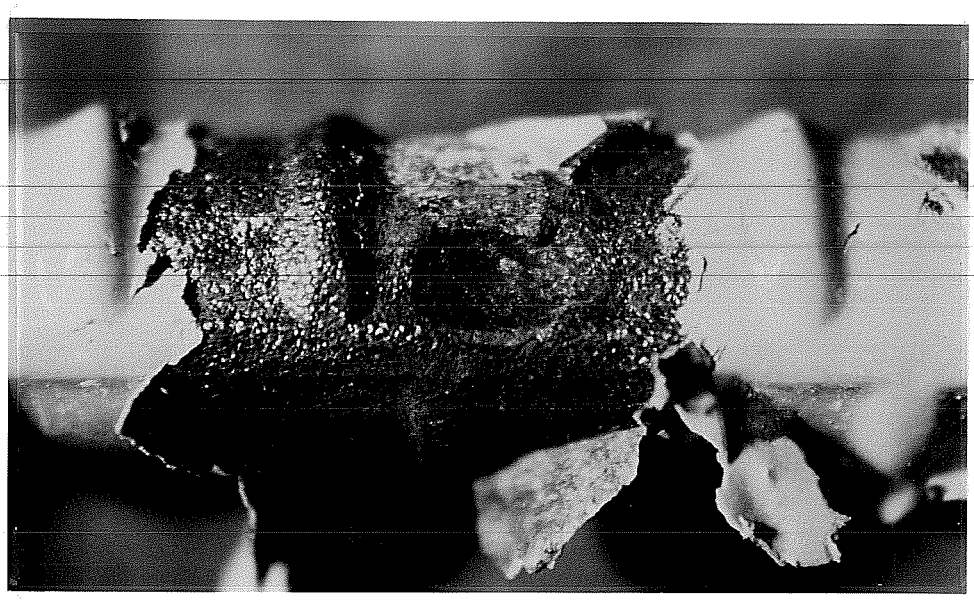

(b) Pitting on Lower Longitudinal Bar

Figure 11.30 Pitting on Exposed Steel Areas of Bars Removed from Cracked Loaded Beam B11 After One Year of Exposure.

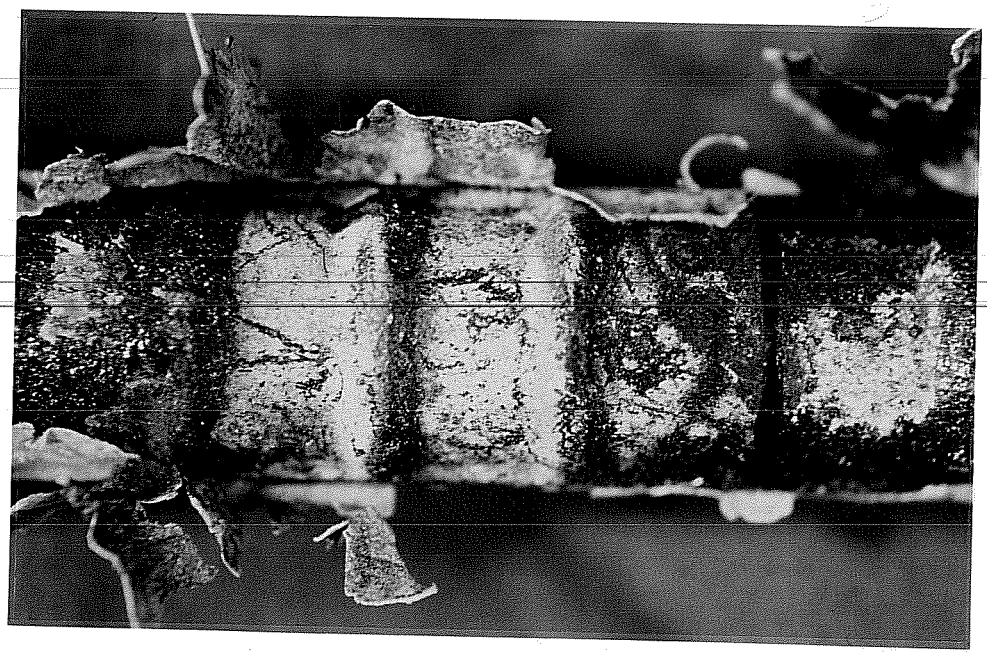

Figure 11.31 White Residue of Dried Solution Trapped Beneath Coating.

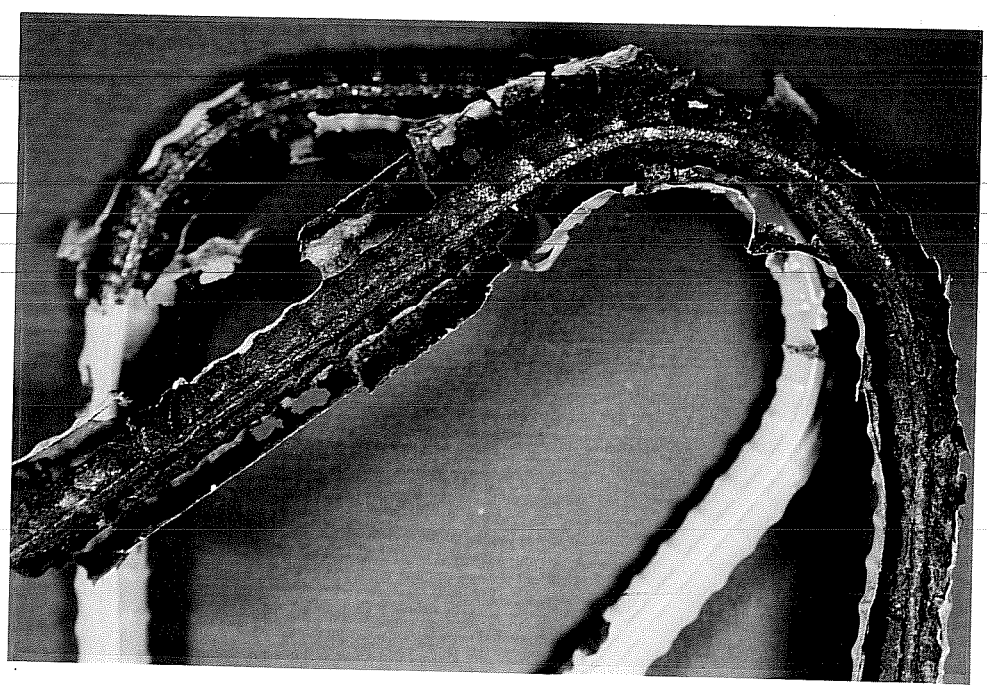

Figure 11.32 Example of Undercutting on Stirrup with 3% Patched Damage After One Year of Exposure.

Figure 11.33 Undercutting Along Splice Bar at Patched Cut End After One Year of Exposure.

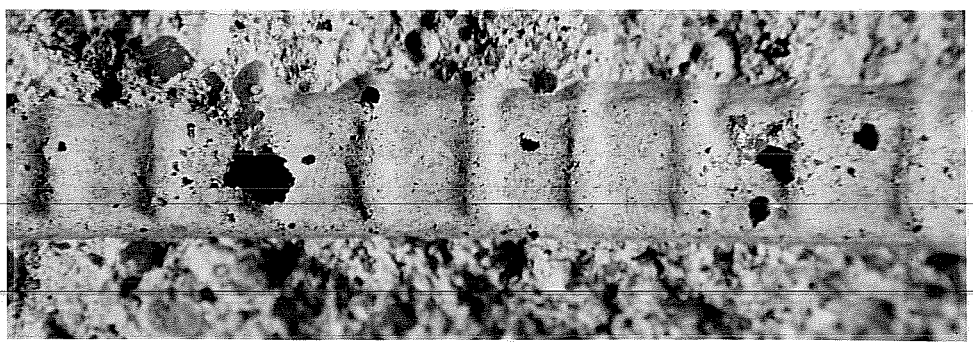

Figure 11.34 Stirrup Trace in Concrete.

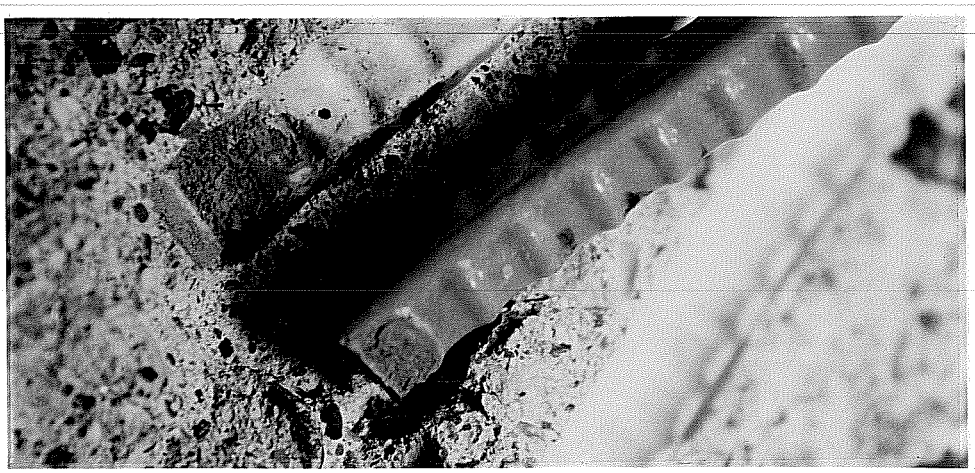

Figure 11.35 Patching Material Observed on Stirrup Imprint in Concrete.

CHAPTER 12
BEAM EXPOSURE STUDY:
ANALYSIS AND DISCUSSION OF TEST RESULTS

12.1 General

The beam exposure study involved many variables in a unique exposure test. The interaction of coating damage level and loading condition on the following aspects of performance of epoxy-coated reinforcement was of special interest:

- Time-to-corrosion initiation.
- Electrical potential of steel.
- Corrosion progression.
- Corrosion mechanism.

Data were collected during exposure testing to show the influence of the following factors on corrosion performance of coated reinforcement:

- Concrete cracking and crack width.
- Concrete quality around reinforcement.
- Chloride concentration and distribution at steel level.

Design and layout of the beam exposure test was primarily driven by the incidence of premature failure of coated reinforcement in bridge substructures in the Florida Keys. Damage was first noted on fabricated bars (ties, stirrups, bent bars) and subsequently on straight bars as well. Corrosion was characterized by the formation of large pits on steel surface.[42] The results presented in Chapter 11 agree with these field observations to a great extent: corrosion was particularly extensive on fabricated bars; and severe pitting occurred on straight bars.

In the following discussion, steel potential data were analyzed to relate the potentials and their changes to corrosion initiation and state or level of activity. Conclusions were drawn as to the causes of coating debonding and loss of coating integrity which led to corrosion of the metal substrate. The data and observations were used to develop a hypothesis for the corrosion mechanism.

Forensic examinations were carried out on only half of the beams in order to continue testing the other half for an extended period. The remaining beams will provide more information in the future about long-term performance of coated bars and protection offered by epoxy coating.

12.2 Time-to-Corrosion

12.2.1 General. Although highly negative potentials were considered to be an indicator of corrosion initiation, it must be remembered that they may also result from progressive restriction in oxygen supply. For example, a potential of -900 mV was reached in a totally saturated structure without corrosion.[22] For this reason, the following discussion refers to suspected corrosion indicated by measured half-cell potentials.

12.2.2 Longitudinal Bars. Time-to-onset of suspected corrosion as indicated by half-cell measurements varied among beams with different coating damage and loading condition. Table 11.3 in Chapter 11 indicates that as received bars delayed corrosion more than bars with 3% damage to coating. In other words, the more steel area that was exposed, the earlier was the shift of potential to more negative values. Interestingly, corrosion of bars in cracked beams was suspected to initiate after the first wetting period; *i.e.* after the first salt application. Bars with patched damage showed comparable time-to-corrosion as bars with unrepaired damage suggesting that patching was not effective.

In general, similar periods to suspected corrosion initiation were listed for bars in beams with opened and unopened cracks. The similarity means that crack width did not

affect the time to active conditions for corrosion. Rostam,[60] on the other hand, revealed that the larger the crack width, the shorter the time to steel depassivation.

12.2.3 Stirrups. Similar to the longitudinal bars, time-to-corrosion of stirrups varied with level of coating damage and loading condition. Table 11.4 showed that corrosion of stirrups in uncracked beams was either uncertain or delayed. In contrast, stirrups in cracked beams may have started to corrode as early as the first wetting period. The potentials tended to drop at a slightly later date for as received stirrups with patched bends compared to those as received without patching or 3% damage and patching. Further, stirrups located at cracks in loaded beams seemed to be the first to corrode regardless of the coating condition.

12.3 Corrosion Activity

12.3.1 General. Half-cell potentials were always measured while concrete was still wet. It was suspected that measuring potentials after drying would lead to unreliable measurements since concrete conductivity would be reduced.

Highly negative potentials generally indicate corrosion but not the rate of corrosion. Half-cell potentials are directly related to changes in steel condition or corrosion state, whereas the corrosion rate is directly proportional to corrosion current. Furthermore, measured potentials do not demonstrate whether macro-galvanic or micro-galvanic corrosion cells exist on a bar. Coupling of corroding and non corroding portions of the same bar will develop a potential difference regardless of the electrode size, *i.e.* macro-electrode or micro-electrode.[105] Since corrosion activity will generally vary with time of exposure, the cathodic and anodic areas, and the cathode to anode ratio, will also change with time. Therefore, the same potential is likely to develop in different arrangements of the participating electrodes.

In the beam exposure study, the layout of the longitudinal bar with respect to exposure area influenced the development of the steel potential. A predominantly anodic behavior prevailed at the middle region of the beam subjected to wetting and drying. Exposed metal on the bar surface became anodic upon contact with chlorides penetrating

through concrete and cracks. Other steel areas in regions outside the exposure zone were predominantly cathodic in relatively less contaminated or chloride-free concrete. The farther the distance from the anodic zone, the more steel passivity was maintained. In addition, the low moisture content of concrete surrounding cathodic spots promoted oxygen transport to the metal surface, thereby facilitating the cathodic reactions. Potential variation between duplicate beams reflected mainly the degree of polarization of these cathodic reactions.

*12.3.2 **Half-Cell Potential Readings.*** It has been suggested that half-cell potentials can be a good indicator of whether or not corrosive levels of chloride have reached the reinforcement level.[30] Therefore, the following analysis of the thermodynamic behavior of tested bars, in terms of the measured potentials and potential change with time, was related to chloride effects on the corrosion process. Data supporting the relation between corrosion and potential measurements for the three beam groups in the test are presented in Tables 12.1 through 12.3.

At the beginning of the exposure test, half-cell potentials were not stable. Wheat and Eliezer[105] noted that days, weeks, and even months were required for reinforced concrete samples to go from a potential of approximately -100 mV to a more stable potential of about -600 mV. Reaching a stable potential corresponds to electrochemical equilibrium. It means that electrochemical activities during the transitory period to a more stable condition may be associated with corrosion initiation.

Despite the instability of the initial potentials, the potentials measured on all uncracked beams were between approximately -50 and -200 mV SCE. This potential range reflects steel passivity. According to Aguilar *et al*,[124] passive steel bars acquire open-circuit potentials typically between +100 and -100 mV SCE. Wheat and Eliezer,[105] and Arup[52] suggested that the range for steel passivity in aerated concrete lies between +100 and -200 mV SCE.

Table 12.1 Relation of Corrosion to Potential Measurements on Beam Specimens Group I, Longitudinal Bars (Upper-Up, and Lower-Lw)

Beam No.	Maximum Diff. of Avg. Mid and End Potential (mV)	Final Average Mid Potential (mV)	Percentage of Rust Area Along 0.9 m of Midspan (%)	Steel Corrosion Condition (Only Autopsied Beams)
B1-Up	150	-180		
B1-Lw	200	-140		
B2-Up	145	-55	0.0	No corrosion
B2-Lw	235	-215	0.0	Negligible
B3-Up	235	-590		
B3-Lw	330	-600		
B4-Up	205	-550	1.5	Minor
B4-Lw	300	-585	6.0	Minor+1 slight pit
B5-Up	220	-355	0.5	Negligible
B5-Lw	325	-630	0.5	Minor
B6-Up	255	-570		
B6-Lw	330	-505		
B7-Up	140	-350	2.5	Minor
B7-Lw	190	-420	4.0	Minor+2 slight pits
B8-Lw	130	-365		
	230	-400		
B9-Up	195	-500	8.0	Minor+7 slight pits
B9-Lw	250	-525	5.5	Minor+5 slight pits
B10-Up	255	-520		
B10-Lw	285	-575		
B11-Up	275	-560	3.0	5 slight+1 severe pit
B11-Lw	360	-585	5.0	5 slight+1 severe pit
B12-Up	260	-525		
B12-Lw	335	-560		
B13-Up	175	-535	9.0	Minor+5 slight pits
B13-Lw	285	-560	6.0	Minor+4 slight pits
B14-Up	145	-555		
B14-Lw	195	-575		

Table 12.2 Relation of Corrosion to Potential Measurements on Beam Specimens Group II, Stirrups

Beam No.	Final Average Potential (mV)	Percentage of Rust Area Along Stirrup (%)	Steel Corrosion Condition (Only Autopsied Beams)
B15	-80		
B16	-415	6.5	Minor rust
B17	-535		
B18	-430	22.0	Minor rust
B19	-525		
B20	-570	22.0	Moderate
B21	-225	0.0	Negligible
B22	-110		
B23	-360		
B24	-460	20.5	Moderate
B25	-355		
B26	-485	23.0	Severe, pitting
B27	-325		
B28	-535	28.0	Severe, pitting

Table 12.3 Relation of Corrosion to Potential Measurements on Beam Specimens Group III, Longitudinal/Splice Bars (Upper-Up, and Lower-Lw) and Stirrups

Beam No.	Maximum Diff. of Avg. Mid and End Potential (mV)	Final Average Mid Potential (mV)	Percentage of Rust Area (%)	Steel Corrosion Condition (Only Autopsied Beams)
		Longitudinal Bars Including Splice Bars		
B29-Up	140	-570	6.0	Minor +3 slight pits
B29-Lw	220	-575	6.0	Minor +3 slight pits
B30-Up	155	-525		
B30-Lw	190	-555		
B31-Up	270	-550	-	Minor
B31-Lw	340	-625	-	Minor
B32-Up	325	-465		
B32-Lw	275	-565		
B33-Up	320	-600	-	Minor
B33-Lw	395	-620	-	Minor
B34-Up	295	-640		
B34-Lw	375	-615		
		Stirrups		
B29		-505	23.5	Severe, pitting
B30		-495		
B31		-545	53.5	Severe, pitting
B32		-510		
B33		-520	56.5	Severe, pitting
B34		-530		

The initial potentials for all cracked beams, however, ranged between approximately -50 and -500 mV SCE. The cause of the different initial potential values is usually attributed to early contact of steel with chlorides penetrating through the cracks. The potentials also tended to be slightly more negative at crack locations relative to adjacent uncracked concrete even away from the exposure area, *i.e.* chloride zone. This variation in steel potential may be caused by concrete carbonation which can easily reach the steel surface at crack locations causing a potential shift. Lehmann[123] suggested that when carbonation of concrete is prevalent, the potential of corroded and noncorroded sites may shift electronegatively as much as 100 mV. Direct contact of steel with chlorides at crack locations in the exposure area caused an immediate shift of potential to more negative values.

The potential readings dropped after the beginning of the test for some uncracked beams. The drop was relatively large in the order of about 300 to 400 mV and sudden in a few cases. This drop indicated the arrival of chloride ions at the steel surface. Potential fluctuations which sometimes followed the drop could be related to unsteady conditions marking the transformation of steel from a passive to an active state. As more chlorides accumulated at the bar surface, the steel was depassivated and metal dissociation was enhanced. For cracked beams, such conditions prevailed either at the beginning of the test or shortly after with drops as large as 500 mV. Beams including patched bar ends in splice zones exhibited large, early drops indicating quick breakdown of the patching material.

The mechanism by which the half-cell potential of iron/ferrous ion Fe/Fe^{+2} shifts to a more negative value is related to chloride reaction with ferrous ions produced by corrosion.[46] When ferrous ion concentration is lowered, further iron oxidation commences. Hence, potential shifts to more negative values are indicative of operational corrosion cells and not necessarily of more rust or ferrous ion accumulation. Consequently, the same potential may have been reached whether corrosion was confined to a minute holiday or spread over a large surface area. Therefore, highly negative potentials should not be construed as definite indicators of significant corrosion.

During the period of potential fluctuation, the corrosion process was controlled by the amount of chloride ions available and the rate of oxygen reduction. Lack of both oxygen and available surfaces for oxygen reduction limited the cathodic reaction and slowed down the dissociation process, particularly for as received bars. If measurements of half-cell potentials were taken in the field on structures undergoing similar potential fluctuations, the results would be highly inconsistent: Corrosion may or may not be found! That is why single potential measurements may not be useful. Potential monitoring needs to be carried out over some time to establish a clear trend.

After an initial or delayed potential drop, or fluctuations, the potential remains steady with time. The potential varied consistently within a narrow range of highly negative values which indicated that active conditions persisted for the remainder of the test. Corrosion progression in this situation was almost certain. Sufficient chloride ions were available to maintain activity. The final potentials for uncracked and cracked beams that exhibited an appreciable drop in potential reached about -400 and -650 mV SCE, respectively.

The range of final potentials agrees very well with that presented by Wheat and Eliezer,[105] for general corrosion due to loss of passivity which is -450 to -600 mV. Sagüés[93] also measured potentials in the range of -350 to -475 mV SCE after almost 300 days of exposure of uncracked columns containing coated bars. Furthermore, the measured half-cell potentials generally agree with previous observations by Hededahl and Manning,[81] that the vast majority of readings were more negative than -200 mV SCE, and a significant number of readings were more negative than -350 mV.

Zayed and Sagüés[109] reported a similar trend of measured open-circuit potentials on damaged epoxy-coated bars embedded in concrete and subjected to salt solution as discussed in Chapter 4. For uncracked concrete specimens, the potentials dropped suddenly over 150 to 250 mV after some time of exposure. The potentials then tended to fluctuate before stabilizing near a low value of -400 mV. The initial potentials were typically between -100 and -250 mV. For cracked concrete specimens, the initial potentials were more negative than

for uncracked specimens ranging between -150 and -450 mV. Some potentials, after moderate fluctuations, stabilized in the -350 to -400 mV range.

Erdogdu and Bremner[56] also obtained similar thermodynamic behavior after measuring open-circuit potentials of coated and uncoated bars in uncracked concrete for two years. The first potential drop for coated bars occurred at times equal to or larger than those encountered for uncoated bar specimens. After that, potentials fluctuated and reached a more steady value till the end of the test. Initially undamaged bars exhibited potentials in the low negative range as they remained passive. Some initial potential readings were highly negative. The most notable conclusion of the above test was that no difference practically existed between the behavior of coated bars with 1 or 2 percent damaged surface area.

Due to hydrolysis, the localized lower pH of solution within an active pit encourages further corrosion at the available potential level.[43] This phenomenon explains why corrosion progression and pitting continued on some bars at a stable half-cell potential between -400 and -600 mV SCE. Wheat and Eliezer,[105] and Arup[52] also indicated that pitting condition resulting from chlorides is associated with -200 to -500 mV SCE. Sagüés[114] reported that appreciable coating debonding took place at -500 mV SCE in electrochemical impedance tests.

Based on the discussion above and observations of actual bar condition, electrical half-cell potential values correlated well with the state of corrosion of coated steel. Figure 12.1 summarizes the relation between the ranges of measured potentials and corrosion state. Although the extent of corrosion spreading on the bar surface did not correlate with steel potential, the corroded area tended to increase as corrosion severity increased.

While half-cell potentials may be helpful in detecting state of corrosion, they need to be measured at close points on the concrete surface to detect the exact location of corrosion activity. Notice that some potentials outside the exposure area where corrosion primarily took place were in the high negative range of around -400 mV for example and yet no corrosion was found on the steel at these measurement points. Therefore, highly negative

potentials may indicate corrosion activity close to measurement sites, say within 0.5 to 1.0 m (around 2 to 3 ft.).

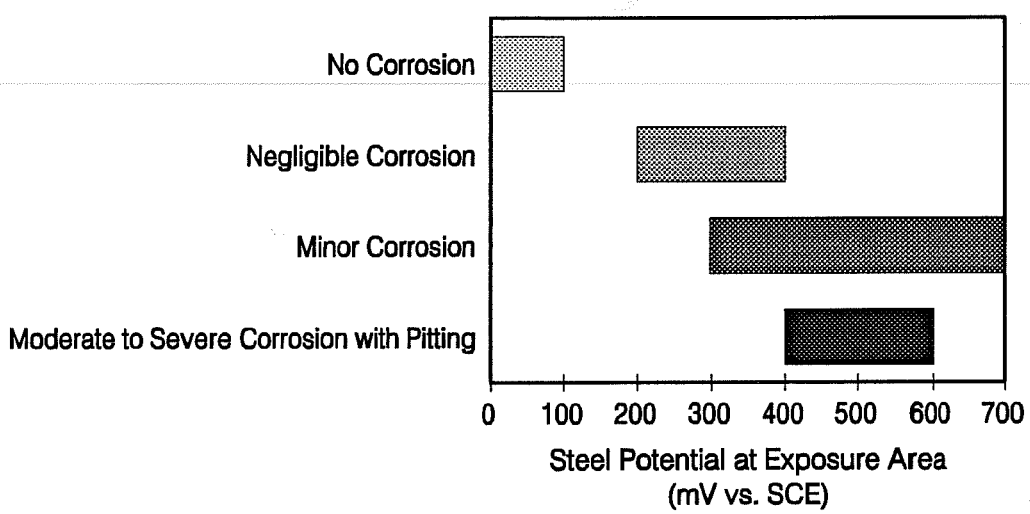

Figure 12.1 Relation Between Corrosion Activity and Steel Potential.

12.3.3 Half-Cell Potential Differences. Since a drop in potential marks a site of possible localized corrosion activity in the vicinity, other parameters were sought to better identify the corrosion state. Experience with uncoated reinforcing bars has shown that dependence on half-cell potentials alone to locate corroded areas was not always reliable when following the ASTM C876[117] assessment criteria. In addition, previous studies have indicated that the electrical potential of an anode cannot be used to indicate rate of corrosion.

Elsener and Böhni[23] found that the local potential gradient was a better way to identify the type of corrosion and to locate corroding sites. Likewise, Clear and Virmani[57] suggested that the difference in anode and cathode potentials was the more important indicator of corrosion activity. Therefore, it is the potential difference between the anode and the cathode, not the magnitude of the anode potential, that relates to corrosion rate. It follows that corrosion severity can be assessed in relation to the difference in potentials. ACI 222-87,[44] agrees and states that the larger the potential difference, the higher the corrosion rate.

A change in potential along a bar creates galvanic cells, with the corrosion occurring at the sites exhibiting higher negative potentials. In effect, a potential drop protects the adjacent noncorroded steel surface which predominantly behaves as a cathode. Large differences of potentials along a concrete member may, then, be used as indicators of macrocell formations.[30]

Lehmann[123] suggested that a difference of 200 mV or more between sites in proximity, within 0.15 to 0.3 m (6 to 12 in.), could be indicative of corrosion activity. However, in the field, the potential differences between anodes and cathodes usually vary between 20 and 500 mV, depending on chloride content, oxygen concentration, and concrete chemistry. Arup[52] suggested that high potential gradients on potential maps are indicative of pitting corrosion of uncoated steel. High negative potentials typically -450 to -600 mV SCE without steep gradients are more indicative of general corrosion. Studies have shown that potential differences rarely exceed 100 mV when corrosion was not active or at extremely low activity.[44] On the other hand, significant corrosion was commonly associated with potential differences over 200 mV.

The closely-spaced potential measurement points along the beam surfaces allowed the identification of predominantly anodic and cathodic sites. Potential differences were studied between adjacent and far points. The maximum differences between average wet (anode) and dry (cathode) potentials are listed in Tables 12.1 through 12.3. The state of corrosion was consistently related to these differences as follows:

- No corrosion was associated with potential gradients less than 150 mV (SCE).
- General corrosion (negligible, minor, or moderate) was associated with potential gradients exceeding 150 mV (SCE).
- Pitting corrosion in presence of chlorides was associated with potential gradients exceeding 200 mV (SCE).

The results listed above agree with suggestions by other researchers even though some were intended for uncoated bars. The potential gradients refer to measurement sites about 0.6 m (2 ft.) apart and a concrete cover of 50 mm (2 in.).

When evaluating potential differences along a corroded coated bar in concrete, it is important to distinguish between measured electrical potentials and what could be actual bar potentials. To illustrate, consider the damaged coated bar shown in Fig. 12.2 with an anodic (corroded) spot in the middle and two adjacent cathodic spots. Any ionic current flow in concrete is coupled with an electric potential field. The potentials change continuously from the anode to the cathode and can be represented by equipotential contours at right angles to the current flow paths.[23] At the concrete surface, potentials measured may be different from those at the steel surface due to cover thickness. Therefore, close anodic and cathodic sites may develop potential differences that cannot be inaccurately estimated from surface potential measurement.

The same reason may explain why potentials measured along the bars in the exposure area were not much different. The interference of equipotential lines from different corrosion cells acting simultaneously next to each other generated mixed surface potentials of the same order. As distance along the bar from the exposure area increased, potential differences between predominantly anodic and predominantly cathodic sites were clearer.

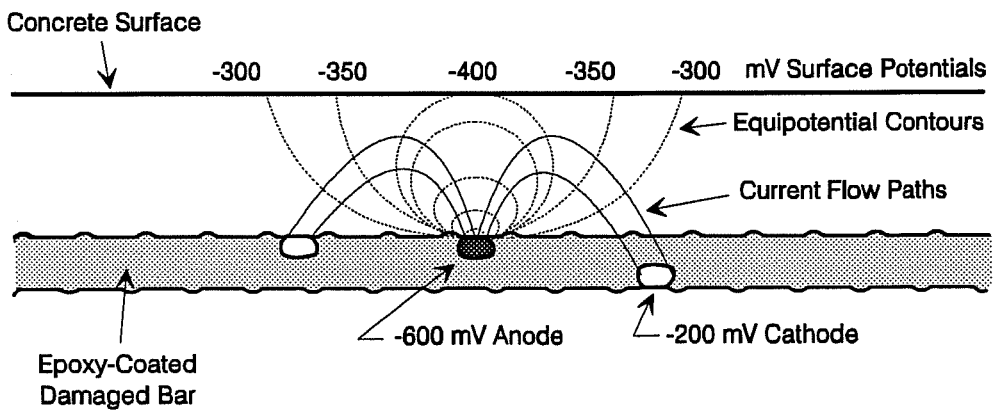

Figure 12.2 Equipotential Contours and Current Flow for Corroded Bar.

12.3.4 Effects of Concrete Cracking. Cracking of concrete has been cited as an important factor affecting the degree of protection of reinforcement. Observations from the beam exposure test confirmed that steel bars either coated or uncoated exhibited the worst corrosion at or near crack locations. In some cases, the localized conditions promoted pitting corrosion that resulted in severe mass losses. If corrosion activity were to continue at these locations, both the strength and fatigue characteristics of the reinforcing bars would have been jeopardized.

Pitting corrosion is characterized by high chloride concentration and low pH, and both occur at a crack tip. Chlorides accumulate at crack sites as a result of frequent wetting by a salt solution, and free access provided by the crack. Concrete alkalinity at a crack location is lowered by carbonation due to exposure to carbon dioxide CO_2. Hence, passivity of bare steel areas, such as damaged spots and pinholes in the immediate vicinity of the cracks, is locally lost and corrosion progresses at an increasing rate.

The uncoated compression bars recovered from tested beams also exhibited significant pitting and substantial metal loss around contact points with coated stirrups at transverse crack locations. Chloride ions were transported through the cracks to the uncoated reinforcement. Corrosion initiated and spread along the bar to a length equivalent to about 8 bar diameters. Poston[4] also reported corrosion spreading over a distance as much as 6 to 10 bar diameters on uncoated reinforcement. Data cited in the literature show that, for cracks perpendicular to the reinforcing bars, the corroded length of intercepted bars is likely to be more than 3 bar diameters.[44]

For coated longitudinal bars, metal loss was less than that observed on uncoated bars and was generally concentrated near crack locations. The maximum propagating length of corrosion at a site was about 6 bar diameters in the vicinity of a crack. The largest pits developed were observed on areas of damaged coating coincident with opened cracks.

Concrete cracking also affected the corrosion process on coated bars by creating different environments along the beam member. Cracks on the outside but close to the

exposure area interrupted chloride paths as shown in Fig. 12.3. Chloride concentrations were considerably different on both sides of the crack as confirmed by the chloride analysis presented in Section 11.6.3. As a result, any exposed steel area located away from the crack and the exposure zone would be predominantly cathodic with respect to those steel areas at the cracks or within the exposure zone.

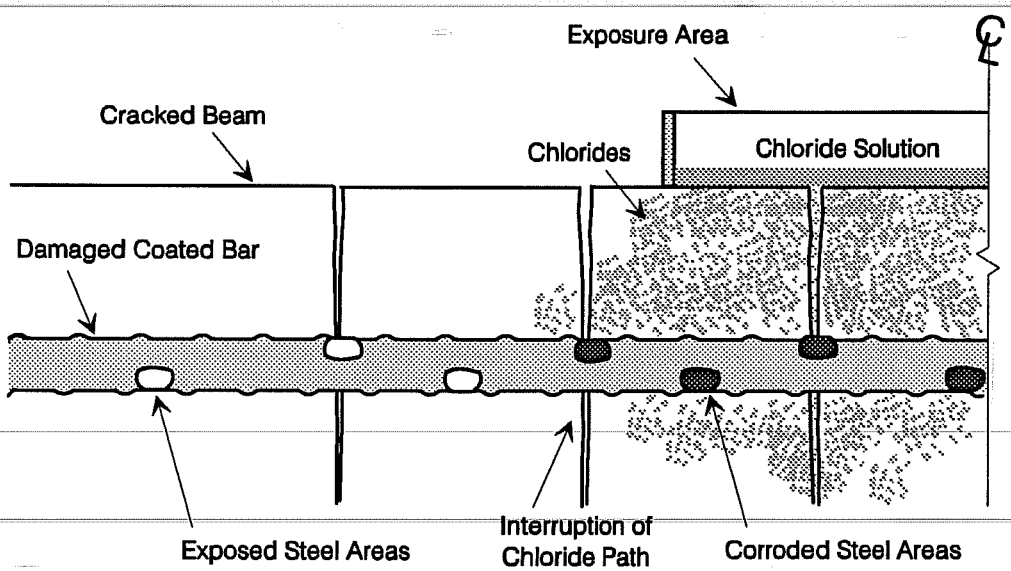

Figure 12.3 Anode-Cathode Development on Longitudinal Bar with Variable Chloride Contamination in Cracked Beam.

The worst corrosive conditions in the test were those associated with coated stirrups lying in the plane of transverse cracks. Corrosion progression and coating debonding were extensive. It is believed that exposure to excessive amounts of chlorides for extended periods and macrocell formation on the stirrups eventually led to corrosion initiation and breakdown of coating.

12.3.5 Effects of Chloride Concentrations. Satake *et al.*[51] suggested that when a crack is produced in a concrete element, the amounts of water, air, and other corrosive elements going into the element are proportional to the width of the crack. The progress of

corrosion was related to wide cracks in the order of 0.15 to 0.5 mm (0.06 to 0.02 in.). In the beam exposure study, the difference in chloride concentration at crack locations between unloaded and loaded beams was not significant at the end of about 400 days of exposure. In both cases, however, the chloride content was more than an order of magnitude higher than the level usually associated with corrosion initiation of uncoated bars.

At crack locations within the exposure area, chloride concentration at the upper longitudinal bar level was slightly higher than that at the lower bar level. The short chloride path between the top concrete surface exposed to salt solution and the upper bar may be one contributing factor. Another factor may be attributed to clogging at deeper levels of the crack with concrete debris washed away by solution during wetting.

However, chloride concentrations determined at uncracked locations within the exposure area were opposite to those described above. It is possible that chlorides were accumulating at the lower bar level by capillary action as the chloride solution was running along the bottom concrete surface before dripping down into the draining system.

Uneven chloride distribution along the coated bar was probably the most significant factor affecting the development of corrosion cells. For longitudinal bars, it was clear that chloride concentrations were substantially different between cracked and uncracked locations and where cracks interrupted the paths as described in the previous section. Similarly, different chloride concentrations were noted between the top and the lower part of the stirrup, and between the front part (within the exposure area in the tension zone) and back part (in the compression zone). These uneven distributions of chloride ions were expected to cause potential differences between the various parts of reinforcement.

12.4 Condition of Reinforcing Steel

12.4.1 Apparent Surface Corrosion. Forensic examination of bar specimens, in general, agreed with the analysis of half-cell potential measurements. No corrosion was observed where potentials were less negative than -100 or -200 mV SCE, whereas corrosion

of variable intensity was found on bars with potentials consistently more negative than -300 mV SCE.

Based on visible surface corrosion of steel, coated bars and stirrups exhibited more corrosion in cracked beams than uncracked beams. The effects of cracks on corrosion spreading along longitudinal bars was generally limited to 40-60 mm (about 1.5-2.5 in.) on either side of the crack. For stirrups, the worst corrosion damage occurred closest to the crack. For illustration, Fig. 12.4 shows traces of two legs of a stirrup in a cracked beam; the stained trace was closer to the crack parallel to the stirrup leg. These findings suggest that performance of coated bars may be affected significantly by concrete cracking in a severely corrosive environment.

Figure 12.4 Stirrup Trace in Concrete Adjacent to Crack.

In general, corrosion was not much different on bars and stirrups in beams with opened and unopened cracks. In some cases, there was a slight tendency for bars and

stirrups in beams with opened cracks to exhibit more corrosion. Thus, whether cracks were wide or narrow had less impact on corrosion performance than whether concrete was cracked or not. It is possible that wider cracks could lead to worse corrosion than narrow cracks; however, even narrow cracks could cause significant corrosion and coating debonding. Rostam[60] recently indicated that after depassivation, crack widths practically do not influence the corrosion rate.

Significant pitting was only observed on damaged longitudinal bars in beams with opened cracks. However, corrosion severity on these coated bars was still less than that observed on uncoated bars recovered from cracked beams. Figure 12.5 shows a close up of one pit that formed on an exposed area of a coated bar at a crack location, and an example of surface degradation of an uncoated bar at another crack location. Hence, coated bars, even with heavy damage, had improved performance relative to uncoated bars.

Generally, the coating of stirrups tended to break down along the longitudinal rib as observed on a number of corroded stirrups. A typical crack in the coating extending along a stirrup leg is shown in Fig. 12.6. The weakness of coating on that bar feature was discussed earlier in Chapters 3 and 8.

The undamaged epoxy-coated bars and stirrups in uncracked beams retained their original appearance with negligible or no corrosion or blistering despite the high chloride content. For these bars, there was no or very limited loss in coating adhesion to substrate steel. These results indicate that originally intact epoxy coating can provide adequate protection to reinforcing steel from chloride-induced corrosion. However, the results were valid for bars embedded in uncracked concrete exposed to chloride concentrations of about 5-6 kg/m^3 (about 8.5-10 lb./yd^3) after one year of testing.

Corrosion was apparent on repaired areas indicating that patching was not effective. Similar findings were noted in the macrocell study and strongly indicate that current materials and techniques for patching require more thorough evaluation.

(a) Pitting on Damaged Longitudinal Bar (B11-Upper)

(b) Pitting on Uncoated Bar (B26)

Figure 12.5 Pitting Corrosion on Coated and Uncoated Bars in Beams with Opened Cracks.

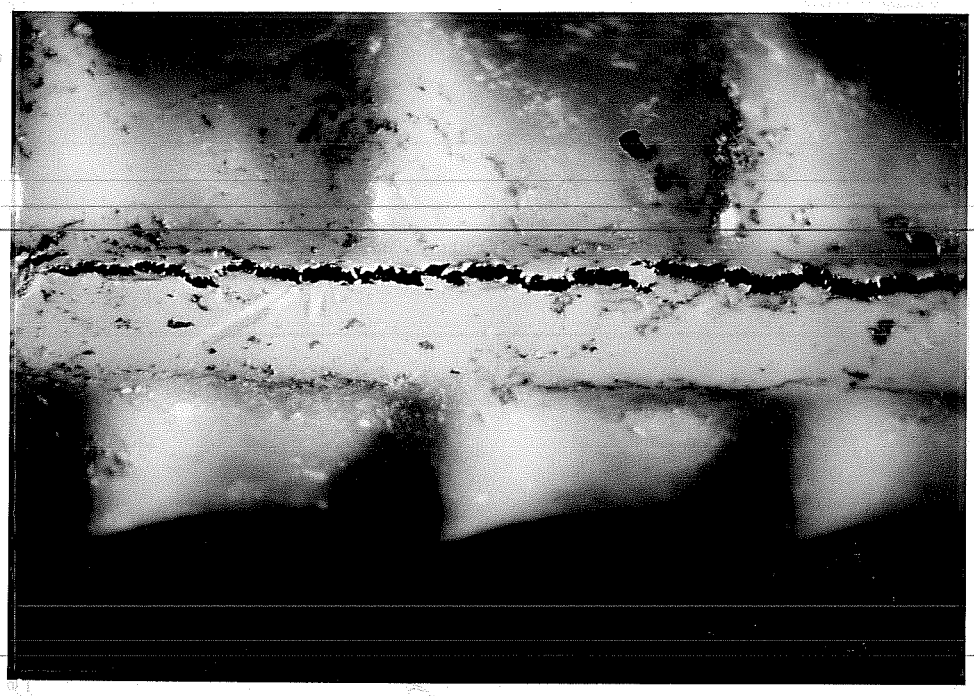

Figure 12.6 Cracking of Coating Along Stirrup Leg.

12.4.2 Coating Adhesion to Steel. The severe corrosion testing conditions for both coated bars and stirrups resulted in significant loss of coating adhesion to steel. Coating debonding occurred around all corroded sites and damaged spots even those remote from the exposure area. The extent of debonding around the damaged spots was larger in cracked beams than uncracked beams. Loss of adhesion associated with bright steel substrate around damaged spots indicated conditions of cathodic debonding. The increased area of debonding with cracking further signified this type of debonding because oxygen had greater access to steel through the cracks.

As expected, coating debonding around corroded sites was more apparent on the bar side facing the concrete surface on the short side of beam. This type of debonding associated with underfilm corrosion indicated conditions of anodic debonding. Hence, both anodic and cathodic conditions prevailed along the damaged longitudinal bars.

The straight portions of stirrups initially had stronger coating adhesion than the bent portions. However, all portions exhibited significant debonding after one year of exposure, particularly in cracked beams. The underlying steel sometimes remained bright, sometimes darkened, and sometimes corroded. These observations again indicate mixed conditions of anodic and cathodic debonding.

Figure 12.7 shows the average amounts of debonding on longitudinal bars and stirrups with different damage levels and under various loading conditions. Coating debonding on longitudinal bars increased when beams were cracked and coating was significantly damaged prior to testing. The results were not much different between cracked unloaded and cracked loaded beams. Coating debonding on stirrups, however, increased significantly when beams were cracked, and more so when the beams were loaded. Stirrups with as received and as received-patched conditions had almost the same amount of debonding indicating that patching was ineffective. Interestingly, there was no substantial difference between debonding on the as received stirrup and that with 3% patched damage in cracked loaded beams. The results indicated the vulnerability of stirrups to significant debonding under service conditions similar to those incorporated in the beam test.

Among the major factors affecting the effectiveness of patching are the thickness of patching material and surface anchor pattern. The thickness of a chipped piece of patch material from a bar cut end was measured and found to be only 75-100 μm (3-4 mils) thick which is approximately one-third of the required fusion-bonded coating thickness. Cut ends of bars are usually not prepared for patching; the steel surface is not roughened to provide an anchor profile. As a result, coating adhesion at cut areas remains weaker than that at bar surface. Figure 12.8 demonstrates the difference in appearance of the backsides of two chipped pieces of coating: one from electrostatically sprayed coating; and the other from brushed patching compound.

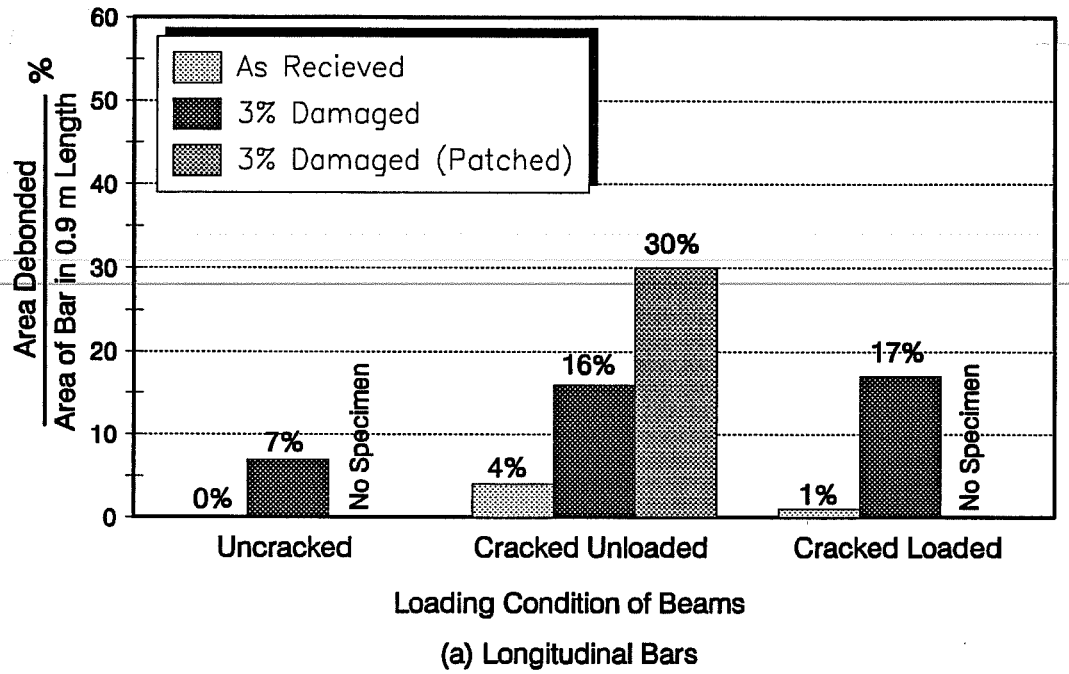

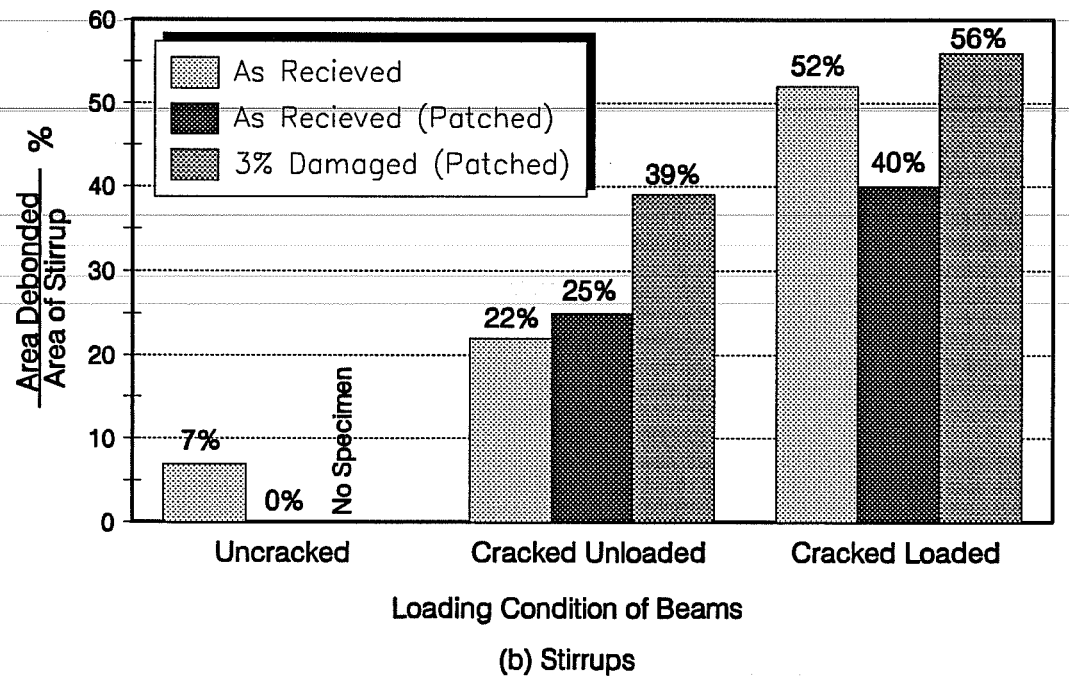

Figure 12.7 Variation of Debonded Area with Bar Damage Level and Loading Condition.

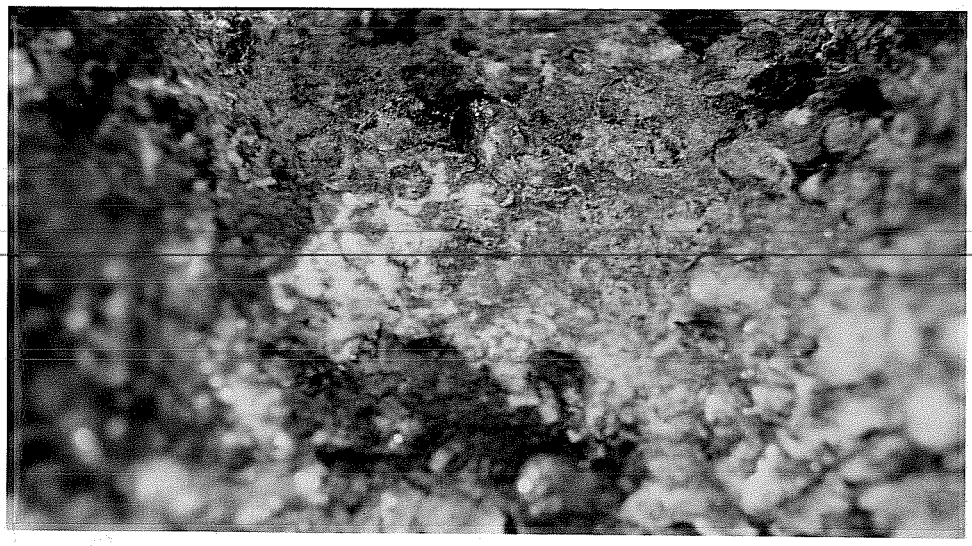

(a) Fusion-Bonded Epoxy Coating

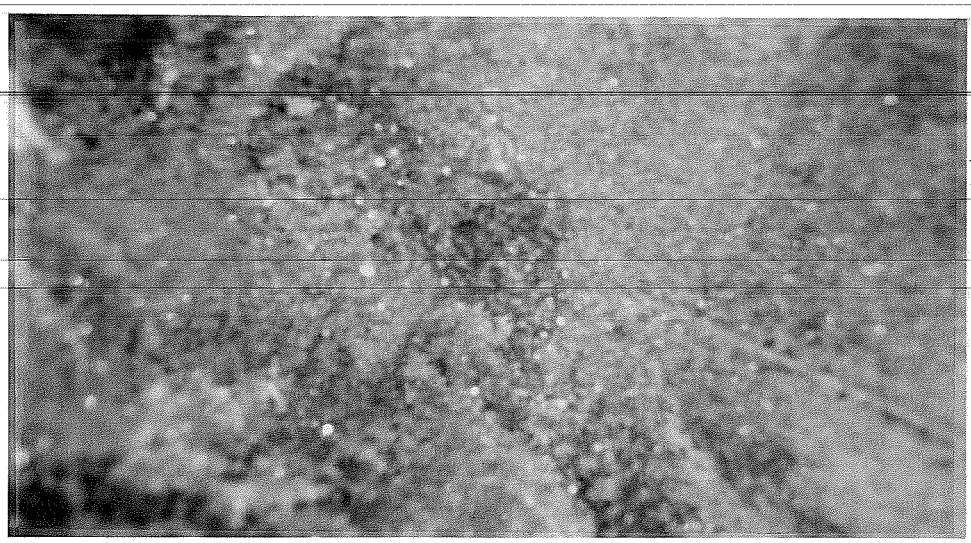

(b) Patching Coating

Figure 12.8 Roughness on Contact Surface of Coating.

12.4.3 Undercutting. Underfilm corrosion was similar in many aspects to that described for macrocell test in Section 10.4.3. For longitudinal bars, after the first year of testing, undercutting was confined to some mill marks and exposed steel areas in uncracked beams. Undercutting increased slightly in cracked beams and spread around the crack locations and areas of no previous damage. The largest pits found in the immediate vicinity of opened cracks were covered with black and brown corrosion products.

The steel substrate away from exposure area was, generally, dull or slightly dark around damaged areas and bright a little further away. These darkened areas could have resulted from some activity that took place immediately after damage was introduced and the steel was exposed to the atmosphere, or upon contact with pore solution when concrete was fresh, or because of cathodic reactions.

For stirrups, undercutting increased noticeably in cracked beams and mostly covered the bends and hook ends. Corrosion spread widely under the film although the coating material itself appeared unaffected over most of the corroded surfaces. This observation was consistent with findings reported in a previous research.[83] The severity of undercutting on stirrups relative to straight bars may be attributed to several factors some of which will be discussed later. These factors are:

- Coating weakness due to fabrication.
- Lesser coating thickness and smaller concrete cover compared to longitudinal bars.
- Exposure to high concentrations of chlorides and oxygen in the same crack plane.
- Crevice effects at points of contact with other bars.
- Intensive macrocell action along stirrup and between stirrup and other bars.

The tendency of coated transverse stirrups or hoops to exhibit widespread corrosion was also observed in field studies. During autopsy of a test pile in Oregon, small corrosion areas were found on only two of the longitudinal bars but on several of the hoop bars.[30]

Figure 12.9 shows the variation of undercutting with bar damage level and loading condition for both longitudinal bars and stirrups. Comparing the results in this figure with those in Fig. 12.8, it was clear that larger crack widths lead to larger debonded areas as a result of greater cathodic activity and not necessarily greater corroded surfaces. In other words, cracks permitted excessive amounts of oxygen to reach the steel surface and to support the cathodic reactions thus resulting in larger debonded areas. Cycling the imposed loads, particularly during drying periods, may then be viewed as an oxygen *pump* that promoted corrosion activity. This observation explains why severe pitting occurred on bars with relatively a high proportion of debonded area to corroded area.

12.4.4 Black Corrosion Products. Thin black sometimes greenish-black corrosion products similar to those described in the macrocell study were formed on the steel surfaces. As mentioned earlier, the black product is indicative of corrosion in a restricted oxygen environment of crevices that form under the coating. However, in cracked beams, oxygen availability in the vicinity of cracks resulted in further oxidation of the corrosion compounds to red rust. Hence, steel surfaces beneath the coating corroded to various levels of oxidation. The relatively short period of exposure (400 days), in addition to the thick concrete cover of 50 mm (2 in.), were the main reasons for delayed staining of concrete surfaces.

12.4.5 Coating Blistering. Blisters spread on the coating surface as previously noted on macrocell bar specimens. Pits associated with blister formation were generally very slight and shallow and were covered with black and brown brittle corrosion products. Blisters formed mainly on the lower half of the bar surface facing concrete cover. As expected, blisters were located at voids in the concrete interface at the underside of the bars.

12.5 Concrete Consolidation Around Reinforcing Bars

12.5.1 General. Observations confirmed that the condition of the concrete in the region surrounding the coated bar played a significant role in the corrosion process. Differences in concrete consolidation above and below the coated bars affected corrosion cell development and the tendency of one side of the bar to degrade more than the other. The

following discussion was based on the main observation that rust spotting and blistering were concentrated on the bar side facing the concrete cover, *i.e.* the bottom side of the bar in the casting position.

12.5.2 Differences in Concrete Consolidation. Referring to the discussion presented in Section 10.5.2, small gaps and air pockets may form under the coated bar during concrete consolidation. By contrast, a smooth and continuous interface layer may form on top of the bar. Such variation in the concrete density was more noticeable for longitudinal bars than for stirrups. Figure 12.10 shows two cross-sections of a beam specimen in the casting position to demonstrate the variation in concrete quality at different regions.

12.5.3 Influence of Concrete Consolidation on Corrosion. Variation in the concrete density surrounding the reinforcing bar creates concentration cells which, in turn, produce differences in potential and lead to macrocell action. Non-uniform chloride concentrations around the bar were probably the most significant contributor to corrosion initiation and acceleration in the beam test. Differences in chloride concentration at the top and bottom of the bar result from variations in chloride penetration as illustrated in Fig. 12.11. In addition, the amount of chloride ions that can accumulate in the zone immediately above the bar may be limited by concrete density. However, the less dense zone beneath the bar can retain more chlorides.

Large macrocell corrosion currents can be produced by the formation of chloride concentration cells. The anodic site is usually associated with the location of higher chloride concentration. One example is that reported in a corrosion test of prestressed pile segments where a single strand was exposed to excessive chlorides through a crack and became anodic with respect to the reinforcement away from the contaminated area.[128]

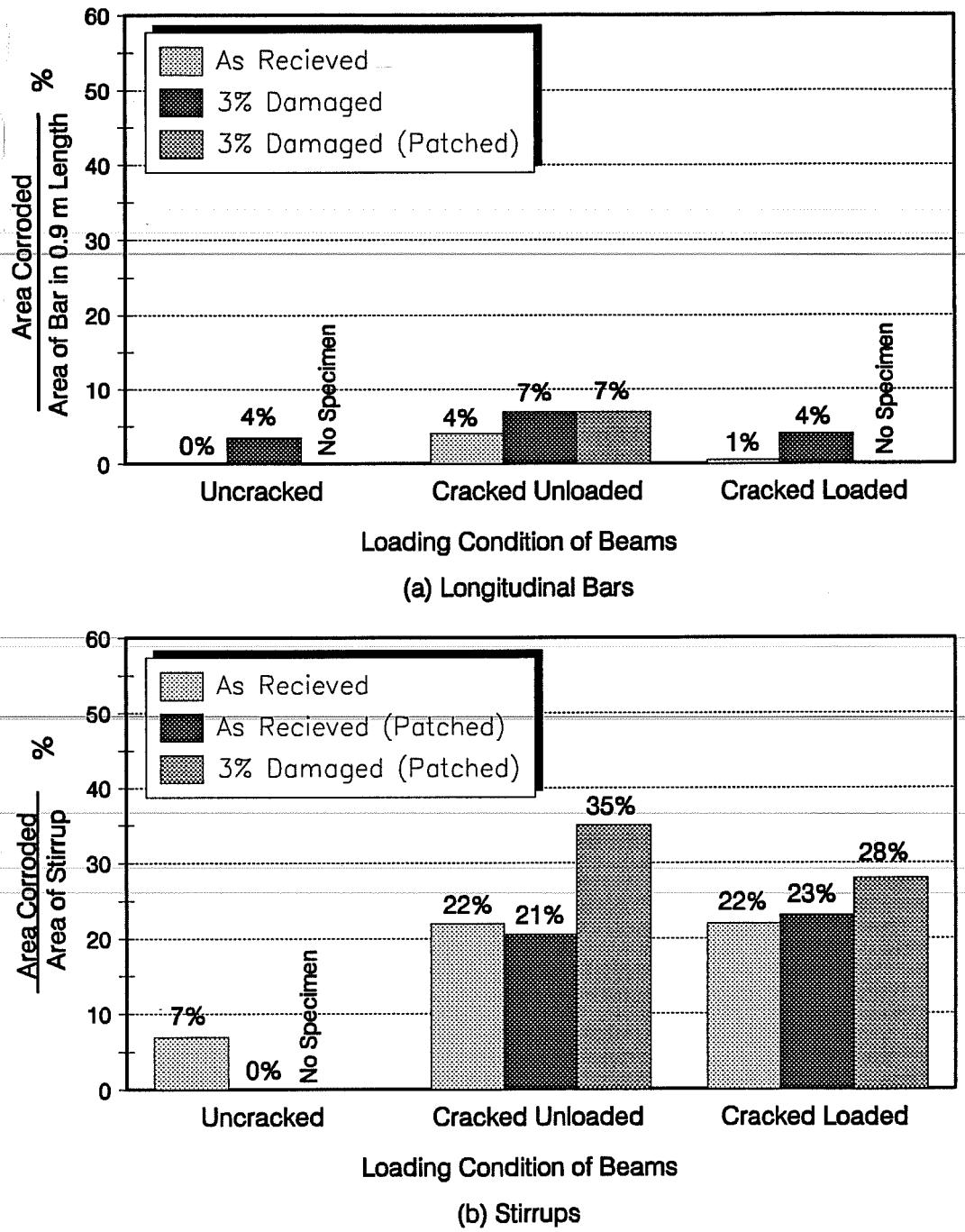

Figure 12.9 Variation of Corroded Area with Bar Damage Level and Loading Condition.

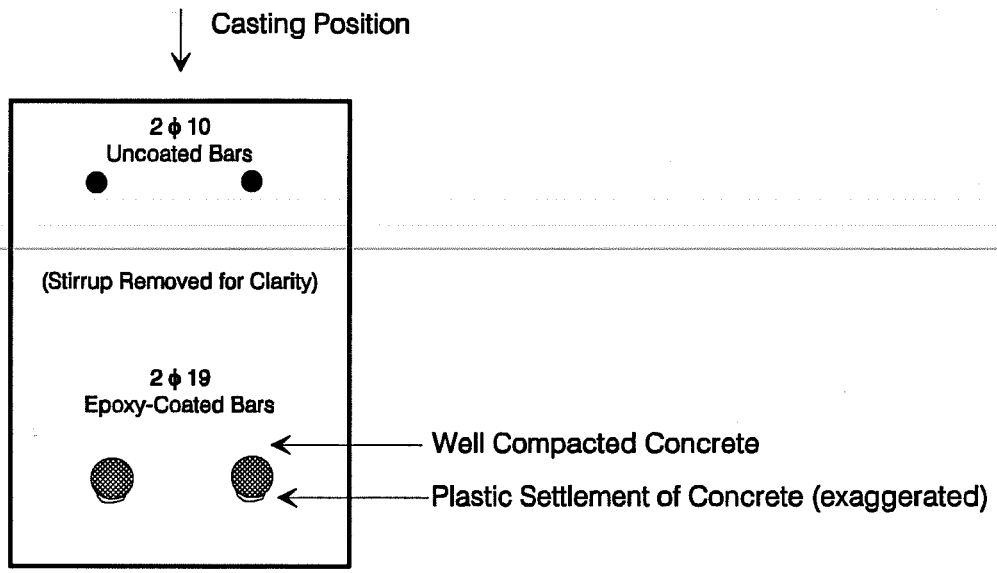

(a) Cross-Section of Beam Showing Longitudinal Bars

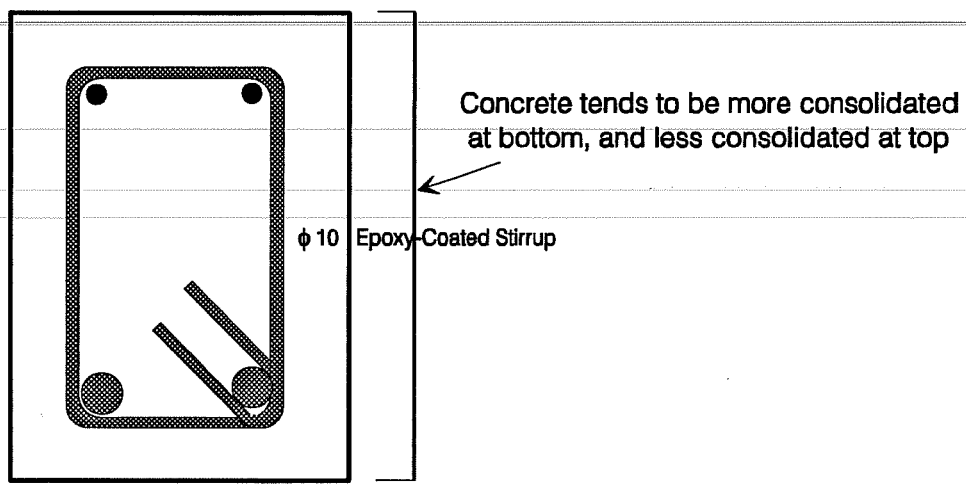

(b) Cross-Section of Beam Showing All Details

Figure 12.10 Variation of Concrete Quality in Beam Cross-Section.

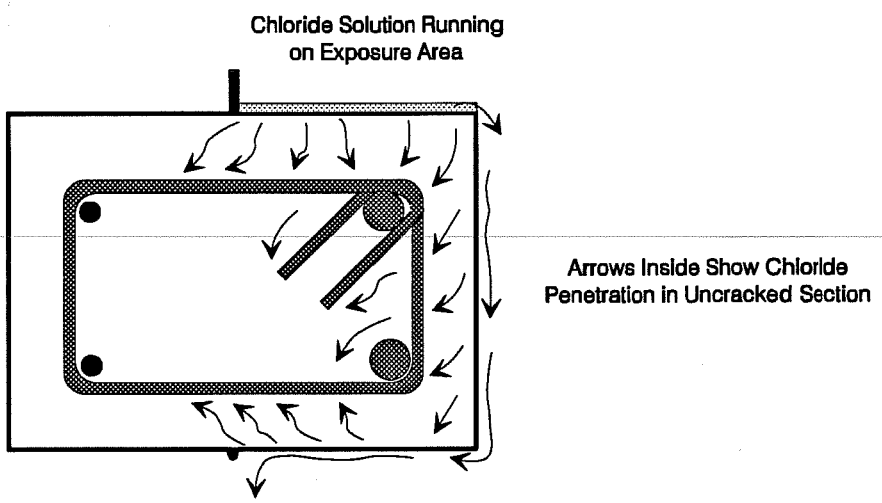

Figure 12.11 Chloride Penetration in Uncracked Beam Cross-Section.

In the beam test, voids at the interface between the concrete and the lower side of the bar in the casting position allowed large amounts of salt water to accumulate and nucleate anodes. The chloride solution served as a strong electrolyte through which ions were transported and corrosion was accelerated. The rate of corrosion was controlled by chloride differential concentration, distance between anodic and cathodic sites, moisture and temperature variations, and concrete resistivity. Buslov[25] estimated that the corrosion rate of a 25 mm (1 in.) diameter bar with 25 mm (1 in.) cover is 6 times faster at the front nearest to the surface (where chlorides concentrated) than at the rear surface.

Corrosion of stirrups was probably influenced by variation in concrete consolidation between the bottom and top sides of the beam. The less dense concrete at the top encouraged chloride diffusion towards the back side of the stirrup away from the exposure area. Cracks in concrete also accelerated chloride migration to those parts of the stirrup not directly under the influence of the exposure area. As a result, corrosion was initiated, sometimes exclusively, at the back side of the stirrup in the vicinity of the contact points with the uncoated bars.

12.6 Corrosion Mechanism

12.6.1 General. The following sections will describe a hypothesis of the corrosion process observed on the bars in the beam exposure test. The scenario of the hypothesis reconstructs the most likely sequence of steps that lead to the observed behavior. There are similarities and differences between this hypothesis and that presented in Section 10.8.3. The beam exposure test added valuable information regarding the performance of coated bars in corrosive environments.

12.6.2 Corrosion Performance of Longitudinal Coated Bars. The midspan region of the beam was subjected to periodic wetting by a salt solution, while those regions near beam ends were continuously dry. Thus, a moisture gradient was created within the beam and the longitudinal bars extended through these different regions. During wetting, the salt solution ran across the top, side, and bottom surfaces, and the chloride ions penetrated through the concrete either by gravity or by capillary action. Cracks facilitated moisture and chloride migration.

During drying, water evaporated from the middle region causing a greater diffusion and accumulation of dissolved chlorides in the concrete pores. The resulting moisture gradient also promoted oxygen transportation to the reinforcing steel surface. The less the concrete pore network was filled with water, the greater the oxygen diffusion. Again, cracks provided direct paths for oxygen; load cycling further *pumped* oxygen along steel surface.

Chloride ions reached the coated bar surface in variable amounts due to the heterogeneous distribution of chlorides and variation of concrete consolidation around the bar. If the steel was exposed where chlorides contacted the bar surface (at holidays or pinholes in the patching material, or at damaged areas), the potential of the steel immediately shifted to more negative values from below -100 mV SCE to more negative than -300 mV SCE. The shift in potential could have different magnitudes and might cause instability of the potential for some time. Potentials fluctuated when holiday emergence commenced and corrosion on the substrate was initiated. Potential drop in cracked beams was almost

instantaneous at first contamination with chlorides. At crack locations, the availability of large amounts of chlorides and oxygen at the bar surface accelerated the onset of corrosion and, thus, reduced potential fluctuation.

Larger amounts of chlorides accumulated in the less dense zone immediately below the bar than in the dense zone above it. The hygroscopic property of salt caused moisture to be retained at the bar surface for an extended time between drying periods. As a result, a strong electrolyte was formed and corrosion microcells were nucleated at the lower half of the bar facing the concrete surface. Corrosion was then accelerated at these sites by several macrocell developments as explained below.

A concentration cell was developed between the two sides of the bar characterized by different chloride concentrations in different concrete mediums. A second concentration cell was developed along the bar in the midspan zone characterized by different chloride concentrations between cracked and uncracked areas. A third strong macrocell was developed along the bar in the midspan region and adjacent regions which were characterized by different ion content and moisture that produced a measurable potential difference. Erlin and Hime[77] emphasized that corrosion occurs due to concentration cells established in wet and dry concrete through which the steel is continuous. Macrocell development at significant interaction distances is possible when concrete resistivity is low.[42] For most of the time, temperature and humidity in the test room were relatively high which may have reduced concrete resistivity.

In effect, anodic activity on the steel was enhanced in the midspan region, particularly along the lower side of the bar. Metal dissociation and pitting were greatest at the exposed steel areas at or near cracks (see Fig. 12.12), at stirrup locations because of crevice effect, and where voids had formed in the concrete. The coating was originally well adhered around the exposed steel areas so corrosion was initially localized before spreading underneath the epoxy film. Figure 12.13 shows a schematic diagram of macrocell corrosion activity on a damaged coated bar with chloride concentration cells and moisture gradient.

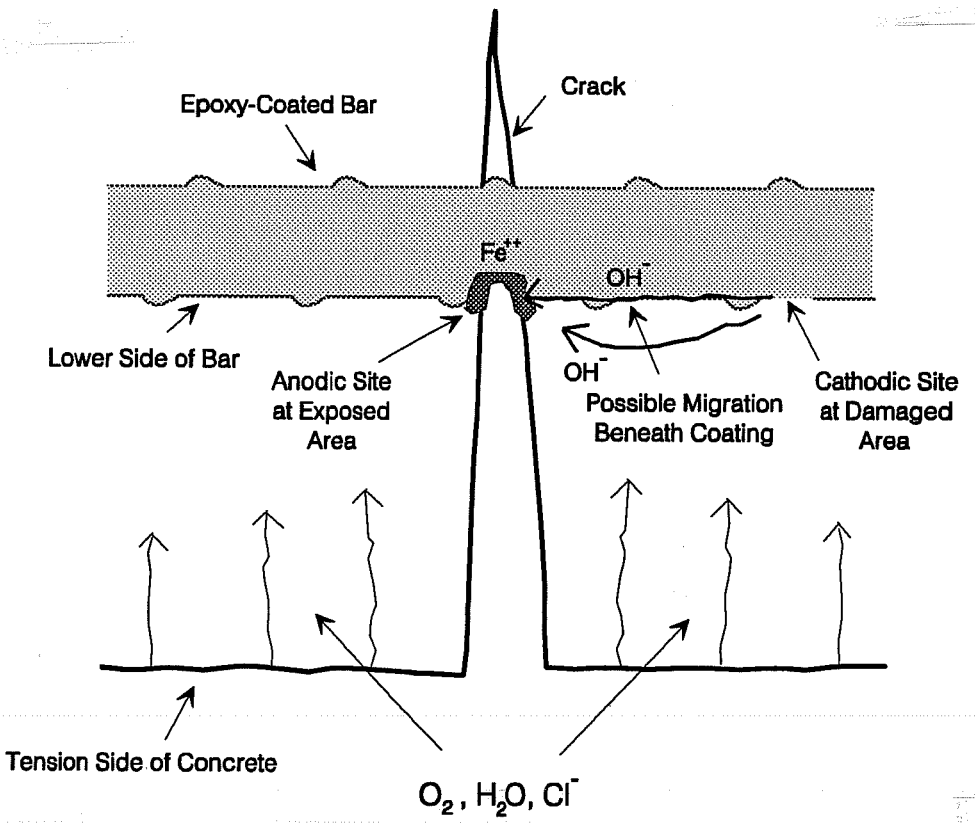

Figure 12.12 Pitting Corrosion on Coated Bar At Crack Location.

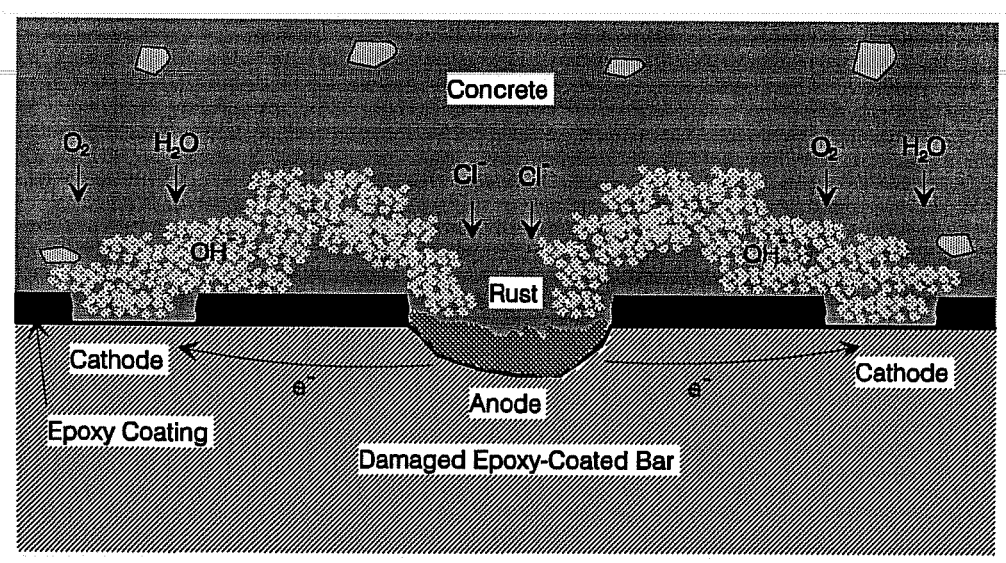

Figure 12.13 Mechanism of Corrosion on Longitudinal Coated Bar.

Oxygen reduction took place preferentially at the exposed steel areas on the top side of the bar, on areas remote from the midspan region, and under the coating where cathodic debonding occurred. The corrosion process was most likely under cathodic control in uncracked beams due to limited oxygen diffusion. In cracked beams, mixed anodic and cathodic control regimes prevailed. Undercutting progressed under mainly stable potentials in the high negative range. Potential differences between predominantly anodic and predominantly cathodic sites were more than 150 to 200 mV in order to sustain corrosion activity.

The electrode kinetics for a corrosion cell are represented in Fig. 12.14. The graph shows how corrosion potential became more negative and corrosion current increases where chloride concentration and oxygen availability are increased. For macrocells, however, the resistance of the electrolyte affects corrosion current as illustrated in Fig. 12.15. The resistance of the electrolyte caused a drop in potential in the corrosion process in the beams (see Fig. 12.16).

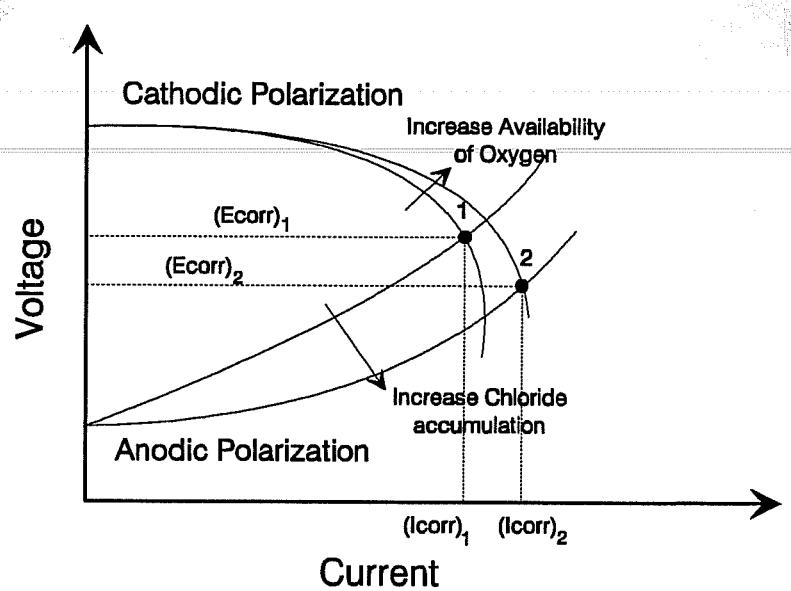

Figure 12.14 Electrode Kinetics for Corrosion Cell.

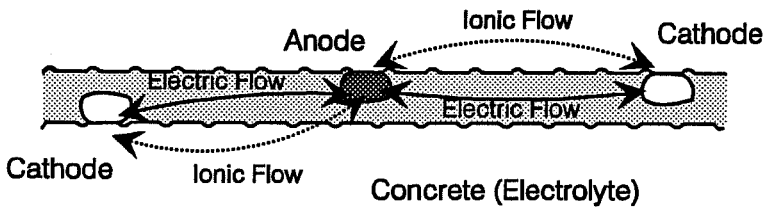

(a) Macro-corrosion Cell

Ra = Resistance of Anode
Rc = Resistance of Cathode
Re = Resistance of electrolyte

Va,c = Voltage Difference Between Anode and Cathode

Icorr = Corrosion Current

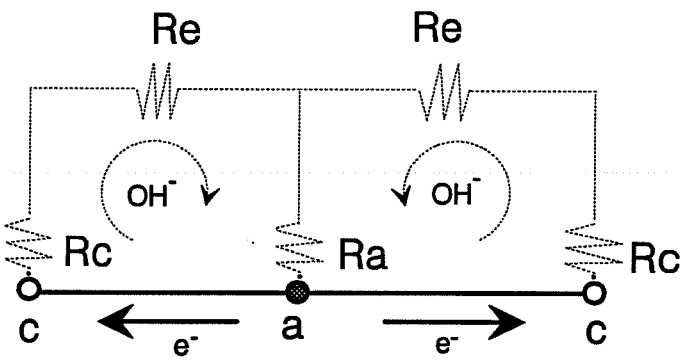

$$Icorr = Va,c / (Ra + Re + Rc)$$

(b) Equivalent Electrical Circuit

Figure 12.15 Macro-Corrosion Cell Representation on Longitudinal Bar.

Corrosion morphology was very similar to that described earlier in the macrocell study. Corrosion products formed in small quantities without large increase in volume. Underfilm corrosion caused minor surface degradation. Under repeated wetting periods, the debonded coating retained an aqueous solution which became acidic. As received bars performed better than those heavily damaged which, again, emphasized the fact that a better initial product results in better corrosion resistance.

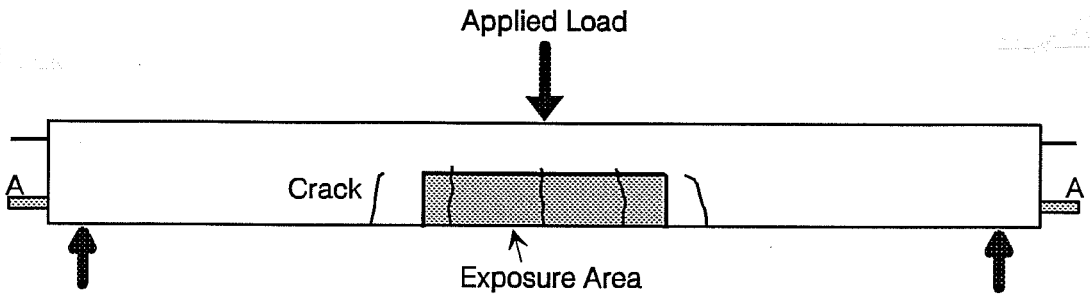

(a) Beam Plan

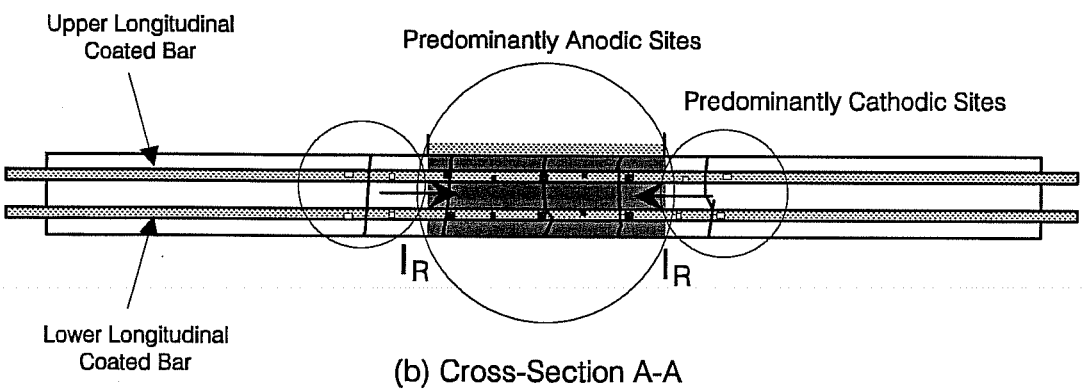

(b) Cross-Section A-A

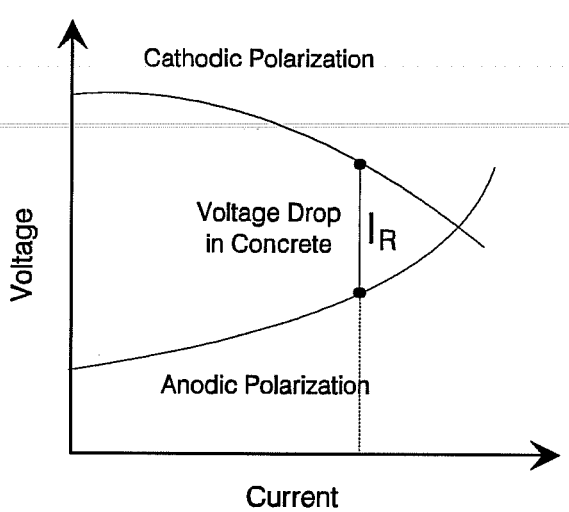

(c) Electrode Kinetics

Figure 12.16 Macrocell Development in Beam Specimen.

12.6.3 Corrosion Performance of Coated Stirrups. Due to the cyclic exposure to salt solution in the beam midspan, the concrete medium around stirrups was always moist. In uncracked beams, chloride ions reached the upper leg of the stirrup primarily by gravity and the lower leg by capillary action. In cracked beams, large amounts of chlorides, oxygen, and moisture surrounded the stirrups. Load cycling further increased the amounts of corrosive substances at the stirrup level.

Chloride ion distribution around the stirrup was non-uniform due to both variations in concrete consolidation and chloride transport mechanisms. As a result, a concentration cell was developed between the parts of the stirrup in different concrete mediums. During the investigation of corrosion of coated bars in Florida bridge substructures, it was stated that enough environmental heterogeneity along the perimeter of the hoop bars can create efficient macrocells.[42] The potential of the steel shifted to more negative values in similar conditions described above for longitudinal bars. Again, the potential drop in cracked beams was almost instantaneous at first contamination with chlorides. Corrosion initiated at holidays and breaks in coating and in patches at bends and hook ends. Corrosion was accelerated most at these sites by a major macrocell development which is explained below.

Electrical continuity between the stirrup and uncoated bars was present through damage at contact points. Damage on the inside of the bend of stirrup was introduced either during fabrication (in the form of mashed spots) or by cutting through the coating during cage assembly. An example of the later is shown in Fig. 12.17. Sometimes, the protected tie wire was stripped under the action of twisting causing the metal to be uncovered. Another possible source of continuity could be overlapping semiconducting corrosion products accumulating in the neighborhood of the contact points (see Fig. 12.18).

A strong macrocell action was developed between the stirrup in a highly contaminated region and uncoated bars stretching along uncontaminated concrete. In many cases, cracks facilitated the ingress of chlorides and oxygen to the contact points and promoted corrosion initiation. The uncoated bars, for the most part, were cathodic with respect to the stirrup and corrosion activity occurred near the contact points because of the distance effect (anodes tend

to locate closest to cathodes). Figure 12.19 demonstrates the macrocell formation for stirrups in cracked beams. Due to availability of a large cathode in the form of the intersecting longitudinal bar, corrosion on stirrups was extensive and anodically controlled.

Figure 12.17 Damage of Coating of Stirrup at Contact with Uncoated Bar.

Figure 12.18 Corrosion at Location of Contact of Coated Stirrup and Uncoated Bar.

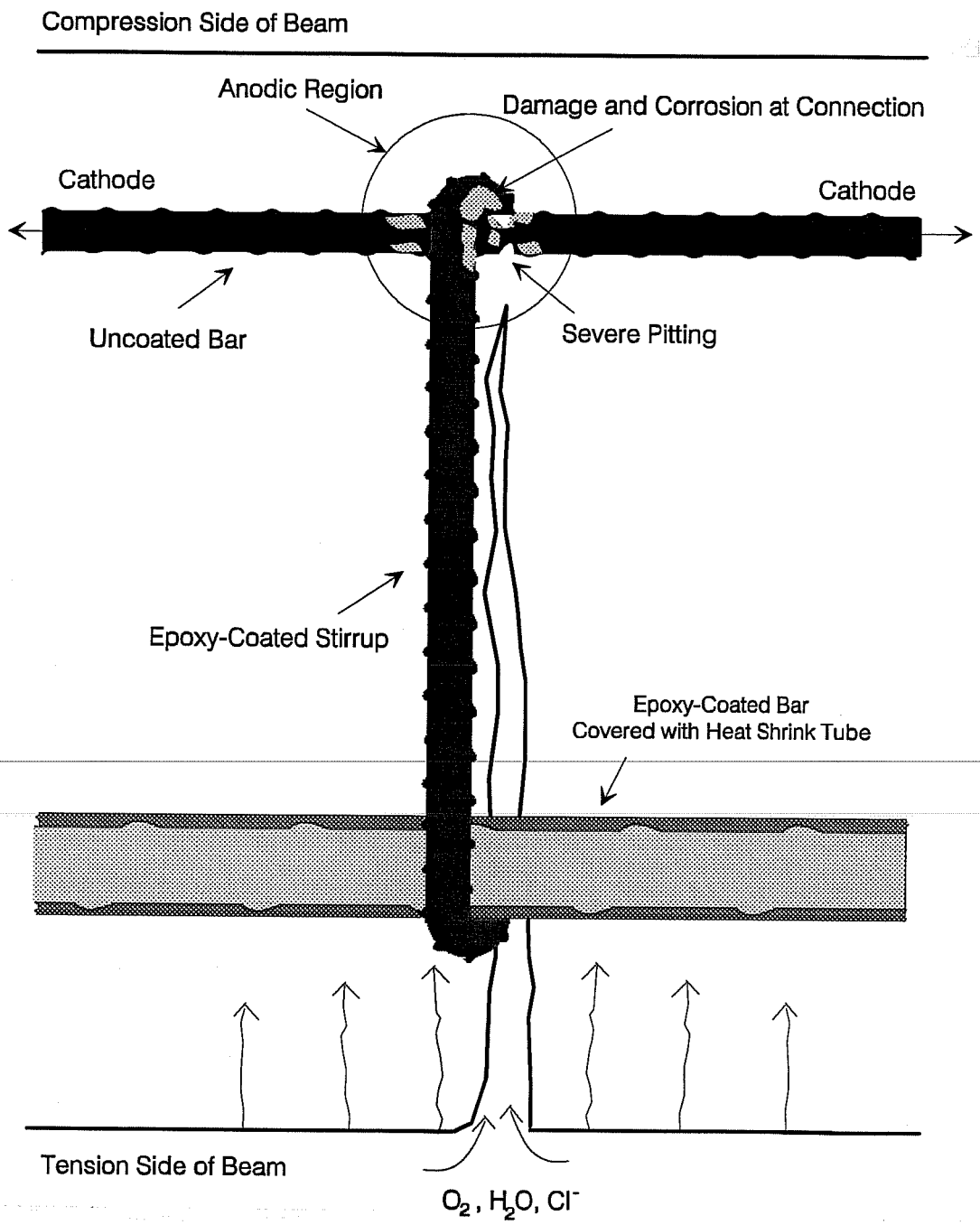

Figure 12.19 Mechanism of Corrosion of Coated Stirrup.

12.6.4 Macrocell Corrosion of Uncoated Bars. Corrosion of uncoated bars located in the compression zone in the cracked beams was due to salt and alkaline concentration macrocell formations. The bar at a crack location was exposed, whereas adjacent surfaces embedded in the concrete were in a highly alkaline environment. Corrosion initiation on the exposed part of bar was accelerated by chloride penetration. The differential alkaline and salt concentrations generated a potential difference between the exposed part and adjacent parts. As a result, galvanic corrosion currents flowed between the small anode and large cathode. Although corrosion spread from the active area at the crack, intensive macrocell action was sufficient to cause severe localized metal consumption in a very small portion.

12.7 Summary and Conclusions

12.7.1 Summary. To study the performance of epoxy-coated bars used as main longitudinal reinforcement or transverse hoops or ties in structural members, a beam exposure experimental program was conducted. The coated bars were tested in separate or mixed arrangements of straight bars, stirrups, and splices. The coating condition was varied to study effects of damage and patching on corrosion performance. Some beams were uncracked while others were cracked and either unloaded or kept under load to maintain the cracks at a maximum allowable crack width. The middle portions of beams were subjected to a chloride solution in a cyclic wet and dry regime. Loads were cycled on the cracked beams during wetting and drying. Half-cell potentials and crack widths were measured through one year of exposure. Selected beams were opened to visually examine the actual bar condition. The main conclusions of this study pertaining to straight bars, stirrups, and cut bar ends are given in the following sections.

12.7.2 Onset of Corrosion. Corrosion of epoxy-coated steel in concrete started much earlier in cracked members than in uncracked members. The impact of crack width on corrosion initiation and later progression was not significant. Corrosion initiation on damaged bars was faster than on those as received. Coated bars tended to resist corrosion at chloride concentration levels exceeding levels normally associated with the onset of corrosion of uncoated steel.

12.7.3 Measuring Half-Cell Potentials. Systematic periodical measurement of half-cell potentials was valuable in predicting the corrosion state of embedded epoxy-coated bars. It was necessary to monitor potentials over a sufficient time to avoid misinterpretations of the results. Measuring potentials on a short-term basis could be misleading. Both the potential value and the changes in potential were important for establishing corrosion initiation. Corrosion was negligible when potentials remained below -400 mV SCE without significant potential gradients along the monitored bar. Pitting corrosion was always associated with potentials in the range of -400 to -600 mV SCE and steep potential gradients in excess of 200 mV. There was no correlation between corrosion spreading (undercutting) and potential readings.

Potentials measured on cracked and uncracked surfaces that had similar exposure conditions were often significantly different. A shift in potential towards more negative values occurred as chlorides reached the bar surface and initiated corrosion in damaged areas.

12.7.4 Effectiveness of Epoxy-Coated Steel. Severity of corrosion on epoxy-coated bars was related to both coating damage level and loading condition. As received bars and stirrups in uncracked members performed well, whereas those with damaged coating in cracked beams showed the worst performance. In a heterogeneous environment, bars and stirrups with excessive damage (many large exposed steel areas), even if patched, were susceptible to macrocell formation. Damage to the coating during fabrication and tying of stirrups to uncoated bars also lead to severe macrocell action. The findings discourage mixing coated and uncoated bars in proximity or in contact.

Patching of damaged coating reduced the severity of corrosion, but did not provide full protection to the bare areas. Both anodic undercutting and cathodic debonding occurred beneath the undamaged coating and patched damage. Patching bar cut ends was ineffective because of the small thickness of patching and lack of surface anchor profile.

Despite the presence of cracks, no staining of the concrete surface was observed. The amount of rust produced on coated steel was small enough to disperse in the concrete

pores. However, coating damage and concrete cracking encouraged significant localized pitting on longitudinal bars. In addition, coating adhesion on stirrups tended to breakdown causing widespread underfilm anodic and cathodic activity. To improve the long-term performance of coated bars and stirrups, damage to coating needs to be reduced, patching requirements need to be modified, quality of coating adhesion to substrate needs to be improved, and treatment of cracked concrete surfaces needs to be considered.

12.7.5 Effects of Concrete Environment. The quality of concrete at the bar interface affected the location where corrosion initiated and progressed. Longitudinal coated bars consistently showed high propensity for corrosion initiation and spreading along the lower side of bar. Rusting of coated stirrups was frequently limited to portions of the stirrup in the less dense concrete. There was a tendency for the epoxy coating to develop blisters and to breakdown at voids in contact with bar surface.

12.7.6 Corrosion Mechanism. In uncracked sections, corrosion commenced at breaks in the coating and exposed steel areas in contact with sufficient amounts of chlorides. In cracked sections, corrosion started at crack locations and spread to adjacent areas undercutting the epoxy coating. Differential chloride distributions and moisture gradients, coupled with damaged coating, generated large potential differences with strong macrocell action. Electrical contact with uncoated steel also caused macrocell formation. Oxygen availability, mostly due to cracking, aggravated corrosion severity. Anodic debonding, underfilm corrosion, and blister formation progressed in a similar manner to that described in the macrocell study.

CHAPTER 13
SUMMARY, CONCLUSIONS, AND RECOMMENDATIONS

13.1 Summary

The main objective of this study was to investigate the integrity and performance of epoxy-coated reinforcement in corrosive environments. An extensive literature review of chloride-induced corrosion and previous studies on durability of coated bars was conducted. The coating process and some inspection techniques for coating application were examined. Damage to coating due to concrete placement and vibration was evaluated experimentally. Finally, a three-part experimental program was established to study performance of coated bars in aggressive environments.

As a result of the literature review, areas of concern were identified about durability of coated reinforcement and major deficiencies in performance. By examining coating, fabrication, handling, transportation, storage, patching and installation procedures, procedures to reduce damage and improve performance were identified. The adequacy of holiday detectors and hot water immersion testing for quality control/quality assurance purposes was studied.

Coating damage during concreting operations was determined by casting a column base and two slab specimens. Coated bars of different sizes, deformation patterns, and spacings were placed at different levels to simulate a variety of steel arrangements. After consolidating concrete using a metal-head vibrator, bars were removed and inspected for damage.

To quickly examine the effectiveness of epoxy coating and patching in protecting underlying steel from corrosion, fabricated bars were periodically immersed in 3.5% NaCl solution. The bars were of different diameters and deformation patterns and were previously damaged to levels comparable with acceptable limits in current specifications. Evaluation of

performance was done visually and forensic examinations were conducted at 8, 18, and 24 months.

Companion fabricated bars were embedded in concrete prisms and linked to uncoated bars to set up macro-corrosion cells. Concrete was contaminated with chlorides by ponding salt water in a cyclic wet and dry regime. Corrosion currents flowing from coated steel to uncoated steel were monitored over a period of two years. The corrosion rate of coated bars was determined and compared to that of uncoated bars. Forensic examinations were conducted at one and two years to relate corrosion rate analysis to actual bar condition.

The performance of coated reinforcement under conditions which simulate a highly corrosive environment and under loading conditions producing concrete cracking was evaluated in a beam exposure test. Various arrangements of longitudinal bars, stirrups, and splices were considered. Coating condition was a variable to assess effects of damage and patching on performance. Some beams were uncracked while others were cracked and either unloaded or kept under load to maintain cracks at a specified maximum allowable crack width. Salt water flowed over the middle portions of beams for a specified length of time. Loads were cycled on the cracked beams during wetting and drying. The state of corrosion activity on steel was monitored by half-cell potential measurements. Beam condition and changes in crack width were observed during exposure. Forensic examinations were conducted after one year to relate corrosion state findings to actual bar condition.

13.2 Conclusions

13.2.1 General Conclusions. The principal conclusion from this study is that *epoxy-coated reinforcement in highly corrosive environments was susceptible to chloride-induced corrosion governed by level of coating damage and extent of debonding of the coating from the reinforcement, degree of concrete consolidation around bars, concrete cracking and macrocell formation.*

Damage to coating and weakening of coating adhesion to steel during fabrication, reduced resistance to corrosion. The larger and more frequent the damage was, the higher was the rate of corrosion. Corrosion activity caused extensive coating debonding and widespread undercutting on bent portions. Although patching of damage reduced the incidence and severity of corrosion, it did not prevent corrosion.

Variations in concrete consolidation around coated bars encouraged corrosion initiation and progression on bar surfaces facing voids in the concrete (normally the underside of the bar). The epoxy coating tended to develop blisters and to break down at air pockets facing bar surface.

Concrete cracking facilitated the ingress of chlorides and oxygen to the bar surface and accelerated the corrosion process. Crack width was not a dominant factor, although wider cracks seemed to aggravate conditions conducive to corrosion.

Performance of coated bars deteriorated progressively during macrocell development. Electrical continuity between coated and uncoated bars in different chloride environments, or exposure of damaged coated bars to chloride concentration cells, promoted macrocell corrosion. Anodic activity on coated bars resulted in metal dissociation and accumulation of corrosion products that breached the coating. Cathodic activity on coated bars resulted in coating debonding.

Corrosion of coated bars was observed more on the underside of the bar than on the topside. For upper bars in slab sections, corrosion would probably ensue without surface staining and the pressure generated due to accumulation of corrosion products below the bar might not result in cracking of the concrete cover. Corrosion of coated bars spread underneath the coating and was more distributed on the steel surface relative to uncoated bars. Concentration of corrosion on small parts of the uncoated bar resulted in severe pitting corrosion and early cracking of concrete. However, lack of oxygen beneath the coating to oxidize the corrosion products to higher oxidation levels suppressed surface damage manifestation.

Despite the susceptibility of coated bars to corrosion, the use of epoxy coating **improved** the performance of reinforcing steel in concrete exposed to aggressive chloride environments. The epoxy coating delayed initiation of corrosion and reduced the severity of bar surface degradation and metal loss. These findings imply that the extent of concrete surface cracking and rate of deterioration of the structure will be reduced.

13.2.2 Specific Conclusions.

Evaluation of Holiday Detectors. Holiday detectors cannot be considered as reliable devices to monitor coating defects. Satisfactory, repeatable responses from the holiday detector for the same test condition could not be achieved.

Evaluation of Hot Water Immersion Test. The hot water immersion test seems to objectively indicate the quality of coating application.

Evaluation of Damage to Coating Due to Concrete Vibration. Vibration equipment used during concrete placement may introduce considerable damage to epoxy coating. Some of the damage was so severe that it exceeded the limit at which repair is required before bars can be placed in forms. There was greater damage with larger size bars and with small clearances between bars and forms.

Salt Water Immersion Test. Even the smallest damage in the coating, such as hairline cracks and pinholes, will initiate corrosion in a severe environment. Long-term cyclic immersion of damaged coated bars in chloride solution resulted in deterioration of the protective qualities of coating. However, the performance of damaged coated bars was qualitatively much better than uncoated bars over two years of testing.

Bars with more complicated rib patterns had more coating defects and were more prone to development of corrosion. The sides of deformation lugs are difficult to coat uniformly and tend to have more coating defects. Quality of base steel, such as rib profile, seemed to significantly affect the corrosion performance of coated bars.

Small-size bars exhibited more hairline cracking in the coating when bent to a smaller radius than large-size bars. Tight bending radii cause more stretching of the coating that may result in damage.

Macrocell study. Corrosion of damaged coated bars in concrete was delayed and started at chloride concentrations around twice the levels associated with the onset of corrosion of uncoated bars.

Corrosion products associated with coated bars were at a low state of oxidation which was accompanied by a small change in volume that suppressed damage visible on the concrete surface. However, the performance of damaged coated bars seemed to be deteriorating with longer periods of exposure.

The limits on allowable damage to coating in current specifications are not strict enough. Damage close to 2% of bar surface area, or approximately 6 x 6 mm (1/4 x 1/4 in.) in size could jeopardize the long-term integrity of coated bars.

Coated bars with smaller diameters exhibited less corrosion than bars with larger diameters. Data on the relative performance of bars with parallel and cross deformations did not show a clear trend.

Epoxy coating was susceptible to debonding under the macrocell setup. Debonding did not correlate with the level of coating damage or extent of undercutting, nor was it a consistent indicator of poor performance.

Beam Exposure study. Corrosion of coated bars started much earlier in cracked members than in uncracked members. Corrosion initiation was detectable by systematic periodical measurement of half-cell potentials and changes thereto.

Corrosion was negligible when potentials remained below -400 mV SCE with potential gradients not exceeding 150 mV along the monitored bar. Pitting corrosion was

always associated with potentials in the range of -400 to -600 mV SCE with steep potential gradients in excess of 200 mV.

Macrocell activity on heavily damaged bars could be severe enough to cause significant localized pitting. Both anodic and cathodic reactions on coated bar surfaces caused coating debonding.

Damage to coating around 3% of bar surface area, even if patched, could reduce the long-term corrosion resistance. Exposure of patched damage to excessive amounts of chlorides near crack locations resulted in corrosion initiation and propagation.

13.3 Recommendations

13.3.1 Quality of Coating. To enhance protection to steel, the formulation of the epoxy coating, the technology used for coating application and curing, and the quality of surface preparation of steel before coating should be constantly improved. Coating imperfections and damage, as well as coating thickness variation, need to be effectively controlled. Only sound steel bars without sharp deformation edges should be coated.

Protective materials, such as high density plastic sleeves, should be used at contact points between the coated bar and bending equipment when bars are fabricated. Use of fluidized beds or conveyor belts carrying items to be coated through the spray chamber to coat bars after fabrication should be considered. The benefits of coating after bending are expected to outweigh the extra cost (about 2-3% of cost of project) in terms of added years of service.

To significantly improve adhesion of coating to substrate, pretreatment of steel is recommended. Pretreatment is a chemical process that enhances adhesion and provides a barrier against the spread of corrosion. Another option is to clean the steel bars twice.

13.3.2 Specifications. Stricter specification requirements regarding coating damage should be considered such as: limiting the number of accepted holidays to 3/m (1/ft.) during coating; patching all visible damage at all stages (at fabrication plant, after arrival to construction site, and before casting); and limiting the percentage of patched damage to a total of 1% of the bar surface area per unit length of coated bar.

Tighter coating thickness tolerances should be required. In addition, procedures for measuring coating thickness should be improved. Coating thickness should be checked at deformations.

Bend test requirements should be modified to encourage improving coating flexibility and adhesion. No signs of damage anywhere on the bar surface should be accepted.

A better repair system (material and procedure) should be specified. Bar cut ends should be treated carefully. For ease of construction and identification of previously repaired areas, it is recommended that the color of the patching material be different from the original coating. The thickness of the coating at the repaired areas should be comparable with the original coating. Procedure for determining the adequacy of repair should be developed.

Additional tests should be specified to check the condition of coating adhesion (as in the cathodic debonding test) and the absorption and water permeability of the epoxy film.

13.3.3 Design Recommendations. To reduce both chloride penetration to coated steel and development of plastic settlement cracking, a thicker concrete cover is required. A proper design strategy would consider eliminating unnecessary joints, and preventing or reducing cracking instead of controlling crack width. A viable option to control cracking in bridge decks is to use transverse prestressing.

Bending epoxy-coated bars to the minimum radii allowed in design may cause damage and weakening of coating adhesion on the outside of bend. Tight bending radii should be avoided unless required for structural purposes. Use of smaller diameter bars is encouraged;

however, spacing between bars should be sufficient to avoid excessive damage caused by vibration. Mixing coated and uncoated bars should be avoided. The cost for using coated bars exclusively in construction would not be prohibitive.

For a coherent service life design, resistance of reinforcing steel to corrosion should be provided by multi-stage protection measures. Epoxy-coated reinforcement can be viewed as a primary protection system with which at least one secondary defence system should be used. Viable alternatives are given in Appendix A.

13.3.4 Field Recommendations. Damage to coating must be kept to a minimum throughout construction. Details to improve field practice, such as using padded materials to protect the bars during handling and transportation, are summarized in Chapter 3.

Tying of coated reinforcement should be done with care not to damage coating even when using protected tie wires. Modified tools and materials for tying and separating bar grids to eliminate metal contact might be needed. A check of electrical continuity before casting is advisable.

To improve concrete consolidation around bars, and to reduce plastic settlement and gap formation underneath the bars, both concrete slump and depth of lifts should be reduced. Careful operation of internal vibrators is required to reduce damage during concrete placement. Vibrators with "soft" heads should be investigated to determine their performance, especially in regard to coating damage. Treatment of cracks on concrete surfaces should be considered. Waterproofing materials and sealants are available for this purpose.

13.3.5 Inspection. A comprehensive quality control plan should be developed to ensure proper production and installation of coated reinforcement. All parties involved should be well educated about the necessity of obtaining a quality product.

The holiday detectors currently used should be modified to increase their reliability. The use of the in-line holiday detector may be continued as a quality indicator during production. For acceptance and rejection purposes, random samples of coated bars should be carefully checked by a hand-held holiday detector using different orientations of the detector and visual inspection. Modifications that might be considered include testing dry bars under a high voltage.

A more reliable defect-monitoring system should be developed. The hot water immersion test may be a viable option but needs to be further investigated before implementation.

13.3.6 Future Research. The reliability of half-cell potential measurement as a monitoring technique for determining the state of corrosion activity on coated bars in concrete needs further investigation. The results of this study encourage using this technique under well controlled environments; however, practical aspects should be studied.

Further research is needed to understand the characteristics of the coating/concrete interface in terms of the role of void formations and the possibility of creating paths for corrosive substances. Corrosion development on coated bars in different concrete micro-structures needs to be studied under various loading conditions.

The corrosion propensity of coated bars that were exposed to ultraviolet for extended periods on site needs to be evaluated. Similarly, the characteristics of coated bar samples extracted from field structures after some years of service need to be assessed.

Future efforts should also focus on developing models for the corrosion behavior of coated bars and means to estimate the service life under defined exposure conditions.

APPENDIX A
CORROSION PHENOMENON

A.1 Corrosion Definition

Corrosion is defined as destruction or deterioration of a material (usually metal) because of reaction with its environment.[14]

A.2 Redox Reactions

Anodic Reactions. When conditions surrounding a steel surface embedded in concrete promote anodic behavior at a spot (the anode), the following reactions take place:

$$Fe^{o} \rightleftarrows Fe^{+2} + 2e^{-}$$
$$Fe^{+2} + 2OH^{-} \rightleftarrows Fe(OH)_2$$
$$Fe(OH)_2 + OH^{-} \rightarrow Fe(OH)_3$$
$$2Fe(OH)_3 \rightarrow Fe_2O_3 + H_2O$$
$$2Fe(OH)_3 + Fe(OH)_2 \rightarrow Fe_3O_4 + 4H_2O$$

When chloride ions are involved in corrosion initiation and progress, complex ions are formed. The expected reactions, in this case, are:[43,46,55,125]

$$2FeCl_3 + 6H_2O \rightleftarrows 2Fe(OH)_3 + 6HCl \text{ (strong acid, pH } \downarrow)$$

or,

$$6(Fe^{+2} + 2Cl^{-}) + O_2 + 6H_2O \rightleftarrows 2Fe_3O_4 + 12H^{+} + 12Cl^{-}.Fe_3O_4$$

or,

$$Fe^{+2} + 4Cl^{-} \rightleftarrows FeCl_4^{-2}$$
$$Fe^{+3} + 6Cl^{-} \rightleftarrows FeCl_6^{-3}$$
$$FeCl_4^{-2} + 2OH^{-} \rightleftarrows Fe(OH)_2 + 4Cl^{-}$$

Cathodic Reactions. The corresponding cathodic reactions at the steel surface are commonly believed to be those reactions involving oxygen reduction as follows:

$$O_2 + 2H_2O + 4e^{-} \rightleftarrows 4(OH)^{-}$$

Normally, concrete retains enough moisture in the pore structure, and oxygen is abundant to facilitate this reduction reaction. However, if oxygen becomes scarce, either this reaction ceases, or other cathodic reactions take place.

A.3 Parameters Affecting Corrosion

General. There are numerous factors which may act separately, or together, causing steel corrosion in concrete. These factors also affect the rate and severity of the corrosion-

induced deterioration of the concrete structure. In general, the factors relate to concrete quality and cover, construction practices, use of deicing salts, and harsh environmental exposures.

Due to its own metallurgical inhomogeneity, reinforcing steel is readily susceptible to corrosion, particularly with respect to oxygen and moisture concentrations.[18] However, the effects of steel composition, grade, or level of stress on corrosion are not considered to be significant.[44]

Corrosion can take place in high quality concrete as well as low quality concrete, although corrosion is more frequent in concrete with inferior quality.[65] A detailed discussion of all the effects of concrete composition and properties on corrosion is beyond the scope of this study. Only a summary of some selected points is included here for completion of the discussion.

Concrete Composition.

Cement Type. The relationship between chloride ion and cement type, and how it affects corrosion, have not yet been clarified. It seems that tricalcium aluminate C_3A content is a key constituent involved in chloride attack. Many researchers believe chloride ions react with the C_3A present in the cement. Others indicated that the total alkalinity, not the C_3A content, is the most important factor.[17] In any case, there is evidence that chlorides diffuse more in cements low in C_3A (such as Type 5- sulphate resistant) compared to cements high in C_3A (such as Type 1).[45] Moreover, Type 1 cement delays the onset of corrosion about 2.8 times more than Type 5.[8]

Concrete Permeability. Permeability is identified as the most important factor in long-term durability. Low w/c is not, by itself, sufficient to insure low permeability. Poor consolidation will lead to very permeable concrete even though the w/c is kept low. Aggregate gradation and proportion are also important.

When w/c is increased, both the porosity and free water will be increased. The result is rapid chloride diffusion, easier ingress of oxygen, and a lower concrete electrical resistivity. In addition, concrete strength will be lowered which reduces the time before cracking occurs under corrosion stresses.

Concrete Consolidation. On the macroscopic scale, the concrete cover provides a protection layer to the embedded reinforcement from the environmental influences. From the corrosion standpoint, it is equally important to evaluate the characteristics of the interface between concrete and steel on the microscopic level. Page studied the environment in the micro-region around the reinforcing bar.[50] He suggested that the buffering action of a lime-rich layer at the steel/mortar interface is responsible for the protection characteristics of concrete surrounding the steel.

Vaysburd,[50] summarized Volmer's conclusions of his corrosion studies related to the condition of bond between concrete and steel. Where concrete was in intimate contact with the reinforcing bar, no corrosion occurred. This observation was the same whether or not

concrete encasing the bar contained calcium chloride. In most cases where corrosion was apparent, the adjacent portion had a void space. The conclusions strongly indicate that voids, cavities, and areas of poor bond have a paramount influence on the corrosion process.

Schupack,[53] did not observe any corrosion on the reinforcement of a 34-year old, 0.18 m (7 in.) thick bridge slab. In fact, there was no chloride ingress nor carbonation detected. The amazing performance of this old and thin concrete member exposed to the environment was attributed to the action of revibrating concrete at the time of placement.

Cover Thickness. The cover to reinforcement is considered to be a critical zone for the corrosion performance of the concrete element. Chlorides penetrate into concrete by diffusion and through cracks. The rate of diffusion depends on the concrete quality of the cover. In one case study, a cover thickness of 75 mm (3 in.) but of poor quality concrete resulted in chloride concentration that is 335 times the known corrosion threshold of 0.2% by weight of cement.[126] As can be expected, severe corrosion and distress occurred.

Diffusion of chloride ions in concrete is non-linear. The penetration rate is nearly proportional to the square-root of the exposure time.[20,44,60] Therefore, a slight increase in the cover thickness may help avoid significant shortening of the service life. An example is shown in Fig. A.1 which illustrates the dominating influence of concrete cover. When the provided cover is half of that specified for a 100 year design life, the actual period to reach an equivalent chloride concentration will be only 15 years. The reduction in service life is 85%. It was found experimentally that a 38 mm (1.5 in.) cover is 6 times more effective in resisting corrosion than 19 mm (0.75 in.) cover.[8]

A.4 Corrosion Detection

Visual Examination. It is difficult to detect the extent and severity of corrosion of embedded reinforcement. To trace corrosion activity, concrete surfaces are often surveyed for special signs such as staining and cracking. Concrete structures incorporating epoxy-coated reinforcement may not show such obvious cues because corrosion could be localized (at breaks in the epoxy film, or beneath the coating) without associated manifestation.

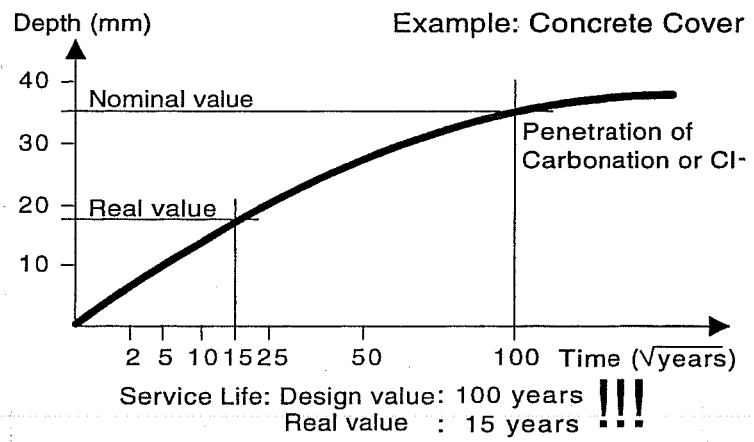

Figure A.1 Concrete Cover Influence on Service Life.[60]

Cracks that are parallel to the direction of the reinforcing bars are more serious than those in the transverse direction. They may evolve corrosion, or may be produced because of corrosion. Crack monitoring, if possible, helps identify the causes of cracking and the crack relation to possible corrosion activity.

Delamination Detection and Coring. In more advanced corrosion cases, spalling or large-scale delamination emanates at the bars. There are several ways to detect delamination or subsurface fracture planes parallel to concrete surface. Chain drags or light-weight hammers are most popular. The chain drag method is widely used on bridge decks.[75] Sometimes, the method is supplemented by hammer-sounding. More sophisticated (automated) devices are available to locate hollow regions in large areas of concrete.

Besides locating cracked and delaminated areas, inspection of the reinforcing steel is possible by taking cores from suspected areas. This is by far the most direct, common, and simple technique to observe the condition of the steel.

Half-Cell Potential Survey. The technique of measuring potentials over concrete areas with respect to a reference electrode has been widely used. Experience shows that the reliability of this technique to detect actual reinforcement corrosion is dependent on the accuracy of testing procedures and the relevance of the evaluation criteria to actual field performance.

The interpretation of half-cell potential is usually related to corrosion activity at the time of measurement. However, Hime,[55] explained that the half-cell potential often represents the chemistry of the solution in contact with the steel which may not relate to corrosion. For instance, as ferrous ion Fe^{+2} concentration is reduced, either by "complexing" with chlorides, or by further oxidation to ferric ion Fe^{+3} in presence of oxygen and water, the potential is shifted to more negative.

Generally, measuring half-cell potentials for detection of corrosion of epoxy-coated bars in bridge decks using ASTM C876[117] has not been successful. Field studies showed no correlation between half-cell readings and visual bar ratings based on ASTM C876 criteria: Bars in excellent condition measured potentials more negative than the limit set in the specification for high probability of corrosion.[73]

The difficulty of using half-cell techniques with coated bars in practice arises when a separate connection is needed for each bar. Moreover, interpretation of the measurements is difficult from a single set of readings. It is necessary to conduct periodic surveys to detect significant changes in potential.

Chloride Analysis. The chloride concentration at the level of reinforcement in concrete is an important indicator of the corrosivity of the environment surrounding the steel. Extraction of chloride ions from concrete can be either by acid or water. In the acid extraction analysis, acid-soluble chlorides are isolated from concrete. The test is simple, relatively fast, and more common in the corrosion investigations. In the water extraction test, water-soluble chlorides are removed. Measuring acid-soluble chloride is favored, and testing for water-soluble chloride may be performed for follow-up studies.[47] The reasons for

considering acid-soluble chlorides as a more reasonable indicator of corrosion potential in concrete are:[77]

- Initial chemically-bound chloride in organic compounds may become unbound.
- Relatively insoluble chloroaluminates formed in fresh concrete may convert, with time and exposure, to sulfoaluminates and carboaluminates releasing the chloride.

Concrete is usually sampled in powder form using impact drilling equipment. Sometimes, cores are extracted from the concrete members and sent back for chloride analysis. In this case, concrete powder is obtained either by dry sawing or other pulverizing techniques.[44] The chloride content in the powder is analyzed following a rapid test procedure or a more electrochemical standard laboratory test procedure (ASTM C114).

The normal way of expressing the chloride content in concrete is as a percentage by weight of cement. When the exact cement content is not known, such as the case in many existing concrete structures, then the percentage is given by weight of concrete or as kg/m^3 ($lb./yd^3$) of concrete. Here, either a concrete unit weight is measured or assumed. Assessment of the actual potential for corrosion at a given chloride concentration is influenced by many other factors such as free moisture and oxygen availability, as well as inhomogeneities in the concrete environment.

Concrete Electrical Resistivity. In general, higher concrete resistivities indicate lower corrosion currents.[106] Where corrosion tends to be severe, concrete resistivity usually falls in the range of 2,000-10,000 ohm.cm.[49,83,93,114,127] The 10,000 ohm.cm limit has been identified as the critical resistivity to support corrosion.[49] Under normal conditions, reinforced concrete possesses a resistance in the range of 10,000-10,000,000 ohm.cm depending on moisture, temperature, and ionic content.[43] ACI 222[44] states that if concrete resistivity exceeds 50,000-70,000 ohm.cm, then corrosion is negligible regardless of the amounts of chloride, oxygen, and moisture.

Concrete Petrographic Analysis. Petrographic microscopy can be used to determine w/c, crack existence, carbonation depth, and corrosion product development.

Miscellaneous Tests. X-ray diffractometry and spectrography can be utilized to determine the constituents of the corrosion products. Infra-red spectroscopy is useful to determine the presence of organic chloride compounds.[77]

A.5 Corrosion Monitoring

General. Preparing schemes for repair or replacement of corrosion-damaged structures can be avoided by corrosion rate measurement. The corrosion rate is useful for determining the onset of corrosion and time to optimum repair.

It is cautioned, however, that monitoring corrosion activity of epoxy-coated reinforcement in concrete may be tedious and, in some cases, misleading.[56] The methods available for corrosion monitoring of uncoated bars may not be valid for coated bars.

However, work is continuing in modifying the existing methods and developing new techniques to overcome this problem.

In the following sections, the most common methods of monitoring corrosion of reinforcing steel in concrete are reviewed. The objective is to study the usefulness and shortcomings of each method. This review is used for selecting the appropriate monitoring systems for the corrosion experimental program of the epoxy-coated reinforcement undertaken in this study.

Macrocell Corrosion Current. A direct measure of the electrons released by the corrosion process is obtained by monitoring the corrosion current in a macrocell setup. This involves measuring the galvanic electrical current passing between a layer of steel in a chloride rich zone (corroding anode) and a low chloride zone (cathode) of the same concrete. A known resistance is used to bridge between the two steel layers, and the macrocell current is determined by measuring the voltage drop across the resistor.

This technique is simple, inexpensive, and is tailored for laboratory use to evaluate different corrosion protective systems (coating materials, corrosion inhibitors, mix additives, *etc.*). The measured current is the best indicator of the metallic iron lost during the corrosion process.[78,128] Since the amount of metal consumed is directly proportional to the corrosion current, the corrosion rate can be evaluated. Each 1.0 Amp.hr of corrosion current consumes 1.04 g (0.015 oz.) of iron.[106]

The major disadvantage of the technique is that it does not detect micro-corrosion cells (localized corrosion); therefore, it may underestimate the corrosion rate. The accuracy of the results may also be questioned if the corrosion rate is very low, and if both connected metals are corroding.[5] Concrete temperature is another factor which affects the corrosion rate significantly.[106] The effect is due primarily to the effect of temperature on concrete resistivity. Hence, corrosion currents measured at different field temperatures need to be adjusted to a base temperature using an experimental formula.

If the voltage of the macrocell is measured an instant after uncoupling the reinforcing bars (the two electrodes), then the reading will be the polarized driving voltage of the corrosion cell. It is also called the open-circuit or instantaneous corrosion voltage because it is measured in the instant-off mode to eliminate the drop of voltage due to path resistance, often known as the IR drop error. A zero driving voltage means no corrosion activity. The higher the voltage, the higher is the corrosion rate at constant circuit resistance.[106]

Standard Half-Cell Potentials. One of the practical and widespread techniques for monitoring the corrosion state of reinforcing bars in concrete is the standard half-cell potential measurement. The technique becomes handy particularly for bridge decks. Measurement is taken by placing the half-cell electrode on the concrete surface and connecting it, via high-input resistance voltmeter, to the reinforcing bar. The measured potential value is used to determine the probability that reinforcement is corroding inside concrete.

The method relies on the measurement of the free corrosion potential E_{corr} of the bar against a standard half-cell electrode. The two commonly used electrodes for detecting and monitoring corrosion activity in reinforced concrete are the copper/copper sulphate electrode (CSE) and the saturated calomel electrode (SCE). The CSE has a fairly slow response to stabilize when measuring the potential. On the other hand, the SCE is a silver/silver chloride half-cell which has a much faster response time, greater stability with respect to time and temperature, and a better reproducibility of the outcome.[21]

The half-cell reference electrode used to measure potentials may be produced in the form of a potential wheel easy to roll on large surfaces. The idea is to speed up potential mapping. Data is stored automatically for later production. Figure A.2 shows a schematic diagram of the tool. For practical purposes, a solid electrolyte rather than a liquid electrolyte is used to ensure proper contact with concrete.

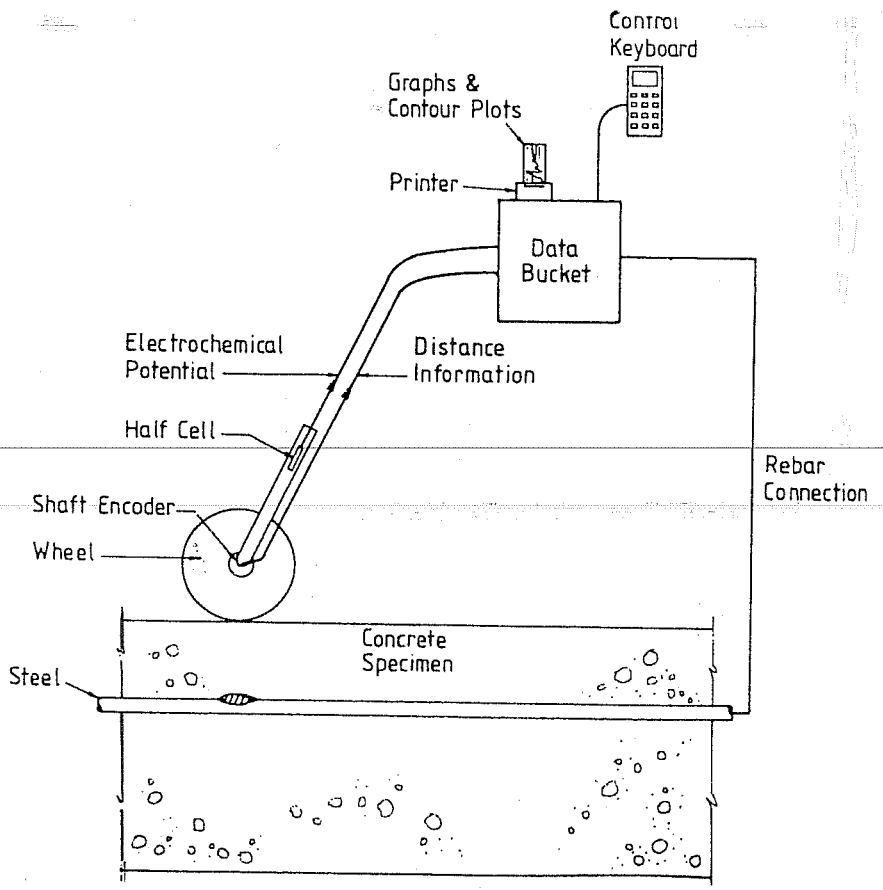

Figure A.2 Schematic Diagram of the Potential Wheel.[21]

Measurement of the potentials is typically done according to ASTM C876[117] which is strictly limited to uncoated reinforcement. The potential readings may have different interpretations. Two oversimplified versions of some established criteria for evaluation are

given in Tables A.1 and A.2. Originally, four states of corrosion of bare steel in concrete were identified. These states are described in Table A.3. According to ASTM C876, a steel potential more negative than -350 mV CSE indicates a high probability of corrosion, whereas a potential less negative than -200 mV CSE indicates a low probability.

The significance of the half-cell potential test is limited to correlating the potential magnitude with corrosion incidence. The potential measurement is, then, an indicator of incidence not rate.[44,129] In other words, half-cell measurement does not give any information on the corrosion kinetics. Highly negative potentials are merely signals of probable greater corrosion activity rather than higher corrosion rate.

The conditions under which the potentials are measured are significant to their interpretation.[105] For example, potentials of bars measured in concrete and in simulated concrete environment will normally give different values. Page and Treadaway, as cited in Ref. 105, note that "in cases where E_{corr} is observed to decrease with time, depassivation may or may not be implied, since the increased cathodic polarization may be associated with either passive film breakdown or the progressive restriction in the supply of oxygen to the surface of the passive steel."

Table A.1 Interpretation of Corrosion Potential Measurements in Terms of Corrosion Probability.[105]

E_{corr}(V vs $Cu/CuSO_4$)	Probability of Corrosion
> -0.20	< 5%
< -0.20 but > -0.35	~50%
< -0.35	>95%

Table A.2 Interpretation of Corrosion Potential Measurements in Terms of Steel Condition.[105]

E_{corr}(V vs SCE)	Condition of Steel
> -0.22	Passive
< -0.22 but > -0.27	Active or Passive
< -0.27	Active

Table A.3 Steel Corrosion States in Concrete.[105]

1. The Passive State

In the absence of chlorides, the passive potential range is very wide, from + 200 mV to − 600 mV SCE at pH 13, but in aerated concrete, steel normally exhibits a potential in the range of + 100 mV to − 200 mV SCE.

2. The Pitting Condition

Pitting typically results from the presence or ingress of chloride ions, and the average potential is typically − 200 to − 500 mV.

3. General Corrosion

General corrosion is the result of a general loss of passivity, resulting from either carbonation or the presence of excessive amounts of chloride, and potentials are typically − 450 mV to − 600 mV SCE.

4. Active, Low-Potential Corrosion

In environments where the access of oxygen is so limited that the passive film cannot be maintained, embedded steel may become active in the still highly alkaline environment exhibiting potentials as low as − 1000 mV.

Pfeifer and Landgren,[78,128] showed extensive data which indicate that a half-cell potential of -240 mV SCE may be the potential at which corrosion of uncoated bars starts. Wheat and Eliezer,[105] on the other hand, found that uncoated steel in concrete immersed in 10% NaCl solution is more passive when the potential is more positive than -300 mV SCE. Conversely, the steel is more active when the potential is more negative than -300 mV SCE. Around -300 mV potential a region of instability between passive and active conditions existed. The findings also show that a potential of -500 mV does not necessarily reflect more active behavior than a potential of -400 mV. However, a potential of -400 mV would be expected to reflect more active behavior than a potential of -200 mV with reference to the above mentioned dividing potential of -300 mV.

Elsner and Böhni,[23] carried out potential mapping and visual inspection of the bars in a bridge deck in Switzerland and found that localized corrosion existed in all the areas with a potential more negative than -300 mV CSE. Had they used the ASTM C876 criterion of probable corrosion at -350 mV, more than 70% of all the corrosion sites would not have been detected.

Based on their findings, Elsner and Böhni demonstrated that an absolute potential value for the identification of active conditions of steel corrosion in concrete does not exist. It follows that the limit given in ASTM C876, which is -350 mV CSE, is not a reliable indicator of corrosion activity on uncoated steel. The following factors were presented as having a significant effect on potential measurement:[23]

- Concrete cover thickness.	The more the depth of concrete cover, the less will be the potential reading. As a result, it becomes more difficult to distinguish the potential values corresponding to active corroding areas.
- Concrete electrical resistivity.	As the concrete resistivity is lowered by moistening and adding chlorides, the absolute potential values are shifted to $\pm$ 50 mV.
- High resistive surface layer.	Surface layers with high resistances enhance the effect of cover depth. Therefore, the potentials become more positive.
- Polarization effects.	Where oxygen supply to the bar surface is restricted, the cathodic reaction is polarized and, therefore, very negative potentials develop despite the limited corrosion activity.

Lambert and Norris,[127] cited other sources of difficulty in obtaining accurate, reliable readings. These are summarized by wide spacing in detection network, dry concrete, surface latence, and inadequate or poorly maintained equipment. The results may vary considerably with different conditions such as temperature and humidity. In addition, surface half-cell measurement may not correctly detect corrosion of deeply embedded bars. To solve this problem, an in-depth technique has been developed in which holes for chloride sampling are made and a three-dimensional or cross-sectional map of the potentials is drawn.

The relevance of the ASTM C876 criteria to epoxy-coated bars has always been controversial. Previous studies had indicated that more negative potential values were recorded when testing epoxy-coated bars compared to uncoated bars in similar concrete.[62,81,85,104] The higher negative potentials should not be misinterpreted as indicating more severe corrosion attack, since the recovered coated bars were nearly in good condition. Typically, corrosion was limited to breaks and defects in the coating with subsequent undercutting. The explanation of this diversity between the potential measurement and the actual extent of corrosion is given in Section 2.9.3.

The discussion above, and other observations, indicate that the applicability of the half-cell technique, using ASTM C876, to field measurements is limited regardless of the type of reinforcing bars. In short, the method may give inconsistent results in field applications. In one study, for example, potential measurements made on a fence wall on a beach in Central California indicated extensive corrosion. Examination of the uncoated metal surface revealed only superficial corrosion.[49] In another study, however, it was found that data from open-circuit potential and electrochemical impedance measurements were mutually consistent.[109]

Linear Polarization. The three electrode linear polarization method (3LP-method) is a corrosion monitoring method used to determine the instantaneous corrosion rate. It is considered to be effective for predicting the behavior of reinforced concrete structures in aggressive environments.[56] However, the technique simulates microscopic corrosion and not macroscopic corrosion conditions. Therefore, assessing the overall effect of corrosion on the

structure is difficult.[44] The method is commonly used in laboratories to compare different protection systems.[5]

The rate of corrosion can be determined in two ways: current-control; and voltage-control. In the first option, small increments of external current ΔI_{app} are applied to the steel electrode (tested bar in concrete) and the corresponding potential shift (polarization) ΔE from the static or equilibrium corrosion potential of the steel E_{corr} is measured.[81] When the polarization resistance ΔE is plotted against the applied current I_{app} the relationship, although not perfect, is linear. The slope is known as the linear polarization resistance R_p. The slope indicates the corrosion activity; the steeper the slope, the less is corrosion activity.

In the second option, the tested bar (working electrode) is polarized in concrete by impressing a voltage and measuring the corresponding current flow.[56] Figure A.3 illustrates the test setup. Before scanning is initiated, the open-circuit potential E_{corr} of the tested reinforcing steel is determined. The system then polarizes the steel anodically and cathodically by changing the potential of steel in concrete. Automated scanning records the change in potential and the corresponding current. Similar to the above, the linear polarization resistance R_p is determined from the plotted ΔE-I diagram.

In any case, the corrosion current density I_{corr} is calculated using Stern and Geary relationship,

$$I_{corr} = \frac{B}{R_p} \tag{A.1}$$

where,

$$R_p = \frac{\Delta E}{I} \tag{A.2}$$

$$B = \frac{\beta_a \beta_c}{2.3(\beta_a + \beta_c)} = \textit{proportionality constant} \tag{A.3}$$

where, β_a and β_c are the anodic and cathodic Tafel constants, respectively. The proportionality constant is equal to 26 for active uncoated steel, and 52 for passive uncoated steel.[63] The expressions provide a linear relationship between the corrosion current I_{corr} and R_p for small shifts in the electrode potential. The range of validity is usually $\pm$ 10 mV more nobel or more active than E_{corr}.[14,56]

The corrosion rate measurement is approximate, and should be extrapolated with caution to estimate steel section loss or predict damage rate. The determined corrosion rate is valid at a given time and location. The accuracy of determining the actual corrosion rate over time has been questioned in a recent study.[6] The results of measurement may also be

inconsistent because of the effects of polarizing an unconfined steel area. The electrical signal vanishes with the distance from the electrode location on concrete surface.[130,131]

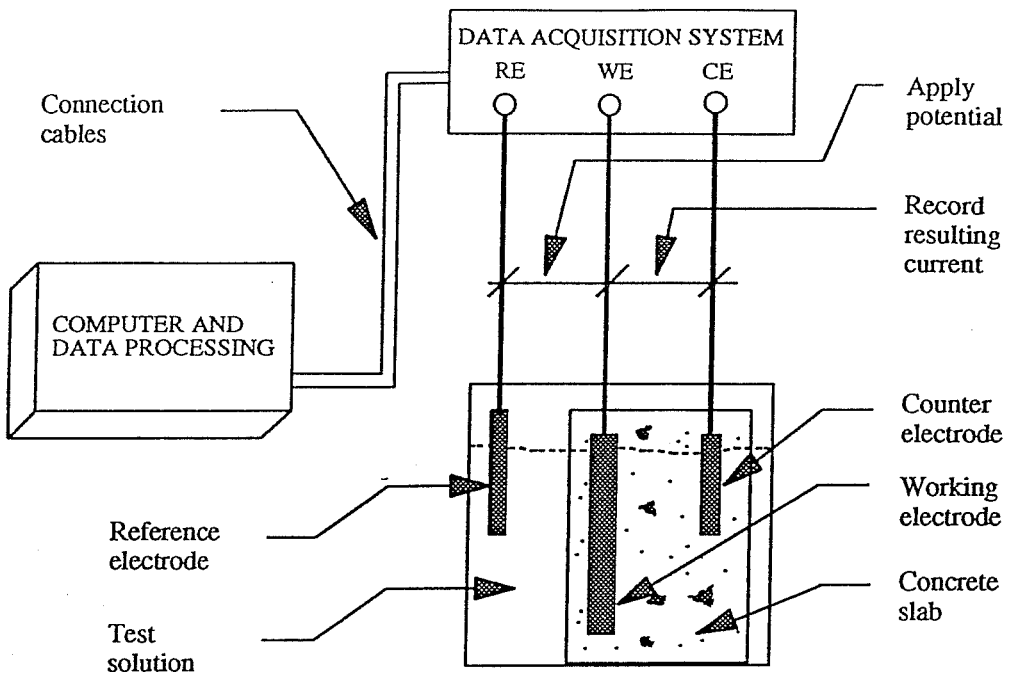

Figure A.3 Schematic Layout of Corrosion Rate Measuring Instrument.[56]

For the case of epoxy-coated bars subjected to increments of applied current, the potential response may be so small and erratic that a reliable calculation of the polarization resistance is not possible.[81] Further, the Tafel constants derived for uncoated reinforcing bars are most likely different for the epoxy-coated bars. These shortcomings may limit the applicability of the 3LP-method to measure corrosion rates of epoxy-coated reinforcement.

AC Impedance Spectroscopy. The AC impedance measurement is a method that allows the characterization of the different mechanisms of corrosion of steel in concrete.[129] It has been used as a laboratory test for corrosion rate determination of small bars in concrete or mortar. It is useful to obtain information on the electrical resistivity and dielectric properties of the cover to reinforcement.[23]

To describe the method in short, a working electrode is maintained at its corrosion potential E_{corr} by a potentiostat of a small amplitude sinusoidal voltage in a wide range of frequencies. The response at every frequency has a signal with a different amplitude measured as ΔI, and a phase shift from the input signal. As an alternative to the applied sinusoidal voltage, potentiodynamic polarization at different sweep rates may be used. Deviations from rest potential are usually restricted to less than 10 mV to minimize non-

linear effects.[84] The signals are then analyzed using a model of assumed equivalent electrical circuit with resistances and capacitors reflecting the actual physical system.

Different circuit models can be used to correlate with such variables as the cover thickness, film at steel/concrete interaction, *etc.* Therefore, the method is useful to study corrosion in concrete structures with different compositions and under varying environmental conditions provided an adequate model is used. More quantitative data is needed to improve reliability of corrosion detection in field structures. A very frequently used circuit is the one proposed by Randles which describes a simple corroding system.[63]

The impedance Z is determined by the ratio,

$$Z = \frac{\Delta E}{\Delta I} \qquad \text{(A.4)}$$

which can also be related to assumed resistances and capacitors. By changing the frequency from zero to infinity and plotting the impedance vector Z, a complex plot is obtained, called the Nyquist diagram. The resulting curve is usually a semicircle the dimensions of which are used to calculate the assumed resistances and capacitors. One of the resistance terms called the charge transfer resistance R_t is equivalent to the polarization resistance described by Stern's formula. This empirically-evaluated resistance is used to calculate the current density and corrosion rate following the steps described in the linear polarization technique.

The AC Impedance method is a relatively new technique for application to the reinforcement corrosion. The complexity of the concrete, and the use of coated reinforcement, have made it difficult to carry out the procedure and to interpret the results correctly. Usually, perfect semicircles are obtained when chlorides are present and pitting is developed. These conditions may not be readily present when bars are epoxy-coated.

Despite the difficulties encountered, the method appears to be promising. Previous experience with electrochemical impedance measurements on epoxy-coated bars indicated the presence of extended crevices underneath cracked coatings on bent bars.[109] Work is being done to improve the validity of the technique on different concrete systems.

The applicability of the method to field measurements has been questioned because of the many technical difficulties. The polarization resistance and the impedance at each position to be measured will not be accurately obtained. This is mainly due to the large area of reinforcement involved. To confine the area of reading and obtain more reliable results, a double-counter electrode method has been proposed.[130] In this method, the reinforcing bars in concrete are polarized by a central electrode together with additional surrounding counter electrodes. This arrangement confines the corrosion resistance measurement to the area under the central electrode.

Electrical Resistivity. The concrete resistivity can be determined by measuring the electrical resistance between two metal inserts using a 1000 cycle AC signal. Measuring AC signals rather than DC signals seems to give better indications.[127] The inserts can be steel wires or hollow cylinders.[44] Conversion factors are needed as multipliers for the measured

resistance to obtain the approximate concrete resistivity. These conversion factors are determined from tests in solutions of known resistivity. Field measurements under variable temperatures should be adjusted to a base temperature value using an experimentally-defined equation given in Ref. 106.

The technique is applicable for predicting macrocell activity. For better accuracy, insert probes must be electrically coupled with the reinforcing steel in concrete, and become equally active with the steel, *i.e.* have similar current flows. The higher the concrete resistivity, under a given potential difference, the smaller the magnitude of corrosion current.[127]

Resistance measurements utilizing AC signals have also been used to monitor the integrity of the epoxy coating on reinforcing bars. Typical use involves measuring the resistance between reinforcement layers to observe any drop indicative of coating deterioration. The resistance, in this case, depends on the concrete resistivity between the reinforcing layers, and on the availability of contact areas, such as holidays, on the bar surface.

The dryer the concrete, the higher is its resistance. The wetter the concrete, especially with an electrically-conductive deicing salt, the lower is the resistivity. Fraczek,[43] found that as the water and ionic content in concrete and temperature increase, the resistance decreases and the conductivity increases. Deterioration of the coating will also increase the exposed steel surface, thereby reducing the resistance.[94]

The above discussion shows that changes in resistance readings may be attributed to changes in either the concrete environment or the coating insulation. The initial findings of a recent study in progress at the University of South Florida suggest that concrete conductivity may vary widely as a result of intrinsic concrete properties and not only because of moisture content.[114] It should be remembered that the epoxy film thickness may affect the measured resistance. Thicker films exhibit higher electrical resistances.[11] The increased resistance is partly due to having a fewer number of pinholes in the thicker film.

Field measurements of the resistance may also be done by surface scanning. A probe and a resistivity bridge are used to measure concrete resistivity by scanning the surface.[93] The measurement is based on 4-pt Wenner array resistivity concept. The probe consists of small copper/copper sulfate electrodes fitted with felt tips. The tips are dipped in a sponge wet with a conductive solution before measurement. If highly resistive surface layers are present, or if bars are closely spaced, then measurements may be disrupted.[127]

Clear,[30] indicated that a resistance number which differentiates a poor quality coating for a good one has not been defined. The problem is even more cumbersome for field measurements because of the variable geometry, concrete cover, and concrete quality. The lack of electrical continuity between coated bars makes it necessary to have a direct attachment of a lead wire to each tested bar.

Galvanostatic Pulse Technique. This is a rapid, nondestructive technique for on site determination of the corrosion state of reinforcement in concrete. The technique uses the

same equipment as for impedance measurement, but a short-time (typically 3 sec.) anodic pulse is imposed onto the reinforcement from an electrode placed on the concrete surface.[23] The potential-time curve is established. The slope of the curve indicates the corrosion state of the reinforcement. Information is also obtained on concrete resistivity.

A.6 Corrosion Assessment

Nondestructive evaluation of corrosion activity in concrete, particularly on epoxy-coated bars, is both difficult and limited in validity. The applicability of some electrochemical methods, such as linear polarization and AC impedance, to measure corrosion activity of coated reinforcing steel is still under investigation.[30] Preliminary data have shown that the electrochemical impedance spectroscopy may be applicable for early detection of the degradation of highly resistive organic coatings on steel. In absence of a more reliable way, visual and delamination surveys of the concrete surface, and destructive examination of the embedded coated steel, remain to be viable means of corrosion evaluation.

From the corrosion standpoint, metals are usually compared on the basis of their corrosion resistance.[14] This requires that the rate of attack be determined for each material. Quantitative expressions of the corrosion rates are frequently in the form of percent weight loss, μm per year or mils per year (mpy), milligrams per square centimeter per day, and grams per square inch per hour. Notice that the weight loss, by calculations, is converted to a uniform reduction in the thickness expressed as μm/yr. It has been proposed that a reduction in bar cross section between 10 and 25% in the critical zones of the structure will mean the depletion of its service life.[132]

One of the best indicators of the corrosion rate and actual mass loss is the value of the average macro-anodic current density. Corrosion development or metal consumed is directly proportional to the magnitude of the current density. For uncoated bars, deterioration of concrete is expected when the average corrosion current varies between 0.1 and 0.2 μA/cm^2 (0.1-0.2 mA/ft^2). In terms of service life, corrosion-induced damage is expected within 10 to 15 years of service in systems that exhibit corrosion currents between 0.2 and 1.0 μA/cm^2 (0.2-1.0 mA/ft^2). These values were based on observations made during experimental polarization measurements.[93] Each 1μA/cm^2 (1 mA/ft^2) is equivalent to 11.6 μm/yr.[22]

For epoxy-coated bars, it is not known whether or not corrosion damage would be associated with levels of corrosion currents similar to those for uncoated bars. Concerns have been expressed about the susceptibility of damaged coated bars to intensified local corrosion activities. If so, then corrosion-induced damage on concrete with coated bars would show up earlier than on concrete with uncoated bars. These concerns, together with the natural low adherence between the coated bars and concrete may aggravate the scale of corrosion-induced structural damage. The early, unexpected deterioration of the Florida Keys bridges, and the severe pitting observed on some coated bars, make these concerns legitimate.

Information is scarce about the limits of corrosion current densities of coated bars related to concrete deterioration. Based on the limited information in Ref. 112, 22, and 6 on the rate of corrosion of reinforcing steel in concrete, corrosion current densities up to 0.1

$\mu A/cm^2$ (0.1 mA/ft^2) denote a negligible corrosion rate, between 0.1 and 0.2 $\mu A/cm^2$ (0.1-0.2 mA/ft^2) indicate a low corrosion rate, and between 0.2 and 0.5 $\mu A/cm^2$ (0.2-0.5 mA/ft^2) disclose a shift to a moderate corrosion rate.

Efforts were made to predict the extent of probable corrosion in structures similar to those in the Florida Keys. One approach to setting guidelines for quantifying expected corrosion on coated reinforcement was studied by the University of South Florida.[93] Both field and laboratory measurements were compiled to develop a model that will replicate the performance of the coated bars in laboratory tested specimens. Equivalent electrical circuits were derived and solved numerically for the corrosion currents passing through different bar sections. The results correlated well with the experimental behavior.

A.7 Corrosion Protection Methods

Implications for Corrosion Protection. In order to take the right measures to stop the corrosion process, the following aspects of the process need to be considered:

- Chlorides perform as catalysts or accelerators to the corrosion reaction. They most likely initiate the corrosion activity and take an active part in fostering the activity.
- Oxygen is mainly involved in the cathodic reactions, not the anodic reactions. Therefore, metal oxidation at the anode does not require oxygen. The only exception is when the corrosion products are oxidized to higher levels, *i.e.* the ferrous ions are converted to ferric ions or red rust. Oxygen at this stage would probably reach the anodic sites through corrosion-induced cracking.
- Moisture is necessary to form the electrolyte which is the conductive medium. Water is also vital for the completion of the cathodic reactions.
- No activity is possible without electrical continuity between the electrodes. The corrosion electrical current will only pass from the anode to the cathode if an electrical link is present.

Principles. To deter the reinforcing steel from corroding, means should be followed to prevent corrosion cell formation. There are several ways to control the anode/cathode cell development. These are grouped under the following:[97]

- Avoid differences in potential in the metal, *e.g.* removing surface contaminants, mill scale, and foreign matter, or isolating dissimilar metals.
- Avoid formation of electrolytes, *e.g.* using protective films that are tough, durable, impervious, and chemically resistant.
- Prevent reaction on the anode or cathode, *e.g.* using rust-inhibiting compounds.

Function. The available techniques of corrosion control are envisaged as means to reduce corrosion or prevent it, if possible. Most of these methods have not been used long enough in actual structures to judge their effectiveness. Whether or not the corrosion of reinforcing steel can be absolutely eliminated for the entire design service life of a structure is not known.

The corrosion control methods may be classified as mechanical or electrochemical, according to their function.[30,111] The mechanical methods use physical barriers to chloride, oxygen, and water penetration. Such methods include: admixtures; sealers and membranes; and steel coatings. The electrochemical methods depend on electrochemical processes to force the steel to remain cathodic. The most common methods are: chloride removal; cathodic protection; and rust-inhibitors. Some of these methods are more suited to remedial and rehabilitation work and will be presented in Section A.8. The following sections highlight the different options available for corrosion control. A thorough discussion of these alternatives falls beyond the scope of this study.

Concrete Surface Coatings, Sealers, and Membranes. The primary function of these methods is to reduce the ingress of the deleterious substances. Coating is defined as a surface treatment (impregnating or film forming) applied in liquid or slurry form.[133] Typical sealants represent a silicate in water, resinous materials in mineral spirits carrier, epoxies, acrylic and ethylene copolymer emulsions, and a methacrylate. Besides concern about their durability, one major problem with their use is that they become ineffective where moisture and chlorides are trapped underneath.[73]

Overlays. Similar to the coating systems, overlays are also used to abate the penetration of the corrosive elements. The most common overlay systems include: portland cement concrete; low-slump, dense concrete; latex-modified concrete; and polymer concrete. Many of these systems have the potential to be a cost effective treatment to repair and extend service life. The main problems associated with overlays are cracking and debonding from the parent concrete.

Thicker Covers of Good Quality Concrete. Thicker covers normally improve the corrosion protection. Increasing the concrete cover by 10 mm (0.4 in.) reduces the corrosion amount by about one third.[11] A less permeable, well-consolidated concrete with rich mortar surrounding the reinforcing bars provides a promising environment for a longer durability. However, the thickness of the cover and the detailing should be such that shrinkage and thermal cracking are controlled and the crack width is limited.

Fly Ash, Slag, and Silica Fume Modified Concrete. Class F fly ash, rice-husk ash, blast-furnace slag, and silica fume are mineral additives used in concrete. Besides economizing the production of concrete, these materials are expected to improve the quality of concrete (strength and durability). Long-term investigations have confirmed that cements containing slag and condensed silica fume impart better resistance to sulphate, chloride, and seawater attack.[134] This is due, in large, to the reduced permeability and increased resistance. The reduction in the permeability of the silica fume concrete may reach a factor of 10 or more, while the increase in its electrical resistance may be a factor of 6 to 16.[135] The literature on the corrosion performance of fly ash or rice-husk ash modified concrete is inconclusive.

Corrosion Inhibitors. Corrosion inhibitors are classified as:[136] anodic; cathodic; and a combination of both. The anodic inhibitors cause an insoluble compound, normally ferric oxide, to precipitate at the anodic sites thereby stifling the anodic reaction and inhibiting corrosion.[16] The cathodic inhibitors, on the other hand, have to act over the whole exposed

surface of the reinforcing steel and are therefore less efficient. They retard corrosion by forming a high electrically resistive film over the surface which prevents the cathodic reactions.[16] The primary compound groups in use are:[44,49] chromates; phosphates; hypophosphates; alkalies; nitrites; and fluorides. The major concern about the use of inhibitors is the adverse effect on concrete physical properties and long-term durability.

Steel Coatings. The main purpose of using steel coatings is to isolate the steel from the aggressive environment. The coatings are either metallic or non-metallic. Of all the non conductive coatings, fusion-bonded epoxy coating is considered to be the most promising. Metallic coatings include: nickel; austenitic stainless steel; zinc; and cadmium. The first two are more nobel than the steel and can be electrochemically active. If defects exist in the coating, a very intense localized attack on the steel occurs. The other two are sacrificial. The effectiveness of galvanized (chromated) bars were investigated by many researchers. The results were not much different: The galvanized reinforcing bars did not provide adequate protection against corrosion.[11,44,57,62,108,112,113]

Noncorrosive steel. Austenitic stainless steel has been used successfully to prevent corrosion; however, the price of employing this material for general use is prohibitive.[29,44,62] Fiber-reinforced plastic (FRP) reinforcement is a recent development for replacement of conventional steel reinforcement in concrete. Since the development of FRP reinforcement is still in infanthood, its disadvantages render it incompetent with steel for "heavy" structural use.[137]

Cathodic Protection. This is a method of "stopping" the corrosion electrical process by simply reversing the process. By polarizing the steel to a more negative potential, the corrosion rate is put under control. The method has been successfully used since the early 1970's.[9] It has gained wide acceptance throughout the world. There are two options for the system: protective galvanic cell, or "sacrificial" anode; and impressed current (requiring an external power supply). The selection of a suitable anode type is crucial to the success of the process. Each application will have its own merits, and the cathodic protection system should be designed accordingly. To have a successful application, the reinforcing steel network should be continuous. The main possible disadvantages of this method are: producing stray corrosion currents[44]; deterioration of the steel/concrete bond[17]; long-term effects on concrete microstructure[45]; and the high cost.

A.8 Corrosion Remedial and Rehabilitation Methods

Principles. The principles of the remedial and rehabilitation methods are summarized by the following:[44]

- Preventing contact of concrete surfaces with the corrosive environment, *e.g.* use of insulative materials, and impermeable dielectric barriers.
- Altering the environment to reduce its corrosivity, *e.g.* chloride extraction.
- Controlling current flow within the environment, *e.g.* cathodic protection.
- Combining some of the above techniques.

Insulative Remedies. Insulative methods include surface coatings and membranes, polyester impregnation and overlays of polymer concrete, low slump concrete, or latex-modified concrete.

Modification of the Environment. To reduce the corrosivity of the environment, certain harmful constituents must be removed from the electrolyte. These constituents are primarily oxygen, water, and chlorides. The most important process in this regard is the electrochemical chloride removal process. Details of the process are given in Ref. 44.

Realkalisation. This is an electrochemical technique to restore alkalinity lost during carbonation. An alkaline solution is introduced into the cover concrete to the reinforcement to arrest and deter further corrosion due to carbonation. More details are given in Ref. 138.

Desalination. This is a modern technique by which penetrated or cast in chlorides are removed electrochemically to arrest corrosion in contaminated concrete. Further information is given in Ref. 138.

Galvanic Control. In this system, an unaided zinc-steel galvanic couple is formed. Zinc anodes are arc-sprayed and deposited directly over the exposed clean bars and surrounding concrete surfaces. A galvanic current flows from zinc anode through concrete and onto steel surface reducing or stopping the corrosion process. The method has been used in Florida to arrest corrosion of the epoxy-coated bars in the Niles Channel bridge.[93]

APPENDIX. B
INFORMATION ON EPOXY-COATED REINFORCEMENT

B.1 Epoxy Coating Material

Generally, the epoxy material used for coating is a bisphenol-amine powder formulation.[42,82,84,109] This epoxy resin is a diglycidyl ether which is a thermosetting material belonging to the polyaddition plastics family.[30,111] The functional chemical groups forming the epoxy consist of carbon and oxygen atoms arranged in various possible structures. The epoxy groups are also termed epoxides -more frequently in Europe- in recognition of their nature as oxides.[97]

Epoxies are classified as thermosetting materials because their cure is accelerated by heat.[85] Upon full curing, they retain their shape up to their decomposition temperatures. Thus, changes in temperature do not readily cause a change in their physical properties.[30] Liquid epoxy paints, on the other hand, are classified as thermoplastic materials.[12] Their exposure to heat may significantly change their physical properties.

Epoxy systems usually consist of two components- an epoxy resin and a curing compound. However, when in powder form, the two components are contained within each powder particle.[85] Therefore, mixing of epoxy powders is unnecessary. Fillers, pigments, and flow control agents can be added in various quantities to the epoxy. The type and quantity of each of these constituents, as well as the blend process, significantly affect the properties of the final product.[30] The fusion blend process (melt mix), in which the solid ingredients of the epoxy are integrated into each particle, yields a product with high potential for good performance.

The epoxy powder is usually applied to the reinforcing steel bars in a process known as fusion bonding. Epoxy fusion bonding is a heat-catalyzed chemical reaction by which epoxy transforms from a hard brittle material into a tough elastic-like material.[12,139] This thermosetting process is an irreversible chemical reaction.[86] It develops molecular or polar bonding between the epoxy and the steel.[41] As a result of this chemical bonding, heating the cured coating will not cause it to soften. In addition to the chemical bonding, physical roughness on the steel surface provides a mechanical anchorage to increase bond between the two materials.

The epoxy powder needs to be maintained in controlled conditions to keep it good for use. There are specific instructions to be followed during handling, storage, shipping, order of use, and feeding the powder into the system. The manufacturer's recommendations, as well as the general rules outlined in Ref. 30 should be closely adhered to for this purpose. One important aspect for assuring good quality epoxy material is to test it whenever in doubt of its condition.

B.2 Epoxy Material Characteristics

Epoxy coating materials have long been known for their excellent characteristics. Some of the most desirable features are:[30,89,97,111]

- excellent adhesion;
- ease of cure;
- mechanical strength;
- high electrical insulation;
- resistance to solvents and chemicals;
- high ductility;
- low shrinkage upon polymerization;
- good heat resistance; and
- low oxygen and chloride ion permeability.

The epoxy coating materials have also some undesirable features. The most pronounced ones are water absorption and water permeability.[29,30,97] Moisture permeation through the epoxy coating has been recognized a long time ago. Exposure of epoxy coatings to moisture greatly reduces the adhesion between the epoxy and the steel. Loss of adhesion, however, does not automatically cause corrosion of the metal. Another undesirable feature is the tendency of the epoxy-coated bars to slip in concrete when subjected to elevated temperatures exceeding 100° C (212° F).[29] Slipping may occur although the epoxy coating can tolerate a temperature increase to about 200° C (392° F).

B.3 Function of Epoxy Coating

The primary function of epoxy coating, as a barrier-type, is to prevent chloride ions from contact with the steel.[96,104,112] However, it has frequently appeared in literature, that epoxy coating works as an isolator for the steel from contact with oxygen, moisture, and chloride ions.[4,44,115,135] While it has been proven experimentally that the epoxy coating is essentially impermeable to chloride ions and to oxygen diffusion, its resistance to moisture penetration has not been established.

The epoxy coating offers corrosion protection to steel in concrete by two main mechanisms: increasing the electrical resistance along the corrosion cell path; and retarding the cathodic reduction process. Epoxy coating on the steel, inherently, increases the macro-corrosion cell resistive path.[30,41,106,112] As a result, the corrosion current flow between adjacent coated steel locations is greatly reduced. As long as this feature is maintained, the risk of developing destructive macrocell action is kept low. The second protective mechanism is attributable to the nonconductive nature of the epoxy coating. The epoxy film prevents the cathodic reactions (mainly oxygen reduction) from taking place on the underlying steel, thereby hindering the corrosion process.[41,106]

In short, the epoxy coating is effective if it abates the driving force for corrosion created by a potential difference in a corrosion cell, and sustained by continuous cathodic reactions. Even if corrosion were to occur, the total metal lost in the concealed iron would be greatly reduced and the risk of concrete disruption would be minimized.

The ability of the epoxy-coated steel to perform well depends on the properties of the epoxy material, as well as the characteristics of the coated steel as a finished product. To best perform its function, the epoxy-coated reinforcement must be defect-free and must satisfy the following requirements:[29,108]

- high coating strength, toughness, and long-term durability;
- high adhesive strength to steel substrate;
- high resistance to alkaline concrete, carbonized concrete, chloride-contaminated concrete;
- high resistance to oxygen and water vapor diffusion; and
- high resistance to normal low and elevated temperatures, such as freeze and hydration heat.

In addition, the coated bars should contribute to satisfactory structural behavior of the concrete members.

B.4 Evolution of Epoxy-Coated Reinforcement

When corrosion-induced deterioration was recognized on bridge decks, research was launched on determining the mechanism of distress and methods of prevention. Efforts were concentrated upon investigation and trial use of moisture barrier systems to prevent the ingress of chloride ions to the embedded reinforcing steel. Other methods or systems to accomplish the same purpose were also identified. Nonmetallic coatings were the primary alternatives. The first use of organic coating to protect against corrosion was in the 1950's.[41] The successful application of epoxy coatings on underground transmission pipes for corrosion prevention encouraged the industry to focus its attention on epoxy resins. Pipe coatings were electrostatically applied powder epoxies.

In March 1973, the Federal Highway Administration (FHWA) initiated the National Experimental and Evaluation Program (NEEP) Project No. 16, Epoxy-Coated Reinforcing Steel. Under this project, the National Bureau of Standards (NBS) and the FHWA, Office of Research and Office of Development, conducted extensive research and set the lead in identifying some epoxy coatings that had promising protective qualities. Based on NBS preliminary tests and evaluation, four epoxy products were pre-qualified for use in the NEEP 16 project. The project then encouraged highway agencies to construct experimental projects to evaluate the coated reinforcement. Information was disseminated to insure that the coated bars used in these projects were equivalent to those that had passed stringent research tests.[19,72,98]

At that time, use of epoxy-coated bars came in lieu of the moisture barrier systems then required on new bridge deck construction. Reinforcing bar coating was done by several companies scattered throughout the nation. These companies were specialized in pipe coating, so they modified their equipment for reinforcing bar coating.[72] The first epoxy powder specifically formulated for reinforcement coating was put on the market in 1976.[122] The industry of coating reinforcing steel grew fast. In 1982, approximately 20 coating applicators were established in the United States and Canada.[86] Because of the special needs

of the developed material, many of the applicators provided a fabrication service, and some were directly involved in field installation of the coated bars.

Recently, the application of epoxy-coated reinforcement in bridge decks and other concrete structures became very widespread. Discussions are almost exclusively limited to non-prestressed type of reinforcement. However, epoxy-coated prestressing strands are also commercially available.[4]

B.5 History of Application of Epoxy-Coated Reinforcement

United States of America. The first bridge deck constructed with epoxy-coated reinforcement is the bridge carrying Route I-576 over the Schuytkill River at West Conshohocken, Philadelphia, Pennsylvania. The construction of the bridge was completed in 1973. Four spans of the 15-span bridge contained epoxy-coated reinforcement.

After the first application of coated reinforcement, subsequent bridge applications were carried out in many states including Florida, Idaho, Delaware, Iowa, and Texas.[4] By the end of 1975, about 40 experimental bridges were constructed using epoxy-coated reinforcement.[1] In 1977, 17 states specified epoxy-coated reinforcing steel as standard procedure in bridge deck construction, and nine more states were carrying out field trials.[2,3,29] Shortly after, the FHWA terminated project NEEP 16 in 1978 ending a successful mission; the majority of the states included epoxy-coated reinforcement in their specifications.

Along with the experimental field applications of epoxy-coated reinforcement, the accelerated corrosion tests of coated bars in concrete slabs conducted by FHWA indicated their long-term effectiveness. The FHWA came to a conclusion in 1981 that the use of epoxy-coated reinforcement is cost-effective and should be adopted as the primary means of corrosion control in bridge decks. In the same year, ASTM produced its first specification to replace the "Interim Specifications for Epoxy-Coated Reinforcing Steel" distributed by FHWA for the NEEP 16 project.

The response of the construction industry and the highway agencies to the new development was warm. By the year 1982, 40 of the 50 state highway agencies specified the use of epoxy-coated reinforcement for new and replacement decks.[19] The snow belt states of the North used the coated bars to protect steel primarily from the deicing salts. However, coastal states, such as Florida, began using the coated bars mainly as a protection from the marine environment. In 1984, the fusion-bonded epoxy-coated welded wire fabric reached the commercial market.[29,57] In 1987, the number of states routinely specifying coated bars in bridges rose to 48.[29] By 1989, 49 states were included.[29]

The use of epoxy-coated reinforcing steel was extended to include many field applications. The following list summarizes these applications:

- Bridge decks, median barriers, and continuously reinforced concrete pavements
- Shafts, piers, and bent caps
- Parking structures
- Foundations, and reinforcement for earth retention

- Seawalls and other marine structures
- Sewage and water treatment plants
- Cooling towers, and power plants
- Chemical plants, and refineries
- Tunnels, end subways

Fusion-bonded epoxy-coated powder coatings became widespread to protect almost any steel reinforcement system embedded in concrete. Reinforcing bars, joint dowels, couplers, welded wire fabric, and prestressing strands can all be provided with epoxy coating.

Florida experience with epoxy-coated bars is unique and is worth reporting. The first sign of corrosion-induced damage on a bridge constructed with epoxy-coated reinforcement in the Florida Keys was observed in 1986. Following some investigations, four major bridges in the Keys were found to have experienced significant corrosion at the substructure.

Fabrication of the coated bars was identified as a major source of deferred corrosion performance in these substructures. Bars bent after coating suffered from damage and debonding of the coating. Corrosion could initiate at the defects and spread under the coating. To prevent recurrence of the problem, the Florida Department of Transportation (FDOT) decided to specify coating after fabrication for the Dodge Island bridge in Miami. However, further investigations have convinced FDOT that epoxy coated reinforcement is inappropriate for marine corrosion protection (splash zone environment).[98]

In 1988, FDOT stopped specifying the use of coated bars in bridge substructures. Four years later, FDOT discontinued the use of epoxy-coated reinforcement in all construction. As a substitute, silica fume concrete is now being used for substructures and calcium nitrite for superstructures exposed to extremely aggressive environments.[98]

Canada. In 1975, research into the reinforcement corrosion problem led to identifying epoxy-coated reinforcement as the most promising solution.[29] Three years later, the Ontario Ministry of Transportation standardized use of epoxy-coated reinforcement for the top mat of bridge decks and in curbs and lane barrier walls.[29,30,81] The implementation was included for bridges under design and in a number of bridges already under contract.

In 1979, the first Canadian bar coating plant was commissioned. Subsequently, use of epoxy-coated reinforcing steel in new bridge structures and in rehabilitation of existing structures increased appreciably. The coated reinforcement was also used in substructure components starting in 1981. At present, there are six Canadian epoxy coating plants.[30] Application of epoxy-coated reinforcement is varied between all steel coated and mixed with uncoated steel. In the world's largest cable-stayed bridge in Vancouver, about 4,000 metric tons (4,400 t) of coated reinforcement were used in the pier and deck.[2]

United Kingdom. The first UK and European production of epoxy-coated reinforcing bars was in Cardiff in 1987.[2,48,115] The pioneer trials were the Colwick Loop Road Bridge in Nottingham, a test section of concrete pavement on motorway M18, and the Cardiff Peripheral Link Road.[2,3,29] Recent applications have included parapets and soffits in bridges,

marine structures for sea defenses and harbor works, silos at chemical plants, pipelines, and water-retaining structures.[2,29]

It was not before the year 1990, when the British standard BS7295 "Fusion Bonded Epoxy-Coated Carbon Steel Bars for the Reinforcement of Concrete" was developed.[29] The published information about this standard indicates that it has, generally, more stringent requirements than its equivalent ASTM (A775 and D3963) specifications.

Germany. The Institute for Reinforcing Steel and Reinforced Concrete Structures (IBS) in Munich, Germany, initiated the first test in Europe to examine the suitability of reinforcing bar coatings as a corrosion protection measure in 1983.[116] The examination of some 40 different coatings showed that fusion-bonded epoxy coatings achieved the best performance with respect to reinforcement corrosion protection. The University of Stuttgart also performed tests with epoxy-coated and PVC-coated reinforcing bars. Tests that followed aimed at identifying the conditions under which epoxy-coated reinforcement should be used and how the quality could be improved.

In the mid 1980's, tests were conducted at the Institute für Bauforschung (Building Research Institute-IBAC) of the RWTH Aachen in cooperation with coating powder manufacturers. The objective was to provide the German market with coatings of improved characteristics.[116]

The Institute für Bautechnik in Berlin (Institute for Building Technology) formed an independent German expert group in 1987 to develop technical guidelines for the production and use of epoxy-coated reinforcement in Germany.[116] The group reviewed the European and American literature and conducted additional tests. Their conclusions were that high powder quality and coating adhesion are the most important parameters for corrosion protection.

German experts discussed issuing harmonized guidelines and standards with Swiss and Dutch groups in the late 1980's. As a result, the published German and Swiss guidelines were very similar. The requirements in these guidelines are close to those in the ASTM A775 standard, but are generally more stringent.[116]

The pioneering and largest project that used epoxy-coated reinforcement in Germany was in cooling towers of a cell re-cooling plant in Ludwigshafen.[116] The second largest project was the Schieβbergstraβe bridge completed in 1990 in Leverkusen. For experimental purposes, bars coated before and after bending were used in the bridge pier caps. Inspection areas were provided to facilitate measurement of macrocell corrosion currents.

Switzerland. The Spiez bridge completed in 1988 was the first civil engineering structure incorporating epoxy-coated bars in the barrier walls.[116] As an exploratory project, the barrier walls were constructed half with coated and half with uncoated reinforcement. Monitoring of the corrosion performance in each half was possible through some inspection areas provided at different levels. Periodic measurements are being taken of the potentials, electric resistances and macrocell currents. Besides acquiring experience in handling and

installation of the coated bars, the project will yield valuable information on the long-term effectiveness of the coated reinforcement.

In 1989, the Swiss Federal Highway Office decided to prepare guidelines for the application of epoxy-coated reinforcing steel.[119] The decision came at a time the industry was fully prepared to produce and supply this material.

Denmark. The first large-scale use of the epoxy-coated reinforcement in Denmark was the Storebaelt railway tunnel, 1990.[116] The tunnel stretches under the Great Belt connecting the Danish Islands of Funen and Zealand. This 7.3 km (4.5 mile), $430 million tunnel is the most extensive pilot project in Europe. A coating plant was constructed on site to deliver approximately 22,000 metric tons (24,200 t) worth $6 million of coated reinforcement. The stringent requirements of minimum damage to coating of reinforcing steel in this project necessitated the use of the fluidized bed dipping process. In this process, full assemblages of welded reinforcement were blasted, heated, dipped in epoxy tanks, and then cooled. Full automation of the coating and quality control checking on coating thickness, holidays, and curing was utilized efficiently.

Middle East. In the Middle East, the use of epoxy-coated reinforcement has spread to many countries along the Arabian Gulf.[7,28,140] The first reinforcing bar coating plant was set up in Abu Dhabi about 10 years ago. Another plant was constructed in Dubai three years later with an initial capacity of 30,000 metric tons (33,000 t) a year. This coating facility in the Jebel Ali free zone has provisions for doubling the initial production capacity. In 1987, a third coating plant was planned for construction near Jubail's steel mill in Saudi Arabia. The new plant was designed to furnish 20,000 metric tons (22,000 t) of coated steel a year for the first phase.

The production of these coating plants was mainly used in the construction of the foundations and lower floors of the buildings. These parts of the construction have the most likelihood of corrosion. Specifying epoxy-coated reinforcing steel in some regions of the Gulf became as a standard for all types of reinforced concrete structures.

B6 Effects Of Epoxy Coating On Structural Behavior

The greatest effect epoxy coating has on the behavior of the composite reinforced concrete member relates to bond strength. Epoxy coating, undoubtedly, reduces the bond strength between concrete and reinforcing steel. Studies have indicated various reduction ranges which were between 5 and 40%.[11,15,29,122,141] Thus, the bond strength loss due to coating is significant. The bond strength reduction depends on the mode of failure whether pullout or splitting. Greater reductions were observed in splitting type bond failures.

Bond between concrete and the reinforcing steel transfers forces between the two materials in the composite section. Force transfer is possible through chemical adhesion, friction and mechanical particle interlock at the concrete/steel interface, and direct bearing of concrete against bar ribs. The epoxy coating diminishes the adhesion and friction between steel and concrete, particularly along the front face of the bar ribs.[122,141,142] Bond strength will thus depend on rib bearing stresses almost exclusively. The coated bars, compared to

uncoated bars, develop higher rib bearing stresses at the same load level. These stresses increase the radial stresses surrounding the bar leading to splitting and early failure.

The contribution of the friction component to the total bond strength depends, primarily, on the bar surface roughness and the irregularities along the concrete/steel interface. Epoxy coating increases the smoothness of the bar surface; breaks the adhesion between concrete particles and the steel; increases the roundness of the ribs; and results in larger apparent slippage deformations due to the low elastic modules of the resin.[11] In effect, the coating eliminates the friction contribution to the bond mechanism resulting in a lower overall bond strength.

Bond strength measurements vary with the type of test and degree of concrete confinement. Reductions of bond strength for coated bars by direct pull out test ranged from 10 to 25%.[122] Splice regions without confining transverse reinforcement failed in splitting at a reduction of about 35%.[29] With the transverse reinforcement, the bond strength reduction was between 15 to 25% depending on bar size.[122]

The effect of bar size on bond strength of the coated reinforcement can be significant. Bond strength reduction is expected to be more pronounced in the case of smaller size bars. The smaller the bar diameter, the smaller the rib height, which will result in less effective rib height and reduced mechanical bond.[29]

The reduction in bond strength of the coated reinforcement was insensitive to variations in coating thickness within the average range of production. For coating thicknesses up to 300 μm (12 mils), the bond strength reductions reported were invariably around 20%.[11,29] Coatings thicker than 375 μm (15 mils) developed unacceptable bond strengths.[15] Excessive coating thicknesses, *i.e.* over 500 μm (20 mils), tend to obscure the deformations of the reinforcing bar which will cause poor bond development between the bar and concrete.[104]

The epoxy coating increases the width and spacing of concrete flexural cracks. The coating causes higher rib-bearing forces to develop that can lead to larger slip, higher bar strain, and eventually wider flexural cracks.[141] The maximum stresses in the coated reinforcement develop at flexural crack locations. Longer transfer lengths are, thus, needed for the coated bars to reduce strain and this systematically increases crack spacing. The amount of increase of crack width and spacing for the coated bars over uncoated bars was about 50%.[29]

The epoxy coating may have a moderate effect on the cracking load and deflections. In one study, the test specimen stiffness measured by cracking load and deflections was not significantly affected by bar coating.[29] In another study, the first crack load was lowered by about 20% for the coated bars compared to uncoated bars. The maximum crack width and deflections were increased by about 10% at design loads.[11]

Tests have indicated that the ultimate load-carrying capacities of the concrete member are not adversely affected by using epoxy-coated reinforcement. Static load tests performed on beam specimens exposed for three years to a marine environment showed that the failure

loads were about 10% higher for the case of coated bars compared to uncoated bars.[11] Under normal laboratory conditions, the ultimate moment capacity was found invariant whether the reinforcement was coated or not.[11] There was also no significant difference in the shear capacity between the two types of reinforcement.[29] The tests showed that the total slip at ultimate load was roughly the same for both coated and uncoated bars.[29]

The effects of repeated loadings on the structural performance of flexural concrete members reinforced with epoxy-coated bars were also investigated. Of particular importance were the load-deflection behavior, flexural crack pattern and width, and bond strength. The investigations usually involve cycling the load between a maximum and a minimum stress level on flexural members and studying the behavior and failure characteristics.

Repetitive load tests on reinforced beams were carried out at Purdue University to study bond behavior of epoxy-coated bars in comparison to uncoated bars. The results showed that specimens with coated reinforcement had fewer flexural cracks at service load conditions.[141,142] The flexural cracks were wider and more widely spaced on the beams containing the coated reinforcement. Such observations were associated with higher stresses in the coated reinforcement at flexural crack locations. As the number of load cycles was increased, the differences in crack widths were reduced. In addition, there was practically no difference in the load-deflection behavior between specimens of both reinforcement types, especially at high number of load cycles.

The concrete cover to bar diameter ratio, and the rib bearing area ratio were found to affect the splitting phenomenon significantly.[141] When the peak repeated stress was increased, the bond strength decreased systematically. A reduction of 10 to 40% was experienced in the bond strength at different stress levels. The epoxy-coated bars themselves do not tend to be affected by repetitive loading. No damage to the coating was observed after two million cycles of loading.[11]

Lower bond strength results in longer transfer lengths. This is currently reflected in the provisions of the design codes for development and splice lengths. The 1989 AASHTO and ACI code ACI 318-89[70] require that the basic development length of an uncoated deformed bar be multiplied by certain factors to get the equivalent for an epoxy-coated bar. Tests on hooked bars in simulated beam-column joints indicated that a 20% increase was necessary.[122] Increasing development lengths to account for bond loss due to coating is more a structural detailing consideration than a major economic impact as far as structural design is concerned. In bridge deck applications, the increase of steel is relatively small since small size bars are usually used.

The outcome of the repetitive load tests indicated that no special precautions are necessary to design members with epoxy-coated reinforcement for fatigue or repeated loading. This is generally true for service load conditions and for cover to bar diameter ratio exceeding 3.0. Concrete cover should be sufficient to provide adequate confinement to the coated bars since their normal and radial stresses are high at the crack locations.[141] The amount of confinement and concrete cover, in turn, have a direct effect on the increase in development length.[142]

B.7 Epoxy Powder Pre-qualification Performance Tests

Accelerated Corrosion and Cathodic Debonding. The test is designed to indicate the resistance of the coated bars to applied voltage. It serves as an accelerated corrosion test and a cathodic debonding test (CDT).[38] The test procedure is derived from ASTM G8 - Part B: Cathodic Disbonding of Pipeline Coatings. Two coated bars (without any detectable holes) are immersed in a strong electrolyte of 7% aqueous NaCl solution. A potential of two volts is applied between the two bars forcing one to be an anode and the other a cathode.

The epoxy film fails the test if evolution of hydrogen gas at the cathode or appearance of corrosion products at the anode is evident during the first hour of testing. The test is run for 30 days. The bars are monitored for holiday development. If holidays occur, no undercutting of the coating at holiday locations is accepted.

If no holidays develop during the test, then single intentional holes 6 mm (0.25 in.) in diameter are made in the coating of both bars. The test is continued for an additional 24 hours in which time no undercutting or loosening of the coating is permitted. The performance of the coated bars in this test correlates well with several coating parameters such as:[30]

- surface preparation and cleanliness;
- degree of coating cure;
- coating application temperature;
- coating thickness; and
- coating foaming (porosity).

The longevity of the test renders it impractical as a routine test in the in-plant quality control program. Since the test has been useful in the pre-qualification program of the epoxy powders, it is suggested that only the last part of the test be evaluated as a potential routine test for inspection or quality control. A new test may then be developed in which the two bar specimens are intentionally damaged, immersed in salt solution, and polarized with a voltage source for only 24 hours. The temperature of the solution, and the voltage applied may also be raised to accelerate the test. In fact, the original CDT test developed for epoxy-coated pipes is run for 24 hours at 65° C (150° F) under 3.5 volts DC.[30] The criteria for the proposed test may be as follows:

- After 24 hours, wedge-shaped cuts should be made in the coating outward from the introduced bare areas.
- Undercutting should not be accepted at the anode bar.
- The debonded region around the bare area on the cathode bar should be measured and recorded (as a radius from the edge of the bare area).
- An evaluation criterion should be developed for the debonded region. The one given for epoxy-coated pipes states that a 10 mm (3/8 in.) radius or less is considered good. A 5 mm (3/16 in.) radius is very good. A region of over 15 mm (9/16 in.) radius is poor.[30]

Chemical Resistance. The chemical resistance of epoxy coatings is evaluated following ASTM G20 by immersing the bars in different solutions simulating different environments. The coating must not blister, soften, loose bond, nor develop holidays during the 45 day test period.[15,38] No undercutting is accepted around intentionally introduced holes, 6 mm (0.25 in.) in diameter, in the coating.

Impact Resistance. The test of coating resistance to mechanical damage is similar to the falling weight test described in ASTM G14. An impact of 9 Nm (80 in.lbf.) should not result in shattering, cracking or debonding of the coating except at the impact area. The impact test results are normally affected by surface preparation, application temperature, and coating cure.

Abrasion Resistance. Coated steel panels are tested for coating abrasion resistance. The test is done with a Taber abrader or its equivalent, using cs-10 wheels and a 1 kg (2.2 lb.) load.[38] After 1000 cycles of abrasion, the measured weight loss must not exceed 100 mg (3.5×10^{-3} oz.).

Coating Hardness. The relative resistance of the epoxy coating to mechanical damage producing scratching, cutting, indentation, *etc.* is assigned a hardness value. Two methods are used to evaluate coating hardness: the pencil method; and the indentation method.[15,30]

The pencil hardness method is used to define coating softening. The procedure is outlined in NACE standard TM 0174-74. The hardness is designated as the softest lead between H and 8H that imparts a scratch in the coating.

The indentation hardness method follows ASTM D1474. The method is based on measuring indentations, using a 0.01 kg (0.022 lb.) weight, which makes it more quantitative and reproducible than the first method.[15,30]

Chloride Permeability. The coating chloride permeability test procedure is given in Report No. FHWA-RD-74-18.[15] The limit of accumulative chloride ion concentration permeability through the film is 1×10^{-4} M.

Bond Strength to Concrete. The bond strength between the coated bars and concrete is determined by pull-out tests as described in Report No. FHWA-RD-74-18.[15] The mean bond strength for coated bars must not fall below 80% of that for uncoated bars.

Creep. The creep test performed on epoxy-coated bar specimens cast in concrete prisms is described in Report No. FHWA-RD-74-18.[15] It is particularly useful when the coating material contains appreciable amounts of additives. The slip-ratio of coated bars to uncoated bars must not exceed 1.3 for free-end slip or 1.6 for loaded-end slip.

B.8 Other Tests

Microscopic Examination. Microscopic examination of the epoxy film underside and cross section can show the foam distribution at surface and through the film (Foam is defined

as porosity divided by voids). The foam level, which correlates with the cured film density, is an indicator of the application temperature.[30] Voids created within the film can affect its adhesion, elasticity, and protective qualities.[12] A foam content rating system has been developed and a guide (shown in Fig. B.1) is used as basis for comparison.

The underside of chipped epoxy pieces can also be examined for the level of contamination (called underfilm or backside contamination). The contaminate is actually the mill scale or remaining material on the reinforcing bat after blast cleaning (in the surface preparation stage). Contamination is visually apparent as dark residue adhered to the epoxy film underside. By microscopic examination and comparison to photographic examples (similar to those shown in Fig. B.2), it is possible to determine the percentage of contamination. Significant backside contamination could lead to poor adhesion.[30]

The microscopic examination is a useful tool to supplement the evaluation of the coating quality and surface preparation. It should be used often in the coating plant to assure proper production.

Scanning Electron Microscopy (SEM). The scanning electron microscope examination of the steel surface is very effective for detecting contamination or flaws, and to study the surface morphology.

Energy Dispersive X-Ray Spectroscopy (EDXS). Chloride residue at the steel/coating interface, and across the film thickness, can be determined by use of the energy dispersive X-ray spectroscopy. Coating impurities can also be found using this technique.

Bond Strength to Steel. There is not a standard test for quantitatively evaluating the adhesion of the epoxy coating to the steel substrate. The bond condition is an important indicator of the quality of protection the coating will offer. The different research studies have only dealt with this aspect qualitatively.

A test device and a test procedure have been developed at the University of Southern Florida to obtain a quantitative measure of the bond.[114] The degree of adhesion between the epoxy coating and the steel is determined by the force applied to pull off a small amount of the coating using the developed device.

AC Resistance. A newly developed test is the AC resistance measurement which yields a quantitative rating of the coating quality and condition.[30] The tested coated reinforcing bar is capped first at one end with a heat shrinking cap and adhesive. Then, it is conditioned in limewater for a certain period of time. Afterwards, a measured surface area of the bar is exposed when placed in a stainless steel beaker filled with limewater. The AC resistance between the bar and the beaker is measured and analyzed. Both straight and bent bars can be tested using this apparatus.

Moisture Permeability. Organic coatings are moisture permeable, and some are water absorbent. Moisture permeation and water absorption tests can be used to determine the sensitivity of the coating to water penetration and weight gain, respectively. The coating might be altered by moisture such that the hardness and adhesion properties are changed.

Softening and blister formation are typical deterioration indicators. Good coatings should retain good adhesion to the underlying steel.

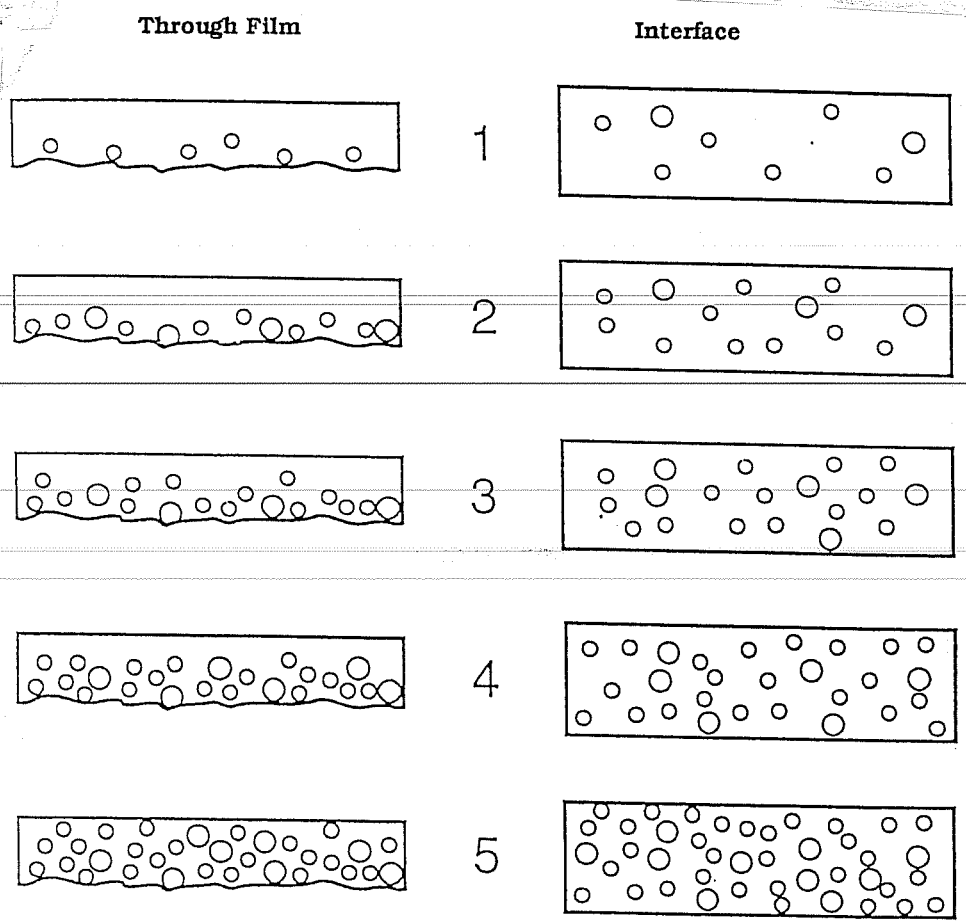

Figure B.1 Foam Evaluation Guide (Bell & Stephens Laboratories).[30]

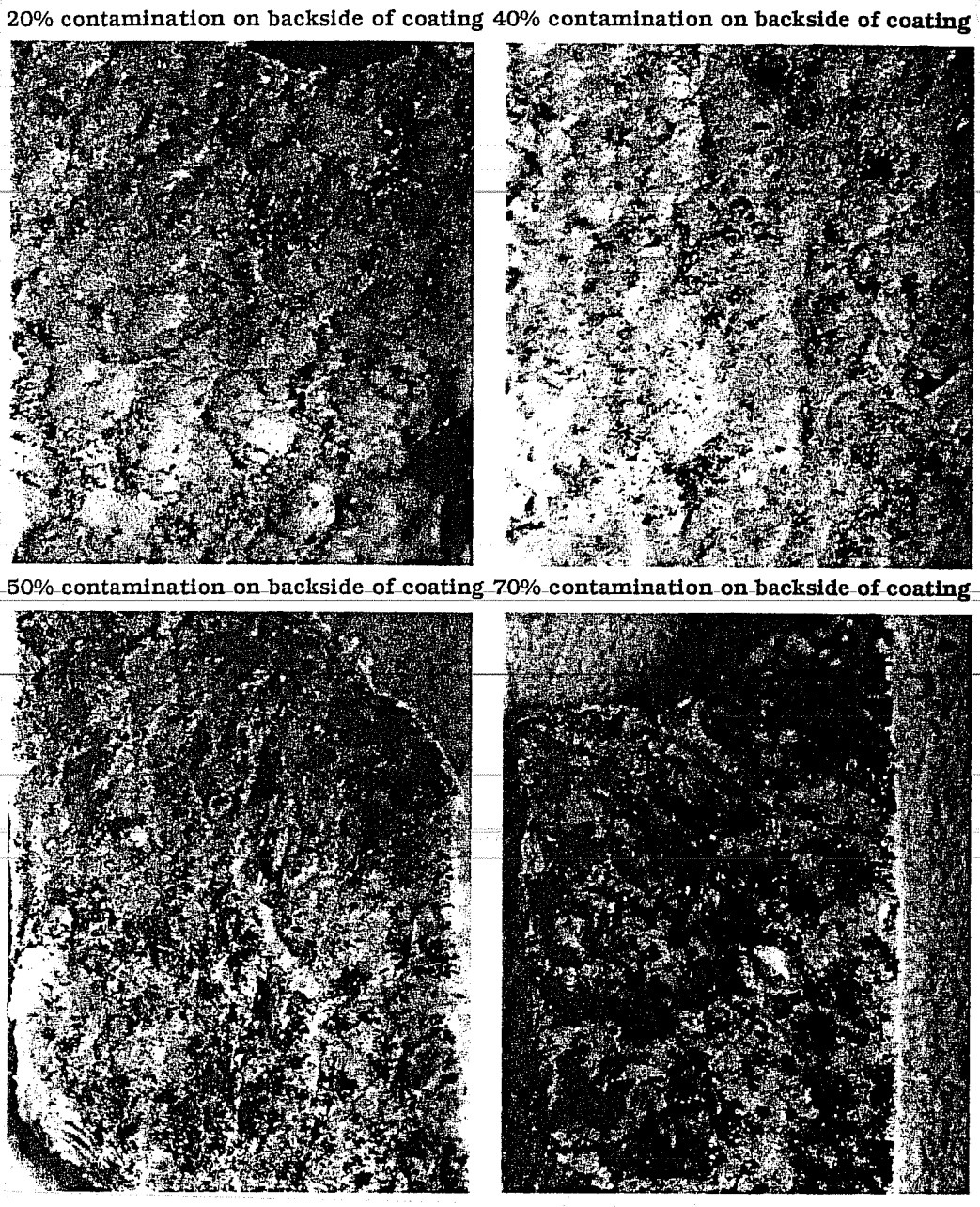

Figure B.2 Examples of Coating Backside Contamination.[30]

Differential Scanning Colorimeter (DSC). The differential scanning colorimeter is a technique based on thermal analysis applicable to both fresh powder and applied coating. The DSC scans can show phase transition, polymerization, curing, thermal degradation, and thermoxidative stability.[30] Although the technique has some pitfalls, it is still considered an option for quality assurance, especially with epoxy-coated pipes.

Fourier Transform Infra-red Spectroscopy (FT-IR). The degree of curing of the fusion-bonded epoxy coating can be determined by thermal analysis using fourier transform infra-red spectroscopy. The epoxy material sample size, stress state (if cured), and impurities do not affect the analysis so that the results are reproducible.[30]

APPENDIX C
DETAILS OF MACROCELL CORROSION TEST

C.1 Test Variables

General. The test variables were selected after reviewing current practice and governing standards and specifications of epoxy-coated reinforcement. Bars with standard bends were used in all the macrocell tests because they represent a category of bars most vulnerable to coating damage and increased susceptibility to corrosion.

Reinforcement. Uncoated and epoxy-coated steel bars were included to compare their corrosion performance. The performance of "as received" uncoated steel was the standard against which the performance of coated steel, with different surface conditions, was compared.

Bar Diameter. Two diameters, 13 mm (#4) and 25 mm (#8) were selected. Small bar represents reinforcement used in bridge construction for decks and for transverse reinforcement (ties and stirrups). The large bars are typical of longitudinal reinforcement in support structures.

Bar Deformation Pattern. Bars with parallel and cross rib patterns were chosen for the study. The deformation pattern may affect the quality of coating and coating defects produced during bending.

Epoxy Coating Damage Level. Previous testing of bent bars reported in the literature has shown that considerable coating damage and debonding may seriously impair the corrosion resistance. Therefore, the degree of mechanical damage to the epoxy coating was the principal variable in the macrocell study.

Current specifications, such as ASTM A775,[38] ASTM D3963,[39] and AASHTO M284,[99] and the CRSI guidelines for inspection and acceptance of epoxy-coated reinforcing bars at the job site,[95] set limits on acceptable coating damage. The limits specified by ASTM D3963 and incorporated in AASHTO M284 (also adopted to a great extent by CRSI guidelines) form the basis of the selected damage for corrosion testing (see Section 3.4.1). The damage level was selected to verify the adequacy of these limits, and to asses whether or not stricter specification requirements were needed.

One category of damage was spots on the outside of bends with a loss of coating slightly greater than 6 x 6 mm (1/4 x 1/4 in.), the acceptable damage size limit. Another category included bars with smaller, but more frequent, damage spots. In this case, the percentage of total damaged area to bar surface area in contact with concrete was slightly above the 2% permissible limit. Hairline cracking along the transverse ribs on the outside of the bend was the third category. Here, the total percentage of damage did not exceed 1% of the bar surface area. Pinholes or small damaged spots, and sometimes the "as received"

condition, constituted the fourth damage category marked by damage percentage less than 1 or 2%. In all cases, damage on the inside of bends, in the form of small mandrel impressions, was included in calculations of percentages.

Repair of Damage. The damaged areas of coating on the outside of the bend were either repaired or left unrepaired as another variable in the test. Repairs (patching) were done according to the manufacturer's instructions using a liquid epoxy patching material and recommended touch-up techniques. To evaluate the effectiveness of repairing, the damaged areas on some bars were repaired while similar damaged areas on other bars were not. The intent was to examine the patched areas because the application process is quite different from the plant-applied, fusion-bonded epoxy coating.

C.2 Specimen Design

General. One of the requirements of this test was to simulate the conditions of concrete bridge deck slabs exposed to chloride-based deicing salts. The primary destructive mechanism of such bridge slabs is the corrosion-induced deterioration related to macrocell action. Corrosion develops as a result of the anodic activity on the top reinforcing layer intercepted by the intruding chlorides, and the cathodic activity on the bottom layer resting in chloride-free concrete.

To simulate such conditions, concrete prisms were designed with two reinforcing layers. The test bars were placed at the top (anode) of the macrocell model. The bottom bars were all uncoated and served as the cathode. A direct electrical link was provided between the two reinforcing layers to allow the corrosion cell to operate. To accelerate corrosion, a wet-dry cyclic exposure regime was selected. The top concrete surface was ponded, intermittently, with chloride solution to supply the chloride ions necessary for accelerated corrosion initiation.

Test bars were divided into two series, denoted A and B, referring to the two bar diameters 13 mm (#4) and 25 mm (#8), respectively. Two different prism configurations were designed for these two series. A third series of smaller plain concrete prisms, denoted C, was designed to provide additional specimens for the determination of chloride content in concrete over the duration of exposure testing.

Series A. The details of Series A test specimen are shown in Fig. C.1. The outer dimensions of the concrete prism were 200 x 200 x 180 (height) mm (8 x 8 x 7 in.). The top reinforcing layer consisted of a single 13 mm (#4) bar with a 180° bend (after rebound on a mandrel diameter of 50 mm (2 in.)). Bending was done in accordance with ACI 318-89[70] requirements for minimum bend diameters for stirrups and ties.

The bottom reinforcing layer consisted of two straight uncoated 19 mm (#6) bars. The choice of the size and number of these bars was based on a calculated surface area ratio of bottom to top steel of approximately 1.4. Only the embedded portions of these bars and their nominal surface areas were considered in the calculations. The ratio provided a theoretical index of the corrosion driving force assuming the total steel surface area beneath the coating to be the anode.

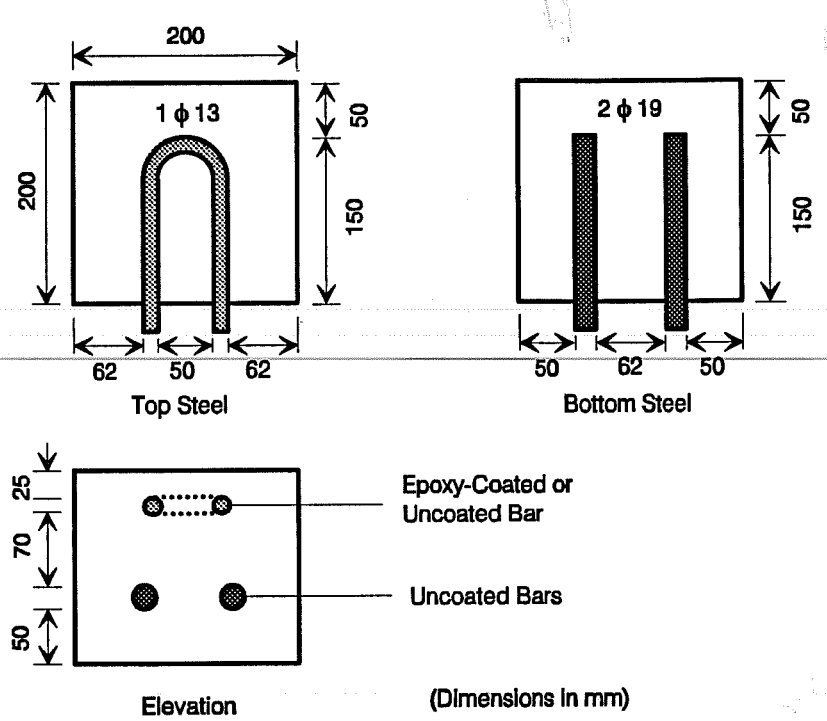

Figure C.1 Details of Series A Macrocell Specimen.

The clear concrete cover over the top bar was only 25 mm (1 in.) to accelerate the onset of corrosion. The distance between the two reinforcing layers was 70 mm (2.75 in.). The concrete cover on all sides and under the bottom bars was 50 mm (2 in.).

Series B. The details of Series B test specimen are shown in Fig. C.2. The outer dimensions of the concrete prism, in this case, were 300 x 230 x 200 (height) mm (12 x 9 x 8 in.). The reinforcement details were similar to those of Series A except for the following: the top reinforcement was a 25 mm (#8) bar bent on a mandrel diameter of 150 mm (6 in.) (a standard in ACI 318-89); the bottom straight reinforcement consisted of three-28 mm (#9) bars; and the clear distance between the two reinforcing layers was 73 mm (2.88 in.).

The ratio of the surface area of bottom steel to top steel embedded in concrete was also 1.4. The ratio was kept a constant for specimens with both bar diameters to provide the same theoretical corrosion driving force. In addition, the distance between the reinforcing layers was roughly equal in both cases in an attempt to maintain similar ionic flow through concrete between layers.

Series C. The determination of chloride content in concrete, particularly at the steel level, is an important consideration in any corrosion study. The chloride concentration was measured periodically to relate changes in the corrosion behavior to variations in chloride level around the steel. Chloride determination requires extracting concrete powder by drilling holes in the specimen. Since this operation is destructive, the test specimens themselves could not be sampled because the salt solution used for contaminating the concrete would accumulate in the hole and disturb the uniformity of exposure.

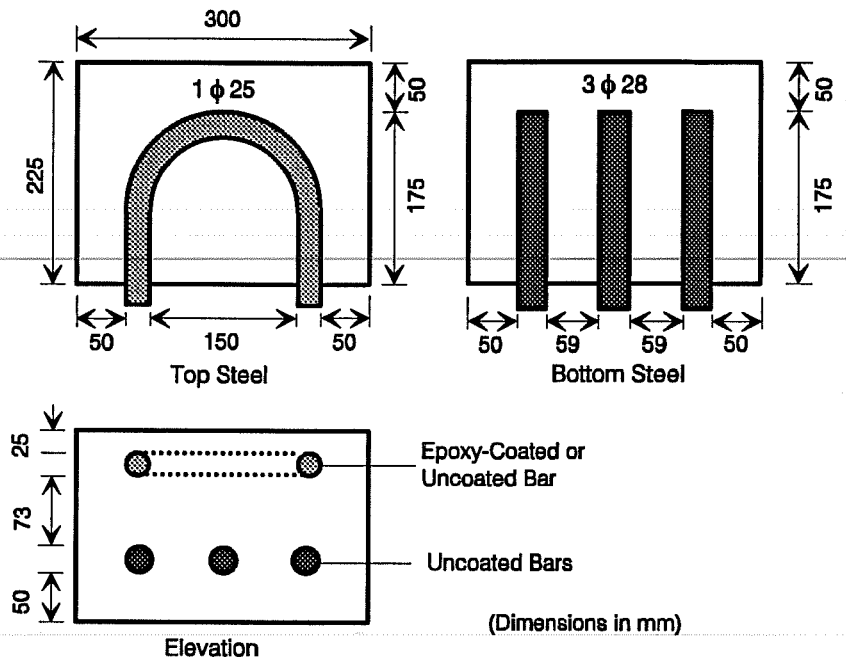

Figure C.2 Details of Series B Macrocell Specimen.

Another series of unreinforced concrete prisms was constructed to enable chloride determination without disturbing the macrocell specimens. The prisms were cast from the same concrete as Series A and B. The dimensions of the prisms were 180 x 170 x 150 (height) mm (7 x 6.75 x 6 in.). The specimens in three series were subjected to the same exposure conditions so that chloride concentrations in the concrete were expected to be nearly the same.

C.3 Epoxy-Coated Reinforcing Steel

Steel Procurement. The epoxy-coated reinforcing bars (12 m (40 ft.) length) used in this test were plant-coated and selected from a normal production run. The coating plant is a major supplier of coated bars to the TxDOT projects. The bars were coated with a commercially available and widely used coating material in the US approved for use by the TxDOT. The coating material was certified as conforming to ASTM A775/A775 M-90, ASTM D3963-86, ASTM A884-88, AASHTO M284-86, and AASHTO M254-77. All bars were Grade 60 meeting ASTM A615-87a.[143]

Uncoated bars from the same heat of steel (for each bar size and rib pattern) were also obtained to be used as control specimens. The chemical analysis of the steel according to certified test reports available at the coating plant is shown in Table C.1. There were no significant differences in steel composition among the different bar groups.

Table C.1 Chemical Analysis of Steel for Macrocell Study
(Mill Test Report: Percent by Weight)

Composition	13 mm Bars Parallel	13 mm Bars Cross	25 mm Bars Parallel	25 mm Bars Cross
C	0.37	0.42	0.43	0.38
Mn	0.85	0.95	0.98	0.89
P	0.017	0.023	0.011	0.031
S	0.037	0.027	0.033	0.054
Si	0.29	0.23	0.29	?
Cu	0.5	0.36	0.48	?
Cr	0.17	0.13	0.14	?
Ni	0.16	0.12	0.19	?
Mo	0.029	0.04	0.05	?
Other	0.007	0.015	0.024	?

The bars were cut in 3 m (10 ft.) lengths by the coating applicator. The bars were bundled and firmly wrapped with protective polyethylene layers to avoid damaging the coating during handling and transportation. At the laboratory, the bars were cut to the required lengths and the coating thickness was measured. Afterwards, the bars were wrapped again and shipped back to the coating plant for fabrication.

At the coating plant, a bar bender equipped with high density plastic sleeves over steel mandrels was used to fabricate the bars into the required "U" shape. During bending, some coating damage was inadvertently introduced, especially on the inside of bends, where ribs were pressed against the mandrels. Damage was in the form of some mashed coating spots on the ribs. The bars were carefully shipped back to the laboratory to avoid further damage to the coating.

Bar Identification. Series A and B each had 11 groups of three replicate specimens distinguished by the test variables summarized in Table C.2. The specimens are identified by a three character label: the order within the group (1-3); series type (A or B), and group number (1-11). For example, specimen 1 A.1 is the first specimen in group 1 of Series A, the 13 mm (#4) bar series, and it is a control specimen. Specimen 3 A.2 is the third replicate in group 2 of Series A and contains an epoxy-coated bar with damaged spots slightly greater than 6 x 6 mm (1/4 x 1/4 in.) patched before concrete placement. Specimen 3 B.2 is similar to 3 A.2 except for the bar size.

Table C.2 Macrocell Test Group Summary

Group Number		Deformation Pattern	Coating Damage[c]	Damage Condition
Series A[a]	Series B[b]			
A.1	B.1	Parallel	"Control" Uncoated Bars	
A.2	B.2	Parallel	Spots > 6 x 6 mm	Patched
A.3	B.3	Parallel	Spots > 6 x 6 mm	Not Patched
A.4	B.4	Parallel	Spots > 2%	Patched
A.5	B.5	Parallel	Spots > 2%	Not Patched
A.6	B.6	Parallel	Cracks < 1%	Not Patched
A.7	B.7	Parallel	Spots < 2%	Not Patched
A.8	B.8	Cross	"Control" Uncoated Bars	
A.9	B.9	Cross	Spots > 6 x 6 mm	Patched
A.10	B.10	Cross	Spots > 6 x 6 mm	Not Patched
A.11	B.11	Cross	As Received < 1%	Not Patched

a 13 mm (#4) bar series.
b 25 mm (#8) bar series.
c Refer to either the size of damaged spots or percentage of damaged area to bar surface area embedded in concrete.

Two more isolated specimens were added to the list of test specimens. The first was a 13 mm (#4) epoxy-coated bar with parallel rib deformations. The bar was bent conventionally on an unprotected metallic mandrel and no additional damage was introduced. The specimen is designated 1 A. and had no replicates. The other added specimen was a 25 mm (#8) epoxy-coated bar with cross rib deformations. The coating of the bar was so thin that the dark steel substrate was partially visible. This specimen was designated 1 B. and also had no replicates.

Steel Tensile Strength. Two coated steel samples of each bar size and deformation pattern were tested to obtain the tensile yield strength, yield strain, and ultimate strength. No significant differences existed between the results of the replicate test samples. Therefore, the average test values were used to construct the stress-strain curves shown in Fig. C.3 and C.4. The measured strengths conformed to the requirements of ASTM A615-87a,[143] as all yield strengths exceeded 414 MPa (60 ksi) and all ultimate strengths exceeded 621 MPa (90 ksi). The average yield strength of the small and large size bars were 486 and 439 MPa (70.4 and 63.6 ksi), respectively.

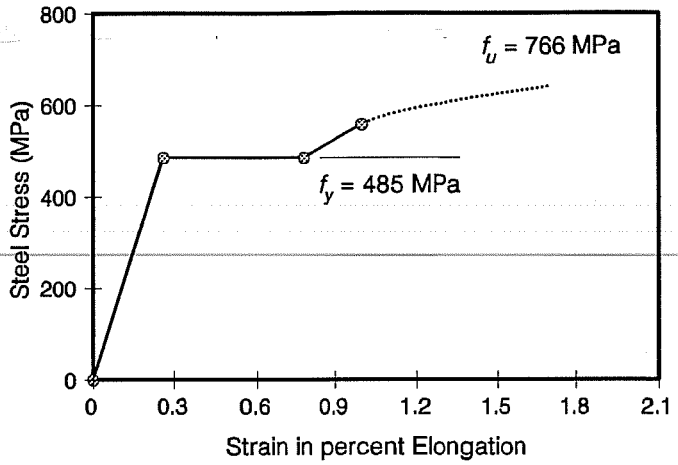

(a) Parallel Deformation Pattern

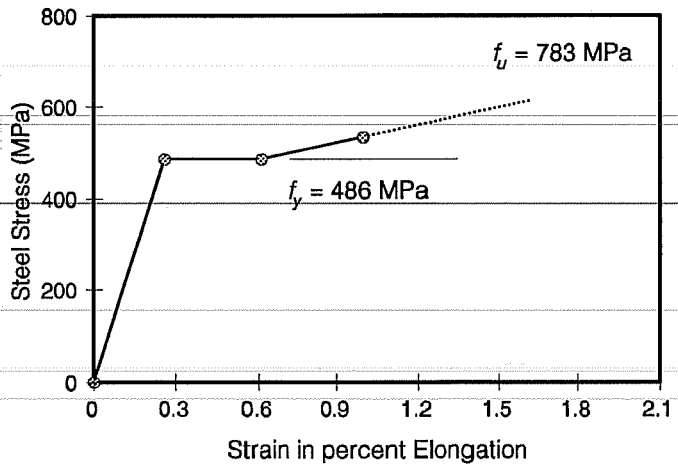

(b) Cross Deformation Pattern

Figure C.3 **Stress-Strain Curves for 13 mm Bars.**

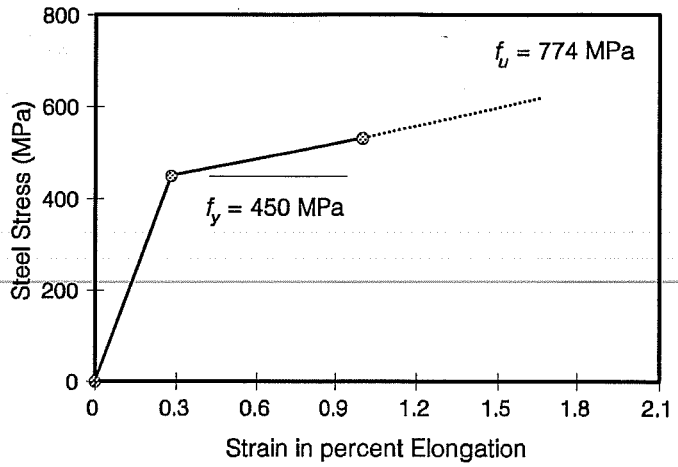

(a) Parallel Deformation Pattern

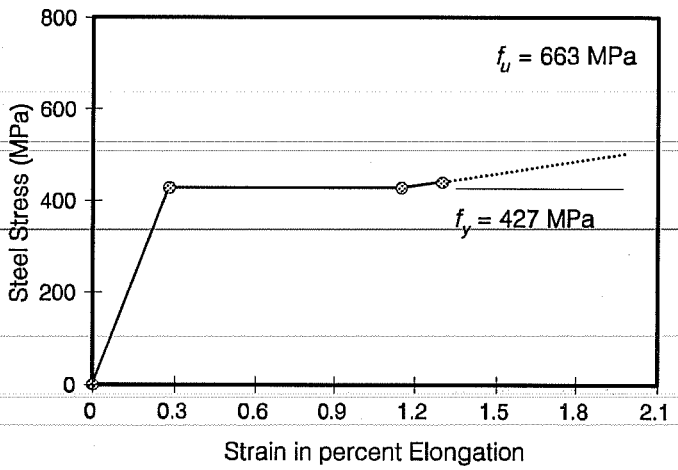

(b) Cross Deformation Pattern

Figure C.4 **Stress-Strain Curves for 25 mm Bars.**

Epoxy-Coating Thickness. A thumbwheel pull-off magnetic gage was used to measure the coating thickness of the epoxy-coated bars before bending (see Fig. C.5). Coating thickness was measured at three locations on each side of the bar; a side being considered the bar surface between longitudinal ribs. The procedure described in ASTM G12-83[144] was followed. Coating thickness was obtained only on areas between the deformations, and ribs, on straight lengths in accordance with ASTM A775[38] and ASTM D3963.[39] For each bar specimen, the average coating thickness of six measurements and the maximum deviation in thickness from the average are reported in Tables C.3 and C.4.

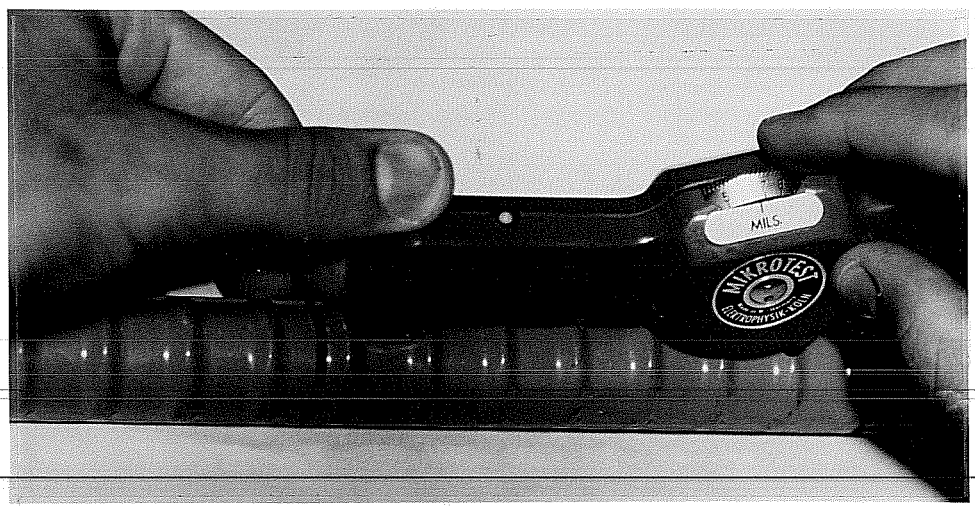

Figure C.5 Coating Thickness Measurement Using a Magnetic Gage.

Both ASTM A775 and ASTM D3963 require that at least 90% of all recorded film thickness measurements be between 130 and 300 μm (5-12 mils). The first specification further requires that the deviation in coating thickness not exceed $\pm$50 μm ($\pm$2 mils) or $\pm$30% from the average thickness, whichever is less. All coating thickness measurements were equal to or greater than 130 μm (5 mils). However, 22 readings, or 18% of all measurements, exceeded 300 μm (12 mils). The maximum thickness was 350 μm (14 mils). In addition, the deviation in coating thickness of almost half of all steel specimens fell beyond the allowable limits. Thus, there was a lack of uniformity in the coating thickness and the specifications were not strictly met.

In general, the 13 mm (#4) bar specimens had slightly thicker coatings than the 25 mm (#8) bar specimens. The average coating thickness of the smaller size bars with parallel and cross deformations were 250 and 270 μm (9.9 and 10.5 mils), respectively. The corresponding average coating thickness of all the larger size bars were 240 μm (9.5 mils). The differences in average coating thickness between bars with different deformation patterns were insignificant, although bars with cross deformations tended to be slightly thicker than those with parallel deformations. The overall average coating thickness was approximately 250 μm (10 mils).

Table C.3 Coating Thickness Measurements, Series A
(130 μm = 5 mils, 300 μm = 12 mils)

Specimen	Average Coating Thickness (μm)	Maximum Deviation from Average	
		(μm)	(%)
1 A.2	250	+85	34
2 A.2	220	+68	30
3 A.2	290	+38	13
1 A.3	280	+55	20
2 A.3	220	+59	27
3 A.3	240	+38	16
1 A.4	240	+42	18
2 A.4	310	+25	8
3 A.4	250	+81	32
1 A.5	230	+46	20
2 A.5	240	+36	15
3 A.5	240	+13	5
1 A.6	270	+40	15
2 A.6	220	+55	25
3 A.6	290	+38	13
1 A.7	240	-40	16
2 A.7	220	+21	10
3 A.7	290	+68	24
1 A.9	270	+85	31
2 A.9	280	-97	35
3 A.9	280	+55	20
1 A.10	260	-55	21
2 A.10	280	+46	16
3 A.10	230	+27	12
1 A.11	250	+85	34
2 A.11	240	+51	21
3 A.11	280	+81	29
1 A.*	280	+55	20

Table C.4 Coating Thickness Measurements, Series B
(130 μm = 5 mils, 300 μm = 12 mils)

Specimen	Average Coating Thickness (μm)	Maximum Deviation from Average	
		(μm)	(%)
1 B.2	290	+66	23
2 B.2	220	-29	13
3 B.2	250	+59	24
1 B.3	270	-61	23
2 B.3	230	-40	17
3 B.3	220	+89	41
1 B.4	260	-27	11
2 B.4	230	-72	31
3 B.4	220	-46	21
1 B.5	250	+53	21
2 B.5	250	-49	19
3 B.5	240	-40	16
1 B.6	240	+68	29
2 B.6	260	+44	17
3 B.6	220	+38	18
1 B.7	280	-51	18
2 B.7	220	+59	27
3 B.7	250	+57	23
1 B.9	260	+42	16
2 B.9	240	+49	20
3 B.9	240	+66	27
1 B.10	240	-27	11
2 B.10	260	+42	16
3 B.10	180	-53	29
1 B.11	230	+51	22
2 B.11	250	+30	12
3 B.11	200	-42	17
1 B.*	170	+64	38

The uniformity of coating thickness did not relate to bar size or deformation pattern. This was concluded from calculations of the difference between the highest and lowest measured coating thickness on each individual bar. The difference was expressed as a percentage of the bar average coating thickness. The results of these calculations were compared between the bars of different sizes and different deformation patterns and no consistent trend was apparent.

The bars in each group of Series A and B were carefully selected in order to minimize the effect of coating thickness variability on the corrosion performance. The criterion of selection was that the average thickness of coating of bars in a group was not significantly different from group to group. Hence, any difference in the corrosion behavior among the groups would be related to the study variables discussed earlier. For example, a difference between the average corrosion rate of bars in A.2 group and that of A.3 group would be due solely to patching the damaged spots on group A.3 bars. The average coating thickness for each group in Series A and B are shown in Table C.5.

Coating Defects And Introduced Damage. The bars were carefully inspected before deliberately introducing further damage. As mentioned earlier, despite the protection on the mandrels used for bending, impressions on the ribs along the inside of bends were introduced. In addition, the backup barrel (a pin which holds the bar straight during bending) generally caused one or two relatively large damaged spots on the outside surface near the beginning of bend. These damage areas, and any others, were included in the calculations of the required additional exposed steel areas to reach the levels of damage set for testing.

The condition of each bar was carefully documented. The documentation included the coating appearance, and the number, approximate size, and location of existing damage. A commercially available holiday detector (SPY Model 67) was used to determine the number and location of holidays. The majority of bars had the same uniform, glossy appearance. Only few bars had either slightly discolored coating, or very thin films through which the dark substrate was visible. Except for this last group of thinly-coated bars, coating coverage was fair and the deformations were well-defined.

Some bars, particularly the 13 mm (#4) bars with parallel deformations, disclosed hairline cracking along the transverse ribs on the outside of bends. The cracks extended between approximately 6 to 12 mm (1/4 to 1/2 in.). Sometimes, these cracks appeared at almost every transverse lug in the bend area. Cracks on bars with cross deformations were generally in the form of very fine intermittent tears (pinholes) concentrated along the rib bases. In all cases, no discernable debonding was detected.

Where additional surface damage was desired, damage was purposely introduced on the outside of bends. File marks were made at the transverse lugs and in between the lugs in small rectangular shapes using a sharp blade. Coating prying was easier on the bar surface than on the lugs, and even easier on the bent portion compared to the straight ends. Generally, the coating on the straight ends was tough and difficult to pry. Some of the coating flakes removed showed dark spotting on the backside.

Table C.5 Group Average Coating Thickness for Macrocell Steel Specimens

Series A		Series B	
Group Number	**Average Coating Thickness (μm)**	**Group Number**	**Average Coating Thickness (μm)**
A.2	250	B.2	250
A.3	250	B.3	240
A.4	260	B.4	240
A.5	240	B.5	250
A.6	260	B.6	240
A.7	250	B.7	250
A.9	270	B.9	250
A.10	260	B.10	230
A.11	250	B.11	220

The introduced damage was documented and each bar was photographed for a record of initial conditions. Tables C.6 to C.9 list descriptions of the introduced damage, the total steel surface area damaged, and the total damage percentage for each bar. Figures C.6 to C.12 show examples of the damaged bars included in the macrocell test.

Only the introduced damaged areas on bar specimens in groups A.2, A.9, B.2, and B.9 were patched. A two-part liquid epoxy, especially formulated for coating repair, was applied by brush. The exposed steel areas were not given any special treatment before patching. Figure C.13 shows examples of patched damaged areas on two test bars.

C.4 Uncoated Reinforcing Steel

Anode Steel Bars. The uncoated bars used as control specimens were left in their "as received" condition, *i.e.* with mill scale. These bars represent, as closely as possible, bars placed in the field.

Cathode Steel Bars. All bars used in the bottom reinforcing layer of the specimens were grade 60 with a parallel deformation pattern. The bars of each size, the 19 and 28 mm diameters (#6 and #9), were obtained from the same heat of steel so that they would have the same chemical composition and mechanical properties. This selection ensured that the rates of corrosion of the anodes were not influenced by differences in the electrical properties of the cathodes.

Table C.6 Description of Coating Damage of Steel Specimens, Series A, Parallel Deformations

Specimen	Introduced Damaged Area		Total Steel Area Damaged[a] (mm^2)	Total Damage Percentage (%)	
	No. and Size (mm)	Condition		Patched[b]	Exposed
1 A.2	1 Spot 10 x 7	Patched	160	0.56	0.64
2 A.2	1 Spot 10 x 9	Patched	160	0.64	0.57
3 A.2	1 Spot 10 x 8	Patched	160	0.58	0.61
1 A.3	1 Spot 10 x 8	Exposed	160	-	1.23
2 A.3	1 Spot 11 x 8	Exposed	160	-	1.22
3 A.3	1 Spot 11 x 8	Exposed	160	-	1.21
1 A.4	7 Spots 5 x 2 8 Spots 5 x 4	Patched	280	1.57	0.54
2 A.4	7 Spots 5 x 2 8 Spots 5 x 4	Patched	280	1.60	0.56
3 A.4	7 Spots 5 x 2 8 Spots 5 x 4	Patched	280	1.56	0.56
1 A.5	7 Spots 5 x 2 8 Spots 5 x 4	Exposed	270	-	2.09
2 A.5	7 Spots 5 x 2 8 Spots 5 x 4	Exposed	270	-	2.08
3 A.5	7 Spots 5 x 2 8 Spots 5 x 4	Exposed	270	-	2.08
1 A.6	(Existing Cracks)	Exposed	80	-	0.65
2 A.6	(Existing Cracks)	Exposed	80	-	0.62
3 A.6	(Existing Cracks)	Exposed	80	-	0.65
1 A.7	3 Spots 5 x 5 5 Spots 2 x 2	Exposed	160	-	1.23
2 A.7	5 Spots 5 x 4	Exposed	160	-	1.22
3 A.7	5 Spots 5 x 4	Exposed	160	-	1.22

a Area includes damage on both the inside and outside of bend.
b Only introduced damaged area on the outside surface of bend was patched.

Table C.7 Description of Coating Damage of Steel Specimens, Series A, Cross Deformations

Specimen	Introduced Damaged Area		Total Steel Area Damaged[a] (mm^2)	Total Damage Percentage (%)	
	No. and Size (mm)	Condition		Patched[b]	Exposed
1 A.9	1 Spot 11 x 10	Patched	160	0.81	0.43
2 A.9	1 Spot 11 x 10	Patched	160	0.81	0.41
3 A.9	1 Spot 11 x 10	Patched	160	0.81	0.46
1 A.10	1 Spot 10 x 10	Exposed	160	-	1.20
2 A.10	1 Spot 11 x 10	Exposed	160	-	1.23
3 A.10	1 Spot 11 x 10	Exposed	160	-	1.20
1 A.11	(Existing Pinholes)	Exposed	90	-	0.68
2 A.11	(Existing Pinholes)	Exposed	80	-	0.57
3 A.11	(Existing Pinholes)	Exposed	80	-	0.64

a Area includes damage on both the inside and outside of bend.
b Only introduced damaged area on the outside surface of bend was patched.

Table C.8 Description of Coating Damage of Steel Specimens, Series B, Parallel Deformations

Specimen	Introduced Damaged Area		Total Steel Area Damaged[a] (mm^2)	Total Damage Percentage (%)	
	No. and Size (mm)	Condition		Patched[b]	Exposed
1 B.2	2(9 x 7) + 2(13 x 4)	Patched	520	0.66	0.85
2 B.2	2(10 x 6) + 2(13 x 5)	Patched	510	0.70	0.79
3 B.2	2(10 x 6) + 2(13 x 6)	Patched	510	0.82	0.64
1 B.3	2(10 x 7) + 2(14 x 4)	Exposed	500	-	1.47
2 B.3	2(10 x 7) + 2(14 x 4)	Exposed	500	-	1.45
3 B.3	2(10 x 6) + 2(14 x 6)	Exposed	500	-	1.46
1 B.4	16(5 x 5) + 12(6 x 2)	Patched	740	1.51	0.65
2 B.4	16(5 x 4) + 12(6 x 2)	Patched	730	1.34	0.76
3 B.4	16(5 x 5) + 12(5 x 2)	Patched	740	1.45	0.70
1 B.5	16(5 x 4) + 12(5 x 2)	Exposed	770	-	2.24
2 B.5	16(5 x 5) + 12(5 x 2)	Exposed	750	-	2.19
3 B.5	16(6 x 5) + 12(5 x 2)	Exposed	740	-	2.13
1 B.6	6 Hairline Cracks	Exposed	300	-	0.89
2 B.6	6 Hairline Cracks	Exposed	300	-	0.84
3 B.6	6 Hairline Cracks	Exposed	300	-	0.86
1 B.7	5(6 x 5) + 6(6 x 2)	Exposed	410	-	1.19
2 B.7	5(5 x 5) + 4(5 x 2)	Exposed	410	-	1.19
3 B.7	5(5 x 5) + 6(6 x 2)	Exposed	390	-	1.11

a Area includes damage on both the inside and outside of bend.
b Only introduced damaged area on the outside surface of bend was patched.

Table C.9 Description of Coating Damage of Steel Specimens, Series B, Cross Deformations

Specimen	Introduced Damaged Area		Total Steel Area Damaged[a] (mm^2)	Total Damage Percentage (%)	
	No. and Size (mm)	Condition		Patched[b]	Exposed
1 B.9	1 Spot 11 x 6 1 Spot 10 x 6 1 Spot 25 x 2 1 Spot 16 x 3	Patched	330	0.64	0.30
2 B.9	1 Spot 11 x 6 1 Spot 10 x 7 1 Spot 29 x 2 1 Spot 13 x 3	Patched	670	0.85	1.10
3 B.9	1 Spot 10 x 6 1 Spot 11 x 6 1 Spot 11 x 6 1 Spot 13 x 3	Patched	500	0.70	0.74
1 B.10	1 Spot 10 x 6 1 Spot 10 x 6 1 Spot 32 x 2 1 Spot 14 x 3	Exposed	580	-	1.69
2 B.10	1 Spot 10 x 6 1 Spot 11 x 6 1 Spot 22 x 2 1 Spot 13 x 3	Exposed	700	-	2.02
3 B.10	1 Spot 10 x 6 1 Spot 10 x 5 1 Spot 25 x 2 1 Spot 19 x 3	Exposed	500	-	1.42
1 B.11	(Existing Pinholes)	Exposed	180	-	0.52
2 B.11	(Existing Pinholes)	Exposed	210	-	0.62
3 B.11	(Existing Pinholes)	Exposed	210	-	0.62

a Area includes damage on both the inside and outside of bend.
b Only introduced damaged area on the outside surface of bend was patched.

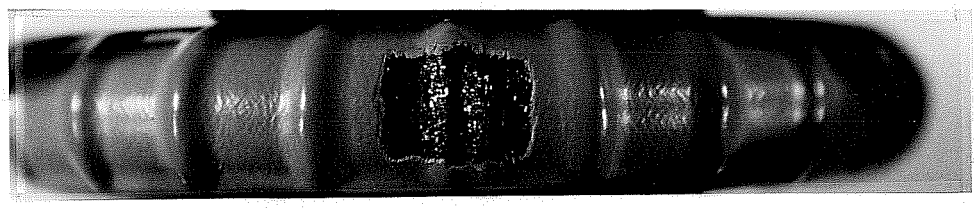

(a) 13 mm Bar (Groups A.2, A.3)

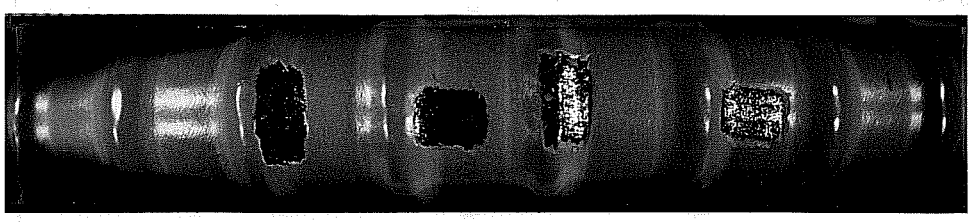

(b) 25 mm Bar (Groups B.2, B.3)

Figure C.6 Damage Spots > 6 x 6 mm, Bars with Parallel Deformations.

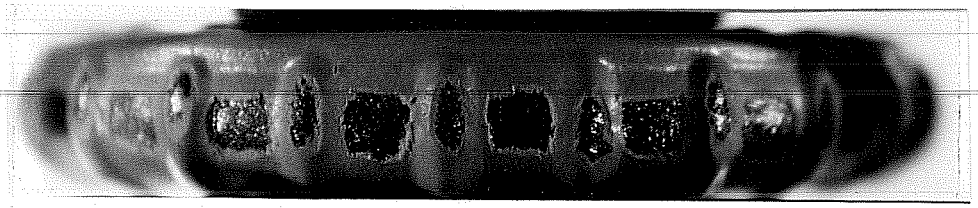

(a) 13 mm Bar (Groups A.4, A.5)

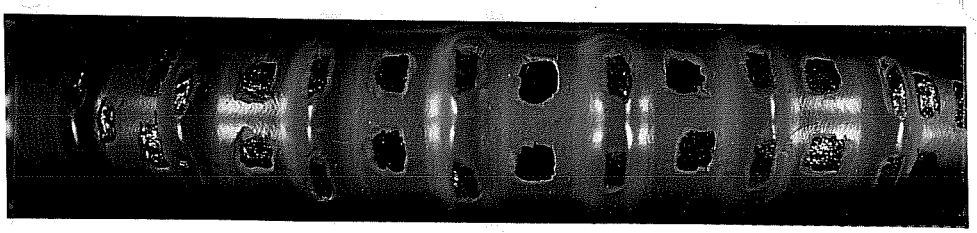

(b) 25 mm Bar (Groups B.4, B.5)

Figure C.7 Damage Spots > 2%, Bars with Parallel Deformations.

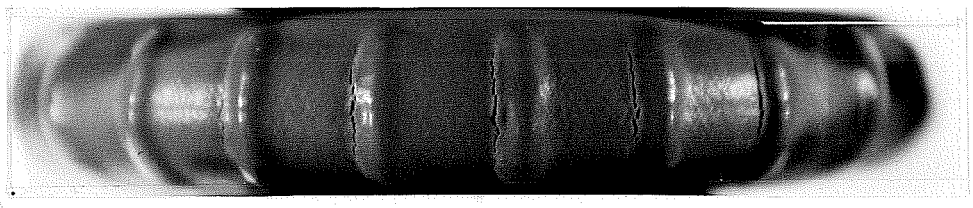

(a) 13 mm Bar (Group A.6)

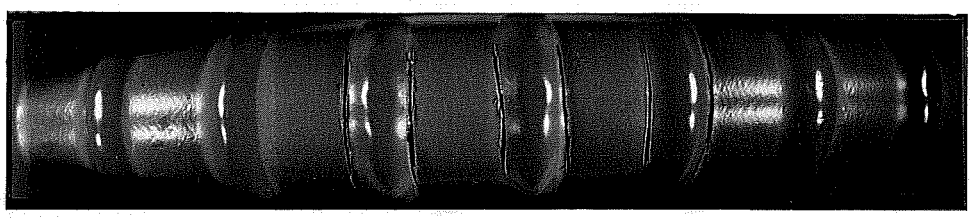

(b) 25 mm Bar (Group B.6)

Figure C.8 Hairline Cracks < 1%, Bars with Parallel Deformations.

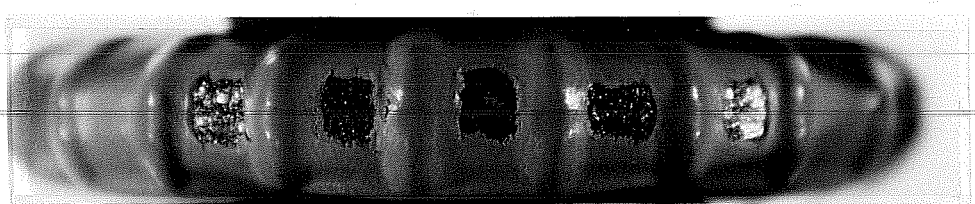

(a) 13 mm Bar (Group A.7)

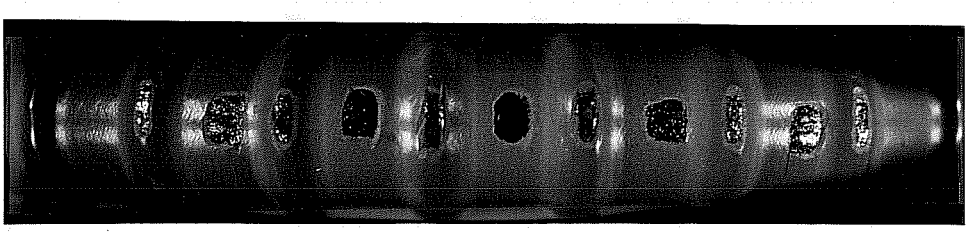

(b) 25 mm Bar (Group B.7)

Figure C.9 Damage Spots < 2%, Bars with Parallel Deformations.

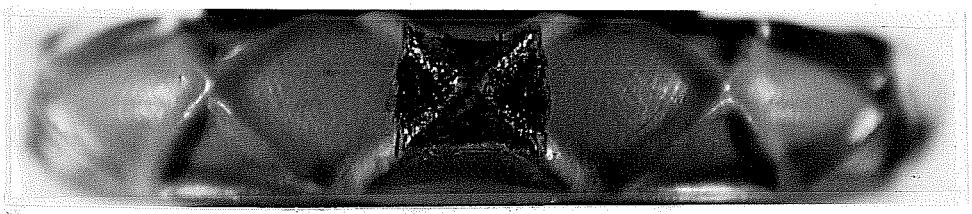

(a) 13 mm Bar (Groups A.9, A.10)

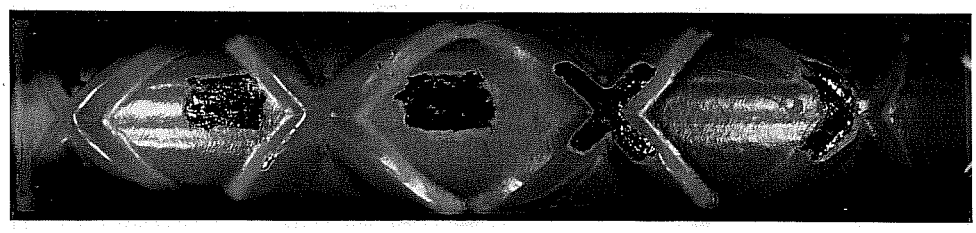

(b) 25 mm Bar (Groups B.9, B.10)

Figure C.10 Damage Spots > 6 x 6 mm, Bars with Cross Deformations.

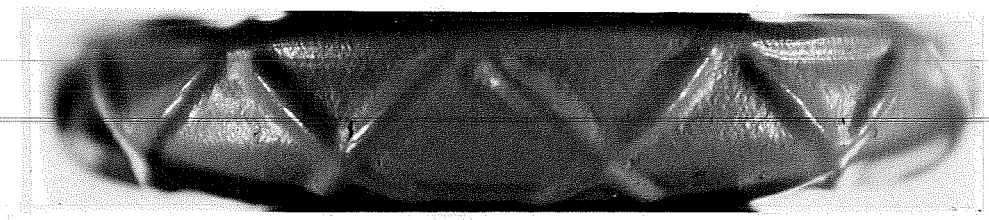

(a) 13 mm Bar (Group A.11)

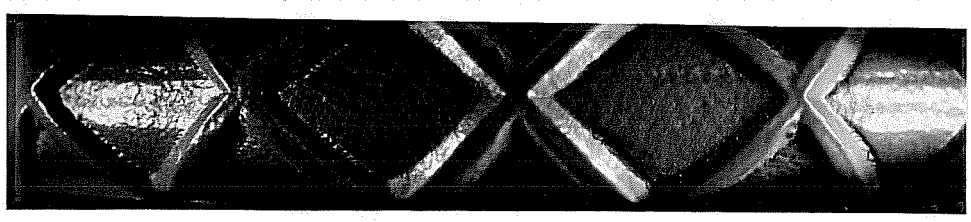

(b) 25 mm Bar (Group B.11)

Figure C.11 As Received (Pinholes) < 1%, Bars with Cross Deformations.

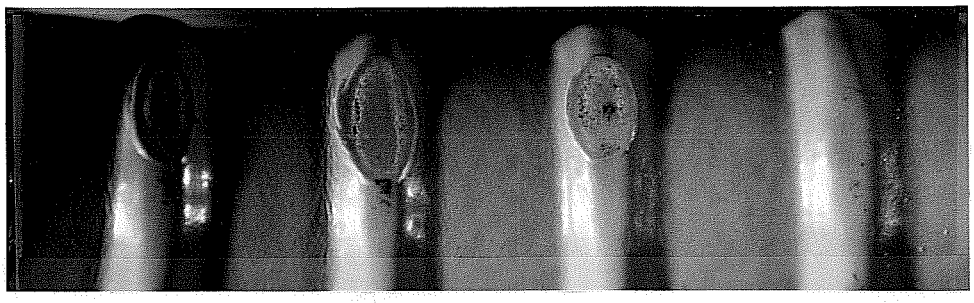

(a) Bar with Parallel Deformations

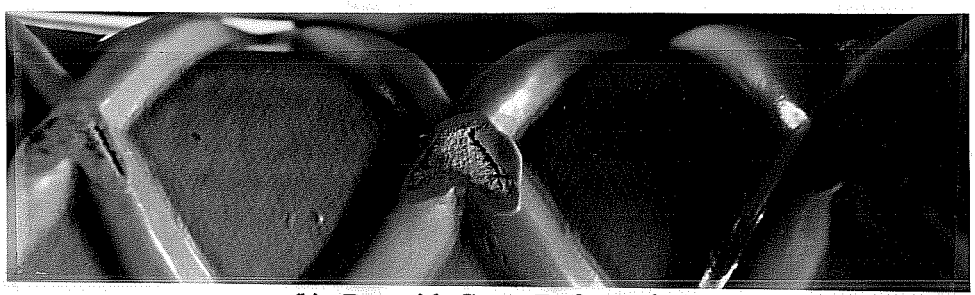

(b) Bar with Cross Deformations

Figure C.12 Typical Damage on the Inside of Bend.

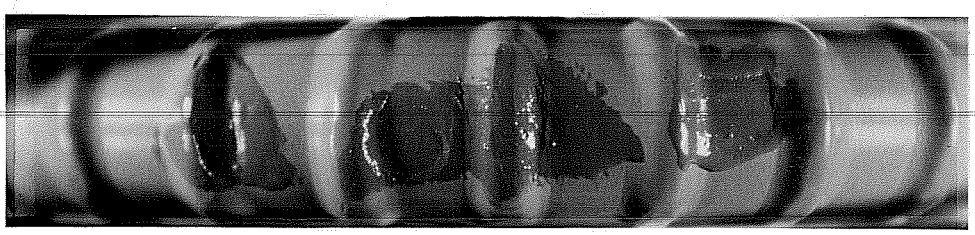

(a) Damage Spots > 6 x 6 mm, Bar with Parallel Deformations

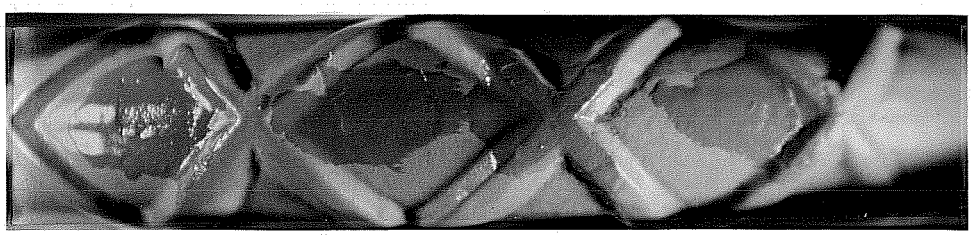

(b) Damage Spots > 6 x 6 mm, Bar with Cross Deformations

Figure C.13 Examples of Pathced Coating Damage.

The bars were further treated chemically by a pickling process as per ASTM G109-92[145] before placement in formwork. The process started with wire brushing and dusting the bars to remove mill scale. The bars were subsequently dipped in a 10% sulfuric acid solution for 15 to 20 minutes. Upon removal, they were rinsed in two baths of clean water for about three minutes each. Finally, the bars were spayed with rubbing alcohol and dried with paper towels.

C.5 Formwork and Steel Installation

Formwork. The formwork for the macrocell specimens consisted of a plywood base with plywood dividers that formed individual compartments (see Fig. C.14). The front plywood panel of each compartment was predrilled to position the top and bottom bars at the proper dimensions. The formwork was completed by placing wales along the top of both sides of the forms and several braces across the forms. The wales and braces maintained the dimensions of specimens during casting.

The formwork for the companion chloride specimens was constructed similarly. These specimens were small and the forms did not require bracing.

Steel Installation. The reinforcement was placed into the formwork by inserting the bars through the front plywood panel as shown in Fig. C.14. The bottom bars were firmly fixed so that their position would not change during concrete placement. The top bars were tightly maintained in position by the front panels and the wales.

C.6 Concrete

Mixture Design. Since concrete of inferior quality will offer less protection against corrosion of the embedded steel, it is often used in corrosion testing to accelerate the corrosion process and produce results within reasonable time limits. Therefore, concrete of reduced strength and increased permeability was used to construct the test specimens. The concrete mixture contained 231 kg/m^3 (389 lb./yd^3) of total cement content, and a maximum aggregate size of 20 mm (3/4 in.). The w/c was fairly high at 0.57 which resulted in a slump of 150 mm (6 in.) without using a water reducing agent. The details of the concrete mixture are shown in Table C.10.

Casting. Concrete was provided by a ready mix supplier. Casting was done indoors by placing concrete with shovels into the forms. The concrete was placed in one lift and consolidated using 50 mm (2 in.) head internal vibrators as shown in Fig. C.15. The vibrators were inserted only at the back sides of Series A specimens to avoid shifting or damaging the steel bars.

The same concrete was used to cast all 68 macrocell specimens in Series A and B, 30 specimens in Series C, and a large number of standard cylinders. The specimens were screeded immediately after placing concrete and trowelled shortly after. The specimens were then covered with plastic sheets to reduce water evaporation.

Table C.10 Concrete Mixture Details for Macrocell Study

Material	Quantity	Unit
20 mm Rock, SSD	1097	kg/m^3
Sand, SSD	875	kg/m^3
Type I Portland Cement	221	kg/m^3
Pozzolana R	10	kg/m^3
Water	132	kg/m^3
Water/Cement Ratio	0.57	
Unit Weight	2278	kg/m^3
Slump	150	mm

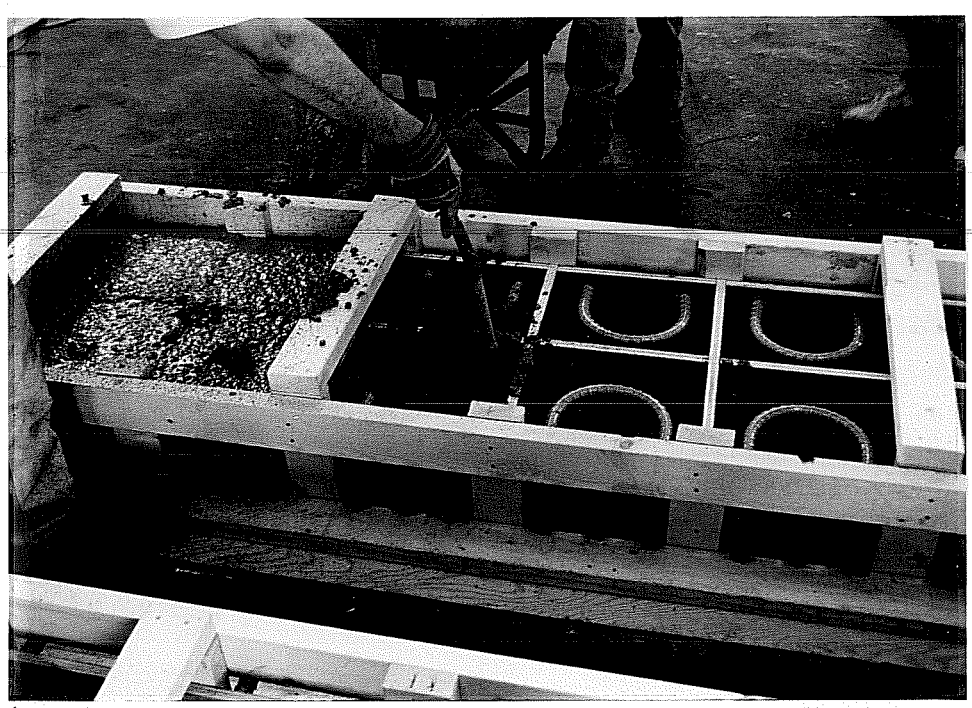

Figure C.15 Casting Macrocell Specimens.

Curing. After two days of casting, the forms and cylinder molds were stripped and no further curing of the specimens was provided. The idea was to slow concrete strength gain which is normally considered an indicator of concrete permeability. Some cylinders were placed in a humidity chamber under standard curing conditions. The rest of the cylinders were exposed to the same atmospheric exposure conditions as the macrocell specimens.

Compressive Strength. Concrete strength was determined at 2, 7, 14, 28, 90, and 365 days after casting. The 28-day strength was determined from both air-cured cylinders and cylinders just removed from the curing chamber which yielded similar results (around 30 MPa (4350 psi)). The strength-gain curve is shown in Fig. C.16.

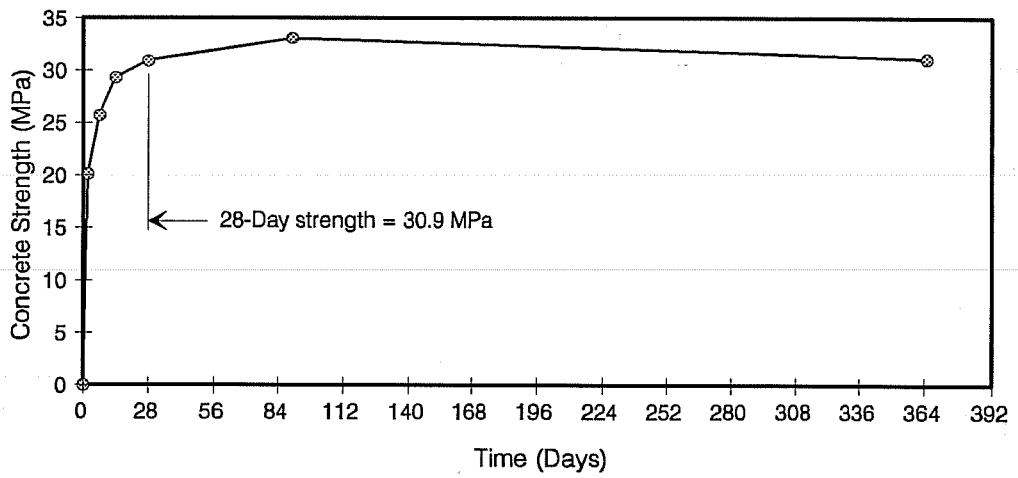

Figure C.16 Compressive Strength Gain of Macrocell Concrete.

Permeability. Concrete permeability was determined from 100 x 200 mm (4 x 8 in.) cylinders using a standard test procedure for Rapid Determination of the Chloride Permeability of Concrete (AASHTO T277-83).[146] The cylinders were air-cured under the same conditions as the macrocell specimens, and tested at ages of 280 and 490 days after casting. The respective permeability measurements were 9360 and 6600 coulombs which fell under the standard classification of "high" permeability.

C.7 Test Setup

Specimen Preparation. The sides of all specimens were sealed to simulate a continuous slab environment. Two coats of a clear waterproof material were applied (brush strokes) at right angles on each side for effective insulation. Plexiglass dikes 75 mm (3 in.) high were mounted with silicon around the edges of the top surfaces to contain the salt solution. The specimens were placed on shelves on narrow wooden strips to allow air circulation under the soffits.

The bottom bars were made electrically continuous by welding a short, 6 mm diameter (#2) bar across the protruding ends. Electrical leads were attached to the top and one of the bottom bars using electrical ground clamps properly secured into the steel metal. A 100 ohm resistor was connected to the two clamps to bridge between the reinforcing layers. This ohmic resistance is in the low range when compared with the internal resistance of concrete. Wires of equal length were used to connect the specimens to the electronic data acquisition equipment to avoid unequal potential drops in the wires between the specimen and the equipment. Figure C.17 shows a schematic view of one of Series B macrocell specimens.

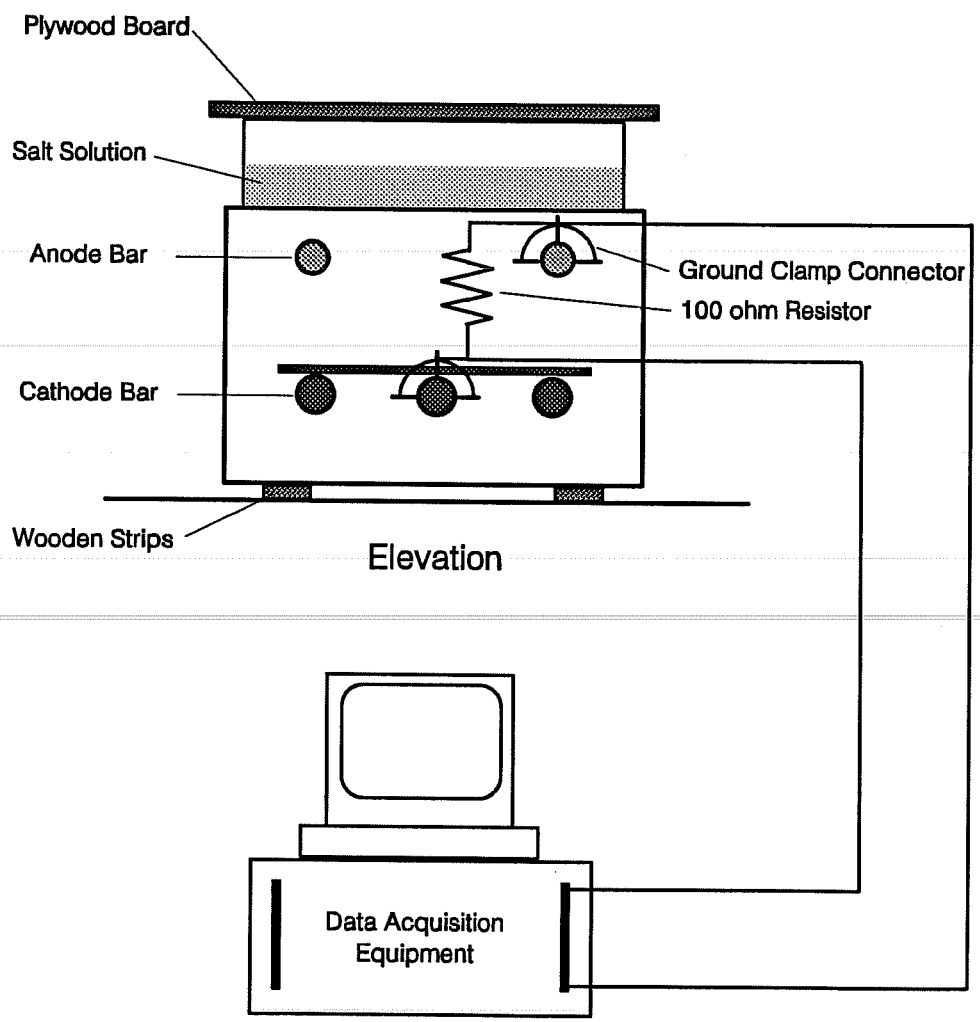

Figure C.17 Schematic View of Macrocell Test Specimen.

The resistors were measured before starting the test and were found to vary by a maximum of about 10%. Therefore, the resistance reading for each specimen was recorded and checked several times at different dates. To read the resistance, one end of each resistor was disconnected from the clamp and a hand-held voltmeter was used for measurement. An average resistance for each resistor was calculated and used for determining the corrosion current passing through the particular specimen.

The attachment areas and the protruding portions of the epoxy-coated bars were coated with a patching epoxy compound. The exposed parts of the uncoated bars were frequently covered with a protective oil.

Exposure Conditions. All macrocell specimens, and the specimens used for chloride determination, were subjected to alternate wetting and drying using a 3.5% NaCl solution. Only the top surfaces were ponded with solution to a depth of about 35 mm (1.5 in.). Evaporation of the solution was minimized by covering the dikes with plywood. The wetting period lasted two weeks, followed by removing the solution and allowing the specimens to dry at room temperature for two more weeks. The four-week exposure cycle was repeated continuously. The first ponding period was started when concrete was 42 days old.

A fresh solution was prepared at the beginning of each wet period. The solution was removed by suction and discarded at the end of the wet period. The top surfaces of the specimens were washed periodically (every 3-4 cycles) with clean water to dissolve any salt buildup or crystallization in the concrete cover.

To avoid varying temperatures, which can alter the electrical resistivity of concrete between the reinforcing layers, and therefore, the corrosion rate, the specimens were placed in a temperature-controlled room. This eliminated the need for adjusting the measured macrocell currents to a uniform base.

C.8 Routine Monitoring

Visual Examination. The macrocell specimens were visually inspected at the beginning of the test and periodically thereafter. Any initial cracks detected on the top concrete surfaces (suspected to be due to plastic settlement), such as those shown in Fig. C.18, were documented before testing. Specimens that exhibited such cracking were the following:

- Series A: 1A.3, 2A.6, 1A.8, 2A.8, 2A.10.
- Series B: 2B.1, 1B.3, 3B.3, 1B.4, 2B.4, 3B.4, 1B.5, 2B.5, 3B.5, 3B.6, 3B.7, 2B.9, 1B.10.

The development of surface staining and new cracks were monitored during the test (see Section 9.5).

Voltage and Current Measurements. A closed electrical circuit was maintained at all times during the test. The voltage drop across the resistor in each macrocell specimen was electronically monitored. A digital data acquisition system was used to scan the voltages periodically. Before starting the test, the initial voltage readings were obtained and stored.

Subsequent voltage measurements were taken every one or two weeks (at the end of each wetting and drying period) for five months. The voltages were, thereafter, measured every week to observe any abrupt changes.

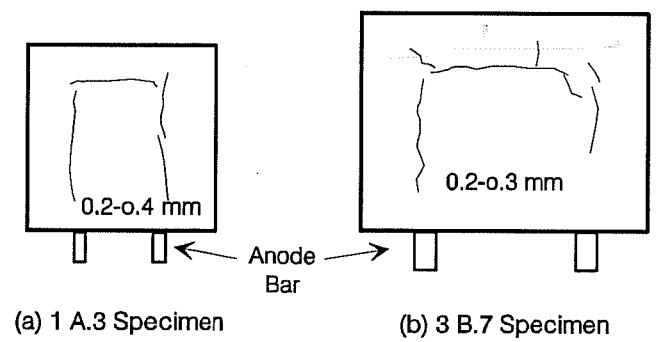

Figure C.18 Examples of Initial Cracks Detected on Top Surfaces of Macrocell Specimens.

A voltage is developed when an electrical current flows through the resistor. Since the only electrical contact between the reinforcing layers was exterior to the specimen, the flowing current was the net corrosion current developed in the macrocell. The measured voltage is related to the current by Ohm's Law,

$$I = \frac{V}{R} \qquad \text{(C.1)}$$

where, I is the electrical current, V is the voltage, and R is the resistance. The voltage data were automatically converted to electrical currents. Adjustment for the initial voltage readings was done by processing the data using an electronic spreadsheet.

The diagrams of the macrocell corrosion currents versus time of exposure up to two years are shown in Fig. C.19 and C.20. Each diagram displays three curves corresponding to the three replicate specimens in a group.

Temperature Measurement. The temperature inside the test room was measured every week at the time of voltage reading. Although the temperature was automatically controlled, slight variations occurred from one season to another. The yearly average temperature was 23° C (73° F). About 90% of the time the temperature remained within ±3° C (±5° F). Therefore, the effects of temperature changes on the corrosion rates during the test period can be neglected.

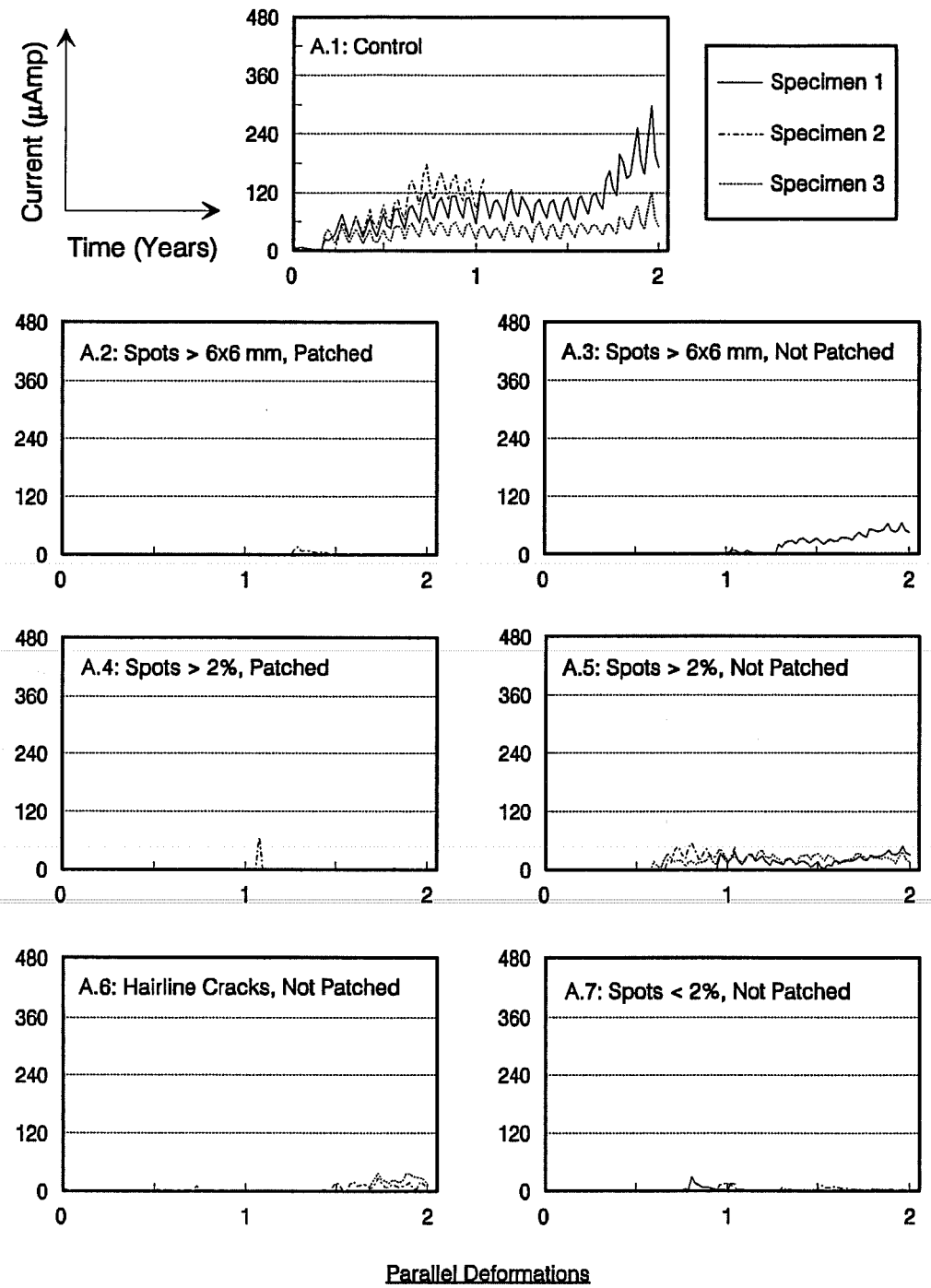

Figure C.19 Macrocell Corrosion Currents for 13-mm Bars (Series A).

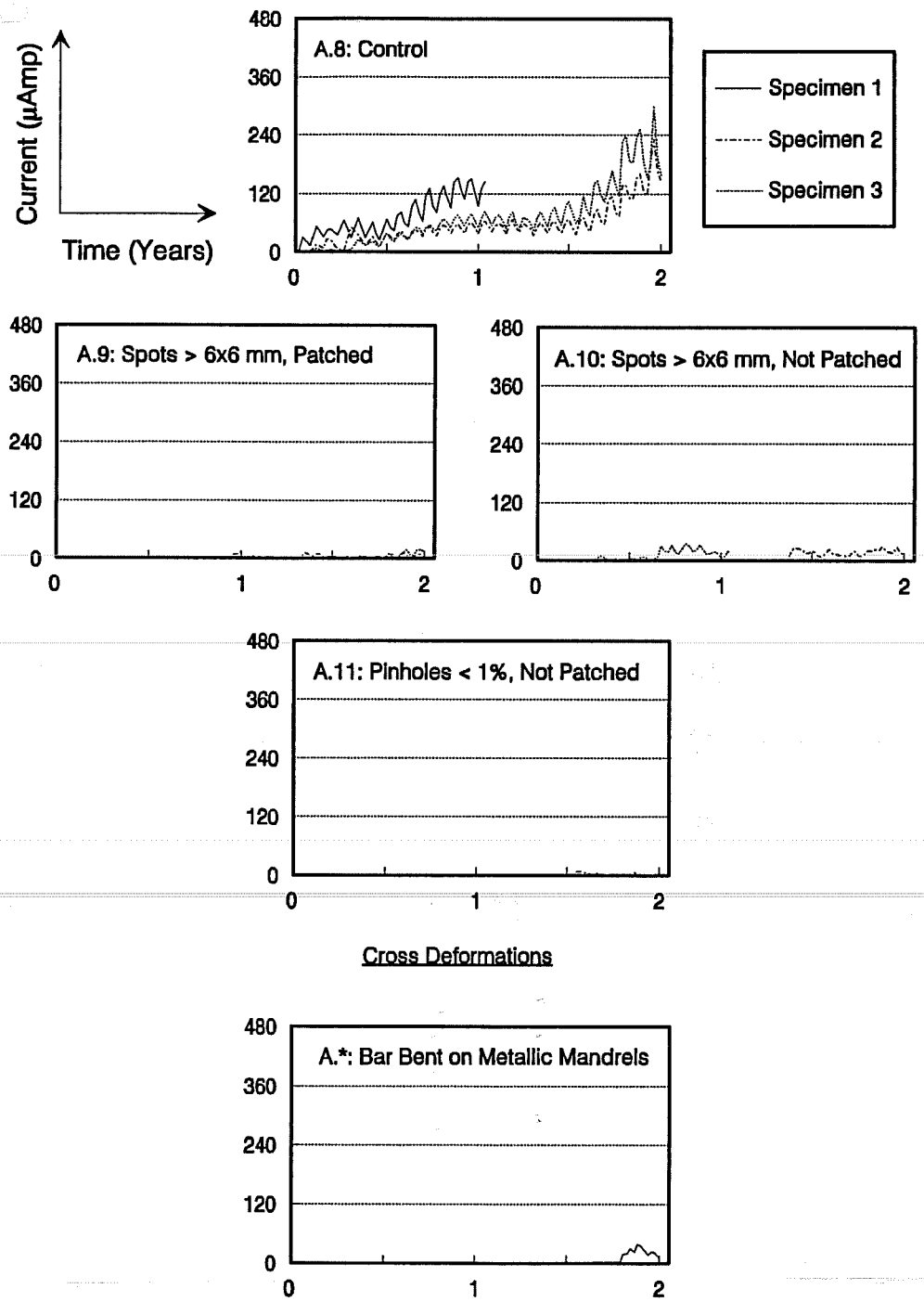

Figure C.19 (Cont'd) Macrocell Corrosion Currents for 13-mm Bars (Series A).

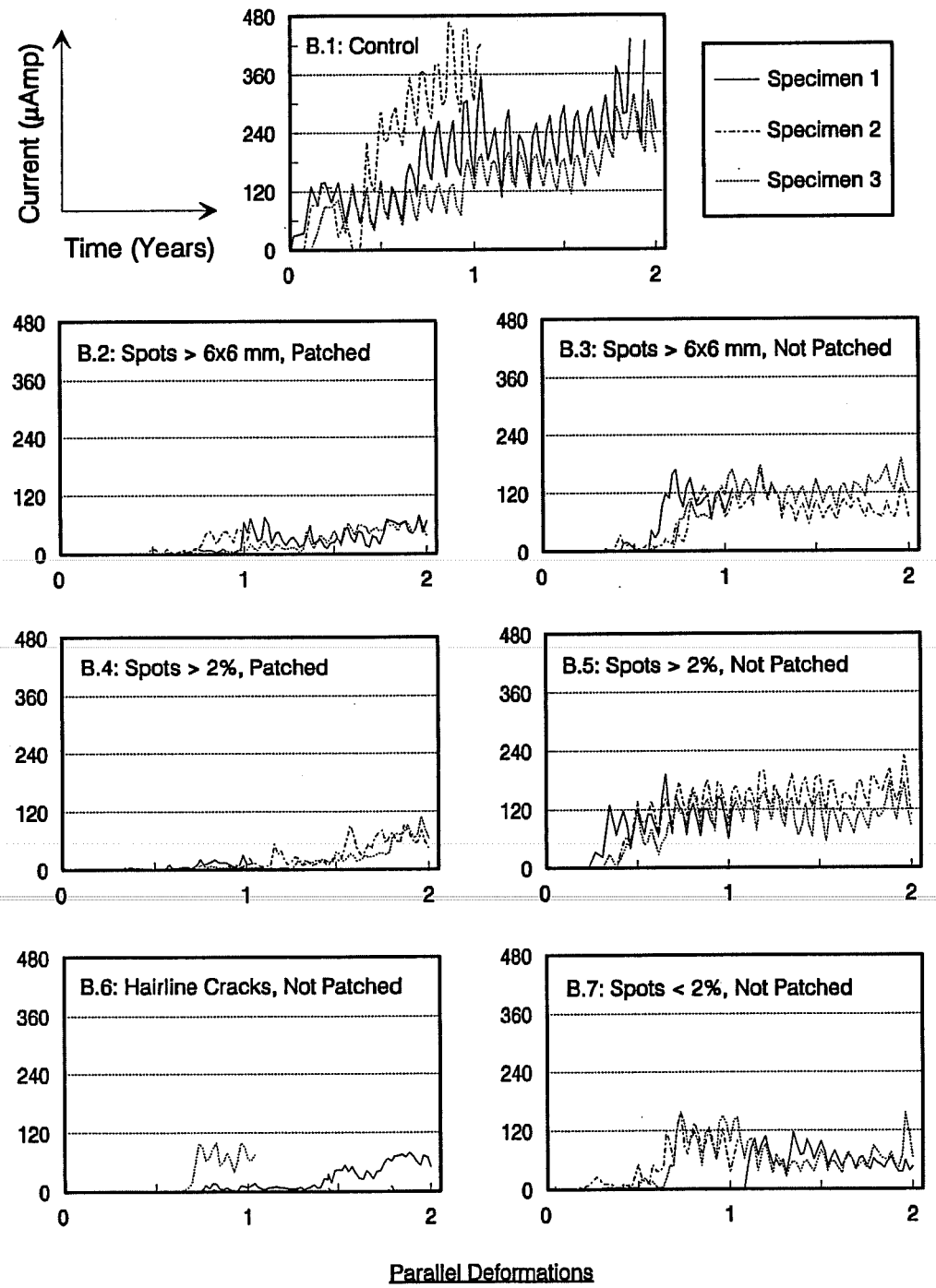

Figure C.20 Macrocell Corrosion Currents for 25-mm Bars (Series B).

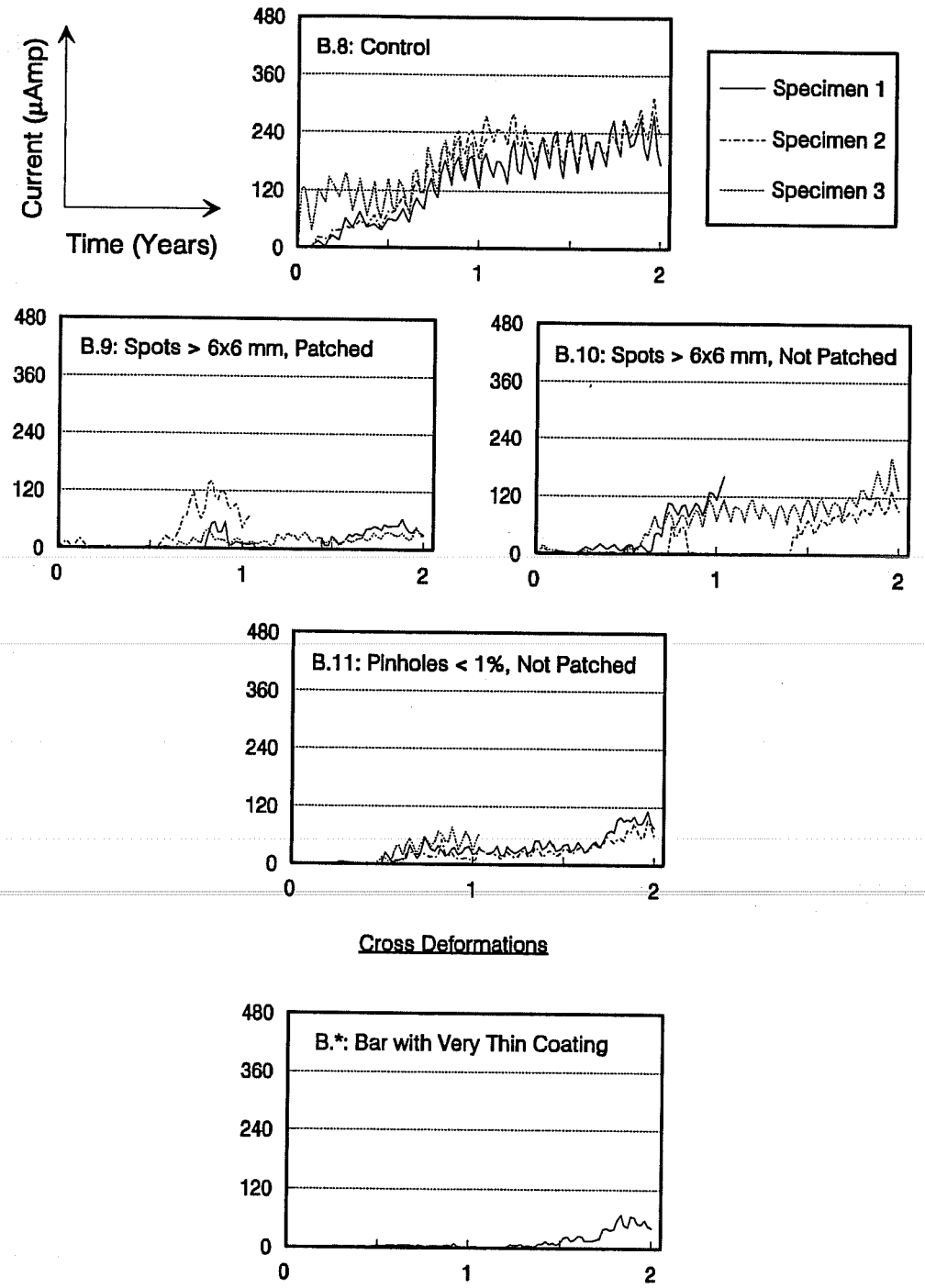

Figure C.20 (Cont'd) Macrocell Corrosion Currents for 25-mm Bars (Series B).

Chloride Content Determination. Chloride levels in concrete were determined every full cycle of exposure, *i.e.* every 28 days. A different specimen from Series C was used every time to extract concrete powder samples used for chloride determination. The concrete samples were collected from multiple holes. The holes were drilled to various depths, at about 6 mm (1/4 in.) intervals, to determine chloride concentrations at different levels of penetration. Two chloride samples were analyzed from each selected depth range. Figure C.21 shows the drilling procedure for concrete sampling.

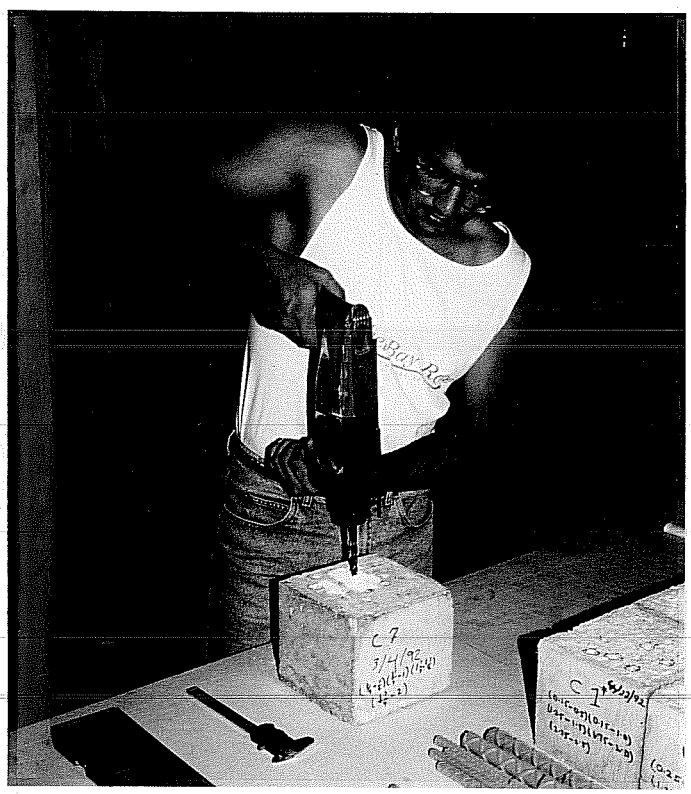

Figure C.21 Extracting Concrete Powder Sample for Chloride Determination.

The acid-soluble chloride content was determined using a rapid method of measuring chlorides in concrete on site. The test has the same accuracy as standard titration made in the laboratory. The chloride concentrations measured with time are shown in Table C.11. These concentrations, particularly at the steel level, were related to corrosion activity (see Chapter 10).

C.9 Postmortem Examination

General. One of the replicate specimens in each group was removed for demolition after one and two years of exposure. Generally, the selected specimen was the one showing maximum corrosion activity indicated by the history of the corrosion current.

Concrete Condition. Prior to destruction, delamination of concrete was checked by hammer sounding. Concrete surfaces were struck with a hammer at several locations to detect any delaminated areas. The results of this inspection are given in Chapter 9. Corrosion-induced cracks and stains on the specimens removed are illustrated in Fig. C.22 and C.23. The condition of the remaining cracked specimens is illustrated in Fig. C.24.

Chloride Content. Chloride samples from each specimen removed were extracted and analyzed to determine the acid-soluble chloride content at various depths. The samples were obtained from a single hole drilled very close to the middle of the inside radius of the embedded bent bar. The chloride contents of the autopsied specimens at one and two years are shown in Tables C.12 and C.13, respectively.

Specimen Destruction. The mechanical removal of concrete was done with great care to avoid damaging the epoxy-coated bars. Saw cuts were made along the sides of the specimen parallel to the top steel bar, and across the top surface. The concrete was then forced to break in the top bar plane by use of a jack hammer along the saw cuts (see Fig. C.25). Additional minor chipping allowed complete removal of the bar from the concrete. The lack of adhesion between the coated bar and concrete greatly facilitated bar retrieval. The bar debonded from the surrounding concrete readily and cleanly.

Visual Inspection. The bars were visually inspected for any evidence of corrosion and blistering. During removal of the coating to examine underfilm corrosion, the ease or difficulty of peeling was reported as an indicator of the degree of debonding. The extent of corrosion on the steel substrate was documented. All observations of the retrieved bars at one and two years are given in Tables C.14 to C.17. In addition, some of the bottom reinforcing bars were exposed to examine their condition (see Chapter 9). Finally, the bar trace on concrete for all recovered bars was carefully inspected for the presence of voids, dried solution deposits, and corrosion products. The observations of the bar trace for the autopsied specimens at one and two years are given in Table C.18.

Table C.11 Acid-Soluble Chloride Concentrations in Concrete During Macrocell Exposure Testing
(Percentage by Weight of Concrete)

Days of Exposure	Sampling Depth Ranges (mm)					
	6-12	19-25	32-38	45-51	57-63	70-76
28	0.25	0.09				
56	0.56	0.16				
84	0.42	0.20	0.09			
112	0.47	0.27	0.15			
140	0.43	0.20	0.08			
168	0.62	0.28	0.17	0.10		
196	0.62	0.34	0.20	0.09		
224	0.49	0.32	0.18	0.10		
252	0.53	0.34	0.20	0.11	0.07	
280	0.40	0.28	0.20	0.09	0.06	
308	0.63	0.31	0.29	0.16	0.07	0.07
336	0.40	0.28	0.21	0.07	0.00	0.00
364	0.38	0.25	0.17	0.06	0.00	0.00
392	0.40	0.25	0.20	0.17	0.07	0.00
420	0.35	0.29	0.22	0.13	0.03	0.00
448	0.28	0.18	0.10	0.04	0.00	0.00
476	0.38	0.21	0.17	0.12	0.01	0.00
504	0.33	0.18	0.15	0.12	0.00	0.00
532	0.31	0.29	0.15	0.10	0.04	0.00
560	0.34	0.29	0.18	0.10	0.02	0.00
588	0.44	0.28	0.17	0.12	0.02	0.00
616	0.41	0.38	0.19	0.20	0.13	0.05
644	0.34	0.17	0.22	0.26	0.13	0.04
672	0.37	0.25	0.18	0.12	0.07	0.02
700	0.34	0.24	0.25	0.19	0.12	0.05
728	0.38	0.22	0.18	0.16	0.15	0.06

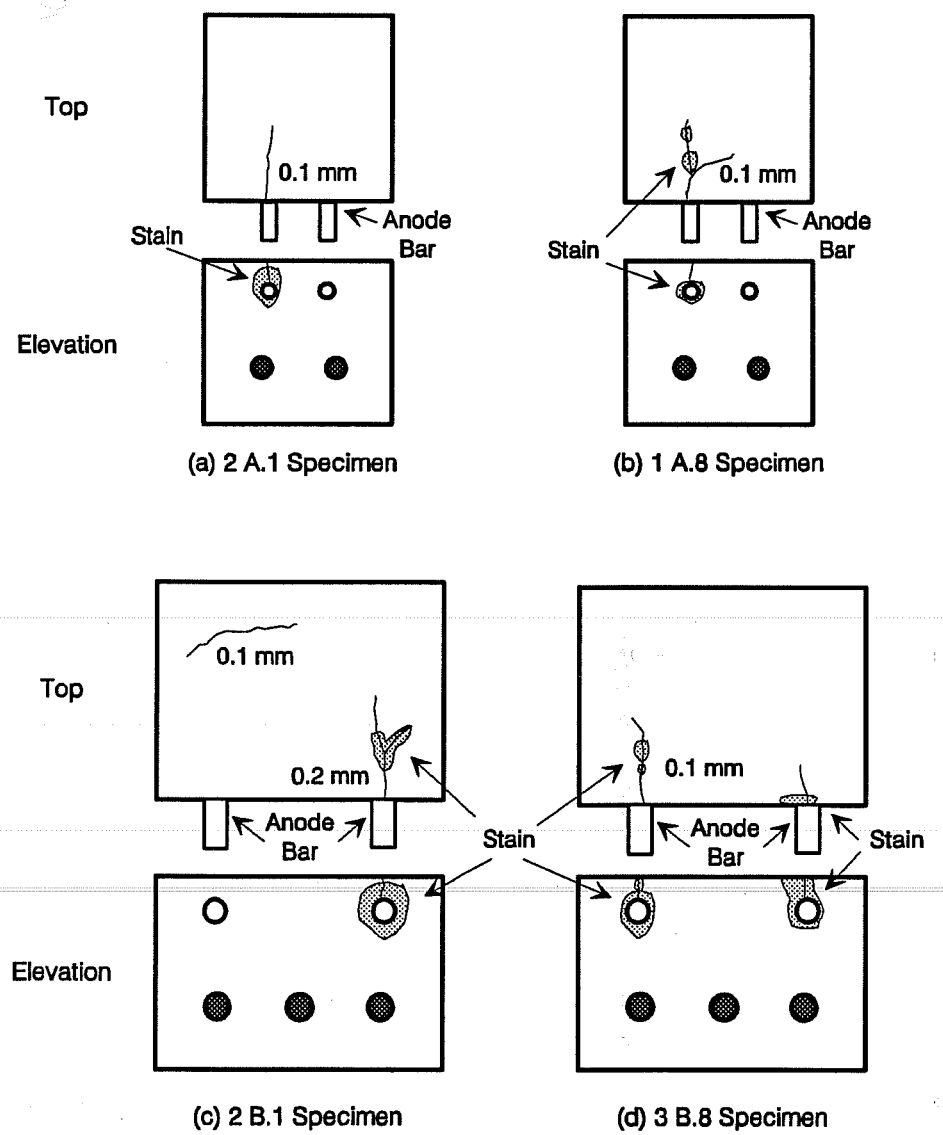

Figure C.22 Cracks and Stains on Macrocell Specimens Autopsied After One Year of Exposure.

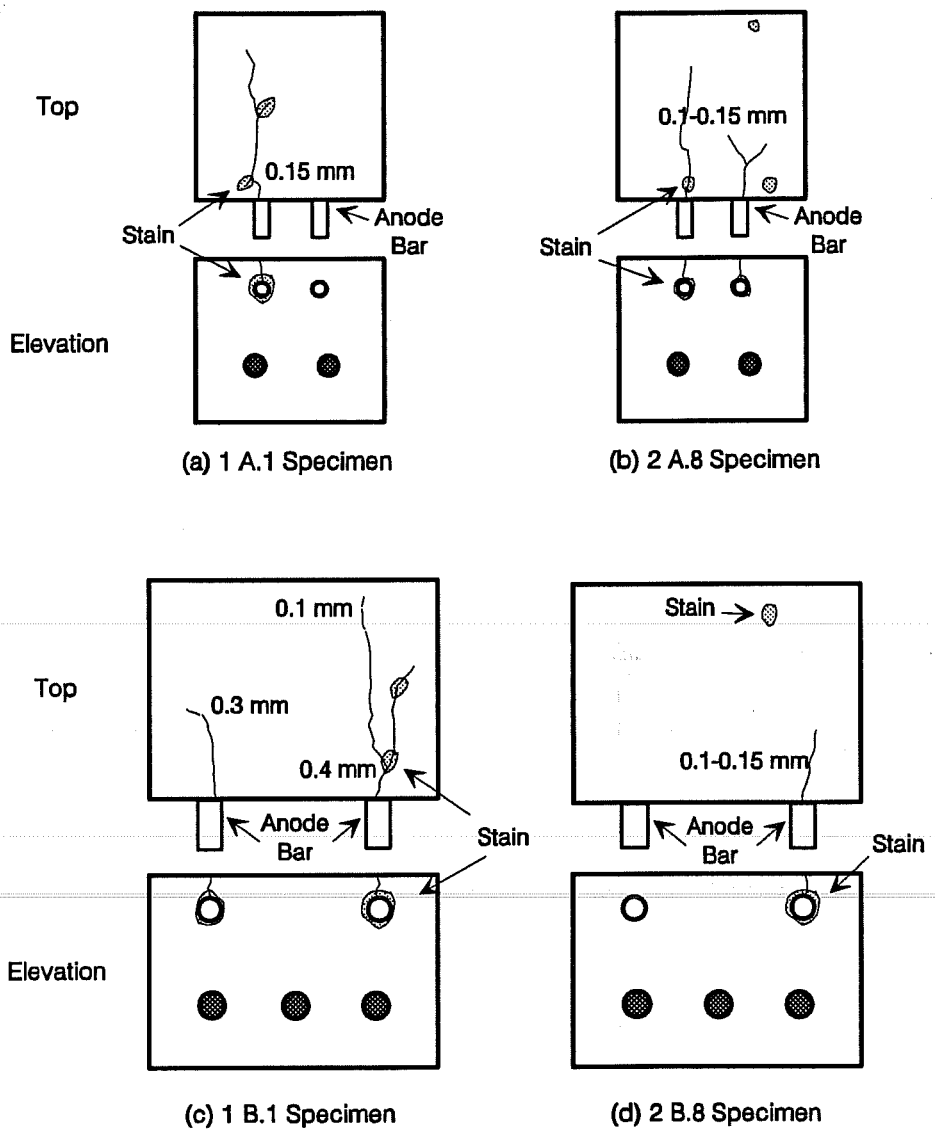

Figure C.23 Cracks and Stains on Macrocell Specimens Autopsied After Two Years of Exposure.

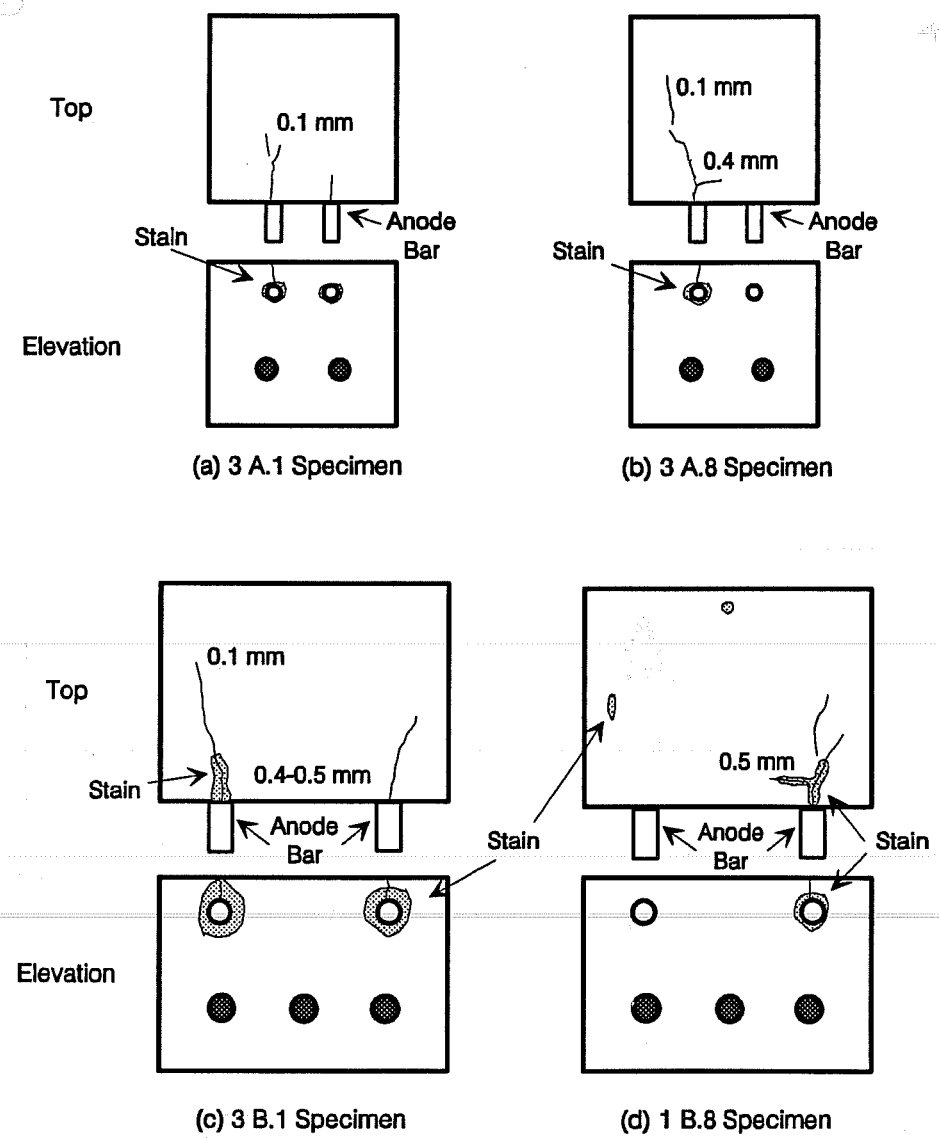

Figure C.24 Cracks and Stains on Continuing Macrocell Specimens Inspected After Two Years of Exposure.

Table C.12 Acid-Soluble Chloride Concentrations in Autopsied Macrocell Specimens After One Year of Exposure
(Percentage by Weight of Concrete)

Specimen	Sampling Depth Ranges (mm)				
	6-12	19-25	32-38	45-51	57-63
2 A.1	0.49	0.35	0.18	0.15	0.05
1 A.2	0.21	0.24	0.16	0.07	0.03
2 A.3	0.42	0.35	0.19	0.10	0.05
1 A.4	0.35	0.26	0.23	0.10	0.02
2 A.5	0.32	0.23	0.20	0.14	0.07
1 A.6	0.30	0.24	0.19	0.08	0.01
1 A.7	0.408	0.24	0.12	0.10	0.03
1 A.8	0.42	0.30	0.21	0.19	0.10
1 A.9	0.41	0.25	0.12	0.09	0.01
3 A.10	0.39	0.32	0.14	0.12	0.01
1 A.11	0.39	0.26	0.15	0.07	0.00
2 B.1	0.41	0.29	0.20	0.11	0.05
2 B.2	0.39	0.27	0.24	0.17	0.08
1 B.3	0.49	0.28	0.19	0.18	0.07
1 B.4	0.45	0.25	0.17	0.10	0.09
1 B.5	0.44	0.29	0.22	0.17	0.11
3 B.6	0.55	0.27	0.20	0.30	0.14
2 B.7	0.59	0.41	0.27	0.20	0.08
3 B.8	0.42	0.28	0.20	0.10	0.05
2 B.9	0.34	0.23	0.20	0.14	0.11
1 B.10	0.39	0.30	0.26	0.17	0.10
3 B.11	0.30	0.30	0.21	0.12	0.08

Table C.13 Acid-Soluble Chloride Concentrations in Autopsied Macrocell Specimens After Two Year of Exposure (Percentage by Weight of Concrete)

Specimen	Sampling Depth Ranges (mm)			
	19-32	32-38	38-51	76-89
1 A.1	0.24	0.30	-	0.05
2 A.2	0.22	0.19	-	0.00
1 A.3	0.17	0.17	-	0.07
2 A.4	0.22	0.14	-	0.00
3 A.5	0.23	0.23	-	0.00
3 A.6	0.25	0.27	-	0.00
2 A.7	0.22	0.20	-	0.00
2 A.8	0.34	0.31	-	0.08
2 A.9	0.19	0.17	-	0.00
2 A.10	0.33	0.24	-	0.00
2 A.11	0.37	0.22	-	0.00
1 B.1	0.26	-	0.19	0.05
1 B.2	0.27	-	0.19	0.06
3 B.3	0.20	-	0.20	0.03
2 B.4	0.23	-	0.18	0.05
2 B.5	0.19	-	0.22	0.09
1 B.6	0.25	-	0.24	0.08
3 B.7	0.28	-	0.22	0.09
2 B.8	0.19	-	0.16	0.07
1 B.9	0.33	-	0.20	0.05
3 B.10	0.14	-	0.10	0.09
1 B.11	0.28	-	0.22	0.07

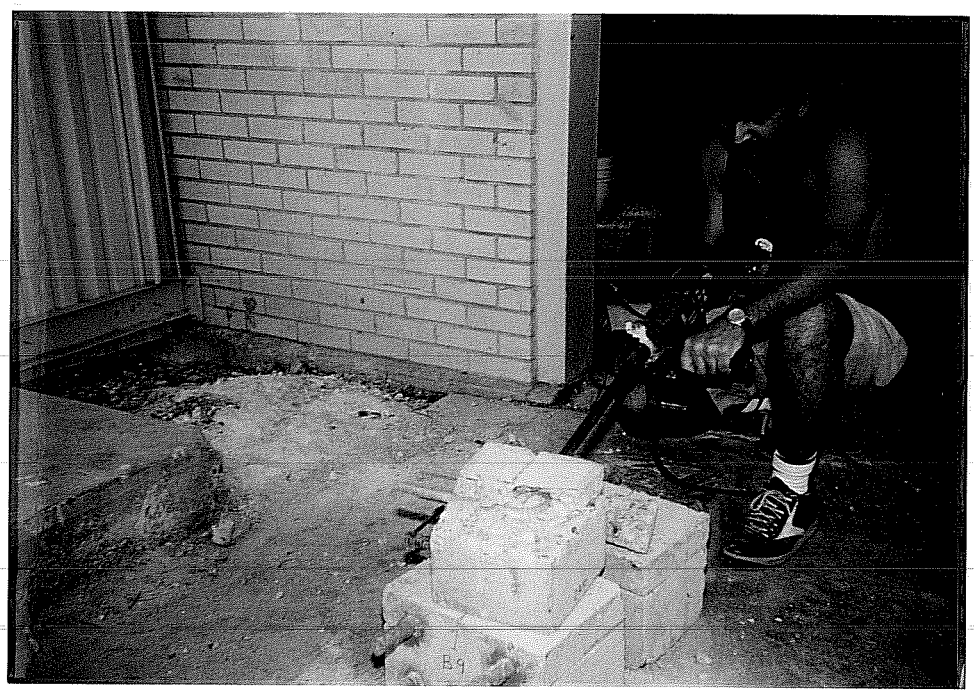

Figure C.25 Demolishing Macrocell Specimens.

Table C.14 Observations of Macrocell 13 mm Bar Specimens, One Year Exposure

Specimen	Bar Surface Condition	Coating Adhesion	Undercutting
2 A.1	Concentrated rib and surface degradation and pitting (0.8 mm deep). Equal corrosion on top and bottom sides.		
1 A.2	No apparent corrosion.	Poor bond on bent portion only.	Bright steel, no visible metal loss.
2 A.3	Minor surface corrosion (very shallow metal loss)	Poor bond on bent portion only.	Slight spreading (6 mm) from edges of damaged spot.
1 A.4	No apparent corrosion.	Poor bond on bent portion only.	Bright steel, no visible metal loss.
2 A.5	Minor pitting, small blisters.	Very poor bond on bent portion only.	Moderate spreading on bent portion, trapped solution.
1 A.6	No apparent corrosion.	Poor bond on bent portion only.	Bright steel, no visible metal loss.
1 A.7	Minor surface corrosion, small blisters.	Very poor bond on bent portion only.	Moderate spreading on bent portion, trapped solution.
1 A.8	Concentrated rib and surface degradation and pitting. More corrosion on top than on bottom side.		
1 A.9	No apparent corrosion.	Poor bond on bent portion only.	Slight spreading around patched area.
3 A.10	Minor surface corrosion.	Poor bond on bent portion and partly on straight ends.	Moderate spreading on bent portion.
1 A.11	No apparent corrosion.	Poor bond on bent portion only.	Bright steel, no visible metal loss.

Table C.15 Observations of Macrocell 25 mm Bar Specimens, One Year Exposure

Specimen	Bar Surface Condition	Coating Adhesion	Undercutting
2 B.1	Concentrated rib and surface degradation and moderate pitting (1-1.2 mm deep). Slightly more corrosion on top than on bottom side.		
2 B.2	Very minor surface corrosion, small blisters.	Poor bond on bent portion only.	Thin black layer, very shallow metal loss, trapped solution.
1 B.3	Minor pitting, small blisters.	Poor bond on bent portion only.	Thin black layer, shallow metal loss, trapped solution.
1 B.4	Very minor surface corrosion.	Poor bond on bent portion only.	Mostly bright steel, no visible metal loss, trapped solution.
1 B.5	Minor surface corrosion, small and large blisters.	Very poor bond on bent portion and partly on straight ends.	Extensive spreading, thin black layer, very shallow metal loss.
3 B.6	Very minor surface corrosion, many blisters.	Poor bond on bent portion and partly on straight ends.	Mostly bright steel, no visible metal loss, thin black layer.
2 B.7	Minor surface corrosion, many variable size blisters.	Very poor bond on bent portion and most of straight ends.	Moderate spreading, very shallow metal loss, trapped solution.
3 B.8	Concentrated rib and surface degradation and pitting on straight ends. More corrosion on top than on bottom side.		
2 B.9	Very minor surface corrosion, many blisters.	Slightly poor bond on bent portion only.	Slight spreading, no visible metal loss.
1 B.10	Minor surface corrosion, many variable size blisters.	Poor bond on bent portion and partly on straight ends.	Moderate spreading, no visible metal loss, thin black layer, trapped solution.
3 B.11	Very minor surface corrosion, many blisters.	Slightly poor bond on bent portion only.	Mostly bright steel, shallow metal loss.

Table C.16 Observations of Macrocell 13 mm Bar Specimens, Two Year Exposure

Specimen	Bar Surface Condition	Coating Adhesion	Undercutting
1 A.1	Concentrated rib and surface degradation and pitting (0.8 mm deep). Equal corrosion on top and bottom sides. Brown-black products.		
2 A.2	No apparent corrosion.	Poor bond on bent portion only.	Mostly bright steel, some darkening, no visible metal loss.
1 A.3	Minor pitting, cracking along continuous rib, blisters.	Very poor bond on bent portion and on most of straight ends.	Black layer around damage, some surface darkening away, stain along continuous rib.
2 A.4	No apparent corrosion.	Poor bond on bent portion only.	Mostly bright steel, no visible metal loss.
3 A.5	Minor pitting, small blisters.	Very poor bond on bent portion only.	Extensive spreading on bent portion, trapped solution.
3 A.6	No apparent corrosion, small blisters.	Very poor bond on bent portion only.	Extensive spreading, no visible metal loss.
2 A.7	Minor surface corrosion, small blisters.	Very poor bond on bent portion only.	Extensive spreading on bent portion, worse on bottom side.
2 A.8	Concentrated rib and surface degradation and moderate pitting (around 1 mm). More corrosion on bottom than on top side. Brown-black products.		
2 A.9	Very minor corrosion, small and large blisters.	Poor bond on bent portion and partly on straight ends.	Mostly bright steel, some darkening, trapped solution.
2 A.10	Minor surface corrosion, numerous corrosion spotting.	Poor bond on bent portion and on most of straight ends.	Black layer around damage, some surface darkening away, stain along continuous rib.
2 A.11	Very minor corrosion, small blisters.	Poor bond on bent portion only.	Mostly bright steel, no visible metal loss.

Table C.17 Observations of Macrocell 25 mm Bar Specimens, Two Year Exposure

Specimen	Bar Surface Condition	Coating Adhesion	Undercutting
1 B.1	Concentrated rib and surface degradation with severe pitting (1.5 mm) and significant loss of section. More corrosion on top than on bottom side.		
1 B.2	Very minor surface corrosion, small blisters.	Very poor bond on bent portion and most of straight ends.	Top side black, bottom side dull, very shallow metal loss, trapped solution.
3 B.3	Moderate pitting (1-1.2 mm deep), small blisters.	Very poor bond on bent portion and half of straight ends.	Top side black, bottom side dull, shallow metal loss, trapped solution.
2 B.4	Very minor surface corrosion, small blisters.	Very poor bond on bent portion and straight ends.	Top side black, bottom side dull, very shallow metal loss, corrosion deposits.
2 B.5	Slight pitting (0.8-1 mm deep), small and large blisters.	Very poor bond on bent portion and straight ends.	Top side black, bottom side dull, shallow metal loss, trapped solution.
1 B.6	Very minor surface corrosion inside of bend, many blisters.	Extremely poor bond on bent portion and straight ends.	Top side black, bottom side dull, very shallow metal loss, trapped solution.
3 B.7	Slight pitting (0.8-1 mm deep), small and large blisters.	Very poor bond on bent portion and straight ends.	Top side black, bottom side brown or dull, shallow metal loss,trapped solution.
2 B.8	Concentrated rib and surface degradation with severe pitting (1.5 mm) and significant loss of section. More corrosion on top than on bottom side.		
1 B.9	Very minor surface corrosion, small and large blisters.	Poor bond on bent portion and most of straight ends.	Top side black, bottom side dull, very shallow metal loss, trapped solution.
3 B.10	Slight pitting (0.8-1 mm deep), large number of blisters.	Poor bond on bent portion and half of straight ends.	Top side black, bottom side dull, very slight pitting, trapped solution.
1 B.11	Large number of pinhole corrosion.	Very poor bond on bent portion.	Black and dull steel, very shallow metal loss.

Table C.18 Observations of Bar Trace on Macrocell Concrete Specimens

Specimen	Concrete on Top Side of Bar	Concrete on Bottom Side of Bar
A series - Control bars	Porous, dusty, adhering to bar, exudation of corrosion products.	More porous and dusty than on top side, adhering to bar, exudation of corrosion products.
A series - Coated bars	Smooth, shiny (glossy), minimum pores, clear rib marks, lack of bond with bar.	More pores than on top, less clear rib marks, sometimes with latence or whitish deposits adhering to bar, minor corrosion products at locations of exposed steel areas, few blisters developed at voids or air pockets.
B series - Control bars	Porous, dusty, adhering to bar, exudation of corrosion products.	More porous and dusty than on top side, surface latence filling rib marks, adhering to bar, exudation of corrosion products.
B series - Coated bars	Smooth, shiny (glossy), minimum pores, clear rib marks, lack of bond with bar, surface cracks not reaching bar level.	More pores than on top, less clear rib marks, sometimes with latence or whitish deposits adhering to bar, corrosion products at locations of exposed steel areas, blisters of variable sizes developed at voids or air pockets.

APPENDIX D
DETAILS OF BEAM EXPOSURE TEST

D.1 Test Variables

General. The variables selected for this test cover different usages of coated reinforcement, different loading conditions, different damage levels to epoxy coating, and different conditions of damage. These variables enable an assessment of the durability of coated bars under conditions simulating loaded structural elements. The limits selected for coating damage and repair relate to allowable levels proposed in several specifications.

Reinforcement Usage. Corrosion performance of straight bars and bent stirrups or ties may depend on bar geometry, concrete cover, and location in the structural element. Additionally, cut bar ends at splice regions may be a weak spot at which corrosion starts and propagates. In order to study all these concerns, three sets of beams were designed for testing: beams with longitudinal bars monitored; beams with stirrups monitored; and beams with mixed longitudinal bars and stirrups (some at splice regions). The intent was to examine the different performance of these bars and to identify the factors that promote corrosion or improve resistance to corrosion.

Loading Conditions. Three conditions were selected to simulate conditions in which the loads have caused cracking. The following load histories were considered:

- No imposed load; the beam supports only its own weight during exposure.
- Load applied to produce a crack of specified width; load removed during exposure.
- Load applied to produce a crack of specified width; load held during exposure.

The maximum crack width selected was 0.33 mm (0.013 in.) as permitted by ACI 318-89[70] for exterior exposure. Such a crack width may allow excessive amounts of chlorides to penetrate to the reinforcing steel during exposure to corrosive environments. Load cycling during exposure was considered a factor to promote corrosion of reinforcement in the cracked beams.

Epoxy Coating Damage Level. As for the macrocell study, coating damage was an important variable for evaluating the corrosion performance of epoxy-coated reinforcement. Damage level up to or exceeding current specification limits may occur in field applications; therefore, damage level needs to be included as a variable in the durability study. As received bars and bars intentionally damaged to 3% of bar surface area were studied.

The 3% limit of coating damage was introduced based on proposed modifications to current specifications governing use of epoxy-coated reinforcing bars. This limit has been proposed as the maximum allowable limit of patched surface area of bar. Accordingly, a damage level of 3% was selected for testing to cover the worst situation of possible damage that can be patched.

Repair of Damage. The damaged coating areas introduced on the test bars, and stirrup bends were either repaired or left unrepaired as another variable to examine the effectiveness of patching. Repairs were done according to the manufacturer's instructions using a liquid epoxy patching material and following recommended touch-up techniques.

D.2 Specimen Design

General. The key feature of this program was to assess the durability of coated bars when incorporated in elements under conditions simulating loaded structural elements. The three main purposes of the beam tests were:

- Group I: Longitudinal main reinforcement (straight bars) subjected to tensile stresses in a flexural mode.
- Group II: Fabricated transverse reinforcement (closed hoops) simulating stirrups or ties at a corner of a column, pier or beam.
- Group III: Splice zones (cut bar ends) in maximum moment regions.

By imposing flexural loads on the beams, the conditions associated with cracks in the concrete around bent transverse bars located close to the surface were reproduced. These conditions have been neglected in previous studies.

The reinforced concrete beams were designed with two reinforcing layers; the top layer consisted of two 10 mm (#3) uncoated bars, and the bottom layer consisted of two 19 mm (#6) epoxy-coated bars. The stirrups were also epoxy-coated 10 mm (#3) bars with 135° hooks. The dimensions of the beam cross section were approximately 0.2 x 0.3 m (8 x 12 in.) as shown in Fig. D.1. The clear concrete cover to reinforcement was 50 mm (2 in.) on all sides. The length of the beam was about 2.9 m (9.5 ft.).

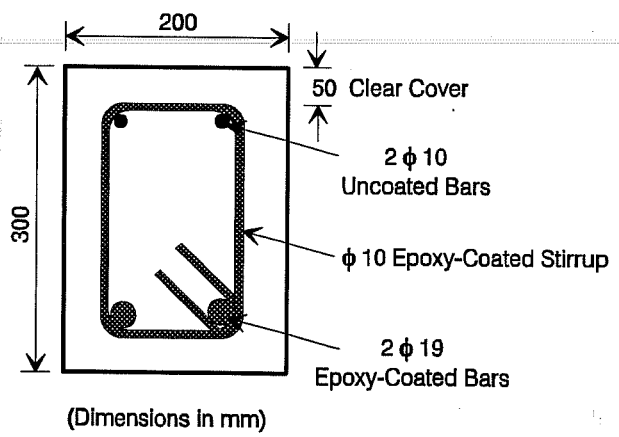

Figure D.1 Cross-Section of Beam Specimen.

Group I. The details of Group I beams are shown in Fig. D.2. The bottom reinforcing bars were completely isolated from contact with any other metal. Only one coated stirrup was placed at midspan of beam as a crack inducer. To ensure no electrical contact between the stirrup and longitudinal bars, the stirrup was encased in a heat shrink tube.

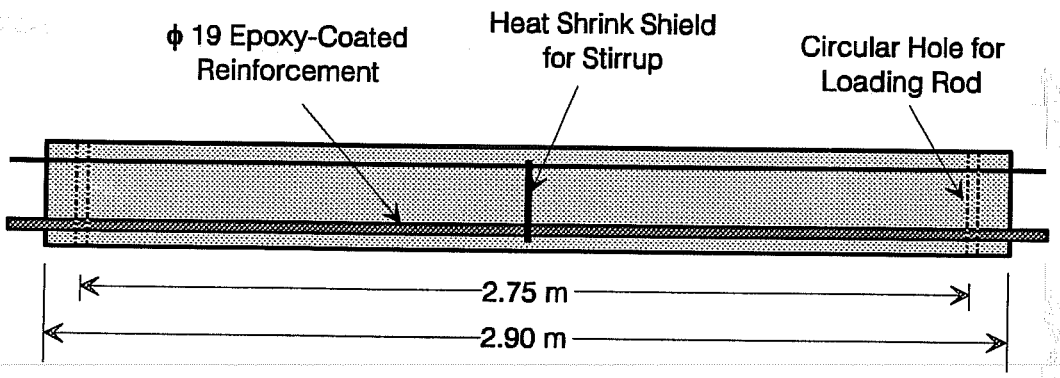

Figure D.2 Details of Group I Beam Specimen.

Group II. The details of Group II beams are shown in Fig. D.3. The bottom reinforcing bars were isolated from the single stirrup at midspan of the beam by encasing the longitudinal bars in heat shrink tubes. No similar precaution was introduced for the top reinforcement at the location of the stirrup. A plastic-covered wire was used to tie the coated stirrup to all longitudinal bars. This arrangement is similar to that at curbs of bridge decks where uncoated bent bars rise up and are tied to coated bars using a protected wire.

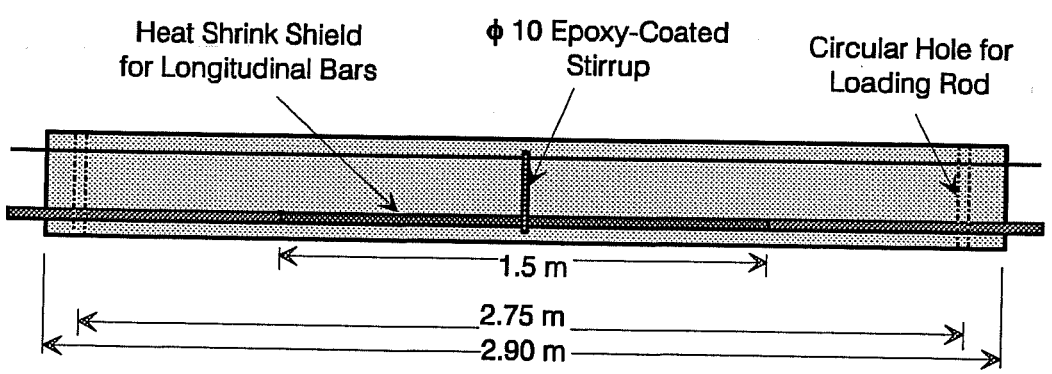

Figure D.3 Details of Group II Beam Specimen.

Group III. The details of Group III beams are typical of those shown for the other groups except that no attempt was made to provide isolation between the straight bars and the stirrups. In this case, the coated longitudinal and transverse reinforcement was tied with plastic-covered wire. This group was intended to determine the influence of connecting all bars, as in practice, on their corrosion performance.

Group III beam bars also included spliced bars to test corrosion initiation and propagation at cut ends of coated bars. The bottom reinforcement was spliced as shown in Fig. D.4 with bar ends at midspan in the high moment region. Three stirrups were provided within the splice zone with one stirrup about 50 mm (2 in.) from the end of splice in the middle of the beam.

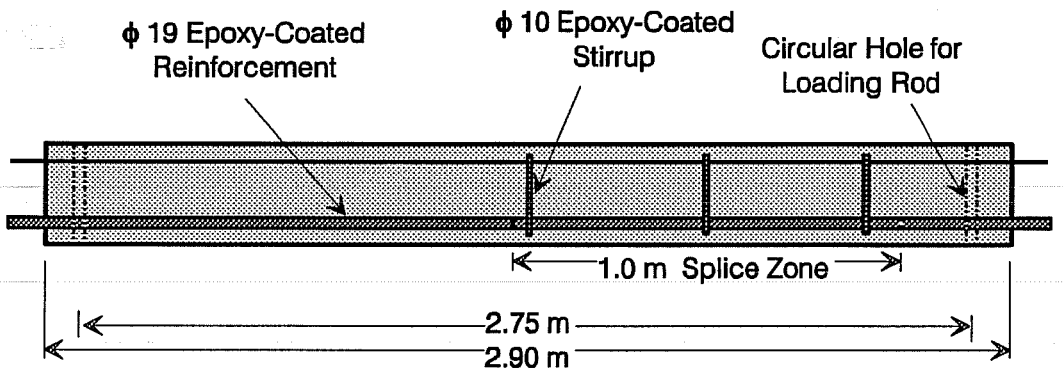

Figure D.4 Details of Group III Beam Specimen.

D.3 Epoxy-Coated Reinforcing Steel

Steel Procurement. The epoxy-coated reinforcing bars used in this test were coated and procured in a manner similar to the bars used in the macrocell test as described in Section C.3. However, the bars were coated with a different commercially available epoxy coating material approved for use by TxDOT. The coating material was certified as conforming to ASTM A775/A775 M-90, ASTM D3963-86, ASTM A884-88, Class A, AASHTO M284/M284-87I, and AASHTO M254-77 (1986) Type B. The straight bars were cut in 3 m (10 ft.) lengths, while stirrups were fabricated and patched (at bar ends and around some of the corners) at the plant.

Bar Identification. Groups I and II each consists of a total of 14 beams arranged in duplicates. Group III has 6 beams, again in duplicates, with two beams of mixed longitudinal bars and stirrups, and four beams with splices. Table D.1 summarizes the variables involved in each pair of beams. The beams are identified by a sequential number and the initials of the variables involved such as the bar monitored, loading condition, and damage level and condition. Each of the coated longitudinal bars is identified by its position in the beam during exposure such as "upper" or "lower" bar (see Section D.7) Additionally for the splice

bars, the terms "long" and "short" are used to distinguish between bars that passed the beam mid section or ended there, respectively.

Table D.1 Summary of Beam Exposure Study Variables

Beam No.	Bar Monitored	Loading Condition[a]	Damage Level and Condition
B1, B2	Longit.	Uncracked, Unloaded	As Received[b]
B3, B4	Longit.	Cracked, Unloaded	As Received
B5, B6	Longit.	Cracked, Loaded	As Received
B7, B8	Longit.	Uncracked, Unloaded	3% Damaged
B9, B10	Longit.	Cracked, Unloaded	3% Damaged
B11, B12	Longit.	Cracked, Loaded	3% Damaged
B13, B14	Longit.	Cracked, Unloaded	3% Damaged (Patched)
B15, B16	Stirrup	Uncracked, Unloaded	As Received[c]
B17, B18	Stirrup	Cracked, Unloaded	As Received
B19, B20	Stirrup	Cracked, Loaded	As Received
B21, B22	Stirrup	Uncracked, Unloaded	As Received (Patched)
B23, B24	Stirrup	Cracked, Unloaded	As Received (Patched)
B25, B26	Stirrup	Cracked, Loaded	As Received (Patched)
B27, B28	Stirrup	Cracked, Unloaded	3% Damaged (Patched)
B29, B30	L / St	Cracked, Unloaded	Both 3% Damaged (Patched)
B31, B32	Splice	Cracked, Unloaded	Stirrup 3% Damaged (Stirrup & Bar End Patched)
B33, B34	Splice	Cracked, Loaded	Stirrup 3% Damaged (Stirrup & Bar End Patched)

a Loading and Unloading refer to imposed loads causing bending about the strong axis.
b No visible damage.
c No patch on bends.

Steel Tensile Strength. Two coated steel samples of the longitudinal bars were tested to obtain the tensile yield strength, yield strain, and ultimate strength. No significant differences existed between the results of the replicate test samples. Therefore, the average test values were used to construct the stress-strain curve shown in Fig. D.5. The measured strengths conformed to the requirements of ASTM A615-87a.[143] The average yield strength was 437 MPa (63 ksi) exceeding 414 MPa (60 ksi) and the average ultimate strength was 701 MPa (102 ksi) exceeding 621 MPa (90 ksi).

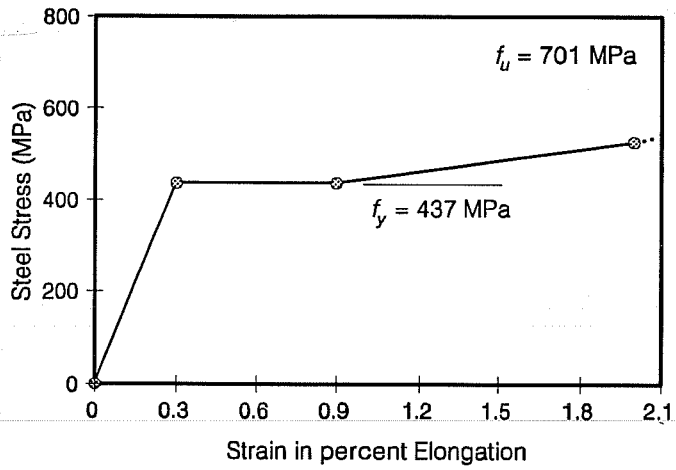

Figure D.5 Stress-Strain Curve for the 19 mm Bars.

Epoxy-Coating Thickness. A thumbwheel pull-off magnetic gage was used to measure the coating thickness on straight lengths of the epoxy-coated bars and stirrups. The procedure described in Section C.3 for the macrocell specimens was followed. For each bar specimen, the average coating thickness of six measurements and the maximum deviation in thickness from the average are reported in Tables D.2 to D.4.

As mentioned previously, both ASTM A775 and ASTM D3963 require that at least 90% of all recorded film thickness measurements must be between 130 and 300 μm (5-12 mils). ASTM A775 further requires that the deviation in coating thickness not exceed $\pm$50 μm ($\pm$2 mils) or deviate $\pm$30% from the average thickness, whichever is less. All coating thickness measurements on longitudinal bars and stirrups were within the specified range. However, 13 readings, or 31% of all longitudinal bar measurements and 15% of all stirrup measurements, did not satisfy the deviation requirements. Thus, there was lack of uniformity in the coating thickness and not all bars met the specification requirements.

In general, the 19 mm (#6) bar specimens had thicker coatings than the 10 mm (#3) stirrups. The average coating thickness of the larger and smaller size bars were 240 and 190 μm (9.4 and 7.4 mils), respectively. However, the uniformity of coating thickness of the smaller bars was better than that of the larger bars.

Table D.2 Coating Thickness Measurements of Beam Steel Specimens, Longitudinal Bars - Group I (130 μm = 5 mils, 300 μm = 12 mils)

Specimen	Average Coating Thickness (μm)	Maximum Deviation from Average	
		(μm)	(%)
B1-L-UU-AR	270	+85	31
	190	23	12
B2-L-UU-AR	230	-51	22
	190	-47	24
B3-L-CU-AR	250	-42	17
	270	+66	25
B4-L-CU-AR	260	-47	18
	190	-40	21
B5-L-CL-AR	240	-38	16
	270	-53	20
B6-L-CL-AR	220	+59	27
	190	+61	32
B7-L-UU-D	200	+53	26
	310	-25	8
B8-L-UU-D	290	+42	15
	280	-28	10
B9-L-CU-D	190	-13	7
	270	-44	16
B10-L-CU-D	290	+68	24
	270	+53	20
B11-L-CL-D	270	-13	5
	230	+47	20
B12-L-CL-D	210	+15	7
	280	+55	20
B13-L-CU-D(P)	260	-44	17
	260	-34	12
B14-L-CU-D(P)	180	-19	10
	250	-36	14

Table D.3 Coating Thickness Measurements of Beam Steel Specimens, Stirrups - Group II (130 μm = 5 mils, 300 μm = 12 mils)

Specimen	Average Coating Thickness (μm)	Maximum Deviation from Average	
		(μm)	(%)
B15-L-UU-AR	230	**-51**	22
B16-ST-UU-AR	170	-19	11
B17-ST-CU-AR	180	-25	14
B18-ST-CU-AR	180	+22	12
B19-ST-CL-AR	190	-41	21
B20-ST-CL-AR	180	-25	14
B21-ST-UU-AR(P)	160	**-60**	**37**
B22-ST-UU-AR(P)	210	+29	13
B23-ST-CU-AR(P)	200	**-76**	**38**
B24-ST-CU-AR(P)	190	+35	18
B25-ST-CL-AR(P)	210	+22	11
B26-ST-CL-AR(P)	200	-25	13
B27-ST-CU-D(P)	180	-25	14
B28-ST-CU-D(P)	200	+29	14

Table D.4 Coating Thickness Measurements of Beam Steel Specimens, Longitudinal Bars and Stirrups - Group III (130 μm = 5 mils, 300 μm = 12 mils)

Specimen	Average Coating Thickness (μm)	Maximum Deviation from Average (μm)	Maximum Deviation from Average (%)
Longitudinal Bars			
B29-L/ST-CU-D(P)	190	+38	20
	200	+30	15
B30-L/ST-CU-D(P)	240	-19	8
	200	-19	10
Stirrups			
B29-L/ST-CU-D(P)	200	-19	10
B30-L/ST-CU-D(P)	190	+16	8
B31-SP-CU-D(P)	170	-19	11
B32-SP-CU-D(P)	170	+32	19
B33-SP-CL-D(P)	170	0	0
B34-SP-CL-D(P)	160	-44	27

Coating Defects and Introduced Damage. The condition of the bars was carefully inspected and documented before deliberately introducing any damage. The documentation included the coating appearance, and the number and location of existing damage. All bars had the same uniform, glossy appearance, with fair coating coverage and well-defined deformations. Fabrication of stirrups resulted in only minor damage to coating concentrated inside the bends.

A predetermined amount of damage was introduced in the coating on some bars using a sharp blade. Damage was in the form of small rectangles that exposed approximately 3% of the bar surface area at a specific location. For the longitudinal reinforcement, damage was estimated and distributed along the middle 0.91 m (3 ft.) of the bar. Damage spots were located between transverse lugs and at the lugs themselves. Some of the spots were offset from the center to include some of the longitudinal continuous ribs.

The number and size of damage spots were approximately as follows: 11- 13 x 10 mm (1/2 x 3/8 in.); 7- 6 x 6 mm (1/4 x 1/4 in.); and 3- 3 x 3 (1/8 x 1/8 in.). For the stirrups, damage was estimated for roughly half the length of the stirrup, and was distributed along the outer surfaces of the bends at one side of the stirrup. A total of 10 damage spots with an approximate size of 6 x 6 mm (1/4 x 1/4 in.) was introduced.

The introduced damage was also documented and each bar was photographed to keep a record of the initial condition. A two-part liquid epoxy, compatible with the coating material, was used for repair where desired. The exposed steel areas were not given any special treatment before applying the patching material by brush. The cut bar ends in the splice zone were also patched in a similar manner. Stirrups which were previously patched at the plant were patched again around the bends were damage was not adequately repaired. Figures D.6 to D.8 show examples of the bars included in the beam exposure study.

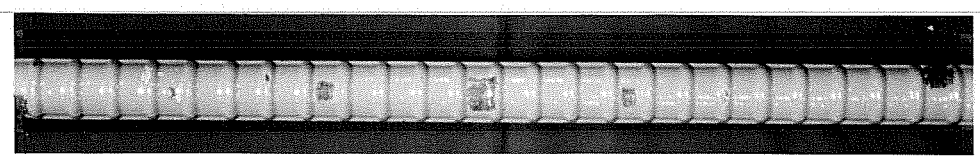

(a) 3% Damage in Middle Segment of Bar

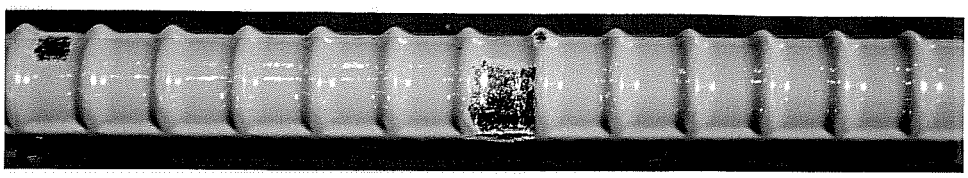

(b) Close Up of the Damaged Area

Figure D.6 Damage Spots on 19 mm Longitudinal Bar.

(a) As Received Condition of Bends

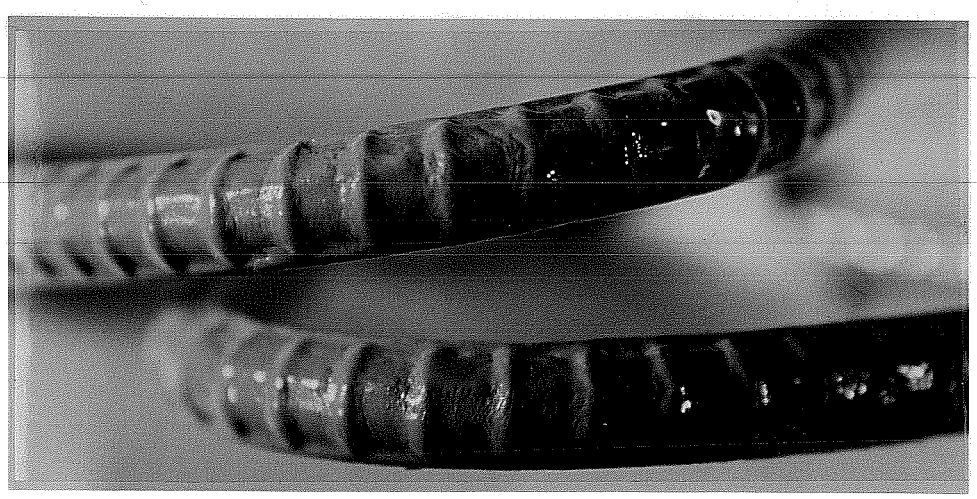

(b) As Received, Patched Condition of Bends

Figure D.7 Stirrup Condition without Introduced Damage.

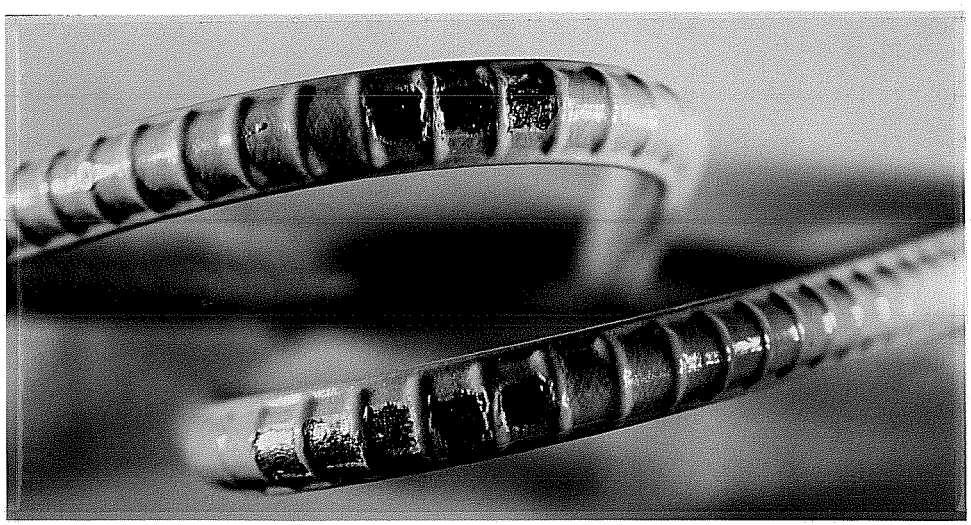

(a) 3% Damaged Bends

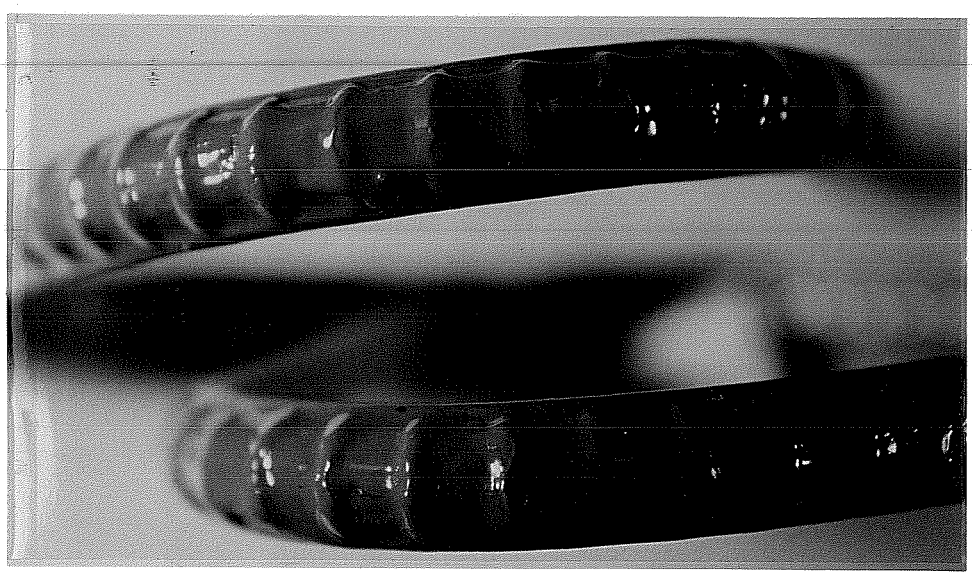

(b) 3% Damaged and Patched Bends

Figure D.8 Stirrup Condition with Introduced Damage.

D.4 Uncoated Reinforcing Steel

The grade 60 uncoated bars used at the top of beam were left "as received".

D.5 Formwork and Steel Installation

Formwork. The formwork for the beam specimens consisted of a plywood base with double plywood dividers for adjacent beams as shown in Fig. D.9. The short side plywood panel of each beam compartment was predrilled to position the top and bottom bars at the proper dimensions. All sides of the formwork were secured in place by bolts and tied threaded rods. Joints between formwork parts were sealed with silicone. One transverse wood brace was used across the middle of the forms to facilitate tying the stirrup and to ensure a constant beam dimensions during casting. Enough forms were built to cast 14 beams at one time, so beam groups were cast at different times.

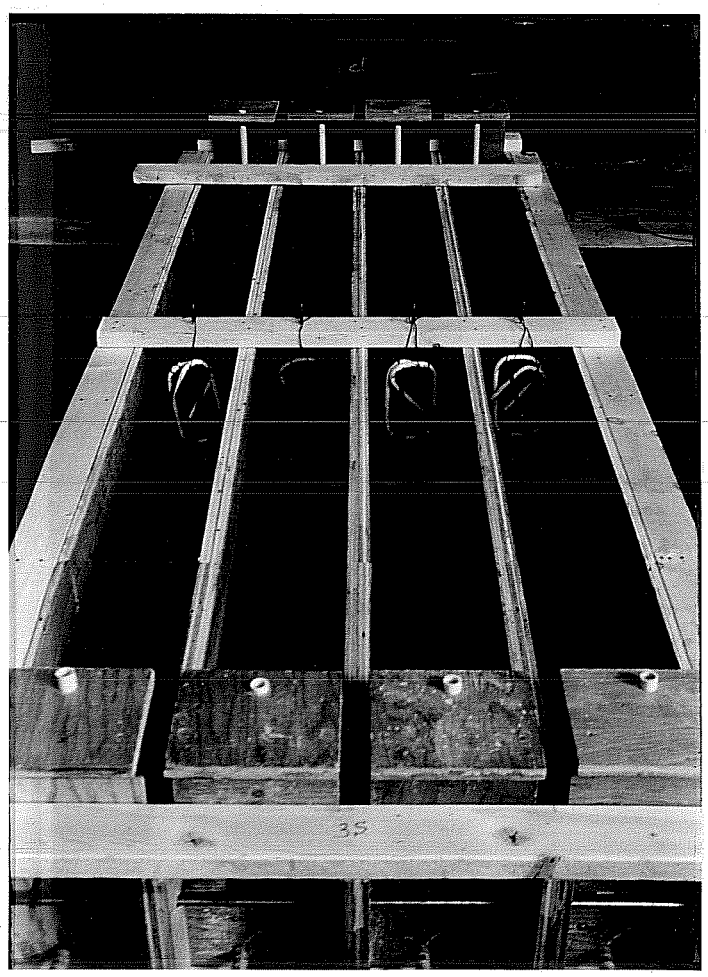

Figure D.9 Formwork for Beam Specimens.

Steel Installation. The reinforcement was placed by inserting the bars through the end plywood panel as shown in Fig. D.9. No chairs were necessary to support the longitudinal bars. Plastic pipes were positioned vertically near the ends of the forms for passing threaded bars through the beams for loading during exposure testing.

Coated stirrups Group I beams were insulated with heat shrink tubes as shown in Fig. D.10, and their ends sealed with silicone, before placement in forms. Longitudinal bars for Group II beams were also insulated with heat shrink tubes over a length of about 1.5 m (5 ft.) along the middle section. Wire connections were installed on the stirrups of group II and III beams to facilitate half-cell measurement during exposure as shown in Fig. D.11. These connections were patched with epoxy before casting to prevent undesired galvanic action. Figure D.12 shows steel installation at one splice of Group III beams.

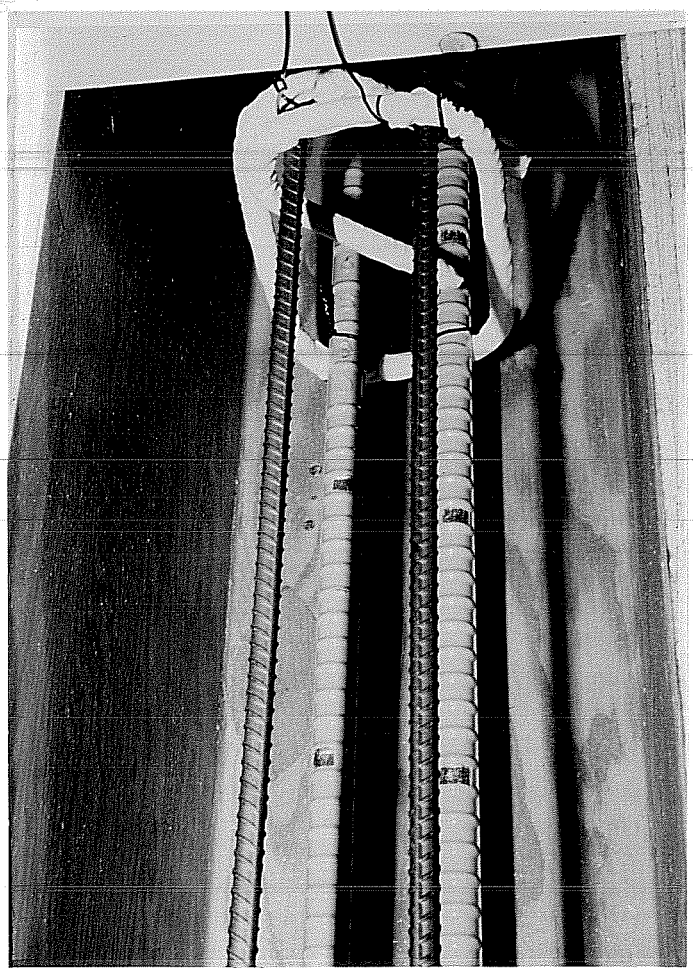

Figure D.10 Steel Detailing of Group I Beam Specimen.

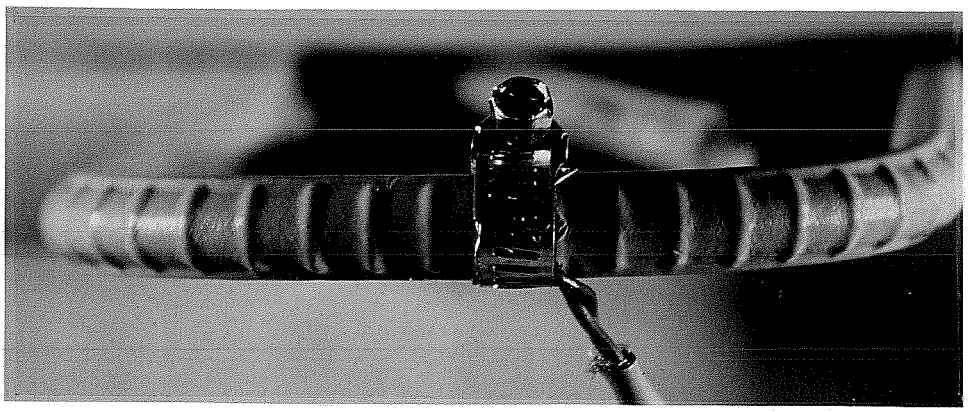

Figure D.11 Internal Stirrup Connection for Group II Beam Specimen.

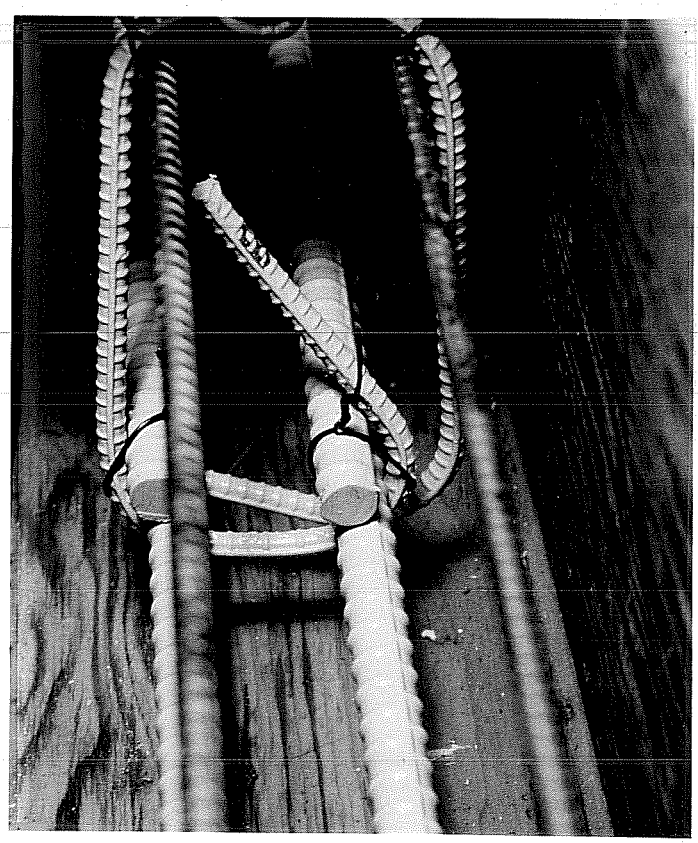

Figure D.12 Steel Detailing of Group III Beam Specimen.

D.6 Concrete

Mixture Design. Similar to the requirements of the macrocell study, concrete of reduced strength and increased permeability was used to construct the test beams. Three similar concrete batches were ordered at different times to cast the three groups of beams. The details of the concrete mixtures are shown in Table D.5.

Casting. Concrete was batched and supplied by a commercial ready mix supplier. Casting was done indoors directly from the truck into the forms. The concrete was placed in one lift and consolidated using 50 mm (2 in.) ϕ head internal vibrators as shown in Fig. D.13. The vibrators were inserted mainly along the middle of the beam to avoid shifting or damaging the steel bars.

During each casting, the same concrete was used to cast all beams within a group and a large number of standard cylinders. The specimens were screeded immediately after placing concrete and trowelled shortly after. The specimens were then covered with plastic sheets for a short time to reduce water evaporation.

Curing. After a period varying between 5 and 12 days of casting, the forms and cylinder molds were stripped and no further curing of the beam specimens was provided. Some cylinders were placed in a humidity chamber under standard moist curing conditions. The rest of the cylinders were exposed to the same ambient conditions as the beams.

Compressive Strength. Concrete strength was determined at 2, 7, 14, 28, 90, and 365 days after casting. The 28-day strength was determined from both air-cured cylinders and moist-cured cylinders and was on the average about 26, 28, and 22 MPa (3750, 4050, and 3200 psi) for Groups I, II, and III, respectively. The strength-gain curves for concrete at the various ages are shown in Fig. D.14.

Permeability. Concrete permeability was determined from 100 x 200 mm (4 x 8 in.) cylinders using a standard test procedure for Rapid Determination of the Chloride Permeability of Concrete (AASHTO T277-83).[146] Some cylinders were kept air dry and some were soaked in water whenever the beams were undergoing a wet period during the exposure cycle.

Cylinders from the three groups were tested for permeability at four different ages within 15 months from casting. The average permeability measurements for the air-dried cylinders for all tests were approximately 8200, 5700, and 11500 coulombs for the three groups in order. Similarly, the average permeability measurements for the wetted cylinders were approximately 6500, 5600, and 7200 coulombs in the same order. Although the results of the wetted cylinders were, as expected, less than those of the air-dried cylinders, all values fell under the standard classification of "high" permeability.

Table D.5 Concrete Mixture Details for the Beam Exposure Study

Material	Quantity	Unit
	Group I	
20 mm Rock, SSD	1120	kg/m^3
Sand, SSD	828	kg/m^3
Type I Portland Cement	222	kg/m^3
Pozzolana R	10	kg/m^3
Water	145	kg/m^3
W/C Ratio, by weight	0.62	
Unit Weight	2217	kg/m^3
Slump	150-175	mm
	Group II	
20 mm Rock, SSD	1088	kg/m^3
Sand, SSD	833	kg/m^3
Type I Portland Cement	222	kg/m^3
Pozzolana R	10	kg/m^3
Water	144	kg/m^3
W/C Ratio, by weight	0.62	
Unit Weight	2268	kg/m^3
Slump	150-175	mm
	Group III	
20 mm Rock, SSD	1090	kg/m^3
Sand, SSD	840	kg/m^3
Type I Portland Cement	221	kg/m^3
Pozzolana R	10	kg/m^3
Water	145	kg/m^3
W/C Ratio, by weight	0.63	
Unit Weight	2197	kg/m^3
Slump	175	mm

Figure D.13 Casting Beam Specimens.

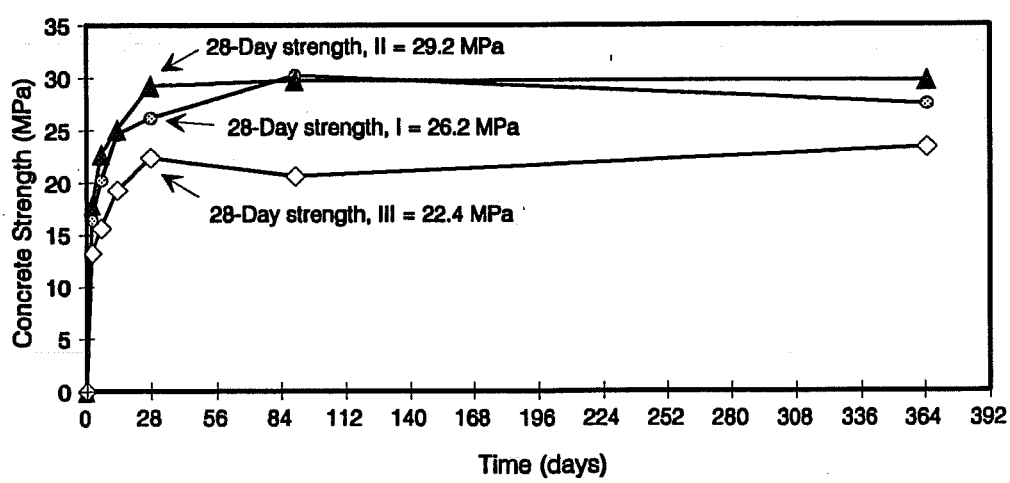

Figure D.14 Compressive Strength Gain of Concrete for Beam Groups.

D.7 Test Setup

Specimen and Test Preparation. The beams were moved carefully to a large testing room on the second floor of a different building. Wood supports were built and arranged in a manner to hold the beams in pairs placed back to back resting on their 300 mm (12 in.) long sides. The bottom of the beams as cast faced out as shown in Fig. D.15. Solid steel bars, 50 x 50 mm (2 in.) in section, separated the beams at mid span.

Due to space limitations, the 34 beams were laid out in three rows over four parallel lines of supports. The two middle lines of supports were loaded first. These supports were lower than the outer ones so that the ends of the beams resting on them served as supports for the higher level beams on either side.

In order to crack the beams and open cracks to the desired width, loads were applied with threaded rods which extended through the beams at the ends. A center-hole hydraulic ram and a pump were used to load the beams as shown in Fig. D.16. A pressure transducer was attached to the pump to monitor the load. This system permitted loading a pair of beams by applying a tension force to the rod at one end and causing reactions at the other end and at the middle through the separator bar.

An exposure area on the top surface at the middle of each beam was defined. The area was 150 x 600 mm (6 x 24 in.) for beams in which corrosion of the longitudinal bars was monitored, and 0.15 x 0.3 m (6 x 12 in.) for beams in which corrosion of the stirrups or splice ends was monitored. Plexiglass dikes 38 mm (1.5 in.) high were mounted with silicon around the three sides of the exposure area to confine the salt solution during wetting and allow the solution to flow over the free edge of the beam. Silicone was also applied to make small dams along the borders of the area exposed directly to the solution on the vertical surface and on the bottom surface for a distance of 150 mm (6 in.) from the edge.

Electrical connections were mounted on the protruding ends of each longitudinal epoxy-coated bar in groups I and III. The epoxy coating was chipped from a small area before installing the connection to ensure good electrical contact. At first, hose clamps were used but they were replaced by ground clamps properly secured into the steel as shown in Fig. D.17.

Lines parallel to the embedded coated reinforcement were drawn on the concrete surfaces to mark points for half-cell measurement. The points were spaced 0.15 m (6 in.) along 0.75 m (2.5 ft.) on either side of the middle of the longitudinal bar. The points (a total of 11) were numbered 0 at the middle, positively to the right, and negatively to the left. Seven points were marked along the stirrup, with 0 at the middle of the vertical surface, positively upward, and negatively downward. The points in each direction coincided with the near corner of the stirrup, the middle point along the leg, and the far corner. Figure D.18 shows an isometric drawing of the coupled beams with the marked lines and points of measurement. The longitudinal bar which faces up in this arrangement was labeled "upper" and the bar below "lower".

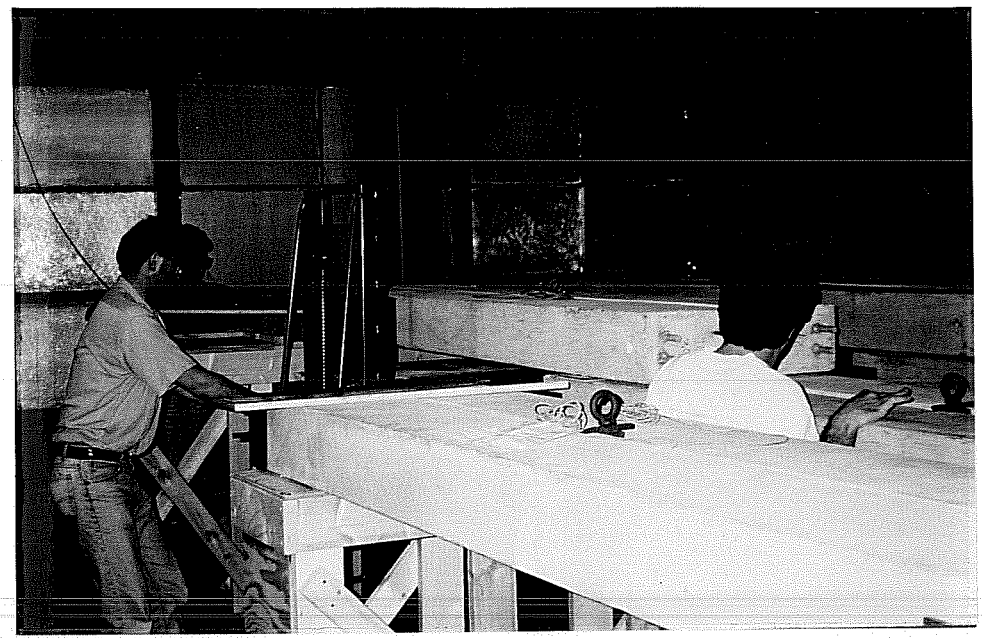

Figure D.15 Laying Out Beams in Testing Room.

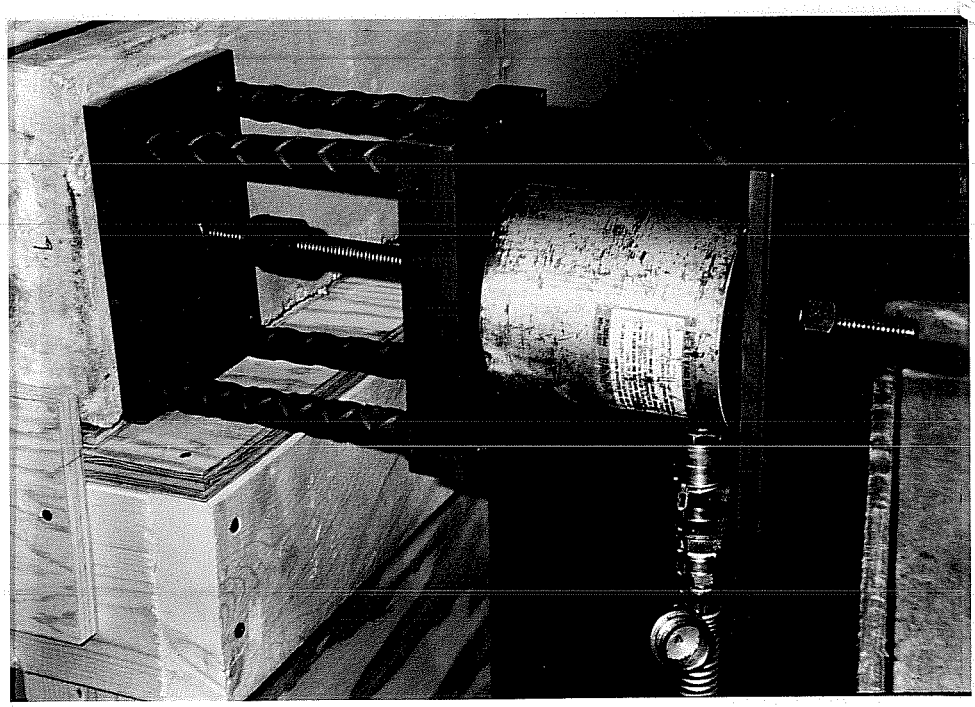

Figure D.16 Beam Loading System.

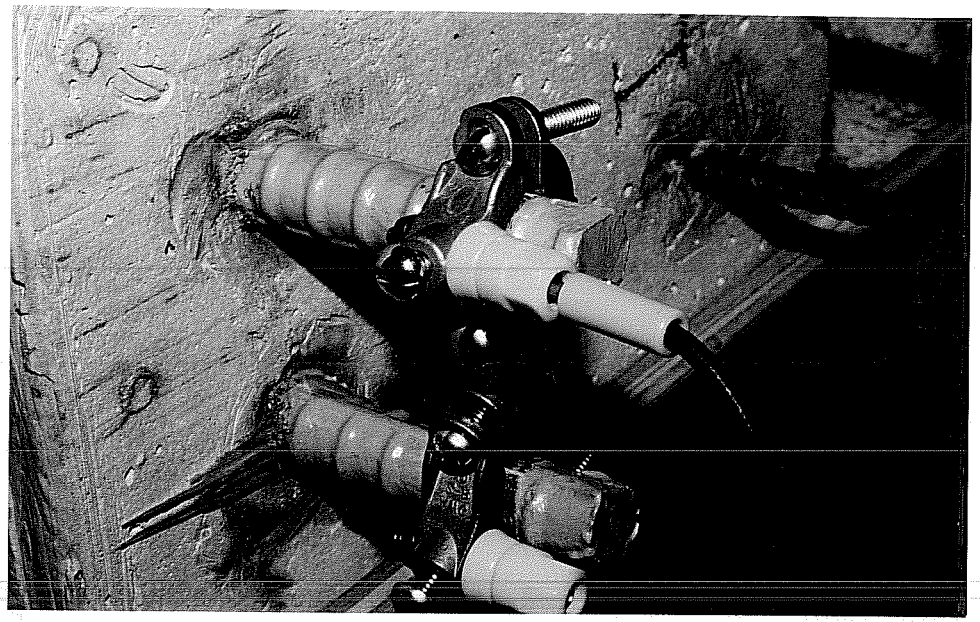

Figure D.17 External Bar Connection For Half-Cell Measurement.

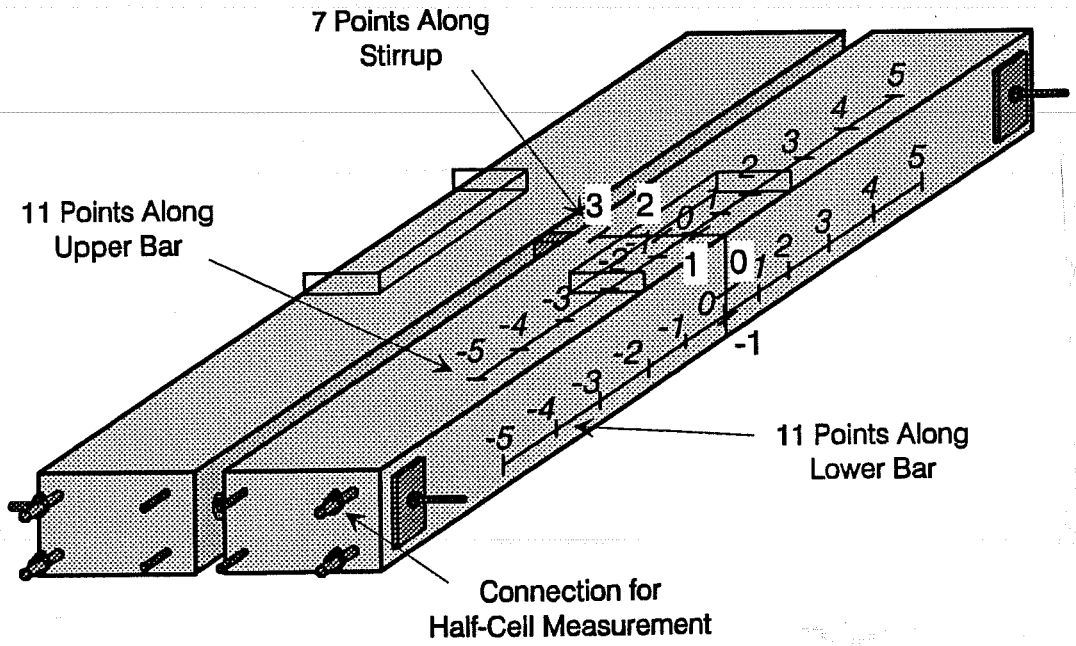

Figure D.18 Points of Half-Cell Measurement.

A salt water distribution network made of PVC pipes was installed above and between the coupled beams. At the starting point near the center, an open plastic tank was placed on the floor below the beams and a stainless steel, end suction, single stage centrifugal pump was mounted. A flow control system was provided to distribute the salt solution at the exposure area of each beam. The system consisted of bubblers (flow control devices operating under pressure) and small diameter flexible tubing. The tubes were clamped to the plexiglass dikes to direct the flow over the exposure area.

Finally, a collecting system was prepared and installed beneath the beams to transfer the solution back to the tank by gravity. Wooden collectors covered with plastic sheets were assembled with tilting bases to drain the solution from each pair of beams to a network of open PVC channels running beneath the supports. The system was simple, rust-free, and easy to maintain.

Cracking of Beams. Before exposure testing was started, beams were loaded and cracked as required. When both beams in a loaded setup cracked, the load was removed and cracks were marked. Beams were then reloaded gradually until the maximum crack width roughly reached the desired surface crack width. After unloading the beams, any additional cracks that occurred during this loading stage were also marked and mapped. Beams to be kept under load during exposure were not unloaded; instead, the nuts were tightened on the threaded rods to maintain beam curvature.

It was interesting to note that cracking of Group II beams was louder and more sudden than that of the other groups and resulted immediately in a wide crack near midspan. Beams in the other groups showed narrower first cracks and gradually formed multiple cracks distributed along the beam. It is believed that the heat shrink tube used to isolate the longitudinal reinforcement destroyed mechanical bond along the bar. In effect, there was no stress transferred from the longitudinal bar to the concrete and a crack formed suddenly at stirrup location.

Calculated stresses in the epoxy-coated bars corresponding to a crack width of 0.33 mm (0.013 in.) were around 60% of steel yield strength. Stresses calculated from applied loads were in agreement with anticipated loads at the desired crack width.

Exposure Conditions. All exposure areas on the beam specimens were subjected to alternate wetting and drying using a 3.5% NaCl solution. A complete exposure cycle consisted of three days of continuous wetting followed by eleven days of air drying at room temperature. Figure D.19 illustrates the exposure cycle including load cycling. The first wetting period was started when all concrete beams were between 115 and 140 days old. Figure D.20 shows an overview of the beams during exposure to salt solution.

To compensate for evaporation and for solution permeating into concrete, the level of solution in the tank was monitored and adjusted during each wetting period. The solution was replaced every few cycles to maintain a constant salt concentration. Concrete surfaces at the exposed areas were washed periodically (every 2-3 cycles) with clean water to dissolve any salt buildup or crystallization in the concrete cover.

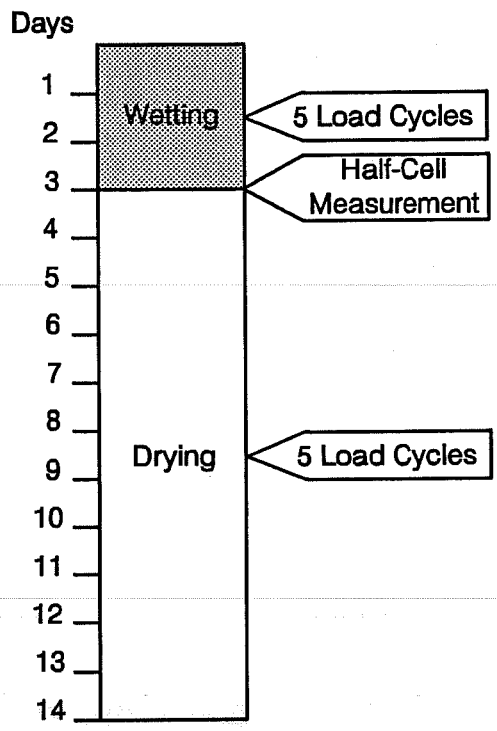

Figure D.19 Exposure Cycle for Beam Test.

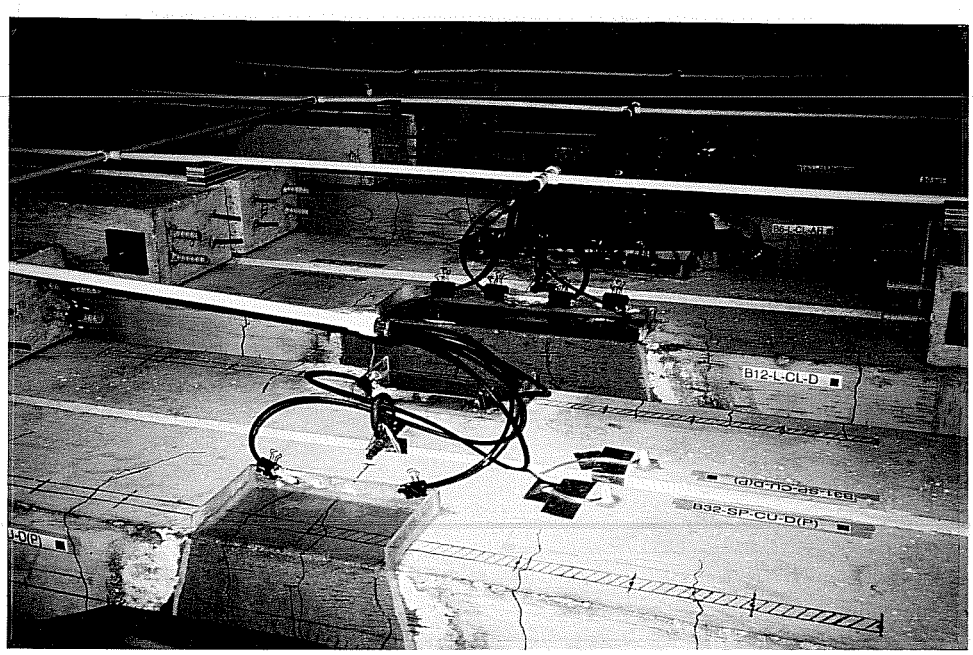

Figure D.20 View of Beams in Exposure Room.

To promote corrosion during exposure to salt solution and drying, the cracked beams were subjected to cycles of loading and unloading following a sequence used previously by Poston.[4] On the second day of wetting, beams were subjected to five repeated loading cycles up to a load equal to that producing the desired crack width as determined during the initial cracking stage. During each load cycle, the maximum applied load was held constant for approximately five seconds before release. These load cycles *pumped* salt solution into the cracks to aggravate chloride accumulation at the reinforcement surface. On the same day of the following week (ninth day of exposure cycle) during drying, five additional load cycles were applied to each cracked beam. These load cycles increased oxygen supply to the reinforcement to enhance oxygen reduction and corrosion product oxidation.

D.8 Routine Monitoring

Visual Examination. Beam specimens were visually inspected at the beginning of the test and periodically thereafter. The purpose of the examination was to observe any development of surface stains and corrosion-induced cracking.

Half-Cell Potential Measurement. Half-cell potentials of the coated bars were measured against a saturated calomel electrode (SCE). The calomel electrode is a mercury/mercury chloride half-cell reference electrode. Measurements were made by connecting the reinforcing bar to the positive terminal of a high impedance DC voltmeter and the reference electrode to the negative terminal. The voltmeter displays potentials in the range 0-1000 mV with 1 mV precision. However, the values were recorded to the nearest multiple of 5 mV. A schematic diagram of the measuring circuit is shown in Fig. D.21. An open cell sponge pad was secured around the electrical base of the electrode to improve conductivity. Measurement procedure was in accordance with ASTM C876.[117]

At first, measurements were made after each wetting period. After the fourth cycle, however, measurements were made at the completion of every two wetting periods. Measuring potentials right after wetting was helpful because the beams were already damp and good concrete conductivity was achieved. However, to improve concrete conductivity in parts not exposed to NaCl, a wetting solution (water and detergent) was used at all points of measurement prior to taking the readings. The potential records were transferred to an electronic spreadsheet for further analysis.

The diagrams of steel potential versus time of exposure up to about 400 days are shown in Fig. D.22 to D.55. These figures correspond to the beams that were removed for autopsy. Exposure testing of the remaining beams continues and results will be reported in a later report. No major differences of performance existed between the replicate beams; therefore, the diagrams shown here are representative of the performance of each pair.

The potentials at points ± 4, and ± 5 along the longitudinal bars were roughly similar but distinctly different from those at points near the beam midspan. The potentials at points within the exposure area were also very similar to each other. Therefore, the average potentials of the four end "dry" points and the five mid "wet" points were calculated and displayed in the same figures mentioned above. In order to monitor any abrupt changes in potentials with time, the step or successive change of average potentials was calculated and

plotted as well. The same procedure was followed for stirrups except that all points were grouped together as their potentials were not considerably different.

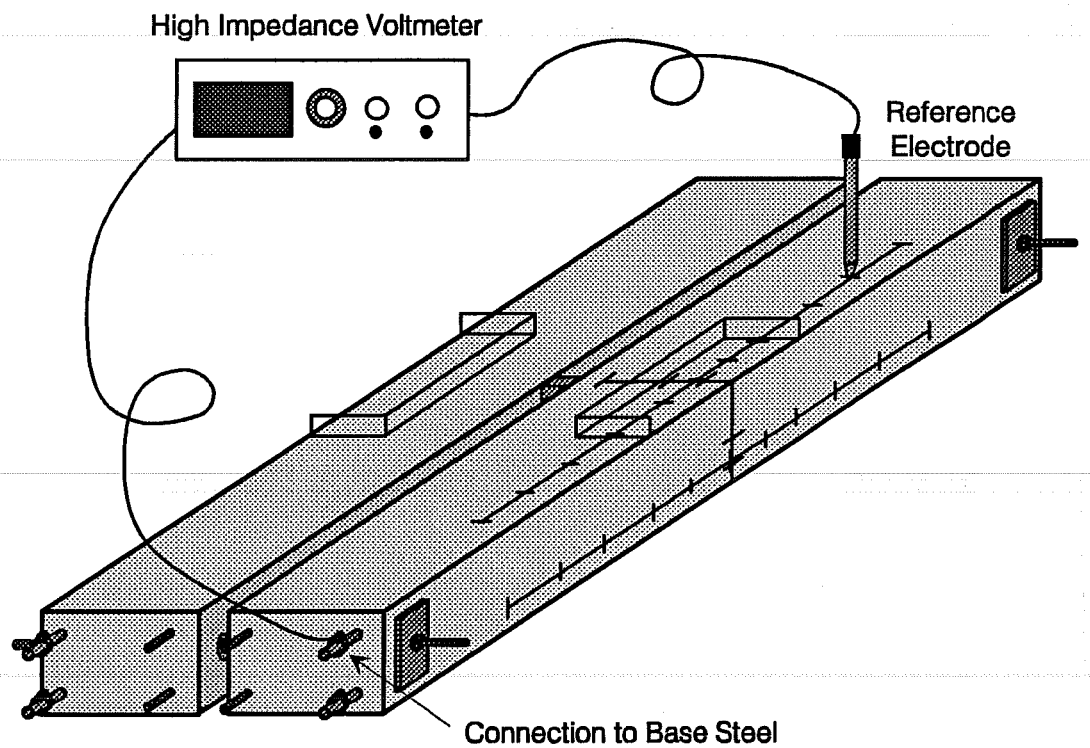

Figure D.21 Schematic Diagram of Half-Cell Measuring Circuit.

Temperature Measurement. The temperature in the test room was measured every time potentials were obtained. Although the temperatures varied between 19° C (66° F) and 32° C (90° F) over a period of one year, the effects of such variation on measured potentials are not significant. Potentials are ideally determined at a temperature of 22.2° C (72° F), and are corrected by a factor of -0.66 mV/C°. Thus, the maximum deviation of potential due to extreme temperature changes is only -6.5 mV. ASTM C876 requires that potentials be reported to the nearest 10 mV because of uncertainty inherent in the procedure. Hence, correcting the measured potentials to a base temperature was unnecessary.

Crack Width Measurement. Crack maps and crack widths were documented and updated during the exposure period. It was desired to detect any crack development or movement due to corrosion activity. For practical purposes, only selected cracks were monitored and measured every two cycles to detect changes in crack width. Three or four cracks at the midspan region were usually monitored. The crack width was measured using a graduated magnifying lens but most often using a crack comparator. Crack was measured at two points on the vertical surface; one point near the top and the other near the bottom with respect to the viewer. Figures D.56 to D.72 show the surface condition and crack maps

of all beams removed after approximately one year of testing. Tables D.6 to D.13 list the average crack widths of those cracks marked on the maps.

D.9 Postmortem Examination

General. One of each pair of beams from the 34 beams was removed for demolition after 392 days of exposure. Generally, the selected beam was the one showing the most negative potentials although differences between the replicate beams were minimal.

Concrete Condition. Prior to destruction, delamination of concrete was checked by hammer sounding. Concrete surfaces were struck with a ball-peen hammer at several locations to detect any delaminated areas. The results of this inspection are given in Chapter 11. No corrosion-induced cracks or stains were observed on any of the test beams during the first year of exposure.

Chloride Content. Chloride samples from each beam were extracted and analyzed to determine the acid-soluble chloride content at various depths including reinforcement levels. The samples were obtained from a number of holes drilled at cracks and in uncracked concrete along and across the beam. The locations of the holes were very close to the embedded reinforcement to determine the chloride concentration most representative of that at the bar level. These locations are shown in Fig. D.56 to D.72. Drilling concrete surfaces for chloride sampling is shown in Fig. D.73. The chloride contents of the autopsied beams are shown in Tables D.14 to D.16.

Specimen Destruction. In order to visually examine the reinforcement at the midspan region, partial and complete saw cuts were made to recover a length of 1.25 m (4 ft.) of the longitudinal bars and the full stirrups. Prior to cutting, lines were drawn to mark the cuts made to facilitate bar removal. Several beams were cut as a group using the concrete saw as shown in Fig. D.74.

The mechanical removal of concrete between the cut lines was done carefully to avoid damaging the epoxy-coated bars. Concrete was forced to break in the longitudinal bar plane or stirrup plane by use of a jack hammer along the grooves as shown in Fig. D.76. Additional minor chipping allowed complete removal of the bar from the concrete. Lack of adhesion between the coated bar and concrete greatly facilitated bar retrieval.

Visual Inspection. The bars were visually inspected for any evidence of corrosion and blistering. During removal of the coating to examine underfilm corrosion, the ease or difficulty of peeling was reported as an indicator of the degree of debonding. The extent of corrosion propagation on the steel substrate was documented, particularly with respect to crack locations. All observations of the retrieved bars are summarized in Tables D.17 to D.19. In addition, some of the uncoated reinforcing bars at the compression side of the beam were exposed to examine their condition. Finally, the bar trace in the concrete was carefully inspected for the presence of voids, dried solution deposits, and corrosion products. These observations are given in Chapter 11.

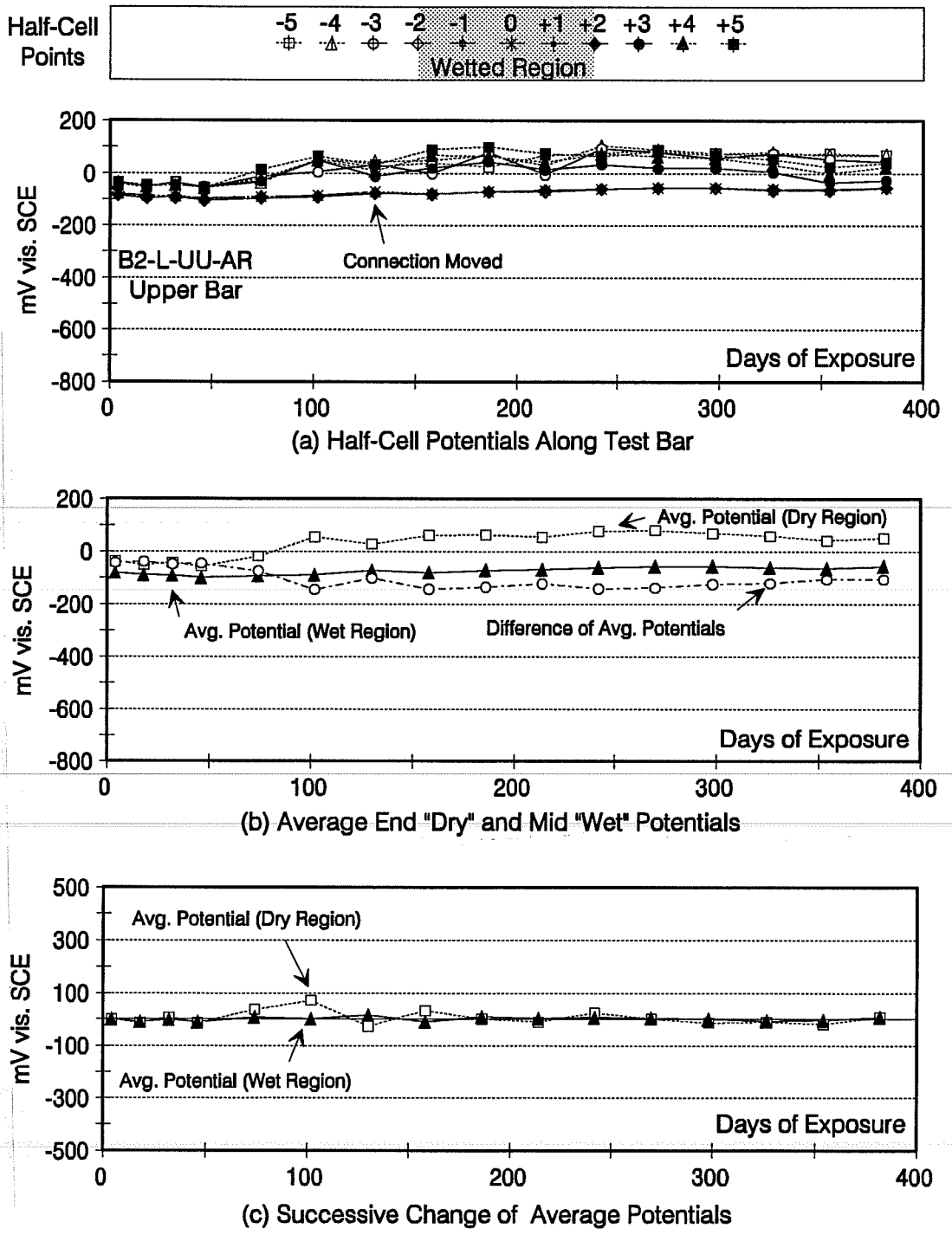

Figure D.22 Half-Cell Potentials for Beam B2-L-UU-AR, Upper Bar.

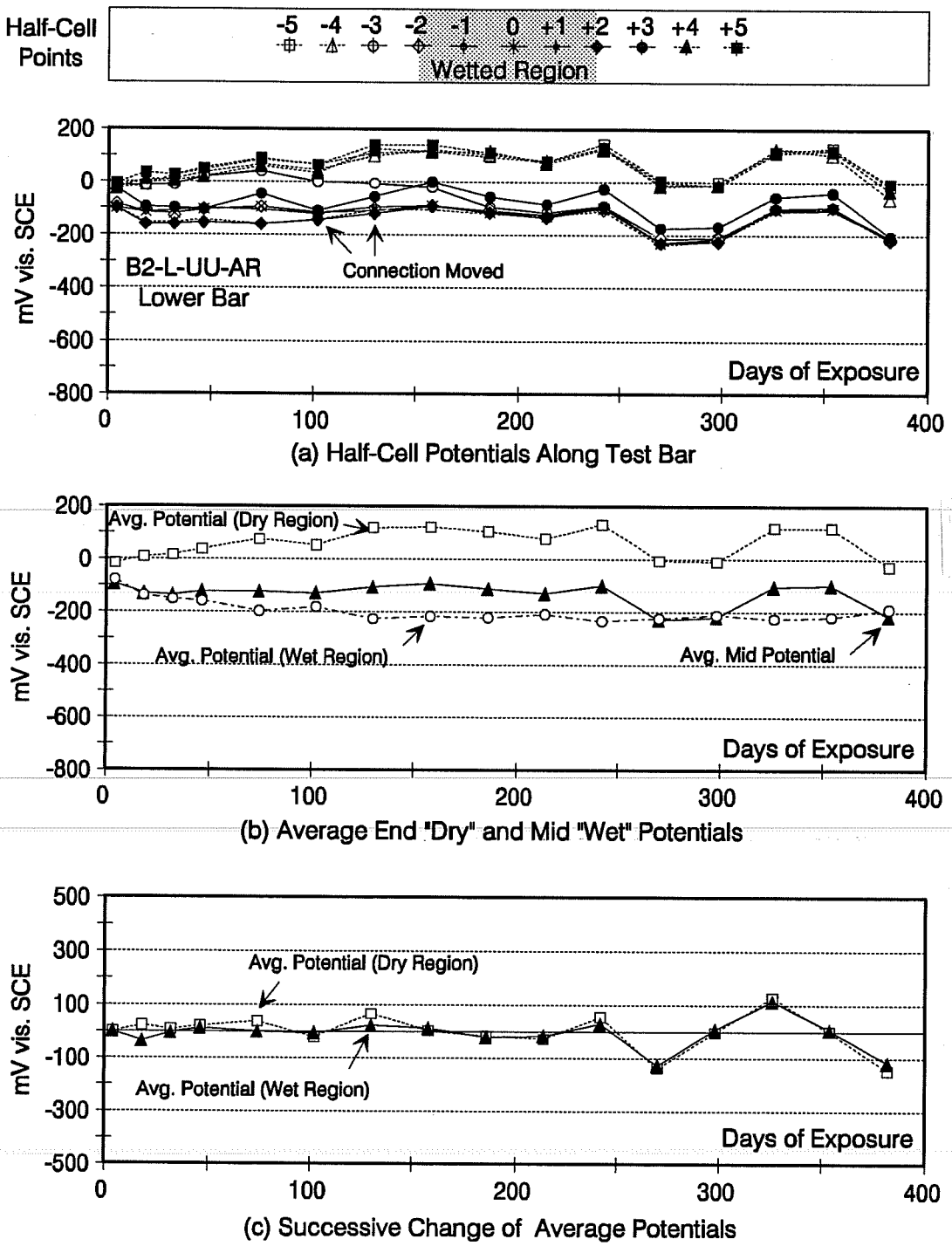

Figure D.23 Half-Cell Potentials for Beam B2-L-UU-AR, Lower Bar.

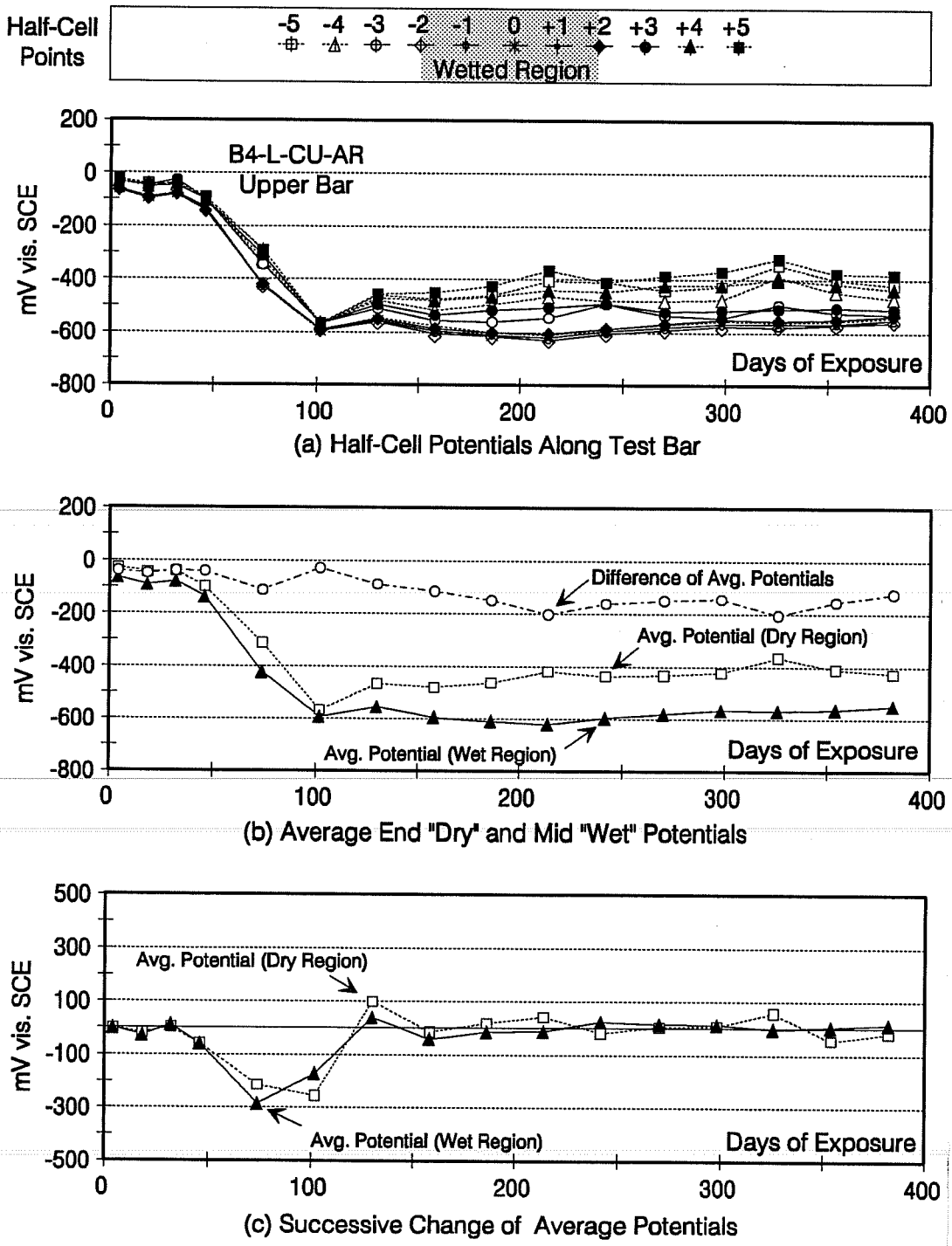

Figure D.24 Half-Cell Potentials for Beam B4-L-CU-AR, Upper Bar.

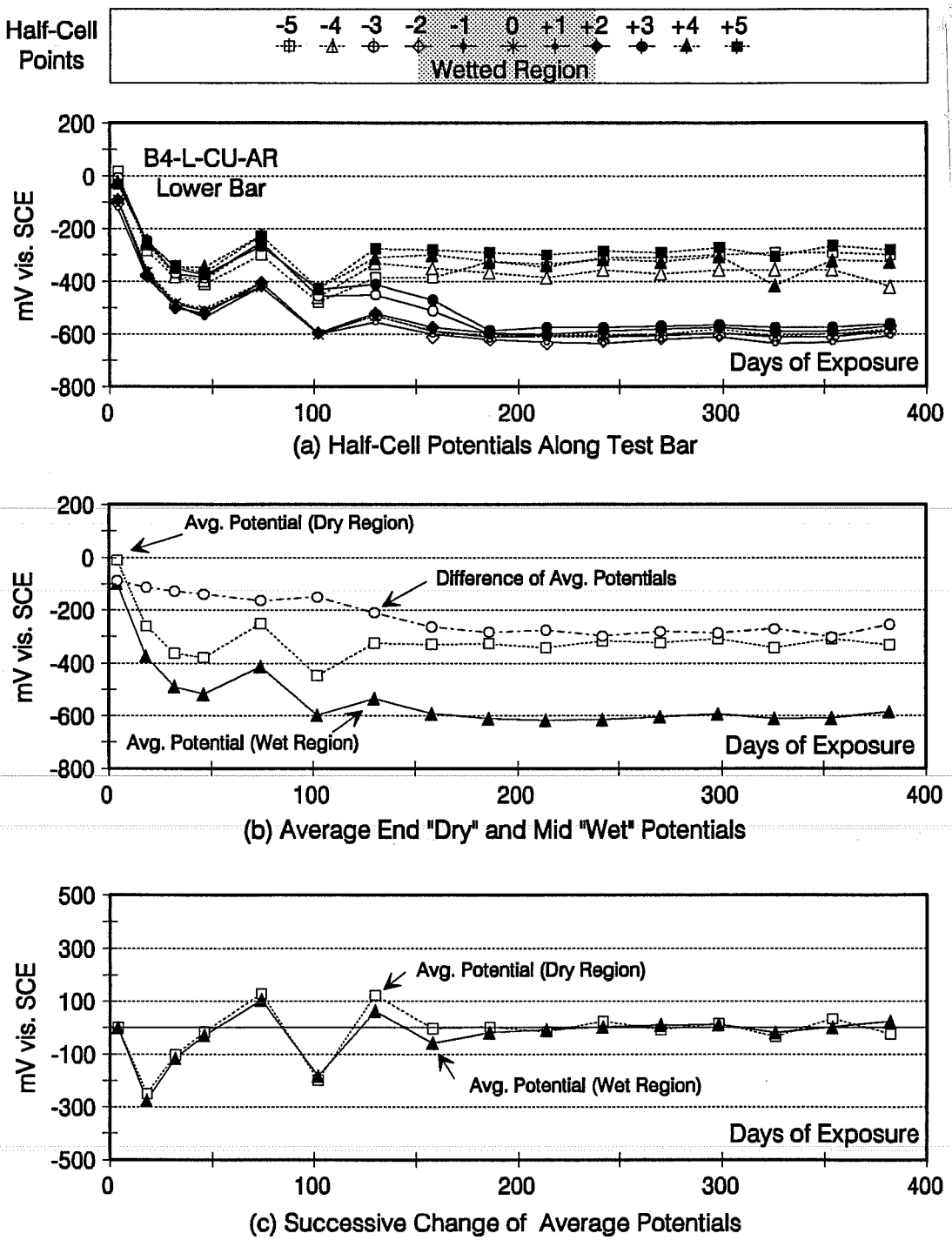

Figure D.25 Half-Cell Potentials for Beam B4-L-CU-AR, Lower Bar.

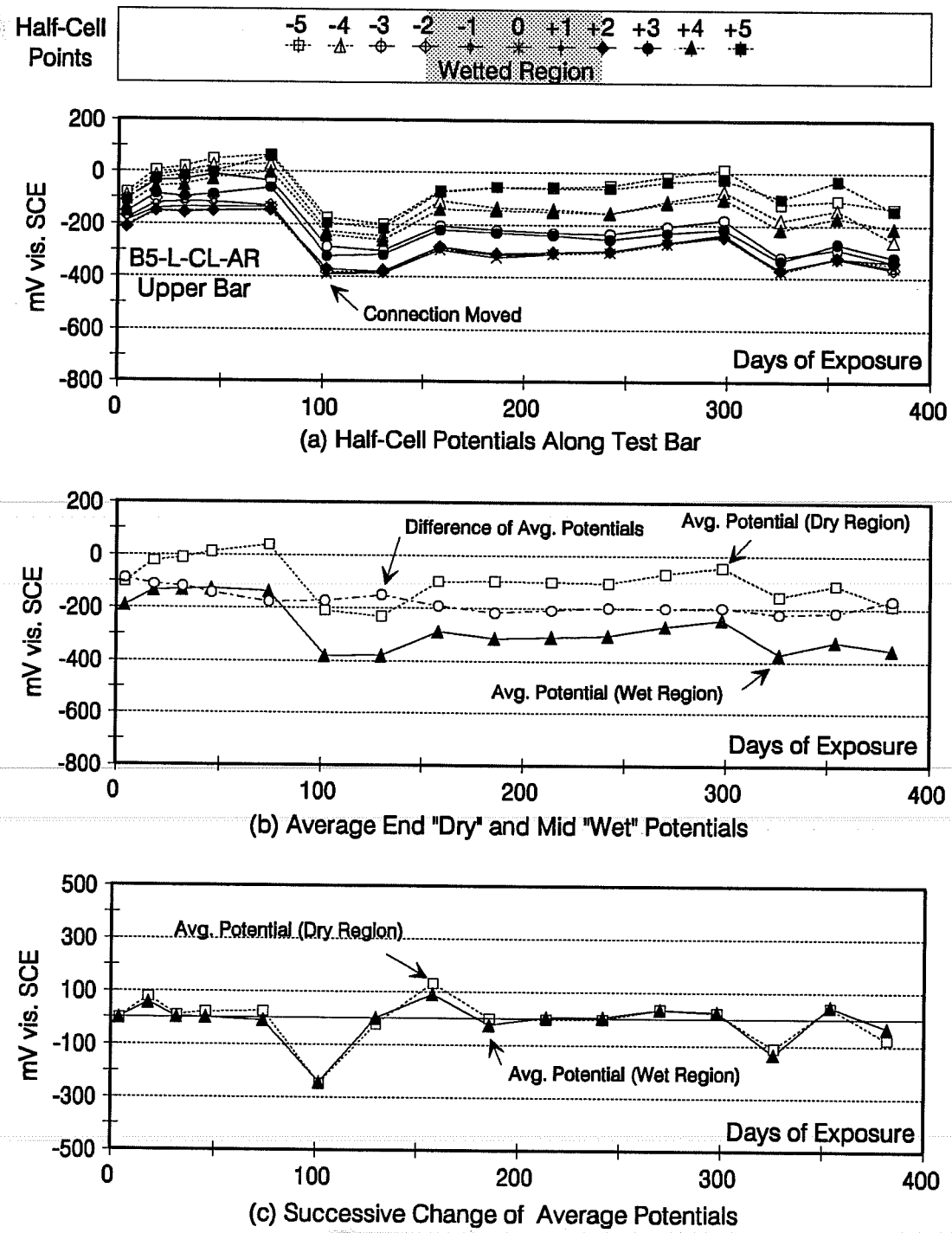

Figure D.26 Half-Cell Potentials for Beam B5-L-CL-AR, Upper Bar.

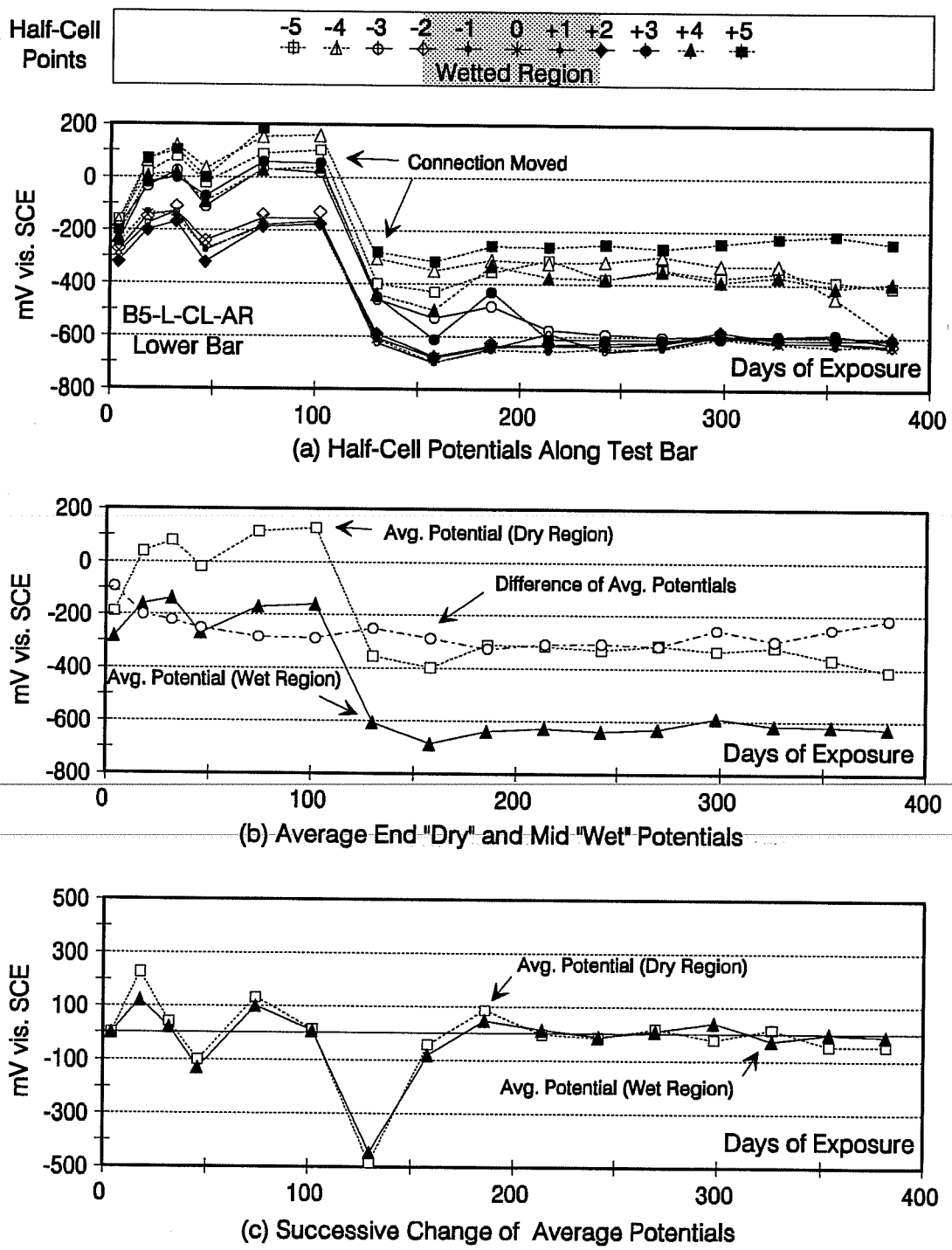

Figure D.27 Half-Cell Potentials for Beam B5-L-CL-AR, Lower Bar.

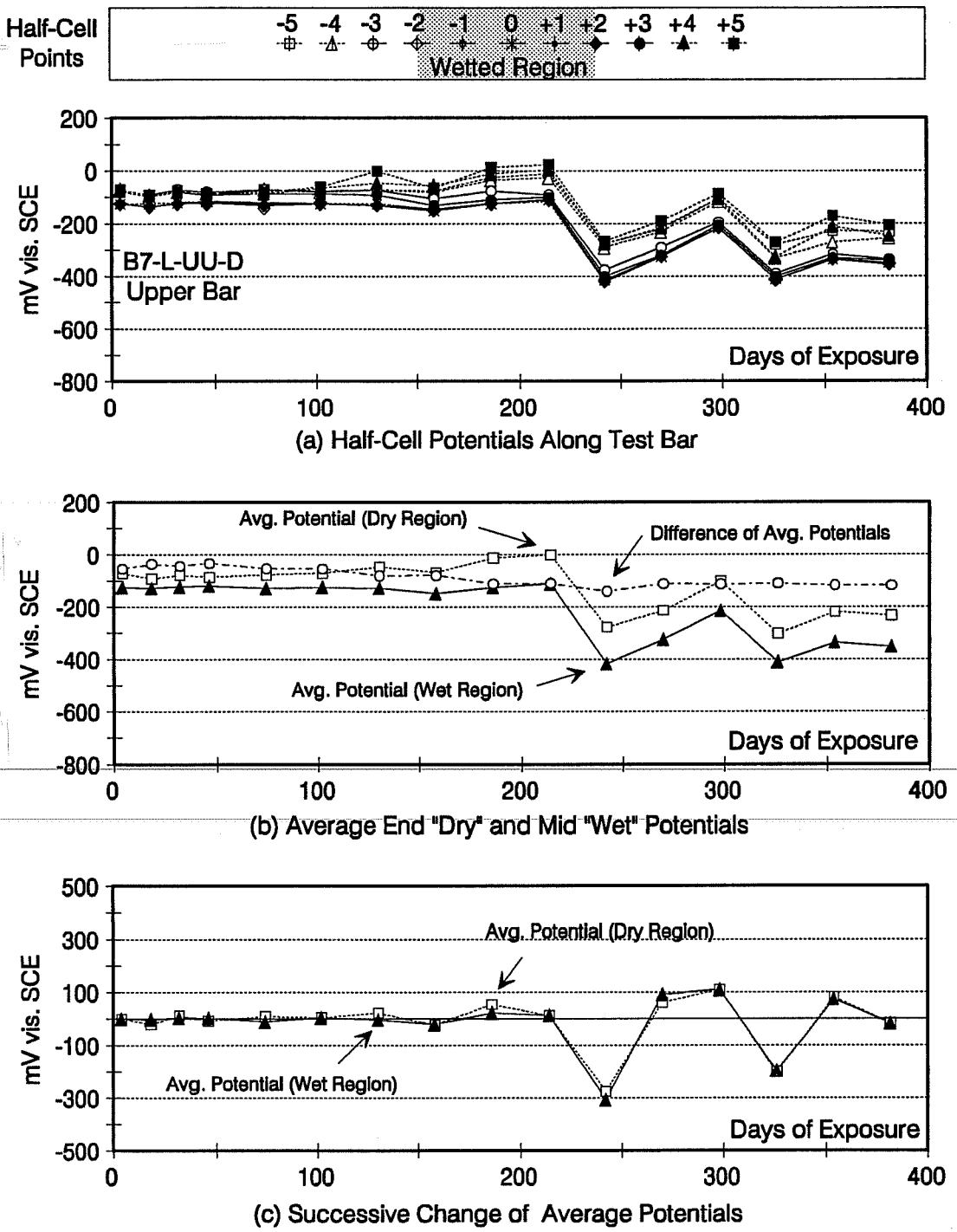

Figure D.28 Half-Cell Potentials for Beam B7-L-UU-D, Upper Bar.

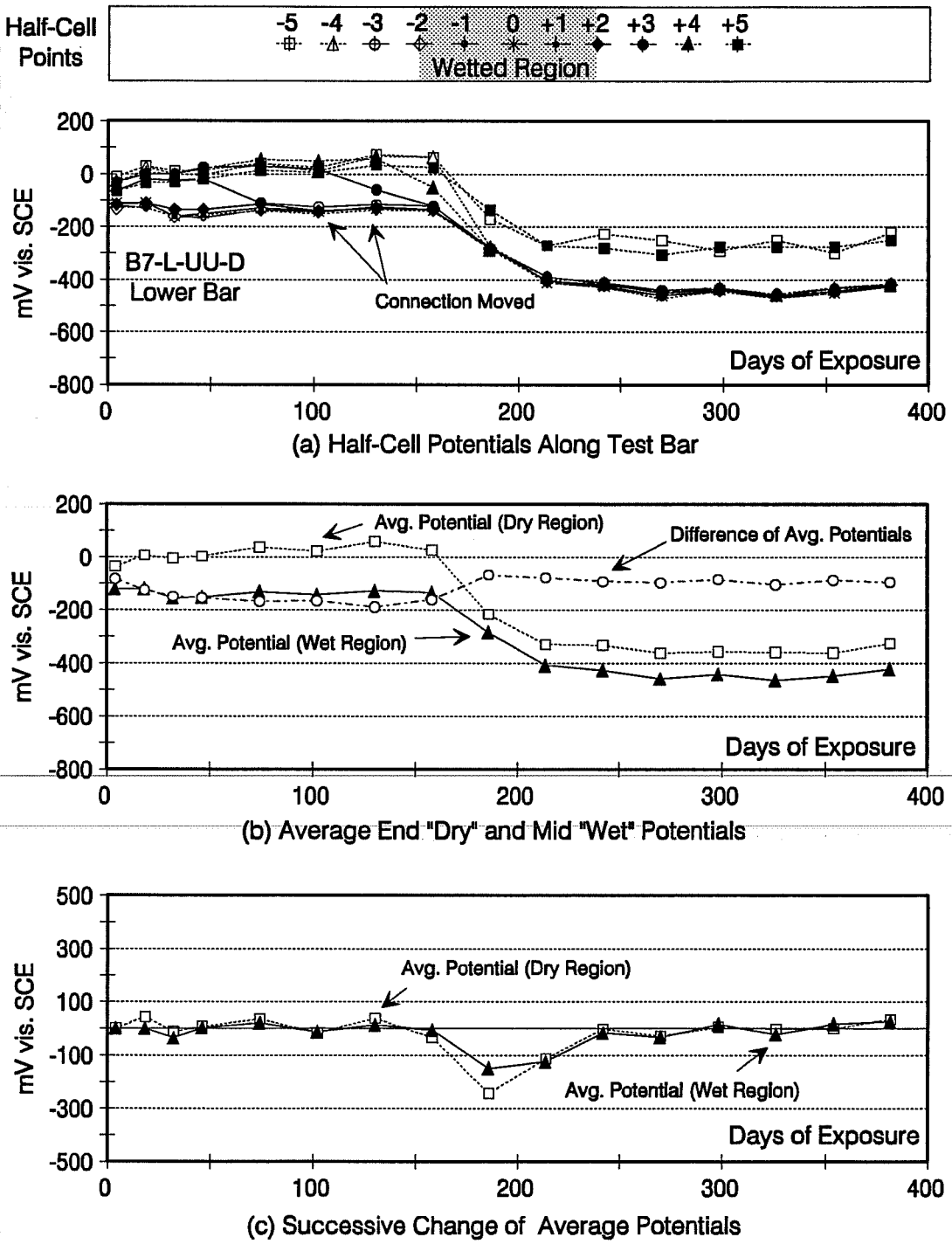

Figure D.29 Half-Cell Potentials for Beam B7-L-UU-D, Lower Bar.

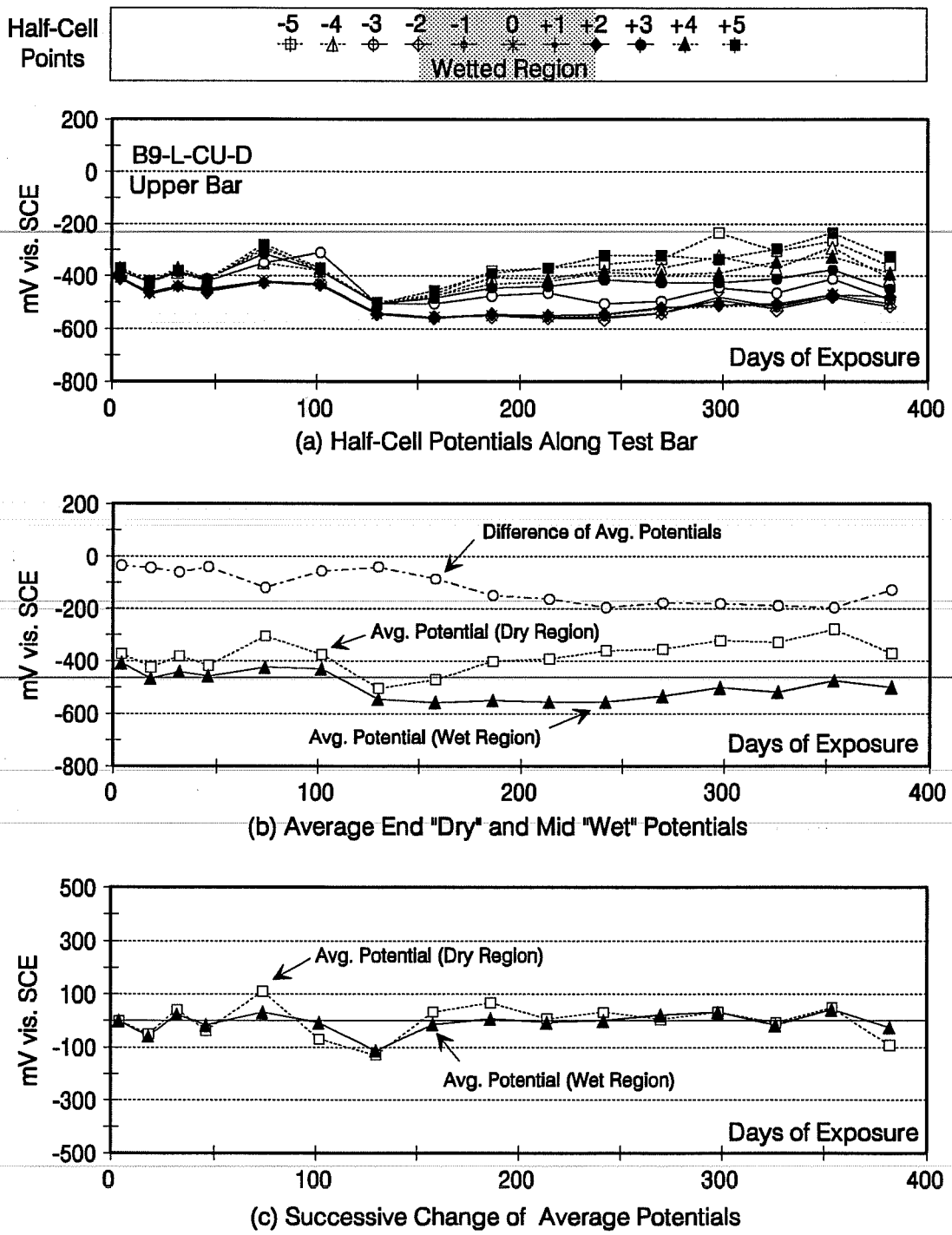

Figure D.30 Half-Cell Potentials for Beam B9-L-CU-D, Upper Bar.

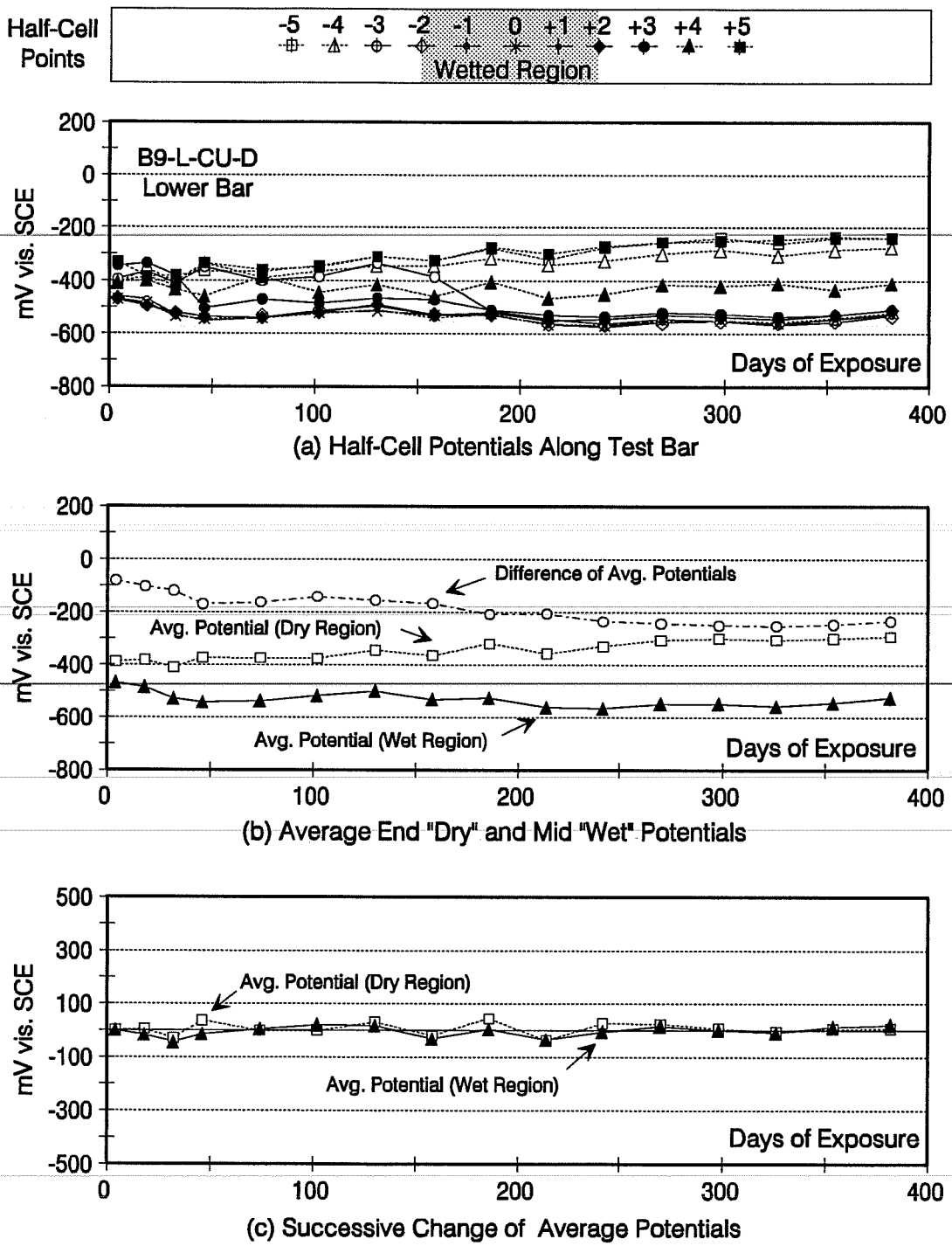

Figure D.31 Half-Cell Potentials for Beam B9-L-CU-D, Lower Bar.

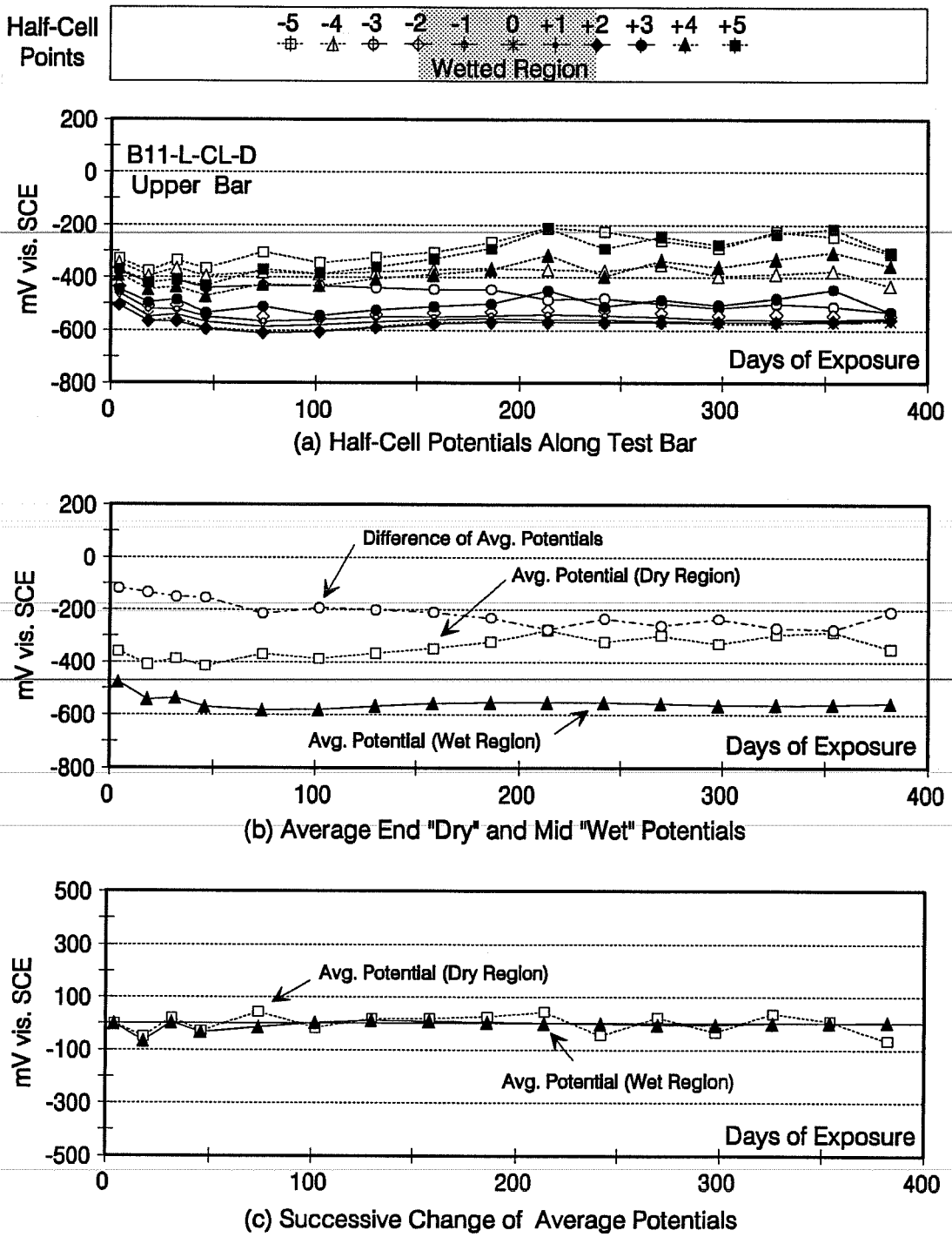

Figure D.32 Half-Cell Potentials for Beam B11-L-CL-D, Upper Bar.

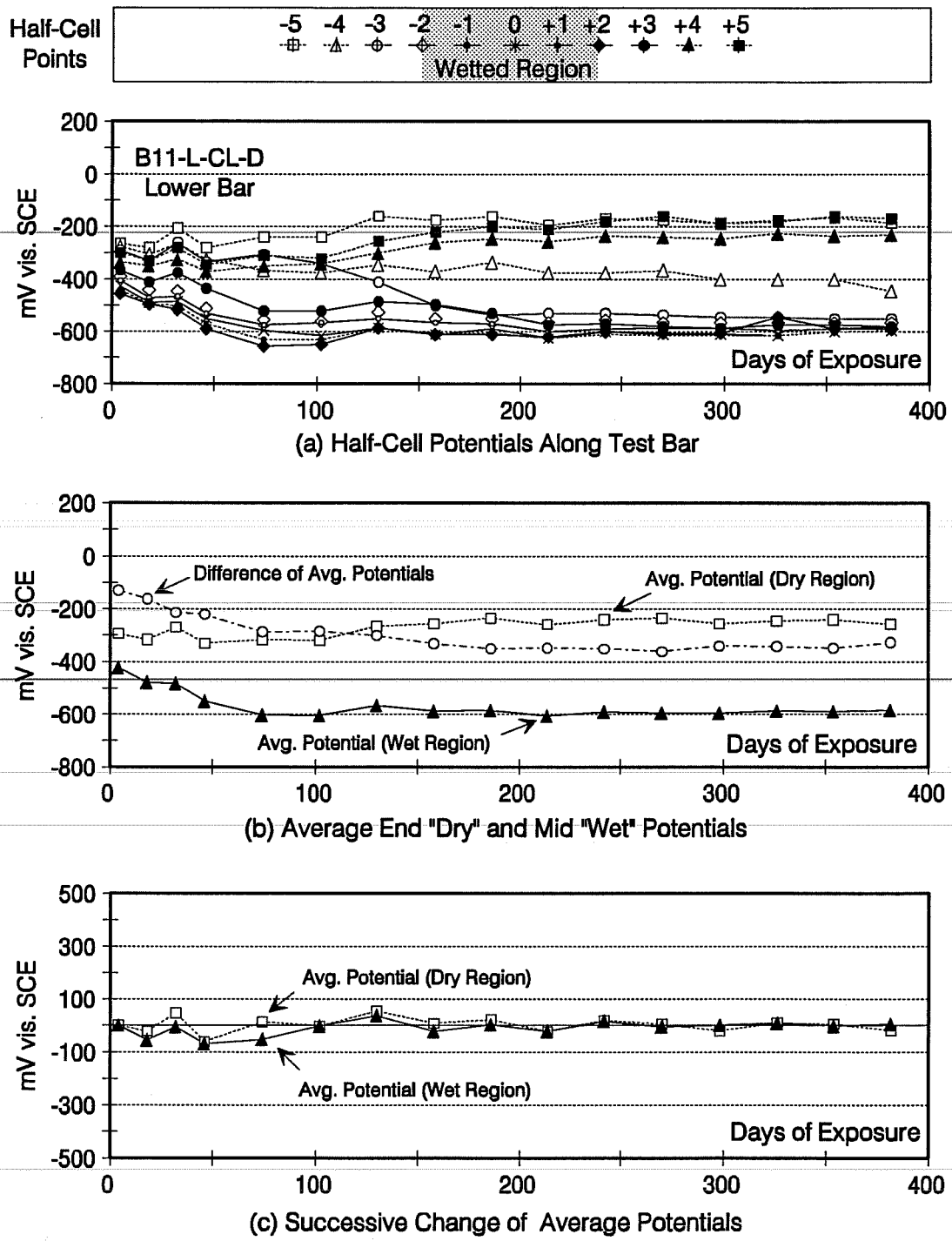

Figure D.33 Half-Cell Potentials for Beam B11-L-CL-D, Lower Bar.

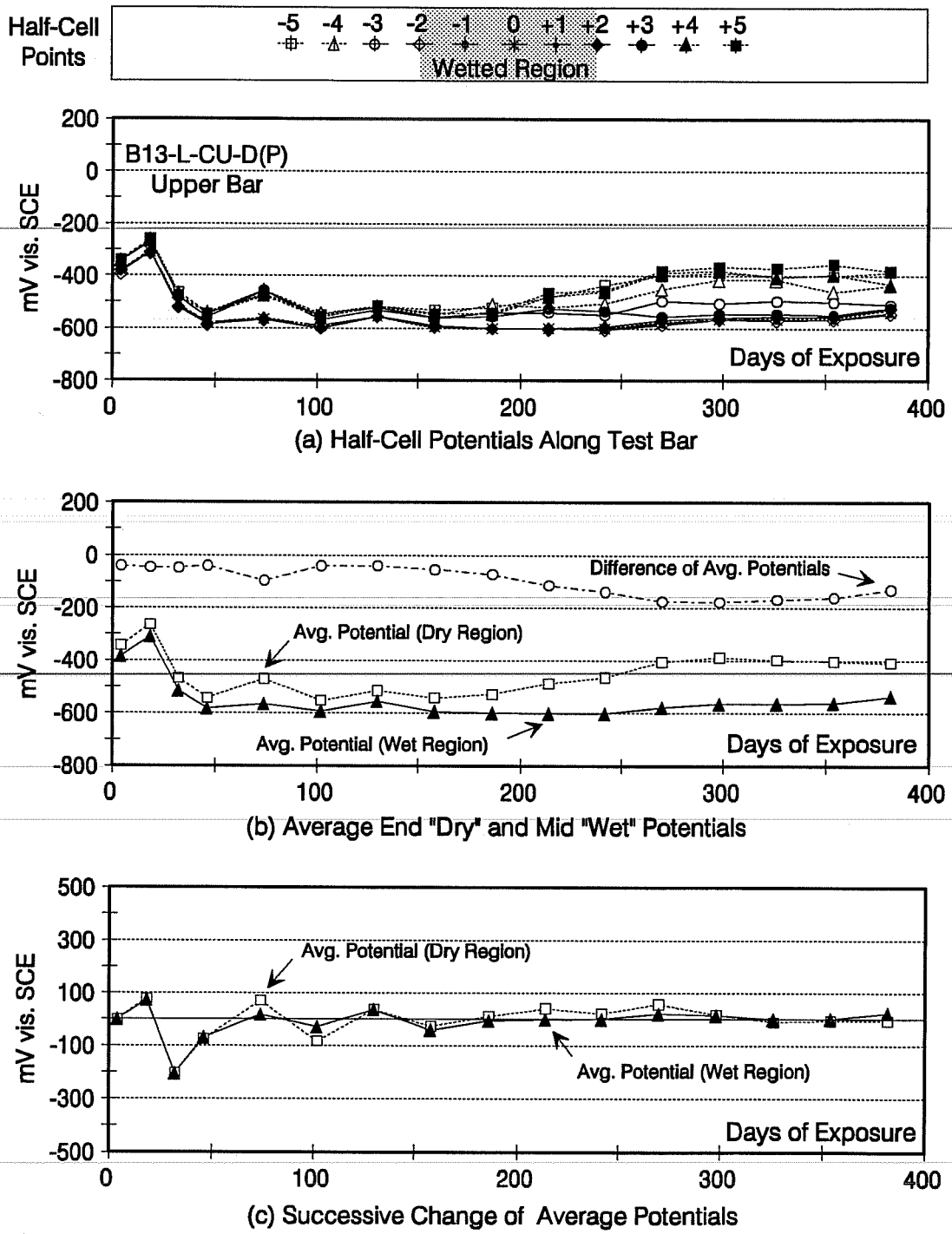

Figure D.34 Half-Cell Potentials for Beam B13-L-CU-D(P), Upper Bar.

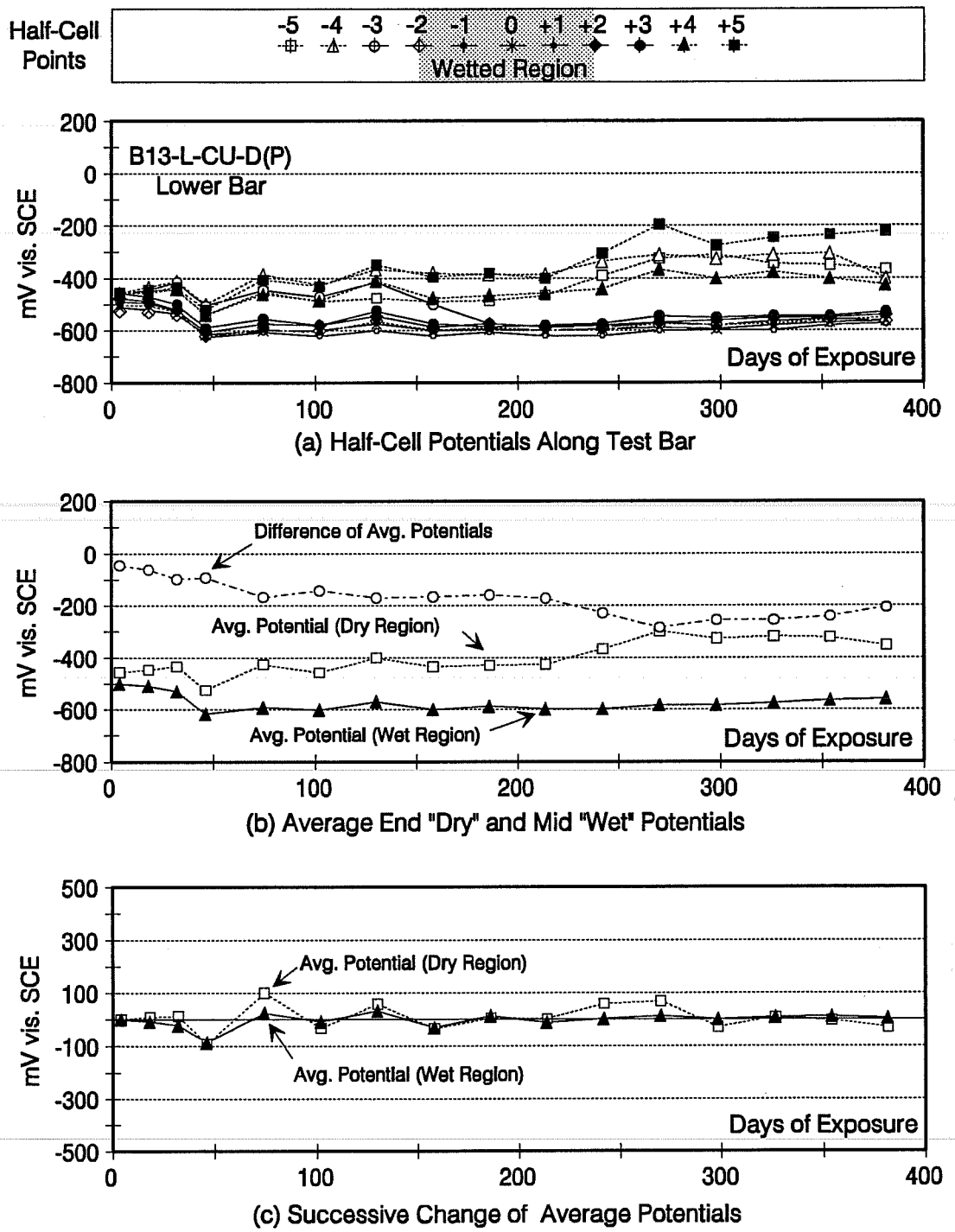

Figure D.35 Half-Cell Potentials for Beam B13-L-CU-D(P), Lower Bar.

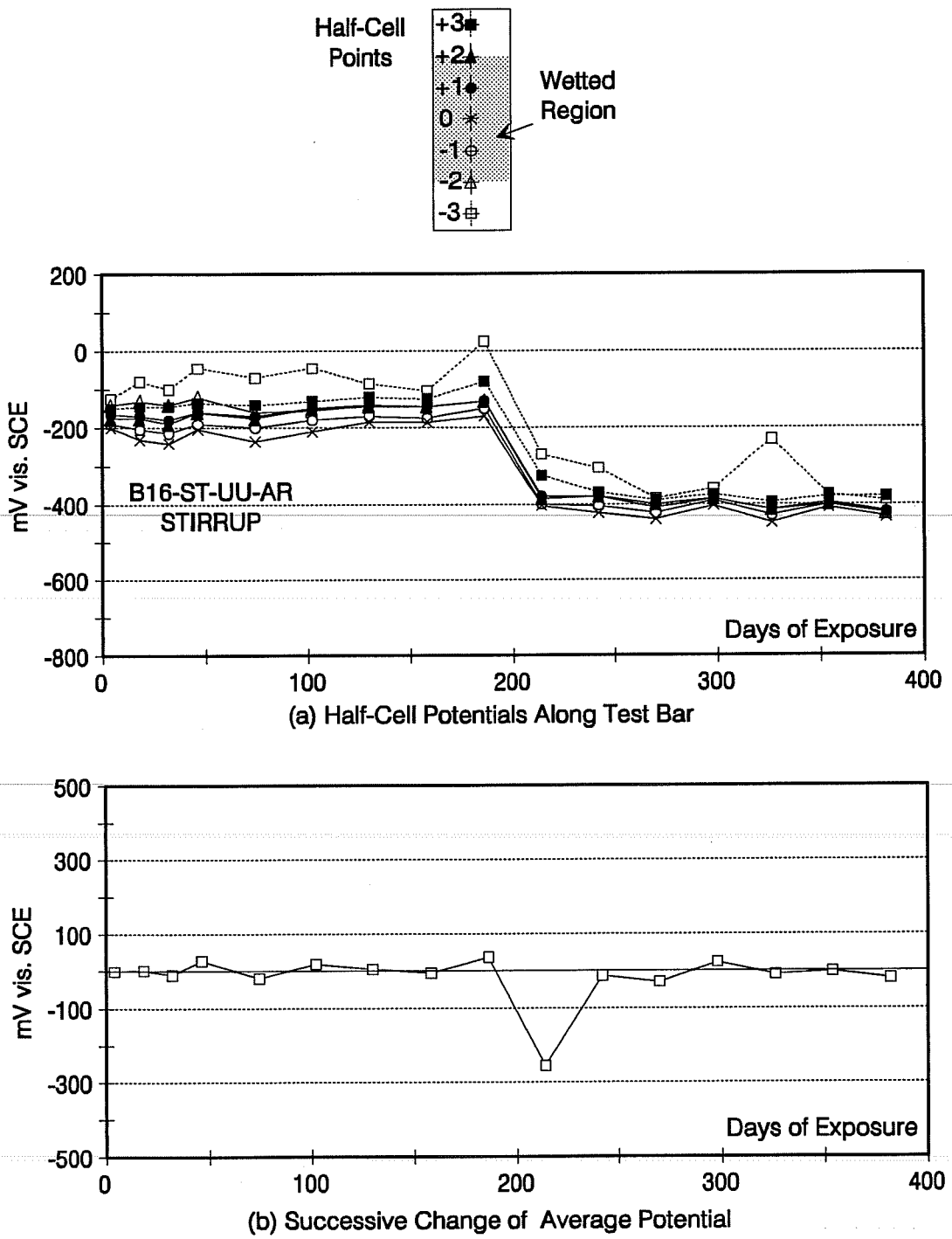

Figure D.36 Half-Cell Potentials for Beam B16-ST-UU-AR, Stirrup.

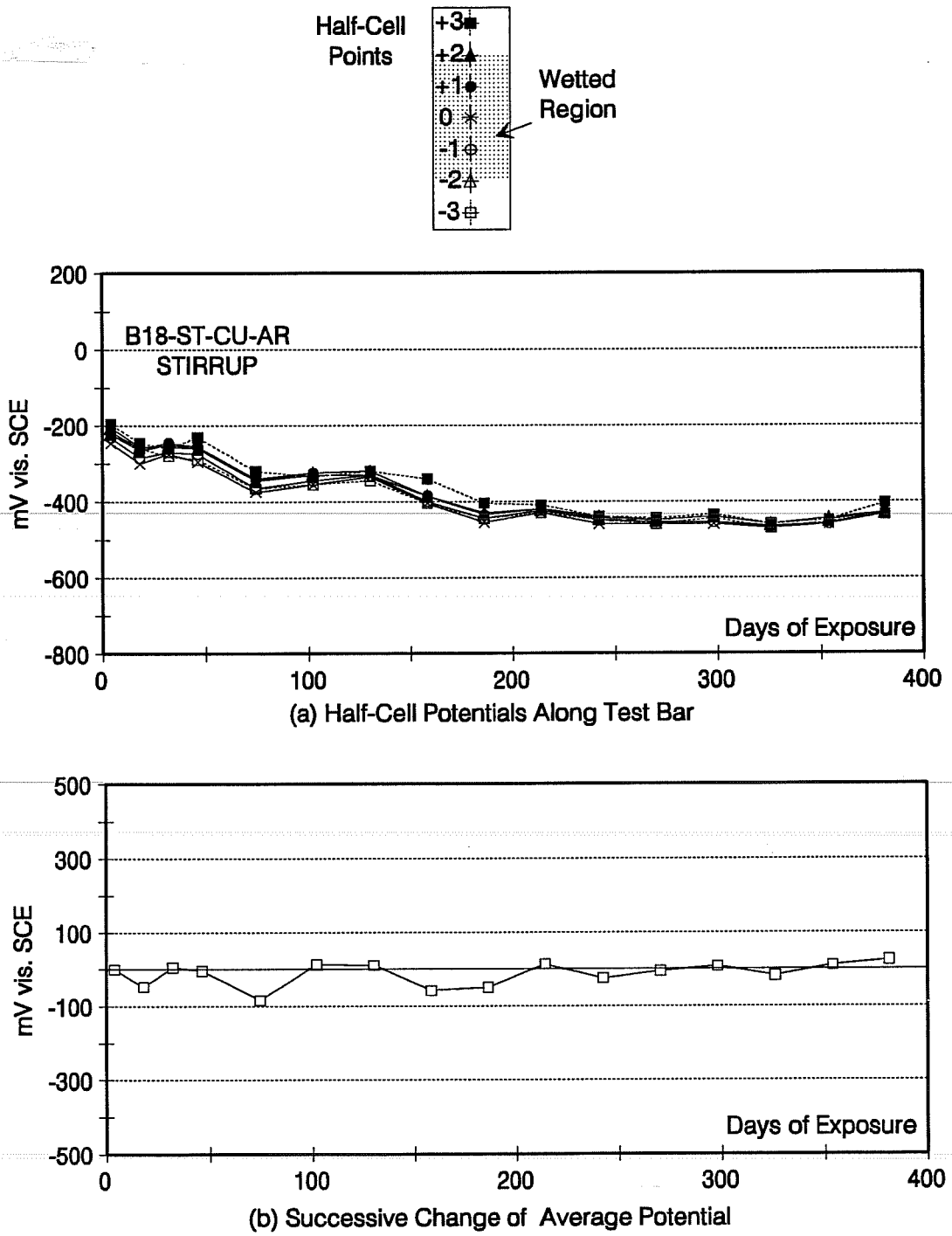

Figure D.37 Half-Cell Potentials for Beam B18-ST-CU-AR, Stirrup.

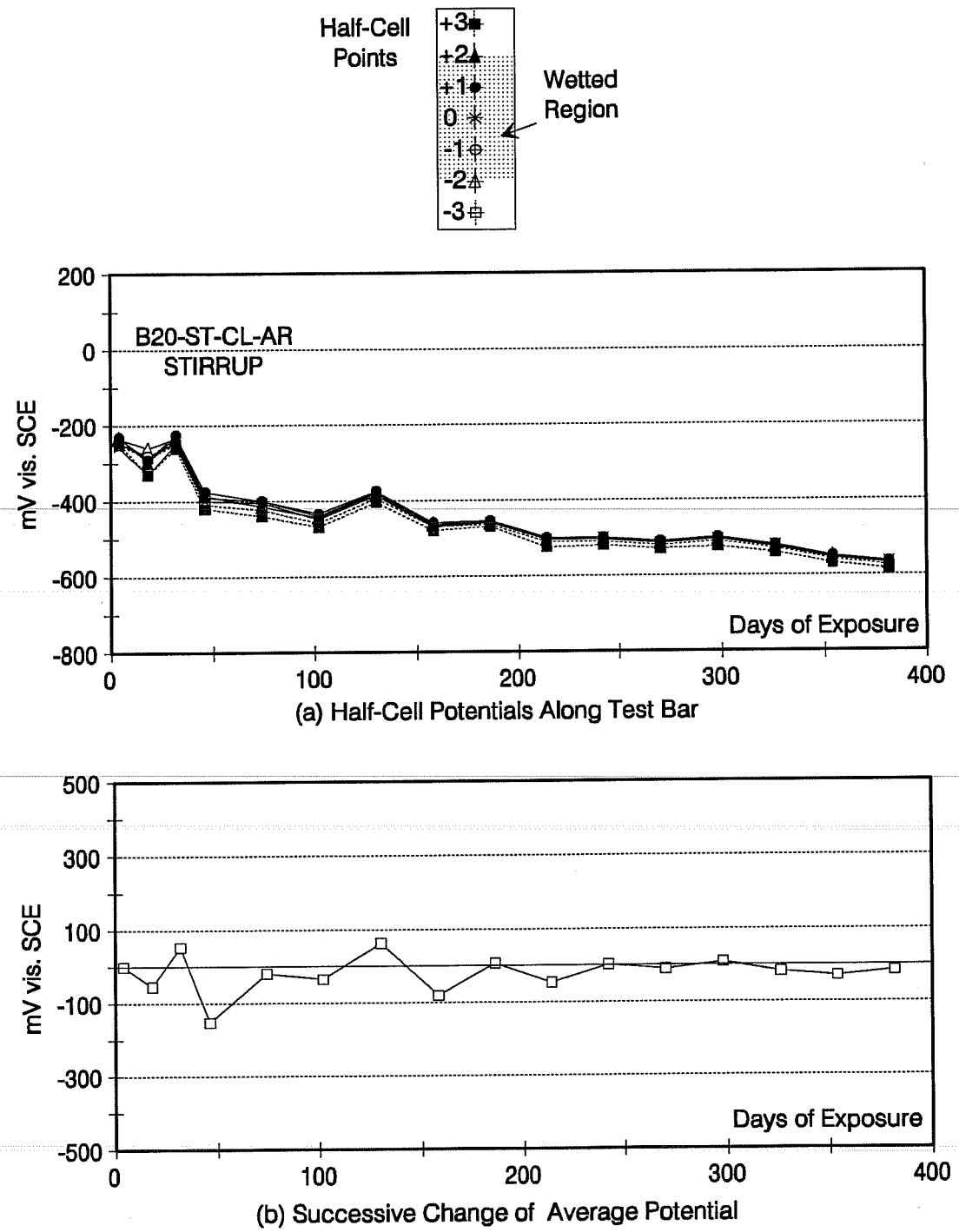

Figure D.38 Half-Cell Potentials for Beam B20-ST-CL-AR, Stirrup.

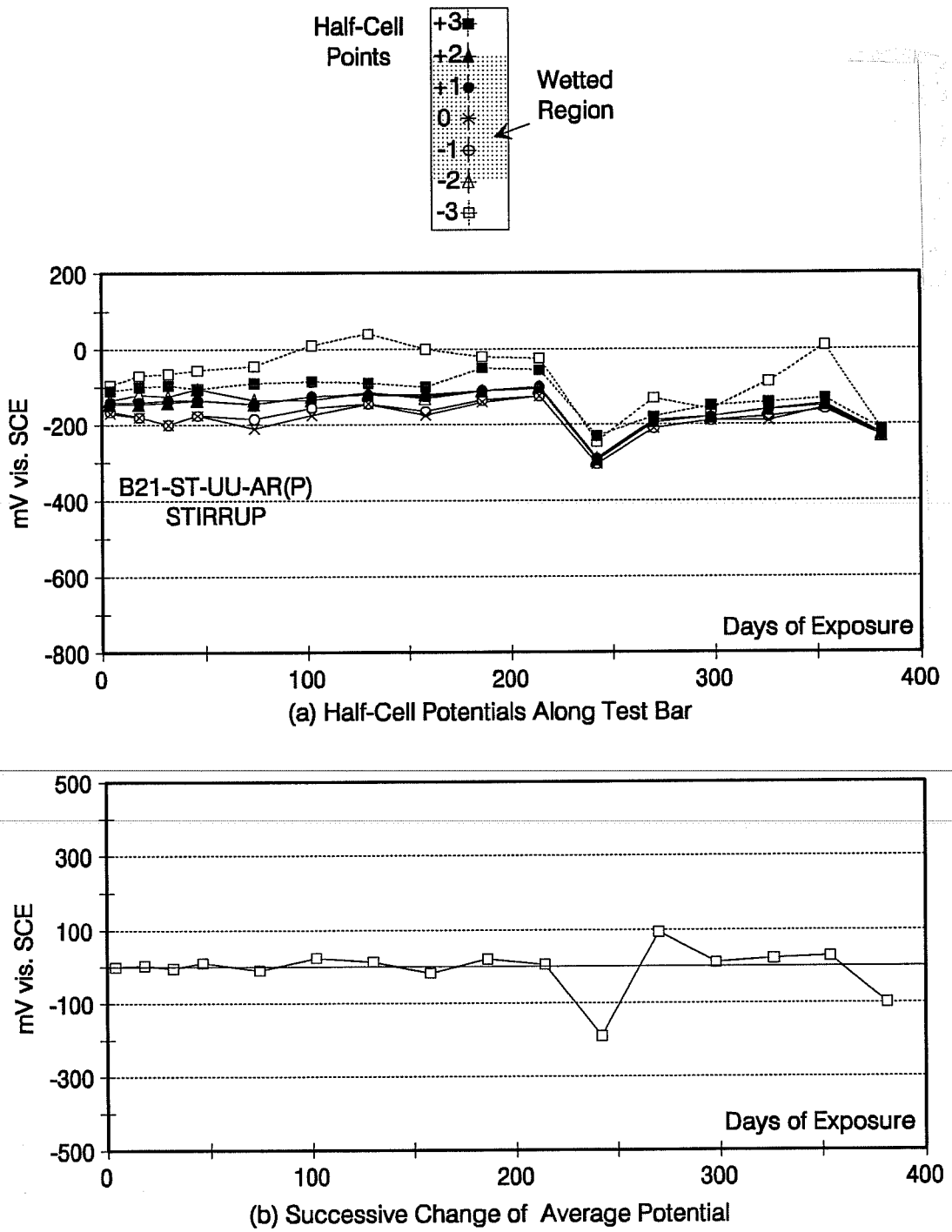

Figure D.39 Half-Cell Potentials for Beam B21-ST-UU-AR(P), Stirrup.

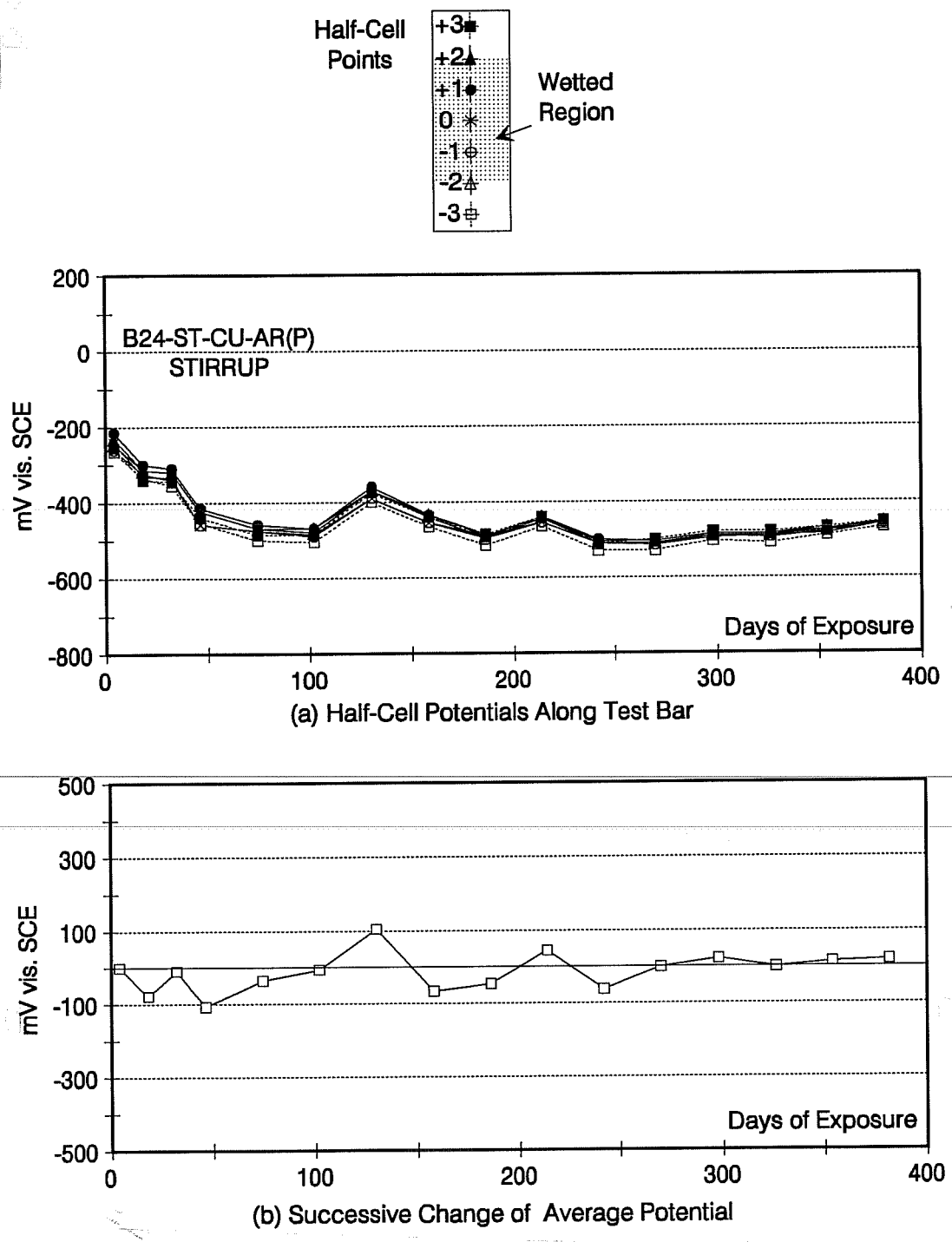

Figure D.40 Half-Cell Potentials for Beam B24-ST-CU-AR(P), Stirrup.

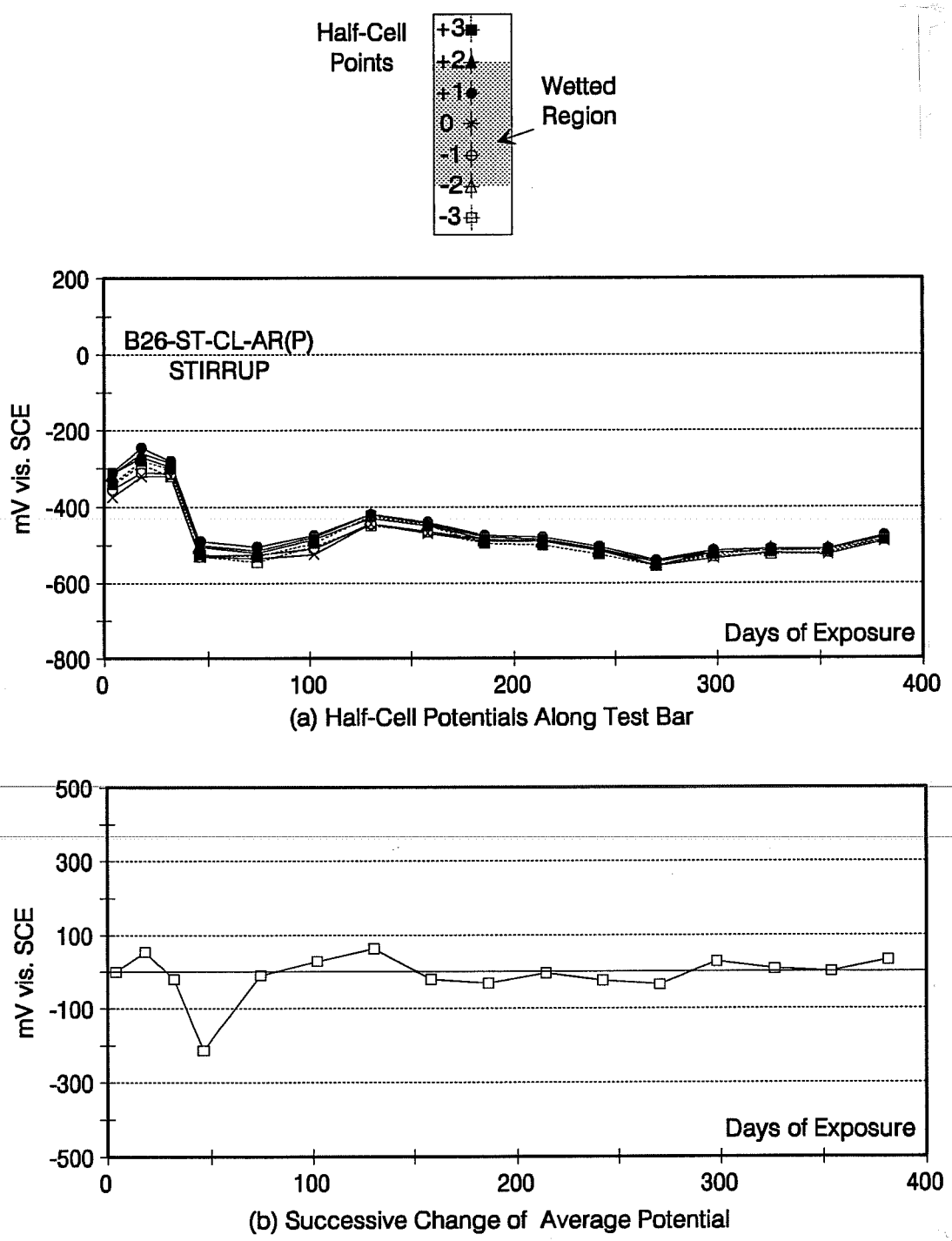

Figure D.41 Half-Cell Potentials for Beam B26-ST-CL-AR(P), Stirrup.

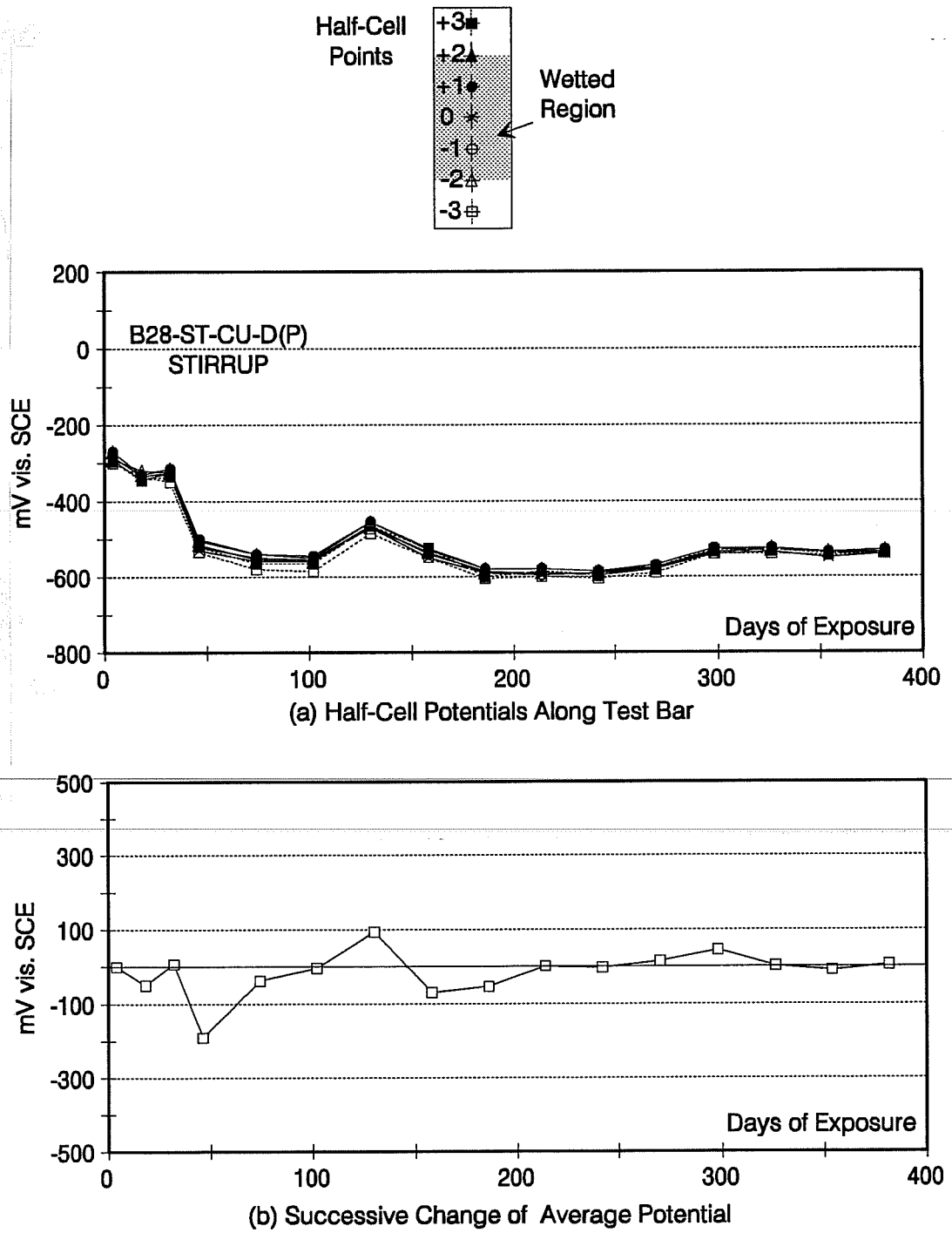

Figure D.42 Half-Cell Potentials for Beam B28-ST-CU-D(P), Stirrup.

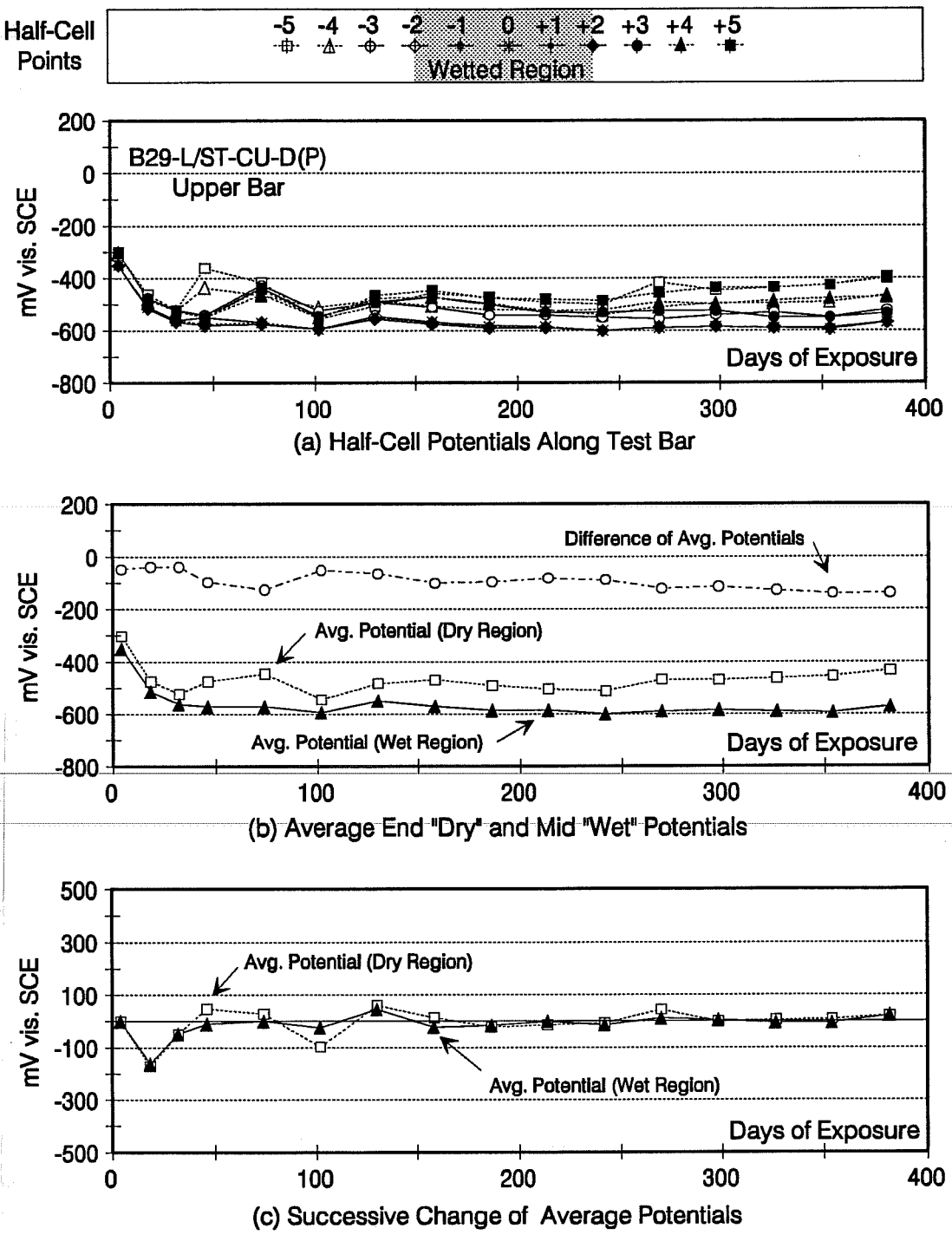

Figure D.43 Half-Cell Potentials for Beam B29-L/ST-CU-D(P), Upper Bar.

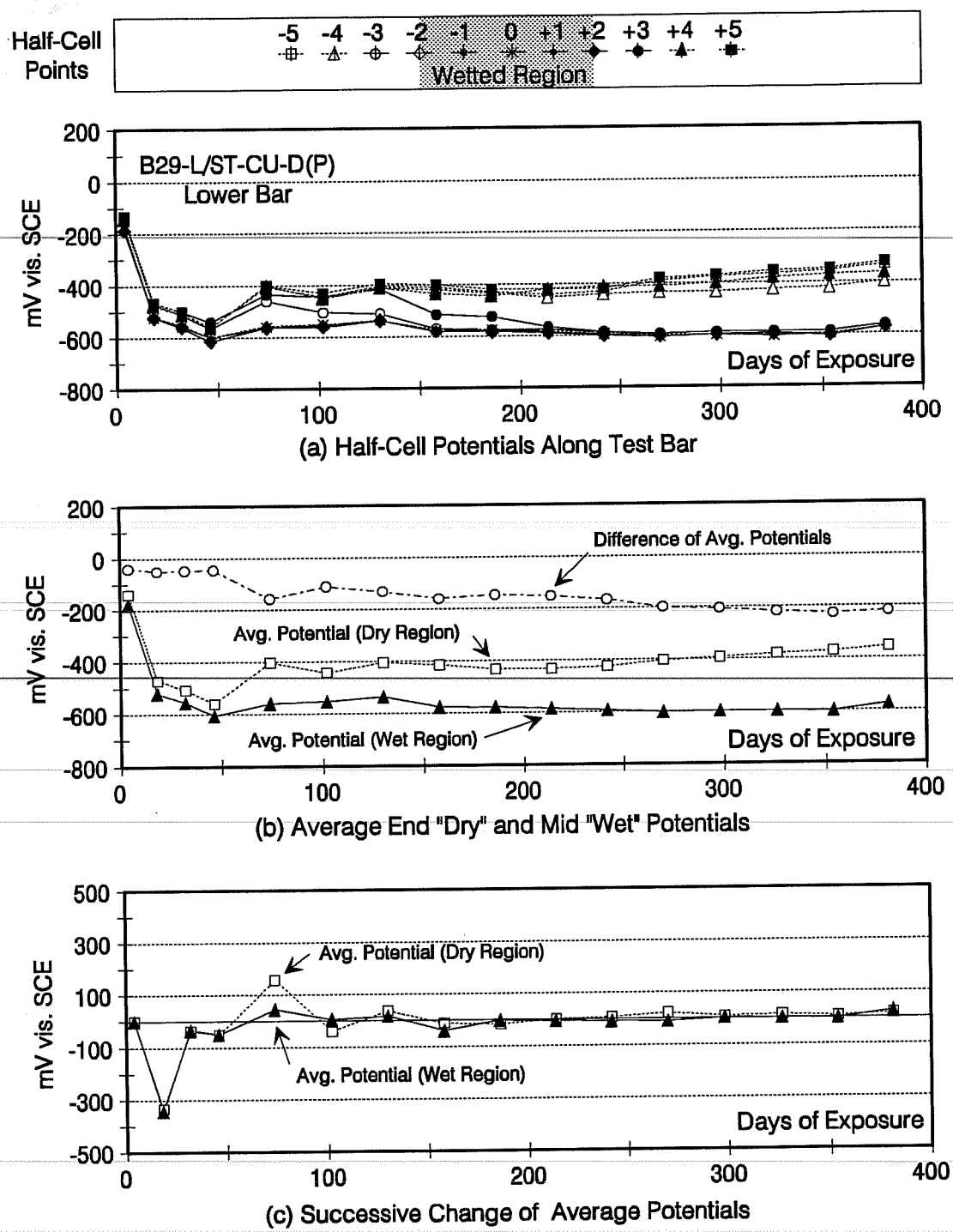

Figure D.44 Half-Cell Potentials for Beam B29-L/ST-CU-D(P), Lower Bar.

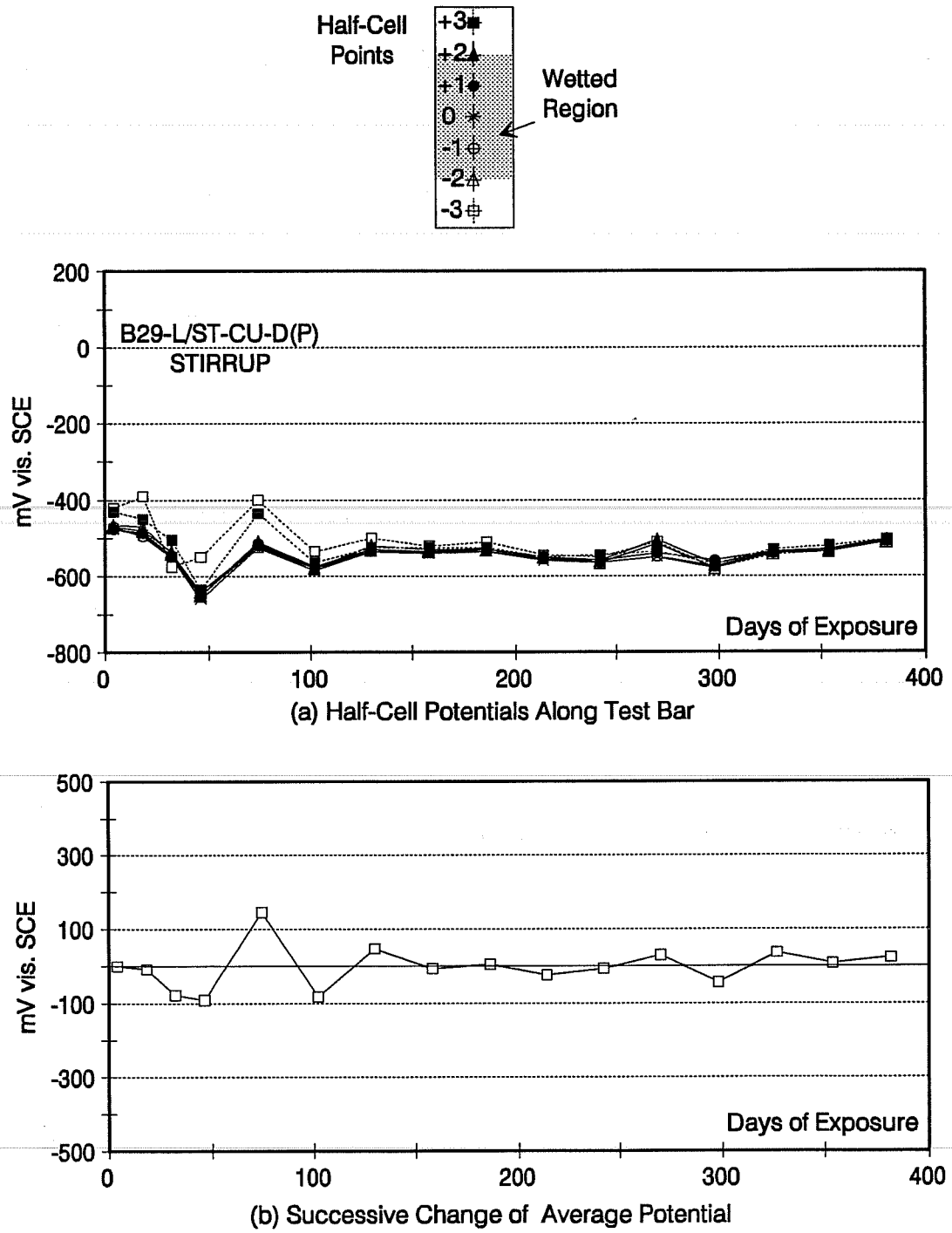

Figure D.45 Half-Cell Potentials for Beam B29-L/ST-CU-D(P), Stirrup.

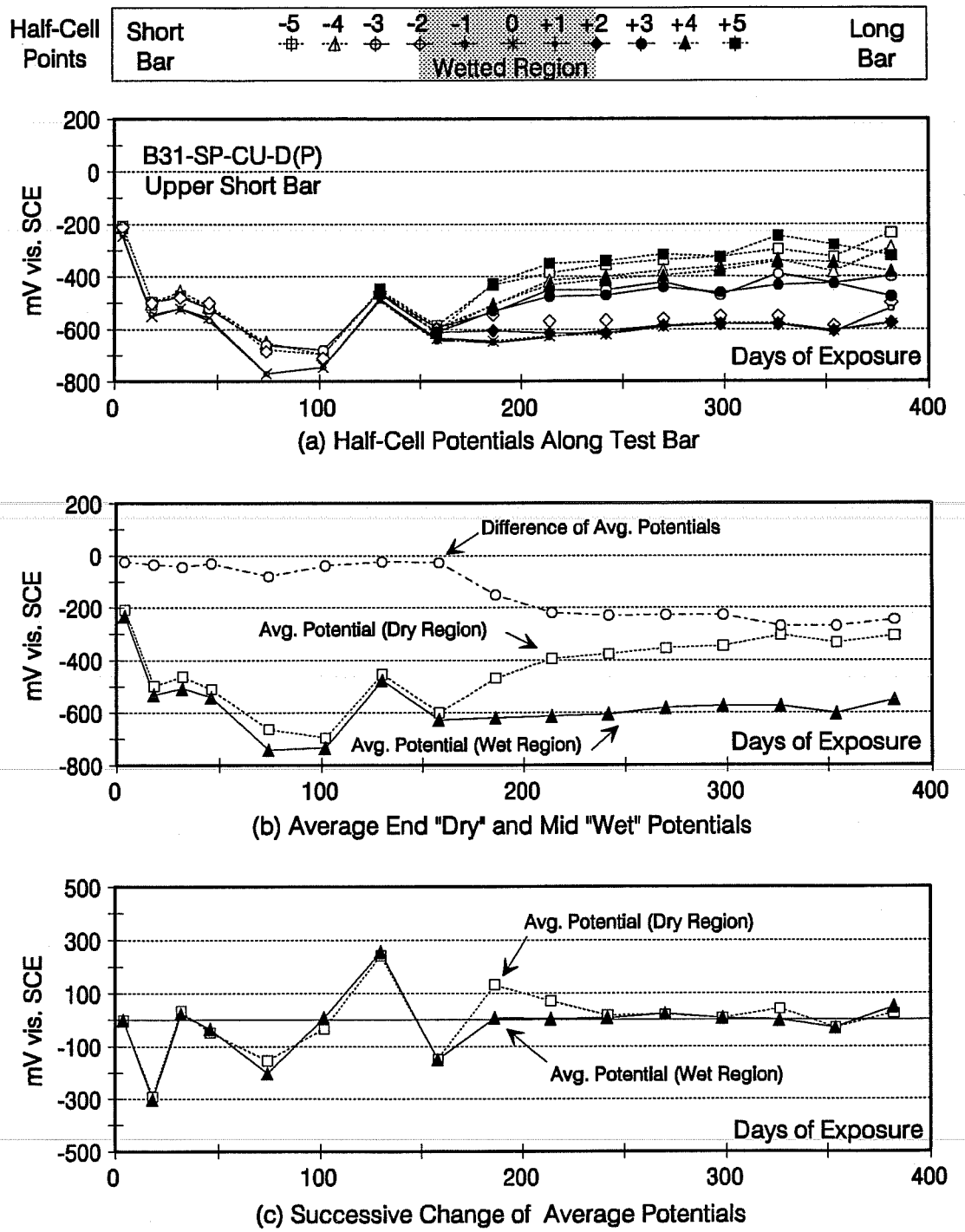

Figure D.46 Half-Cell Potentials for Beam B31-SP-CU-D(P), Upper Short Bar.

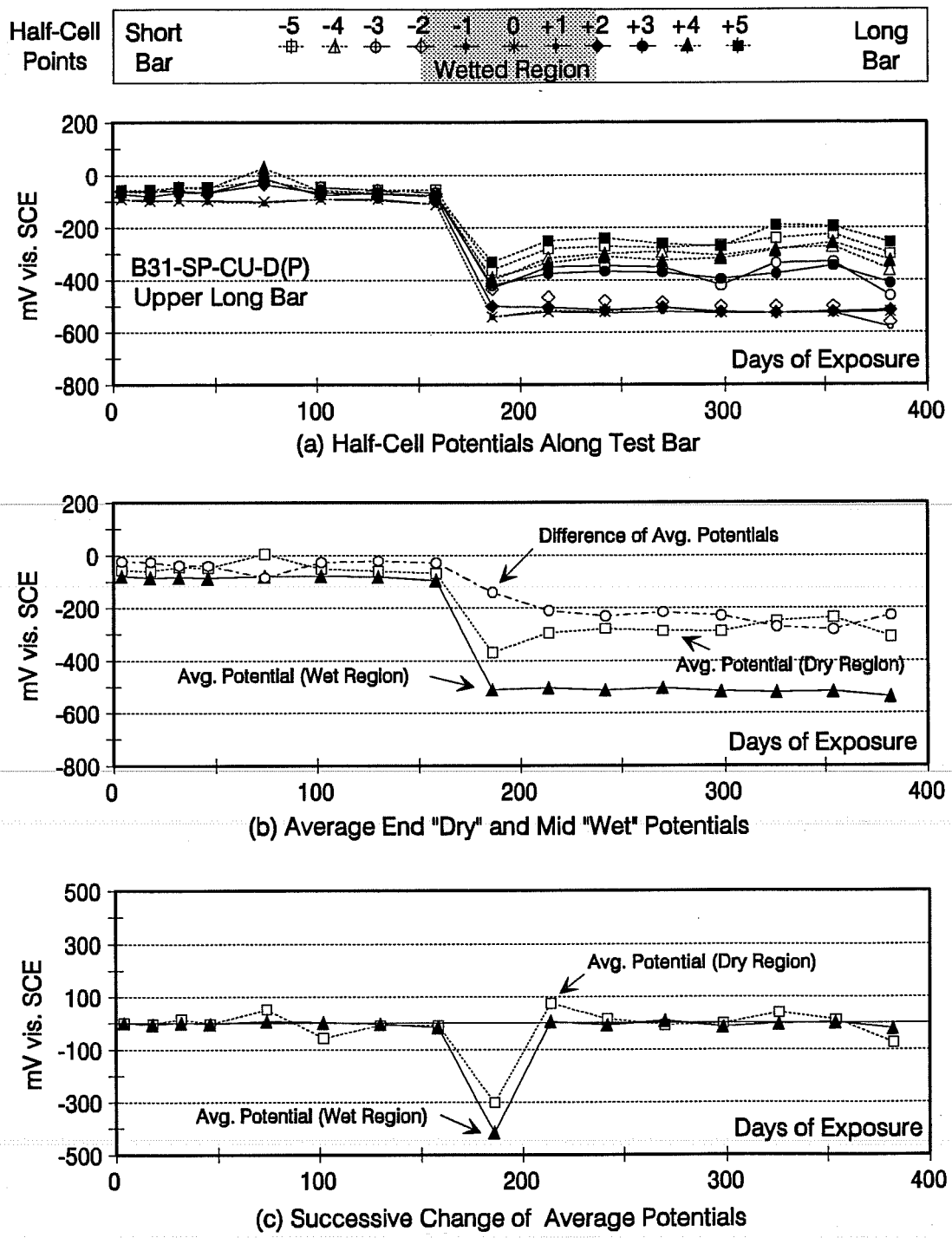

Figure D.47 Half-Cell Potentials for Beam B31-SP-CU-D(P), Upper Long Bar.

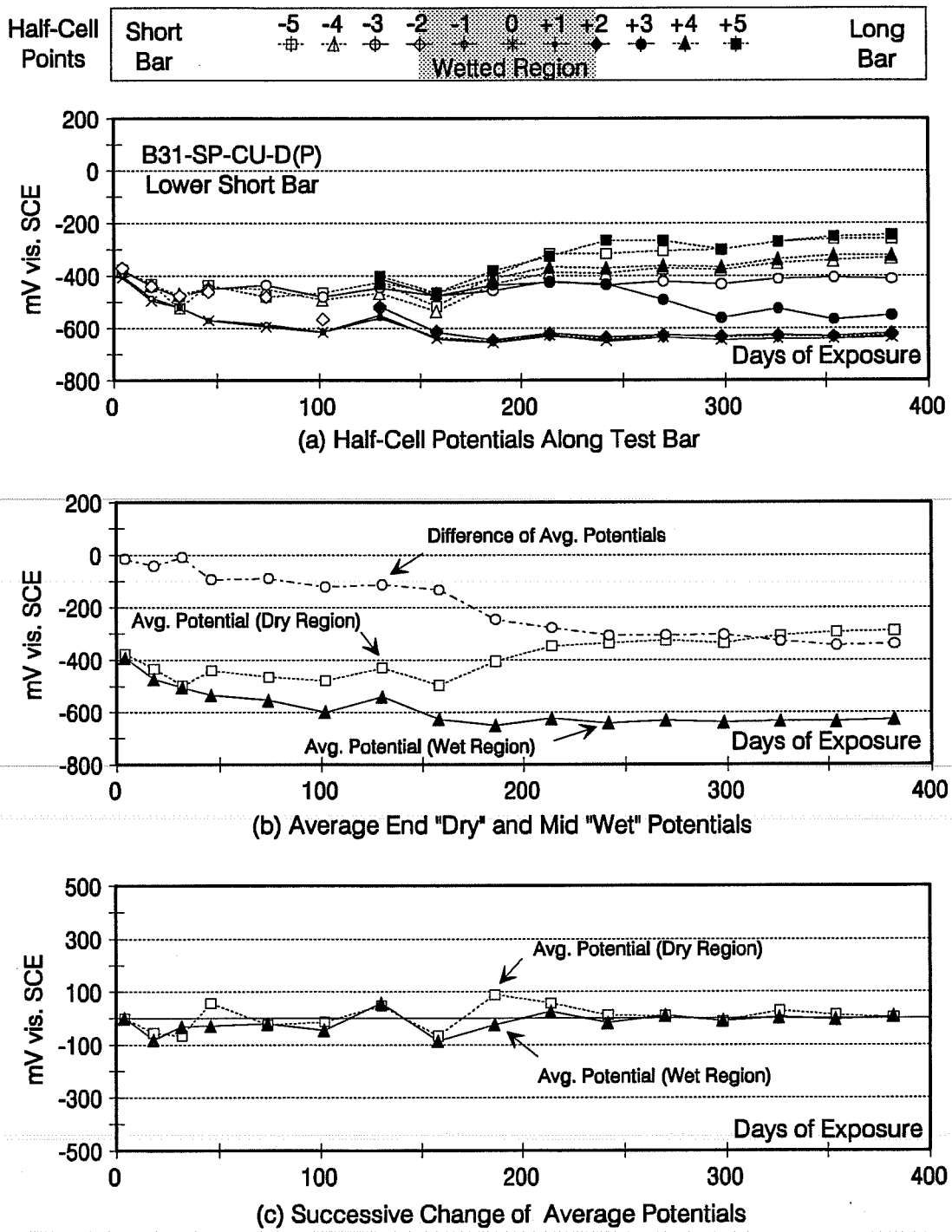

Figure D.48 Half-Cell Potentials for Beam B31-SP-CU-D(P), Lower Short Bar.

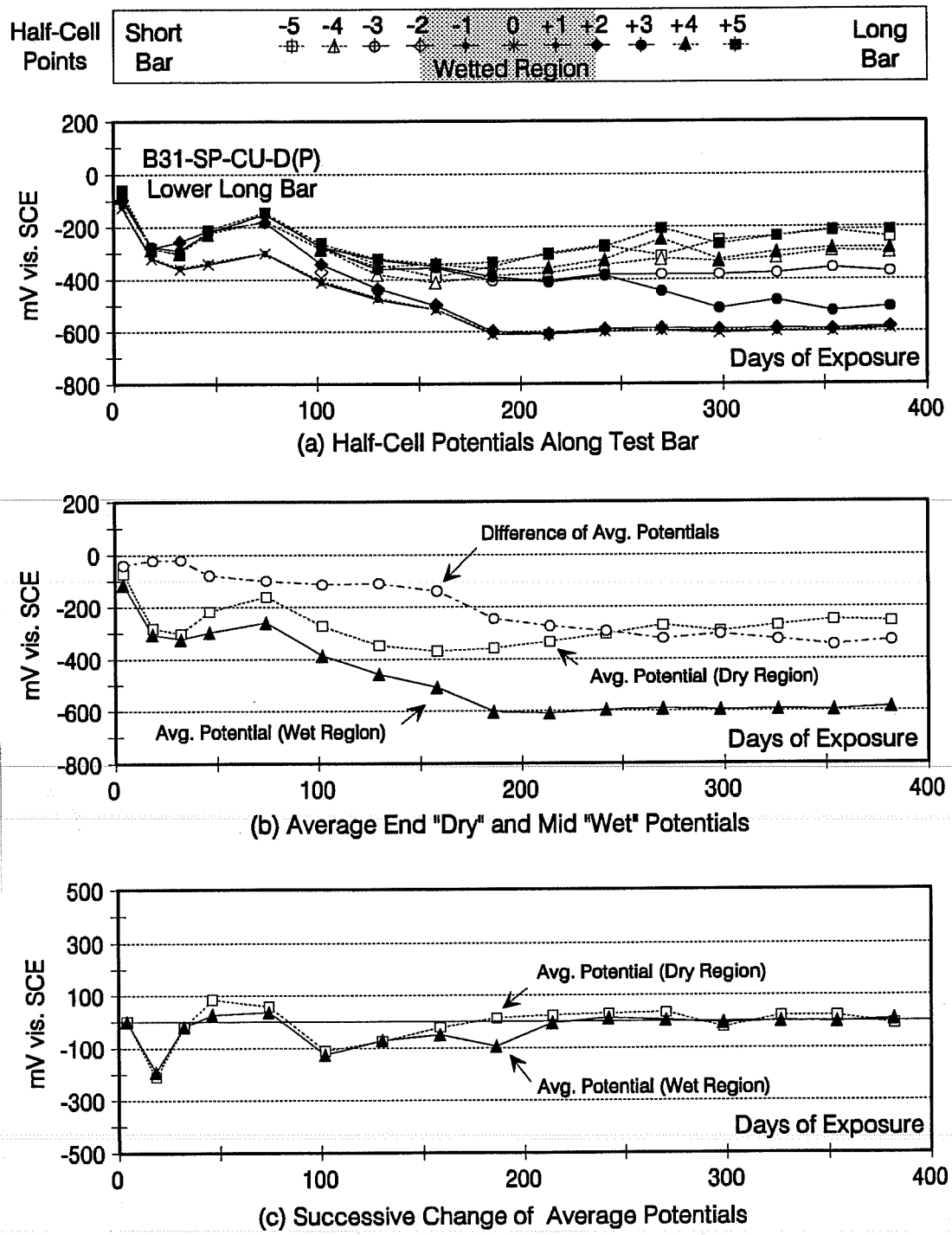

Figure D.49 Half-Cell Potentials for Beam B31-SP-CU-D(P), Lower Long Bar.

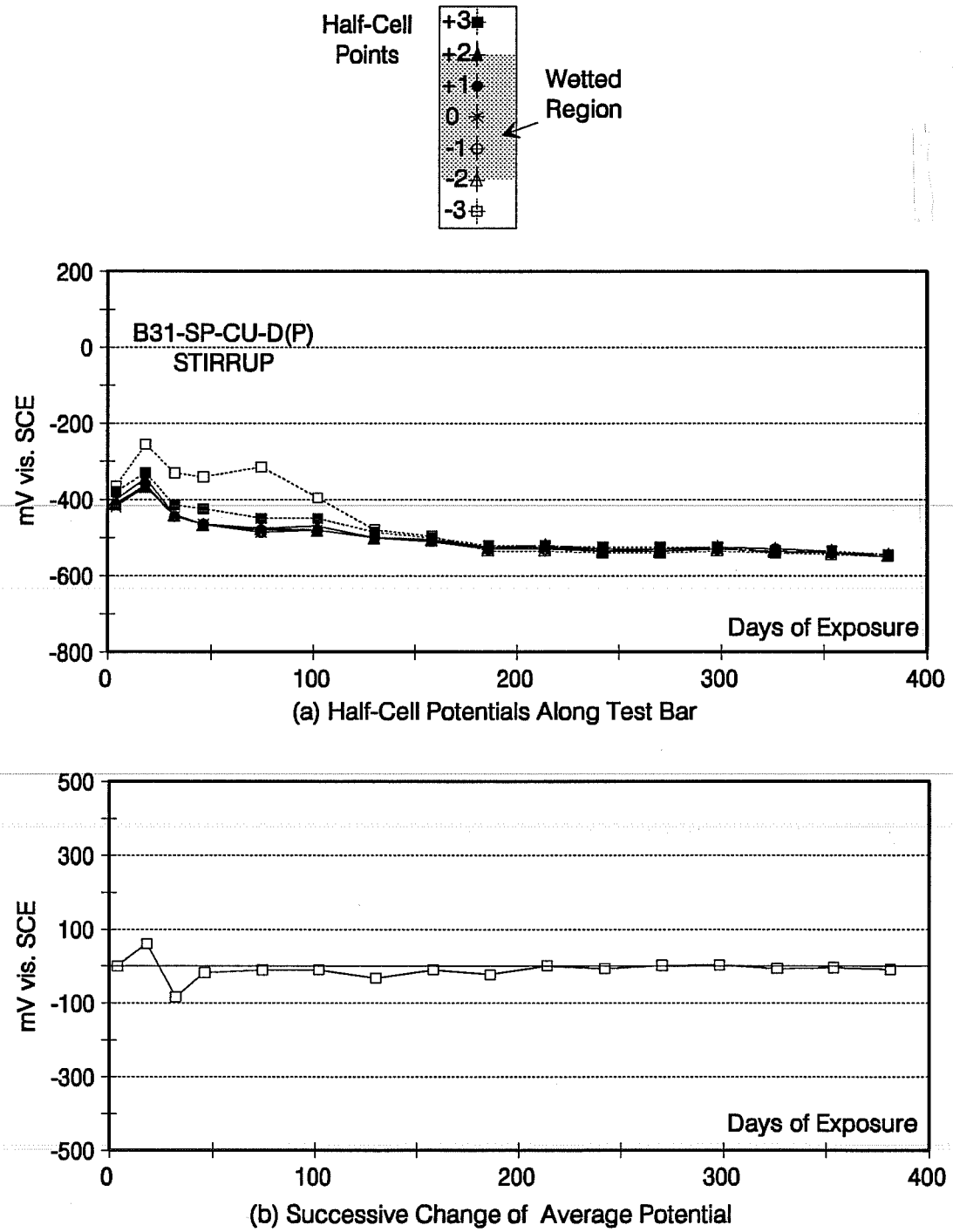

Figure D.50 Half-Cell Potentials for Beam B31-SP-CU-D(P), Stirrup.

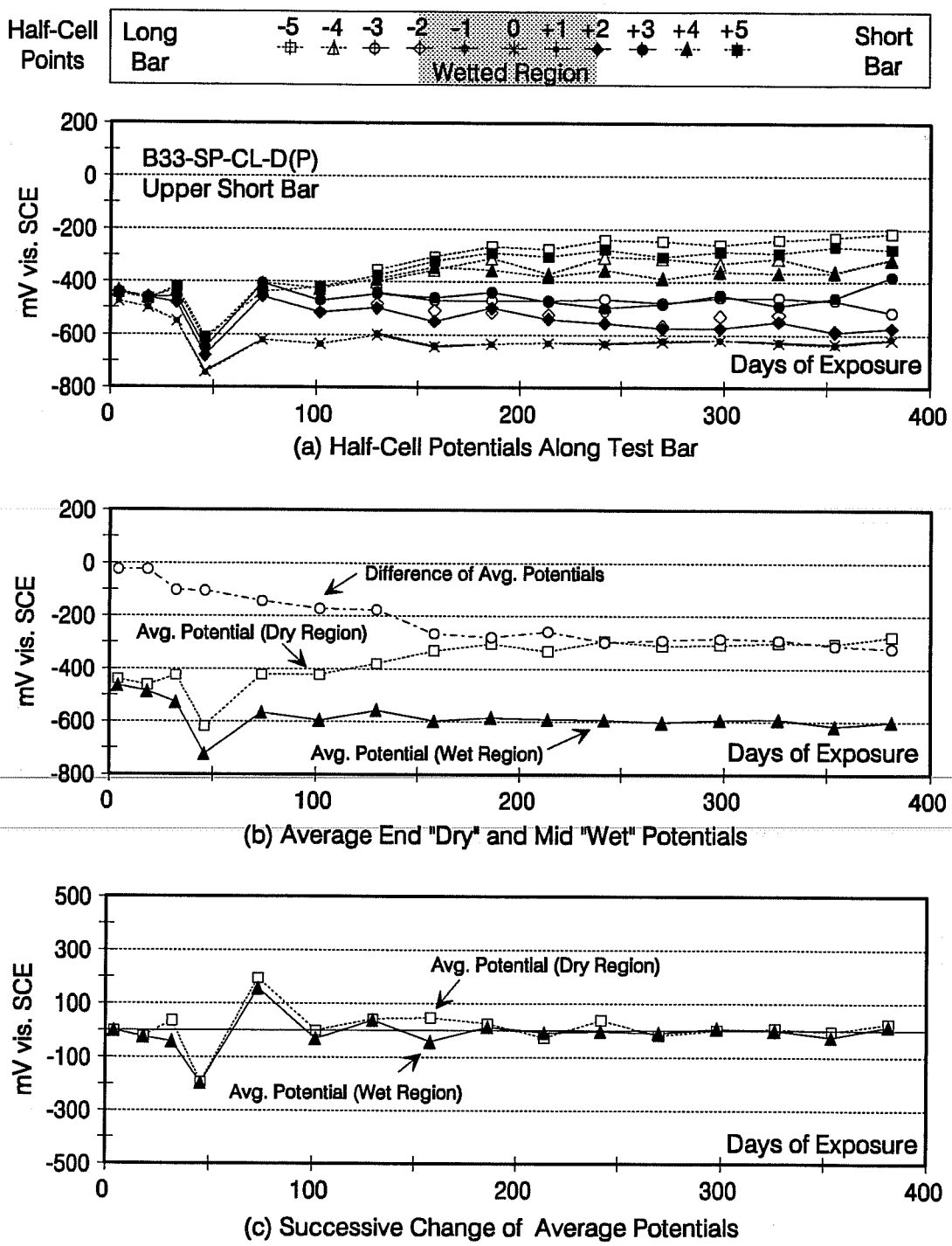

Figure D.51 Half-Cell Potentials for Beam B33-SP-CL-D(P), Upper Short Bar.

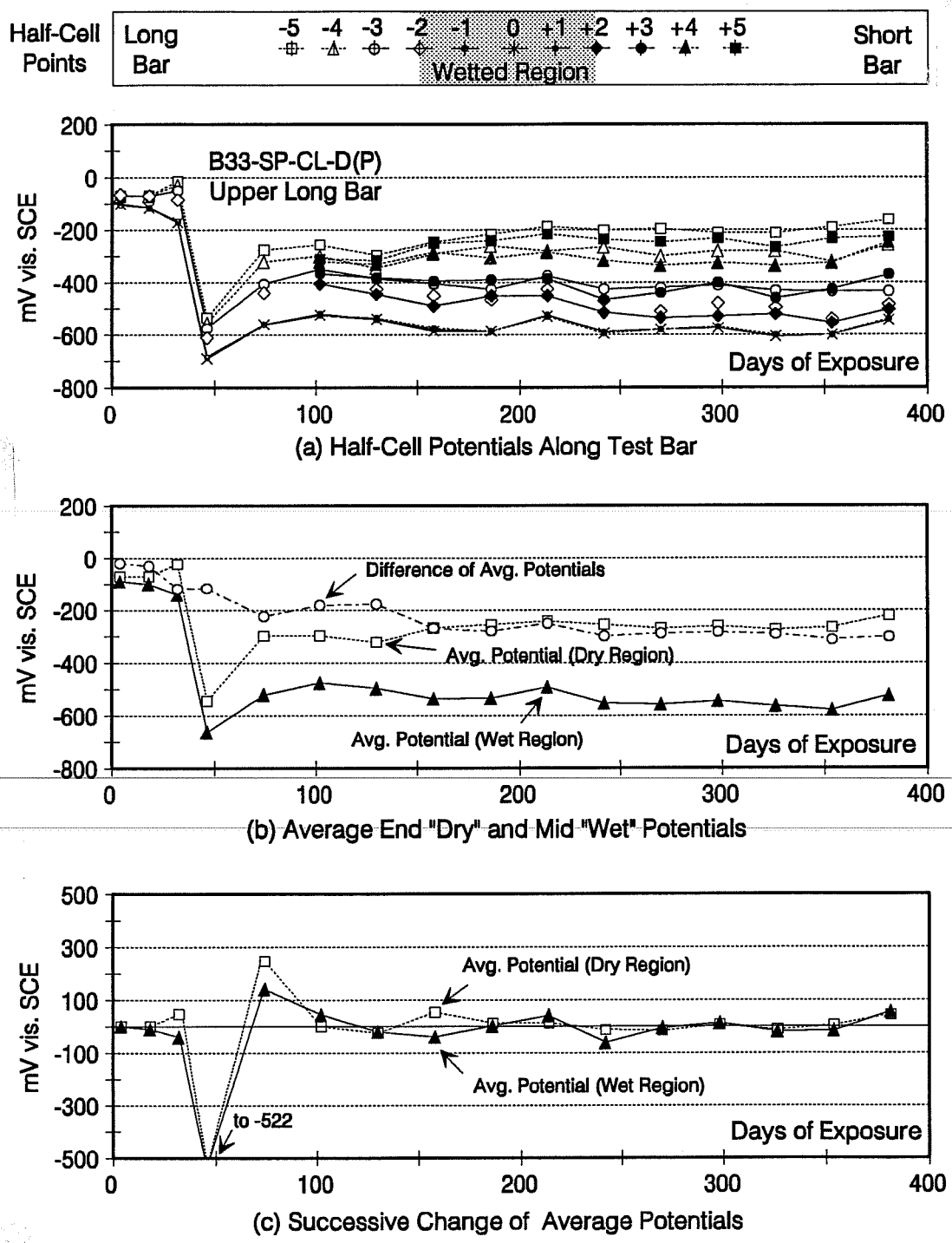

Figure D.52 Half-Cell Potentials for Beam B33-SP-CL-D(P), Upper Long Bar.

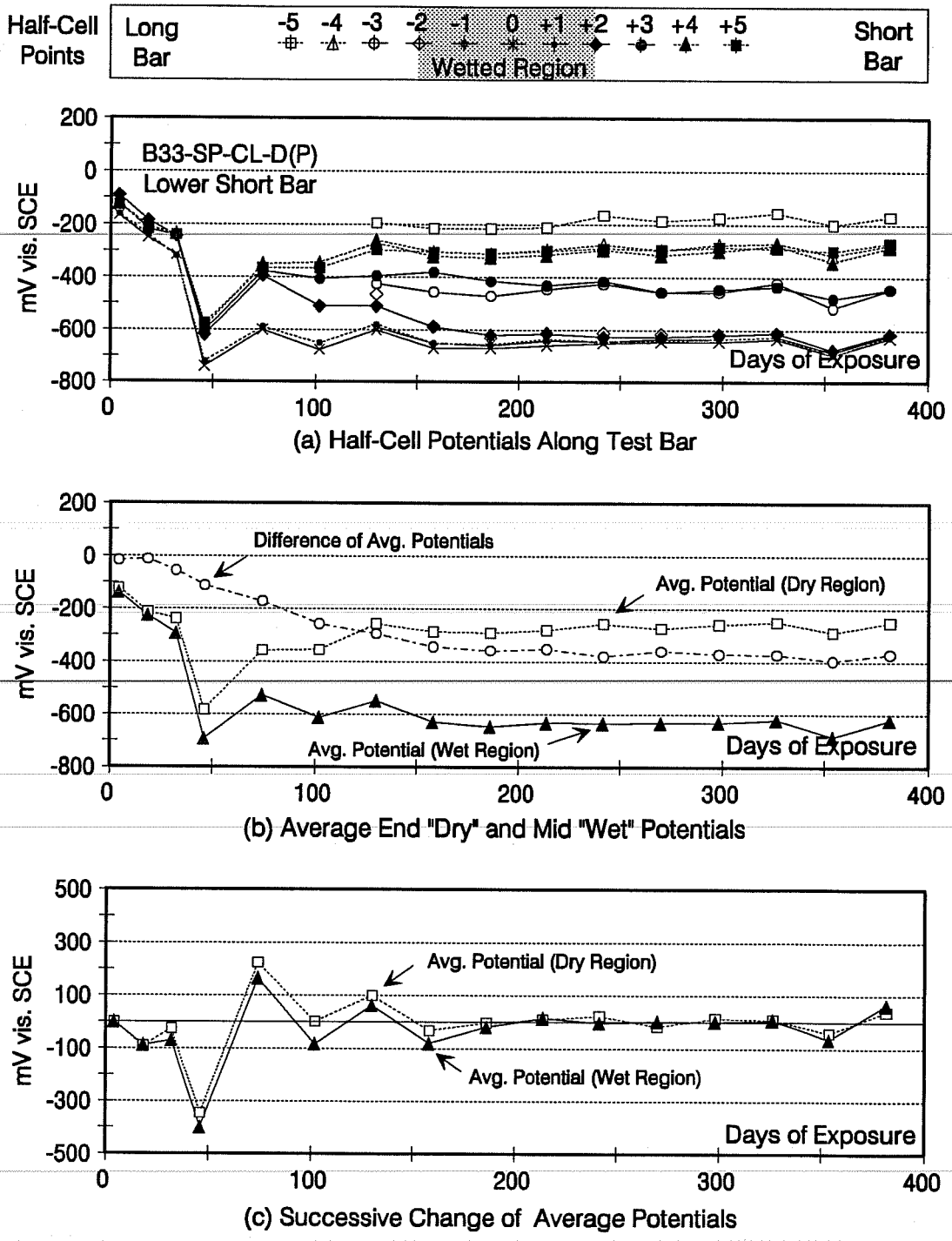

Figure D.53 Half-Cell Potentials for Beam B33-SP-CL-D(P), Lower Short Bar.

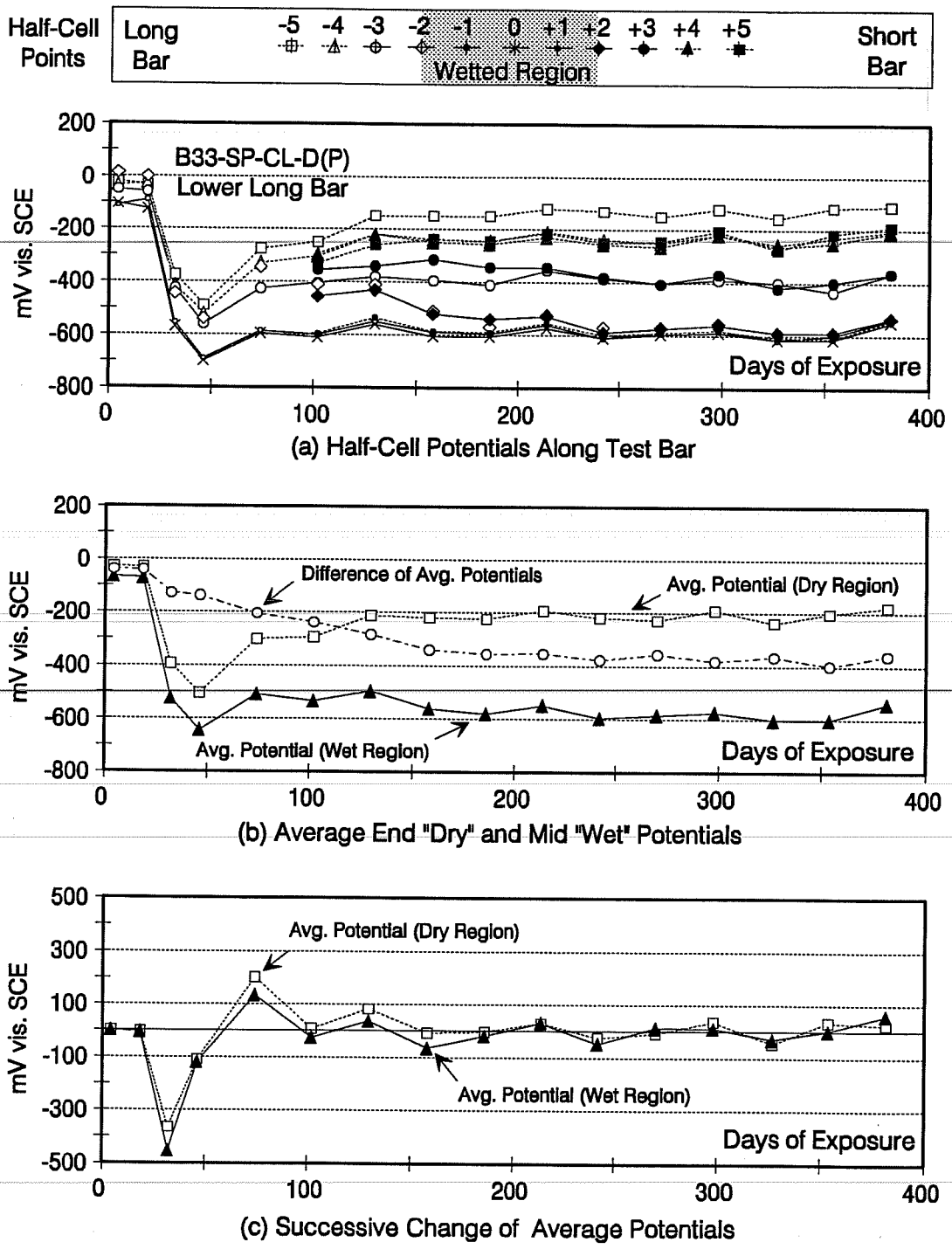

Figure D.54 Half-Cell Potentials for Beam B33-SP-CL-D(P), Lower Long Bar.

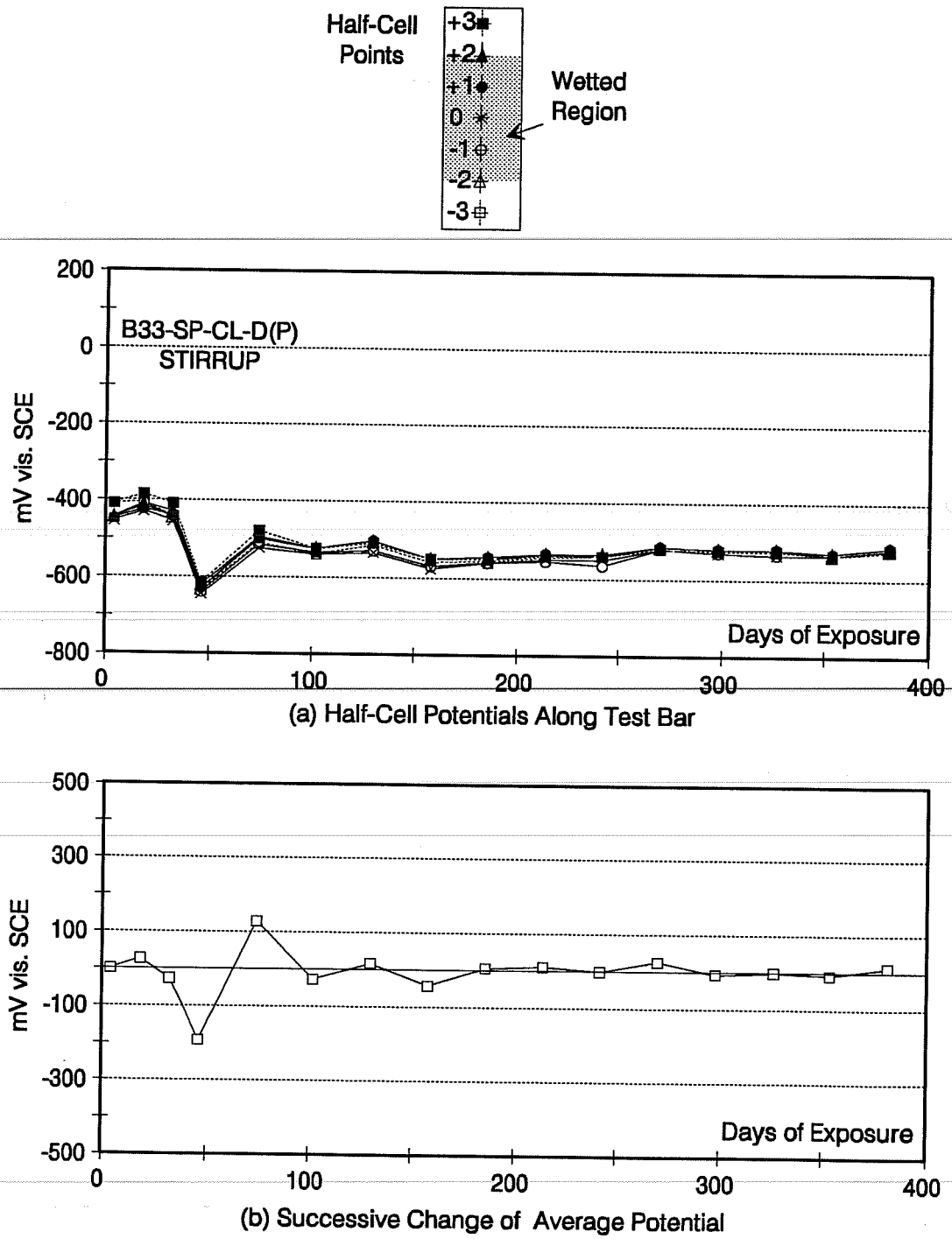

Figure D.55 Half-Cell Potentials for Beam B33-SP-CL-D(P), Stirrup.

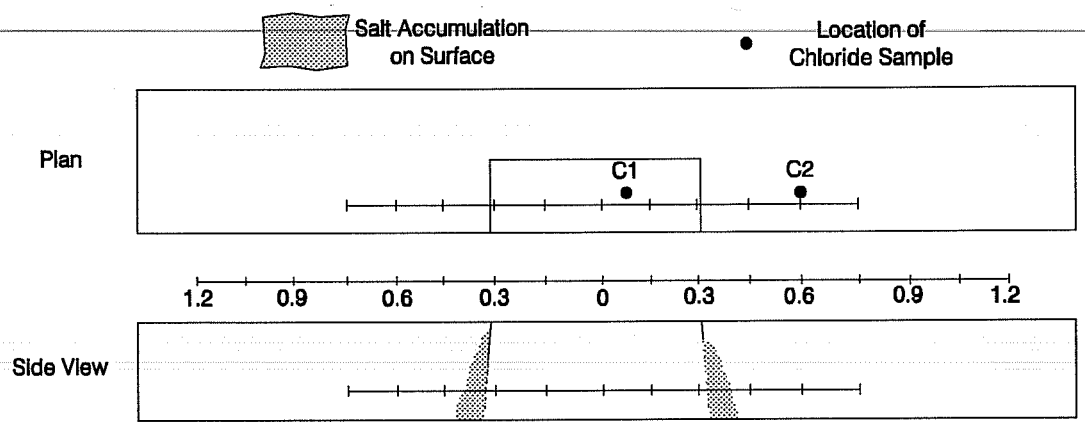

Figure D.56 Surface Condition of Beam B2-L-UU-AR After One Year of Expoure.

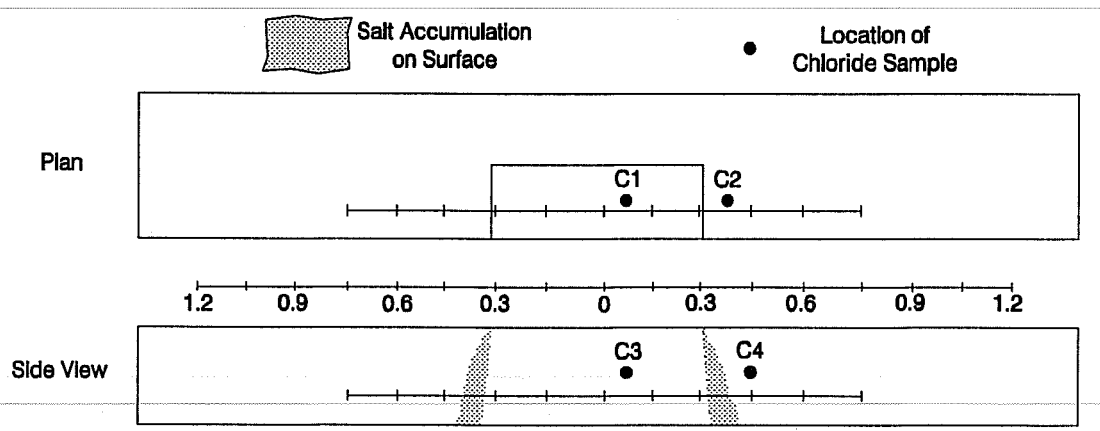

Figure D.57 Surface Condition of Beam B7-L-UU-D After One Year of Expoure.

Table D.6 Average Crack Width Measurement for B4-L-CU-AR

Days	Crack 1, mm	Crack 2, mm	Crack 3, mm
162	0.31	0.26	0.22
193	0.27	0.15	0.17
220	0.30	0.25	0.22
252	0.29	0.15	0.20
277	0.29	0.22	0.20
305	0.30	0.21	0.20
333	0.30	0.22	0.22
361	0.29	0.21	0.21
381	0.27	0.20	0.21

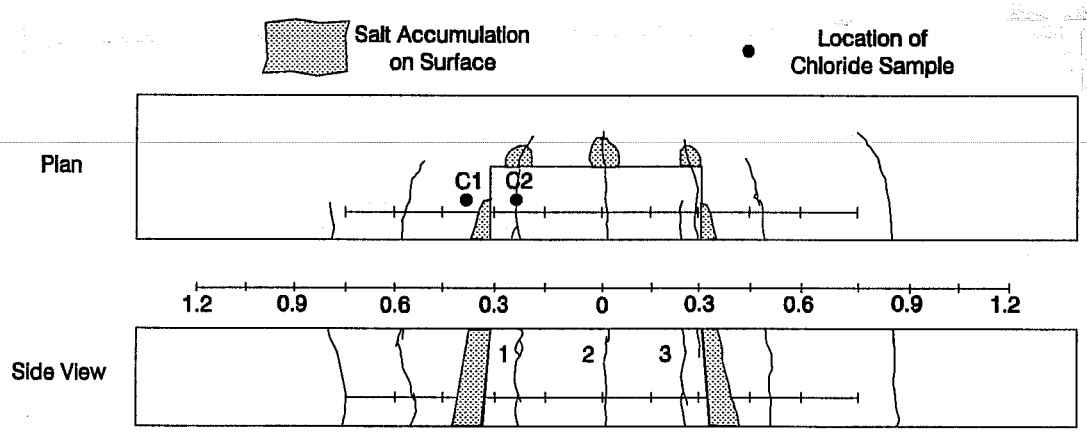

Figure D.58 Surface Condition of Beam B4-L-CU-AR After One Year of Expoure.

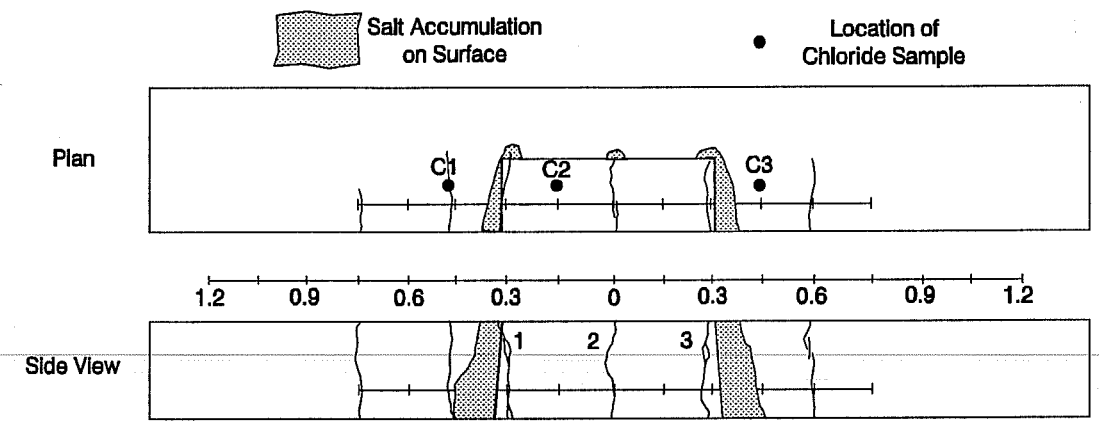

Figure D.59 Surface Condition of Beam B5-L-CL-AR After One Year of Expoure.

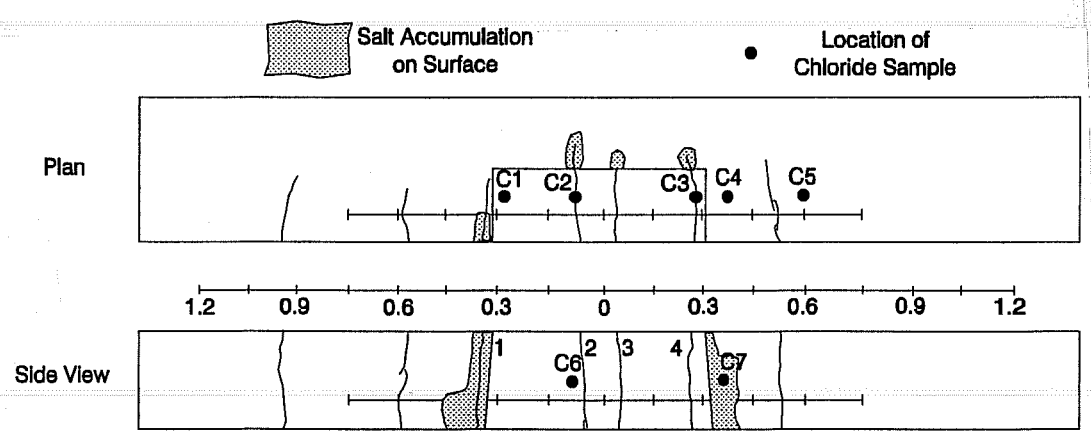

Figure D.60 Surface Condition of Beam B11-L-CL-D After One Year of Expoure.

Table D.7 Average Crack Width Measurement for B9-L-CU-D

Days	Crack 1, mm	Crack 2, mm	Crack 3, mm
162	0.24	0.29	0.33
193	0.24	0.25	0.19
220	0.22	0.22	0.22
252	0.19	0.20	0.16
277	0.24	0.21	0.17
305	0.22	0.24	0.19
333	0.25	0.24	0.17
361	0.22	0.22	0.17
381	0.22	0.20	0.16

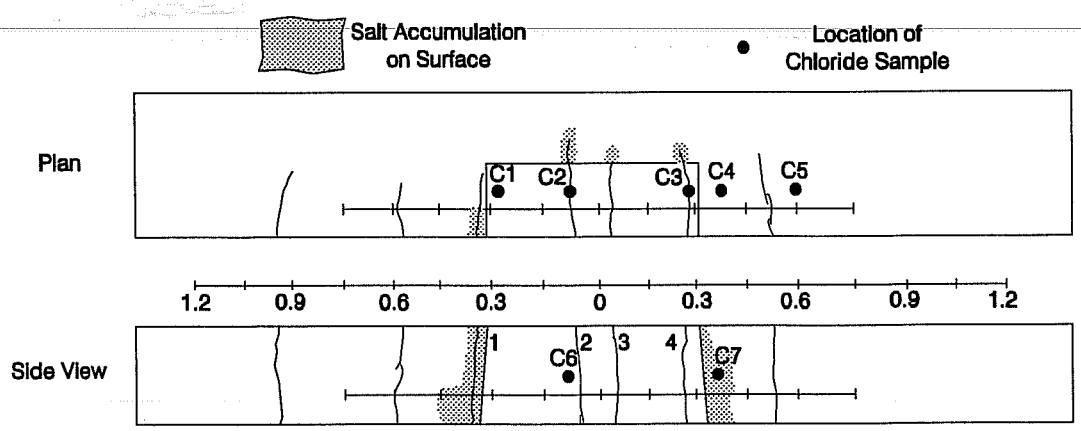

Figure D.61 Surface Condition of Beam B9-L-CU-D After One Year of Expoure.

Table D.8 Average Crack Width Measurement for B13-L-CU-D(P)

Days	Crack 1, mm	Crack 2, mm	Crack 3, mm	Crack 4, mm
162	0.16	0.16	0.20	0.16
193	0.12	0.12	0.17	0.12
220	0.15	0.20	0.17	0.15
252	0.12	0.17	0.17	0.12
277	0.12	0.16	0.16	0.12
305	0.13	0.17	0.16	0.15
333	0.13	0.17	0.16	0.12
361	0.12	0.15	0.15	0.11
381	0.12	0.16	0.13	0.11

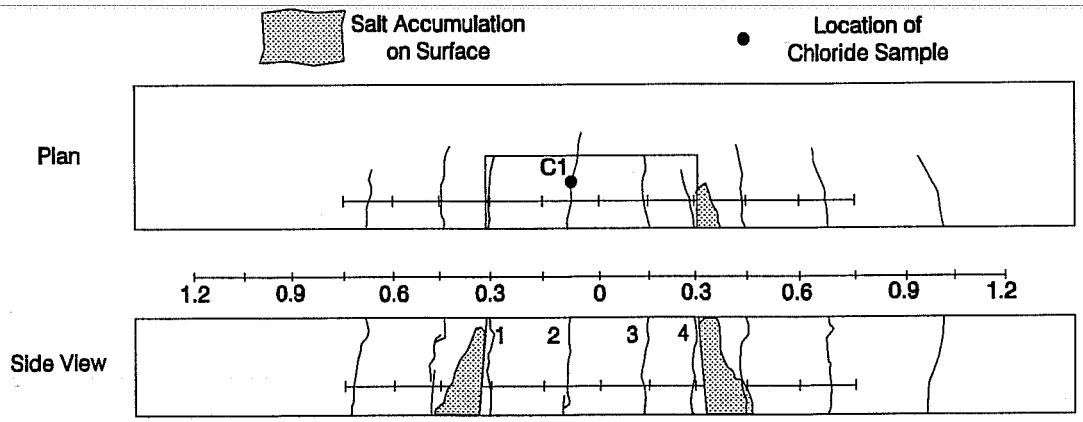

Figure D.62 Surface Condition of Beam B13-L-CU-D(P) After One Year of Expoure.

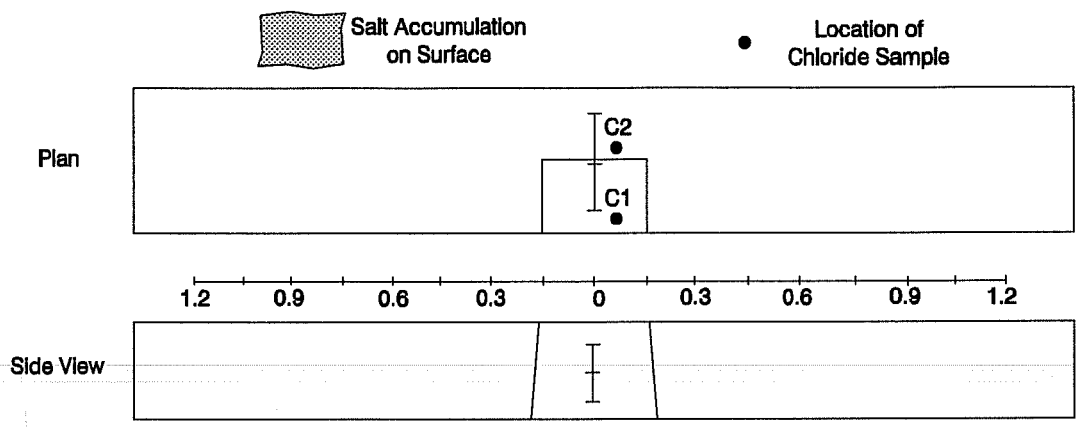

Figure D.63 Surface Condition of Beam B16-ST-UU-AR After One Year of Expoure.

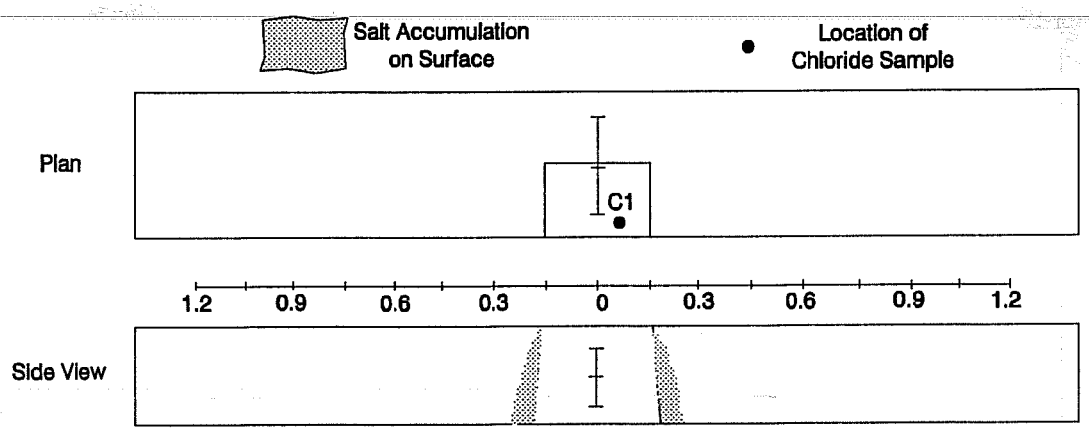

Figure D.64 Surface Condition of Beam B21-ST-UU-AR(P) After One Year of Expoure.

Table D.9 Average Crack Width Measurement for B18-ST-CU-AR

Days	Crack 1, mm
162	0.41
193	0.54
220	0.44
252	0.45
277	0.44
305	0.45
333	0.44
361	0.44
381	0.43

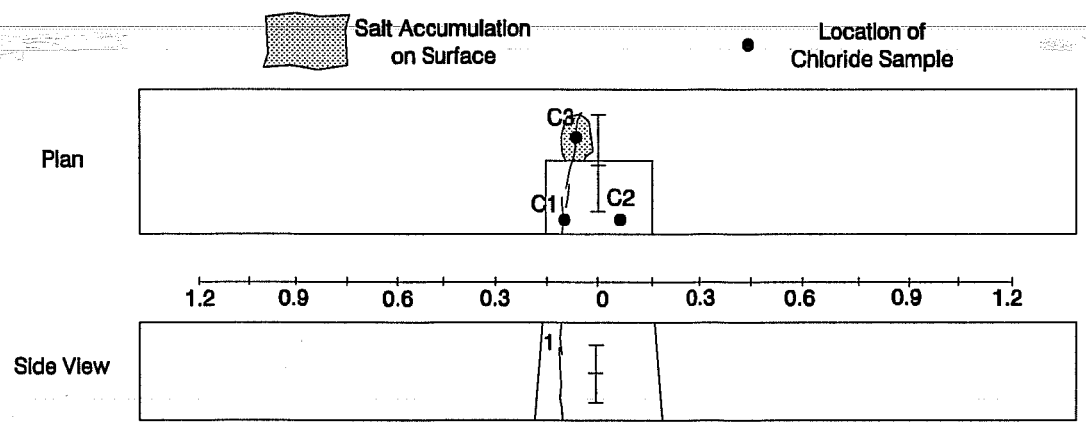

Figure D.65 Surface Condition of Beam B18-ST-CU-AR After One Year of Expoure.

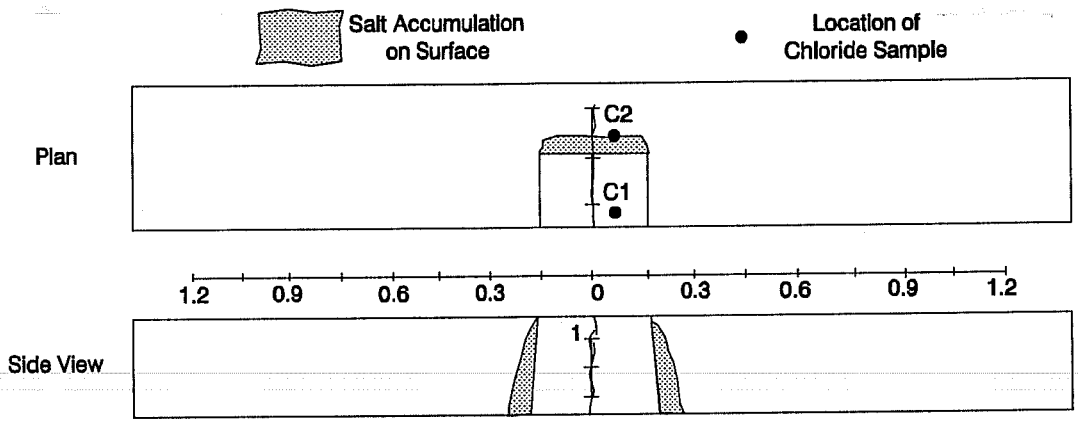

Figure D.66 Surface Condition of Beam B20-ST-CL-AR After One Year of Expoure.

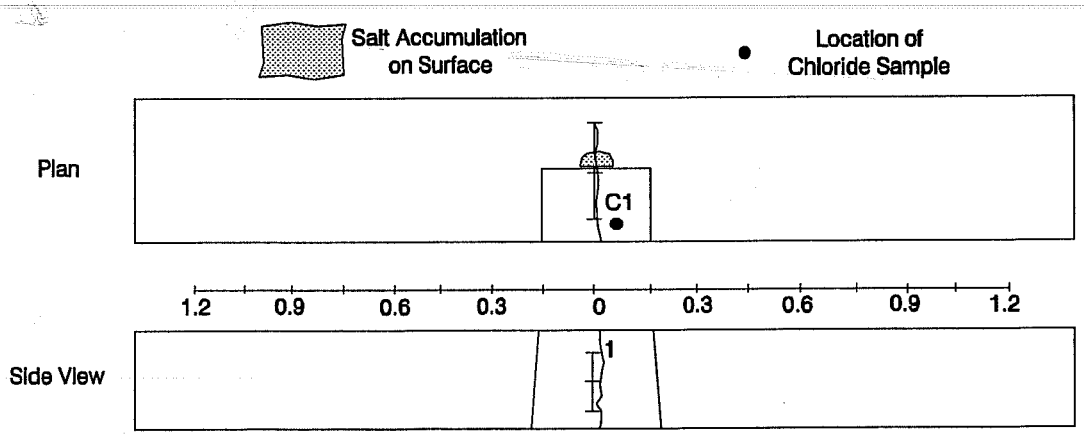

Figure D.67 Surface Condition of Beam B26-ST-CL-AR(P) After One Year of Expoure.

Table D.10 Average Crack Width Measurement for B24-ST-CU-AR(P)

Days	Crack 1, mm
162	0.36
193	0.38
220	0.39
252	0.38
277	0.38
305	0.40
333	0.39
361	0.38
381	0.40

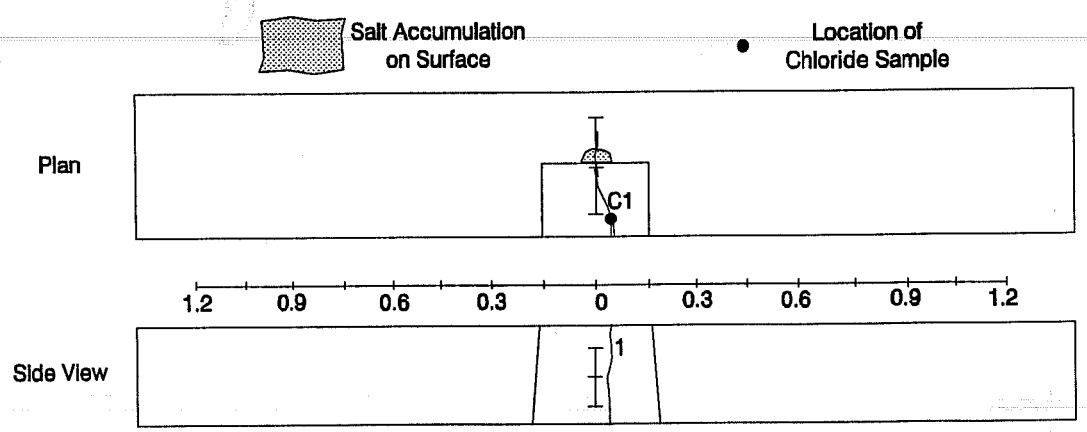

Figure D.68 Surface Condition of Beam B24-ST-CU-AR(P) After One Year of Expoure.

Table D.11 Average Crack Width Measurement for B28-ST-CU-D(P)

Days	Crack 1, mm
162	0.39
193	0.38
220	0.36
252	0.38
277	0.39
305	0.39
333	0.40
361	0.39
381	0.38

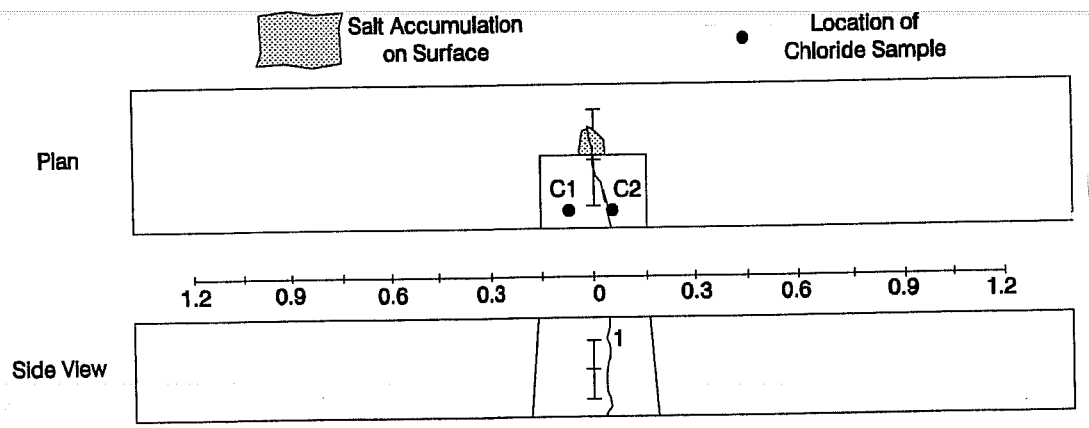

Figure D.69 Surface Condition of Beam B28-ST-CU-D(P) After One Year of Expoure.

Table D.12 Average Crack Width Measurement for B29-L/ST-CU-D(P)

Days	Crack 1, mm	Crack 2, mm	Crack 3, mm	Crack 4, mm
162	0.08	0.17	0.06	0.11
193	0.10	0.20	0.07	0.13
220	0.08	0.19	0.07	0.15
252	0.10	0.20	0.07	0.13
277	0.10	0.19	0.08	0.15
305	0.11	0.20	0.07	0.15
333	0.10	0.19	0.07	0.13
361	0.10	0.17	0.07	0.13
381	0.10	0.17	0.08	0.12

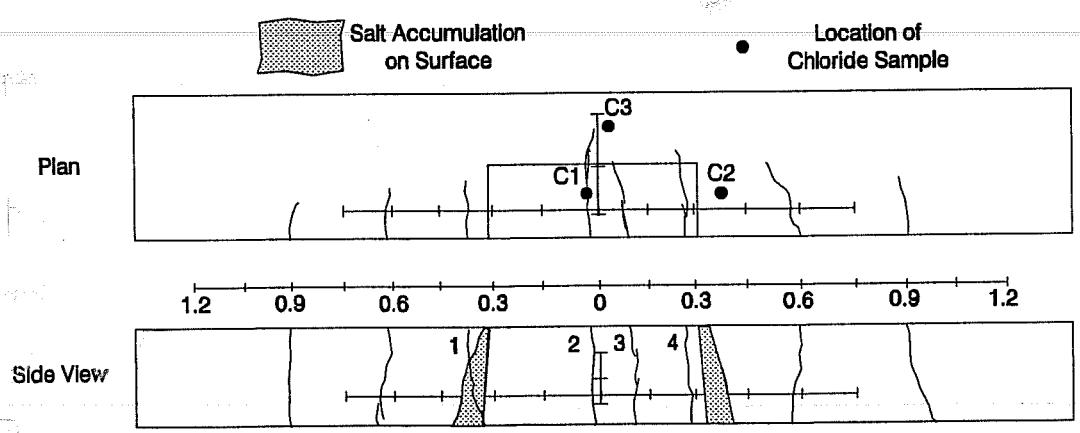

Figure D.70 Surface Condition of Beam B29-L/ST-CU-D(P) After One Year of Expoure.

Table D.13 Average Crack Width Measurement for B31-SP-CU-D(P)

Days	Crack 1, mm	Crack 2, mm	Crack 3, mm
162	0.26	0.19	0.26
193	0.25	0.16	0.21
220	0.30	0.19	0.21
252	0.31	0.22	0.19
277	0.30	0.20	0.20
305	0.31	0.19	0.19
333	0.29	0.19	0.17
361	0.29	0.19	0.17
381	0.30	0.17	0.16

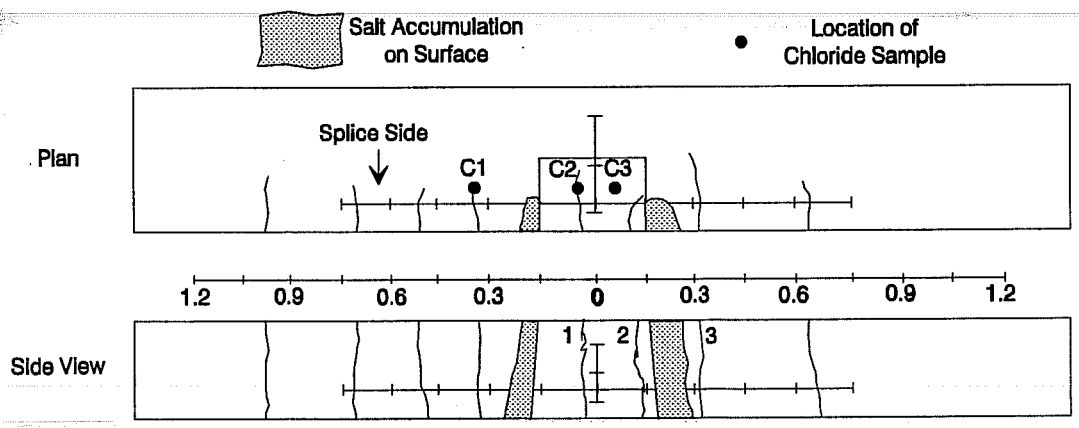

Figure D.71 Surface Condition of Beam B31-SP-CU-D(P) After One Year of Expoure.

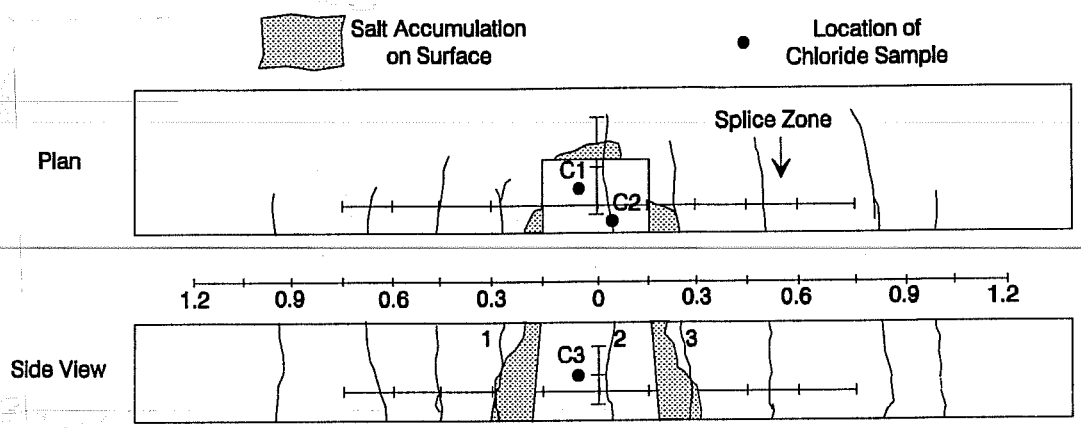

Figure D.72 Surface Condition of Beam B33-SP-CU-D(P) After One Year of Expoure.

Figure D.73 Sampling Chloride from Beams Before Autopsy.

Table D.14 Acid-Soluble Chloride Concentrations in Autopsied Group I Beams After One Year of Exposure (Percentage by Weight of Concrete)

Beam	Location	Sampling Depth Ranges (mm)			
		13-38	51-76	89-114	127-152
B2-L-UU-AR	C1		0.14		0.09
	C2		0.00		0.00
B4-L-CU-AR	C1		0.05		0.14
	C2		0.41		0.47
B5-L-CL-AR	C1		0.00		0.04
	C2	0.36	0.05	0.03	0.08
	C3		0.00		0.00
B7-L-UU-D	C1	0.45	0.09	0.00	0.11
	C2		0.00		0.04
	C3		0.09		
	C4		0.07		
B9-L-CU-D	C1	0.53	0.12	0.03	0.12
	C2		0.01		0.31
	C3	0.42	0.15		
	C4		0.55		
B11-L-CL-D	C1		0.17		0.37
	C2		0.57		0.58
	C3		056		0.49
	C4		0.22		0.29
	C5		0.00		
	C6		0.56		
	C7		0.32		
B13-L-CU-D(p)	C1		0.52		0.39

Table D.15 Acid-Soluble Chloride Concentrations in Autopsied Group II Beams After One Year of Exposure (Percentage by Weight of Concrete)

Beam	Location	Sampling Depth Ranges (mm)			
		13-38	51-76	89-114	127-152
B16-ST-UU-AR	C1	0.52	0.23	0.19	0.24
	C2		0.01		0.00
B18-ST-CU-AR	C1		0.50		0.53
	C2		0.27		0.32
	C3		0.49		0.43
B20-ST-CL-AR	C1		0.29		0.40
	C2		0.34		0.30
B21-ST-UU-AR(P)	C1		0.34		0.33
B24-ST-CU-AR(P)	C1		0.69		0.50
B26-ST-CL-AR(P)	C1		0.68		0.60
B28-ST-CU-D(p)	C1		0.38		0.49
	C2		0.51		0.39

Table D.16 Acid-Soluble Chloride Concentrations in Autopsied Group III Beams After One Year of Exposure (Percentage by Weight of Concrete)

Beam	Location	Sampling Depth Ranges (mm)			
		13-38	51-76	89-114	127-152
B29-L/ST-CU-D(P)	C1		0.47		0.51
	C2		0.31		0.48
	C3		0.00		
B31-SP-CU-D(P)	C1		0.06		
	C2		0.66		0.65
	C3		0.47		0.33
B33-SP-CL-D(P)	C1	0.77	0.71	0.58	0.77
	C2		0.93		0.85
	C3		0.58		0.58

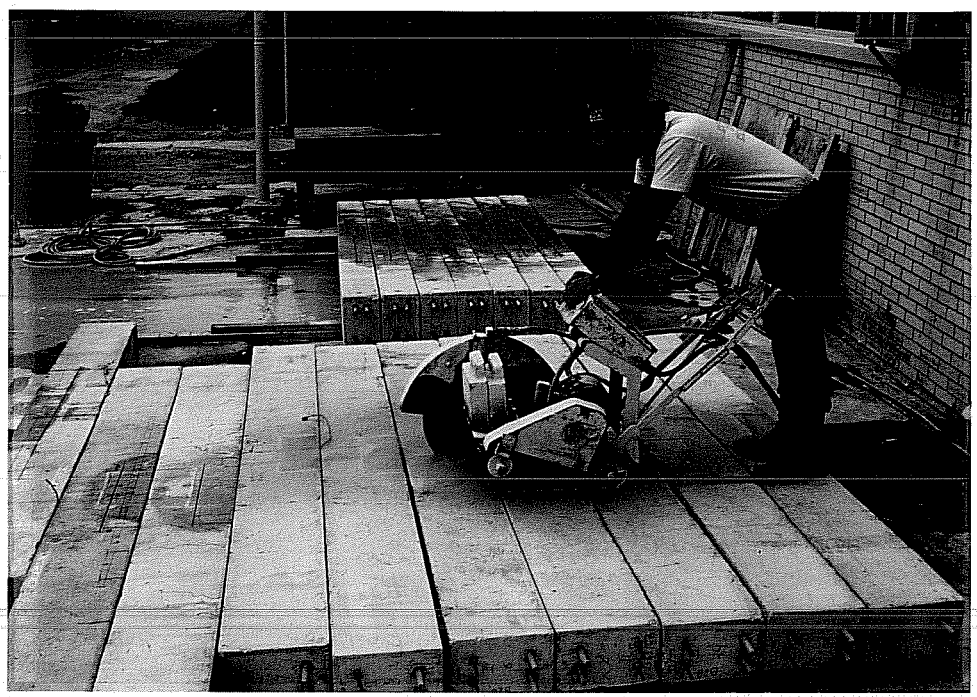

Figure D.74 Saw Used to Crosscut Beams.

Figure D.75 Beam Demolition for Bar Retrieval.

Table D.17 Observations of Longitudinal Bars in Group I Beams, One Year Exposure

Beam No.	Bar Surface Condition	Coating Adhesion	Undercutting
B2-Upper	No apparent corrosion.	Very good adhesion.	Bright steel, as new.
B2-Lower	No apparent corrosion except at one mill mark.	Very good adhesion except at rust spot.	Bright steel, one 3 x 6 mm black rust spot.
B4-Upper	As B2-Lower, rust 13 mm from crack near stirrup.	Very good adhesion except at rust spot.	Black over 25 mm from crack -side facing cover.
B4-Lower	Rust spots at mill marks within 25 mm from cracks.	Debonding along 130 mm around rust spots.	As B4-Upper, but about 50-75 mm from crack.
B5-Upper	No apparent corrosion.	Very good adhesion except at a mill mark.	Bright steel, one 13 x 13 mm black rust spot.
B5-Lower	Rust at one damaged spot 37 mm from crack.	Very good adhesion except at rust spot.	Bright steel, one 22 x 13 mm black rust spot.
B7-Upper	Rust spotting only on steel areas facing cover.	Debonding up to 25 mm around rust areas.	Dark (or black) around damaged (or rust) spots
B7-Lower	As B7-Upper, with 12 blisters.	As B7-Upper.	As B7-Upper, clear fluid in some blisters.
B9-Upper	As B7-Upper, spots 40 mm or less from cracks, 5-6 blisters of variable size.	Debonding up to 9 mm around steel spots, up to 100 mm along rust.	Rust up to 60 mm from crack, (25 mm from steel edge)
B9-Lower	As B9-Upper	As B9-Upper, but up to 75 mm along rust spots.	As B9-Upper, but up to 45 mm from steel edges
B11-Upper	As B7-Upper, 5 blisters of variable size.	As B9-Lower.	As B9-Upper, pits 1.25, 1.05, 0.2 mm deep.
B11-Lower	Rust on areas up to 60 mm from cracks, 5 blisters	As B9-Lower.	As B9-Upper, one pit 6 x 9 x 1.15 (deep) mm.
B13-Upper	As B11-Lower but patched areas, cracking and blistering of coating.	Extensive debonding mostly on side facing cover.	Darker around than under patches, rust up to 50 mm from crack.
B13-Lower	As B13-Upper.	As B13-Upper.	As B13-Upper.

Table D.18 Observations of Stirrups in Group II Beams, One Year Exposure

Beam No.	Bar Surface Condition	Coating Adhesion	Undercutting
B16	Corrosion spots, blisters and coating cracking of hook end near bottom concrete surface.	Poor bond at bent portions (more on outside) and some straight portions.	Mostly bright steel inside and dark outside of stirrup, rust along 90 mm of hook end.
B18	Corrosion spots at areas of contact with uncoated bars, 10 small blisters.	Poor bond as B16 and to about 13 mm from patched ends and along rust areas.	Rust along 0.22 m near contact points with black bars, mostly dark steel elsewhere.
B20	Corrosion along continuous ribs at bend, longitudinal cracking of coating along hook end and inside bends.	As B16 and along rust areas, almost half length of stirrup.	As B16, corrosion concentrated along hook and leg closest to crack.
B21	No apparent corrosion, bright steel at damaged spots in contact with black bars.	No debonding of coating.	Mostly bright steel inside and dark outside of stirrup, minor rust spots at bent areas.
B24	Corrosion and blisters at part close to bottom concrete surface and points of contact with black bars.	As B16 and to about 50 mm from patched ends and along rust areas.	Mostly dark steel except at parts of straight legs, rust concentrated at lower side of stirrup.
B26	As B24 and along hook and inside bends close to upper concrete surface with coating cracking.	As B24.	As B24, black rust inside one bend, slight pits along continuous rib of lower leg (0.2-0.4 mm deep).
B28	As B26, 4 blisters up to 3 x 3 mm.	As B16 and to about 90 mm from patched ends and along rust areas.	As B24, dark steel under patches, rust along hook ends and some bends.

Table D.19 Observations of Longitudinal Bars and Stirrups in Group III Beams, One Year Exposure

Beam No.	Bar Surface Condition	Coating Adhesion	Undercutting
B29-Upper	Minor rust spotting at mill marks and on patched areas facing concrete cover near cracks, blisters.	Debonding up to 13 mm around patched areas and along rust spots.	Rust up to 60 mm from crack, (25 mm from steel edge), slight pits 0.3 mm deep.
B29-Lower	Minor rust spotting on patched areas facing concrete cover 25-50 mm from cracks, blisters.	Debonding up to 13 mm around patched areas and along rust spots.	Rust up to 60 mm from crack, (25 mm from steel edge), bright steel beneath patches.
B29-Stirrup	Rust spotting along leg, bend and hook end with crack along continuous rib	Debonding at bends (more on outside) and along rust portions.	Rusting along leg near crack from front hook to back connection.
B31-Upper Splice End	Surface corrosion (60%) of cut area, cracks and blisters along continuous ribs (140 mm).	Debonding along cracked coating.	Black corrosion product 50-70% of surface around bar (at lower side) up to 165 mm from cut end.
B31-Lower Splice End	Surface corrosion (20%), slight cracking along rib, 2 rust spots 50-75 mm from cut end.	Debonding along cracked coating.	Black and brown rust 60% of surface around bar (at lower side) up to 50 mm from cut end.
B31-Stirrup	Breakdown and corrosion on hook end, bends and lower leg near a crack, cracking along continuous ribs and longitudinally.	Extensive debonding (over 65% of stirrup surface) along hook, bends and straight legs.	Black and brown corrosion covering all debonded areas, dark steel beneath intact coating.
B33-Upper Splice End	Surface corrosion (10%) of cut area.	Limited debonding around bar end.	Slight corrosion (70%) under patched end.
B33-Lower Splice End	Surface corrosion (40%) of cut area.	Limited debonding around bar end.	Slight corrosion (100%) under patched end.
B33-Stirrup	AS B31-Stirrup, severe corrosion of patched spots.	Debonding over 50% of stirrup area.	As B31-Stirrup, more rust on outer surfaces of upper and front parts

BIBLIOGRAPHY

1. **Safier, A.S.,** "Development and Use of Electrostatic, Epoxy-Powder Coated Reinforcement," *The Structural Engineer,* Vol. 67, No. 6/21, March 1989, pp 95-98.

2. "Applications of Fusion Bonded Epoxy-Coated Rebar," *Concrete (London),* Vol. 23, No. 4, May 1989, pp 16.

3. "Rebars Protective Coating," *Highways,* Vol. 57, No. 1953, September 1989, pp 16.

4. **Poston, R.W.,** "Improving Durability of Bridge Decks by Transverse Prestressing," Ph.D. Dissertation, Department of Civil Engineering, The University of Texas at Austin, Austin, TX, December 1984.

5. **Berke, N.S., Shen, D.F., and Sandberg, K.M.,** "Comparison of the Polarization Resistance Technique to the Macrocell Corrosion Technique," *Corrosion Rates of Steel in Concrete,* ASTM STP 1065, N.S. Berke, V. Chaker, and D. Whiting, Eds., American Society for Testing and Materials, Philadelphia, PA, 1990, pp 38-51.

6. **Al-Qadi, I.L., Peterson, J.E., and Weyers, R.E.,** "A Time to Cracking Model for Critically Contaminated Reinforced Concrete Structures," Proceedings of 5th International Conference on Structural Faults and Repair held 29 June, 1993, V.3, Venue, University of Edinburgh, pp 91-99.

7. **MEC,** "As Solid as Concrete," *Middle East Construction,* April/May 1987, pp 20-21.

8. **WC,** "Gulf Concrete Under Scrutiny," *World Construction,* July 1986, pp 22-24.

9. **Schutt, W.R.,** "Cathodic Protection of new High-Rise Buildings in Abu Dhabi," *Concrete International,* May 1992, pp 45-46.

10. **Henriksen, C.F., and Stoltzner, E.,** "Chloride Corrosion in Danish Road-Bridge Columns," *Concrete International,* Vol. 15, No. 8, August 1993, pp 55-60.

11. **Kobayashi, K., and Takewaka, K.,** "Experimental Studies of Epoxy-Coated Reinforcing Steel for Corrosion Protection," *The International Journal of Cement Composites and Lightweight Concrete,* Vol. 6, No. 2, May 1984, pp 99-116.

12. **Read, J.A.,** "FBECR- The Need for Correct Specification and Quality Control," Paper Presented at Symposium on FBECR at Sheffield University on Wednesday May 17, 1989, 23 p.

13. **French, E.L.,** "Protection of Concrete and Reinforcement- The Significance of Test Results," *Polymers Paint Colour Journal,* Vol. 177, No. 4204, November 25, 1987, pp 821-822.

14. **Fontana, M.G.,** "Corrosion Engineering," 3rd ed. McGraw-Hill, New York, NY, 1986.

15. **Clifton, J.R., Beeghly, H.F., and Mathey, R.G.,** "Nonmetallic Coatings for Concrete Reinforcing Bars," Report No. NBS BSS-65, Federal Highway Administration, Washington, D.C., August 1975, 44 p.

16. **Collacott, R.A.,** "Structural Integrity Monitoring," Chapman and Hall, Ltd., London-New York, 1985.

17. **Locke, C.E.,** "Corrosion of Steel in Portland Cement Concrete: Fundamental Studies," *Corrosion Effect of Stray Currents and the Techniques for Evaluating Corrosion of Rebars in Concrete,* ASTM STP 906, V. Chaker, Ed., American Society for Testing and Materials, Philadelphia, PA, 1986, pp 5-14.

18. **Pourkhosrow, G.,** "Epoxy-Coated Reinforcing Steel in Bridge Decks," Report No. FHWA/OK-81(3), Oklahoma Department of Transportation, Federal Highway Administration, Oklahoma City, Oklahoma, November 1981, 55 p.

19. **Baldwin, W.R.,** "An Update on Epoxy-Coated Reinforcing Steel," Paper No. 7, Seminar Reprints on *Solving Rebar Corrosion Problems in Concrete,* September 27-29, 1982, Chicago, Ill, NACE, Houston, TX, 1983, 4 p.

20. **Cady, P.D., and Weyers, R.E.,** "Chloride Penetration and the Deterioration of Concrete Bridge Decks," *Cement, Concrete and Aggregates,* CCAGDP, Vol. 5, No. 2, Winter 1983, pp 81-87.

21. **Broomfield, J.P., Langford, P.E., and Ewins, A.J.,** "The Use of a Potential Wheel to Survey Reinforced Concrete Systems," *Corrosion Rates of Steel in Concrete,* ASTM STP 1065, N.S. Berke, V. Chaker, and D. Whiting, Eds., American Society for Testing and Materials, Philadelphia, PA, 1990, pp 157-173.

22. **Broomfield, J.P., Rodriguez, J., Ortega, L.M., and Garcia, A.M.,** "Corrosion Rate Measurement and Life Prediction for Reinforced Concrete Structures," Proceedings of 5th International Conference on Structural Faults and Repair held 29 June, 1993, V.2, Venue, University of Edinburgh, pp 155-163.

23. **Elsener, B., and Böhni, H.,** "Potential Mapping and Corrosion of Steel in Concrete," *Corrosion Rates of Steel in Concrete,* ASTM STP 1065, N.S. Berke, V. Chaker, and D. Whiting, Eds., American Society for Testing and Materials, Philadelphia, PA, 1990, pp 143-156.

24. **Mautner, A.,** "A Failure of Ethics," *Materials Performance,* August 1993, pp 5-6.

25. **Buslov, V.M.,** "Marine Concrete- When to Repair, What to Repair," *Concrete International,* May 1992, pp 36-40.

26. **El-Metwally, S.E., and Schlaich, J.,** "The Design for Repair- Free Structures is the Ideal Approach," Proceedings of 5th International Conference on Structural Faults and Repair held 29 June, 1993, V.3, Venue, University of Edinburgh, pp 21-29.

27. **Clear, K.C., and Hay, R.E.,** "Time-To-Corrosion of Reinforcing Steel in Concrete Slabs, V.2: Electrical Potential Data," Report No. FHWA-RD-73-33, Federal Highway Administration, Washington, D.C., April 1973, 139 p.

28. **Higgins, R.J.,** "Fusion Bonded Epoxy Powder Coating Chosen for Rebar Protection in Dubai," *Corrosion Prevention and Control,* Vol. 34, No. 4, August 1987, pp 102-104.

29. **Andrade, C., Holst, J.D., Nürnberger, U., Whiteley, J.D., and Woodman, N.,** "Protection Systems for Reinforcement," CEB Bulletin D' Information No. 211, Switzerland, February 1992.

30. **Clear, K.C.,** "Effectiveness of Epoxy-Coated Reinforcing Steel- Interim Report," Canadian Strategic Highway Research Program (C-SHRP), Ottawa, Ontario, November 1992, 94 p.

31. **Clear, K.C.,** "Effectiveness of Epoxy-Coated Reinforcing Steel," *Concrete International,* May 1992, pp 58-62.

32. **CRSI,** "CRSI Comments," *Concrete International,* May 1992, pp 59-64.

33. **ENR,** "Top Researcher's Switch Shakes Bridge Deck Design," *Engineering News Record,* The McGraw-Hill Construction Weekly, June 15, 1992.

34. **CE,** "Epoxy-Coated-Rebar, Debate Still Going," *Civil Engineering,* March 1993, pp 22.

35. **ENR,** "Rebar Researcher Cleared," and "Misguided Legal Pursuit," Editorial, *Engineering News Record,* The McGraw-Hill Construction Weekly, November 9, 1992.

36. **CE,** "Researcher Discusses Fallout of Epoxy-Coated-Rebar Case," *Civil Engineering,* January 1993, pp 11.

37. **Clear, K.C.,** "Effectiveness of Epoxy-Coated Reinforcing Steel (C-SHRP Report: Executive Summary)," Transportation Research Circular: Epoxy-Coated Reinforcement in Highway Structures, No. 403, ISSN 0097-8515, National Research Council, Washington, D.C., March 1993, pp 66-67.

38. **American Society for Testing and Materials,** "Standard Specification for Epoxy Coated Reinforcing Steel Bars," ASTM A775/A775M-90, Philadelphia, PA, 1990.

39. American Society for Testing and Materials, "Standard Specification for Epoxy Coated Reinforcing Steel," ASTM D3963/D3963M-87, Philadelphia, PA, 1987.

40. Sarcinella, R.L., "Epoxy-Coated Reinforcing Steel," *TQ7-1/7-2-TXDOT Newsletter,* pp 7-8.

41. Neif, T., "Performance of Epoxy-Coated Bars," A Seminar Presentation at Wyndham Hotel, Austin, TX, November 2, 1991.

42. Sagüés, A.A., Powers, R.G., and Zayed, A.M., "Marine Environment Corrosion of Epoxy-Coated Reinforcing Steel," *Corrosion of Reinforcement in Concrete,* C. Page, K. Treadaway and P. Bamforth, Eds., Elsevier Applied Science, London-New York, 1990, pp 539-549.

43. Fraczek, J., "A Review of Electrochemical Principles as Applied to Corrosion of Steel in a Concrete or Grout Environment," *Corrosion, Concrete and Chlorides, ACI SP 102,* F.W. Gibson, Ed., American Concrete Institute, Detroit, 1987, pp 13-24.

44. ACI Committee 222, "Corrosion of Metals in Concrete," ACI 222R-85, *ACI Manual of Concrete Practice, Part 1, Materials and General Properties of Concrete,* American Concrete Institute, Detroit, 1987, 30 p.

45. Mehta, P.K., "Durability of Concrete Exposed to Marine Environment- A Fresh Look," *Concrete in Marine Environment, Proceedings, 2nd International Conference, St. Andrews by-the-Sea, Canada,* ACI SP 109, V.M. Malhotra, Ed., American Concrete Institute, Detroit, 1988, pp 1-29.

46. Hime, W., and Erlin, B., "Some Chemical and Physical Aspects of Phenomena Associated with Chloride-Induced Corrosion," *Corrosion, Concrete and Chlorides, ACI SP 102,* F.W. Gibson, Ed., American Concrete Institute, Detroit, 1987, pp 1-12.

47. ACI Committee 201, "Guide to Durable Concrete," ACI 201.2R-77 (Revised 1982), *ACI Manual of Concrete Practice, Part 1, Materials and General Properties of Concrete,* American Concrete Institute, Detroit, 1987, 37 p.

48. Read, J.A., "Rebar Corrosion- Coatings a Cure?" *Civil Engineering (England),* November/December 1987, pp 42-48.

49. Borgard, B., Warren, C., Somayaji, S., and Heidersbach, R., "Mechanisms of Corrosion of Steel in Concrete," *Corrosion Rates of Steel in Concrete,* ASTM STP 1065, N.S. Berke, V. Chaker, and D. Whiting, Eds., American Society for Testing and Materials, Philadelphia, PA, 1990, pp 174-188.

50. Vaysburd, A.M., "Some Durability Considerations for Evaluating and Repairing Concrete Structures," *Concrete International,* Vol. 15, No. 3, March 1993, pp 29-35.

51. **Satake, J., Kamakura, M., Shirakawa, K., Mikami, N., and Swamy, N.,** "Long-Term Corrosion Resistance of Epoxy-Coated Reinforcing Bars," *Corrosion of Reinforcement in Concrete Construction,* A.P. Crane, Ed., Ellis Horwood, Ltd., Great Britain, 1983, pp 357-378.

52. **Arup, H.,** "The Mechanisms of the Protection of Steel by Concrete," *Corrosion of Reinforcement in Concrete Construction,* A.P. Crane, Ed., Ellis Horwood, Ltd., Great Britain, 1983, pp 151-158.

53. **Schupack, M.,** "34 Year Old Bridge Durability Study," A Seminar Presentation at The University of Texas at Austin, Austin, TX, October 12, 1992.

54. **Barbera, O.E., Perperez, V.B., Benlloch, M.J., Mas, L.V., and Santatecla, F.R.,** "Planning, Design, Construction and Durability of Concrete Constructions Research into the Causes of Structure Deterioration at the Technical University of Valencia," Proceedings of 5th International Conference on Structural Faults and Repair held 29 June, 1993, V.3, Venue, University of Edinburgh, pp 11-20.

55. **Hime, W.G.,** "The Corrosion of Steel- Random Thoughts and Wishful Thinking," *Concrete International,* Vol. 15, No. 10, October 1993, pp 54-57.

56. **Erdoğdu, S., and Bremner,** "Field and Laboratory Testing of Epoxy-Coated Reinforcing Bars in Concrete," Transportation Research Circular: Epoxy-Coated Reinforcement in Highway Structures, No. 403, ISSN 0097-8515, National Research Council, Washington, D.C., March 1993, pp 5-16.

57. **Clear, K.C., and Virmani, Y.P.,** "Solving Rebar Corrosion Problems in Concrete Research Update: Methods and Materials, " Paper No. 4, Seminar Reprints on *Solving Rebar Corrosion Problems in Concrete,* September 27-29, 1982, Chicago, Ill, NACE, Houston, TX, 1983, 21 p.

58. **Escalante, E., and Ito, S.,** "Measuring the Rate of Corrosion of Steel in Concrete," *Corrosion Rates of Steel in Concrete,* ASTM STP 1065, N.S. Berke, V. Chaker, and D. Whiting, Eds., American Society for Testing and Materials, Philadelphia, PA, 1990, pp 86-102.

59. **Taywood Engineering Laboratories,** "Concrete Protection Evaluation Through Analysis and Engineering," *Polymers Paint Colour Journal,* Vol. 177, No. 4204, November 25, 1987, pp 817-822.

60. **Rostam, S.,** "Service Life Design- The European Approach," *Concrete International,* Vol. 15, No. 7, July 1993, pp 24-32.

61. **Matta, Z.G.,** "Deterioration of Concrete Structures in Arabian Gulf," *Concrete International,* Vol. 15, No. 7, July 1993, pp 33-36.

62. **Treadaway, K.W.J., and Davies, H.,** "Performance of Fusion-Bonded Epoxy-Coated Steel Reinforcement," *The Structural Engineer*, Vol. 67, No. 6/21, March 1989, pp 99-108.

63. **Andrade, C., Castelo, V., Alonso, C., and González, J.A.,** "The Determination of the Corrosion Rate of Steel Embedded in Concrete by the Polarization Resistance and AC Impedance Methods," *Corrosion Effect of Stray Currents and the Techniques for Evaluating Corrosion of Rebars in Concrete,* ASTM STP 906, V. Chaker, Ed., American Society for Testing and Materials, Philadelphia, PA, 1986, pp 43-63.

64. **Hansson, C.M., and Sφrensen, B.,** "The Threshold Concentration of Chloride in Concrete for the Initiation of Reinforcement Corrosion," *Corrosion Rates of Steel in Concrete,* ASTM STP 1065, N.S. Berke, V. Chaker, and D. Whiting, Eds., American Society for Testing and Materials, Philadelphia, PA, 1990, pp 3-16.

65. **ACI Forum:** "Influence of Chlorides in Reinforced Concrete," *Corrosion, Concrete and Chlorides, ACI SP 102*, F.W. Gibson, Ed., American Concrete Institute, Detroit, 1987, pp 143-153.

66. **Barony, S.Y., Elwefati, A.M., and Fadel, M.I.,** "Diagnostic Study of Deteriorated Alcohol Factory Building," Proceedings of 5th International Conference on Structural Faults and Repair held 29 June, 1993, V.2, Venue, University of Edinburgh, pp 343-351.

67. **Petersen, C.G.,** "RCT Profile Grinding Kit for In-situ Evaluation of the Chloride Diffusion Coefficient and the Remaining Service Life of a Reinforced Concrete Structure," *Chloride Ingress in Concrete Structures,* Symposium held at the Chalmers Technical University, Gothenburg, Sweden, January 13-14, 1993.

68. **Gaynor, R.,** "Understanding Chloride Percentages," *Corrosion, Concrete and Chlorides, ACI SP 102*, F.W. Gibson, Ed., American Concrete Institute, Detroit, 1987, pp 161-165.

69. **Nagataki, S., Otsuki, N., Wee, T-H., and Nakashita, K.,** "Condensation of Chloride Ion in Hardened Cement Matrix Materials and on Embedded Steel Bars," *ACI Materials Journal,* Vol. 90, No. 4, July-August 1993, pp 323-332.

70. **ACI Committee 318,** "Building Code Requirements for Reinforced Concrete and Commentary," ACI Standard 318-89, American Concrete Institute, Detroit, 1989.

71. **Matta, Z.G.,** "Chlorides and Corrosion in the Arabian Gulf Environment," *Concrete International,* May 1992, pp 47-48.

72. **Munjal, S.K., Reviewed by Parrish, S.,** "Evaluation of Epoxy-Coated Reinforcing Steel in Bridge Decks," Interim Report No. FHWA-MD-82/03, Maryland State Highway Administration, Federal Highway Administration, Brooklandville, Maryland, March 1981, 137 p.

73. Malasheskie, G.J., Maurer, D.A., Mellott, D.B., and Avellano, J.L., "Bridge Deck Protective Systems- Final Report," Report No. FHWA-PA-88-001+85-17, Federal Highway Administration, Washington, D.C., July 1988, 61 p.

74. Berke, N.S., "The Use of Anodic Polarization to Determine the Effectiveness of Calcium Nitrite as an Anodic Inhibitor," *Corrosion Effect of Stray Currents and the Techniques for Evaluating Corrosion of Rebars in Concrete,* ASTM STP 906, V. Chaker, Ed., American Society for Testing and Materials, Philadelphia, PA, 1986, pp 78-91.

75. Weyers, R.E., and Cady, P.D., "Deterioration of Concrete Bridge Decks from Corrosion of Reinforcing Steel," *Concrete International,* Vol. 9, No. 1, January 1987, pp 15-20.

76. Hagen, M.G., "Bridge Deck Deterioration and Restoration- Final Report," Report No. FHWA/MN/RD-83/01, Federal Highway Administration, Washington, D.C., November 1982, 39 p.

77. Erlin, B., and Hime, W., "Chloride-Induced Corrosion," *Corrosion, Concrete and Chlorides, ACI SP 102,* F.W. Gibson, Ed., American Concrete Institute, Detroit, 1987, pp 155-159.

78. Holm, J., "Comparison of the Corrosion Potential of Calcium Chloride and a Calcium Based Non-Chloride Accelerator- A Macro-Cell Corrosion Approach," *Corrosion, Concrete and Chlorides, ACI SP 102,* F.W. Gibson, Ed., American Concrete Institute, Detroit, 1987, pp 35-48.

79. American Society for Testing and Materials, "Corrosion and Corrosion Testing," ASTM, G15-74, Philadelphia, PA, 1974.

80. Mills, G., "Coating Adhesion is Key to Protection," *Gulf Construction,* June 1987, pp 42-43.

81. Hededahl, P., and Manning, D.G., "Field Investigation of Epoxy-Coated Reinforcing Steel," Report No. MAT-89-02, The Research and Development Branch, Ontario Ministry of Transportation, Ontario, Canada, December 1989, 28 p.

82. Sagüés, A.A., "Evaluation of Corrosion Rate by Electrochemical Impedance in a System With Multiple Polarization Effects," paper no. 25, *Corrosion 89,* NACE, New Orleans Convention Center, New Orleans, Louisiana, April 17-21, 1989, 10 p.

83. Sagüés, A.A., Perez-Duran, H.M., Powers, R.G., "Corrosion Performance of Epoxy-Coated Reinforcing Steel in Marine Substructure Service," a paper prepared at Department of Civil Engineering and Mechanics, University of South Florida, Tampa, Florida, and Materials Office, Florida Department of Transportation, Gainesville, Florida, 17 p.

84. **Zayed, A.M., and Sagüés, A.A.,** "Corrosion at Surface Damage on an Epoxy-Coated Reinforcing Steel," *Corrosion Science,* Vol. 30, No. 10, 1990, pp 1025-1044.

85. **Pike, R.G., Hay, R.E., Clifton, J.R., Beeghly, H.F., and Mathey, R.G.,** "Nonmetallic Coatings for Concrete Reinforcing Bars," *Public Roads,* Vol. 37, No. 5, U.S. Bureau of Public Roads, June 1973, pp 185-197.

86. **McFadden, B.J.,** "Application and Fabrication of Epoxy-Coated Reinforcing Steel," Paper No. 8, Seminar Reprints on *Solving Rebar Corrosion Problems in Concrete,* September 27-29, 1982, Chicago, Ill, NACE, Houston, TX, 1983, 6 p.

87. **Steel Structures Painting Council,** "Near-White Blast Cleaning," SSPC-SP10-85.

88. **Steel Structures Painting Council,** "Pictorial Surface Preparation Standards for Painting Steel Surfaces," SSPC-VIS 1-67T.

89. **Robert, A.G.,** "Organic Coatings: Properties, Selection and Use," NBS, Building Science Series 7, National Bureau of Standards, Washington, D.C., 1968.

90. **Concrete Reinforcing Steel Institute,** "Voluntary Certification Program for Fusion Bonded Epoxy Coating Application Plants," CRSI, Schaumburg, Ill, 1991, 97 p.

91. **Concrete Reinforcing Steel Institute,** "Standard Specification for Epoxy-Coated Reinforcing Steel," CRSI Draft of the Revised ASTM Specification D3963, Schaumburg, Ill, 1991.

92. **National Association of Corrosion Engineers,** "Proposed NACE Standard Recommended Practice: Epoxy-Coated Steel Reinforcing Bars," NACE, Houston, TX, 1989.

93. **Sagüés, A.A.,** "Mechanism of Corrosion of Epoxy-Coated Reinforcing Steel in Concrete- Final Report," Report No. FL/DOT/RMC/0543-3296, University of South Florida, Tampa, Florida, April 1991, 75 p.

94. **Pfeifer, D.W., Landgren, R., and Krauss, P.,** "Performance of Epoxy-Coated Rebars: A Review of CRSI Research Studies," Transportation Research Circular: Epoxy-Coated Reinforcement in Highway Structures, No. 403, ISSN 0097-8515, National Research Council, Washington, D.C., March 1993, pp 57-65.

95. **Concrete Reinforcing Steel Institute,** "Guidelines for Inspection and Acceptance of Epoxy-Coated Reinforcing Bars at the Job Site," CRSI, Schaumburg, Ill, 1986.

96. **Mckeel, W.T., Jr.,** "Evaluation of Epoxy-Coated Reinforcing Steel," Report No. VHTRC 77-R56, Virginia Highway and Transportation Research Council, Federal Highway Administration, Charlottesville, Virginia, June 1977, 26 p.

97. **Lee, H., and Neville, K.,** "Handbook of Epoxy Resins," 2nd ed., McGraw-Hill, Inc., New York, NY, 1982.

98. Smith, L.L., Kessler, R.J., and Powers, R.G., "Corrosion of Epoxy-Coated Rebar in a Marine Environment," Transportation Research Circular: Epoxy-Coated Reinforcement in Highway Structures, No. 403, ISSN 0097-8515, National Research Council, Washington, D.C., March 1993, pp 36-45.

99. American Association of State Highway Transportation Officials, "Standard Specification for Epoxy-Coated Reinforcing Bars," AASHTO M284-86, Washington, D.C., 1986.

100. Texas Department of Transportation, "Epoxy Coating of Reinforcing Steel," Special Specification Item 4785, TXDOT, 4 p.

101. Texas Department of Transportation, "Standard Specifications for Construction of Highways, Streets and Bridges," TXDOT, march 1993, pp 730-744.

102. National Association of Corrosion Engineering, "Holiday Detection of Fusion-Bonded Epoxy External Pipeline Coatings of 10 to 30 Mils (0.25 to 0.76 mm)," NACE, Standard RP 0490-90, Houston, TX, April 1990.

102. National Association of Corrosion Engineering, "Holiday Detection of Fusion-Bonded Epoxy External Pipeline Coatings of 10 to 30 Mils (0.25 to 0.76 mm)," NACE, Standard RP 0490-90, Houston, TX, April 1990.

103. ENR, "Rebar Coating Plants to be Certified," *Engineering News Record,* The McGraw-Hill Construction Weekly, July 29, 1991, p 8.

104. Clifton, J.R., "Protection of Reinforcing Bars with Organic Coatings," *Materials Performance,* Vol. 15, No. 5, May 1976, pp 14-17.

105. Wheat, H.G., and Eliezer, Z., "Some Electrochemical Aspects of Corrosion of Steel in Concrete," *Corrosion,* NACE, Vol. 41, No. 11, November 1985, pp 640-645.

106. Virmani, Y.P., Clear, K.C., and Pasko, T.J., Jr., "Time-To-Corrosion of Reinforcing Steel in Concrete Slabs, V.5: Calcium Nitrite Admixture or Epoxy-Coated Reinforcing Bars as Corrosion Protection Systems," Report No. FHWA/RD-83/012, Federal Highway Administration, Washington, D.C., September 1983, 71 p.

107. Clear, K.C., and Virmani, Y.P., "Corrosion of Nonspecification Epoxy-Coated Rebars in Salty Concrete," *Public Roads,* Vol. 47, No. 1, June 1983, 10 p.

108. Swamy, R.N., Koyama, S., Arai, T., and Mikami, N., "Durability of Steel Reinforcement in Marine Environment," *Concrete in Marine Environment, Proceedings, 2nd International Conference, St. Andrews by-the-Sea, Canada,* ACI SP 109, V.M. Malhotra, Ed., American Concrete Institute, Detroit, 1988, pp 147-161.

109. Zayed, A.M., Sagüés, A.A., and Powers, R.G., "Corrosion of Epoxy-Coated Reinforcing Steel in Concrete," paper no. 379, *Corrosion 89,* NACE, New Orleans Convention Center, New Orleans, Louisiana, April 17-21,1989, 20 p.

110. Sagüés, A.A., and Powers, R.G., "Effect of Concrete Environment on the Corrosion Performance of Epoxy-Coated Reinforcing Steel," paper no. 311, *Corrosion 90,* NACE, Bally's Hotel, Las Vegas, Nevada, April 23-27, 1990, 15 p.

111. Sohanghpurwala, A., and Clear, K.C., "Effectiveness of Epoxy Coatings on Minimizing Corrosion of Reinforcing Steel in Concrete," Paper No. 890432, Transportation Research Board, 69th Annual Meeting, Washington, D.C., January 1990, 9 p.

112. Concrete Reinforcing Steel Institute, "CRSI Performance Research: Epoxy-Coated Reinforcing Steel," Interim Report, CRSI, Schaumburg, Ill, January 1992.

113. Rasheeduzzafar, Dakhil, F.H., Bader, M.A., and Khan, M.M., "Performance of Corrosion Resisting Steels in Chloride-Bearing Concrete," *ACI Materials Journal,* Vol. 89, No. 5, September-October 1992, pp 439-448.

114. Sagüés, A.A., "Corrosion of Epoxy-Coated Rebar in Florida Bridges," Interim Summary Report, State Job No. 99700-7556-010, University of South Florida, Tampa, Florida, April 1992, 42 p.

115. McKenzie, M., "The Effect of Defects on the Durability of Epoxy-Coated Reinforcement," Transportation Research Circular: Epoxy-Coated Reinforcement in Highway Structures, No. 403, ISSN 0097-8515, National Research Council, Washington, D.C., March 1993, pp 17-28.

116. Schiessl, P., and Renter, C., "Epoxy-Coated Rebars in Europe: Research Projects, Requirements and Use," Transportation Research Circular: Epoxy-Coated Reinforcement in Highway Structures, No. 403, ISSN 0097-8515, National Research Council, Washington, D.C., March 1993, pp 29-35.

117. American Society for Testing and Materials, "Half-Cell Potentials of Uncoated Reinforcing Steel in Concrete," ASTM C876-87, Philadelphia, PA, 1987.

118. Kahhaleh, K.Z., Chao, H.Y., Jirsa, J.O., Carrasquillo, R.L., and Wheat, H.G., "Studies on Damage and Corrosion Performance of Fabricated Epoxy-Coated Reinforcement," Report No. FHWA/TX-93+1265-1, National Technical Information Service, Spingfield, Varginia, January 1993, 80 p.

119. "Epoxy-Coated Rebars- Swiss Guidelines," **Peter Matt,** Private Communications, February 1992, 9 p.

120. Mindess, S., and Young, J.F., "Concrete," Prentice-Hall, N.J., 1981.

121. **Neif, T.,** Private Communication at The University of Texas at Austin, Austin, TX, November 1, 1991.

122. **Hamad, B.S., Jirsa, J.O., and D'Abreu D'Paolo, N.J.,** "Effect of Epoxy Coating on Bond and Anchorage of Reinforcement in Concrete Structures," Research Report No. 1181-1F, Center for Transportation Research, The University of Texas at Austin, Austin, TX, November 1990, 258 p.

123. **Lehmann, J.,** "Cathodic Protection (Corrosion Control) of Reinforced Concrete Structures Using Conductive Coatings," *Corrosion, Concrete and Chlorides, ACI SP 102,* F.W. Gibson, Ed., American Concrete Institute, Detroit, 1987, pp 127-141.

124. **Aguilar, A., Sagüés, A.A., and Powers, R.G.,** "Corrosion Measurements of Reinforcing Steel in Partially Submerged Concrete Slabs," *Corrosion Rates of Steel in Concrete,* ASTM STP 1065, N.S. Berke, V. Chaker, and D. Whiting, Eds., American Society for Testing and Materials, Philadelphia, PA, 1990, pp 66-85.

125. **Jones, L.W.,** "Corrosion and Water Technology for Petroleum Producers," Oil & Gas Consultants International, Inc., Tulsa, Oklahoma, 1988.

126. **Paul, J.H., and Keyvan, N.R.,** "Parking Structure Repair by Full-Slab Replacement," *Concrete International,* Vol. 15, No. 3, March 1993, pp 36-38.

127. **Lambert, P., and Norris, P.,** "Investigation and Structural Consequences of Reinforcement Corrosion in Concrete Structures," Proceedings of 5th International Conference on Structural Faults and Repair held 29 June, 1993, V.1, Venue, University of Edinburgh, pp 111-117.

128. **Pfeifer, D.W., and Landgren, J.R.,** "Protective Systems for New Prestressed and Substructure Concrete," Proceedings, 5th International Bridge Conference, Paper No. IBC-88-29, Pittsburgh, PA, June 1988, pp 146-153.

129. **Lemoine, L., Weger, F., and Galland, J.,** "Study of the Corrosion of Concrete Reinforcement by Electrochemical Impedance Measurement," *Corrosion Rates of Steel in Concrete,* ASTM STP 1065, N.S. Berke, V. Chaker, and D. Whiting, Eds., American Society for Testing and Materials, Philadelphia, PA, 1990, pp 118-133.

130. **Matsuoka, K., Kihira, H., Ito, S., and Murata, T.,** "Corrosion Monitoring for Reinforcing Bars in Concrete," *C Corrosion Rates of Steel in Concrete,* ASTM STP 1065, N.S. Berke, V. Chaker, and D. Whiting, Eds., American Society for Testing and Materials, Philadelphia, PA, 1990, pp 103-117.

131. **Andrade, C., Macias, A., Feliu, S., Escudero, M.L., and González, J.A.,** "Quantitative Measurement of the Corrosion Rate Using a Small Counter Electrode in the Boundary of Passive and Corroded Zones of a Long Concrete Beam," *Corrosion Rates of Steel in Concrete,* ASTM STP 1065, N.S. Berke, V. Chaker, and D. Whiting, Eds., American Society for Testing and Materials, Philadelphia, PA, 1990, pp 134-142.

132. Andrade, C., Alonso, M.C., and González, J.A., "An Initial Effort to Use the Corrosion Rate Measurements for Estimating Rebar Durability," *Corrosion Rates of Steel in Concrete,* ASTM STP 1065, N.S. Berke, V. Chaker, and D. Whiting, Eds., American Society for Testing and Materials, Philadelphia, PA, 1990, pp 29-37.

133. Thompson, D.M., "Coatings for Concrete Bridges," *Polymers Paint Colour Journal,* Vol. 177, No. 4204, November 25, 1987, pp 815-816.

134. Malhotra, V.M., "Fly Ash, Slag, Silica, Fume and Rice-Husk Ash in Concrete: A Review," *Concrete International,* Vol. 15, No. 4, April 1993, pp 23-28.

135. Sherman, M.R., "Field Evaluation of Bridge Corrosion Protection Measures," A Master of Science Thesis, The University of Texas at Austin, Austin, TX, May 1993, 266 p.

136. Tourney, P., and Berke, N., "Put to the Test," *Civil Engineering,* December 1992, pp 62-63.

137. Erki, M.A., and Rizkalla, S.H., "FRP Reinforcement of Concrete Structures," *Concrete International,* Vol. 15, No. 6, June 1993, pp 48-53.

138. Hammond, A.D., "Electrochemical Techniques for the Repair of Concrete," Proceedings of 5th International Conference on Structural Faults and Repair held 29 June, 1993, V.2, Venue, University of Edinburgh, pp 181-198.

139. Gustafson, D.P., and Edgell, T.W., "Epoxy-Coated Rebars Provides Rehab Relief," *Roads and Bridges,* Vol. 27, No. 8, August 1989, pp 51-53.

140. MEC, "Total Protection," *Middle East Construction,* April/May 1987, p 26.

141. Hasan, H., and Ramirez, J.A., "Effects of Static and Repeated Loadings on Concrete Bridge Decks and Slabs Reinforced with Epoxy-Coated Bars," Transportation Research Circular: Epoxy-Coated Reinforcement in Highway Structures, No. 403, ISSN 0097-8515, National Research Council, Washington, D.C., March 1993, pp 46-56.

142. Cleary, D.B., and Ramirez, J.A., "Bond of Epoxy-Coated Reinforcement Under Repeated Loading," Report No. CE-STR-92-13, School of Civil Engineering, Purdue University, West Lafayette, 1992.

143. American Society for Testing and Materials, "Standard Specification for Deformed and Plain Billet-Steel Bars for Concrete Reinforcement," ASTM A615- 87a, Philadelphia, PA, 1987.

144. American Society for Testing and Materials, "Standard Method for Nondestructive Measurement of Film Thickness of Pipeline Coatings on Steel," ASTM G12-83, Philadelphia, PA, 1983.

145. American society for Testing and Materials, "Standard Test Methods for Determining the Effects of Chemical Admixtures on the Corrosion of Embedded Steel Reinforcement in Concrete Exposed to Chloride Environment," ASTM G109-92, Philadelphia, PA, 1992.

146. American Association of State Highway Transportation Officials, "Rapid Determination of the Chloride Permeability of Concrete," AASHTO T277-83, Washington, D.C., 1983.

VITA

Khaled Zuhair Kahhaleh was born in Amman, Jordan, on February 13, 1960, the son of Zuhair and Sabah Kahhaleh. After completing his work at The Islamic Educational School, Amman, Jordan, in 1978, he entered The University of Jordan. He received the degree of Bachelor of Science in Civil Engineering from The University of Jordan in June 1983. During the following year, he worked on different design and construction projects in Amman. In September 1984, he entered the Graduate School of The University of Texas at Austin and was granted the degree of Master of Science in Engineering in August 1985. In February 1986, he joined The Royal Scientific Society in Amman, Jordan, and held the position of the head of the Engineering Consultations Unit at the Building Research Center. He prepared and participated in the preparation of more than 70 technical reports on various studies performed between 1986 and 1990. In September 1990, he was readmitted to the Graduate School of the University of Texas.

Permanent address: P. O. Box 385
P. C. 11118
Amman, Jordan

This dissertation was typed by the author.